Springer Series in Optical Sciences 145

Tom Rother
Michael Kahnert

Electromagnetic Wave Scattering on Nonspherical Particles

Basic Methodology and Simulations

2nd Edition

Springer

Springer Series in Optical Sciences

Volume 145

Founded by
H. K. V. Lotsch

Editor-in-Chief
W. T. Rhodes

For further volumes:
http://www.springer.com/series/624

Springer Series in Optical Sciences

The Springer Series in Optical Sciences, under the leadership of Editor-in-Chief William T. Rhodes, Georgia Institute of Technology, USA, provides an expanding selection of research monographs in all major areas of optics: lasers and quantum optics, ultrafast phenomena, optical spectroscopy techniques, optoelectronics, quantum information, information optics, applied laser technology, industrial applications, and other topics of contemporary interest.

With this broad coverage of topics, the series is of use to all research scientists and engineers who need up-to-date reference books.

The editors encourage prospective authors to correspond with them in advance of submitting a manuscript. Submission of manuscripts should be made to the Editor-in-Chief or one of the Editors. See also www.springer.com/series/624

Tom Rother · Michael Kahnert

Electromagnetic Wave Scattering on Nonspherical Particles

Basic Methodology and Simulations

Second Edition

Springer

Tom Rother
Inst. Methodik der Fernerkundung
Deutsches Zentrum für Luft- und Raumfahrt (DLR)
Neustrelitz
Germany

Michael Kahnert
Swedish Meteorological and Hydrological Institute
Norrköping
Sweden

Additional material to this book can be downloaded from http://extras.springer.com.

ISSN 0342-4111 ISSN 1556-1534 (electronic)
ISBN 978-3-642-36744-1 ISBN 978-3-642-36745-8 (eBook)
DOI 10.1007/978-3-642-36745-8
Springer Heidelberg New York Dordrecht London

Library of Congress Control Number: 2013937605

Printed on acid-free paper

Springer is part of Springer Science+Business Media (www.springer.com)

The photo shows a 22-degree Halo phenomenon with sun dogs. It was taken by the author in March 1998 at the DLR site in Neustrelitz. This phenomenon is caused by light scattering on hexagonal ice columns (the 22-degree Halo) and ice plates (the sun dogs) in Cirrus clouds

Preface to the Second Edition

Advantage has been taken in the preparation of the second edition of this book to eliminate several errors and misprints as well as to add a chapter on group theory. The importance of such group theoretical considerations has been proven in recent applications for particles with discrete boundary symmetries. To demonstrate this benefit we included an additional subsection in Chap. 9 where we consider light scattering on Chebyshev particles of higher order. The reference chapter was updated accordingly.

The simulation software which was provided on a CD-ROM with the first edition can now be obtained via download from Springer's web site or on request from the authors. Besides the program *mieschka* and the scattering database of the first edition, the program *Tsym* for non-axisymmetric particles is also included. Its usage is described in detail in Chap. 9 of this second edition. Heikki Laitinen, Kari Lumme, Dan Mackowski, Michael Mishchenko, Karri Muinonen, and Timo Nousiainen are gratefully acknowledged for their kind permission to include various Fortran routines from their respective programs in the distribution of *Tsym*.

Neustrelitz, Germany — T. Rother
Norrköping, Sweden — M. Kahnert

Preface to the First Edition

Scattering of electromagnetic waves on three-dimensional, dielectric structures is a basic interaction process in physics, which is also of great practical importance. Most of our visual impressions are caused not by direct but by scattered light, as everybody can experience by looking directly at the sun. Several modern measurement technologies in technical and medical diagnostics are also based on this interaction process. Atmospheric remote sensing with lidar and radar as well as nephelometer instruments for measuring suspended particulates in a liquid or gas colloid are only a few examples where scattered electromagnetic waves provide us with information concerning the structure and consistence of the objects under consideration. Using the information of the elastically scattered electromagnetic wave is a common ground for most of those measuring methods. The phrase "elastically scattered" expresses the restriction that we consider such interaction processes only where the scattered wave possesses the same wavelength as the primary incident wave. This book addresses this special scattering problem.

The methodology part of this book is concerned with the solution of the partial differential equations underlying this scattering process. These are especially the scalar Helmholtz equation and the vector-wave equation. From the mathematical point of view, we are faced with the solution of boundary value problems. This becomes especially simple if the boundary values are given along a constant coordinate line in one of the coordinate systems that allow a separation of the partial differential equation. Such problems are sometimes called "separable boundary value problems" in the literature. The applied method is the so-called "Separation of Variables method". It reduces the primary partial differential equation to a set of ordinary differential equations whose eigensolutions serve afterwards as expansion functions to approximate the sought solution appropriately. Scattering of light on dielectric and ideal metallic spheres was first solved by this method in 1908 by Gustav Mie. The Mie theory, as it is called nowadays, forms the basis in many applications even today.

On the other hand, not the least due to the possibilities of modern computers, there can be observed a growing interest in modelling more and more realistic scattering scenarios which goes beyond the conventional Mie theory for spherical scatterers. If the geometry of the scatterer differs only slightly from that of a separable geometry simpler perturbation methods may be applied successfully. But

more often the deviation from such a separable geometry is much stronger so that we are forced to apply more rigorous numerical methods to solve the problem. A large variety of such methods have been developed in the past. Differing in concept and execution these methods start from the common assumption that it is no longer possible to apply the Separation of Variables method. A critical discussion of this assumption is a major objective of this book. The Green functions are of special importance for this discussion. Based on these functions, we will show that there can be established a formalism which provides a common methodological background for a variety of different numerical methods. But the so-called "T-matrix" method is within the focus of our interest. This special solution method was developed by Waterman at the end of the 1960s and the beginning of the 1970s of the twentieth century. It has been proved to be very successful in many applications.

This book at hand is restricted to the relatively simple case of modelling electromagnetic wave scattering on single, homogeneous, but nonspherical particles in spherical coordinates. Nevertheless, it provides a sound basis to develop the methods for more complex situations as we have, if scattering on an ensemble of objects or on inhomogeneous objects (like multilayered particles, for example) is considered.

The basic methodological considerations of this book are complemented in the penultimate chapter with numerical simulations of a few typical scattering scenarios. For these simulations we have developed a specific T-matrix code which can be found in the enclosed CD. Its structure and usage is presented in detail. This program will enable the reader who is more interested in tangible calculations, to perform quickly his own numerical simulations, and, most important, to estimate the accuracy and usefulness of the obtained results. This software can also be used in university lectures to demonstrate the principal aspects of light scattering. Some parts of this book began as notes of a special lecture given by the author at the Meteorological Institute of the University Leipzig. The considerations in the penultimate chapter should reveal some of the numerical problems which must be solved if one tries to develop a certain T-matrix code.

Naturally, this book is not the result of only my efforts. For the multitude of (partly very heavily) discussions over the years I sincerely thank my two colleagues at the Remote Sensing Technology Institute, Dr. K. Schmidt and Dr. J. Wauer. Special thanks are due to Dr. J. Wauer for his numerical work on the Rayleigh hypothesis as discussed in Chap. 6, and for his work on the software package *mieschka* and the database. Special thanks are due also to the German Aerospace Center (DLR) for the confidence in my work over the years, and for the financial as well as administrative support which cannot be taken for granted nowadays.

C. Ascheron at Springer deserves a word of thanks for his continuous interest, support, and encouragement after the manuscript appeared via email for the first time suddenly in his office.

My gratitude is deepest, however, to my parents, who supported me in manifold ways and pushed me into the direction of science, and to my wife Doreen, who helped me without complaint through the nearly 7 years of writing this book. She also carefully read the manuscript and wiped out a lot of needless "m"-dashes—thus demonstrating that a musician and a physicist can really benefit from each other.

Neustrelitz, Germany, June 2009 T. Rother

Contents

1 Scattering as a Boundary Value Problem 1
1.1 Introduction 1
1.2 Formulation of the Boundary Value Problems. 5
1.3 Solving the Boundary Value Problems with the Rayleigh Method 8
1.3.1 The Outer Dirichlet Problem 10
1.3.2 The Outer Transmission Problem 12

2 Filling the Mathematical Tool Box 17
2.1 Introduction 17
2.2 Approximation of Functions and Fields at the Scatterer Surface 18
2.2.1 Approximation by Finite Series Expansions 19
2.2.2 Best Approximation 21
2.2.3 The Transformation Character of the T-Matrix 24
2.3 Eigensolutions of the Scalar Helmholtz Equation in Spherical Coordinates. 29
2.3.1 The Eigensolutions 31
2.3.2 The Combined Summation Index 36
2.3.3 Properties of the Scalar Eigensolutions 37
2.3.4 Expansion of a Scalar Plane Wave 39
2.4 Eigensolutions of the Vector-Wave Equation in Spherical Coordinates. 42
2.4.1 The Vectorial Eigensolutions 42
2.4.2 Properties of the Vectorial Eigensolutions 47
2.4.3 Expansion of a Linearly Polarized Plane Wave. 52
2.5 Green Theorems and Green Functions Related to the Scalar Boundary Value Problems 59
2.5.1 The Green Theorems. 60
2.5.2 The Free-Space Green Function 61
2.5.3 The Green Functions Related to the Outer Dirichlet and Transmission Problem 67

2.6 Green Theorems and Green Functions Related to the Vectorial Boundary Value Problems 69
2.6.1 Dyadics 69
2.6.2 The Green Theorems 72
2.6.3 The Dyadic Free-Space Green Function 73
2.6.4 The Dyadic Green Functions Related to the Outer Dirichlet and Transmission Problem 77

3 First Approach to the Green Functions: The Rayleigh Method . . . 81
3.1 Introduction 81
3.2 The Scalar Delta Distribution at the Scatterer Surface 83
3.3 The Scalar Green Functions Related to the Helmholtz Equation 84
3.3.1 The Outer Dirichlet Problem 84
3.3.2 The Outer Transmission Problem 92
3.4 The Dyadic Delta Distribution at the Scatterer Surface 94
3.5 The Dyadic Green Functions Related to the Vector-Wave Equation 95
3.5.1 The Outer Dirichlet Problem 95
3.5.2 The Outer Transmission Problem 102

4 Second Approach to the Green Functions: The Self-Consistent Way 105
4.1 Introduction 105
4.2 The Scalar Green Functions Related to the Helmholtz Equation 106
4.2.1 The Outer Dirichlet Problem 106
4.2.2 The Outer Transmission Problem 109
4.3 The Dyadic Green Functions Related to the Vector-Wave Equation 111
4.3.1 The Outer Dirichlet Problem 111
4.3.2 The Outer Transmission Problem 113
4.4 Symmetry and Unitarity 115
4.4.1 Symmetry 116
4.4.2 Unitarity 119

5 Other Solution Methods 129
5.1 Introduction 129
5.2 T-Matrix Methods 130
5.2.1 The Extended Boundary Condition Method 130
5.2.2 Point Matching Methods 136
5.3 The Method of Lines as a Special Finite-Difference Method . . . 137
5.3.1 Discretization of the Scalar Helmholtz Equation and its Solution 138
5.3.2 The Limiting Behaviour of the Method of Lines 146

5.4 Integral Equation Methods 151
5.4.1 Boundary Integral Equation Method Related to the Outer Dirichlet Problem 153
5.4.2 Boundary Integral Equation Method Related to the Outer Transmission Problem 158
5.4.3 Volume Integral Equation Method Related to the Outer Transmission Problem 160
5.5 Lippmann-Schwinger Equations 164
5.5.1 The Scalar Problem 164
5.5.2 The Dyadic Problem 167

6 The Rayleigh Hypothesis 171
6.1 Introduction 171
6.2 Plane Wave Scattering on Periodic Gratings 174
6.2.1 Conventional Formulation of the Scattering Problem 174
6.2.2 Formulation in Terms of Green Functions 177
6.2.3 T-Matrix Solution 182
6.2.4 Rayleigh's Hypothesis According to Petit, Cadilhac, and Millar 185
6.2.5 Rayleigh's Hypothesis According to Lippmann, and a Corresponding Boundary Integral Solution 188
6.3 Numerical Near-Field Analysis 191
6.4 Summary 195

7 Physical Basics of Electromagnetic Wave Scattering 203
7.1 Introduction 203
7.2 The Electromagnetic Scattering Problems 204
7.2.1 Maxwell's Equations and Boundary Conditions 204
7.2.2 Vector Wave Equations of the Electromagnetic Fields . . . 208
7.2.3 Helmholtz Equation of the Debye Potentials and Mie Theory 214
7.3 The Far-Field and the Scattering Quantities 221
7.3.1 The Far-Field 222
7.3.2 Definition of Scattering Quantities 230
7.4 Scalability of the Scattering Problem 237

8 Scattering on Particles with Discrete Symmetries 241
8.1 Introduction 241
8.1.1 Symmetry Relations 241
8.2 Explicit Commutation Relations of the T-Matrix 251
8.2.1 Unitary Representations of Symmetry Operations 251
8.2.2 Commutation Relations 261
8.2.3 Simplification of Scalar Products 263

8.3 Symmetry Groups 265
8.3.1 Groups and Generators 265
8.3.2 Conjugate Elements and Classes 268
8.3.3 Linear Representations of a Group 269
8.4 Irreducible Representations 270
8.4.1 Motivation 271
8.4.2 Basic Definitions 273
8.4.3 The Great Orthogonality Theorem. 277
8.4.4 Projection Operators into the Invariant Subspaces 277
8.4.5 Construction of the Basis Transformation from the Reducible to the Irreducible Basis 280

9 Numerical Simulations of Scattering Experiments 287
9.1 Introduction 287
9.2 Numerical Simulations with *mieschka* 288
9.2.1 Single Particles in Fixed Orientations 288
9.2.2 Single Particles in Random Orientation 302
9.2.3 Database for Spheroidal Particles and Size Averaging . . . 313
9.2.4 Morphology Dependent Resonances 315
9.3 High-Order Chebyshev Particles 319
9.3.1 Perturbation Approach of the T-Matrix 320
9.3.2 Results. 322
9.4 Description of Program *mieschka* 324
9.4.1 Convergence Strategy Used in *mieschka* 325
9.4.2 Functionality and Usage of *mieschka*. 329
9.4.3 Content of the Software Package 335
9.5 Description of Program *Tsym* 336
9.5.1 Compilation and Input Parameters. 337
9.5.2 Convergence Tests 339
9.5.3 Result Files 340
9.5.4 Resources. 342

10 Recommended Literature 345
10.1 Mie Theory 345
10.2 Mathematical Aspects of Scattering 346
10.3 Green Functions. 347
10.4 T-Matrix Methods 348
10.5 Method of Lines 349
10.6 Integral Equation Methods and Singularities 350
10.7 Rayleigh's Hypothesis 351
10.8 Electromagnetic Wave Theory 352
10.9 Scattering of Electromagnetic Waves and Applications. 352

10.10 Group Theory 354
10.11 Miscellaneous 355

Index 357

Chapter 1
Scattering as a Boundary Value Problem

1.1 Introduction

If we speak about scattering in this book it is tacitly meant that we consider the interaction of a plane electromagnetic wave with a three-dimensional structure. The latter is characterized by its dielectric property, and the geometry of its boundary surface. A corresponding scattering theory interrelates the asymptotic free states before and after the interaction of the primary incoming plane wave with the scattering structure, whereas the incoming plane wave represents the asymptotic free state before the interaction. If we know the asymptotic free state after the interaction we can derive and define quantities which are appropriate to measure. Moreover, we restrict our considerations to the steady state of scattering with an assumed time dependence of $exp(-i\omega t)$. The asymptotic free states correspond in this case to spatial distances large compared to a characteristic distance of the scattering structure, i.e., we look at the free states in the far field. Due to this understanding of scattering we have to consider processes taking place at different spatial scales. These are the interaction between the incoming plane wave and the scatterer on the local scale of the scatterer, and the behaviour of the electromagnetic fields in the nonlocal far-field. An exception is only made in Chap. 6, when we examine the near-field of a two-dimensional, ideal metallic grating.

The scattering efficiency of a spherical scatterer as a function of the size parameter is presented in Fig. 1.1. The size parameter denotes the ratio of a characteristic length of the scatterer to the wavelength of the incoming plane wave (the exact definitions of the "scattering efficiency" and the "size parameter" will be given in Chap. 7!). If the scatterer is small compared to the wavelength we can observe a continuously increasing scattering efficiency. This is the well-known region of Rayleigh scattering, which is characterized by the scattering behaviour of a dipole. If we increase the size of the sphere but retain the wavelength of the incoming plane wave we arrive at a region with pronounced resonances. This region, not surprisingly, is therefore called "resonance region". These resonances become less pronounced if we increase the size of the sphere further until we arrive at the region where the geometric optics approximation

T. Rother and M. Kahnert, *Electromagnetic Wave Scattering on Nonspherical Particles*, Springer Series in Optical Sciences 145, DOI: 10.1007/978-3-642-36745-8_1,

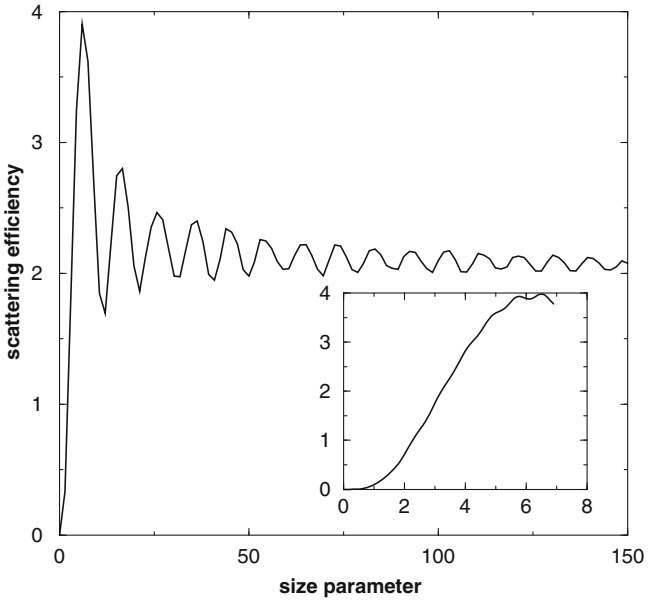

Fig. 1.1 Scattering efficiency of a dielectric sphere with a refractive index of $n = 1.33$ as a function of the size parameter. The included figure is a zoom in onto the Rayleigh region, and on the transition of the resonance region

can be applied. This approximation neglects diffraction and replaces the incoming plane wave by a bundle of rays propagating through the scatterer according to the laws of reflection and refraction. The qualitative dependence of the scattering efficiency on the size parameter shown in Fig. 1.1 is typical for every scatterer and not restricted to spheres. But, of course, the quantitative behaviour in each region as well as the location of the transitions between the regions are still dependent on the geometry and permittivity of the scatterer. The Rayleigh region and the geometric optics region are characterized by the physical simplifications which can be made when initially formulating the scattering problem. In the resonance region, on the other hand, we have to consider the full Maxwell equations and the wave nature of the fields. As a result, we have to solve the more complicate boundary value problems related to the Helmholtz equation and the vector-wave equation, respectively. In this book, we will look rather closely at some of the solution techniques developed especially for these boundary value problems. Strictly speaking, we should be able to derive the solutions within the Rayleigh region and the geometric optics region from limiting considerations of the general solution methods developed for the resonance region. This is indeed possible for the Rayleigh region. Regarding higher size parameters this can be done only in some exceptional cases, so far (for spherical particles, for example). The development of appropriate solution methods for the resonance region which can be applied also at higher size parameters is therefore an important and ambitious goal of recent research in this area.

In general, scattering of electromagnetic waves on three-dimensional structures requires the solution of the boundary value problems related to the vector-wave equation. Only in specific situations, as it happens for spherical scatterers or if we consider infinitely extended cylinders with noncircular cross-sections normally illuminated by a plane wave, for example, we can benefit from the solution of two independent but scalar boundary value problems related to the scalar Helmholtz equation (see also Chap. 7). Another example of such a situation is discussed in Chap. 6. The detailed considerations of the boundary value problems related to the scalar Helmholtz equation carried out in this book are therefore attributed primarily to the didactic aspect that most of the derivations become even simpler. The dyadic nature of the relevant Green functions resulting in an increased complexity can be neglected in this case, for example. But there are also essential differences between the scalar and dyadic formulation, as will be shown later. One of such differences is the singular behaviour of the free-space Green's function in the source region with corresponding consequences for the general solution methods and their numerical realizations. But, on the other hand, there are other physical disciplines where the scalar boundary value problems considered herein are of direct importance. This applies to acoustic wave scattering and to certain problems in quantum and fluid mechanics, to mention only a few examples. The parameter "k" occurring in the Helmholtz equation has merely a different physical meaning in these cases.

In Sects. 1.2 and 1.3 of this chapter, we will formulate the boundary value problems of our interest and later discuss very formally a solution scheme which was already established by Rayleigh.

It is the general intention of all our efforts in this book to approximate the unknown solution of the boundary value problems in terms of an appropriate finite series expansion. The mathematical tools which are required for this purpose are examined in Chap. 2. In Chap. 2, we will also try to define the term "appropriate" more precisely.

Chapter 3 represents a first step toward the relevant Green functions. Once we have found the finite series expansion for the sought solution we are able to derive the equivalent approximation of the Green function belonging to the considered boundary value problem. This is accomplished by employing Green's theorem appropriately. However, the most important result of this chapter, from the authors point of view, is the verification of the fact that Waterman's T-matrix is a substantial part of this Green function. This result is derived again but on a different way in Chap. 4. Starting point is the definition of the so-called "interaction operator". This definition can be considered as a special formulation of the Huygens principle for Green functions. Chapter 4 deals exclusively with the Green functions related to the boundary value problems of our interest, without any recourse to the underlying physical problem. This is the deeper reason why we called the resulting formalism the "self-consistent Green's function formalism". In this chapter we will express our firm conviction that, from a methodical point of view, the Green functions form a suitable starting point for the treatment of different scattering problems as well as for the development of numerical procedures. The advantage of using Green functions is moreover demonstrated by deriving those important mathematical properties like symmetry and unitarity.

These properties will be related later on to the physical experience of reciprocity and energy conservation.

In Chap. 5 we will demonstrate how one can find other known solution methods in this self-consistent Green's function formalism. Amongst others we discuss in this chapter the advantages and disadvantages of a special Finite-Difference technique, the so-called "Method of Lines". Regarding this method there exist several misunderstandings concerning its nature, and its assumed difference compared to the T-matrix methods. These misunderstandings will be clarified. To reveal the relation of the Green's function formalism to the conventional boundary and volume integral equation methods as well as to derive the so-called "Lippmann-Schwinger equations" we have to perform a slight but important change in the definition of the interaction operators introduced in Chap. 4.

This slight change in the definition of the interaction operator is strongly related to the controversial and still ongoing discussion of "Rayleigh's hypothesis". Rayleigh's hypothesis has such an interesting history that we dedicate this aspect its own chapter—Chap. 6. We are also not able to provide a final and satisfactory answer to this problem. But the Green functions point of view may add some interesting aspects on it. Additionally, we present a numerical answer to that problem originally considered in the famous 1907 paper of Rayleigh.

In Chap. 7 we will take a closer look onto the electromagnetic theory as needed to formulate the scattering process and to define suitable quantities in the far-field which will help us to establish the link to real measurements. Especially, the nature of the far-field and the somehow strange nature of a plane wave is considered in detail here. Thus, this chapter forms the physical basis for the numerical simulations in Chap. 9.

Essential simplifications in the calculation of the T-matrix can be achieved if the particle geometry under consideration exhibits a certain symmetry. This aspect is considered in detail in Chap. 8 where we discuss group theoretical approaches to particles with discrete boundary symmetries.

In Chap. 9 we will condense the theoretical considerations of the former chapters into basic numerical simulations of selected scattering scenarios which are of importance in recent measurement techniques. Our main focus here is on the difference of the scattering behaviour of nonspherical but rotationally symmetric particles in fixed and random orientation vs. spherical particles. The restriction to rotationally symmetric boundaries is abandoned in Sect. 9.3 where we consider scattering on higher-order Chebyshev particles. This reveals the benefit one may gain if combining the group theoretical results of Chap. 8 with an iteration procedure to calculate the T-matrix.

The book is completed with a reference chapter. Only those references which have been found most useful for the authors are mentioned. This chapter reflects the very personal preferences of the authors and should be understood neither as complete nor as a ranking!

1.2 Formulation of the Boundary Value Problems

Regarding the scalar Helmholtz equation and the vector-wave equation, respectively, we are essentially interested in two special boundary value problems. These are the outer Dirichlet problem and the outer transmission problem. "Outer" problems because we are only considering sources $\rho(x)$ of the primary unperturbed field which are located outside the scatterer. Moreover, we are only interested in the fields outside the scatterer. The basic geometrical configuration of these scattering problems are depicted in Fig. 1.2. The finite volume Γ_- of the scatterer is enclosed by its boundary surface $\partial\Gamma = S$ and physically characterized by the constant k. The origin of the coordinate system is located somewhere inside the scatterer. $\hat{n}$ denotes the unit normal vector at the boundary surface $\partial\Gamma$ pointing into the outer region Γ_+. The outer region Γ_+ itself is physically characterized by the constant k_0, i.e., it is assumed to be vacuum. The spherical surface S_∞ at infinity represents its outer boundary surface. $\hat{n}_-$ is the unit normal vector belonging to the boundary surface of Γ_+. Along its inner boundary surface $\partial\Gamma$ this vector is pointing into Γ_-, i.e., we have the relation $\hat{n}_- = -\hat{n}$ at $\partial\Gamma$. Along S_∞, $\hat{n}_-$ is pointing outward into the radial direction. Each of these regions, the region inside and outside the scatterer, can be considered as a simply connected region bounded by different boundary surfaces. Γ_- is simply bounded by $\partial\Gamma$. Γ_+, on the other hand, is bounded by $\partial\Gamma$, S_∞, and C. The cut C must be considered twice but with opposite sign for a closed orbit of Γ_+. Each point $\mathbf{x}$ in Γ_- as well as in Γ_+ is represented by its coordinates (r, θ, ϕ), i.e., the scattering problems will be treated in a spherical coordinate system. An exception from this is only made in Chap. 6. There, we consider a specific scattering problem in Cartesian coordinates.

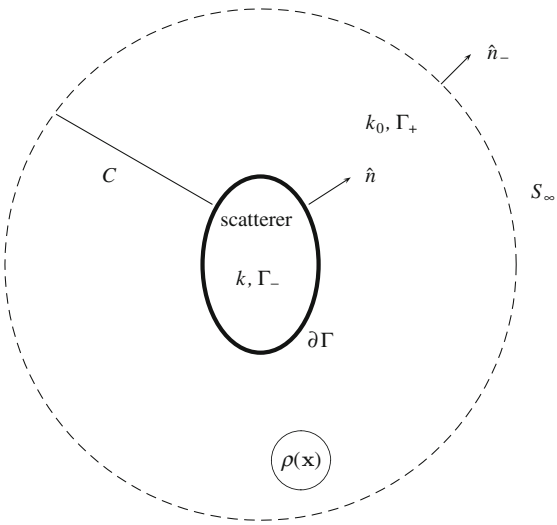

Fig. 1.2 Underlying geometry of the scattering problems

With respect to the scalar Helmholtz equation, we are interested in the following two boundary value problems:

- Solving the inhomogeneous Helmholtz equation in the outer region Γ_+ in conjunction with the fulfilment of the homogeneous boundary condition along $\partial\Gamma$ (the outer Dirichlet problem of the Helmholtz equation):

$$\left(\nabla^2 + k_0^2\right) u_t(\mathbf{x}) = -\rho(\mathbf{x}); \quad \mathbf{x} \in \Gamma_+ \tag{1.1}$$

$$u_t(\mathbf{x}) = 0; \quad \mathbf{x} \in \partial\Gamma. \tag{1.2}$$

- Solving the inhomogeneous Helmholtz equation in the outer region Γ_+ as well as the homogeneous Helmholtz equation inside the scatterer in conjunction with the fulfilment of the transmission conditions along $\partial\Gamma$ (the outer transmission problem of the Helmholtz equation):

$$(\nabla^2 + k_0^2)\, u_t(\mathbf{x}) = -\rho(\mathbf{x}); \quad \mathbf{x} \in \Gamma_+ \tag{1.3}$$

$$(\nabla^2 + k^2)\, u_{int}(\mathbf{x}) = 0; \quad \mathbf{x} \in \Gamma_- \tag{1.4}$$

$$u_t(\mathbf{x}) = u_{int}(\mathbf{x}); \quad \mathbf{x} \in \partial\Gamma \tag{1.5}$$

$$\frac{\partial u_t(\mathbf{x})}{\partial \hat{n}_-} = \frac{\partial u_{int}(\mathbf{x})}{\partial \hat{n}_-}; \quad \mathbf{x} \in \partial\Gamma. \tag{1.6}$$

The normal derivative at the scatterer surface is defined according to

$$\frac{\partial u(\mathbf{x})}{\partial \hat{n}_-} := \hat{n}_- \cdot \nabla u(\mathbf{x}). \tag{1.7}$$

u_t is the total field existing in the outer region. Due to the linearity of the Helmholtz equation we can represent this total field by the sum of the primary incident field u_{inc} and the scattered field u_s, i.e., by

$$u_t(\mathbf{x}) = u_{inc}(\mathbf{x}) + u_s(\mathbf{x}). \tag{1.8}$$

The primary incident field is a solution of the inhomogeneous Helmholtz equation

$$(\nabla^2 + k_0^2)\, u_{inc}(\mathbf{x}) = -\rho(\mathbf{x}); \quad \mathbf{x} \in \Gamma_+. \tag{1.9}$$

Its inhomogeneity $\rho(\mathbf{x})$ is the generating source distribution of this primary field. On account of (1.1) and (1.3), respectively, the scattered field must be a solution of the corresponding homogeneous Helmholtz equation. According to this, we can replace the homogeneous boundary condition (1.2) of the outer Dirichlet problem for the total field by the corresponding inhomogeneous boundary condition

$$u_s(\mathbf{x}) = -u_{inc}(\mathbf{x}); \quad \mathbf{x} \in \partial\Gamma \tag{1.10}$$

for the scattered field.

The two boundary value problems of our interest related to the vector-wave equation can be formulated in close analogy to the scalar problems:

- Solving the inhomogeneous vector-wave equation in the outer region Γ_+ in conjunction with the fulfilment of the homogeneous boundary condition along $\partial\Gamma$ (the outer Dirichlet problem of the vector-wave equation):

$$\left(\nabla \times \nabla \times -k_0^2\right) \vec{u}_t(\mathbf{x}) = \vec{\rho}(\mathbf{x}); \quad \mathbf{x} \in \Gamma_+ \tag{1.11}$$

$$\hat{n}_- \times \vec{u}_t(\mathbf{x}) = \vec{0}; \quad \mathbf{x} \in \partial\Gamma. \tag{1.12}$$

- Solving the inhomogeneous vector-wave equation in the outer region Γ_+ as well as the homogeneous vector-wave equation inside the scatterer in conjunction with the fulfilment of the transmission conditions along $\partial\Gamma$ (the outer transmission problem of the vector-wave equation):

$$\left(\nabla \times \nabla \times -k_0^2\right) \vec{u}_t(\mathbf{x}) = \vec{\rho}(\mathbf{x}); \quad \mathbf{x} \in \Gamma_+ \tag{1.13}$$

$$\left(\nabla \times \nabla \times -k^2\right) \vec{u}_{int}(\mathbf{x}) = \vec{0}; \quad \mathbf{x} \in \Gamma_- \tag{1.14}$$

$$\hat{n}_- \times \vec{u}_t(\mathbf{x}) = \hat{n}_- \times \vec{u}_{int}(\mathbf{x}); \quad \mathbf{x} \in \partial\Gamma \tag{1.15}$$

$$\hat{n}_- \times \nabla \times \vec{u}_t(\mathbf{x}) = \hat{n}_- \times \nabla \times \vec{u}_{int}(\mathbf{x}); \quad \mathbf{x} \in \partial\Gamma. \tag{1.16}$$

The total field $\vec{u}_t$ outside the scatterer can again be represented by the sum of the primary incident and scattered field with the primary incident field $\vec{u}_{inc}$ being a solution of the inhomogeneous vector-wave equation

$$\left(\nabla \times \nabla \times -k_0^2\right) \vec{u}_{inc}(\mathbf{x}) = \vec{\rho}(\mathbf{x}); \quad \mathbf{x} \in \Gamma_+. \tag{1.17}$$

Because of (1.11) and (1.13), respectively, the scattered field $\vec{u}_s$ must then be a solution of the homogeneous vector-wave equation. Thus, the homogeneous boundary condition (1.12) of the outer Dirichlet problem for the total field can again be replaced by the inhomogeneous boundary condition

$$\hat{n}_- \times \vec{u}_s(\mathbf{x}) = -\hat{n}_- \times \vec{u}_{inc}(\mathbf{x}); \quad \mathbf{x} \in \partial\Gamma \tag{1.18}$$

for the scattered field. It should be emphasized that the primary incident fields u_{inc} and $\vec{u}_{inc}$ are taken for given quantities. The unknown fields are the scattered fields u_s and $\vec{u}_s$.

However, the above formulated boundary value problems are not complete. To get a unique solution of the scattering problems we need beside the behaviour at the scatterer surface $\partial\Gamma$ an additional condition at the outer boundary surface S_∞. The field generated by a source distribution within Γ_+ and within a finite distance from the origin has to fulfil the so-called "radiation condition" at infinity, or, more

precisely, at an infinite distance from the source distribution. This condition expresses the physical requirement that energy which is radiated from the source distribution must radiate away from this source to infinity. No energy may be reflected from infinity into the direction of the source distribution. In the scalar case this condition is also known as the "Sommerfeld's radiation condition" and for three-dimensional problems given by

$$\lim_{|\mathbf{x}|\to\infty}\left(\frac{\mathbf{x}}{|\mathbf{x}|}\cdot\nabla - ik_0\right)u(\mathbf{x}) = 0\left(\frac{1}{|\mathbf{x}|}\right). \tag{1.19}$$

It must hold uniformly for any direction $\mathbf{x}/|\mathbf{x}|$. In the vector case we have

$$\lim_{|\mathbf{x}|\to\infty}\left(\nabla\times\ -ik_0\frac{\mathbf{x}}{|\mathbf{x}|}\times\right)\vec{u}(\mathbf{x}) = 0\left(\frac{1}{|\mathbf{x}|}\right), \tag{1.20}$$

which is also known as the "Silver-Mueller radiation condition". This condition must also hold uniformly for any direction $\mathbf{x}/|\mathbf{x}|$. It is important to note here that the plane wave solutions of the scalar Helmholtz and vector-wave equation do not apply to these radiation conditions. Thus, if a plane wave is considered as the primary incident field the earlier formulated radiation conditions can only be applied to the scattered field! We will see later in Chap. 7, why especially this situation represents the real scattering problem.

From a more physical point of view it makes also sense to require that the scattered field is a smooth function in Γ_+, i.e., that it is a two times continuously differentiable function. The same should hold for the internal field within Γ_- if the outer transmission problem is considered. Moreover, the internal field should be regular, i.e., it must be free of singularities especially at the origin of the coordinate system.

1.3 Solving the Boundary Value Problems with the Rayleigh Method

Only in a very few cases we are able to derive a closed analytical solution of the above formulated boundary value problems. Therefore we will restrict all our effort to obtain "only" an approximate solution in terms of the following series expansion:

$$|\, u_s^{(N)}(\mathbf{x})\,> = \sum_{\tau=1}^{2}\sum_{i=0}^{N} a_{i,\tau}^{(N)}\cdot|\,\varphi_{i,\tau}(k_0,\mathbf{x})\,>; \quad \mathbf{x}\in\Gamma_+. \tag{1.21}$$

The expansion functions $|\,\varphi_{i,\tau}(k_0,\mathbf{x})\,>$ are assumed to be known quantities. With this expansion goes our hope that an increasing number of expansion terms will more precisely approach the sought solution $|\,u_s(\mathbf{x})\,>$. For the time being we will leave open what "more precisely" means precisely. In the above series expansion we have

used a compact notation for the approximate solution $| u_s^{(N)}(\mathbf{x}) >$ and the expansion functions $| \varphi_{i,\tau}(k_0, \mathbf{x}) >$. These are the "bra" (symbol "$< ...|$") and "ket" (symbol "$|... >$") symbols known from quantum mechanics. These symbols are used here to make the derivations in the following sections independent of whether continuously varying functions, continuously varying vector functions, or finite-dimensional vectors are considered. That is, the abstract vector $| u_s(\mathbf{x}) >$ may represent the quantities

$$| u_s(\mathbf{x}) > = u_s(\mathbf{x}) \tag{1.22}$$

$$\begin{aligned} | u_s(\mathbf{x}) > &= u_{s_1}(\mathbf{x}) \cdot \hat{x}_1 + u_{s_2}(\mathbf{x}) \cdot \hat{x}_2 + u_{s_3}(\mathbf{x}) \cdot \hat{x}_3 \\ &= (u_{s_1}(\mathbf{x}), u_{s_2}(\mathbf{x}), u_{s_3}(\mathbf{x})) = \vec{u}_s(\mathbf{x}) \end{aligned} \tag{1.23}$$

$$| u_s(\mathbf{x}) > = (u_{s_1}, u_{s_2}, ..., u_{s_n}) = \vec{u}_s. \tag{1.24}$$

$\hat{x}_1$, $\hat{x}_2$, and $\hat{x}_3$ are orthonormal unit vectors of the three-dimensional space, and each point $\mathbf{x}$ of this space is given by its components (x_1, x_2, x_3). The abstract "bra"-vector denotes the corresponding conjugate-complex quantities, i.e.,

$$< u_s(\mathbf{x}) | = u_s^*(\mathbf{x}) \tag{1.25}$$

$$\begin{aligned} < u_s(\mathbf{x}) | &= u_{s_1}^*(\mathbf{x}) \cdot \hat{x}_1 + u_{s_2}^*(\mathbf{x}) \cdot \hat{x}_2 + u_{s_3}^*(\mathbf{x}) \cdot \hat{x}_3 \\ &= (u_{s_1}^*(\mathbf{x}), u_{s_2}^*(\mathbf{x}), u_{s_3}^*(\mathbf{x})) = \vec{u}_s^*(\mathbf{x}) \end{aligned} \tag{1.26}$$

$$< u_s(\mathbf{x}) | = (u_{s_1}^*, u_{s_2}^*, ..., u_{s_n}^*) = \vec{u}_s^*. \tag{1.27}$$

Representation (1.22) is needed in connection with the boundary value problems of the scalar Helmholtz equation. The corresponding boundary value problems of the vector-wave equation makes it necessary to apply representation (1.23). Finite-dimensional vectors of type (1.24) are exclusively used in the context of the Method of Lines considered in Chap. 5. Moreover, the sum $\sum_{\tau=1}^{2}$ which appears in (1.21) is only needed if the boundary value problems of the vector-wave equation are considered. It can be neglected in the scalar case.

In 1907, Lord Rayleigh published a paper in the Proceedings of the Royal Society London (see the reference chapter for details) where he presented a method to analyse the scattering of a plane electromagnetic wave on an ideal metallic and periodic surface. This problem can be formulated exclusively in Cartesian coordinates, as already mentioned in Sect. 1.2. Interestingly, this paper was published one year before the famous paper of Gustav Mie, where he solved the more simple problem of light scattering on spherical particles. More simple because the latter problem can be treated in a straightforward way by use of the conventional Separation of Variables method in spherical coordinates (see Chap. 7). In Chap. 6, in the context of Rayleigh's hypothesis, we consider Rayleigh's approach in more detail. It is of our interest in this introductory chapter since this approach offers already a pragmatic way for the solution of the above formulated boundary value problems, and since it results directly into the T-matrix methods, derived later on by Waterman on a total different way. It should also be remarked at this point that all expansion and weighting functions are left undefined in this chapter, except some of their general

properties needed for the derivations in the following sections. Explicit expressions for these quantities will be given in Chap. 2 of this book.

1.3.1 The Outer Dirichlet Problem

Let us assume that the expansion functions $|\,\varphi_{i,\tau}(k_0,\mathbf{x})>$ in Eq. (1.21) are the so-called radiating eigensolutions of the scalar Helmholtz and vector-wave equation, respectively. Radiating eigensolutions means that these are solutions of the corresponding homogeneous equation subject to the radiation condition at S_∞. We assume further that we have a similar expansion for the primary incident field (which must be not necessarily a plane wave at this point!)

$$|\,u_{inc}^{(N)}(\mathbf{x})> \;=\; \sum_{\tau=1}^{2}\sum_{i=0}^{N} b_{i,\tau}\cdot|\,\psi_{i,\tau}(k_0,\mathbf{x})>; \quad \mathbf{x}\in\Gamma_+\cup\Gamma_- \tag{1.28}$$

with known expansion coefficients $b_{i,\tau}$ and known regular eigensolutions $|\,\psi_{i,\tau}(k_0,\mathbf{x})>$ of the homogeneous Helmholtz and vector-wave equation, respectively. It is then possible to determine the unknown expansion coefficients $a_{i,\tau}^{(N)}$ in expansion (1.21) by applying the boundary conditions (1.10) or (1.18) appropriately. Due to these conditions we have at the scatterer surface

$$\sum_{\tau=1}^{2}\sum_{i=0}^{N} a_{i,\tau}^{(N)}\cdot|\,\varphi_{i,\tau}(k_0,\mathbf{x})>_{\partial\Gamma} \;=\; -\sum_{\tau=1}^{2}\sum_{i=0}^{N} b_{i,\tau}\cdot|\,\psi_{i,\tau}(k_0,\mathbf{x})>_{\partial\Gamma}; \quad \mathbf{x}\in\partial\Gamma \tag{1.29}$$

where

$$|\,\varphi_{i,\tau}(k_0,\mathbf{x})>_{\partial\Gamma} = \delta_{1,\tau}\cdot\varphi_i(k_0,\mathbf{x}); \quad \mathbf{x}\in\partial\Gamma \tag{1.30}$$

$$|\,\psi_{i,\tau}(k_0,\mathbf{x})>_{\partial\Gamma} = \delta_{1,\tau}\cdot\psi_i(k_0,\mathbf{x}); \quad \mathbf{x}\in\partial\Gamma \tag{1.31}$$

and

$$|\,\varphi_{i,\tau}(k_0,\mathbf{x})>_{\partial\Gamma} \;=\; \hat{n}_-\times\vec{\varphi}_{i,\tau}(k_0,\mathbf{x}) \;=\; \vec{\varphi}_{i,\tau}^{\,\hat{n}_-}(k_0,\mathbf{x}); \quad \mathbf{x}\in\partial\Gamma \tag{1.32}$$

$$|\,\psi_{i,\tau}(k_0,\mathbf{x})>_{\partial\Gamma} \;=\; \hat{n}_-\times\vec{\psi}_{i,\tau}(k_0,\mathbf{x}) \;=\; \vec{\psi}_{i,\tau}^{\,\hat{n}_-}(k_0,\mathbf{x}); \quad \mathbf{x}\in\partial\Gamma, \tag{1.33}$$

respectively, depending on whether boundary condition (1.10) of the boundary value problem related to the scalar Helmholtz equation or boundary condition (1.18) of the boundary value problem related to the vector-wave equation is employed. The Kronecker symbol $\delta_{1,\tau}$ in Eqs. (1.30) and (1.31) suppresses the τ-summation in the scalar case. In the vector case we have only to consider the projections of the vector functions into the tangential planes in each point at the scatterer surface. Next, we define the following three scalar products for the quantities given in (1.22–1.24):

$$< v(\mathbf{x}) \,|\, u(\mathbf{x}) >_{\partial\Gamma} := \oint_{\partial\Gamma} v^*(\mathbf{x}) \cdot u(\mathbf{x})\, dS(\mathbf{x}) \tag{1.34}$$

$$< v(\mathbf{x}) \,|\, u(\mathbf{x}) >_{\partial\Gamma} := \oint_{\partial\Gamma} \vec{v}^{\,*}(\mathbf{x}) \cdot \vec{u}(\mathbf{x})\, dS(\mathbf{x}) \tag{1.35}$$

$$< v(\mathbf{x}) \,|\, u(\mathbf{x}) >_{\partial\Gamma} := \sum_{i=1}^{n} v_i^* \cdot u_i. \tag{1.36}$$

Now, if we apply a scalar multiplication to (1.29) with the weighting functions $| g_{j,\tau'}(\mathbf{x}) >_{\partial\Gamma}$ $(j = 0, \ldots, N; \tau' = 1, 2)$ given by

$$| g_{j,\tau'}(\mathbf{x}) >_{\partial\Gamma} = \delta_{1,\tau'} \cdot g_j(\mathbf{x}); \quad \mathbf{x} \in \partial\Gamma \tag{1.37}$$

and

$$| g_{j,\tau'}(\mathbf{x}) >_{\partial\Gamma} = \vec{g}_{j,\tau'}(\mathbf{x}); \quad \mathbf{x} \in \partial\Gamma, \tag{1.38}$$

depending on whether we consider the scalar or vectorial boundary value problem, and if introducing the definitions

$$\left[A_{\partial\Gamma}^{(g,\varphi_0)}\right]_{j,i}^{\tau',\tau} := < g_{j,\tau'}(\mathbf{x}) \,|\, \varphi_{i,\tau}(k_0, \mathbf{x}) >_{\partial\Gamma} \tag{1.39}$$

$$\left[B_{\partial\Gamma}^{(g,\psi_0)}\right]_{j,i}^{\tau',\tau} := < g_{j,\tau'}(\mathbf{x}) \,|\, \psi_{i,\tau}(k_0, \mathbf{x}) >_{\partial\Gamma}, \tag{1.40}$$

of the matrix elements of the two matrices $\mathbf{A}_{\partial\Gamma}^{(g,\varphi_0)}$ and $\mathbf{B}_{\partial\Gamma}^{(g,\psi_0)}$ we get from (1.29) the equation

$$\mathbf{A}_{\partial\Gamma}^{(g,\varphi_0)} \cdot \vec{a}^{\,(N)\,tp} = -\mathbf{B}_{\partial\Gamma}^{(g,\psi_0)} \cdot \vec{b}^{\,tp} \tag{1.41}$$

in matrix notation. The upper index "tp" denotes the transpose of the row vector. The expressions φ_0 and ψ_0 in the superscript brackets attached to the matrices as well as to the matrix elements should indicate that the expansion functions are used with the parameter k_0 in their arguments. This is not really important at this point since we have no explicit expressions for the expansion functions, so far. But regarding the outer transmission problem we will consider shortly, we have to distinguish between expansion functions with k_0 and k!

Concerning the scalar case of the Helmholtz equation the coefficients in (1.41) are condensed into a column vector with $(N + 1)$ components. The corresponding matrices are square matrices of the order $(N + 1) \times (N + 1)$. But if we look at the problems related to the vector-wave equation, due to the additional τ-summation we have column vectors with $2 \times (N + 1)$ components and 2×2 block matrices with each single matrix being of the size $(N + 1) \times (N + 1)$. The formal inversion of (1.41) results in the expression

$$\vec{a}^{\,(N)\,tp} = -\mathbf{T}_{\partial\Gamma} \cdot \vec{b}^{\,tp}, \tag{1.42}$$

for the unknown expansion coefficients. The matrix $\mathbf{T}_{\partial\Gamma}$ reads

$$\mathbf{T}_{\partial\Gamma} \;=\; \mathbf{A}_{\partial\Gamma}^{(g,\varphi_0)^{-1}} \cdot \mathbf{B}_{\partial\Gamma}^{(g,\psi_0)} \tag{1.43}$$

and is called "transition matrix" or "T-matrix" since it transforms the known expansion coefficients of the primary incident field into the expansion coefficients of the scattered field, or, better, of its approximation.

Provided that the inverse of the matrix $\mathbf{A}_{\partial\Gamma}^{(g,\varphi_0)^{-1}}$ in (1.43) exists we have obtained an approximate solution for the scattered field of the outer Dirichlet problem. More precisely: with the approximation (1.21) and the expansion coefficients (1.42) we have obtained an expression solving exactly the corresponding partial differential equation as well as the required radiation condition. The additional boundary condition at the scatterer surface, on the other hand, is fulfilled only approximately.

The following tip may be helpful for the ongoing derivations where we perform the transition to the matrix notation many times. It is advantageous to write down (1.29) in the form of a conventional scalar product according to

$$\vec{\varphi}_0 \cdot \vec{a}^{\,(N)^{tp}} \;=\; -\vec{\psi}_0 \cdot \vec{b}^{\,tp}. \tag{1.44}$$

$\vec{a}^{\,(N)^{tp}}$ and $\vec{b}^{\,tp}$ are the column vectors containing the expansion coefficients as components. $\vec{\varphi}_0$ and $\vec{\psi}_0$ are row vectors with components given by the expansion functions with arguments restricted to the boundary surface $\partial\Gamma$ of the scatterer.

1.3.2 The Outer Transmission Problem

The formal solution of the outer transmission problem can be treated in a similar manner. Boundary conditions (1.10) or (1.18) have now to be replaced by the conditions (1.5)/(1.6) or (1.15)/(1.16). Beside the representations (1.21) and (1.28) of the scattered and primary incident field we have to take the internal field additionally into account. For this field we assume a representation in terms of the expansion

$$|\, u_{int}^{(N)}(\mathbf{x}) > \;=\; \sum_{\tau=1}^{2} \sum_{i=0}^{N} c_{i,\tau}^{(N)} \cdot |\, \psi_{i,\tau}(k,\mathbf{x}) >; \quad \mathbf{x} \in \Gamma_{-} \tag{1.45}$$

with unknown coefficients $c_{i,\tau}^{(N)}$. The appropriate expansion functions $|\, \psi_{i,\tau}(k,\mathbf{x}) >$ are the regular eigensolutions of the Helmholtz and vector-wave equation, respectively, but now with the parameter k in their arguments. We will see that the coefficients $c_{i,\tau}^{(N)}$ are not needed explicitly to solve the outer transmission problem. Now, if the transmission conditions are imposed, then we may write

$$\sum_{\tau=1}^{2}\sum_{i=0}^{N} b_{i,\tau}\cdot \mid \psi_{i,\tau}(k_0,\mathbf{x}) >_{\partial\Gamma} \; + \sum_{\tau=1}^{2}\sum_{i=0}^{N} a_{i,\tau}^{(N)}\cdot \mid \varphi_{i,\tau}(k_0,\mathbf{x}) >_{\partial\Gamma}$$
$$= \sum_{\tau=1}^{2}\sum_{i=0}^{N} c_{i,\tau}^{(N)}\cdot \mid \psi_{i,\tau}(k,\mathbf{x}) >_{\partial\Gamma}; \quad \mathbf{x}\in\partial\Gamma, \tag{1.46}$$

and

$$\sum_{\tau=1}^{2}\sum_{i=0}^{N} b_{i,\tau}\cdot \mid \partial_{\hat{n}}\psi_{i,\tau}(k_0,\mathbf{x}) >_{\partial\Gamma} \; + \sum_{\tau=1}^{2}\sum_{i=0}^{N} a_{i,\tau}^{(N)}\cdot \mid \partial_{\hat{n}}\varphi_{i,\tau}(k_0,\mathbf{x}) >_{\partial\Gamma}$$
$$= \sum_{\tau=1}^{2}\sum_{i=0}^{N} c_{i,\tau}^{(N)}\cdot \mid \partial_{\hat{n}}\psi_{i,\tau}(k,\mathbf{x}) >_{\partial\Gamma}; \quad \mathbf{x}\in\partial\Gamma. \tag{1.47}$$

In close analogy to the outer Dirichlet problem the expansion functions at the scatterer surface are given by

$$\mid \varphi_{i,\tau}(k_0,\mathbf{x}) >_{\partial\Gamma} = \delta_{1,\tau}\cdot\varphi_i(k_0,\mathbf{x}); \quad \mathbf{x}\in\partial\Gamma \tag{1.48}$$
$$\mid \psi_{i,\tau}(k_0,\mathbf{x}) >_{\partial\Gamma} = \delta_{1,\tau}\cdot\psi_i(k_0,\mathbf{x}); \quad \mathbf{x}\in\partial\Gamma \tag{1.49}$$
$$\mid \psi_{i,\tau}(k,\mathbf{x}) >_{\partial\Gamma} = \delta_{1,\tau}\cdot\psi_i(k,\mathbf{x}); \quad \mathbf{x}\in\partial\Gamma \tag{1.50}$$
$$\mid \partial_{\hat{n}}\varphi_{i,\tau}(k_0,\mathbf{x}) >_{\partial\Gamma} = \delta_{1,\tau}\cdot\left[\hat{n}_-\cdot\nabla\varphi_i(k_0,\mathbf{x})\right]; \quad \mathbf{x}\in\partial\Gamma \tag{1.51}$$
$$\mid \partial_{\hat{n}}\psi_{i,\tau}(k_0,\mathbf{x}) >_{\partial\Gamma} = \delta_{1,\tau}\cdot\left[\hat{n}_-\cdot\nabla\psi_i(k_0,\mathbf{x})\right]; \quad \mathbf{x}\in\partial\Gamma \tag{1.52}$$
$$\mid \partial_{\hat{n}}\psi_{i,\tau}(k,\mathbf{x}) >_{\partial\Gamma} = \delta_{1,\tau}\cdot\left[\hat{n}_-\cdot\nabla\psi_i(k,\mathbf{x})\right]; \quad \mathbf{x}\in\partial\Gamma \tag{1.53}$$

and

$$\mid \varphi_{i,\tau}(k_0,\mathbf{x}) >_{\partial\Gamma} = \vec{\varphi}_{i,\tau}^{\,\hat{n}_-}(k_0,\mathbf{x}); \quad \mathbf{x}\in\partial\Gamma \tag{1.54}$$
$$\mid \psi_{i,\tau}(k_0,\mathbf{x}) >_{\partial\Gamma} = \vec{\psi}_{i,\tau}^{\,\hat{n}_-}(k_0,\mathbf{x}); \quad \mathbf{x}\in\partial\Gamma \tag{1.55}$$
$$\mid \psi_{i,\tau}(k,\mathbf{x}) >_{\partial\Gamma} = \vec{\psi}_{i,\tau}^{\,\hat{n}_-}(k,\mathbf{x}); \quad \mathbf{x}\in\partial\Gamma \tag{1.56}$$
$$\mid \partial_{\hat{n}}\varphi_{i,\tau}(k_0,\mathbf{x}) >_{\partial\Gamma} = \hat{n}_-\times\nabla\times\vec{\varphi}_{i,\tau}(k_0,\mathbf{x}); \quad \mathbf{x}\in\partial\Gamma \tag{1.57}$$
$$\mid \partial_{\hat{n}}\psi_{i,\tau}(k_0,\mathbf{x}) >_{\partial\Gamma} = \hat{n}_-\times\nabla\times\vec{\psi}_{i,\tau}(k_0,\mathbf{x}); \quad \mathbf{x}\in\partial\Gamma \tag{1.58}$$
$$\mid \partial_{\hat{n}}\psi_{i,\tau}(k,\mathbf{x}) >_{\partial\Gamma} = \hat{n}_-\times\nabla\times\vec{\psi}_{i,\tau}(k,\mathbf{x}); \quad \mathbf{x}\in\partial\Gamma \tag{1.59}$$

depending on whether the outer transmission problem of the scalar Helmholtz or vector-wave equation is considered. We apply a scalar multiplication with the weighting functions (1.37) or (1.38–1.46), and with the weighting functions

$$\mid h_{j,\tau'}(\mathbf{x}) >_{\partial\Gamma} = \; \delta_{1,\tau'}\cdot h_j(\mathbf{x}); \quad \mathbf{x}\in\partial\Gamma \tag{1.60}$$

or

$$|\, h_{j,\tau'}(\mathbf{x}) >_{\partial\Gamma} = \vec{h}_{j,\tau'}(\mathbf{x}); \quad \mathbf{x} \in \partial\Gamma \tag{1.61}$$

to (1.47). This results in the two matrix equations

$$\mathbf{A}_{\partial\Gamma}^{(g,\varphi_0)} \cdot \vec{a}^{\,(N)^{tp}} + \mathbf{B}_{\partial\Gamma}^{(g,\psi_0)} \cdot \vec{b}^{\,tp} = \mathbf{C}_{\partial\Gamma}^{(g,\psi)} \cdot \vec{c}^{\,(N)^{tp}} \tag{1.62}$$

and

$$\mathbf{A}_{\partial\Gamma}^{(h,\partial_{\hat{n}}\varphi_0)} \cdot \vec{a}^{\,(N)^{tp}} + \mathbf{B}_{\partial\Gamma}^{(h,\partial_{\hat{n}}\psi_0)} \cdot \vec{b}^{\,tp} = \mathbf{C}_{\partial\Gamma}^{(h,\partial_{\hat{n}}\psi)} \cdot \vec{c}^{\,(N)^{tp}}. \tag{1.63}$$

The matrix elements of the matrices in these two equations are now determined by the scalar products

$$\left[A_{\partial\Gamma}^{(g,\varphi_0)}\right]_{j,i}^{\tau',\tau} := < g_{j,\tau'}(\mathbf{x}) \,|\, \varphi_{i,\tau}(k_0,\mathbf{x}) >_{\partial\Gamma} \tag{1.64}$$

$$\left[B_{\partial\Gamma}^{(g,\psi_0)}\right]_{j,i}^{\tau',\tau} := < g_{j,\tau'}(\mathbf{x}) \,|\, \psi_{i,\tau}(k_0,\mathbf{x}) >_{\partial\Gamma} \tag{1.65}$$

$$\left[C_{\partial\Gamma}^{(g,\psi)}\right]_{j,i}^{\tau',\tau} := < g_{j,\tau'}(\mathbf{x}) \,|\, \psi_{i,\tau}(k,\mathbf{x}) >_{\partial\Gamma} \tag{1.66}$$

$$\left[A_{\partial\Gamma}^{(h,\partial_{\hat{n}}\varphi_0)}\right]_{j,i}^{\tau',\tau} := < h_{j,\tau'}(\mathbf{x}) \,|\, \partial_{\hat{n}}\varphi_{i,\tau}(k_0,\mathbf{x}) >_{\partial\Gamma} \tag{1.67}$$

$$\left[B_{\partial\Gamma}^{(h,\partial_{\hat{n}}\psi_0)}\right]_{j,i}^{\tau',\tau} := < h_{j,\tau'}(\mathbf{x}) \,|\, \partial_{\hat{n}}\psi_{i,\tau}(k_0,\mathbf{x}) >_{\partial\Gamma} \tag{1.68}$$

$$\left[C_{\partial\Gamma}^{(h,\partial_{\hat{n}}\psi)}\right]_{j,i}^{\tau',\tau} := < h_{j,\tau'}(\mathbf{x}) \,|\, \partial_{\hat{n}}\psi_{i,\tau}(k,\mathbf{x}) >_{\partial\Gamma}\,. \tag{1.69}$$

If both equations (1.62) and (1.63) are solved for the unknown expansion coefficients $\vec{c}^{\,(N)^{tp}}$ we end up again with a relation between the unknown coefficients $\vec{a}^{\,(N)^{tp}}$ of the scattered field and the known coefficients $\vec{b}^{\,tp}$ of the primary incident field:

$$\vec{a}^{\,(N)^{tp}} = -\mathbf{T}_{\partial\Gamma}^{(d)} \cdot \vec{b}^{\,tp}, \tag{1.70}$$

where

$$\begin{aligned}\mathbf{T}_{\partial\Gamma}^{(d)} = &\left[\mathbf{C}_{\partial\Gamma}^{(g,\psi)^{-1}} \cdot \mathbf{A}_{\partial\Gamma}^{(g,\varphi_0)} - \mathbf{C}_{\partial\Gamma}^{(h,\partial_{\hat{n}}\psi)^{-1}} \cdot \mathbf{A}_{\partial\Gamma}^{(h,\partial_{\hat{n}}\varphi_0)}\right]^{-1} \\ &\cdot \left[\mathbf{C}_{\partial\Gamma}^{(g,\psi)^{-1}} \cdot \mathbf{B}_{\partial\Gamma}^{(g,\psi_0)} - \mathbf{C}_{\partial\Gamma}^{(h,\partial_{\hat{n}}\psi)^{-1}} \cdot \mathbf{B}_{\partial\Gamma}^{(h,\partial_{\hat{n}}\psi_0)}\right].\end{aligned} \tag{1.71}$$

$\mathbf{T}_{\partial\Gamma}^{(d)}$ is the transition matrix now related to the outer transmission problem. In the course of derivation it was again tacitly assumed that all necessary matrix inversions may be performed without any problems.

Of course, the solution of the boundary value problems were not given in this general form in the paper of Rayleigh mentioned at the beginning. But the essential two steps:

- Expansion of the scattered field in terms of those eigensolutions of the underlying partial differential equation which are in accordance with the required radiation condition and
- Using the boundary conditions at the scatterer surface in conjunction with a scalar multiplication with some weighting functions

are already included there. The derived transition matrices (or T-matrices) have been proven in the past to be very powerful tools for solving the scattering problems in the resonance region. Hence we could finish at this point our methodical considerations, could represent explicit expressions for the expansion and weighting functions, could define the physical quantities of our interest, and could then immediately start with the numerical simulations to see the T-matrices in action. But, interestingly, the approach presented by Rayleigh remained not undisputed, and alternative approaches have been developed. The advantages and disadvantages of those methods have been and are still discussed controversial to some extent. Therefore, using Green functions, we will try to give this discussion a firm methodological basis. The Green functions are also helpful to derive those quantities that are able to characterize the scattering process physically, and to derive some important properties of these quantities. Moreover, they provide an appropriate starting point for iterative solution schemes, as we will see later.

Chapter 2
Filling the Mathematical Tool Box

2.1 Introduction

Regarding the approximations of the fields in terms of finite series expansions specified in Chap. 1 the question of how to estimate their accuracy is of considerable interest. Unfortunately, there is no unique answer to this question satisfying all demands. As it happens frequently in physics we are moving with this question in the no man's land in-between our physical experience made by experiments, that is scattering of electromagnetic waves on nonspherical particles in our case, and our claim to condense this experience into a rigorous mathematical model. This situation is nicely expressed by the statement (was it Einstein?) that mathematics, where it is exact, it gives not an account to reality, and, contrary, where it gives an account to reality, it is not exact. Thus, we are often forced to take up a pragmatic position concerning the question of the accuracy of a certain approximation which must focus on the practical requirements of a specific task.

The accuracy problem is considered especially in Sect. 2.2 of this chapter. But we will come back to this aspect also in subsequent discussions. Explicit expressions for the formally introduced expansion and weighting functions of Chap. 1 are discussed in the two afterward sections together with their relevant properties. Being as mathematical complete and accurate as possible is not the goal of both these sections. We are more interested in the composition of those aspects which are of importance for the solution concept we pursue, for the development of the self-consistent Green's function formalism, and for the conceptual discussions of other solution techniques. Sections 2.5 and 2.6 of this chapter introduce the required Green theorems as well as the definitions and properties of the Green functions related to the scattering problems of our interest.

T. Rother and M. Kahnert, *Electromagnetic Wave Scattering on Nonspherical Particles*, Springer Series in Optical Sciences 145, DOI: 10.1007/978-3-642-36745-8_2,

2.2 Approximation of Functions and Fields at the Scatterer Surface

In the classical theory of approximations, we are faced with the problem of expanding a known function into a series of other known functions, among other things. In the classical Fourier theory, these expansion functions are sine and cosine functions, for example. The expansion coefficients of such an expansion are determined afterwards by some requirements applied to the expansion. Minimizing the mean square error or minimizing the maximum error in the considered interval and for a given number of expansion terms are two well-known examples of such requirements. How can this be related to our scattering problem? The function of the left hand side of expansion (1.21) is not known in our case. It is the solution we are looking for. But, fortunately, according to the formulated boundary conditions we know its behaviour at the scatterer surface as well as the primary incident field. These boundary conditions interrelate the unknown solution with the known primary field at the scatterer surface. As demonstrated in the foregoing chapter this interrelation allowed us to determine the unknown expansion coefficients in a certain way. At first, it seems to be obvious to use the accuracy of the fulfilment of the required boundary condition to estimate the accuracy of the scattering solution. On the other hand, for the primary incident field we assumed the existence of a series expansion

$$\mid u_{inc}^{(N)}(\mathbf{x}) >_{\partial\Gamma} \;=\; \sum_{\tau=1}^{2}\sum_{i=0}^{N} b_{i,\tau}^{(N)} \cdot \mid \psi_{i,\tau}(k_0,\mathbf{x}) >_{\partial\Gamma} ; \quad \mathbf{x} \in \partial\Gamma \tag{2.1}$$

at the scatterer surface with already known expansion coefficients $b_{i,\tau}^{(N)}$. Please, note that in contrast to the foregoing chapter the known expansion coefficients in (2.1) are now characterized by the additional upper index "(N)". The meaning of this index is clarified in the Sect. 2.2.2 concerning the "best approximation". It should also be emphasized once more that for the boundary value problems related to the vector-wave equation the abstract quantities $\mid u_{inc}^{(N)}(\mathbf{x}) >_{\partial\Gamma}$ and $\mid \psi_{i,\tau}(k_0,\mathbf{x}) >_{\partial\Gamma}$ represent the tangential projections $\hat{n} \times \vec{u}_{inc}^{(N)}(\mathbf{x})$ and $\hat{n} \times \vec{\psi}_{i,\tau}(k_0,\mathbf{x})$ at the scatterer surface!

Statements concerning the accuracy of the scattering solution at the scatterer surface $\partial\Gamma$ are therefore strongly related to the accuracy of the approximation (2.1) of the primary incident field at the scatterer surface. Therefore, we will concentrate on approximating a given field at the scatterer surface in Sects. 2.2.1–2.2.3. In doing so, we will discover a quite interesting relation between this aspect and the T-matrices derived in the foregoing chapter by use of Rayleigh's method. How the knowledge of the behaviour of the scattered field at the scatterer surface is used to represent this field everywhere in the outer space Γ_+ will be discussed in Chap. 3.

2.2.1 Approximation by Finite Series Expansions

The characteristic restriction of approximation (2.1) to a finite number of expansion terms appears very naturally nowadays, since we are used to adopt a computer-oriented view of solving a certain problem. This restriction is also naturally from a mathematical point of view for the finite-dimensional vectors given in representation (1.24). But as one can find, usually in the mathematical literature, the approximations of a continuously varying scalar or vector function start from infinite series expansions owing to the analysis of their convergence behaviour. For example, we say that the series (2.1) converges uniformly against $|\, u_{inc}(\mathbf{x}) >_{\partial\Gamma}$ if for any $\mathbf{x} \in \partial\Gamma$ and for any value $\varepsilon > 0$ there exist a natural number N for which

$$\left| \, |\, u_{inc}(\mathbf{x}) >_{\partial\Gamma} \; - |\, u_{inc}^{(N)}(\mathbf{x}) >_{\partial\Gamma} \right| < \varepsilon \tag{2.2}$$

holds. That is the strongest demand we can impose on series expansion (2.1), since we require that it converges in every point at the boundary surface $\partial\Gamma$. Another possibility represents the convergence with respect to a certain norm defined according to

$$M = \| \; |\, u_{inc}(\mathbf{x}) >_{\partial\Gamma} \; - |\, u_{inc}^{(N)}(\mathbf{x}) >_{\partial\Gamma} \| \to 0, \quad \text{if } N \to \infty. \tag{2.3}$$

This convergence, sometimes also called "strong convergence", is less restrictive than the uniform convergence. For a fixed number N of expansion terms M^2 is nothing but the mean square error of approximation (2.1). The norm "$\| \cdots \|$" therein is related to the scalar product calculated via the definition

$$\| \; |\, f(\mathbf{x}) >_{\partial\Gamma} \| := \sqrt{< f(\mathbf{x}) \,|\, f(\mathbf{x}) >_{\partial\Gamma}}, \tag{2.4}$$

with the scalar products given by (1.34–1.36), for example. Beside this strong convergence we know the "weak convergence". It requires that the scalar product of an arbitrary function $|\, g(\mathbf{x}) >_{\partial\Gamma}$ defined on the boundary surface $\partial\Gamma$ with the approximation $|\, u_{inc}^{(N)}(\mathbf{x}) >_{\partial\Gamma}$ converges against the scalar product of $|\, g(\mathbf{x}) >_{\partial\Gamma}$ with $|\, u_{inc}(\mathbf{x}) >_{\partial\Gamma}$ if N tends to infinity, i.e., if we have

$$< g(\mathbf{x}) \,|\, u_{inc}^{(N)}(\mathbf{x}) >_{\partial\Gamma} \to < g(\mathbf{x}) \,|\, u_{inc}(\mathbf{x}) >_{\partial\Gamma}, \quad \text{if } N \to \infty. \tag{2.5}$$

As a criterion for the number of expansion terms which have to be used in the finite series (2.1) we can then choose the "quality" with which the known quantity $|\, u_{inc}(\mathbf{x}) >_{\partial\Gamma}$ is approximated, for example. This quality may be a certain value of ε which should not be exceeded according to (2.2), (2.3), and (2.5), respectively. In close analogy we could formulate a quality criterion for the behaviour of the approximation (1.21) of the scattered field at the boundary surface since this is known from the required boundary conditions. But in most of the applications we have in mind there is no need to know the behaviour of the scattered field at the scatterer surface

exactly. More often we are interested in quantities within Γ_+ which are derived by certain mathematical procedures from the scattered field. In scattering measurements these quantities are the angular dependent intensities of the scattered wave in the far-field, for example. Depending on the specific task one has to solve this may result in very different requirements concerning the accuracy of approximation (1.21). From our physical experience, we know that in some circumstances the observed scattering quantities must exhibit certain properties like symmetry properties or properties which can be related to energy conservation in the case of a non-absorbing scatterer, for example. Sometimes, it is more appropriate to use the fulfilment of these properties as a quality criterion for the accuracy of a certain approximation. Moreover, we know from our numerical experience that a series which has been proven to converge in a certain sense mathematically may not be automatically helpful in practical applications. These are the reasons for we will not insist in the mathematical rigour concerning the convergence behaviour of approximations (2.1) and (1.21), as well. As it will be demonstrated with the numerical simulations presented in Chap. 9 it is more convenient to determine the truncation parameter "N" of the series expansions according to the practical requirements. This is our pragmatic position with respect to the convergence behaviour of the scattering solution if it is approximated by a finite series expansion. But we can benefit from a finite series expansion even more. In the ongoing derivations we have to interchange frequently summation and integration. If we consider an infinite series expansion this is only justified if it is uniformly convergent. But for a finite series, this can be carried out without any problems if the quality of the resulting expressions is estimated again from our pragmatic point of view.

The expansion functions $|\,\psi_{i,\tau}(k_0, \mathbf{x})\,>_{\partial\Gamma}$ in (2.1) are assumed to be known, as already mentioned. For the following considerations we will assume further that these functions form a linear independent set of functions at the scatterer surface. This means that the zero-vector has only the trivial representation in terms of a series expansion with zero expansion coefficients or, in other words, that none of the expansion functions can be expressed by a linear combination of all other expansion functions. The linear independence of a given set of functions can be tested numerically by looking at Gram's matrix. If the determinant of this matrix is $\neq 0$, then its constitutive functions are linearly independent. But, concerning this question, it may also happen that a set of functions which is mathematically known to be linearly independent may behave numerically like a linearly dependent system with all resulting consequences for solving a linear equation system like a hardly invertible coefficient matrix. Completeness is an additional mathematical aspect which is of some importance if infinite series expansions are considered. A set of functions is called complete if for any function $|\,u_{inc}(\mathbf{x})\,>_{\partial\Gamma}$ and for any $\varepsilon > 0$ there exists a natural number N and a corresponding set of expansion coefficients $\{b_{i,\tau}^{(N)}\}_{i=0}^{N}$ so that

$$\| \,|\,u_{inc}(\mathbf{x})\,>_{\partial\Gamma} \; - |\,u_{inc}^{(N)}(\mathbf{x})\,>_{\partial\Gamma}\| \;<\; \varepsilon \tag{2.6}$$

holds for the approximation (2.1) at the scatterer surface. In a finite dimensional vector-space completeness is trivial since N linearly independent vectors are always complete in $I\!R^N$!

There is a last remark we want to add before dealing with the determination of the expansion coefficients. It is concerned with the nature of expansion functions used throughout this book. In the literature, one can find two different classes of expansion functions. These are subdomain expansion functions like overlapping triangles or step functions, for example, and expansion functions which are defined on the entire surface domain $\partial\Gamma$, on the other hand. The former are often used in Electrodynamics to approximate the unknown surface currents or surface charges, for example. But here we will consider only the entire surface domain expansion functions which can be derived from the continuous eigensolutions of the relevant partial differential equation, not least because these functions exhibit already some important properties we require for the final solution. Moreover, the linearly independence and completeness of the eigensolutions is already known in advance in some circumstances.

2.2.2 Best Approximation

Now, we want to answer the question how one can determine the expansion coefficients $b_{i,\tau}^{(N)}$ of approximation (2.1). For this, we assume first that $\mid u_{inc}(\mathbf{x}) >_{\partial\Gamma}$ is a sufficient smooth function. This assumption is justified by the physical experience that all the electromagnetic fields are smooth and differentiable quantities outside their sources. In the classical Fourier theory one uses the minimization of the mean square error M^2 with M according to (2.3) to determine the expansion coefficients. But in this classical theory we usually impose a further restriction on the expansion functions. They are assumed to be orthogonal, i.e., for the scalar product of any two expansion functions holds the relation

$$< \psi_{0_{j,\tau'}} \mid \psi_{0_{i,\tau}} >_{\partial\Gamma} = c_{i,\tau} \cdot \delta_{ij} \cdot \delta_{\tau\tau'} \tag{2.7}$$

with $c_{i,\tau}$ being a certain normalization constant. With this constant the expansion functions can be normalized to unity. This requirement of orthogonality is strongly related to the so-called requirement of finality of the expansion coefficients. What does it means? It means that once we have calculated a certain number of expansion coefficients there is no need to recalculate these coefficients if it becomes necessary (due to an unsatisfactory convergence behaviour, for example) to take more expansion terms in approximation (2.1) into account. If the coefficients are final we have just to calculate the additional coefficients. Of course, this would be a huge numerical advantage if applicable. Here, we do not want to insist on this claim since it is unsustainable in all the scattering problems of our interest as well as in every boundary value problem which can not be formulated along boundary surfaces coinciding with

a constant coordinate line. The abandonment of the requirement of orthogonality of the expansion functions and the resulting non-finality of the expansion coefficients is the deeper reason for adding the upper index "(N)" to the expansion coefficients in (2.1). But the finality of the expansion coefficients in the approximation of the scattered field appears in the subsequent relations as the limiting case of a spherical boundary surface. For the plane wave, on the other hand, we know an infinite series expansion with final expansion coefficients which holds everywhere in the free space $\Gamma = \Gamma_- \cup \Gamma_+$, and which is independent of the geometry of the scatterer. This expansion was already introduced in Chap. 1 when dealing with the formal solution of the outer Dirichlet and transmission problem.

All the functions we are using in this book are complex-valued functions, in general. Therefore, we will first consider the so-called "best approximation" to determine the unknown expansion coefficients of expansion (2.1). This special approximation is identical with the method of minimization of the mean square error for real-valued functions. Let $\mid u_{inc} >_{\partial\Gamma}$ be the function in an infinite-dimensional Hilbert space $\mathcal{H}$ we want to approximate. Furthermore, let $\mathcal{H}^{(N)}$ be a finite-dimensional subspace $\mathcal{H}^{(N)} \subset \mathcal{H}$ of $\mathcal{H}$. Then, we call $\mid u_{inc}^{(N)} >_{\partial\Gamma}$ a best approximation of $\mid u_{inc} >_{\partial\Gamma}$ with respect to $\mathcal{H}^{(N)}$ if

$$< u_{inc} - u_{inc}^{(N)} \mid v >_{\partial\Gamma} = 0; \quad \forall \mid v >_{\partial\Gamma} \in \mathcal{H}^{(N)} \tag{2.8}$$

holds. If $\mid u_{inc}^{(N)} >_{\partial\Gamma}$ is given by the representation (2.1), and if the expansion functions $\mid \psi_{0_{i,\tau}} >_{\partial\Gamma}$ are linearly independent in the subspace $\mathcal{H}^{(N)}$ it can be shown that $\mid u_{inc}^{(N)} >_{\partial\Gamma}$ is best approximation if and only if the corresponding expansion coefficients $b_{i,\tau}^{(N)}$ are the solutions of the equation system

$$\sum_{\tau=1}^{2}\sum_{i=0}^{N} b_{i,\tau}^{(N)} \cdot < \psi_{0_{j,\tau'}} \mid \psi_{0_{i,\tau}} >_{\partial\Gamma} = < \psi_{0_{j,\tau'}} \mid u_{inc} >_{\partial\Gamma},$$
$$j = 0, \ldots, N\,;\ \tau' = 1, 2. \tag{2.9}$$

The elements of the coefficient matrix we will denote with $\mathbf{A}_{\partial\Gamma}^{(\psi_0,\psi_0)}$ are calculated via the scalar product of the expansion functions among themselves, i.e., by

$$\left[A_{\partial\Gamma}^{(\psi_0,\psi_0)}\right]_{j,i}^{\tau',\tau} = < \psi_{0_{j,\tau'}} \mid \psi_{0_{i,\tau}} >_{\partial\Gamma}. \tag{2.10}$$

This is nothing but the earlier mentioned Gram's matrix. We want to emphasize once again that we have to take the τ, τ'-summation into account if considering vector functions. Thus, the Gram's matrix becomes a 2×2 block matrix with each single square matrix within this block matrix being of the size $(N+1) \times (N+1)$. The inhomogeneity on the right hand side of (2.9) results from the scalar product of the known function $\mid u_{inc} >_{\partial\Gamma}$ with the expansion functions $\mid \psi_{0_{i,\tau}} >_{\partial\Gamma}$. It becomes a

$2 \times (N+1)$-dimensional block vector if again vector functions are considered. In the scalar case, however, all matrices and vectors become simple matrices and vectors. To check that approximation (2.1) together with the coefficients resulting from (2.9) is indeed best approximation we start from the fact that any function $\mid v >_{\partial\Gamma} \in \mathcal{H}^{(N)}$ can be represented by the linear combination

$$\mid v >_{\partial\Gamma} = \sum_{\tau=1}^{2} \sum_{i=0}^{N} v_{i,\tau} \cdot \mid \psi_{0_{i,\tau}} >_{\partial\Gamma} \tag{2.11}$$

with non-vanishing expansion coefficients $v_{i,\tau}$. If we insert this representation together with (2.1) into the scalar product $< u_{inc} - u_{inc}^{(N)} \mid v(\mathbf{x}) >_{\partial\Gamma}$ it becomes obvious that it vanishes identical if the coefficients $b_{i,\tau}^{(N)}$ are the solutions of the equation system (2.9).

There exists a more straightforward way to derive the equation system (2.9). For this we must simply replace $\mid u_{inc}^{(N)} >_{\partial\Gamma}$ by $\mid u_{inc} >_{\partial\Gamma}$ on the left hand side of approximation (2.1). Then, we apply a scalar multiplication with the functions $\mid \psi_{0_{j,\tau'}} >_{\partial\Gamma}$ to the thus modified equation. Since this way is more clearly and much simpler we will use it more often in the ongoing discussions.

Now, from (2.9) we get formally

$$b_{i,\tau}^{(N)} = \sum_{\tau'=1}^{2} \sum_{j=0}^{N} \left[A_{\partial\Gamma}^{(\psi_0,\psi_0)^{-1}} \right]_{i,j}^{\tau,\tau'} \cdot < \psi_{0_{j,\tau'}} \mid u_{inc} >_{\partial\Gamma} \tag{2.12}$$

for the expansion coefficients where $\left[A_{\partial\Gamma}^{(\psi_0,\psi_0)^{-1}} \right]_{i,j}^{\tau,\tau'}$ are the elements of the inverse $\mathbf{A}_{\partial\Gamma}^{(\psi_0,\psi_0)^{-1}}$ of matrix (2.10). The existence of this inverse matrix is ensured due to the assumed linearly independence of the expansion functions $\mid \psi_{0_{i,\tau}} >_{\partial\Gamma}$.

The matrix (2.10) is fully occupied, in general. This means that all expansion coefficients have to be calculated once again if additional expansion terms are considered in approximation (2.1). Only if we have orthogonal expansion functions $\mid \psi_{0_{i,\tau}} >_{\partial\Gamma}$ matrix $\mathbf{A}_{\partial\Gamma}^{(\psi_0,\psi_0)}$ as well as its inverse become diagonal matrices because of relation (2.7), as known from the conventional Fourier theory. In this special case, we end up with the simpler equation

$$b_{i,\tau} = \frac{1}{c_{i,\tau}} \cdot < \psi_{0_{i,\tau}} \mid u_{inc} >_{\partial\Gamma} \tag{2.13}$$

for the expansion coefficients. Now, we can omit the upper index "(N)" since these coefficients are final.

Are there other possibilities to determine the expansion coefficients? According to our remark following Eq. (2.11) we can answer this question with "yes". If we replace again $\mid u_{inc}^{(N)} >_{\partial\Gamma}$ by $\mid u_{inc} >_{\partial\Gamma}$ on the left hand side of (2.1), and apply a

scalar multiplication not with the expansion functions $|\,\psi_{0_{j,\tau'}}\,>_{\partial\Gamma}$ but with some arbitrary weighting functions $|\,g_{j,\tau'}\,>_{\partial\Gamma}$ we get instead of (2.12)

$$b_{i,\tau}^{(N)} = \sum_{\tau'=1}^{2}\sum_{j=0}^{N}\left[A_{\partial\Gamma}^{(g,\psi_0)^{-1}}\right]_{i,j}^{\tau,\tau'} \cdot <\, g_{j,\tau'}\,|\,u_{inc}\,>_{\partial\Gamma} \tag{2.14}$$

with

$$\left[A_{\partial\Gamma}^{(g,\psi_0)}\right]_{j,i}^{\tau',\tau} = <\, g_{j,\tau'}\,|\,\psi_{0_{i,\tau}}\,>_{\partial\Gamma} \tag{2.15}$$

being the elements of the more general coefficient matrix $\mathbf{A}_{\partial\Gamma}^{(g,\psi_0)}$. Of course, the functions $|\,g_{j,\tau'}\,>_{\partial\Gamma}$ must again be chosen in such a way that the matrix inversion can be performed without any problems. In doing so, we abandon the framework of the best approximation. But it does not mean that the resulting approximation converges worse than the best approximation! The contrary may happen since we have now an additional degree of freedom. In accordance with our pragmatic point of view concerning the question of convergence we can try to choose the weighting functions in such a way that the resulting equation system fits better to the requirements of a certain application. The appropriate choice of weighting functions is of course a question of experience in a certain field and a none too simple task.

2.2.3 The Transformation Character of the T-Matrix

Up to this point we used (2.1) with the known expansion functions $|\,\psi_{i,\tau}(k_0,\mathbf{x})\,>_{\partial\Gamma}$ $(\tau = 1,2;\, i = 0,\ldots,N)$ as a starting point to approximate the primary incident field $|\,u_{inc}\,>_{\partial\Gamma}$ at the scatterer surface. Let us now assume that there exists an additional set of linearly independent expansion functions $|\,\varphi_{i,\tau}(k_0,\mathbf{x})\,>_{\partial\Gamma}$ $(\tau = 1,2;i = 0,\ldots,N)$. Then, we may ask how one can change from representation (2.1) (which is now assumed to be known!) to the new representation

$$|\,u_{inc}^{(N)}(\mathbf{x})\,>_{\partial\Gamma} = \sum_{\tau=1}^{2}\sum_{i=0}^{N} a_{i,\tau}^{(N)} \cdot |\,\varphi_{i,\tau}(k_0,\mathbf{x})\,>_{\partial\Gamma};\quad \mathbf{x}\in\partial\Gamma \tag{2.16}$$

in terms of the new expansion functions? Or, more precisely, how one can calculate the new and unknown coefficients $a_{i,\tau}^{(N)}$ of approximation (2.16) from the known coefficients $b_{i,\tau}^{(N)}$ of approximation (2.1)? To answer this question we must first transform the new expansion functions into the old one, i.e., we introduce the transformation matrix $\tilde{\mathbf{T}}_{\partial\Gamma}$ according to

$$| \psi_{0_{i,\tau}} >_{\partial\Gamma} = \sum_{\tau'=1}^{2} \sum_{k=0}^{N} \left[\tilde{T}_{\partial\Gamma} \right]_{i,k}^{\tau,\tau'} \cdot | \varphi_{0_{k,\tau'}} >_{\partial\Gamma}; \quad i = 0, \ldots, N; \quad \tau = 1, 2. \tag{2.17}$$

This reads in matrix notation

$$\vec{\psi}_0^{\,tp} = \tilde{\mathbf{T}}_{\partial\Gamma} \cdot \vec{\varphi}_0^{\,tp}. \tag{2.18}$$

Taking the transpose of this equation, and after scalar multiplication with the weighting functions $| g_{j,\tau''} >_{\partial\Gamma}$ we get the following matrix equation for the transpose $\mathbf{T}_{\partial\Gamma} = \tilde{\mathbf{T}}_{\partial\Gamma}^{tp}$ of the above introduced transformation matrix $\tilde{\mathbf{T}}_{\partial\Gamma}$:

$$\mathbf{T}_{\partial\Gamma} = \mathbf{A}_{\partial\Gamma}^{(g,\varphi_0)^{-1}} \cdot \mathbf{B}_{\partial\Gamma}^{(g,\psi_0)}. \tag{2.19}$$

Please, note that the transpose of a block matrix is given by

$$\begin{pmatrix} \mathbf{X_{11}} & \mathbf{X_{12}} \\ \mathbf{X_{21}} & \mathbf{X_{22}} \end{pmatrix}^{\mathbf{tp}} = \begin{pmatrix} \mathbf{X_{11}^{tp}} & \mathbf{X_{21}^{tp}} \\ \mathbf{X_{12}^{tp}} & \mathbf{X_{22}^{tp}} \end{pmatrix}. \tag{2.20}$$

The matrix elements of the matrices appearing in (2.19) are given by the expressions

$$\left[A_{\partial\Gamma}^{(g,\varphi_0)} \right]_{i,j}^{\tau,\tau'} = < g_{i,\tau} | \varphi_{0_{j,\tau'}} >_{\partial\Gamma} \tag{2.21}$$

and

$$\left[B_{\partial\Gamma}^{(g,\psi_0)} \right]_{i,j}^{\tau,\tau'} = < g_{i,\tau} | \psi_{0_{j,\tau'}} >_{\partial\Gamma} . \tag{2.22}$$

Surprisingly, expressions (2.19), (2.21), and (2.22) are identical with the expressions we have already derived in Chap. 1 when dealing with the formal solution of the outer Dirichlet problem by use of Rayleigh's method, with the exception of sign (see (1.39), (1.40), and (1.43) in Chap. 1). If we insert (2.17) into (2.1) we end up with the following relation between the new expansion coefficients $a_{i,\tau}^{(N)}$ of approximation (2.16) and the old coefficients $b_{i,\tau}^{(N)}$ of the original representation (2.1):

$$\vec{a}^{\,(N)^{tp}} = \mathbf{T}_{\partial\Gamma} \cdot \vec{b}^{\,(N)^{tp}}. \tag{2.23}$$

Except the sign this is again identical with Eq. (1.42)! Thus we can state: **The matrix we have obtained from the formal application of the Rayleigh method to solve the outer Dirichlet problem allowed us to calculate the expansion coefficients of the unknown scattered field from the known expansion coefficients of the primary incident field. This matrix is identical with the matrix whose transpose transforms the expansion functions** $| \varphi_{0_{i,\tau}} >_{\partial\Gamma}$ **into the expansion functions** $| \psi_{0_{i,\tau}} >_{\partial\Gamma}$ **at the scatterer surface. Moreover, this matrix allows us to change**

from approximation (2.1) to approximation (2.16) of the primary incident field at the scatterer surface. This remarkable transformation character of the T-matrix becomes of special importance later on when dealing with its mathematical properties like unitarity, with the resulting properties of the physical quantities calculated by use of this matrix, and with the related properties of the Green functions.

For using the equal sign in (2.17) we should turn to pink under the watchful eyes of the mathematicians. Equation (2.17) is not really an equation but only an approximation of the old expansion functions $\mid \psi_{0_{i,\tau}} >_{\partial\Gamma}$, i.e., on the left hand side we should write $\mid \psi_{0_{i,\tau}}^{(N)} >_{\partial\Gamma}$ more precisely. But once again: according to our pragmatic point of view concerning the convergence behaviour of an approximation we will ignore this mathematical distinction. Not least because in contrast to the unknown scattering solution we know the old expansion functions $\mid \psi_{0_{i,\tau}} >_{\partial\Gamma}$. Thus, we are able to verify the accuracy of (2.17) and the transformation matrix in advance and to determine the number of expansion terms appropriately. In this context, we want to point out that there exists again an easier way to derive relation (2.23). First, regarding representation (2.16), we have to start from Eq. (2.14) but with $b_{i,\tau}^{(N)}$ replaced by $a_{i,\tau}^{(N)}$ on its left hand side. On the right hand side we have to replace the matrix elements $\left[A_{\partial\Gamma}^{(g,\psi_0)^{-1}}\right]_{i,j}^{\tau,\tau'}$ by $\left[A_{\partial\Gamma}^{(g,\varphi_0)^{-1}}\right]_{i,j}^{\tau,\tau'}$. On the right hand side of (2.14) appears also the known function $\mid u_{inc} >$ in the scalar product. This function is now replaced by the approximation (2.1) which is again assumed to be known. From this procedure (2.23) follows directly. In contrast to the former derivation the finite series (2.1) is now taken as the primary given field $\mid u_{inc} >$, and this finite series itself is approximated afterwards by (2.16) with expansion coefficients resulting from (2.23).

Now, in close analogy to (2.17), we may ask for the two transformation matrices $\mathbf{T}_{\varphi_0}$ and $\mathbf{T}_{\psi}$ transforming the expansion functions $\vec{\varphi}_0$, $\vec{\psi}$, $\partial_{\hat{n}}\vec{\varphi}_0$, and $\partial_{\hat{n}}\vec{\psi}$ into the expansion functions $\vec{\psi}_0$ and $\partial_{\hat{n}}\vec{\psi}_0$ according to

$$\vec{\psi}_0 = \vec{\varphi}_0 \cdot \mathbf{T}_{\varphi_0} \; + \; \vec{\psi} \cdot \mathbf{T}_{\psi} \tag{2.24}$$

and

$$\partial_{\hat{n}}\vec{\psi}_0 = \partial_{\hat{n}}\vec{\varphi}_0 \cdot \mathbf{T}_{\varphi_0} \; + \; \partial_{\hat{n}}\vec{\psi} \cdot \mathbf{T}_{\psi}. \tag{2.25}$$

Please, note that we used now right from the start the matrix notation! The expansion functions $\partial_{\hat{n}}\vec{\varphi}_0$, $\partial_{\hat{n}}\vec{\psi}_0$, and $\partial_{\hat{n}}\vec{\psi}$ are defined in (1.51), (1.52), (1.53), (1.57), (1.58), and (1.59), respectively. Scalar multiplication of (2.24) with the weighting functions (1.37) or (1.38), and of (2.25) with the weighting functions (1.60) or (1.61) results in the two equations

$$\mathbf{C}_{\partial\Gamma}^{(g,\psi)} \cdot \mathbf{T}_{\psi} = -\,\mathbf{A}_{\partial\Gamma}^{(g,\varphi_0)} \cdot \mathbf{T}_{\varphi_0} \; + \; \mathbf{B}_{\partial\Gamma}^{(g,\psi_0)} \tag{2.26}$$

and

$$\mathbf{C}_{\partial\Gamma}^{(h,\partial_{\hat{n}}\psi)} \cdot \mathbf{T}_{\psi} = -\,\mathbf{A}_{\partial\Gamma}^{(h,\partial_{\hat{n}}\varphi_0)} \cdot \mathbf{T}_{\varphi_0} \; + \; \mathbf{B}_{\partial\Gamma}^{(h,\partial_{\hat{n}}\psi_0)}. \tag{2.27}$$

The matrix elements of the matrices $\mathbf{A}_{\partial\Gamma}^{(g,\varphi_0)}$, $\mathbf{B}_{\partial\Gamma}^{(g,\psi_0)}$, and $\mathbf{C}_{\partial\Gamma}^{(g,\psi)}$ as well as of $\mathbf{A}_{\partial\Gamma}^{(h,\partial_{\hat{n}}\varphi_0)}$, $\mathbf{B}_{\partial\Gamma}^{(h,\partial_{\hat{n}}\psi_0)}$, and $\mathbf{C}_{\partial\Gamma}^{(h,\partial_{\hat{n}}\psi)}$ are now identical to these one defined in (1.64–1.69). Solving both (2.26) and (2.27) for $\mathbf{T}_{\psi}$ we get immediately the relation

$$\mathbf{T}_{\varphi_0} = \mathbf{T}_{\partial\Gamma}^{(d)} \tag{2.28}$$

for the remaining transformation matrix $\mathbf{T}_{\varphi_0}$. But $\mathbf{T}_{\partial\Gamma}^{(d)}$ on the right hand side is identical with the T-matrix (1.71) of the outer transmission problem we have already derived in Chap. 1. There exists an alternative way to solve both equations for $\mathbf{T}_{\varphi_0}$. First, we eliminate in both equations the quantity $\mathbf{T}_{\varphi_0}$. This results in

$$\begin{aligned}\mathbf{T}_{\psi} = &\left[\mathbf{A}_{\partial\Gamma}^{(g,\varphi_0)^{-1}} \cdot \mathbf{C}_{\partial\Gamma}^{(g,\psi)} - \mathbf{A}_{\partial\Gamma}^{(h,\partial_{\hat{n}}\varphi_0)^{-1}} \cdot \mathbf{C}_{\partial\Gamma}^{(h,\partial_{\hat{n}}\psi)}\right]^{-1} \\ &\cdot \left[\mathbf{A}_{\partial\Gamma}^{(g,\varphi_0)^{-1}} \cdot \mathbf{B}_{\partial\Gamma}^{(g,\psi_0)} - \mathbf{A}_{\partial\Gamma}^{(h,\partial_{\hat{n}}\varphi_0)^{-1}} \cdot \mathbf{B}_{\partial\Gamma}^{(h,\partial_{\hat{n}}\psi_0)}\right]\end{aligned} \tag{2.29}$$

for the transformation matrix $\mathbf{T}_{\psi}$. In analogy to (2.18) we can next define a transformation matrix which transforms the expansion functions $\vec{\psi}_0$ into the expansion functions $\vec{\psi}$ at the scatterer surface, i.e., for which

$$\vec{\psi}^{\,tp} = \tilde{\mathbf{T}}_{\psi_0/\psi} \cdot \vec{\psi}_0^{\,tp} \tag{2.30}$$

holds or, which is one and the same,

$$\vec{\psi} = \vec{\psi}_0 \cdot \mathbf{T}_{\psi_0/\psi}. \tag{2.31}$$

$\mathbf{T}_{\psi_0/\psi}$ is again the transpose of $\tilde{\mathbf{T}}_{\psi_0/\psi}$. By use of (2.18) and (2.30) we can generally pass in (2.24) into the expansion functions $\vec{\varphi}_0$. Then we end up with the alternative relation

$$\mathbf{T}_{\varphi_0} = \mathbf{T}_{\partial\mathbf{\Gamma}} \cdot \left[\mathbf{E} - \mathbf{T}_{\psi_0/\psi} \cdot \mathbf{T}_{\psi}\right] \tag{2.32}$$

for the transformation matrix $\mathbf{T}_{\varphi_0}$. If we have $\mathbf{T}_{\psi} \equiv \mathbf{0}$, then $\mathbf{T}_{\varphi_0}$ becomes identical with the transformation matrix $\mathbf{T}_{\partial\mathbf{\Gamma}}$ of the outer Dirichlet problem.

There is a possibility to manipulate the T-matrix further which can be used to make it numerically more appropriate, and to get an approximation of the scattered field which exhibits already some properties required from a physical point of view like the energy conservation in the case of non-absorbing particles, for example. To discuss this possibility let us rewrite (2.23) in the following way:

$$\vec{a}^{\,(N)\,tp} = \mathbf{Z} \cdot \mathbf{Z}^{-1} \cdot \mathbf{T}_{\partial\mathbf{\Gamma}} \cdot \mathbf{Z} \cdot \mathbf{Z}^{-1} \cdot \vec{b}^{\,(N)\,tp}, \tag{2.33}$$

i.e., we have just multiplied in (2.23) the old T-matrix from the left and the right with the unit matrix $\mathbf{E} = \mathbf{Z} \cdot \mathbf{Z}^{-1}$. With the definitions

$$\vec{\tilde{a}}^{\,(N)\,tp} := \mathbf{Z}^{-1} \cdot \vec{a}^{\,(N)\,tp}, \tag{2.34}$$

$$\vec{\tilde{b}}^{\,(N)^{tp}} := \mathbf{Z^{-1}} \cdot \vec{b}^{\,(N)^{tp}}, \tag{2.35}$$

and with

$$\mathbf{T}_{\partial\Gamma}^{(Z)} = \mathbf{Z^{-1}} \cdot \mathbf{T}_{\partial\mathbf{\Gamma}} \cdot \mathbf{Z} \tag{2.36}$$

we get from (2.33)

$$\vec{\tilde{a}}^{\,(N)^{tp}} = \mathbf{T}_{\partial\Gamma}^{(Z)} \cdot \vec{\tilde{b}}^{\,(N)^{tp}}. \tag{2.37}$$

Now, we can try to choose matrix $\mathbf{Z}$ in such a way that it provides the transformation matrix $\mathbf{T}_{\partial\Gamma}$ with a certain property. For example, if the original transformation matrix is a real and symmetric matrix we can first solve the eigenvalue problem

$$[\mathbf{T}_{\partial\mathbf{\Gamma}} - \lambda\mathbf{E}] \cdot \vec{x} = \vec{0}. \tag{2.38}$$

These eigenvectors are then used as the columns of the matrix $\mathbf{Z}$. In this way $\mathbf{Z}$ becomes an orthogonal transformation matrix, and the new transformation matrix $\mathbf{T}_{\partial\Gamma}^{(Z)}$ becomes a diagonal matrix. In Chap. 5 , in the context of the Method of Lines, we will discuss this situation. The same can be done if $\mathbf{T}_{\partial\Gamma}$ is a hermitian matrix. In this case, $\mathbf{Z}$ becomes a unitary transformation matrix and (2.33–2.36) must be modified accordingly, i.e., $\mathbf{Z^{-1}}$ must be replaced by $\mathbf{Z}^{\dagger}$. The latter denotes the transpose and conjugate-complex of $\mathbf{Z}$. But the matrix $\mathbf{Z}$ can also be chosen to exploit particle symmetries in the transformation matrix $\mathbf{T}_{\partial\Gamma}$. This can be related to the irreducible representation of group theory, as will be demonstrated in Chap. 8. These manipulations of the T-matrix are equivalent to respective manipulations of the expansion functions. Starting from (2.34) and (2.35) we may write contrary

$$\vec{a}^{\,(N)^{tp}} = \mathbf{Z} \cdot \vec{\tilde{a}}^{\,(N)^{tp}} \tag{2.39}$$

and

$$\vec{b}^{\,(N)^{tp}} = \mathbf{Z} \cdot \vec{\tilde{b}}^{\,(N)^{tp}}. \tag{2.40}$$

If we insert these expressions into the original expansion

$$\begin{aligned} \mid u_{inc}^{(N)}(\mathbf{x}) >_{\partial\Gamma} &= \sum_{\tau=1}^{2} \sum_{i=0}^{N} b_{i,\tau}^{(N)} \cdot \mid \psi_{i,\tau}(k_0, \mathbf{x}) >_{\partial\Gamma} \\ &= \sum_{\tau=1}^{2} \sum_{i=0}^{N} a_{i,\tau}^{(N)} \cdot \mid \varphi_{i,\tau}(k_0, \mathbf{x}) >_{\partial\Gamma} \end{aligned} \tag{2.41}$$

we get

$$
\begin{aligned}
|\, u_{inc}^{(N)}(\mathbf{x}) >_{} &= \sum_{\tau=1}^{2} \sum_{i=0}^{N} \tilde{b}_{i,\tau}^{(N)} \cdot |\, \psi_{i,\tau}^{(Z)}(k_0, \mathbf{x}) >_{\partial\Gamma} \\
&= \sum_{\tau=1}^{2} \sum_{i=0}^{N} \tilde{a}_{i,\tau}^{(N)} \cdot |\, \varphi_{i,\tau}^{(Z)}(k_0, \mathbf{x}) >_{\partial\Gamma}
\end{aligned}
\tag{2.42}
$$

with

$$
|\, \psi_{i,\tau}^{(Z)}(k_0, \mathbf{x}) >_{\partial\Gamma} = \sum_{\tau'=1}^{2} \sum_{j=0}^{N} \left[\tilde{Z}\right]_{i,j}^{\tau,\tau'} \cdot |\, \psi_{j,\tau'}(k_0, \mathbf{x}) >_{\partial\Gamma} \tag{2.43}
$$

and

$$
|\, \varphi_{i,\tau}^{(Z)}(k_0, \mathbf{x}) >_{\partial\Gamma} = \sum_{\tau'=1}^{2} \sum_{j=0}^{N} \left[\tilde{Z}\right]_{i,j}^{\tau,\tau'} \cdot |\, \varphi_{j,\tau'}(k_0, \mathbf{x}) >_{\partial\Gamma}. \tag{2.44}
$$

Thus, the new expansion functions $|\, \psi_{i,\tau}^{(Z)}(k_0, \mathbf{x}) >_{\partial\Gamma}$ and $|\, \varphi_{i,\tau}^{(Z)}(k_0, \mathbf{x}) >_{\partial\Gamma}$ turn out to be linear combinations of the old expansion functions $|\, \psi_{j,\tau'}(k_0, \mathbf{x}) >_{\partial\Gamma}$ and $|\, \varphi_{j,\tau'}(k_0, \mathbf{x}) >_{\partial\Gamma}$ accomplished with the matrix elements $[\tilde{Z}]_{i,j}^{\tau,\tau'}$ of the transpose of matrix $\mathbf{Z}$. The new expansion functions are then related to each other via Eq. (2.37).

While reading this section it may happen that for the attentive reader the following question arises: If the linearly independence of the expansion functions was assumed in advance, why we do not pass into orthogonal expansion functions by use of the Gram-Schmidt process? This should ease the foregoing considerations considerably. This is indeed possible and has been practised in the past for some simple scattering problems. But, on the other hand, this requires an additional numerical effort which can be spent just as well to calculate the inverse matrices defined above by use of only linearly independent functions. Moreover, as it can be seen from Eq. (2.29), for example, we have to consider different systems of expansion functions within one equation. This will again increase the numerical effort. For these reasons non-orthogonal but linearly independent functions are often more appropriate for practical problems.
In all the foregoing considerations we have used the expansion and weighting functions very formally. Becoming acquainted with explicit expressions together with the relevant properties of these functions is therefore in the focus of Sects. 2.3 and 2.4.

2.3 Eigensolutions of the Scalar Helmholtz Equation in Spherical Coordinates

In the relevant literature, the Separation of Variables method is customarily restricted from the beginning to certain boundary value problems of the partial differential equations underlying the scattering process. Three quotations should confirm this statement:

For example, if the equation is the scalar Helmholtz equation, the method of separation of variables can be used in only 11 coordinate systems. If the surface upon which boundary conditions are to be satisfied is not one of these coordinate surfaces, ..., the method of separation fails wrote P. M. Morse and H. Feshbach in Chap. 9 of their two books "Methods of Theoretical Physics" (see the reference chapter for details).

In H. C. van de Hulst's famous book "Light Scattering by Small Particles" (see the reference chapter for details) we can find the sentence *The method used for spheres ... and cylinders ... was to separate the vector-wave equation in curvilinear coordinates which have been chosen in such a way that the surface of the particle coincides with one of the coordinate surfaces* in Sect. 16.11.

And, finally, in the book "Absorption and Scattering of Light by Small Particles" of C. F. Bohren and D. R. Huffman (see the reference chapter for details) we can find the following statement in Sect. 8.6.1 concerning the applicability of the Separation of Variables method: *it is applicable to particles with boundaries coinciding with coordinate surfaces of coordinate systems in which the wave equation is separable*.

These citations manifest the point of view that the Separation of Variables method is only applicable if the boundary surface of the scatterer coincides with a constant coordinate line in one of the coordinate systems allowing the separation of the underlying partial differential equation. Starting from this assumption a variety of different numerical methods have been developed in the past which are not only restricted to those separable geometries. But this assumption deserves a certain correction in our opinion. According to our understanding the Separation of Variables method is essentially a method for providing a pool of potential expansion functions, namely independent of the geometry of a certain boundary surface and the physical conditions which have to be fulfilled along these boundaries. Replacing the original partial differential equation by an appropriate number of ordinary differential equations and exploiting their eigensolutions are the main objectives of this method. The physical problem, on the other hand, consists of the formulation of the underlying partial differential equation **and** the boundary conditions which have to be fulfilled additionally. The latter enables us to choose from the pool of eigensolutions provided by the Separation of Variables method the appropriate expansion functions which can be used to approximate the sought solution of the physical problem in terms of series expansion (1.21), for example.

Therefore, we will first discuss the relevant eigensolutions of the scalar Helmholtz equation in the spherical coordinates (r, θ, ϕ) together with some of their properties along the boundary surface of the scatterer. We will see moreover that the selected eigensolutions correspond already with some of the additional conditions resulting from the physical requirements of the scattering problem, except the behaviour of the physical fields across the boundary surface. This last behaviour will be taken into account later on. But we will see on the other hand how one can expand a plane wave in the whole free space $\Gamma = \Gamma_- \cup \Gamma_+$ into an appropriate series expansion with final expansion coefficients.

Table 2.1 Relations between the unit vectors in Cartesian and spherical coordinates

	$\hat{x}$	$\hat{y}$	$\hat{z}$
$\hat{r}$	$\sin\theta\cos\phi$	$\sin\theta\sin\phi$	$\cos\theta$
$\hat{\theta}$	$\cos\theta\cos\phi$	$\cos\theta\sin\phi$	$-\sin\theta$
$\hat{\phi}$	$-\sin\phi$	$\cos\phi$	0

Most of the following considerations are well-known, of course. But we thought that it would be helpful to gather together the mathematical material seen from the point of view of scattering.

2.3.1 The Eigensolutions

The relations between the Cartesian and spherical coordinates are given by

$$\begin{aligned} x &= r \cdot \sin\theta \cdot \cos\phi \\ y &= r \cdot \sin\theta \cdot \sin\phi \\ z &= r \cdot \cos\theta. \end{aligned} \tag{2.45}$$

The values of the elevation angle θ are restricted to the interval $[0, \pi]$, and the values of the azimuthal angle ϕ are within the interval $[0, 2\pi]$. The corresponding relations between the unit vectors of both coordinate systems can be taken from Table 2.1. The homogeneous Helmholtz equation reads

$$\left(\nabla^2 + k^2\right) u(r, \theta, \phi) = 0 \tag{2.46}$$

with the Laplace operator given by

$$\nabla^2 = \frac{1}{r^2}\frac{\partial}{\partial r}\left(r^2 \frac{\partial}{\partial r}\right) + \frac{1}{r^2 \sin\theta}\frac{\partial}{\partial\theta}\left(\sin\theta \frac{\partial}{\partial\theta}\right) + \frac{1}{r^2 \sin^2\theta}\frac{\partial^2}{\partial\phi^2} \tag{2.47}$$

in spherical coordinates. The boundary surface $\partial\Gamma = S$ enclosing the finite volume Γ_- is given by the parameter representation

$$\vec{r} = r(\theta, \phi) \cdot \hat{r}. \tag{2.48}$$

$\hat{r}$ denotes the unit vector in the radial direction and $\vec{r}$ is the vector to a certain point on the boundary surface. Due to this representation we get the following expression for the surface elements in the two definitions (1.34) and (1.35) of the scalar product:

$$dS = \left| \frac{\partial\vec{r}}{\partial\theta} \times \frac{\partial\vec{r}}{\partial\phi} \right| \mathrm{d}\theta\, \mathrm{d}\phi \tag{2.49}$$

with

$$\frac{\partial \vec{r}}{\partial \theta} \times \frac{\partial \vec{r}}{\partial \phi} = r^2 \sin\theta \cdot \hat{r} - r \sin\theta \cdot \frac{\partial r}{\partial \theta} \cdot \hat{\theta} - r \cdot \frac{\partial r}{\partial \phi} \cdot \hat{\phi}. \tag{2.50}$$

In the special case of a spherical boundary surface with the radius $r = a$ this reduces to

$$dS = a^2 \sin\theta \, \mathrm{d}\theta \, \mathrm{d}\phi. \tag{2.51}$$

The unit vector $\hat{n}$ at the boundary surface $\partial\Gamma$ pointing into the outer volume Γ_+ is calculated according to

$$\hat{n} = \frac{\frac{\partial \vec{r}}{\partial \theta} \times \frac{\partial \vec{r}}{\partial \phi}}{\left| \frac{\partial \vec{r}}{\partial \theta} \times \frac{\partial \vec{r}}{\partial \phi} \right|}. \tag{2.52}$$

How can we solve the Helmholtz equation (2.46)? The Separation of Variables method is based on the Bernoulli ansatz

$$u(r, \theta, \phi) \;=\; R(r) \cdot \Theta(\theta) \cdot \Phi(\phi) \tag{2.53}$$

for the unknown function $u(r, \theta, \phi)$. This will allow us to separate the above given Helmholtz equation. Using (2.53) in (2.46) and introducing the at first arbitrary separation constants α and β converts the original Helmholtz equation into three ordinary differential equations of second order, i.e., into

$$\left[\frac{d^2}{dr^2} + k^2 - \frac{\beta}{r^2}\right] r \cdot R(r) = 0 \tag{2.54}$$

$$\left[\frac{1}{\sin\theta}\frac{d}{d\theta}\left(\sin\theta \frac{d}{d\theta}\right) + \beta - \frac{\alpha}{\sin^2\theta}\right] \Theta(\theta) = 0 \tag{2.55}$$

$$\left[\frac{d^2}{d\phi^2} + \alpha\right] \Phi(\phi) = 0. \tag{2.56}$$

Each of these ordinary differential equations provides us with two linearly independent solutions. But regarding the scattering problem we are only interested in the following eigensolutions:

$$\psi_{l,n}(r, \theta, \phi) = j_n(kr) \cdot Y_{l,n}(\theta, \phi) \tag{2.57}$$

$$\varphi_{l,n}(r, \theta, \phi) = h_n^{(1)}(kr) \cdot Y_{l,n}(\theta, \phi) \tag{2.58}$$

$$\chi_{l,n}(r, \theta, \phi) = h_n^{(2)}(kr) \cdot Y_{l,n}(\theta, \phi). \tag{2.59}$$

$Y_{l,n}(\theta, \phi)$ are the spherical harmonics

$$Y_{l,n}(\theta, \phi) \;:=\; \sqrt{\frac{2n+1}{4\pi}\frac{(n-l)!}{(n+l)!}} \cdot P_n^l(\cos\theta)\, e^{il\phi} \tag{2.60}$$

which are normalized to unity. They obey the orthogonality relation

$$\int_0^{2\pi} d\phi \int_0^{\pi} d\theta \sin\theta \; Y^*_{l',n'}(\theta,\phi)\, Y_{l,n}(\theta,\phi) = \delta_{ll'}\delta_{nn'} \tag{2.61}$$

as well as the following relations:

$$Y^*_{l,n}(\theta,\phi) = (-1)^l \cdot Y_{-l,n}(\theta,\phi), \tag{2.62}$$

$$Y_{l,n}(\pi-\theta,\phi\pm\pi) = (-1)^n \cdot Y_{l,n}(\theta,\phi), \tag{2.63}$$

$$\sum_{n=0}^{\infty}\sum_{l=-n}^{n} Y^*_{l,n}(\theta,\phi)\cdot Y_{l,n}(\theta',\phi') = \delta(\cos\theta-\cos\theta')\cdot\delta(\phi-\phi'). \tag{2.64}$$

The latter is the relation of completeness . Index n is restricted to the natural numbers $n = 0, 1, 2, \ldots \infty$, and index l takes the integer numbers $l = -n, -n+1, \ldots, n-1, n$. These indices are related to the separation constants α and β according to $n(n+1) = \beta$ and $l = \sqrt{\alpha}$.

j_n in (2.57), $h_n^{(1)}$ in (2.58), and $h_n^{(2)}$ in (2.59) are the spherical Bessel functions, the spherical Hankel functions of first kind, and the spherical Hankel functions of second kind, respectively. All these functions are possible solutions of equation (2.54) and are related to the corresponding functions with fractional orders according to

$$j_n(kr) = \sqrt{\frac{\pi}{2kr}}\cdot J_{n+1/2}(kr) \tag{2.65}$$

$$h_n^{(1)}(kr) = \sqrt{\frac{\pi}{2kr}}\cdot H^{(1)}_{n+1/2}(kr) \tag{2.66}$$

$$h_n^{(2)}(kr) = \sqrt{\frac{\pi}{2kr}}\cdot H^{(2)}_{n+1/2}(kr). \tag{2.67}$$

The functions $P_n^l(\cos\theta)$ in (2.60) are the associated Legendre polynomials. They form one of the two linearly independent solutions of the ordinary differential Eq. (2.55). At the elevation angles $\theta = 0$ and $\theta = \pi$ they fulfil the homogeneous Neumann condition if $l = 0$ and the homogeneous Dirichlet condition if $l \neq 0$:

$$\frac{d}{d\theta}P_n^l(1) = \frac{d}{d\theta}P_n^l(-1) = 0\,; \quad l = 0 \tag{2.68}$$

$$P_n^l(1) = P_n^l(-1) = 0\,; \quad l \neq 0. \tag{2.69}$$

Moreover, these functions are orthogonal in the sense

$$\int_0^{\pi} d\theta \sin\theta \cdot P_n^l(\cos\theta)\, P_{n'}^l(\cos\theta) = \frac{2}{2n+1}\frac{(n+l)!}{(n-l)!}\cdot\delta_{nn'}. \tag{2.70}$$

$$P_n^{-l}(\cos\theta) = (-1)^l \cdot \frac{(n-l)!}{(n+l)!} \cdot P_n^l(\cos\theta) \tag{2.71}$$

is the relation between the associated Legendre polynomials with positive and negative index l. The associated Legendre polynomials may be calculated from the conventional Legendre polynomials $P_n(x)$ by use of the relation

$$P_n^l(x) = (-1)^l \cdot (1-x^2)^{l/2} \cdot \frac{d^l P_n(x)}{dx^l} \tag{2.72}$$

with the $P_n(x)$ given by

$$P_n(x) = \frac{1}{2^n n!}\left(\frac{d}{dx}\right)^n (x^2-1)^n. \tag{2.73}$$

It should be noted that one can find in the literature relation (2.72) also without the prefactor $(-1)^l$. This is important since making the intercomparison of analytical results sometimes not a simple task. We will further see how one can expand a plane wave into regular eigensolutions. As a consequence of the mentioned difference in relation (2.72) we get expansion coefficients which may differ in sign from these one given in the literature, for example. Here, we use (2.72) throughout this book. The associated Legendre polynomials of second kind are the other linearly independent functions of the ordinary differential Eq. (2.55). But since these functions exhibit a logarithmic singularity if $\theta = 0, \pi$ they are not of our interest here.

The functions $e^{il\phi}$ solving the ordinary differential Eq. (2.56) are periodic functions with respect to 2π,

$$\Phi(\phi) = \Phi(\phi + 2\pi l). \tag{2.74}$$

They are two times continuously differentiable functions for every $\phi \in [0, 2\pi]$ and obey the orthogonality relation

$$\int_0^{2\pi} d\phi e^{il\phi} e^{-il'\phi} \;=\; 2\pi\delta_{ll'}. \tag{2.75}$$

When formulating the boundary value problems in Chap. 1 we have already introduced Sommerfeld's radiation condition (1.19) which has to be applied to the scattered field at the outer boundary S_∞ of Γ_+. This condition reads in spherical coordinates

$$\lim_{r\to\infty}\left(\frac{\partial}{\partial r} - ik\right) u_s(r,\theta,\phi) \;=\; 0\left(\frac{1}{r}\right). \tag{2.76}$$

A closer look at the asymptotic behaviour

$$\lim_{r\to\infty} j_n(kr) = \frac{1}{kr} \cdot \cos\left[kr - \frac{\pi}{2}(n+1)\right] \tag{2.77}$$

$$\lim_{r\to\infty} h_n^{(1)}(kr) = (-i)^{n+1} \cdot \frac{e^{ikr}}{kr} \tag{2.78}$$

$$\lim_{r\to\infty} h_n^{(2)}(kr) = (i)^{n+1} \cdot \frac{e^{-ikr}}{kr} \tag{2.79}$$

of the Bessel and Hankel functions for large arguments reveals that only the Hankel functions $h_n^{(1)}$ of the first kind are in accordance with the radiation condition (2.76). The functions $\varphi_{l,n}(r, \theta, \phi)$ in (2.58) are therefore called "radiating functions" or "radiating solutions" of the Helmholtz equation. Inside the scatterer we assumed a regular field with no singularities especially at the origin of the coordinate system. The functions $\psi_{l,n}(r, \theta, \phi)$ in (2.57) are the only functions subject to this requirement. Correspondingly, we will call these functions the "regular solutions" of Helmholtz' equation. The remaining functions $\chi_{l,n}(r, \theta, \phi)$ in (2.59) are called the "incoming solutions". The radiation condition does not apply to these functions, and they are not really needed for the approximation of the scattering solution. But they can be very helpful for some derivations and definitions. Since being two times continuously differentiable everywhere in Γ_+ they will be used later on in the representation of the total field outside the scatterer, for example. Moreover, in conjunction with the transformation character of the T-matrix these functions provide an easy access to the proof of the unitarity of the T-matrix if an ideal metallic scatterer is considered.

Both types of Hankel functions can be expressed by the combination

$$h_n^{(1)}(kr) = j_n(kr) + iy_n(kr) \tag{2.80}$$

$$h_n^{(2)}(kr) = j_n(kr) - iy_n(kr). \tag{2.81}$$

of the Bessel and Neumann functions. The Neumann functions $y_n(kr)$ are also possible solutions of the ordinary differential Eq. (2.54). Thus, we can represent the regular solutions as a superposition of the radiating and incoming solutions according to

$$\psi_{l,n}(r, \theta, \phi) = \frac{1}{2} \cdot \left[\varphi_{l,n}(r, \theta, \phi) + \chi_{l,n}(r, \theta, \phi)\right]. \tag{2.82}$$

The Bessel and Neumann functions are real-valued functions if the parameter k in their arguments becomes also real-valued.

What makes all these functions so well-suited for our purposes? By use of these functions we are now able to approximate a smooth function $u(r, \theta, \phi)$ outside or inside the scatterer by series

$$u^{(N)}(r, \theta, \phi) = \sum_{n=0}^{N} \sum_{l=-n}^{n} a_{l,n}^{(N)} \cdot \varphi_{l,n}(kr, \theta, \phi) \tag{2.83}$$

or series

$$u^{(N)}(r,\theta,\phi) = \sum_{n=0}^{N} \sum_{l=-n}^{n} a_{l,n}^{(N)} \cdot \psi_{l,n}(kr,\theta,\phi) \tag{2.84}$$

respectively, depending on whether the radiation condition or the regularity requirement must be additionally fulfilled.

For later purposes we introduce additionally the auxiliary functions

$$\tilde{\varphi}_{l,n}(kr,\theta,\phi) := (-1)^l \cdot \varphi_{-l,n}(kr,\theta,\phi) \tag{2.85}$$

$$\tilde{\chi}_{l,n}(kr,\theta,\phi) := (-1)^l \cdot \chi_{-l,n}(kr,\theta,\phi). \tag{2.86}$$

$$\tilde{\psi}_{l,n}(kr,\theta,\phi) := (-1)^l \cdot \psi_{-l,n}(kr,\theta,\phi) \tag{2.87}$$

where for a real-valued parameter k

$$\tilde{\psi}_{l,n}(kr,\theta,\phi) = \psi_{l,n}^{*}(kr,\theta,\phi) \tag{2.88}$$

holds. ψ^* denotes the conjugate-complex of ψ.

Dealing with the numerical realization of all the functions introduced in this section is outside the scope of this book. We will tacitly assume that this can be done without any difficulties. We refer the reader who may be interested in those numerical aspects to the reference chapter.

2.3.2 The Combined Summation Index

Sometimes it is more useful to write down the series expansions (2.83) and (2.84) in a more compact form with only one summation index. This can be accomplished with the index i combining the two indices n and l according to

$$i = n(n+1) + l. \tag{2.89}$$

Table 2.2 illustrates the relation (2.89) explicitly. Using this index we can write instead of (2.83) and (2.84)

Table 2.2 Relation between the combined summation index i and the original indices n and l

i	0	1	2	3	4	5	6	7	8	9	10	11	12	13	14	15	⋯
n	0	1	1	1	2	2	2	2	2	3	3	3	3	3	3	3	⋯
l	0	−1	0	1	−2	−1	0	1	2	−3	−2	−1	0	1	2	3	⋯

$$u^{(N)}(r,\theta,\phi) = \sum_{i=0}^{N} a_i^{(N)} \cdot \varphi_i(kr,\theta,\phi) \tag{2.90}$$

$$u^{(N)}(r,\theta,\phi) = \sum_{i=0}^{N} a_i^{(N)} \cdot \psi_i(kr,\theta,\phi). \tag{2.91}$$

Conversely, the two indices n and l can be recalculated from the relations

$$n(i) = nint\left[\frac{1}{2}\left(-1+\sqrt{1+4i}\right)\right] \tag{2.92}$$

$$l(i) = i - n(i)\cdot[n(i)+1] \tag{2.93}$$

with $nint(a)$ being the integer number closest to the real number a. Equation (2.92) can be inferred from the solution of the quadratic equation resulting from (2.89) for $l = 0$. Next, if $n(i)$ has been determined for a given i, then (2.93) provides the corresponding $l(i)$ in a unique way.

2.3.3 Properties of the Scalar Eigensolutions

If restricting the arguments of the functions defined in (2.57) and (2.58) to the boundary surface $\partial\Gamma$ of the scatterer we are able to make the following mathematical statements:

- The families of functions $\{\varphi_i(kr,\theta,\phi)\}$ and $\{\partial\varphi_i(kr,\theta,\phi)/\partial\hat{n}\}$ are linearly independent in the space $L_2(\partial\Gamma)$ (that is the space of the square-integrable functions at $\partial\Gamma$). Moreover, if k^2 is not an eigenvalue of the interior Dirichlet problem then the set of functions $\{\psi_i(kr,\theta,\phi)\}$ becomes linearly independent in space $L_2(\partial\Gamma)$. On the other hand, if k^2 is not an eigenvalue of the interior Neumann problem the linearly independence in $L_2(\partial\Gamma)$ holds for the set of functions $\{\partial\psi_i(kr,\theta,\phi)/\partial\hat{n}\}$. The interior Dirichlet and Neumann problem are two internal resonance problems with discrete solutions at the resonance frequencies (their eigenvalues). The mathematical proofs can be found, for example, in the paper of R. E. Kleinman et al., 1984 (see the reference Sect. 10.2 for details). For the proofs it is assumed that $\partial\Gamma$ is a two times continuously differentiable surface (a C^2 surface). Sometimes one can also find a weakening of this assumption by assuming that the surface is of a Liapounoff type. Liapounoff type surfaces are only one times continuously differentiable, sufficiently smooth, and not ambiguous surfaces. The terminus square-integrable is related to the scalar product defined in (1.34).
- The families of functions $\{\varphi_i(kr,\theta,\phi)\}$ and $\{\partial\varphi_i(kr,\theta,\phi)/\partial\hat{n}\}$ are complete in $L_2(\partial\Gamma)$. Moreover, if k^2 is not an eigenvalue of the interior Dirichlet problem then the set of functions $\{\psi_i(kr,\theta,\phi)\}$ becomes complete in $L_2(\partial\Gamma)$. On the other hand, if k^2 is not an eigenvalue of the interior Neumann problem the completeness in $L_2(\partial\Gamma)$ holds for the set of functions $\{\partial\psi_i(kr,\theta,\phi)/\partial\hat{n}\}$.

The mathematical proofs can be found, for example, in the paper of R. F. Millar, 1973 (see the reference Sect. 9.7), and in the book of A. Doicu et al., 2000 (see the reference Sect.. 9.2).

Thus, if the boundary surface of the scatterer belongs to a C^2 or Liapounoff type surface, and if we choose the regular and radiating solutions as expansion and weighting functions we know the invertability of the finite-dimensional matrices considered in Sect. 1.3 in advance. In all other cases we have to prove the invertability of the relevant matrices numerically.

We have mentioned earlier that the limiting case of a spherical scatterer is always incorporated in our methods. This will be demonstrated explicitly later on in conjunction with the relevant Green functions. But for this discussion we need the orthogonality relations of the scalar eigensolutions $\varphi_i(\kappa a, \theta, \phi)$ and $\psi_i(\kappa a, \theta, \phi)$ at a spherical surface with the radius $r = a$. These are based on the orthogonality relation (2.61) of the spherical harmonics. In what follows κ and κ' stand for one of the two parameters k and k_0 characterizing the regions Γ_- and Γ_+ physically. Then the orthogonality relations read

$$\int_0^{2\pi} d\phi \int_0^{\pi} d\theta a^2 \sin\theta \, \varphi_i^*(\kappa a, \theta, \phi) \cdot \varphi_j(\kappa' a, \theta, \phi) = a^2 \cdot c_i^{(\varphi,\varphi)}(\kappa, \kappa') \cdot \delta_{ij} \quad (2.94)$$

$$\int_0^{2\pi} d\phi \int_0^{\pi} d\theta a^2 \sin\theta \, \varphi_i^*(\kappa a, \theta, \phi) \cdot \psi_j(\kappa' a, \theta, \phi) = a^2 \cdot c_i^{(\varphi,\psi)}(\kappa, \kappa') \cdot \delta_{ij} \quad (2.95)$$

$$\int_0^{2\pi} d\phi \int_0^{\pi} d\theta a^2 \sin\theta \, \psi_i^*(\kappa a, \theta, \phi) \cdot \psi_j(\kappa' a, \theta, \phi) = a^2 \cdot c_i^{(\psi,\psi)}(\kappa, \kappa') \cdot \delta_{ij} \quad (2.96)$$

$$\int_0^{2\pi} d\phi \int_0^{\pi} d\theta a^2 \sin\theta \, \psi_i^*(\kappa a, \theta, \phi) \cdot \varphi_j(\kappa' a, \theta, \phi) = a^2 \cdot c_i^{(\psi,\varphi)}(\kappa, \kappa') \cdot \delta_{ij}. \quad (2.97)$$

The normalization constants c_i are given by the following expressions:

$$c_i^{(\varphi,\varphi)}(\kappa, \kappa') = \left(h_{n_i}^{(1)}(\kappa a)\right)^* \cdot h_{n_i}^{(1)}(\kappa' a) \quad (2.98)$$

$$c_i^{(\varphi,\psi)}(\kappa, \kappa') = \left(h_{n_i}^{(1)}(\kappa a)\right)^* \cdot j_{n_i}(\kappa' a) \quad (2.99)$$

$$c_i^{(\psi,\psi)}(\kappa, \kappa') = j_{n_i}^*(\kappa a) \cdot j_{n_i}(\kappa' a) \quad (2.100)$$

$$c_i^{(\psi,\varphi)}(\kappa, \kappa') = j_{n_i}^*(\kappa a) \cdot h_{n_i}^{(1)}(\kappa' a). \quad (2.101)$$

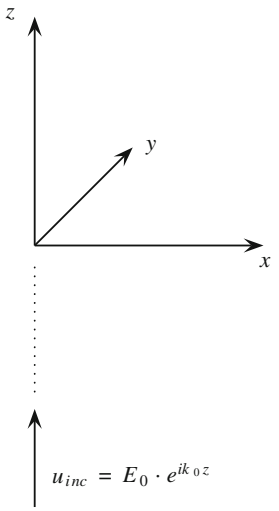

Fig. 2.1 u_{inc} represents a scalar plane wave travelling along the positive z-axis

2.3.4 Expansion of a Scalar Plane Wave

$$u_{inc}(k_0 r, \theta, \phi) = E_0 \cdot e^{ik_0 r \cos\theta} \tag{2.102}$$

represents the scalar plane wave $E_0 \cdot e^{ik_0 z}$ in spherical coordinates travelling along the positive z-axis in a Cartesian coordinate system (see Fig. 2.1). E_0 is its arbitrary amplitude. This plane wave solves the homogeneous Helmholtz's equation but it does not fulfil the radiation condition at S_∞ as already mentioned. We will now demonstrate how one can approximate this wave by an infinite series in terms of the regular solutions $\psi_{l,n}(k_0 r, \theta, \phi)$ valid everywhere in the free space. That is, we are asking for the expansion coefficients $c_{l,n}$ of expansion

$$E_0 \cdot e^{ik_0 r \cos\theta} = E_0 \sum_{n=0}^{N} \sum_{l=-n}^{n} c_{l,n} \cdot \psi_{l,n}(k_0 r, \theta, \phi). \tag{2.103}$$

First, we multiply this equation from the left with the functions $\psi^*_{l,n}(k_0 r, \theta, \phi)$ and integrate afterwards over the entire free space. In this way we get

$$\begin{aligned} &\int_0^{2\pi} d\phi \int_0^{\pi} d\theta \sin\theta \int_0^{\infty} dr\, r^2\, j^*_{n'}(k_0 r) Y^*_{l',n'}(\theta, \phi)\; e^{ik_0 r \cos\theta} \\ &= \sum_{n=0}^{N} \sum_{l=-n}^{n} c_{l,n} \int_0^{2\pi} d\phi \int_0^{\pi} d\theta \sin\theta \int_0^{\infty} dr\, r^2 \\ &\quad \cdot j^*_{n'}(k_0 r)\, j_n(k_0 r) Y^*_{l',n'}(\theta, \phi)\, Y_{l,n}(\theta, \phi). \end{aligned} \tag{2.104}$$

Applying the orthogonality relation (2.61) we can perform the ϕ- and θ-integration on the right hand side immediately. The same can be done for the ϕ-integration on the left hand side if applying the orthogonality relation (2.75) but for the special case $l = 0$,

$$\int_0^{2\pi} d\phi e^{-il'\phi} = 2\pi\delta_{0l'}. \tag{2.105}$$

If we rename n' as n and l' as l we arrive at the expression

$$\begin{aligned}\delta_{0l}\sqrt{\pi(2n+1)}\int_0^{\pi} d\theta \sin\theta \int_0^{\infty} dr\, r^2\, j_n^*(k_0 r)\, P_n^l(\cos\theta)\; e^{ik_0 r\cos\theta} \\ = c_{l,n}\int_0^{\infty} dr\, r^2\, j_n^*(k_0 r)\, j_n(k_0 r).\end{aligned} \tag{2.106}$$

Due to the independence of the plane wave (2.102) of the azimuthal angle ϕ the expansion coefficients are only dependent via the Kronecker δ_{0l} on the azimuthal modes l. As a consequence, only the Legendre polynomials $P_n(\cos\theta)$ must be taken into account in the approximation. Using Gegenbauer's representation

$$j_n(z) = \frac{1}{2}(-i)^n \int_0^{\pi} d\theta\; \sin\theta\, P_n(\cos\theta)\; e^{iz\cos\theta} \tag{2.107}$$

of the Poisson integral (see "Pocketbook of Mathematical Functions", for example) we obtain on the left hand side of (2.106) the same integral with respect to r as we have on the right hand side. Thus, we get finally

$$c_{l,n} = \delta_{0l} \cdot i^n \cdot \sqrt{4\pi(2n+1)} \tag{2.108}$$

for the expansion coefficients $c_{l,n}$ of the approximation (2.103). And, moreover, these coefficients are final and thus independent on the truncation parameter N of this approximation.

Representation (2.102) is a special case of the more general plane wave

$$u_{inc}(k_0 r, \theta, \phi, \theta_i, \phi_i) = E_0 \cdot e^{i\vec{k}_i\cdot\vec{r}} \tag{2.109}$$

with

$$\vec{k}_i = k_0 \cdot \hat{k} = k_{x_i}\cdot\hat{x} + k_{y_i}\cdot\hat{y} + k_{z_i}\cdot\hat{z} \tag{2.110}$$

$$\vec{r} = r\cdot\hat{r} = x\cdot\hat{x} + y\cdot\hat{y} + z\cdot\hat{z} \tag{2.111}$$

and

$$\begin{aligned} k_{x_i} &= k_0\cdot\sin\theta_i\cdot\cos\phi_i \\ k_{y_i} &= k_0\cdot\sin\theta_i\cdot\sin\phi_i \\ k_{z_i} &= k_0\cdot\cos\theta_i \end{aligned} \tag{2.112}$$

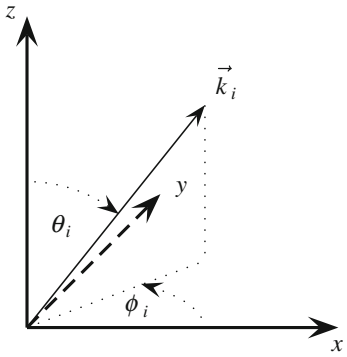

Fig. 2.2 u_{inc} represents a scalar plane wave travelling into the direction specified by $\vec{k}_i$

(see Fig. 2.2) if choosing $(\theta_i = 0, \phi_i)$ as the direction of propagation. $\hat{k}_i$ and $\hat{r}$ denote the corresponding unit vectors in the direction of $\vec{k}_i$ and $\vec{r}$, respectively. We can also approximate the plane wave (2.109) in the entire free space into an infinite series of regular solutions with final expansion coefficients. This approximation reads

$$u_{inc}(k_0 r, \theta, \phi, \theta_i, \phi_i) = E_0 \, 4\pi \sum_{l,n} \psi_{l,n}(k_0 r, \theta, \phi) \cdot \tilde{Y}^*_{l,n}(\theta_i, \phi_i). \tag{2.113}$$

The modified spherical harmonics $\tilde{Y}_{l,n}$ are related to the spherical harmonics given in (2.60) by

$$\tilde{Y}_{l,n}(\theta_i, \phi_i) = (-i)^n \cdot Y_{l,n}(\theta_i, \phi_i). \tag{2.114}$$

It is not difficult to show that we get indeed series expansion (2.103) with coefficients (2.108) from the more general expansion (2.113) if choosing $(\theta_i = 0^o, \phi_i)$. With the definitions

$$Y_{l,n}(\hat{k}_i) := Y_{l,n}(\theta_i, \phi_i) \tag{2.115}$$

$$Y_{l,n}(\hat{r}) := Y_{l,n}(\theta, \phi) \tag{2.116}$$

and because of (2.57) we may alternatively write instead of (2.113)

$$u_{inc}(k_0 r, \hat{r}, \hat{k}_i) = E_0 \, 4\pi \sum_{l,n} j_n(k_0 r) \cdot Y_{l,n}(\hat{r}) \cdot \tilde{Y}^*_{l,n}(\hat{k}_i). \tag{2.117}$$

This last expression can be found frequently in the literature. The derivation of expression (2.117) which was omitted here will be discussed in more detail in Sect. 3.3.1.

2.4 Eigensolutions of the Vector-Wave Equation in Spherical Coordinates

Now, we will consider the relevant eigensolutions of the homogeneous vector-wave equation. These solutions can be determined from the earlier discussed scalar eigensolutions of the Helmholtz equation. As in the scalar case, we are only interested in non-singular and two times continuously differentiable functions in regions Γ_+ and Γ_-, respectively. It should be mentioned that one can find several different representations of these eigensolutions in the relevant literature. And it is not even a simple task to convince oneself from the equivalence of these representations. However, here we will discuss again only those representations, relations, and properties which are most important for our purposes. We refer the reader who may be interested in further details on these aspects to the reference chapter at the end of this book.

2.4.1 The Vectorial Eigensolutions

The relevant eigensolutions of the vector-wave equation

$$\left(\nabla \times \nabla \times - k^2\right) \vec{u}(r, \theta, \phi) = \vec{0} \tag{2.118}$$

with the Nabla operator given by

$$\nabla = \frac{\partial}{\partial r} \cdot \hat{r} \; + \; \frac{1}{r} \frac{\partial}{\partial \theta} \cdot \hat{\theta} \; + \; \frac{1}{r \sin\theta} \frac{\partial}{\partial \phi} \cdot \hat{\phi} \tag{2.119}$$

in spherical coordinates are calculated in the following way from the scalar eigensolutions (2.57–2.59) of the Helmholtz equation:

$$\vec{\psi}_{l,n,1}(r, \theta, \phi) = \frac{1}{\sqrt{n(n+1)}} \nabla \times \left(\hat{r} \cdot r \cdot \psi_{l,n}(r, \theta, \phi)\right) \tag{2.120}$$

$$\vec{\psi}_{l,n,2}(r, \theta, \phi) = \frac{1}{\sqrt{n(n+1)}} \frac{1}{k} \nabla \times \nabla \times \left(\hat{r} \cdot r \cdot \psi_{l,n}(r, \theta, \phi)\right) \tag{2.121}$$

$$\vec{\varphi}_{l,n,1}(r, \theta, \phi) = \frac{1}{\sqrt{n(n+1)}} \nabla \times \left(\hat{r} \cdot r \cdot \varphi_{l,n}(r, \theta, \phi)\right) \tag{2.122}$$

$$\vec{\varphi}_{l,n,2}(r, \theta, \phi) = \frac{1}{\sqrt{n(n+1)}} \frac{1}{k} \nabla \times \nabla \times \left(\hat{r} \cdot r \cdot \varphi_{l,n}(r, \theta, \phi)\right) \tag{2.123}$$

$$\vec{\chi}_{l,n,1}(r, \theta, \phi) = \frac{1}{\sqrt{n(n+1)}} \nabla \times \left(\hat{r} \cdot r \cdot \chi_{l,n}(r, \theta, \phi)\right) \tag{2.124}$$

$$\vec{\chi}_{l,n,2}(r, \theta, \phi) = \frac{1}{\sqrt{n(n+1)}} \frac{1}{k} \nabla \times \nabla \times \left(\hat{r} \cdot r \cdot \chi_{l,n}(r, \theta, \phi)\right). \tag{2.125}$$

Employing the explicit expressions of the scalar eigenfunctions given in the foregoing section and introducing the constant

$$\gamma_{l,n} := \sqrt{\frac{2n+1}{4\pi n(n+1)} \frac{(n-l)!}{(n+l)!}} \tag{2.126}$$

as well as the vector spherical harmonics

$$\vec{P}_{l,n}(\theta,\phi) := \hat{r}\ P_n^l(\cos\theta) \cdot e^{il\phi} \tag{2.127}$$

$$\vec{C}_{l,n}(\theta,\phi) := \left[\hat{\theta}\,\frac{il}{\sin\theta} \cdot P_n^l(\cos\theta) \ - \ \hat{\phi}\,\frac{dP_n^l(\cos\theta)}{d\theta}\right] \cdot e^{il\phi} \tag{2.128}$$

$$\vec{B}_{l,n}(\theta,\phi) := \left[\hat{\theta}\,\frac{dP_n^l(\cos\theta)}{d\theta} \ + \ \hat{\phi}\,\frac{il}{\sin\theta} \cdot P_n^l(\cos\theta)\right] \cdot e^{il\phi}, \tag{2.129}$$

results in the following expressions:

$$\vec{\psi}_{l,n,1}(r,\theta,\phi) = \gamma_{l,n} \cdot j_n(kr) \cdot \vec{C}_{l,n}(\theta,\phi) \tag{2.130}$$

$$\begin{aligned}\vec{\psi}_{l,n,2}(r,\theta,\phi) = \gamma_{l,n} \ \cdot \Bigg[&\frac{n(n+1)}{kr} \cdot j_n(kr) \cdot \vec{P}_{l,n}(\theta,\phi) \\ &+ \frac{1}{kr}\frac{\partial}{\partial r}\left(rj_n(kr)\right) \cdot \vec{B}_{l,n}(\theta,\phi)\Bigg].\end{aligned} \tag{2.131}$$

$$\vec{\varphi}_{l,n,1}(r,\theta,\phi) = \gamma_{l,n} \cdot h_n^{(1)}(kr) \cdot \vec{C}_{l,n}(\theta,\phi) \tag{2.132}$$

$$\begin{aligned}\vec{\varphi}_{l,n,2}(r,\theta,\phi) \ = \gamma_{l,n} \cdot \Bigg[&\frac{n(n+1)}{kr} \cdot h_n^{(1)}(kr) \cdot \vec{P}_{l,n}(\theta,\phi) \\ &+ \frac{1}{kr}\frac{\partial}{\partial r}\left(rh_n^{(1)}(kr)\right) \cdot \vec{B}_{l,n}(\theta,\phi)\Bigg].\end{aligned} \tag{2.133}$$

The corresponding expressions for the vector functions $\vec{\chi}_{l,n,1}(r,\theta,\phi)$ and $\vec{\chi}_{l,n,2}(r,\theta,\phi)$ are obtained from (2.132) and (2.133) by replacing the Hankel functions $h_n^{(1)}(kr)$ of the first kind appearing in both of these expressions by the Hankel functions $h_n^{(2)}(kr)$ of the second kind.

The vector spherical harmonics defined in (2.127–2.129) obey the symmetry relations

$$\vec{C}_{l,n}^{*}(\theta,\phi) = (-1)^l \cdot \frac{(n+l)!}{(n-l)!} \cdot \vec{C}_{-l,n}(\theta,\phi) \tag{2.134}$$

$$\vec{B}^*_{l,n}(\theta,\phi) = (-1)^l \cdot \frac{(n+l)!}{(n-l)!} \cdot \vec{B}_{-l,n}(\theta,\phi) \tag{2.135}$$

$$\vec{C}_{l,n}(\pi-\theta,\phi\pm\pi) = (-1)^n \cdot \vec{C}_{l,n}(\theta,\phi) \tag{2.136}$$

$$\vec{B}_{l,n}(\pi-\theta,\phi\pm\pi) = (-1)^{n+1} \cdot \vec{B}_{l,n}(\theta,\phi) \tag{2.137}$$

as well as the orthogonality relations

$$\begin{aligned}
&\int_0^{2\pi} d\phi \int_0^{\pi} d\theta \sin\theta\ \vec{B}^*_{l,n}(\theta,\phi)\,\vec{C}_{l,n}(\theta,\phi) \\
&\quad = \int_0^{2\pi} d\phi \int_0^{\pi} d\theta \sin\theta\ \vec{B}^*_{l,n}(\theta,\phi)\,\vec{P}_{l,n}(\theta,\phi) \\
&\quad = \int_0^{2\pi} d\phi \int_0^{\pi} d\theta \sin\theta\ \vec{C}^*_{l,n}(\theta,\phi)\,\vec{P}_{l,n}(\theta,\phi) = 0,
\end{aligned} \tag{2.138}$$

and

$$\begin{aligned}
&\int_0^{2\pi} d\phi \int_0^{\pi} d\theta \sin\theta\ \vec{B}^*_{l,n}(\theta,\phi)\,\vec{B}_{l,n}(\theta,\phi) \\
&\quad = \int_0^{2\pi} d\phi \int_0^{\pi} d\theta \sin\theta\ \vec{C}^*_{l,n}(\theta,\phi)\,\vec{C}_{l,n}(\theta,\phi) = \frac{1}{\gamma^2_{l,n}} \cdot \delta_{ll'}\delta_{nn'}
\end{aligned} \tag{2.139}$$

$$\int_0^{2\pi} d\phi \int_0^{\pi} d\theta \sin\theta\ \vec{P}^*_{l,n}(\theta,\phi)\,\vec{P}_{l,n}(\theta,\phi) = \frac{1}{n(n+1)\cdot\gamma^2_{l,n}} \cdot \delta_{ll'}\delta_{nn'}. \tag{2.140}$$

They become especially simple if choosing $\theta = 0^o$. In this case, we get

$$\vec{C}_{l,n}(\theta=0^o,\phi) = \frac{il}{\gamma_{l,n}} \cdot \sqrt{\frac{2n+1}{8\pi}} \cdot \hat{e}_l; \quad l = \pm 1 \tag{2.141}$$

$$\vec{B}_{l,n}(\theta=0^o,\phi) = \frac{1}{\gamma_{l,n}} \cdot \sqrt{\frac{2n+1}{8\pi}} \cdot \hat{e}_l; \quad l = \pm 1 \tag{2.142}$$

with

$$\hat{e}_1(\theta=0^o) = -\frac{1}{\sqrt{2}} e^{i\phi} \cdot \left(\hat{\theta} + i\,\hat{\phi}\right) \tag{2.143}$$

$$\hat{e}_{-1}(\theta=0^o) = \frac{1}{\sqrt{2}} e^{-i\phi} \cdot \left(\hat{\theta} - i\,\hat{\phi}\right), \tag{2.144}$$

i.e., for this special choice we have to consider the azimuthal modes $l = \pm 1$ only.

The following relations become obvious from (2.120) to (2.125):

$$\vec{\psi}_{i,2}(r,\theta,\phi) = \frac{1}{k}\nabla \times \vec{\psi}_{i,1}(r,\theta,\phi). \tag{2.145}$$

$$\vec{\varphi}_{i,2}(r,\theta,\phi) = \frac{1}{k}\nabla \times \vec{\varphi}_{i,1}(r,\theta,\phi) \tag{2.146}$$

$$\vec{\chi}_{i,2}(r,\theta,\phi) = \frac{1}{k}\nabla \times \vec{\chi}_{i,1}(r,\theta,\phi). \tag{2.147}$$

If using these relations together with the vector-wave equation we can show that conversely

$$\vec{\psi}_{i,1}(r,\theta,\phi) = \frac{1}{k}\nabla \times \vec{\psi}_{i,2}(r,\theta,\phi) \tag{2.148}$$

$$\vec{\varphi}_{i,1}(r,\theta,\phi) = \frac{1}{k}\nabla \times \vec{\varphi}_{i,2}(r,\theta,\phi) \tag{2.149}$$

$$\vec{\chi}_{i,1}(r,\theta,\phi) = \frac{1}{k}\nabla \times \vec{\chi}_{i,2}(r,\theta,\phi) \tag{2.150}$$

hold (please, note that we have now used the combined summation index i).

The Silver-Mueller radiation condition (1.20) is given in spherical coordinates by the expression

$$\lim_{r\to\infty} \left(\nabla \times -ik\hat{r}\times\right)\vec{u}(r,\theta,\phi) = \vec{0}\left(\frac{1}{r}\right) \tag{2.151}$$

and applies to the two vector functions $\vec{\varphi}_{i,1}$ and $\vec{\varphi}_{i,2}$. In close analogy to the scalar case these two eigensolutions are therefore called "radiating vector solutions" of the vector-wave equation. Correspondingly, $\vec{\psi}_{i,1}$ and $\vec{\psi}_{i,2}$ are called the "regular vector solutions", and $\vec{\chi}_{i,1}$ and $\vec{\chi}_{i,2}$ are the "incoming vector solutions" .

The following asymptotic behaviour is needed later on if expanding a linearly polarized plane wave, and for the proof of unitarity of the S-matrix in Chap. 4:

$$\lim_{r\to\infty} \vec{\varphi}_{l,n,1}(r,\theta,\phi) = \frac{(-i)^{n+1}e^{ikr}}{kr} \cdot \gamma_{l,n} \cdot \vec{C}_{l,n}(\theta,\phi) \tag{2.152}$$

$$\lim_{r\to\infty} \vec{\varphi}_{l,n,2}(r,\theta,\phi) = \frac{(-i)^{n}e^{ikr}}{kr} \cdot \gamma_{l,n} \cdot \vec{B}_{l,n}(\theta,\phi). \tag{2.153}$$

From the above considerations, it becomes clear why we have introduced the additional τ-summation in the formal series expansions for the vector fields in Chap. 1. To each of the additional requirements (i.e., the radiation condition and the requirement of regularity) there exist two different sets of eigensolutions obeying these requirements. Furthermore, in the vectorial case there exist two additional sets of eigensolutions which can be obtained from employing the gradient operation $\nabla\psi_i$ and $\nabla\varphi_i$ to the scalar eigensolutions ψ_i and φ_i of the scalar Helmholtz equation. These two sets are useful to approximate longitudinal fields with non-vanishing divergence which may exist in regions with non-vanishing sources like free electric charges, for example. But since we are dealing in this book exclusively with

solenoidal fields in source-free regions these two sets of functions are not needed here. Because of the identity

$$\nabla \cdot \nabla \times \vec{u} \;\equiv\; 0 \tag{2.154}$$

one can immediately see from (2.145) to (2.150) that these fields are indeed solenoidal.

For later purposes let us define additionally the auxiliary vector functions

$$\vec{\tilde{\psi}}_{i,\tau}(r,\theta,\phi) = \vec{\tilde{\psi}}_{l,n,\tau}(r,\theta,\phi) \;:=\; (-1)^l \cdot \vec{\psi}_{-l,n,\tau}(r,\theta,\phi) \tag{2.155}$$

$$\vec{\tilde{\varphi}}_{i,\tau}(r,\theta,\phi) = \vec{\tilde{\varphi}}_{l,n,\tau}(r,\theta,\phi) \;:=\; (-1)^l \cdot \vec{\varphi}_{-l,n,\tau}(r,\theta,\phi) \tag{2.156}$$

$$\vec{\tilde{\chi}}_{i,\tau}(r,\theta,\phi) = \vec{\tilde{\varphi}}_{l,n,\tau}(r,\theta,\phi) \;:=\; (-1)^l \cdot \vec{\chi}_{-l,n,\tau}(r,\theta,\phi) \tag{2.157}$$

and

$$\vec{\psi}_{i,\tau}^{\,\hat{n}_-}(r,\theta,\phi) := \hat{n}_- \times \vec{\psi}_{i,\tau}(r,\theta,\phi)\;;\; r \in \partial\Gamma \tag{2.158}$$

$$\vec{\varphi}_{i,\tau}^{\,\hat{n}_-}(r,\theta,\phi) := \hat{n}_- \times \vec{\varphi}_{i,\tau}(r,\theta,\phi)\;;\; r \in \partial\Gamma \tag{2.159}$$

$$\vec{\chi}_{i,\tau}^{\,\hat{n}_-}(r,\theta,\phi) := \hat{n}_- \times \vec{\chi}_{i,\tau}(r,\theta,\phi)\;;\; r \in \partial\Gamma, \tag{2.160}$$

with $\tau = 1, 2$. In close analogy to the scalar case we have

$$\vec{\tilde{\psi}}_{i,\tau}(r,\theta,\phi) = \vec{\psi}_{i,\tau}^{\,*}(r,\theta,\phi) \tag{2.161}$$

for a real-valued parameter k. The last three definitions are the projections of the original vector solutions into the tangential planes at each point of the scatterer surface. Due to the relations (2.80) and (2.81) it is possible to express the regular vector solutions as a superposition of the radiating and incoming vector solutions according to

$$\vec{\psi}_{i,\tau}(r,\theta,\phi) = \frac{1}{2} \cdot \left[\vec{\varphi}_{i,\tau}(r,\theta,\phi) \;+\; \vec{\chi}_{i,\tau}(r,\theta,\phi)\right], \tag{2.162}$$

as already done in the scalar case.

With the above defined vector functions we are now able to approximate a smooth vector function $\vec{u}(r,\theta,\phi)$ given in region Γ_- or Γ_+ by the series expansion

$$\vec{u}^{\,(N)}(r,\theta,\phi) = \sum_{\tau=1}^{2} \sum_{n=0}^{N} \sum_{l=-n}^{n} a_{l,n,\tau}^{(N)} \cdot \vec{\psi}_{l,n,\tau}(kr,\theta,\phi) \tag{2.163}$$

or

$$\vec{u}^{\,(N)}(r,\theta,\phi) = \sum_{\tau=1}^{2} \sum_{n=0}^{N} \sum_{l=-n}^{n} a_{l,n,\tau}^{(N)} \cdot \vec{\varphi}_{l,n,\tau}(kr,\theta,\phi) \tag{2.164}$$

subject to the regularity requirement and radiation condition, respectively.

2.4.2 Properties of the Vectorial Eigensolutions

Concerning the linearly independence and completeness of the vector functions (2.158) and (2.159) defined in the tangential planes at the scatterer surface $\partial\Gamma$ we are able to make the following mathematical statements:

- The vector functions $\vec{\varphi}_{i,\tau}^{\,\hat{n}_-}(r,\theta,\phi)\}$, $\tau = 1,2$; $(r,\theta,\phi) \in \partial\Gamma$ are linearly independent in the space $\mathcal{L}_2^{tan}(\partial\Gamma)$. If k^2 is not an eigenvalue of the interior Dirichlet problem then the vector functions $\vec{\psi}_{i,\tau}^{\,\hat{n}_-}(r,\theta,\phi)\}$, $\tau = 1,2$; $(r,\theta,\phi) \in \partial\Gamma$ are also linearly independent in $\mathcal{L}_2^{tan}(\partial\Gamma)$.
- The vector functions $\vec{\varphi}_{i,\tau}^{\,\hat{n}_-}(r,\theta,\phi)\}$, $\tau = 1,2$; $(r,\theta,\phi) \in \partial\Gamma$ are complete in the space $\mathcal{L}_2^{tan}(\partial\Gamma)$. If k^2 is not an eigenvalue of the interior Dirichlet problem then the vector functions $\vec{\psi}_{i,\tau}^{\,\hat{n}_-}(r,\theta,\phi)\}$, $\tau = 1,2$; $(r,\theta,\phi) \in \partial\Gamma$ are also complete in $\mathcal{L}_2^{tan}(\partial\Gamma)$. Here it is again assumed that the surface $\partial\Gamma$ is a two times continuously differentiable surface (a C^2 surface). $\mathcal{L}_2^{tan}(\partial\Gamma)$ is now the space of the complex-valued and square-integrable vector functions $\vec{F}^{\,\hat{n}_-} = \hat{n}_- \times \vec{F}$ at the boundary surface $\partial\Gamma$, and the terminus square-integrable relates to the scalar product defined in (1.35). The mathematical proofs can again be found in the book of A. Doicu et al., 2000 (see the reference Sect. 10.2).

Choosing the vector functions (2.158) and (2.159) as expansion and weighting functions and restricting the boundary surface of the scatterer to a C^2 surface ensures the invertability of all the matrices discussed in Sect. 1.3 from the beginning.

For the discussion of the limiting case of electromagnetic wave scattering on a spherical scatterer we need again the orthogonality relations of the vector functions which hold at the surface of a sphere with radius $r = a$. As it already happened in the scalar case κ and κ' are related to one of the two parameters k and k_0 characterizing the regions Γ_- and Γ_+ physically. The corresponding orthogonality relations for the vector functions $\vec{\varphi}_{i,\tau}(r,\theta,\phi)$ and $\vec{\psi}_{i,\tau}(r,\theta,\phi)$ read

$$\int_0^{2\pi} d\phi \int_0^{\pi} d\theta\, a^2 \sin\theta\, \vec{\varphi}_{i,\tau}^{\,*}(\kappa a,\theta,\phi)\, \vec{\varphi}_{j,\tau'}(\kappa' a,\theta,\phi) = a^2 \cdot c_{i,\tau}^{(\varphi,\varphi)}(\kappa,\kappa') \cdot \delta_{ij}\delta_{\tau\tau'} \tag{2.165}$$

$$\int_0^{2\pi} d\phi \int_0^{\pi} d\theta\, a^2 \sin\theta\, \vec{\varphi}_{i,\tau}^{\,*}(\kappa a,\theta,\phi)\, \vec{\psi}_{j,\tau'}(\kappa' a,\theta,\phi) = a^2 \cdot c_{i,\tau}^{(\varphi,\psi)}(\kappa,\kappa') \cdot \delta_{ij}\delta_{\tau\tau'} \tag{2.166}$$

$$\int_0^{2\pi} d\phi \int_0^{\pi} d\theta\, a^2 \sin\theta\, \vec{\psi}^*_{i,\tau}(\kappa a, \theta, \phi)\, \vec{\psi}_{j,\tau'}(\kappa' a, \theta, \phi) = a^2 \cdot c_{i,\tau}^{(\psi,\psi)}(\kappa, \kappa') \cdot \delta_{ij}\delta_{\tau\tau'} \tag{2.167}$$

$$\int_0^{2\pi} d\phi \int_0^{\pi} d\theta\, a^2 \sin\theta\, \vec{\psi}^*_{i,\tau}(\kappa a, \theta, \phi)\, \vec{\varphi}_{j,\tau'}(\kappa' a, \theta, \phi) = a^2 \cdot c_{i,\tau}^{(\psi,\varphi)}(\kappa, \kappa') \cdot \delta_{ij}\delta_{\tau\tau'}. \tag{2.168}$$

The normalization constants $c_{i,\tau}$ herein are given by the expressions

$$c_{i,1}^{(\varphi,\varphi)}(\kappa, \kappa') = \left(h_{n_i}^{(1)}(\kappa a)\right)^* \cdot h_{n_i}^{(1)}(\kappa' a) \tag{2.169}$$

$$c_{i,1}^{(\varphi,\psi)}(\kappa, \kappa') = \left(h_{n_i}^{(1)}(\kappa a)\right)^* \cdot j_{n_i}(\kappa' a) \tag{2.170}$$

$$c_{i,1}^{(\psi,\psi)}(\kappa, \kappa') = j_{n_i}^*(\kappa a) \cdot j_{n_i}(\kappa' a) \tag{2.171}$$

$$c_{i,1}^{(\psi,\varphi)}(\kappa, \kappa') = j_{n_i}^*(\kappa a) \cdot h_{n_i}^{(1)}(\kappa' a) \tag{2.172}$$

$$c_{i,2}^{(\varphi,\varphi)}(\kappa, \kappa') = \frac{1}{\kappa^*\kappa' a^2}\left[n(n+1)\left(h_{n_i}^{(1)}(\kappa a)\right)^* \cdot h_{n_i}^{(1)}(\kappa' a) + \left(\frac{\partial}{\partial r}\left(r \cdot h_{n_i}^{(1)}(\kappa r)\right)\right)^*_{r=a} \cdot \left(\frac{\partial}{\partial r}\left(r \cdot h_{n_i}^{(1)}(\kappa' r)\right)\right)_{r=a}\right] \tag{2.173}$$

$$c_{i,2}^{(\varphi,\psi)}(\kappa, \kappa') = \frac{1}{\kappa^*\kappa' a^2}\left[n(n+1)\left(h_{n_i}^{(1)}(\kappa a)\right)^* \cdot j_{n_i}(\kappa' a) + \left(\frac{\partial}{\partial r}\left(r \cdot h_{n_i}^{(1)}(\kappa r)\right)\right)^*_{r=a} \cdot \left(\frac{\partial}{\partial r}\left(r \cdot j_{n_i}(\kappa' r)\right)\right)_{r=a}\right] \tag{2.174}$$

$$c_{i,2}^{(\psi,\psi)}(\kappa, \kappa') = \frac{1}{\kappa^*\kappa' a^2}\left[n(n+1) j_{n_i}^*(\kappa a) \cdot j_{n_i}(\kappa' a) + \left(\frac{\partial}{\partial r}\left(r \cdot j_{n_i}(\kappa r)\right)\right)^*_{r=a} \cdot \left(\frac{\partial}{\partial r}\left(r \cdot j_{n_i}(\kappa' r)\right)\right)_{r=a}\right] \tag{2.175}$$

$$c_{i,2}^{(\psi,\varphi)}(\kappa, \kappa') = \frac{1}{\kappa^*\kappa' a^2}\left[n(n+1) j_{n_i}^*(\kappa a) \cdot h_{n_i}^{(1)}(\kappa' a) + \left(\frac{\partial}{\partial r}\left(r \cdot j_{n_i}(\kappa r)\right)\right)^*_{r=a} \cdot \left(\frac{\partial}{\partial r}\left(r \cdot h_{n_i}^{(1)}(\kappa' r)\right)\right)_{r=a}\right]. \tag{2.176}$$

Furthermore, we need the orthogonality relations of the vector functions $\vec{\varphi}_{i,\tau}^{\,\hat{n}_-}(\kappa a, \theta, \phi)$ and $\vec{\psi}_{i,\tau}^{\,\hat{n}_-}(\kappa a, \theta, \phi)$ at the same spherical surface:

$$\int_0^{2\pi} d\phi \int_0^{\pi} d\theta\, a^2 \sin\theta \left[\vec{\varphi}_{i,\tau}^{\,\hat{n}_-}(\kappa a, \theta, \phi)\right]^* \cdot \vec{\varphi}_{j,\tau'}^{\,\hat{n}_-}(\kappa' a, \theta, \phi) = a^2 \cdot d_{i,\tau}^{(\varphi,\varphi)}(\kappa, \kappa') \cdot \delta_{ij}\delta_{\tau\tau'} \tag{2.177}$$

$$\int_0^{2\pi} d\phi \int_0^{\pi} d\theta\, a^2 \sin\theta \left[\vec{\varphi}_{i,\tau}^{\,\hat{n}_-}(\kappa a, \theta, \phi)\right]^* \cdot \vec{\psi}_{j,\tau'}^{\,\hat{n}_-}(\kappa' a, \theta, \phi) = a^2 \cdot d_{i,\tau}^{(\varphi,\psi)}(\kappa, \kappa') \cdot \delta_{ij}\delta_{\tau\tau'} \tag{2.178}$$

$$\int_0^{2\pi} d\phi \int_0^{\pi} d\theta\, a^2 \sin\theta \left[\vec{\psi}_{i,\tau}^{\,\hat{n}_-}(\kappa a, \theta, \phi)\right]^* \cdot \vec{\psi}_{j,\tau'}^{\,\hat{n}_-}(\kappa' a, \theta, \phi) = a^2 \cdot d_{i,\tau}^{(\psi,\psi)}(\kappa, \kappa') \cdot \delta_{ij}\delta_{\tau\tau'} \tag{2.179}$$

$$\int_0^{2\pi} d\phi \int_0^{\pi} d\theta\, a^2 \sin\theta \left[\vec{\psi}_{i,\tau}^{\,\hat{n}_-}(\kappa a, \theta, \phi)\right]^* \cdot \vec{\varphi}_{j,\tau'}^{\,\hat{n}_-}(\kappa' a, \theta, \phi) = a^2 \cdot d_{i,\tau}^{(\psi,\varphi)}(\kappa, \kappa') \cdot \delta_{ij}\delta_{\tau\tau'}\,. \tag{2.180}$$

For the spherical surface we have $\hat{n}_- = -\hat{r}$. The normalization constants $d_{i,\tau}$ are now given by

$$d_{i,1}^{(\varphi,\varphi)}(\kappa, \kappa') = \left(h_{n(i)}^{(1)}(\kappa a)\right)^* \cdot h_{n(i)}^{(1)}(\kappa' a) \tag{2.181}$$

$$d_{i,1}^{(\varphi,\psi)}(\kappa, \kappa') = \left(h_{n(i)}^{(1)}(\kappa a)\right)^* \cdot j_{n(i)}(\kappa' a) \tag{2.182}$$

$$d_{i,1}^{(\psi,\psi)}(\kappa, \kappa') = j_{n(i)}^*(\kappa a) \cdot j_{n(i)}(\kappa' a) \tag{2.183}$$

$$d_{i,1}^{(\psi,\varphi)}(\kappa, \kappa') = j_{n(i)}^*(\kappa a) \cdot h_{n(i)}^{(1)}(\kappa' a) \tag{2.184}$$

$$d_{i,2}^{(\varphi,\varphi)}(\kappa, \kappa') = \frac{1}{\kappa^* \kappa' a^2} \left[\left(\frac{\partial}{\partial r}\left(r \cdot h_{n_i}^{(1)}(\kappa r)\right)\right)_{r=a}^* \cdot \left(\frac{\partial}{\partial r}\left(r \cdot h_{n_i}^{(1)}(\kappa' r)\right)\right)_{r=a}\right] \tag{2.185}$$

$$d_{i,2}^{(\varphi,\psi)}(\kappa,\kappa') = \frac{1}{\kappa^*\kappa' a^2}\left[\left(\frac{\partial}{\partial r}\left(r\cdot h_{n_i}^{(1)}(\kappa r)\right)\right)_{r=a}^{*} \cdot \left(\frac{\partial}{\partial r}\left(r\cdot j_{n_i}(\kappa' r)\right)\right)_{r=a}\right] \tag{2.186}$$

$$d_{i,2}^{(\psi,\psi)}(\kappa,\kappa') = \frac{1}{\kappa^*\kappa' a^2}\left[\left(\frac{\partial}{\partial r}\left(r\cdot j_{n_i}(\kappa r)\right)\right)_{r=a}^{*} \cdot \left(\frac{\partial}{\partial r}\left(r\cdot j_{n_i}(\kappa' r)\right)\right)_{r=a}\right] \tag{2.187}$$

$$d_{i,2}^{(\psi,\varphi)}(\kappa,\kappa') = \frac{1}{\kappa^*\kappa' a^2}\left[\left(\frac{\partial}{\partial r}\left(r\cdot j_{n_i}(\kappa r)\right)\right)_{r=a}^{*} \cdot \left(\frac{\partial}{\partial r}\left(r\cdot h_{n_i}^{(1)}(\kappa' r)\right)\right)_{r=a}\right]. \tag{2.188}$$

Another important property of the vector solutions is their transformation behaviour with respect to rotation of the underlying coordinate system about its origin. This becomes of special importance in Chap. 7 when considering a certain particle in different orientations with respect to the primary incident field. The rotation of the coordinate system is depicted in Fig. 2.3. The Cartesian coordinate system (x', y', z') is the result of three consecutive rotations of the original coordinate system (x, y, z). These three rotations may be expressed by the Eulerian angles (α, β, γ). The first rotation is the rotation about the z-axis of the original system expressed by the angle $\alpha \in [0, 2\pi]$. This rotation is performed in such a way that the new y'-axis coincides with the nodal line. The second rotation is the rotation about the new y'-axis through the angle $\beta \in [0, \pi]$. The last rotation is the rotation about the new z'-axis through an angle $\gamma \in [0, 2\pi]$. If we consider $\mathbf{x}$ to be a fixed point with components (r, θ, ϕ) in the original coordinate system, and with components (r, θ', ϕ') in the rotated coordinate system then the vectorial eigensolutions are transformed according to

$$\vec{\xi}_{l,n,\tau}(r,\theta',\phi') = \sum_{l'=-n}^{n} D_{l,l'}^{(n)}(\alpha,\beta,\gamma)\cdot\vec{\xi}_{l',n,\tau}(r,\theta,\phi) \tag{2.189}$$

with respect to this point. The vector $\vec{\xi}$ represents one of the eigensolutions $\vec{\psi}$, $\vec{\varphi}$, or $\vec{\chi}$. The transformation coefficients $D_{l,l'}^{(n)}(\alpha,\beta,\gamma)$ in (2.189) are the elements of the rotation matrix $\mathbf{D}^{(n)}$ and therefore functions of the Eulerian angles (α, β, γ). They are also called "Wigner functions" or "Wigner D" functions . For these functions we know the relation

$$D_{l,l'}^{(n)}(\alpha,\beta,\gamma) = e^{il\alpha}\cdot d_{l,l'}^{(n)}(\beta)\cdot e^{il'\gamma} \tag{2.190}$$

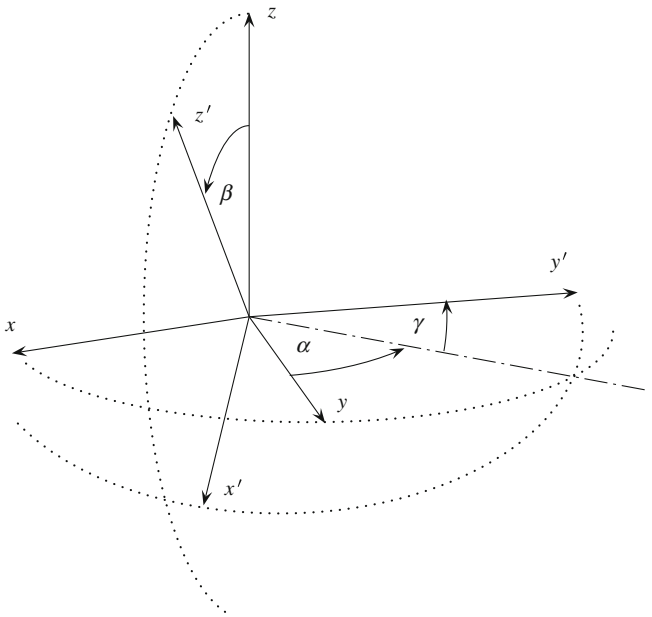

Fig. 2.3 The three Eulerian angles (α, β, γ) of rotation. The nodal line (*dash-point-line*) represents the intersection between the $x-y$- and $x'-y'$-plane and runs into the direction of $\hat{z} \times \hat{z}'$, i.e., it is perpendicular to the $z-z'$-plane

with the functions $d_{l,l'}^{(n)}(\beta)$ given by

$$d_{l,l'}^{(n)}(\beta) = \sum_{\sigma=\sigma_{min}}^{\sigma_{max}} \frac{\left[(n+l)!(n-l)!(n+l')!(n-l')!\right]^{1/2}}{\sigma!(l+l'+\sigma)!(n-l-\sigma)!(n-l'-\sigma)!} \cdot (-1)^{n-l'-\sigma} \left[\sin\frac{\beta}{2}\right]^{2n-2\sigma-l-l'} \left[\cos\frac{\beta}{2}\right]^{2\sigma+l+l'}. \quad (2.191)$$

These real-valued functions are the "Wigner d"-functions. The summation within these functions runs from $\sigma_{min} = \max\left(0, -l-l'\right)$ to $\sigma_{max} = \min\left(n-l, n-l'\right)$. The inverse transformation of (2.189) are accomplished by the three consecutive rotations about the Eulerian angles $(-\gamma, -\beta, -\alpha)$ in reversed order. Thus, with

$$\left[\mathbf{D}^{(n)}(\alpha, \beta, \gamma)\right]^{-1} = \mathbf{D}^{(n)}(-\gamma, -\beta, -\alpha) \quad (2.192)$$

we get

$$\vec{\xi}_{l',n,\tau}(r, \theta, \phi) = \sum_{l=-n}^{n} D_{l',l}^{(n)}(-\gamma, -\beta, -\alpha) \cdot \vec{\xi}_{l,n,\tau}(r, \theta', \phi'). \quad (2.193)$$

Moreover, it is known that the matrix $\mathbf{D}^{(n)}$ is a unitary matrix, i.e., it obeys the relation

$$\left[\mathbf{D}^{(n)}\right]^{\dagger} = \left[\mathbf{D}^{(n)}\right]^{-1}. \tag{2.194}$$

Therefore, we may also write

$$\vec{\xi}_{l',n,\tau}(r,\theta,\phi) = \sum_{l=-n}^{n} D^{(n)}_{l,l'}(-\alpha,\beta,-\gamma)\cdot\vec{\xi}_{l,n,\tau}(r,\theta',\phi') \tag{2.195}$$

for the inverse transformation (2.193). There exist different representations of the Wigner functions in the literature. The above given representation was implemented in our numerical realization we will consider in more detail in Chap. 9. We have tested this representation against the conventional Euler transformation of the relevant fields to verify its correctness. For example, if we have the original field $\vec{F}(r,\theta,\phi)$ given in the coordinate system (x, y, z) then the transformed field in the rotated system (x', y', z') reads

$$\vec{F}(r,\theta',\phi') = \mathbf{M}\cdot\vec{F}(r,\theta,\phi) \tag{2.196}$$

with

$$\begin{aligned}
M_{11} &= \cos\alpha\cos\beta\cos\gamma - \sin\alpha\sin\gamma\\
M_{12} &= \sin\alpha\cos\beta\cos\gamma + \cos\alpha\sin\gamma\\
M_{13} &= -\sin\beta\cos\gamma\\
M_{21} &= -\cos\alpha\cos\beta\sin\gamma - \sin\alpha\cos\gamma\\
M_{22} &= -\sin\alpha\cos\beta\sin\gamma + \cos\alpha\cos\gamma\\
M_{23} &= \sin\beta\sin\gamma\\
M_{31} &= \cos\alpha\sin\beta\\
M_{32} &= \sin\alpha\sin\beta\\
M_{33} &= \cos\beta
\end{aligned} \tag{2.197}$$

being the elements of the Euler matrix. Now, if expanding the field $\vec{F}(r,\theta,\phi)$ in terms of the vectorial eigensolutions and applying the transformation (2.189) afterwards we can compare the transformed expansion with the result of the Euler transformation (2.196). For this intercomparison one must have in mind, of course, that the transformed expansion is only an approximation of the transformed field.

2.4.3 Expansion of a Linearly Polarized Plane Wave

As in the scalar case we will now use some of the above given material to approximate a linearly polarized plane wave with polarization $\hat{\mathbf{e}}_0$ (it is exactly this polarization

which turns the scalar plane wave $e^{ik_0 r\cos\theta}$ into a vector field) travelling along the positive z-direction into a series expansion in terms of the regular vector solutions (2.130) and (2.131) with final expansion coefficients. This is not even a simple task if using the direct way, as we will see now. It is already described in the book "Absorption and Scattering of Light by Small Particles" of Bohren and Huffman (see the reference chapter for details). But for a better understanding, we will outline some aspects in more detail here.

The linearly polarized plane wave we intend to expand is given by the equation

$$\vec{u}_{inc}(k_0 r,\theta,\phi) = \hat{e}_0 \cdot E_0 \cdot e^{ik_0 r\cos\theta} \tag{2.198}$$

with E_0 being again an arbitrary amplitude. We will consider the two polarization states $\hat{e}_0 = \hat{x}$ and $\hat{e}_0 = \hat{y}$ separately. $\hat{x}$ and $\hat{y}$ are the corresponding unit vectors belonging to the x- and y-axis, respectively. These two cases are of some importance in real applications. On the other hand, one can represent any linear polarization state by a linear combination of these two cases. From Table 2.1 we get the relations

$$\hat{x} = \Big(\hat{r}\sin\theta\cos\phi + \hat{\theta}\cos\theta\cos\phi - \hat{\phi}\sin\phi\Big), \tag{2.199}$$

$$\hat{y} = \Big(\hat{r}\sin\theta\sin\phi + \hat{\theta}\cos\theta\sin\phi + \hat{\phi}\cos\phi\Big). \tag{2.200}$$

We are now asking for the coefficients $c_{l,n,\tau}$ of the expansion

$$\hat{e}_0 \cdot E_0 \cdot e^{ik_0 r\cos\theta} = E_0 \cdot \sum_{\tau=1}^{2}\sum_{n=0}^{\infty}\sum_{l=-n}^{n} c_{l,n,\tau}\cdot\vec{\psi}_{l,n,\tau}(r,\theta,\phi) \tag{2.201}$$

related to a given polarization state $\hat{e}_0$. We multiply this equation with $\vec{\psi}^{*}_{l',n',\tau'}(r,\theta,\phi)$ and integrate afterwards over the entire free space to obtain

$$\begin{aligned}&\int_0^{2\pi} d\phi \int_0^{\pi} d\theta\sin\theta \int_0^{\infty} dr\, r^2\, \vec{\psi}^{*}_{l',n',\tau'}(r,\theta,\phi)\,\hat{e}_0\, e^{ik_0 r\cos\theta}\\ &= \sum_{\tau=1}^{2}\sum_{n=0}^{\infty}\sum_{l=-n}^{n} c_{l,n,\tau}\int_0^{2\pi} d\phi\int_0^{\pi} d\theta\sin\theta\int_0^{\infty} dr\, r^2\\ &\quad\cdot\vec{\psi}^{*}_{l',n',\tau'}(r,\theta,\phi)\,\vec{\psi}_{l,n,\tau}(r,\theta,\phi).\end{aligned} \tag{2.202}$$

Taking the orthogonality relation (2.167) into account we can perform the ϕ and θ integration on the right hand side (the radius r is kept constant, at first. At the end of this derivation we will arrive at the same radial dependence on both sides of this equation, as already done in the scalar case!). Renaming n' as n, l' as l, and τ' as τ in the resulting expression provides

$$\int_0^{2\pi} d\phi \int_0^{\pi} d\theta \sin\theta \int_0^{\infty} dr\, r^2\, \vec{\psi}^*_{l,n,\tau}(r,\theta,\phi)\, \hat{e}_0\, e^{ik_0 r\cos\theta} = c_{l,n,\tau} \int_0^{\infty} dr\, r^2\, c^{(\psi,\psi)}_{l,n,\tau}(k_0,k_0). \tag{2.203}$$

Let us consider the left hand side of (2.203). The dependence on $\cos\phi$ and $\sin\phi$ of the polarization states (2.199) and (2.200) together with the $e^{-il\phi}$ dependence of the weighting functions $\vec{\psi}^*_{l,n,\tau}(r,\theta,\phi)$ result in the two integrals

$$\int_0^{2\pi} d\phi\, e^{-il\phi}\, \cos\phi$$
$$\int_0^{2\pi} d\phi\, e^{-il\phi}\, \sin\phi.$$

Since the summation index l is running from $-n$ to n we get for the integrals

$$\int_0^{2\pi} d\phi\, e^{-il\phi}\, \cos\phi = \pi\delta_{1|l|} \tag{2.204}$$

$$\int_0^{2\pi} d\phi\, e^{-il\phi}\, \sin\phi = \left\{ \begin{array}{r} -1,\ l \geq 0 \\ 1,\ l < 0 \end{array} \right\} i\pi\delta_{1|l|} \tag{2.205}$$

depending on whether l is positive or negative. Due to the special l dependence of (2.205) a similar distinction becomes necessary on the left-hand side of (2.203). Therefore, let us consider the two cases $\pm l$ separately. If $\tau = 1$ we obtain by use of the vector functions (2.130), the expressions (2.199) and (2.200), and the two integrals (2.204) and (2.205) the relation

$$\begin{aligned} & c_{l,n,1} \int_0^{\infty} dr\, r^2\, c^{(\psi,\psi)}_{l,n,1}(k_0,k_0) \\ & = \pi \int_0^{\pi} d\theta \int_0^{\infty} dr\, r^2\, j^*_n(k_0 r)\, e^{ik_0 r\cos\theta} \left[\cos\theta + \sin\theta \frac{\partial}{\partial\theta}\right] \\ & \cdot \left\{ \begin{array}{r} -i\gamma_{1,n} P^1_n(\cos\theta)\ ;\ \hat{e}_0 = \hat{x},\ l = 1 \\ i\gamma_{-1,n} P^{-1}_n(\cos\theta)\ ;\ \hat{e}_0 = \hat{x},\ l = -1 \\ -\gamma_{1,n} P^1_n(\cos\theta)\ ;\ \hat{e}_0 = \hat{y},\ l = 1 \\ -\gamma_{-1,n} P^{-1}_n(\cos\theta)\ ;\ \hat{e}_0 = \hat{y},\ l = -1 \end{array} \right\} \end{aligned} \tag{2.206}$$

According to relation (2.71) we can express the associated Legendre polynomials with negative l values by the associated Legendre polynomials with positive l values. Taking additionally (2.126) into account provides finally

$$
\begin{aligned}
& c_{l,n,1} \int_0^\infty dr\, r^2\, c_{l,n,1}^{(\psi,\psi)}(k_0, k_0) \\
& = \frac{1}{2n(n+1)} \sqrt{\pi(2n+1)} \int_0^\pi d\theta \int_0^\infty dr\, r^2\, j_n^*(k_0 r) e^{ik_0 r \cos\theta} \\
& \quad \cdot \left[\cos\theta + \sin\theta \frac{\partial}{\partial\theta} \right] P_n^1(\cos\theta) \left\{ \begin{array}{r} -i\ ;\ \hat{e}_0 = \hat{x},\ l = 1 \\ -i\ ;\ \hat{e}_0 = \hat{x},\ l = -1 \\ -1\ ;\ \hat{e}_0 = \hat{y},\ l = 1 \\ 1\ ;\ \hat{e}_0 = \hat{y},\ l = -1 \end{array} \right\}. \qquad (2.207)
\end{aligned}
$$

If $\tau = 2$ we get in the same way from (2.203) together with the vector functions (2.131)

$$
\begin{aligned}
& c_{l,n,2} \int_0^\infty dr\, r^2\, c_{l,n,2}^{(\psi,\psi)}(k_0, k_0) = \frac{1}{2n(n+1)} \sqrt{\pi(2n+1)} \\
& \cdot \int_0^\pi d\theta \int_0^\infty dr\, r^2 \frac{1}{k_0 r} e^{ik_0 r \cos\theta} \left[n(n+1) \sin^2\theta\, j_n^*(k_0 r) \right. \\
& \left. + \frac{\partial}{\partial r} (r j_n(k_0 r))^* \cdot \left(\sin\theta \cos\theta \frac{\partial}{\partial\theta} + 1 \right) \right] P_n^1(\cos\theta) \\
& \cdot \left\{ \begin{array}{r} 1\ ;\ \hat{e}_0 = \hat{x},\ l = 1 \\ -1\ ;\ \hat{e}_0 = \hat{x},\ l = -1 \\ -i\ ;\ \hat{e}_0 = \hat{y},\ l = 1 \\ -i\ ;\ \hat{e}_0 = \hat{y},\ l = -1 \end{array} \right\}. \qquad (2.208)
\end{aligned}
$$

The remaining θ integrals

$$
\Theta_1 = \int_0^\pi d\theta\, e^{ik_0 r \cos\theta} \left[\cos\theta + \sin\theta \frac{\partial}{\partial\theta} \right] P_n^1(\cos\theta) \qquad (2.209)
$$

$$
\Theta_2 = \int_0^\pi d\theta\, e^{ik_0 r \cos\theta} \sin^2\theta\, P_n^1(\cos\theta) \qquad (2.210)
$$

$$
\Theta_3 = \int_0^\pi d\theta\, e^{ik_0 r \cos\theta} \left[\sin\theta \cos\theta \frac{\partial}{\partial\theta} + 1 \right] P_n^1(\cos\theta) \qquad (2.211)
$$

are solved as follows: Using the relation

$$
P_n^1(\cos\theta) = \frac{d}{d\theta} P_n(\cos\theta) \qquad (2.212)
$$

(see (2.72)!) we can write instead of (2.209)

$$
\Theta_1 = \int_0^\pi d\theta\, e^{ik_0 r \cos\theta} \left[\cos\theta \frac{\partial}{\partial\theta} + \sin\theta \frac{\partial^2}{\partial\theta^2} \right] P_n(\cos\theta). \qquad (2.213)
$$

Now, there appear a higher derivative in the integrand. With the help of the ordinary Legendre differential equation

$$\left[\sin\theta\frac{d^2}{d\theta^2}+\cos\theta\frac{d}{d\theta}+n(n+1)\sin\theta\right]P_n(\cos\theta)=0 \tag{2.214}$$

we can next transform (2.213) into the simpler expression

$$\Theta_1=-n(n+1)\int_0^\pi d\theta\, e^{ik_0r\cos\theta}\,\sin\theta\,P_n(\cos\theta). \tag{2.215}$$

Comparing this with (2.107) provides finally

$$\Theta_1=-2i^n n(n+1)j_n(k_0r). \tag{2.216}$$

The integral (2.210) can be solved by partial integration applied to the functions

$$\sin\theta\cdot P_n^1(\cos\theta) \tag{2.217}$$

and

$$\sin\theta\cdot e^{ik_0r\cos\theta}=\frac{d}{d\theta}\left(-e^{ik_0r\cos\theta}/ik_0r\right). \tag{2.218}$$

In this way, (2.210) can be traced back to the integral (2.209). We obtain finally

$$\Theta_2=-2i^{(n-1)}n(n+1)\frac{1}{k_0r}j_n(k_0r). \tag{2.219}$$

Using again relations (2.212) and (2.214) allow us to transform the remaining integral (2.211) into

$$\Theta_3=\int_0^\pi d\theta\, e^{ik_0r\cos\theta}\left[\sin^2\theta\,P_n^1(\cos\theta)-n(n+1)\sin\theta\cos\theta\,P_n(\cos\theta)\right]. \tag{2.220}$$

The first part on the right hand side is nothing but the already solved integral Θ_2. Therefore we may write

$$\Theta_3=\Theta_2-n(n+1)\Theta_4 \tag{2.221}$$

with

$$\Theta_4=\int_0^\pi d\theta\, e^{ik_0r\cos\theta}\sin\theta\cos\theta\,P_n(\cos\theta). \tag{2.222}$$

To solve the integral Θ_4 we first multiply (2.107) with z and differentiate with respect to z afterwards. Thus, the integral is

$$\frac{\partial}{\partial z}(zj_n(z))=\frac{1}{2}(-i)^n\int_0^\pi d\theta\,\sin\theta\,P_n(\cos\theta)\,e^{iz\cos\theta}\,[1+iz\cos\theta]. \tag{2.223}$$

The first term on the right hand side is again $j_n(z)$, because of (2.107). The second term on the right hand side provides $\frac{1}{2}(-i)^{n-1}k_0 r \cdot \Theta_4$ if $z = k_0 r$. This can be compared with expression (2.222). For Θ_4 we get therefore

$$\Theta_4 = 2i^{(n-1)}\frac{1}{k_0 r}\left[\frac{\partial}{\partial r}\left(r j_n(k_0 r)\right) - j_n(k_0 r)\right]. \tag{2.224}$$

Together with (2.219), (2.221), and (2.224) it follows finally

$$\Theta_3 = -2i^{(n-1)}n(n+1)\frac{1}{k_0 r}\frac{\partial}{\partial r}\left(r j_n(k_0 r)\right). \tag{2.225}$$

After performing the θ integration (2.209–2.211) successfully we are now able to determine the expansion coefficients $c_{l,n,\tau}(\tau = 1, 2)$. Inserting (2.216) into equation (2.207) and taking the normalization constant $c_{l,n,1}^{(\psi,\psi)}(k_0, k_0)$ according to (2.171) into account produces the same radial dependence on both sides. From this we can deduce the coefficients $c_{l,n,1}$:

$$c_{l,n,1} = i^n\sqrt{\pi(2n+1)}\cdot\left\{\begin{array}{c} i\ ;\ \hat{e}_0 = \hat{x},\ l = 1 \\ i\ ;\ \hat{e}_0 = \hat{x},\ l = -1 \\ 1\ ;\ \hat{e}_0 = \hat{y},\ l = 1 \\ -1\ ;\ \hat{e}_0 = \hat{y},\ l = -1 \end{array}\right\}. \tag{2.226}$$

On the other hand, from equations (2.208), (2.219), and (2.225) in conjunction with the normalization constant $c_{l,n,2}^{(\psi,\psi)}(k_0, k_0)$ according to (2.175) we get the following expression for the remaining expansion coefficients $c_{l,n,2}$:

$$c_{l,n,2} = i^{n+1}\sqrt{\pi(2n+1)}\cdot\left\{\begin{array}{c} 1\ ;\ \hat{e}_0 = \hat{x},\ l = 1 \\ -1\ ;\ \hat{e}_0 = \hat{x},\ l = -1 \\ -i\ ;\ \hat{e}_0 = \hat{y},\ l = 1 \\ -i\ ;\ \hat{e}_0 = \hat{y},\ l = -1 \end{array}\right\}. \tag{2.227}$$

These results can be more clearly represented by

$$c_{l,n,1} = i^{n+1}\sqrt{\pi(2n+1)}\cdot\left(\delta_{1l} + \delta_{-1,l}\right) \tag{2.228}$$

$$c_{l,n,2} = i^{n+1}\sqrt{\pi(2n+1)}\cdot\left(\delta_{1l} - \delta_{-1,l}\right) \tag{2.229}$$

if the polarization state $\hat{e}_0 = \hat{x}$ is considered, and by

$$c_{l,n,1} = i^{n}\sqrt{\pi(2n+1)}\cdot\left(\delta_{1l} - \delta_{-1,l}\right) \tag{2.230}$$

$$c_{l,n,2} = i^{n}\sqrt{\pi(2n+1)}\cdot\left(\delta_{1l} + \delta_{-1,l}\right) \tag{2.231}$$

if we have $\hat{e}_0 = \hat{y}$.

The linearly polarized plane wave (2.198) is again a special case of the more general plane wave

$$\vec{u}_{inc}(k_0 r, \theta, \phi, \theta_i, \phi_i) \;=\; \vec{E}_0 \cdot e^{i\vec{k}_i \cdot \vec{r}} \;=\; \left(\hat{\phi}_i \cdot E_{\phi_i} \;+\; \hat{\theta}_i \cdot E_{\theta_i}\right) \cdot e^{i\vec{k}_i \cdot \vec{r}} \qquad (2.232)$$

with the vector $\vec{k}_i$ given by expression (2.112). Moreover, according to Table 2.1

$$\hat{\phi}_i = -\sin\phi_i \cdot \hat{x} \;+\; \cos\phi_i \cdot \hat{y} \qquad (2.233)$$

$$\hat{\theta}_i = \cos\theta_i \cdot \cos\phi_i \cdot \hat{x} \;+\; \cos\theta_i \cdot \sin\phi_i \cdot \hat{y} \;-\; \sin\theta_i \cdot \hat{z} \qquad (2.234)$$

hold for the unit vectors $\hat{\phi}_i$ and $\hat{\theta}_i$ in spherical coordinates. Employing these relations in conjunction with (2.112) reveals that the scalar product of the vector $\vec{k}_i$ with the polarization vector $\vec{E}_0$ becomes zero which is a characteristic property of a plane wave (see also Chap. 7). The special case of the plane wave expanded above results from the choice $\theta_i = \phi_i = 0^o$ and $E_{\phi_i} = 0, E_{\theta_i} = E_0$ or $E_{\phi_i} = E_0, E_{\theta_i} = 0$, respectively, depending on its polarization state $\hat{e}_0$. In the literature one can find the following expansion of the plane wave (2.232) with polarization $\vec{E}_0$:

$$\vec{u}_{inc}(k_0 r, \theta, \phi, \theta_i, \phi_i) = \sum_{\tau=1}^{2} \sum_{l,n} c_{l,n,\tau} \cdot \vec{\psi}_{l,n,\tau}(r, \theta, \phi) \qquad (2.235)$$

with

$$c_{l,n,1} = (-1)^l \cdot \frac{i^n}{\gamma_{l,n}} \cdot \frac{(2n+1)}{n(n+1)} \cdot \vec{E}_0 \cdot \vec{C}_{-l,n}(\theta_i, \phi_i) \qquad (2.236)$$

$$c_{l,n,2} = (-1)^l \cdot \frac{i^{n-1}}{\gamma_{l,n}} \cdot \frac{(2n+1)}{n(n+1)} \cdot \vec{E}_0 \cdot \vec{B}_{-l,n}(\theta_i, \phi_i) \qquad (2.237)$$

and the vector spherical harmonics $\vec{C}_{l,n}$ and $\vec{B}_{l,n}$ given by (2.128) and (2.129). The derivation of this expansion is omitted here but we will come back to this aspect at the end of Sect. 3.5.1. Due to the relations (2.141) and (2.142) only the modes $l = \pm 1$ must be taken into account in expansion (2.235) if the special case with $\theta_i = 0^o$ is considered. From this, and if choosing $\phi_i = 0^o$ the expansion coefficients (2.228)/(2.229) and (2.230)/(2.231) can be derived immediately. It should be also emphasized that the expansion coefficients $c_{l,n,\tau}$ in (2.201) as well as in (2.235) are identical to zero if $n = 0$.

In the foregoing two sections, we became acquainted with the most important properties of the relevant eigensolutions of the Helmholtz and vector-wave equation. In the remaining two sections of this chapter we will now concentrate on the mathematical aspects of the Green functions related to the scattering problems of our interest.

2.5 Green Theorems and Green Functions Related to the Scalar Boundary Value Problems

Since their introduction in the nineteenth century, the Green functions have become a powerful mathematical tool for solving boundary value problems . Freeman Dyson has compared the importance of these functions in a historical overview with the methodical revolution in science caused by the invention of modern computers in our days (see section "Miscellaneous" in the reference chapter for details). They became of special importance in modern quantum mechanics because they made new scientific insights possible in the first place. But beside their importance as a mathematical tool in modern physical theories these functions are also of importance for the solution of more practical problems like electromagnetic wave scattering on nonspherical particles, as it will be even demonstrated with this book. What makes these functions so useful for our purposes? Mathematically seen, with the help of these functions we are able to transform the formulation of the scattering problem in terms of partial differential equations discussed in Chap. 1 into an equivalent formulation in terms of integral equations. The accent here is on the phrase *equivalent* since the integral point of view provides finally exactly the same solution as the differential point of view does if no additional physical approximations are applied in one of these two point of views. The Green functions, while being itself a solution of a partial differential equation, are the linking elements between the integral and the differential (i.e. local) point of view. This is the essential aspect for we choose these functions as a methodological basis to discuss some of the rigorous methods which have been developed in the past for solving the scattering problems formulated in Chap. 1.

From a physical point of view these functions describe the field in space point $\mathbf{x}$ caused by a unit source located in a different space point $\mathbf{x}'$. A given source, on the other hand, can be considered as a distribution of unit sources within a confined area in space. The field of this given source is simply the sum of the fields of all unit sources. In this way the Green functions are able to decouple the properties of the source from the properties of the space where the latter is characterized by the properties (i.e., by the geometry and permittivity) of the scatterer. Thus, if only the given source will change, the Green function remains still the same and must be calculated only ones. Last but not least, Green functions can be used to express the fundamental Huygens principle in terms of an integral equation which serves as a powerful starting point for solving scattering problems.

In Sects. 2.5.1–2.5.3 we restrict our considerations to the scalar problems related to the Helmholtz equation. We will present the relevant Green theorems needed frequently for the ongoing analysis, the definitions of the Green functions belonging to our boundary value problems, but, most important, basic properties of the free-space Green function.

2.5.1 The Green Theorems

The basic geometry of the scattering problems was already given in Sect. 1.2 (see Fig. 1.2). In each of the simply connected regions we can formulate Green's theorem. By use of these theorems, and with the corresponding Green functions we are able to establish the integral representations of the boundary value problems formulated in Sect. 1.2.

Green's theorem for the two scalar but arbitrary functions Ψ and Φ is given in Γ_- by

$$\int_{\Gamma_-} \left[\Psi(\mathbf{x}) \nabla^2 \Phi(\mathbf{x}) - \Phi(\mathbf{x}) \nabla^2 \Psi(\mathbf{x}) \right] dV(\mathbf{x}) = \oint_{\partial\Gamma} \left[\Psi(\mathbf{x}) \frac{\partial \Phi(\mathbf{x})}{\partial \hat{n}} - \Phi(\mathbf{x}) \frac{\partial \Psi(\mathbf{x})}{\partial \hat{n}} \right] dS(\mathbf{x}), \tag{2.238}$$

and in Γ_+ by

$$\int_{\Gamma_+} \left[\Psi(\mathbf{x}) \nabla^2 \Phi(\mathbf{x}) - \Phi(\mathbf{x}) \nabla^2 \Psi(\mathbf{x}) \right] dV(\mathbf{x}) = \oint_{\partial\Gamma + S_\infty} \left[\Psi(\mathbf{x}) \frac{\partial \Phi(\mathbf{x})}{\partial \hat{n}_-} - \Phi(\mathbf{x}) \frac{\partial \Psi(\mathbf{x})}{\partial \hat{n}_-} \right] dS(\mathbf{x}). \tag{2.239}$$

The boundary integral $\oint_{\partial\Gamma + S_\infty}$ on the right-hand side of (2.239) represents the sum of two separate boundary integrals over the surfaces $\partial\Gamma$ and S_∞. The contribution of the boundary integral along the cut C in Γ_+ can be neglected since it appears twice but with opposite sign. The corresponding Green theorem in the entire space $\Gamma = \Gamma_- \cup \Gamma_+$ without any scatterer can be expressed as follows:

$$\int_{\Gamma} \left[\Psi(\mathbf{x}) \nabla^2 \Phi(\mathbf{x}) - \Phi(\mathbf{x}) \nabla^2 \Psi(\mathbf{x}) \right] dV(\mathbf{x}) = \oint_{S_\infty} \left[\Psi(\mathbf{x}) \frac{\partial \Phi(\mathbf{x})}{\partial \hat{n}} - \Phi(\mathbf{x}) \frac{\partial \Psi(\mathbf{x})}{\partial \hat{n}} \right] dS(\mathbf{x}). \tag{2.240}$$

When formulating Green's theorem in a certain region it is usually assumed that both functions Ψ and Φ are two times continuously differentiable functions. On the other hand, in the context of this book we are especially interested in employing Green's theorem with the Green functions, i.e., with functions which become singular if the observation point becomes identical with the source point. We will see later that all the T-matrix approaches avoid this critical situation. But in Chap. 5 we will discuss other solution methods which have to take this singularity into account.

2.5.2 The Free-Space Green Function

Before dealing with the Green functions belonging to our boundary value problems formulated in Chap. 1 we first want to dwell on the free-space Green function $G_0(\mathbf{x}, \mathbf{x}')$ because it is of special importance for our purposes. This Green function solves the inhomogeneous Helmholtz equation

$$(\nabla_{\mathbf{x}}^2 + k_0^2)\, G_0(\mathbf{x}, \mathbf{x}') = -\,\delta(\mathbf{x} - \mathbf{x}') \tag{2.241}$$

and is defined everywhere in the entire free space (as its name expresses already) physically characterized by the parameter k_0. An elementary source in space point $\mathbf{x}'$ is the inhomogeneity on the right hand side of this equation. This elementary source produces a disturbance (a field) $G_0(\mathbf{x}, \mathbf{x}')$ in observation point $\mathbf{x}$. In the limiting case of $|\mathbf{x}| \to \infty$ this field has to fulfil the radiation condition (1.19).

The free-space Green function exhibits an important symmetry property. For its derivation let us consider the additional free-space Green function $G_0(\mathbf{x}, \mathbf{x}'')$ with a unit source in space point $\mathbf{x}''$. It is a solution of the corresponding Helmholtz equation

$$(\nabla_{\mathbf{x}}^2 + k_0^2)\, G_0(\mathbf{x}, \mathbf{x}'') = -\,\delta(\mathbf{x} - \mathbf{x}''). \tag{2.242}$$

Multiplying (2.241) with $G_0(\mathbf{x}, \mathbf{x}'')$, and, conversely, (2.242) with $G_0(\mathbf{x}, \mathbf{x}')$, taking the difference of the resulting equations and integrating afterwards over the entire free space provides

$$\begin{aligned}
&\int_\Gamma \left[G_0(\mathbf{x}, \mathbf{x}'') \cdot \nabla_{\mathbf{x}}^2 G_0(\mathbf{x}, \mathbf{x}') - G_0(\mathbf{x}, \mathbf{x}') \cdot \nabla_{\mathbf{x}}^2 G_0(\mathbf{x}, \mathbf{x}'') \right] dV(\mathbf{x}) \\
&= \oint_{S_\infty} \left[G_0(\mathbf{x}, \mathbf{x}'') \cdot \frac{\mathbf{x}}{|\mathbf{x}|} \cdot \nabla_{\mathbf{x}} G_0(\mathbf{x}, \mathbf{x}') - G_0(\mathbf{x}, \mathbf{x}') \cdot \frac{\mathbf{x}}{|\mathbf{x}|} \nabla_{\mathbf{x}} G_0(\mathbf{x}, \mathbf{x}'') \right] dS(\mathbf{x}) \\
&= \int_\Gamma \left[\delta(\mathbf{x} - \mathbf{x}'') \cdot G_0(\mathbf{x}, \mathbf{x}') - \delta(\mathbf{x} - \mathbf{x}') \cdot G_0(\mathbf{x}, \mathbf{x}'') \right] dV(\mathbf{x})
\end{aligned} \tag{2.243}$$

if taking the relation $\hat{\mathbf{n}} = \hat{\mathbf{r}} = \mathbf{x}/|\mathbf{x}|$ for the outward directed unit normal vector at the surface S_∞ and Green's theorem (2.240) additionally into account. Since the radiation condition (1.19) applies to both free-space Green functions the boundary integral over the surface S_∞ vanishes. Due to the definition

$$\int_\Gamma \delta(\mathbf{x} - \mathbf{x}_j) \cdot f(\mathbf{x})\, dV(\mathbf{x}) \;:=\; f(\mathbf{x}_j) \tag{2.244}$$

of Dirac's delta distribution we get in a straightforward way the following remarkable symmetry relation

$$G_0(\mathbf{x}'', \mathbf{x}') = G_0(\mathbf{x}', \mathbf{x}''). \tag{2.245}$$

That is, the free-space Green function with source point $\mathbf{x}'$ and observation point $\mathbf{x}''$ is identical with the free-space Green function with source point $\mathbf{x}''$ and observation point $\mathbf{x}'$. This symmetry relation is of some importance for the physical experience of reciprocity as we will see later on.

Fortunately, we know a closed analytical expression for the free-space Green function $G_0(\mathbf{x}, \mathbf{x}')$. We will present its derivation here for two reasons. First because it nicely demonstrates the application of the residual method and second because it provides us with an interesting point of view on the radiation condition. Instead of (2.241) we start with

$$(\nabla_{\mathbf{x}}^2 + [k_0^2 + i\epsilon])\, G_0(\mathbf{x}, \mathbf{x}') = -\delta(\mathbf{x} - \mathbf{x}'); \quad \epsilon > 0. \tag{2.246}$$

ϵ therein is a small parameter which tends to zero at the end of the analysis. A further simplification can be achieved if we put the origin of the coordinate system into the source point $\mathbf{x}'$ thus transforming (2.246) into

$$(\nabla_{\mathbf{x}}^2 + [k_0^2 + i\epsilon])\, G_0(\mathbf{x}) = -\delta(\mathbf{x}). \tag{2.247}$$

The Fourier transformation of the quantities G_0, $\nabla^2 G_0$, and δ are given in a three-dimensional space by

$$G_0(\mathbf{x}) = \int \frac{d\mathbf{k}}{(2\pi)^3}\, e^{i\mathbf{k}\,\mathbf{x}} \cdot \tilde{G}_0(\mathbf{k}) \tag{2.248}$$

$$\nabla_{\mathbf{x}}^2\, G_0(\mathbf{x}) = \int \frac{d\mathbf{k}}{(2\pi)^3}\, e^{i\mathbf{k}\,\mathbf{x}} \cdot (-k^2) \cdot \tilde{G}_0(\mathbf{k}) \tag{2.249}$$

and

$$\delta(\mathbf{x}) = \int \frac{d\mathbf{k}}{(2\pi)^3}\, e^{i\mathbf{k}\,\mathbf{x}}. \tag{2.250}$$

The three-dimensional vector $\mathbf{k}$ has components (k_x, k_y, k_z). Applying the Fourier transformation to (2.247) provides therefore

$$\tilde{G}_0(\mathbf{k}) = \frac{1}{k^2 - \kappa_0^2} = \frac{1}{(k - \kappa_0) \cdot (k + \kappa_0)} \tag{2.251}$$

with

$$\kappa_0^2 = k_0^2 + i\epsilon. \tag{2.252}$$

From (2.248) we get

$$G_0(\mathbf{x}) = \int \frac{d\mathbf{k}}{(2\pi)^3}\, \frac{e^{i\mathbf{k}\,\mathbf{x}}}{k^2 - \kappa_0^2}. \tag{2.253}$$

To perform the $\mathbf{k}$-integration we pass into spherical coordinates with respect to $\mathbf{k}$. The k_z-axis is put into the direction of the vector $\mathbf{x}$. Due to this choice angle θ forms

the angle between the vectors **k** and **x**. Thus we get

$$G_0(\mathbf{x}) = \int_0^{\infty} \frac{dk}{(2\pi)^3}\, k^2 \int_0^{2\pi} d\phi \int_0^{\pi} d\theta\, \sin\theta\, \frac{e^{ik\,x\,\cos\theta}}{k^2 - \kappa_0^2}. \tag{2.254}$$

If we substitute $w = \cos\theta$ the θ-integration yields

$$G_0(\mathbf{x}) = \frac{1}{i\,x\,(2\pi)^2} \int_0^{\infty} dk\, k \cdot \frac{e^{ik\,x} - e^{-ik\,x}}{k^2 - \kappa_0^2}. \tag{2.255}$$

This result can be manipulated further to provide

$$G_0(\mathbf{x}) = \frac{1}{i\,x\,(2\pi)^2} \int_{-\infty}^{\infty} dk\, \frac{k \cdot e^{ik\,x}}{(k - \kappa_0)\cdot(k + \kappa_0)}. \tag{2.256}$$

The remaining integration with respect to k will be performed in the complex k-plane. The closed path of integration in the upper complex k-plane is depicted in Fig. 2.4. The two poles $\pm\kappa_\epsilon$ are shown in Fig. 2.4, too. For small values of the parameter ϵ they are approximately given by

$$\kappa_0 \cong \pm\left[k_0 + i\frac{\epsilon}{2k_0}\right] = \pm\,\kappa_\epsilon. \tag{2.257}$$

The contribution of the upper half circle ($Im(k) \to \infty$) vanishes so that

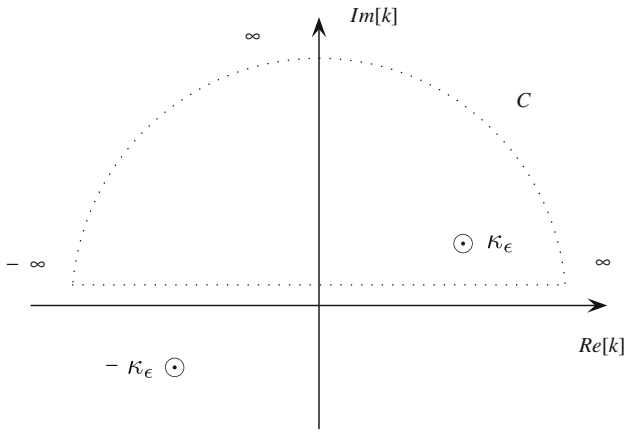

Fig. 2.4 The path of integration in the upper complex k-plane and the location of poles to calculate G_0

$$\int_{-\infty}^{\infty} dk \ \cdots = \oint_C dk \ \cdots \tag{2.258}$$

holds. That is, inside the region of integration we have only to consider the single pole at $+\kappa_0$. Employing the residual method we obtain

$$\int_{-\infty}^{\infty} dk \ \frac{k \cdot e^{ik\,x}}{(k\ -\ \kappa_0) \cdot (k\ +\ \kappa_0)} = 2\pi i \lim_{k \to \kappa_0} \left[\frac{(k\ -\ \kappa_0) \cdot k \cdot e^{ik\,x}}{(k\ -\ \kappa_0) \cdot (k\ +\ \kappa_0)} \right] = \pi i \ e^{i\kappa_0\,x} \tag{2.259}$$

and, thus, for the free-space Green function in the limiting case $\epsilon \to 0$

$$G_0(\mathbf{x}) = \frac{e^{ik_0\,x}}{4\pi x}. \tag{2.260}$$

Now, we can revert to the original vector $\mathbf{x} - \mathbf{x}'$ by replacing x by $|\mathbf{x} - \mathbf{x}'|$. In doing so, we get finally

$$G_0(\mathbf{x}, \mathbf{x}') = \frac{e^{ik_0|\mathbf{x}-\mathbf{x}'|}}{4\pi|\mathbf{x} - \mathbf{x}'|} \tag{2.261}$$

for the free-space Green function $G_0(\mathbf{x}, \mathbf{x}')$ which is in accordance with the radiation condition.

This solution is sometimes called the fundamental solution of Helmholtz's equation. It represents an outgoing spherical wave starting from source point $\mathbf{x}'$ (if a time dependence $e^{-i\omega t}$ is assumed), and subject to the radiation condition at S_∞. This solution exhibits obviously a singularity if $\mathbf{x} = \mathbf{x}'$.

The following aspect should be emphasized: If we would have used the expression $-i\epsilon$ instead of $+i\epsilon$ in (2.246) then the two poles in the complex k-plane would read $\kappa_0 \ \cong \ \pm\left[k_0 \ - \ i\,\frac{\epsilon}{2k_0} \right]$. But then only the pole $-\kappa_0$ would contribute to the k integration. In this case, the Green function would take the form

$$G_0(\mathbf{x}, \mathbf{x}') = \frac{e^{-ik_0|\mathbf{x}-\mathbf{x}'|}}{4\pi|\mathbf{x} - \mathbf{x}'|} \tag{2.262}$$

which is **not** in accordance with the required radiation condition. Thus, we can state that the choice $+i\epsilon$ of the additional term in (2.246) provides the Green function which agrees with the radiation condition. This relation between an appropriate choice of the additional term in (2.246) and the fulfilment of the radiation condition is employed with benefit in recent numerical realizations of Finite Element methods, for example, to take the radiation condition for boundary value problems in open spaces approximately into account.

Assuming that the two conditions

$$\begin{aligned} |\mathbf{x}'| &>> |\mathbf{x}| \\ k_0 \cdot |\mathbf{x}'| &>> (k_0 \cdot |\mathbf{x}|)^2 \end{aligned} \tag{2.263}$$

hold we can approximate (2.261) by

$$\lim_{|\mathbf{x}'|\to\infty} G_0(\mathbf{x},\mathbf{x}') = \frac{e^{ik_0|\mathbf{x}'|}}{4\pi\,|\mathbf{x}'|}\cdot e^{-ik_0\hat{e}_{x'}\cdot\mathbf{x}} = \frac{e^{ik_0|\mathbf{x}'|}}{4\pi\,|\mathbf{x}'|}\cdot e^{i\mathbf{k_0}\cdot\mathbf{x}} \tag{2.264}$$

with

$$\hat{e}_{x'} = \frac{\mathbf{x}'}{|\mathbf{x}'|}. \tag{2.265}$$

Please, note that the second condition in (2.263) is used to approximate the phase term appropriately. $\hat{e}_{x'}$ is identical with the unit vector $\hat{r}'$ in the radial direction in spherical coordinates. $\mathbf{k_0}$ can then be expressed by

$$\mathbf{k_0} = k_0\cdot\hat{k} = -\,k_0\cdot\hat{r}'. \tag{2.266}$$

For example, if $\mathbf{x}$ and $\mathbf{x}'$ are the two special vectors

$$\mathbf{x} \;=\; (x,y,z)\;; \quad \mathbf{x}' = (0,0,-b) \tag{2.267}$$

in Cartesian coordinates we may ask for the field in observation point $\mathbf{x}$ produced by a unit source located at the z-axis in point $-b$ if $b >> |\mathbf{x}|$ holds. The denominator of (2.261) can be approximated in this case according to (2.264) by $|\mathbf{x}-\mathbf{x}'| = \sqrt{x^2+y^2+(z+b)^2} = b$. For the phase term, on the other hand, we have to consider the approximation $ik_0|\mathbf{x}-\mathbf{x}'| \approx ik_0(z+b)$. Because of $\hat{e}_{x'} = -\hat{z}$ we get as the corresponding approximation of the free-space Green function

$$G_0(\mathbf{x},-b) = \frac{e^{ik_0 b}}{4\pi b}\cdot e^{ik_0 z}. \tag{2.268}$$

This is nothing but a plane wave with the constant amplitude $e^{ik_0 b}/(4\pi b)$ travelling along the positive z-axis.

By use of the free-space Green function we are able to express the solution u_0 of the inhomogeneous Helmholtz equation

$$(\nabla^2 \;+\; k_0^2)\; u_0(\mathbf{x}) = -\;\rho(\mathbf{x}) \tag{2.269}$$

which also fulfils the radiation condition (1.19) in terms of an integral relation. This is achieved by applying Green's theorem (2.240) with the two functions $\Psi(\mathbf{x}) = u_0(\mathbf{x})$ and $\Phi(\mathbf{x}) = G_0(\mathbf{x},\mathbf{x}')$. This results at first in

$$u_0(\mathbf{x}') = \int_\Gamma G_0(\mathbf{x},\mathbf{x}')\cdot\rho(\mathbf{x})\;dV(\mathbf{x}). \tag{2.270}$$

Since, we are bothered to denote the observation point with $\mathbf{x}$ and the source point with $\mathbf{x}'$ throughout this book we have to apply symmetry relation (2.245) to (2.270)

with $\mathbf{x}$ and $\mathbf{x}'$ interchanged in the latter equation. From this procedure we get the integral representation

$$u_0(\mathbf{x}) = \int_\Gamma G_0(\mathbf{x}, \mathbf{x}') \cdot \rho(\mathbf{x}') \, dV(\mathbf{x}') \tag{2.271}$$

for the field in observation point $\mathbf{x}$ in the free space caused by the source $\rho(\mathbf{x}')$. Let us assume further that this source is known and given by

$$\rho(\mathbf{x}') = 4\pi E_0 \, |\mathbf{x}'| \cdot e^{-ik_0|\mathbf{x}'|} \cdot \delta(\mathbf{x}' - \mathbf{x}'_\mathbf{q}). \tag{2.272}$$

For large distances of the observation point $\mathbf{x}$ from this source, i.e., if

$$|\mathbf{x}'_\mathbf{q}| >> |\mathbf{x}| \tag{2.273}$$

holds, and if taking the asymptotic behaviour (2.264) of the free-space Green function into account we get from representation (2.271) just the plane wave (2.109) with $\hat{k}_i$ according to

$$\hat{k}_i = -\hat{e}_{x'_q} = -\hat{r}'_q. \tag{2.274}$$

Beside the closed analytical expression we know also an approximation of the free-space Green function in terms of the scalar eigensolutions of Helmholtz's equation, given by

$$G_0(\mathbf{x}, \mathbf{x}') = ik_0 \cdot \sum_{n=0}^{\infty} \sum_{l=-n}^{n} \begin{cases} \varphi_{l,n}(k_0, \mathbf{x}) \cdot \tilde{\psi}_{l,n}(k_0, \mathbf{x}') \; ; \; |\mathbf{x}| > |\mathbf{x}'| \\ \psi_{l,n}(k_0, \mathbf{x}) \cdot \tilde{\varphi}_{l,n}(k_0, \mathbf{x}') \; ; \; |\mathbf{x}| < |\mathbf{x}'|. \end{cases} \tag{2.275}$$

This approximation will become a decisive element in Chaps. 3 and 4 when discussing the interrelation between the T-matrix and the Green function. The functions $\varphi_{l,n}(k_0, \mathbf{x})$, $\psi_{l,n}(k_0, \mathbf{x})$, $\tilde{\psi}_{l,n}(k_0, \mathbf{x}')$, and $\tilde{\varphi}_{l,n}(k_0, \mathbf{x}')$ are the eigensolutions introduced in (2.58), (2.57), (2.87), and (2.85) (please, note that the arguments $(k_0, \mathbf{x})$ and $(k_0, \mathbf{x}')$ have to be replaced by the arguments $(k_0 r, \theta, \phi)$ and $(k_0 r', \theta', \phi')$ in spherical coordinates). Approximation (2.275) can be brought into the shorter form

$$G_0(\mathbf{x}, \mathbf{x}') = \begin{cases} G_0^{>}(\mathbf{x}, \mathbf{x}') \; ; \; |\mathbf{x}| > |\mathbf{x}'| \\ G_0^{<}(\mathbf{x}, \mathbf{x}') \; ; \; |\mathbf{x}| < |\mathbf{x}'| \end{cases} \tag{2.276}$$

with

$$G_0^{>}(\mathbf{x}, \mathbf{x}') = (ik_0) \cdot \sum_{i=0}^{\infty} \varphi_i(k_0, \mathbf{x}) \cdot \tilde{\psi}_i(k_0, \mathbf{x}') \tag{2.277}$$

$$G_0^{<}(\mathbf{x}, \mathbf{x}') = (ik_0) \cdot \sum_{i=0}^{\infty} \psi_i(k_0, \mathbf{x}) \cdot \tilde{\varphi}_i(k_0, \mathbf{x}') \tag{2.278}$$

if using the combined index i (which should not be confused with the imaginary quantity i in the prefactor ik_0!) instead of both indices n and l. If we take only a finite number N of expansion terms in theses approximations into account we will denote this with $G_0^{(N)}(\mathbf{x}, \mathbf{x}')$ in the future. It should be noted that both functions $G_0^{>}(\mathbf{x}, \mathbf{x}')$ and $G_0^{<}(\mathbf{x}, \mathbf{x}')$ are solutions of the corresponding homogeneous Helmholtz equation. This is not surprising since the additional conditions $|\mathbf{x}| > |\mathbf{x}'|$ and $|\mathbf{x}| < |\mathbf{x}'|$ appearing in (2.275) and (2.276) exclude the singular point $\mathbf{x} = \mathbf{x}'$.

2.5.3 The Green Functions Related to the Outer Dirichlet and Transmission Problem

Let us now consider the Green function G_{Γ_+} which is related to the outer Dirichlet problem and the Green function $G_{\Gamma_+}^{(d)}$ which belongs to the outer transmission problem (the upper index "(d)" at $G_{\Gamma_+}^{(d)}$ should indicate that the outer transmission problem is related to the scattering problem on **d**ielectric particles). Both Green functions are exclusively defined in the outer region Γ_+ and are solutions of the inhomogeneous Helmholtz equations

$$\begin{aligned}(\nabla_{\mathbf{x}}^2 + k_0^2)\, G_{\Gamma_+}(\mathbf{x}, \mathbf{x}') &= -\delta(\mathbf{x} - \mathbf{x}') \\ (\nabla_{\mathbf{x}}^2 + k_0^2)\, G_{\Gamma_+}^{(d)}(\mathbf{x}, \mathbf{x}') &= -\delta(\mathbf{x} - \mathbf{x}'); \quad \mathbf{x}, \mathbf{x}' \in \Gamma_+. \end{aligned} \tag{2.279}$$

It is also required that the radiation condition (1.19) applies to both of these functions. But moreover and as distinguished from the free-space Green function we require additionally the fulfilment of

- the homogeneous Dirichlet condition

$$G_{\Gamma_+}(\mathbf{x}, \mathbf{x}') = 0 \tag{2.280}$$

  if $\mathbf{x} \in \partial\Gamma$, and
- the transmission conditions

$$G_{\Gamma_+}^{(d)}(\mathbf{x}, \mathbf{x}') = G^{(-/+)}(\mathbf{x}, \mathbf{x}') \tag{2.281}$$

$$\frac{\partial G_{\Gamma_+}^{(d)}(\mathbf{x}, \mathbf{x}')}{\partial \hat{n}_-} = \frac{\partial G^{(-/+)}(\mathbf{x}, \mathbf{x}')}{\partial \hat{n}_-} \tag{2.282}$$

  if $\mathbf{x} \in \partial\Gamma$, respectively, depending on whether the outer Dirichlet or transmission problem is considered .

The auxiliary Green function $G^{(-/+)}$ in (2.281) and (2.282) has its source point always outside the scatterer. Its observation point, on the other hand, is generally located inside the scatterer (this should be indicated by the upper mark "$(-/+)$").

Due to this general placement of the source and observation point this Green function solves the homogeneous Helmholtz equation

$$(\nabla_{\mathbf{x}}^2 + k_s^2)\, G^{(-/+)}(\mathbf{x}, \mathbf{x}') = 0 \quad ; \quad \mathbf{x} \in \Gamma_- \; ; \; \mathbf{x}' \in \Gamma_+ \tag{2.283}$$

subject to the regularity requirement. That is, there are no sources assumed inside the scatterer, in general.

Both Green functions G_{Γ_+} and $G_{\Gamma_+}^{(d)}$ obey the same important symmetry relation (2.245) as the free-space Green function G_0 does, i.e., we have

$$G_{\Gamma_+}(\mathbf{x}'', \mathbf{x}') = G_{\Gamma_+}(\mathbf{x}', \mathbf{x}'') \tag{2.284}$$

and

$$G_{\Gamma_+}^{(d)}(\mathbf{x}'', \mathbf{x}') = G_{\Gamma_+}^{(d)}(\mathbf{x}', \mathbf{x}''). \tag{2.285}$$

To prove (2.284) we may simply employ Green theorem (2.239) in the outer region Γ_+ with both functions $\Psi(\mathbf{x}) = G_{\Gamma_+}(\mathbf{x}, \mathbf{x}')$ and $\Phi(\mathbf{x}) = G_{\Gamma_+}(\mathbf{x}, \mathbf{x}'')$. If taking the Helmholtz equation (2.279), the homogeneous Dirichlet condition (2.280) as well as the radiation condition into account (2.284) follows in a straightforward way. To prove (2.285) we have to apply Green's theorem twice. First again in Γ_+ with both functions $\Psi(\mathbf{x}) = G_{\Gamma_+}^{(d)}(\mathbf{x}, \mathbf{x}')$ and $\Phi(\mathbf{x}) = G_{\Gamma_+}^{(d)}(\mathbf{x}, \mathbf{x}'')$, and second inside the scatterer with both functions $\Psi(\mathbf{x}) = G^{(-/+)}(\mathbf{x}, \mathbf{x}')$ and $\Phi(\mathbf{x}) = G^{(-/+)}(\mathbf{x}, \mathbf{x}'')$. Then relation (2.285) follows in conjunction with both Helmholtz equations (2.279) and (2.283), the radiation condition as well as the transmission conditions (2.281) and (2.282) at the boundary surface. This analysis can be performed without any difficulties by the reader himself.

In contrast to the free-space Green function there are no closed analytical expressions known for the two Green functions G_{Γ_+} and $G_{\Gamma_+}^{(d)}$. Due to this reason the following integral representations of the solutions of the related boundary value problems are at first very formally. For the total field in the outer region Γ_+ related to the outer Dirichlet problem we obtain

$$u_t(\mathbf{x}) = \int_{\Gamma_+} G_{\Gamma_+}(\mathbf{x}, \mathbf{x}') \cdot \rho(\mathbf{x}')\, dV(\mathbf{x}'). \tag{2.286}$$

The analogue representation for the total field in Γ_+ related to the outer transmission problem reads

$$u_t(\mathbf{x}) = \int_{\Gamma_+} G_{\mathbf{\Gamma}_+}^{(d)}(\mathbf{x}, \mathbf{x}') \cdot \rho(\mathbf{x}')\, dV(\mathbf{x}'). \tag{2.287}$$

The proofs of these representations are quite similar to the proofs of the symmetry relations. To show (2.286) we have to apply again Green's theorem in Γ_+ but now with the two functions $\Psi(\mathbf{x}) = u_t(\mathbf{x})$ and $\Phi(\mathbf{x}) = G_{\Gamma_+}(\mathbf{x}, \mathbf{x}')$. Together with the inhomogeneous Helmholtz equations related to u_t and G_{Γ_+}, the required boundary

conditions (1.2) and (2.280), the radiation condition at S_∞, and, not at least, with the symmetry relation (2.284) we end up with (2.286).

To derive representation (2.287) we must again apply Green's theorem twice. Once with $\Psi(\mathbf{x}) = u_t(\mathbf{x})$ and $\Phi(\mathbf{x}) = G^{(d)}_{\mathbf{\Gamma}_+}(\mathbf{x}, \mathbf{x}')$ in Γ_+, and once with $\Psi(\mathbf{x}) = u_{int}(\mathbf{x})$ and $\Phi(\mathbf{x}) = G^{(-/+)}(\mathbf{x}, \mathbf{x}')$ inside the scatterer. Taking again the relevant Helmholtz equations, transmission conditions, radiation condition as well as symmetry relation (2.285) into account provides (2.287). This is again a not to difficult exercise for the reader to become acquainted with the usage of Green's theorems.

2.6 Green Theorems and Green Functions Related to the Vectorial Boundary Value Problems

In this last tray of our mathematical tool box we want to sort the same instruments as treated in the foregoing section but now applicable to the vector case. The Green theorems introduced in Sect. 2.5.1 express at first relations between scalar quantities calculated via volume integrals on one side and boundary integrals on the other side of the relevant equations. Only after introducing the Green functions depending on the two variables $\mathbf{x}$ and $\mathbf{x}'$ we could express the field u_0 of (2.269) for example in space point $\mathbf{x}$ in terms of the volume integral Eq. (2.271). Its integrand consists of the product of the scalar source distribution $\rho(\mathbf{x}')$ with the scalar free-space Green function $G_0(\mathbf{x}, \mathbf{x}')$. In the vector case, however, we have to consider the vector source $\vec{\rho}(\mathbf{x}')$. Each component of this vector source produces a vector field $\vec{u}(\mathbf{x})$ with components $(u_{x_1}, u_{x_2}, u_{x_3})$ in observation point $\mathbf{x}$. To express this vector field again by use of a volume integral containing the product of the vector source and a Green function the latter quantity must become a dyadic. Therefore, we have to deal first with some important definitions and relations regarding the dyadic analysis.

2.6.1 Dyadics

Let us assume that we have the vector source

$$\vec{\rho} = \rho_x\,\hat{x} \;+\; \rho_y\,\hat{y} \;+\; \rho_z\,\hat{z} \tag{2.288}$$

with components (ρ_x, ρ_y, ρ_z). This vector source produces the field

$$\vec{E} = E_x\,\hat{x} \;+\; E_y\,\hat{y} \;+\; E_z\,\hat{z} \tag{2.289}$$

with components (E_x, E_y, E_z). Between the components of the vector source and the components of the generated field we assume further the linear relations

$$\begin{aligned} E_x &= \phi_{xx} \cdot \rho_x \; + \; \phi_{xy} \cdot \rho_y \; + \; \phi_{xz} \cdot \rho_z \\ E_y &= \phi_{yx} \cdot \rho_x \; + \; \phi_{yy} \cdot \rho_y \; + \; \phi_{yz} \cdot \rho_z \\ E_z &= \phi_{zx} \cdot \rho_x \; + \; \phi_{zy} \cdot \rho_y \; + \; \phi_{zz} \cdot \rho_z . \end{aligned} \tag{2.290}$$

According to these relations! each component of the vector source contributes to all components E_x, E_y and E_z of the field. To bring these linear relations into the more comfortable form

$$\vec{E} = \mathbf{\Phi} \cdot \vec{\rho} \tag{2.291}$$

we define the dyadic quantity $\mathbf{\Phi}$ in the following way:

$$\mathbf{\Phi} \; := \; \hat{x} \odot \vec{\phi}_x \; + \; \hat{y} \odot \vec{\phi}_y \; + \; \hat{z} \odot \vec{\phi}_z \tag{2.292}$$

where the vectors $\vec{\phi}_x, \vec{\phi}_y, \vec{\phi}_z$ are given by the expressions

$$\begin{aligned} \vec{\phi}_x &= \phi_{xx} \, \hat{x} \; + \; \phi_{xy} \, \hat{y} \; + \; \phi_{xz} \, \hat{z} \\ \vec{\phi}_y &= \phi_{yx} \, \hat{x} \; + \; \phi_{yy} \, \hat{y} \; + \; \phi_{yz} \, \hat{z} \\ \vec{\phi}_z &= \phi_{zx} \, \hat{x} \; + \; \phi_{zy} \, \hat{y} \; + \; \phi_{zz} \, \hat{z} . \end{aligned} \tag{2.293}$$

(Please, note that a dyadic quantity will be denoted by bold capital letters, as we have already done for matrices. But from the context it should become clear whether dyadics or matrices are meant!). The symbol "$\odot$" in (2.292) denotes the dyadic product of the vectors. The dyadic $\mathbf{\Phi}$ reads explicitly

$$\begin{aligned} \mathbf{\Phi} \; := \; & \phi_{xx} \, \hat{x} \odot \hat{x} \; + \; \phi_{xy} \, \hat{x} \odot \hat{y} \; + \; \phi_{xz} \, \hat{x} \odot \hat{z} \; + \\ & \phi_{yx} \, \hat{y} \odot \hat{x} \; + \; \phi_{yy} \, \hat{y} \odot \hat{y} \; + \; \phi_{yz} \, \hat{y} \odot \hat{z} \; + \\ & \phi_{zx} \, \hat{z} \odot \hat{x} \; + \; \phi_{zy} \, \hat{z} \odot \hat{y} \; + \; \phi_{zz} \, \hat{z} \odot \hat{z} . \end{aligned} \tag{2.294}$$

$\mathbf{\Phi}$ is symmetric if

$$\mathbf{\Phi} = \mathbf{\Phi}^{tp} \tag{2.295}$$

with

$$\mathbf{\Phi}^{tp} \; := \; \vec{\phi}_x \odot \hat{x} \; + \; \vec{\phi}_y \odot \hat{y} \; + \; \vec{\phi}_z \; \odot \; \hat{z} \tag{2.296}$$

as the transpose dyadic.

The scalar product of a dyadic $\left(\vec{\phi}^{\,(1)} \odot \vec{\phi}^{\,(2)} \right)$ with an arbitrary vector $\vec{f}$ is defined according to

$$\left(\vec{\phi}^{\,(1)} \odot \vec{\phi}^{\,(2)} \right) \cdot \vec{f} \; := \; \vec{\phi}^{\,(1)} \cdot \left(\vec{\phi}^{\,(2)} \cdot \vec{f} \right) . \tag{2.297}$$

From this definition (2.291) follows immediately. It follows also that $\mathbf{\Phi} \cdot \vec{f} \neq \vec{f} \cdot \mathbf{\Phi}$ holds, in general. The dyadic $\mathbf{\Phi}$ of (2.292–2.294) can be represented by the matrix

$$\begin{pmatrix} \phi_{xx} & \phi_{xy} & \phi_{xz} \\ \phi_{yx} & \phi_{yy} & \phi_{yz} \\ \phi_{zx} & \phi_{zy} & \phi_{zz} \end{pmatrix}. \tag{2.298}$$

We can represent correspondingly the transpose dyadic by the transpose of this matrix. In close analogy to (2.297), we define the vector product of a vector with a dyadic according to

$$\left(\vec{\phi}^{\,(1)} \odot \vec{\phi}^{\,(2)}\right) \times \vec{f} \;:=\; \vec{\phi}^{\,(1)} \odot \left(\vec{\phi}^{\,(2)} \times \vec{f}\right). \tag{2.299}$$

As for the scalar product $\mathbf{\Phi} \times \vec{f} \neq \vec{f} \times \mathbf{\Phi}$ holds, in general. The sum of the dyadic products of the unit vectors $\hat{\mathbf{x}}_i$ represents a special dyadic, the so-called "idem factor" $\mathbf{I}$,

$$\mathbf{I} \;:=\; \sum_{i=1}^{3} \hat{\mathbf{x}}_i \odot \hat{\mathbf{x}}_i. \tag{2.300}$$

The idem factor is characterized by its property

$$\mathbf{I} \cdot \vec{f}(\mathbf{x}) = \vec{f}(\mathbf{x}) \cdot \mathbf{I} = \vec{f}(\mathbf{x}). \tag{2.301}$$

Taking the gradient of a vector $\vec{f}$ will also produce a dyadic. In Cartesian coordinates, this operation provides

$$\nabla \vec{f} = \hat{x} \odot \frac{\partial \vec{f}}{\partial x} \;+\; \hat{y} \odot \frac{\partial \vec{f}}{\partial y} \;+\; \hat{z} \odot \frac{\partial \vec{f}}{\partial z}, \tag{2.302}$$

where $\vec{f} = f_x \cdot \hat{x} + f_y \cdot \hat{y} + f_z \cdot \hat{z}$. In spherical coordinates, if the vector $\vec{f}$ is given by $\vec{f} = f_r \cdot \hat{r} + f_\theta \cdot \hat{\theta} + f_\phi \cdot \hat{\phi}$, we have correspondingly

$$\nabla \vec{f} = \hat{r} \odot \frac{\partial \vec{f}}{\partial r} \;+\; \hat{\theta} \odot \frac{1}{r} \frac{\partial \vec{f}}{\partial \theta} \;+\; \hat{\phi} \odot \frac{1}{r \sin\theta} \frac{\partial \vec{f}}{\partial \phi}. \tag{2.303}$$

It must be taken into account that in spherical coordinates not only the components f_r, f_θ, f_ϕ but also the unit vectors must be differentiated with respect to θ and ϕ. According to Table 2.1, we have

$$\frac{\partial \hat{r}}{\partial r} = 0, \quad \frac{\partial \hat{r}}{\partial \theta} = \hat{\theta}, \quad \text{and} \quad \frac{\partial \hat{r}}{\partial \phi} = \sin\theta \, \hat{\phi}, \tag{2.304}$$

for example. Thus the gradient of the radial unit vector produces the dyadic

$$\nabla \hat{r} = \frac{1}{r} \left(\hat{\theta} \odot \hat{\theta} \;+\; \hat{\phi} \odot \hat{\phi}\right). \tag{2.305}$$

Furthermore, taking the gradient of the product of a scalar function f with a vector $\vec{\phi}$ provides the dyadic

$$\nabla(f\vec{\phi}) = (\nabla f) \odot \vec{\phi} \; + \; f \cdot \nabla(\vec{\phi}). \tag{2.306}$$

The curl of the dyadic $\mathbf{\Phi}$ in (2.292) is defined according to

$$\nabla \times \mathbf{\Phi} \; := \; \hat{x} \odot \left[\nabla \times \vec{\phi}_x\right] \; + \; \hat{y} \odot \left[\nabla \times \vec{\phi}_y\right] \; + \; \hat{z} \odot \left[\nabla \times \vec{\phi}_z\right]. \tag{2.307}$$

In spherical coordinates this becomes

$$\nabla \times \mathbf{\Phi} \; := \; \hat{r} \odot \left[\nabla \times \vec{\phi}_r\right] \; + \; \hat{\theta} \odot \left[\nabla \times \vec{\phi}_\theta\right] \; + \; \hat{\phi} \odot \left[\nabla \times \vec{\phi}_\phi\right] \tag{2.308}$$

with $\nabla \times \vec{\phi}_r$, $\nabla \times \vec{\phi}_\theta$, and $\nabla \times \vec{\phi}_\phi$ being the curl of the vector functions $\vec{\phi}_r$, $\vec{\phi}_\theta$, and $\vec{\phi}_\phi$ in spherical coordinates.

The following identities are of some importance for the ongoing considerations:

$$\vec{a} \cdot [\vec{b} \times \mathbf{C}] = -\vec{b} \cdot [\vec{a} \times \mathbf{C}] = [\vec{a} \times \vec{b}] \cdot \mathbf{C} \tag{2.309}$$

$$\vec{a} \cdot \mathbf{B} = \mathbf{B}^{tp} \cdot \vec{a} \tag{2.310}$$

$$\vec{a} \times \mathbf{B} = -\,[\mathbf{B}^{tp} \times \vec{a}]^{tp} \tag{2.311}$$

$$\mathbf{C}^{tp} \cdot [\vec{a} \times \mathbf{B}] = -\,[\vec{a} \times \mathbf{C}]^{tp} \cdot \mathbf{B} \tag{2.312}$$

$$[\mathbf{A} \times \vec{b}] \cdot \mathbf{C} = \mathbf{A} \cdot [\vec{b} \times \mathbf{C}] \tag{2.313}$$

$$-\,[\vec{a} \times \mathbf{C}^{tp}]^{tp} = \mathbf{C} \times \vec{a} \tag{2.314}$$

$$[\mathbf{A} \cdot \mathbf{B}]^{tp} = \mathbf{B}^{tp} \cdot \mathbf{A}^{tp}. \tag{2.315}$$

2.6.2 The Green Theorems

Green's theorem for the two arbitrary vector functions $\vec{\psi}$ and $\vec{\phi}$ is given in Γ_+ by

$$\begin{aligned} &\int_{\Gamma_+} \left[\vec{\psi}(\mathbf{x}) \cdot \nabla \times \nabla \times \vec{\phi}(\mathbf{x}) - \vec{\phi}(\mathbf{x}) \cdot \nabla \times \nabla \times \vec{\psi}(\mathbf{x})\right] dV(\mathbf{x}) \\ &= \oint_{\partial\Gamma \cup S_\infty} \hat{n}_- \cdot \left\{\vec{\phi}(\mathbf{x}) \times \left[\nabla \times \vec{\psi}(\mathbf{x})\right] \; - \; \vec{\psi}(\mathbf{x}) \times \left[\nabla \times \vec{\phi}(\mathbf{x})\right]\right\} dS(\mathbf{x}). \end{aligned} \tag{2.316}$$

Obviously, this theorem relates two scalar quantities. To get a corresponding theorem which allows us to represent vector functions we have to introduce dyadic quantities into this theorem. This can be achieved by taking the scalar product of a dyadic with a constant vector into account, i.e., we use

$$\mathbf{\Phi}(\mathbf{x}, \mathbf{x}') \cdot \vec{c} \tag{2.317}$$

instead of the dyadic $\mathbf{\Phi}(\mathbf{x}, \mathbf{x}')$. Since this operation yields a vector according to definition (2.297) we can use such a scalar product within (2.316). The constant vector can be rejected afterwards.

By means of this procedure we can derive the vector-dyadic Green theorem

$$\begin{aligned}\int_{\Gamma_+} \Big\{ \Big[\nabla \times \nabla \times \vec{\Psi}(\mathbf{x})\Big] \cdot \mathbf{Q}(\mathbf{x}, \mathbf{x}') - \vec{\Psi}(\mathbf{x}) \cdot \big[\nabla_x \times \nabla_x \times \mathbf{Q}(\mathbf{x}, \mathbf{x}')\big] \Big\}\, dV(\mathbf{x}) \\ = \oint_{\partial\Gamma + S_\infty} \hat{n}_- \cdot \Big\{ \vec{\Psi}(\mathbf{x}) \times \big[\nabla_x \times \mathbf{Q}(\mathbf{x}, \mathbf{x}')\big] \\ + \Big[\nabla \times \vec{\Psi}(\mathbf{x})\Big] \times \mathbf{Q}(\mathbf{x}, \mathbf{x}') \Big\}\, dS(\mathbf{x})\end{aligned} \tag{2.318}$$

as well as the dyadic-dyadic Green theorem

$$\begin{aligned}\int_{\Gamma_+} \Big\{ \big[\nabla_x \times \nabla_x \times \mathbf{Q}(\mathbf{x}, \mathbf{x}')\big]^{tp} \cdot \mathbf{P}(\mathbf{x}, \mathbf{x}'') \\ - \mathbf{Q}^{tp}(\mathbf{x}, \mathbf{x}') \cdot \big[\nabla_x \times \nabla_x \times \mathbf{P}(\mathbf{x}, \mathbf{x}'')\big] \Big\}\, dV(\mathbf{x}) \\ = \oint_{\partial\Gamma + S_\infty} \Big\{ \big[\hat{n}_- \times \mathbf{Q}(\mathbf{x}, \mathbf{x}')\big]^{tp} \cdot \big[\nabla_x \times \mathbf{P}(\mathbf{x}, \mathbf{x}'')\big] \\ - \big[\nabla_x \times \mathbf{Q}(\mathbf{x}, \mathbf{x}')\big]^{tp} \cdot \big[\hat{n}_- \times \mathbf{P}(\mathbf{x}, \mathbf{x}'')\big] \Big\}\, dS(\mathbf{x})\end{aligned} \tag{2.319}$$

valid in Γ_+. Similar theorems can be derived in Γ_- which differs only in the surface integral on the right hand side of (2.318) and (2.319) (in Γ_- we have to consider only the surface $\partial\Gamma$), and in the use of the unit normal vector $\hat{n}$ instead of $\hat{n}_-$. Contrary, for the free space without any scatterer, we have to consider only the surface integral over S_∞. The derivation of these theorems will be omitted here. The interested reader is referred to the relevant literature cited in the reference chapter.

2.6.3 The Dyadic Free-Space Green Function

We start again with the free-space Green function of the entire free space $\Gamma = \Gamma_- \cup \Gamma_+$ which is now a dyadic and, therefore, a solution of the inhomogeneous equation

$$[\,\nabla_{\mathbf{x}} \times \nabla_{\mathbf{x}} \times \; - k_0^2\,]\,\mathbf{G_0}(\mathbf{x}, \mathbf{x}') = \mathbf{I}\delta(\mathbf{x} - \mathbf{x}') \tag{2.320}$$

with $\mathbf{I}$ being the idem factor defined in (2.300). We require additionally the fulfilment of the radiation condition (1.20) at S_∞ with respect to the variable $\mathbf{x}$. Levine and Schwinger could show (see the reference chapter for details) that the solution of this equation can be expressed in terms of the scalar free-space Green function (2.261) according to

$$\mathbf{G_0}(\mathbf{x}, \mathbf{x}') = \left[\mathbf{I} + \frac{1}{k_0^2} \nabla_{\mathbf{x}} \nabla_{\mathbf{x}} \right] G_0(\mathbf{x}, \mathbf{x}'). \tag{2.321}$$

The first term $\mathbf{I}G_0(\mathbf{x}, \mathbf{x}')$ on the right hand side of this expression is the free-space Green function which solves the dyadic form of Helmholtz's equation

$$[\, \nabla_{\mathbf{x}}^2 + k_0^2 \,]\, \mathbf{G}_{\mathbf{0}}^{(\mathbf{H})}(\mathbf{x}, \mathbf{x}') = -\mathbf{I}\delta(\mathbf{x} - \mathbf{x}'). \tag{2.322}$$

Since the Nabla operator operates twice on the scalar G_0 in the second term on the right hand side of (2.321) the dyadic $\mathbf{G_0}$ has a pole of order 3 at $\mathbf{x} = \mathbf{x}'$, i.e., it exhibits a much stronger singularity than the scalar G_0 and the first term $\mathbf{I}G_0$ of (2.321) in the same point. To make this singularity more obvious let us calculate the expression $\nabla_R \nabla_R G_0$ explicitly in spherical coordinates. For simplicity we assume that the origin of the coordinate system coincides with the location of the source point $\mathbf{r}'$, as already done when deriving the analytical expression of the scalar free-space Green function G_0 in Sect. 2.5.2. In this system $\mathbf{R}$ denotes the vector to the observation point. Now, taking into account that applying ∇_R to the scalar G_0 provides the vector

$$\frac{\partial}{\partial R} \left(\frac{e^{ik_0 R}}{4\pi r} \right) \cdot \hat{R}, \tag{2.323}$$

we obtain in conjunction with relations (2.305) and (2.306) the following matrix:

$$\begin{pmatrix} \frac{\partial^2}{\partial^2 R} & 0 & 0 \\ 0 & \frac{1}{R}\frac{\partial}{\partial R} & 0 \\ 0 & 0 & \frac{1}{R}\frac{\partial}{\partial R} \end{pmatrix} \frac{e^{ik_0 R}}{4\pi R}. \tag{2.324}$$

This matrix is nothing but the representation of the dyadic $\nabla_R \nabla_R G_0(\mathbf{R})$ in spherical coordinates. If performing the differentiations with respect to R, and after some simple algebra we get the explicit expression

$$\begin{aligned} \mathbf{G_0}(\mathbf{R}) = & \left[\mathbf{I} \left(1 + \frac{i}{k_0 R} - \frac{1}{k_0^2 R^2} \right) \right. \\ & \left. + \hat{R} \odot \hat{R} \left(-1 - \frac{3i}{k_0 R} + \frac{3}{k_0^2 R^2} \right) \right] \frac{e^{ik_0 R}}{4\pi R} \end{aligned} \tag{2.325}$$

for the dyadic (2.321) in spherical coordinates. For large distances R and if neglecting all contributions $1/R^n$ with $n > 2$ we obtain the asymptotic behaviour

$$\lim_{R\to\infty} \mathbf{G_0}(\mathbf{R}) = \left[\mathbf{I} - \hat{R} \odot \hat{R}\right] \frac{e^{ik_0 R}}{4\pi R}, \tag{2.326}$$

or, if going back to the original vectors $\mathbf{x}$ and $\mathbf{x}'$ and assuming $|\mathbf{x}'| >> |\mathbf{x}|$ (i.e., the distance to the source point is assumed to be much larger than the distance to the observation point),

$$\lim_{|\mathbf{x}'|\to\infty} \mathbf{G_0}(\mathbf{x}, \mathbf{x}') = \left[\mathbf{I} - \hat{e}_{x'} \odot \hat{e}_{x'}\right] \frac{e^{ik_0|\mathbf{x}'|}}{4\pi|\mathbf{x}'|} \cdot e^{-ik_0 \hat{e}_{x'}\cdot\mathbf{x}}. \tag{2.327}$$

$\hat{e}_{x'}$ agrees with the unit vector $\hat{\mathbf{r}}'$ in spherical coordinates. This asymptotic expression will help us to define the scattering quantities appropriately as we will see later on in Chap. 7.

Moreover, by use of (2.321) together with relation

$$\nabla_{\mathbf{x}} \nabla_{\mathbf{x}} G_0(\mathbf{x}, \mathbf{x}') = \nabla_{\mathbf{x}'} \nabla_{\mathbf{x}'} G_0(\mathbf{x}, \mathbf{x}') \tag{2.328}$$

and in conjunction with the dyadic-dyadic Green theorem if applied in the entire free space we are able to prove the following symmetry relations regarding the commutation of arguments:

$$\mathbf{G_0^{tp}}(\mathbf{x}', \mathbf{x}'') = \mathbf{G_0}(\mathbf{x}'', \mathbf{x}') = \mathbf{G_0}(\mathbf{x}', \mathbf{x}''). \tag{2.329}$$

Now, looking for the solution of the inhomogeneous vector-wave equation

$$\left[\nabla \times \nabla \times - k_0^2\right] \vec{u}_0(\mathbf{x}) = \vec{\rho}(\mathbf{x}) \tag{2.330}$$

in the entire free space we get in close analogy to the scalar case by use of Green's theorem (2.318) if applied with the vector function $\vec{\psi}(\mathbf{x}) = \vec{u}_0(\mathbf{x})$ and the dyadic $\mathbf{Q}(\mathbf{x}, \mathbf{x}') = \mathbf{G_0}(\mathbf{x}, \mathbf{x}')$

$$\vec{u}_0(\mathbf{x}) = \int_\Gamma \mathbf{G_0}(\mathbf{x}, \mathbf{x}') \cdot \vec{\rho}(\mathbf{x}')\, dV(\mathbf{x}')\,; \quad \mathbf{x}, \mathbf{x}' \in \Gamma \tag{2.331}$$

if the radiation condition (1.20) applies also to $\vec{u}_0(\mathbf{x})$. In deriving (2.331) we made use of the symmetry relation (2.329) to denote again the source point by $\mathbf{x}'$ and the observation point by $\mathbf{x}$. For example, if we have the specific source vector

$$\vec{\rho}(\mathbf{x}') = 4\pi|\mathbf{x}'| \cdot e^{-ik_0|\mathbf{x}'|} \cdot \delta(\mathbf{x}' - \mathbf{x}'_\mathbf{q}) \cdot \vec{E}_0 \tag{2.332}$$

with

$$|\mathbf{x}'_{\mathbf{q}}| >> |\mathbf{x}| \tag{2.333}$$

and the $\vec{k}_i$ vector given by

$$\vec{k}_i = -k_0\, \hat{e}_{x'_q} \tag{2.334}$$

then the plane wave with polarization $\vec{E}_0$ we have already considered in (2.232) follows immediately from (2.331) and (2.327).

Regarding representation (2.331) it should be emphasized that due to the strong singularity of $\mathbf{G_0}$ this expression can be applied without problems only for observation points $\mathbf{x}$ outside the source region. But there exist some methods which makes it necessary to go into the source region, as we will see especially in Chap. 5. This step requires some care since it may easily result in an erroneous numerical analysis, for example. On the other hand, we can benefit from the fact that although $\mathbf{G_0}$ exhibits this strong singularity the same does not hold for the rotation of this quantity, i.e., for

$$\nabla_{\mathbf{x}} \times \mathbf{G_0}(\mathbf{x}, \mathbf{x}') = \nabla_{\mathbf{x}} \times \mathbf{I} G_0(\mathbf{x}, \mathbf{x}') = \nabla_{\mathbf{x}} G_0(\mathbf{x}, \mathbf{x}') \times \mathbf{I} = -\nabla_{\mathbf{x}'} G_0(\mathbf{x}, \mathbf{x}') \times \mathbf{I}. \tag{2.335}$$

We will come back to this aspect in Sect. 7.2.2. The T-matrix methods avoid this situation, as already mentioned. But this advantage is gained with the discussion concerning Rayleigh's hypothesis and their influence on the T-matrix methods. In Chap. 6 we will resume discussing this aspect.

For many electromagnetic wave problems it is convenient to split a general vector field $\vec{f}$ into two parts according to

$$\vec{f} = \vec{f}_t + \vec{f}_l, \tag{2.336}$$

i.e., into a transverse or solenoidal part $\vec{f}_t$ with $\nabla \cdot \vec{f}_t = 0$, and into a longitudinal part $\vec{f}_l$ with $\nabla \times \vec{f}_l = 0$. The same can be done with the dyadic delta distribution $\mathbf{I}\delta(\mathbf{x} - \mathbf{x}') = \mathbf{D_t}(\mathbf{x} - \mathbf{x}') + \mathbf{D_l}(\mathbf{x} - \mathbf{x}')$. In accordance with the general definition

$$\int_\Gamma \mathbf{I}\delta(\mathbf{x} - \mathbf{x}') \cdot \vec{f}(\mathbf{x}')\, dV(\mathbf{x}') := \vec{f}(\mathbf{x}) \tag{2.337}$$

the transverse part $\mathbf{D_t}(\mathbf{x} - \mathbf{x}')$ of the delta distribution provides the transverse part $\vec{f}_t$ if applied to the vector field $\vec{f}$. Correspondingly, its longitudinal part $\mathbf{D_l}(\mathbf{x} - \mathbf{x}')$ provides the longitudinal part $\vec{f}_l$ of $\vec{f}$. Then we can write

$$\mathbf{G_0}(\mathbf{x}, \mathbf{x}') = \mathbf{G_t}(\mathbf{x}, \mathbf{x}') - \frac{1}{k_0^2} \cdot \mathbf{D_l}(\mathbf{x} - \mathbf{x}') \tag{2.338}$$

with $\mathbf{G_t}$ being the transverse part of the dyadic free-space Green function obeying the equation

$$[\,\nabla_{\mathbf{x}} \times \nabla_{\mathbf{x}} \times \; - k_0^2\,]\,\mathbf{G_t}(\mathbf{x}, \mathbf{x}') \;=\; \mathbf{D_t}(\mathbf{x} - \mathbf{x}'), \tag{2.339}$$

unlike (2.320) of $\mathbf{G_0}$. And, as we have already discussed for the fields, the longitudinal part of $\mathbf{G_0}$ exists only in the source region, if applicable. But concerning the scattering problems of our interest we are faced exclusively with transverse fields and induced but transverse sources.

In the scalar case we presented already a series expansion of the free-space Green function in terms of appropriate eigensolutions of the scalar Helmholtz equation. For the transverse part of the dyadic free-space Green function we know a corresponding expansion given by

$$\mathbf{G_t}(\mathbf{x}, \mathbf{x}') = (ik_0) \cdot \sum_{\tau=1}^{2} \sum_{i=0}^{\infty} \begin{cases} \vec{\varphi}_{i,\tau}(k_0, \mathbf{x}) \odot \vec{\tilde{\psi}}_{i,\tau}(k_0, \mathbf{x}'); & |\mathbf{x}| > |\mathbf{x}'| \\ \vec{\psi}_{i,\tau}(k_0, \mathbf{x}) \odot \vec{\tilde{\varphi}}_{i,\tau}(k_0, \mathbf{x}'); & |\mathbf{x}| < |\mathbf{x}'|. \end{cases} \tag{2.340}$$

Here, we will use the similar notation $\mathbf{G_t^>}(\mathbf{x}, \mathbf{x}')$ if $|\mathbf{x}| > |\mathbf{x}'|$, and $\mathbf{G_t^<}(\mathbf{x}, \mathbf{x}')$ if $|\mathbf{x}| < |\mathbf{x}'|$ (in close analogy to (2.276)!), where $\mathbf{G_t^>}$ and $\mathbf{G_t^<}$ are again solutions of the homogeneous Eq. (2.320).

2.6.4 The Dyadic Green Functions Related to the Outer Dirichlet and Transmission Problem

Finally, let us consider the two Green functions which can be related to the two vectorial scattering problems. As in the case of the dyadic free-space Green function the Green function $\mathbf{G}_{\mathbf{\Gamma}_+}$ belonging to the ideal metallic scatterer as well as the Green function $\mathbf{G}^{(\mathbf{d})}_{\mathbf{\Gamma}_+}$ belonging to the dielectric scatterer are solutions of the inhomogeneous equations

$$\begin{aligned} \left[\nabla_{\mathbf{x}} \times \nabla_{\mathbf{x}} \times \; - k_0^2\right] \mathbf{G}_{\mathbf{\Gamma}_+}(\mathbf{x}, \mathbf{x}') &= \mathbf{I}\delta(\mathbf{x} - \mathbf{x}') \\ \left[\nabla_{\mathbf{x}} \times \nabla_{\mathbf{x}} \times \; - k_0^2\right] \mathbf{G}^{(\mathbf{d})}_{\mathbf{\Gamma}_+}(\mathbf{x}, \mathbf{x}') &= \mathbf{I}\delta(\mathbf{x} - \mathbf{x}'); \quad \mathbf{x}, \mathbf{x}' \in \Gamma_+. \end{aligned} \tag{2.341}$$

They are defined in the outer region Γ_+ only subject to the radiation condition (1.20) with respect to $\mathbf{x}$. But at the scatterer surface they have to fulfil additionally

- the homogeneous Dirichlet condition

$$\hat{n} \times \mathbf{G}_{\mathbf{\Gamma}_+}(\mathbf{x}, \mathbf{x}') = 0; \quad \mathbf{x} \in \partial\Gamma \tag{2.342}$$

  if we are interested in solving the outer Dirichlet problem (the vectorial case), or
- the transmission conditions

$$\hat{n}_- \times \mathbf{G}^{(\mathbf{d})}_{\mathbf{\Gamma}_+}(\mathbf{x}, \mathbf{x}') = \hat{n}_- \times \mathbf{G}^{(-/+)}(\mathbf{x}, \mathbf{x}') \tag{2.343}$$

$$\hat{n}_- \times \left[\nabla \times \mathbf{G}^{(\mathbf{d})}_{\mathbf{\Gamma}_+}(\mathbf{x}, \mathbf{x}')\right] = \hat{n}_- \times \left[\nabla \times \mathbf{G}^{(-/+)}(\mathbf{x}, \mathbf{x}')\right] \tag{2.344}$$

if we are interested in solving the outer transmission problem (the vectorial case).

$\mathbf{G}^{(-/+)}$ is again an auxiliary dyadic Green function with its source point outside the scatterer and the observation point inside, in general. Thus it is a solution of the homogeneous equation

$$\left[\nabla_{\mathbf{x}} \times \nabla_{\mathbf{x}} \times - k_s^2\right] \mathbf{G}^{(-/+)}(\mathbf{x}, \mathbf{x}') = 0; \quad \mathbf{x} \in \Gamma_-; \ \mathbf{x}' \in \Gamma_+ \tag{2.345}$$

within Γ_- subject to the regularity requirement.

Employing the dyadic-dyadic Green theorem we are able to prove the symmetry relations

$$\left[\mathbf{G}_{\mathbf{\Gamma}_+}(\mathbf{x}, \mathbf{x}')\right]^{tp} = \mathbf{G}_{\mathbf{\Gamma}_+}(\mathbf{x}', \mathbf{x}) \tag{2.346}$$

$$\left[\mathbf{G}^{(\mathbf{d})}_{\mathbf{\Gamma}_+}(\mathbf{x}, \mathbf{x}')\right]^{tp} = \mathbf{G}^{(\mathbf{d})}_{\mathbf{\Gamma}_+}(\mathbf{x}', \mathbf{x}). \tag{2.347}$$

The at first formal integral representation of the total field related to the outer Dirichlet and transmission problem is thus given by

$$\vec{u}_t(\mathbf{x}) = \int_{\Gamma_+} \mathbf{G}_{\mathbf{\Gamma}_+}(\mathbf{x}, \mathbf{x}') \cdot \vec{\rho}(\mathbf{x}')\, dV(\mathbf{x}') \tag{2.348}$$

and

$$\vec{u}_t(\mathbf{x}) = \int_{\Gamma_+} \mathbf{G}^{(\mathbf{d})}_{\mathbf{\Gamma}_+}(\mathbf{x}, \mathbf{x}') \cdot \vec{\rho}(\mathbf{x}')\, dV(\mathbf{x}'), \tag{2.349}$$

respectively. These integral representations can be derived in the same way as already done in conjunction with (2.286) and (2.287) in the scalar case but now by use of the vector-dyadic Green theorem. Concerning representation (2.348) and symmetry relation (2.346) this prove can be performed without any difficulties by the reader himself. To prove (2.349) as well as symmetry relation (2.347) requires a little bit more effort for which reason we will indicate the necessary steps in what follows:

At first we employ the vector-dyadic Green theorem with the quantities $\vec{\Psi}(\mathbf{x}) = \vec{u}_t(\mathbf{x})$ and $\mathbf{Q}(\mathbf{x}, \mathbf{x}') = \mathbf{G}^{(\mathbf{d})}_{\mathbf{\Gamma}_+}(\mathbf{x}, \mathbf{x}')$ in region Γ_+ thus providing

$$\begin{aligned}\vec{u}_t(\mathbf{x}') \ = & \int_{\Gamma_+} \vec{\rho}(\mathbf{x}) \cdot \mathbf{G}^{(\mathbf{d})}_{\mathbf{\Gamma}_+}(\mathbf{x}, \mathbf{x}')\, dV(\mathbf{x}) \\ & - \oint_{\partial\Gamma} \left\{\left[\hat{n}_- \times (\nabla \times \vec{u}_t(\mathbf{x}))\right] \cdot \mathbf{G}^{(\mathbf{d})}_{\mathbf{\Gamma}_+}(\mathbf{x}, \mathbf{x}') \right. \\ & \left. + \left[\hat{n}_- \times \vec{u}_t(\mathbf{x})\right] \cdot \left[\nabla_x \times \mathbf{G}^{(\mathbf{d})}_{\mathbf{\Gamma}_+}(\mathbf{x}, \mathbf{x}')\right]\right\} dS(\mathbf{x}).\end{aligned} \tag{2.350}$$

To show the vanishing of the boundary integral on the right hand side of (2.350) we use next the vector-dyadic Green theorem with the quantities $\vec{\Psi}(\mathbf{x}) = \vec{u}_{int}(\mathbf{x})$ and $\mathbf{Q}(\mathbf{x}, \mathbf{x}') = \mathbf{G}^{(-/+)}(\mathbf{x}, \mathbf{x}')$ in Γ_-. In doing so we obtain the expression

$$\oint_{\partial\Gamma} \Big\{ \Big[\hat{n} \times (\nabla \times \vec{u}_{int}(\mathbf{x}))\Big] \cdot \mathbf{G}^{(-/+)}(\mathbf{x}, \mathbf{x}') + \Big[\hat{n} \times \vec{u}_{int}(\mathbf{x})\Big] \cdot \Big[\nabla_x \times \mathbf{G}^{(-/+)}(\mathbf{x}, \mathbf{x}')\Big] \Big\} dS(\mathbf{x}) = 0 \tag{2.351}$$

since both quantities are solutions of the homogeneous vector-wave equation. Taking the transmission conditions (1.15), (1.16), (2.343), and (2.344) into account and employing identity (2.309) it can be shown that the boundary integrals in (2.350) and (2.351) are identical. But from this identity the vanishing of the boundary integral in (2.350) follows immediately. Then, if interchanging the variables $\mathbf{x}$ and $\mathbf{x}'$, and by use of symmetry relation (2.347) it follows (2.349).

The prove of symmetry relation (2.347) itself runs along the same track but with the difference that now the dyadic-dyadic Green theorem with the quantities $\mathbf{Q}(\mathbf{x}, \mathbf{x}') = \mathbf{G}^{(\mathbf{d})}_{\mathbf{\Gamma}_+}(\mathbf{x}, \mathbf{x}')$ and $\mathbf{P}(\mathbf{x}, \mathbf{x}'') = \mathbf{G}^{(\mathbf{d})}_{\mathbf{\Gamma}_+}(\mathbf{x}, \mathbf{x}'')$, or rather $\mathbf{Q}(\mathbf{x}, \mathbf{x}') = \mathbf{G}^{(-/+)}(\mathbf{x}, \mathbf{x}')$ and $\mathbf{P}(\mathbf{x}, \mathbf{x}'') = \mathbf{G}^{(-/+)}(\mathbf{x}, \mathbf{x}'')$ together with identity (2.312) must be employed.
Herewith we have reached the end of Chap.2. Now, let us shoulder the filled mathematical tool box and set of for discovering the so far formal Green functions related to the scattering problems of our interest. This will keep us busy during Chaps. 3 and 4.

Chapter 3
First Approach to the Green Functions: The Rayleigh Method

3.1 Introduction

In Sect. 1.3 we have considered a solution method for the scattering problems which was already used by Rayleigh to solve plane wave scattering on periodic gratings. Starting point was the approximation (1.21) of the scattered field by a finite series expansion in terms of any appropriate expansion functions. This approximation was assumed to hold everywhere in the outer region Γ_+. The unknown expansion coefficients in this approximation have been determined afterwards by use of the additional boundary conditions at the scatterer surface $\partial\Gamma$ (see (1.29), for example, if the outer Dirichlet problem is considered). Hereby it was assumed that the primary incident field is the known quantity. But if we look closer on (1.21) and (1.29) we can recognize two different sets of expansion functions. In (1.21), we have the expansion functions $|\,\varphi_{i,\tau}(k_0, \mathbf{x})\rangle$ defined everywhere in the outer region Γ_+. On the other hand, concerning equation (1.29) we used the expansion functions $|\,\varphi_{i,\tau}(k_0, \mathbf{x})\rangle_{\partial\Gamma}$ defined exclusively at the scatterer surface $\partial\Gamma$. The expansion coefficients resulting from the corresponding continuity conditions at the scatterer surface should have their meaning only for the approximation of the scattered field at this surface, as one might expect. Therefore, we have to clarify whether these expansion coefficients can be used also in approximation (1.21) or not. Before going into the details of deriving the Green function related to the outer Dirichlet problem of the Helmholtz and vector-wave equation we will clarify this aspect first.

The Green functions form the decisive link between the differential equation and integral equation formulation of the scattering problems, as we pointed out already in Sect. 2.5. It is exactly this property which will be used in this chapter to approximate the Green functions of the scattering problems by finite series expansions. The procedure is very similar to what is known for the corresponding approximation of Dirac's delta distribution. What does it mean? Let us consider for simplicity the one-dimensional problem with real-valued functions $f(x)$ defined in the interval $x \in [a, b]$. We can expand the function $f(x)$ in terms of some appropriate expansion

T. Rother and M. Kahnert, *Electromagnetic Wave Scattering on Nonspherical Particles*, Springer Series in Optical Sciences 145, DOI: 10.1007/978-3-642-36745-8_3,

functions $\varphi_i(x)$ according to

$$f^{(N)}(x) = \sum_{i=0}^{N} a_i \cdot \varphi_i(x). \tag{3.1}$$

Let us assume furthermore that these expansion functions form an orthogonal basis in the functional space of square-integrable functions defined on the interval $x \in [a, b]$ like the sine and cosine functions of the conventional Fourier method, for example. Then, if minimizing the mean square error, we can calculate the expansion coefficients of the approximation $f^{(N)}$ from

$$a_i = \int_a^b \varphi_i(x) \cdot f(x)\, dx. \tag{3.2}$$

Due to the assumed orthogonality of the expansion functions these expansion coefficients are final, i.e., they are independent of the truncation parameter N in the finite series (3.1) (see the remarks in Sect. 2.2.2 concerning the best approximation). Inserting (3.2) into (3.1) results in

$$f^{(N)}(x_j) = \sum_{i=0}^{N} \int_a^b \varphi_i(x_j) \cdot \varphi_i(x) \cdot f(x)\, dx \tag{3.3}$$

as the approximation of $f(x)$ in point $x_j \in [a, b]$. Dirac's delta distribution, on the other hand, is defined according to

$$\int_a^b \delta(x - x_j) \cdot f(x)\, dx := f(x_j). \tag{3.4}$$

Replacing $f(x_j)$ on the right hand side of this definition by expression (3.3), and after interchanging integration and summation (this can be done since we restrict our consideration to a finite series expansion) we get finally

$$\delta^{(N)}(x - x_j) = \sum_{i=0}^{N} \varphi_i(x) \cdot \varphi_i(x_j) \tag{3.5}$$

as the corresponding approximation of Dirac's delta distribution. That is the strategy we want to pursue in this chapter to get an approximation of the Green functions related to the scattering problems. Beside the clarification of the interrelation between the expansion coefficients in the approximations of the scattered field at the scatterer surface and in the outer region Γ_+ there is just one additional complication resulting from the assumed non-orthogonality but linearly independence of the relevant expansion functions. But before going into the details of this analysis we will start with the introduction and approximation of the scalar delta distribution at the scatterer

surface. This quantity becomes of interest when proving the continuity condition which has to be fulfilled by the Green function related to the outer Dirichlet problem, and in conjunction with the Lippmann-Schwinger equations we will derive at the end of Chap. 5.

3.2 The Scalar Delta Distribution at the Scatterer Surface

For a moment we keep staying at the scatterer surface $\partial\Gamma$ and consider sufficiently smooth functions $f(\mathbf{x})$ defined on this surface. In close analogy to (3.4) in the above considered one-dimensional case we define the scalar delta distribution $\delta_{\partial\Gamma}(\mathbf{x}' - \mathbf{x})$ at the scatterer surface according to

$$\oint_{\partial\Gamma} \delta_{\partial\Gamma}(\mathbf{x}' - \mathbf{x}) \cdot f(\mathbf{x}')\, dS(\mathbf{x}') \;:=\; f(\mathbf{x}); \quad \mathbf{x} \in \partial\Gamma. \tag{3.6}$$

Now, we look back to the results of Sect. 2.2 and use expansion (2.1) as an approximation of the function $f(\mathbf{x})$ in terms of the linearly independent functions $\varphi_i(\mathbf{x})$ (which must not necessarily be the radiating solutions of Helmholtz's equation):

$$f^{(N)}(\mathbf{x}) \;=\; \sum_{i=0}^{N} b_i^{(N)} \cdot \varphi_i(\mathbf{x}); \quad \mathbf{x} \in \partial\Gamma. \tag{3.7}$$

The expansion coefficients are calculated from Eq. (2.14). Taking the definition (1.34) of the scalar product into account we obtain

$$b_i^{(N)} \;=\; \sum_{j=0}^{N} [A_{\partial\Gamma}^{(g,\varphi)^{-1}}]_{i,j} \cdot \oint_{\partial\Gamma} g_j^*(\mathbf{x}') \cdot f(\mathbf{x}')\, dS(\mathbf{x}') \tag{3.8}$$

for the coefficients. Inserting these coefficients into (3.7), interchanging summation and integration, and comparing the resulting expression with (3.6) where we have again replaced on the right hand side of this latter equation $f(\mathbf{x})$ by its approximation (3.7) we end up with

$$\delta_{\partial\Gamma}^{(N)}(\mathbf{x}' - \mathbf{x}) \;=\; \sum_{i,j=0}^{N} \left[A_{\partial\Gamma}^{(g,\varphi)^{-1}}\right]_{i,j} \cdot \varphi_i(\mathbf{x}) \cdot g_j^*(\mathbf{x}'); \quad \mathbf{x}, \mathbf{x}' \in \partial\Gamma \tag{3.9}$$

as an appropriate approximation of the scalar surface delta distribution. That is,

$$\oint_{\partial\Gamma} \delta_{\partial\Gamma}^{(N)}(\mathbf{x}' - \mathbf{x}) \cdot f(\mathbf{x}')\, dS(\mathbf{x}') \;:=\; f^{(N)}(\mathbf{x}); \quad \mathbf{x} \in \partial\Gamma \tag{3.10}$$

was used as the corresponding definition of this approximation.

3.3 The Scalar Green Functions Related to the Helmholtz Equation

3.3.1 The Outer Dirichlet Problem

Now, we will answer the question if the expansion coefficients $a_i^{(N)}$ of approximation (1.21) of the scattered field $u_s(\mathbf{x})$ in the outer region Γ_+ are identical to the expansion coefficients $\alpha_i^{(N)}$ of approximation

$$u_s^{(N)}(\mathbf{x}) \;=\; \sum_{i=0}^{N} \alpha_i^{(N)} \cdot \varphi_i(k_0, \mathbf{x}); \quad \mathbf{x} \in \partial\Gamma \tag{3.11}$$

which holds for the scattered field at the scatterer surface. It is moreover assumed that in both approximations the radiating solutions (2.58) of the scalar Helmholtz equation are used as expansion functions (we would like to recall that in the scalar case considered in the following analysis we can neglect the τ-summation in (1.21)!). As frequently done, we employ again Green's theorem (2.239) but now with the two quantities $\Psi(\mathbf{x}) = u_s(\mathbf{x})$ and $\Phi(\mathbf{x}) = \varphi_i(k_0, \mathbf{x})$. Since u_s as well as φ_i are solutions of the homogeneous Helmholtz equation we get

$$\oint_{\partial\Gamma} \left[u_s(\mathbf{x}) \cdot \frac{\partial \varphi_i(k_0, \mathbf{x})}{\partial \hat{n}_-} \;-\; \varphi_i(k_0, \mathbf{x}) \cdot \frac{\partial u_s(\mathbf{x})}{\partial \hat{n}_-} \right] dS(\mathbf{x}) \;=\; 0. \tag{3.12}$$

$u_s(\mathbf{x})$ in the boundary integral on the right-hand side is next replaced by its approximation (3.11) valid at the scatterer surface. For its normal derivative $\partial u_s(\mathbf{x})/\partial \hat{n}_-$, on the other hand, we have to use approximation (1.21) instead. This is essential since according to the definition (1.7) we have to apply the ∇-operation on $u_s^{(N)}$ first. But this operation must be performed inside Γ_+ and can not be restricted to the scatterer surface. Only then we can apply the scalar multiplication with the normal vector $\hat{n}_-$. Thus, we have

$$\sum_{j=0}^{N} \oint_{\partial\Gamma} \left[\alpha_j^{(N)} \cdot \varphi_j(k_0, \mathbf{x}) \cdot \frac{\partial \varphi_i(k_0, \mathbf{x})}{\partial \hat{n}_-} \right.$$
$$\left. -a_j^{(N)} \cdot \varphi_i(k_0, \mathbf{x}) \cdot \frac{\partial \varphi_j(k_0, \mathbf{x})}{\partial \hat{n}_-} \right] dS(\mathbf{x}) \;=\; 0. \tag{3.13}$$

Furthermore, if employing Green's theorem (2.239) with the two quantities $\Psi(\mathbf{x}) = \varphi_i(k_0, \mathbf{x})$ and $\Phi(\mathbf{x}) = \varphi_j(k_0, \mathbf{x})$ it is easy to show that one gets the relation

$$\oint_{\partial\Gamma} \varphi_j(k_0, \mathbf{x}) \cdot \frac{\partial \varphi_i(k_0, \mathbf{x})}{\partial \hat{n}_-} \, dS(\mathbf{x}) = \oint_{\partial\Gamma} \varphi_i(k_0, \mathbf{x}) \cdot \frac{\partial \varphi_j(k_0, \mathbf{x})}{\partial \hat{n}_-} \, dS(\mathbf{x}). \tag{3.14}$$

Together with (3.13) this results into

$$\sum_{j=0}^{N} \left[\alpha_j^{(N)} - a_j^{(N)} \right] \cdot \oint_{\partial\Gamma} \varphi_j(\mathbf{x}) \cdot \frac{\partial \varphi_i(k_0, \mathbf{x})}{\partial \hat{n}_-} \, dS(\mathbf{x}) = 0 \tag{3.15}$$

which holds for all $i = 0, \ldots, N$. The boundary integral on the right hand side defines the elements $m_{i,j}$ of a matrix $\mathbf{M}$. If this matrix is invertible then we have for the expansion coefficients in the square brackets

$$a_j^{(N)} = \alpha_j^{(N)}. \tag{3.16}$$

That is, we can indeed use the coefficients resulting from the application of the continuity condition (1.29) in approximation (1.21). Since every linear combination of the radiating solutions of Helmholtz's equation is a radiating solution itself relation (3.16) holds also if we use the new expansion functions

$$\xi_i(k_0, \mathbf{x}) = \sum_{k=0}^{N} c_{i,k} \cdot \varphi_k(k_0, \mathbf{x}); \quad i = 0, \ldots, N \tag{3.17}$$

instead of the old functions φ_i, and if the resulting matrix $\mathbf{M}$ is again invertible. The invertability of the infinite-dimensional matrix $\mathbf{M}$ (i.e., for the matrix with elements $m_{i,j}$; $i, j = 0, \ldots, N$, and N tends to infinity) can be ensured mathematically only if the radiating solutions form a basis in the functional space $L_2(\partial\Gamma)$. The invertibility of the finite-dimensional matrix, on the other hand, requires only the linearly independence of the expansion functions as it was already discussed in Sect. 2.3.3. But if we have a scatterer geometry whose surface is not of C^2 or Liapounoff type then we can prove the invertibility of the finite-dimensional matrix only by a numerical procedure according to our pragmatic point of view on the convergence behaviour formulated in Sect. 2.3.1. This situation belongs to most of the realistic problems. But it should be also emphasized at this point that the usage of approximation (1.21) for the scattered field everywhere outside the scatterer is not without controversy and strongly related to the problem of the Rayleigh hypothesis we will discuss throughout Chap. 6.

Now we are prepared to approximate the Green function G_{Γ_+} belonging to the outer Dirichlet problem. The cooking recipe for this undertaking is as follows:

First step:

We expand the primary incident field u_{inc} at the scatterer surface according to (2.1) into a series in terms of the functions $\psi_i(k_0, \mathbf{x})$. These could be the regular

eigensolutions of Helmholtz's equation, for example, but not necessarily. The corresponding expansion coefficients $b_i^{(N)}$ are then calculated according to (2.14) and (2.15).

Second step:

Utilizing the transformation character (2.18) of the T-matrix (2.19) we accomplish the transition from the expansion functions $\psi_i(k_0, \mathbf{x})$ to the radiating solutions $\varphi_i(k_0, \mathbf{x})$ in the approximation of the primary incident field at the scatterer surface. The new expansion coefficients $a_i^{(N)}$ are calculated according to (2.23) from the old coefficients $b_i^{(N)}$. Due to the identical definitions (2.15) and (2.22) of both matrices $\mathbf{A}_{\partial\Gamma}^{(g,\psi_0)}$ and $\mathbf{B}_{\partial\Gamma}^{(g,\psi_0)}$ which appear in equations (2.14) and (2.19) we get from the continuity condition (1.29) and from the above derived relation (3.16) the following approximation for the scattered field u_s in the outer region Γ_+:

$$u_s^{(N)}(\mathbf{x}) \;=\; -\sum_{i,j=0}^{N} \left[A_{\partial\Gamma}^{(g,\varphi_0)^{-1}}\right]_{i,j} \cdot < g_j \,|\, u_{inc} >_{\partial\Gamma} \cdot \varphi_i(k_0, \mathbf{x}); \quad \mathbf{x} \in \Gamma_+. \tag{3.18}$$

Let us write the scalar product $< g_j \,|\, u_{inc} >_{\partial\Gamma}$ in this equation more explicitly. With definition (1.34) we obtain

$$\begin{aligned} u_s^{(N)}(\mathbf{x}) = \; -\sum_{i,j=0}^{N} \left[A_{\partial\Gamma}^{(g,\varphi_0)^{-1}}\right]_{i,j} \cdot \oint_{\partial\Gamma} g_j^*(\mathbf{x}') \cdot u_{inc}(\mathbf{x}')\, dS(\mathbf{x}') \\ \cdot \varphi_i(k_0, \mathbf{x}); \quad \mathbf{x} \in \Gamma_+,\ \mathbf{x}' \in \partial\Gamma, \end{aligned} \tag{3.19}$$

or, if interchanging summation and integration, and after a few rearrangements:

$$\begin{aligned} u_s^{(N)}(\mathbf{x}) = \; -\oint_{\partial\Gamma} \sum_{i,j=0}^{N} \left[A_{\partial\Gamma}^{(g,\varphi_0)^{-1}}\right]_{i,j} \cdot \varphi_i(k_0, \mathbf{x}) \cdot g_j^*(\mathbf{x}') \\ \cdot u_{inc}(\mathbf{x}')\, dS(\mathbf{x}'); \quad \mathbf{x} \in \Gamma_+,\ \mathbf{x}' \in \partial\Gamma. \end{aligned} \tag{3.20}$$

The weighting functions $g_j(\mathbf{x})$ are not yet specified, and we will keep this situation to allow for a certain degree of flexibility in the ongoing analysis. But if they are specified, then, with expression (3.20) we have already found an approximate solution of the outer Dirichlet problem! If we choose the same set of functions as weighting and expansion functions, for example, the primary incident field at the scatterer surface is approximated in terms of the best approximation discussed in Sect. 2.2 Replacing $u_{inc}(\mathbf{x}')$ in the boundary integral on the right hand side of (3.20) by the approximation (1.28) we obtain once again the relation (1.42) between the expansion coefficients of the scattered and primary incident field. If the primary incident field is given by the plane wave (2.102), for example, and if we use in approximation (1.28) the regular eigensolutions of the Helmholtz equation, then the expansion coefficients b_i of the plane wave are given by (2.108). But deriving the Green function of the

outer Dirichlet problem (or, better, its approximation) from approximation (3.20) requires some additional steps.

Third step:

We use Green's theorem (2.239) with the two functions $\Psi(\mathbf{x}) = u_s(\mathbf{x})$ and $\Phi(\mathbf{x}) = G_{\Gamma_+}(\mathbf{x}, \mathbf{x}')$. u_s is a solution of the homogeneous Helmholtz equation whereas G_{Γ_+} is a solution of the inhomogeneous Helmholtz equation. Taking the boundary conditions (1.10) and (2.280) as well as the radiation condition at S_∞ into account provides

$$u_s(\mathbf{x}) \;=\; \oint_{\partial\Gamma} \frac{\partial G_{\Gamma_+}(\mathbf{x}', \mathbf{x})}{\partial \hat{n}'_-} \cdot u_{inc}(\mathbf{x}')\, dS(\mathbf{x}') \tag{3.21}$$

as a representation of the scattered field in Γ_+.

$$G_{\partial\Gamma}(\mathbf{x}, \mathbf{x}') \;:=\; \frac{\partial G_{\Gamma_+}(\mathbf{x}', \mathbf{x})}{\partial \hat{n}'_-} \;=\; \hat{n}'_- \cdot \nabla_{x'} G_{\Gamma_+}(\mathbf{x}', \mathbf{x}) \qquad \mathbf{x} \in \Gamma_+,\ \mathbf{x}' \in \partial\Gamma \tag{3.22}$$

is the definition of the surface Green function $G_{\partial\Gamma}$ belonging to the Green function G_{Γ_+}. Please, note that one argument of the surface Green function is always located at the scatterer surface. The other argument can be located everywhere in G_{Γ_+}. With this surface Green function we can reformulate Eq. (3.21) into

$$u_s(\mathbf{x}) \;=\; \oint_{\partial\Gamma} G_{\partial\Gamma}(\mathbf{x}, \mathbf{x}') \cdot u_{inc}(\mathbf{x}')\, dS(\mathbf{x}'). \tag{3.23}$$

Comparing this equation with (3.20) provides

$$G^{(N)}_{\partial\Gamma}(\mathbf{x}, \mathbf{x}') \;=\; -\sum_{i,j=0}^{N} \left[A^{(g,\varphi_0)^{-1}}_{\partial\Gamma}\right]_{i,j} \cdot \varphi_i(k_0, \mathbf{x}) \cdot g^*_j(\mathbf{x}') \;; \qquad \mathbf{x}' \in \partial\Gamma,\ \mathbf{x} \in \Gamma_+. \tag{3.24}$$

as an appropriate approximation of the surface Green function. The corresponding approximation of the Green function G_{Γ_+} is obtained by two additional steps.

Fourth step:

From (1.8), (2.271), (1.286), (3.23), and by assuming that the source $\rho(\mathbf{x})$ of the primary incident field is located somewhere in the outer region Γ_+ we obtain

$$\int_{\Gamma_+} G_{\Gamma_+}(\mathbf{x}, \mathbf{x}') \cdot \rho(\mathbf{x}')\, dV(\mathbf{x}') = \int_{\Gamma_+} G_0(\mathbf{x}, \mathbf{x}') \cdot \rho(\mathbf{x}')\, dV(\mathbf{x}') + \oint_{\partial\Gamma} G_{\partial\Gamma}(\mathbf{x}, \mathbf{x}') \cdot u_{inc}(\mathbf{x}')\, dS(\mathbf{x}'). \tag{3.25}$$

Next, we use again (2.271) to replace $u_{inc}(\mathbf{x}')$ on the right-hand side of this expression. Comparing the integrands on both sides of the resulting equation provides

$$G_{\Gamma_+}(\mathbf{x},\mathbf{x}') \;=\; G_0(\mathbf{x},\mathbf{x}') \;+\; \oint_{\partial\Gamma} G_{\partial\Gamma}(\mathbf{x},\bar{\mathbf{x}})\cdot G_0(\bar{\mathbf{x}},\mathbf{x}')\,dS(\bar{\mathbf{x}}) \tag{3.26}$$

as the relation between the Green function G_{Γ_+} of the outer Dirichlet problem and its surface Green function $G_{\partial\Gamma}$. This relation turns out to be very important for all our ongoing discussions and can be considered as Huygens' principle formulated solely in terms of Green functions. Of course, it is usually not allowed to infer the equality of integrands from the equality of the integrals. The way we used above to derive (3.26) is therefore only a way of plausibility although it is in agreement with the linear superposition of the primary incident and scattered field to the total field. Another possibility to derive (3.26) which avoids this problem is offered with Green's theorem (2.239) employed with the two quantities $\Psi(\mathbf{x}) = G_{\Gamma_+}(\mathbf{x},\mathbf{x}'')$ and $\Phi(\mathbf{x}) = G_0(\mathbf{x},\mathbf{x}')$. We get

$$G_{\Gamma_+}(\mathbf{x}',\mathbf{x}'') \;=\; G_0(\mathbf{x}'',\mathbf{x}') \;+\; \oint_{\partial\Gamma} G_{\partial\Gamma}(\mathbf{x}'',\mathbf{x})\cdot G_0(\mathbf{x},\mathbf{x}')\,dS(\mathbf{x}). \tag{3.27}$$

From this expression (3.26) follows immediately if taking the symmetry relations (2.245) and (2.284) into account.

Fifth step:

We replace the surface Green function on the right-hand side of (3.26) by its approximation (3.24) and obtain

$$\begin{aligned} G^{(N)}_{\Gamma_+}(\mathbf{x},\mathbf{x}') &= G_0(\mathbf{x},\mathbf{x}') \\ &\quad - \sum_{i,j=0}^{N} \left[A_{\partial\Gamma}^{(g,\varphi_0)^{-1}}\right]_{i,j}\cdot \varphi_i(k_0,\mathbf{x})\cdot \tilde{g}_j^*(\mathbf{x}')\;; \quad \mathbf{x},\mathbf{x}'\in\Gamma_+ \end{aligned} \tag{3.28}$$

with $\tilde{g}_j^*(\mathbf{x}')$ therein given by

$$\tilde{g}_j^*(\mathbf{x}') \;=\; \oint_{\partial\Gamma} g_j^*(\bar{\mathbf{x}})\cdot G_0(\bar{\mathbf{x}},\mathbf{x}')\,dS(\bar{\mathbf{x}}). \tag{3.29}$$

Next, let us replace in this last expression the free-space Green function G_0 by the expansion (2.278) of $G_0^<$ thus providing

$$\tilde{g}_j^*(\mathbf{x}') \;=\; (ik_0)\sum_{k=0}^{N}\left[B_{\partial\Gamma}^{(g,\psi_0)}\right]_{j,k}\cdot\tilde{\varphi}_k(k_0,\mathbf{x}') \tag{3.30}$$

with matrix elements $\left[B_{\partial\Gamma}^{(g,\psi_0)}\right]_{j,k}$ defined in (2.22). The usage of $G_0^<$ instead of G_0 in (3.29) is allowed only if **the source point $\mathbf{x}'$ of the primary incident field is located somewhere outside the smallest spherical surface circumscribing the scatterer!** But, as we will see later, this assumption provides no restriction for the plane wave scattering problems. With this replacement we get from (3.28) the final approximation

$$G_{\Gamma_+}^{(N)}(\mathbf{x},\mathbf{x}') = G_0(\mathbf{x},\mathbf{x}') \; - \; (ik_0) \cdot \sum_{i,k=0}^{N} [T_{\partial\Gamma}]_{i,k} \cdot \varphi_i(k_0,\mathbf{x}) \cdot \tilde{\varphi}_k(k_0,\mathbf{x}') \; ; \mathbf{x},\mathbf{x}' \in \Gamma_+ \tag{3.31}$$

of the Green function G_{Γ_+} related to the outer Dirichlet problem. Since the second term on the right-hand side of (3.31) represents the scattering part of the Green function, from which one can calculate the scattered field, we will denote it with $G_s(\mathbf{x},\mathbf{x}')$, i.e., we write

$$G_{\Gamma_+}^{(N)}(\mathbf{x},\mathbf{x}') \; = \; G_0(\mathbf{x},\mathbf{x}') \; + \; G_s^{(N)}(\mathbf{x},\mathbf{x}') \tag{3.32}$$

with G_s given by

$$G_s^{(N)}(\mathbf{x},\mathbf{x}') \; = \; - \, (ik_0) \sum_{i,k=0}^{N} [T_{\partial\Gamma}]_{i,k} \cdot \varphi_i(k_0,\mathbf{x}) \cdot \tilde{\varphi}_k(k_0,\mathbf{x}'). \tag{3.33}$$

This is a remarkable result since the matrix elements

$$[T_{\partial\Gamma}]_{i,k} \; = \; \sum_{j=0}^{N} \left[A_{\partial\Gamma}^{(g,\varphi_0)^{-1}}\right]_{i,j} \cdot \left[B_{\partial\Gamma}^{(g,\psi_0)}\right]_{j,k} \tag{3.34}$$

are nothing but the elements of the transformation matrix (2.19). We can state moreover that $G_{\Gamma_+}^{(N)}(\mathbf{x},\mathbf{x}')$ solves the defining equation (2.279) subject to the radiation condition with respect to $\mathbf{x}$. But what happens with the additional boundary condition (2.280)? Looking back at Huygens' principle (3.26) one can infer that this condition will be fulfilled if

$$G_{\partial\Gamma}(\mathbf{x},\bar{\mathbf{x}}) \; = \; -\delta_{\partial\Gamma}(\bar{\mathbf{x}}-\mathbf{x}) \tag{3.35}$$

holds for every $\mathbf{x} \in \partial\Gamma$. Comparing (3.9) with (3.24) reveals that this is indeed true for the respective approximations, i.e., that

$$G_{\partial\Gamma}^{(N)}(\mathbf{x},\bar{\mathbf{x}}) \; = \; -\delta_{\partial\Gamma}^{(N)}(\bar{\mathbf{x}}-\mathbf{x}) \tag{3.36}$$

holds if the expansion functions in (3.9) are the radiating solutions of Helmholtz's equation. Therefore, with (3.31)/(3.34) we have found an appropriate approximation of the Green function related to the outer Dirichlet problem we were looking for. Its usefulness must be proven in real applications, of course.

Approximation (3.31) of the Green function G_{Γ_+} becomes especially simple if the limiting case of a spherical scatterer geometry is considered. From this limiting expression the result of the conventional Mie theory can be derived without any problems if the primary incident field is given by the plane wave (2.102), and if using the regular solutions $\psi_i(k_0 r, \theta, \phi)$ according to (2.57) as weighting functions. Due to the orthogonality relations (2.96) and (2.97) valid at the surface of a sphere with radius $r = a$ the matrices (1.39) and (1.40) defining the T-matrix become diagonal matrices of the form

$$\left[A_{\partial\Gamma}^{(\psi_0,\varphi_0)}\right]_{i,k} = \delta_{i,k} \cdot \frac{1}{a^2} \cdot j_{n(i)}^*(k_0 a) \cdot h_{n(i)}^{(1)}(k_0 a) \tag{3.37}$$

and

$$\left[B_{\partial\Gamma}^{(\psi_0,\psi_0)}\right]_{i,k} = \delta_{i,k} \cdot \frac{1}{a^2} \cdot j_{n(i)}^*(k_0 a) \cdot j_{n(i)}(k_0 a). \tag{3.38}$$

The scattering part (3.33) of the Green function reads therefore

$$G_s^{(N)}(\mathbf{x}, \mathbf{x}') = -(ik_0) \sum_{i=0}^{N} \frac{j_{n(i)}(k_0 a)}{h_{n(i)}^{(1)}(k_0 a)} \cdot \varphi_i(\mathbf{x}) \cdot \tilde{\varphi}_i(\mathbf{x}'), \tag{3.39}$$

and the corresponding approximation of the surface Green function becomes

$$G_{\partial\Gamma}^{(N)}(\mathbf{x}, \mathbf{x}') = -\frac{1}{a^2} \sum_{i=0}^{N} \left[j_{n(i)}^*(k_0 a) \cdot h_{n(i)}^{(1)}(k_0 a)\right]^{-1} \cdot \varphi_i(k_0, \mathbf{x}) \cdot \psi_i^*(k_0, \mathbf{x}'). \tag{3.40}$$

At the end of this subsection let us consider the scattering problem of a plane wave given by (2.109). Therewith we want to show that (2.286) together with (3.32) provides the representation of the scattered field we have already considered in the first chapter of this book in the context of Rayleigh's method . This ought to convince us from the equivalence of the differential and integral point of views on the level of the respective approximations.

With (1.21), (1.42), and with the radiating solutions (2.58) as expansion functions we get for the scattered field in spherical coordinates

$$u_s^{(N)}(k_0 r, \theta, \phi) = -\sum_{i,k=0}^{N} [T_{\partial\Gamma}]_{i,k} \cdot b_k \cdot \varphi_i(k_0 r, \theta, \phi). \tag{3.41}$$

b_k are the expansion coefficients of the primary incident plane wave (2.109) given by

$$b_k \;=\; E_0\, 4\pi\, \tilde{Y}_k^*(\theta_i, \phi_i) \tag{3.42}$$

according to (2.113). In conjunction with (1.8), (2.286), and (3.33) we get on the other hand

$$u_s^{(N)}(k_0 r, \theta, \phi) = -(ik_0) \sum_{i,k=0}^{N} [T_{\partial\Gamma}]_{i,k} \cdot \varphi_i(k_0 r, \theta, \phi) \cdot \int_{\Gamma_+} \tilde{\varphi}_k(k_0, \mathbf{x}') \cdot \rho(\mathbf{x}')\, dV(\mathbf{x}'). \tag{3.43}$$

Both representations become identical if the coefficients

$$\tilde{b}_k \;=\; (ik_0) \int_{\Gamma_+} \tilde{\varphi}_k(k_0, \mathbf{x}') \cdot \rho(\mathbf{x}')\, dV(\mathbf{x}') \tag{3.44}$$

calculated by use of the source distribution (2.272) are identical with the coefficients b_k of (3.42). Since we have Dirac's delta distribution in (2.272) it follows

$$\tilde{b}_k \;=\; (ik_0)\, 4\pi E_0 \cdot \tilde{\varphi}_k(k_0 r_i, \theta_i, \phi_i) \cdot r_i \cdot e^{-ik_0 r_i} \tag{3.45}$$

Please, mind the difference that we denote $|\mathbf{x}'_\mathbf{q}|$ with r_i in spherical coordinates. Moreover, the subindex k denotes the combined summation index and should not be confused with the parameter k characterizing the region physically. Then, it is not to difficult to show that both sets of expansion coefficients $\tilde{b}_k$ and b_k are indeed identical. For this we have to employ definition (2.85), both relations (2.62) and (2.63) (the latter is necessary because of (2.274) which provides the spherical harmonics with arguments $Y_{l,n}(\pi - \theta_i, \phi_i \pm \pi)$!), and the asymptotic behaviour resulting from (2.78) for large arguments $k_0 r_i$.

With this prove of equivalence we have established at the same time a way to arrive at expansion (2.113) for a general plane wave travelling along an arbitrary direction $\vec{k}_i$, and if starting from the integral representation (2.271) of the primary incident field. In (2.271), we must only replace G_0 by $G_0^<$ according to (2.278). In conjunction with the source distribution (2.272) and the asymptotic behaviour of the radiating expansion functions $\tilde{\varphi}_k(k_0 r_i, \theta_i, \phi_i)$ for large arguments $k_0 r_i$ we end up in a straightforward way with (2.113). This way of deriving the expansion of a plane wave foreshadows already the somehow strange nature of the physical object "plane wave". On the one hand, expansion (2.113) is assumed to hold everywhere in the entire free space Γ. On the other hand, this space must contain somewhere the source distribution (2.272). Then there exist observation points (r, θ, ϕ) nearby the source point (r_i, θ_i, ϕ_i) for which the usage of $G_0^<(\mathbf{x}, \mathbf{x}')$ is actually not allowed since the condition $|\mathbf{x}| < |\mathbf{x}'|$ is violated. From this we would infer that expansion (2.113) is not a valid representation of a plane wave everywhere in Γ. But we know

also that the plane wave solves the homogeneous Helmholtz equation without any source. That is, the plane wave is smoke without fire, so to say. Isn't it a strange situation? We will come back to it in Chap. 7.

3.3.2 The Outer Transmission Problem

With the following two steps we arrive at the approximation of the Green function $G^{(d)}_{\Gamma_+}$ of the outer transmission problem:

First step:

We go back to the transmission conditions (1.46) and (1.47) but by cancelling the additional τ-summation therein due to the restriction to the scalar case. For the expansion functions (1.48)–(1.53) appearing in these conditions we use the regular as well as the radiating eigensolutions of Helmholtz's equation defined in Sect. 2.3.1. Employing the shorter matrix notation introduced in (1.44) we thus have the two equations

$$\vec{\varphi}_0(\mathbf{x}) \cdot \vec{a}^{\,(N)^{tp}} - \vec{\psi}(\mathbf{x}) \cdot \vec{c}^{\,(N)^{tp}} = -\vec{\psi}_0(\mathbf{x}) \cdot \vec{b}^{\,tp} \tag{3.46}$$

$$\partial_{\hat{n}} \vec{\varphi}_0(\mathbf{x}) \cdot \vec{a}^{\,(N)^{tp}} - \partial_{\hat{n}} \vec{\psi}(\mathbf{x}) \cdot \vec{c}^{\,(N)^{tp}} = -\partial_{\hat{n}} \vec{\psi}_0(\mathbf{x}) \cdot \vec{b}^{\,tp}. \tag{3.47}$$

Please, have in mind that the regular functions $\psi_i(\mathbf{x})$ contain the parameter k in their arguments to characterize the physical property of the scatterer. Contrariwise, the regular functions $\psi_{0_i}(\mathbf{x})$ as well as the radiating solutions $\varphi_{0_i}(\mathbf{x})$ contain the parameter k_0 related to the free space which is assumed to be vacuum. According to the procedure described in Sect. 1.3.2. we could apply a scalar multiplication with the weighting functions $g_j(\mathbf{x})$ and $h_j(\mathbf{x})$ $(j = 0, \ldots, N)$ to these two equations to generate the two equation systems (1.62) and (1.63). Eliminating the expansion coefficients $\vec{c}^{\,(N)}$ belonging to the approximation of the internal field would produce the T-matrix to interrelate the expansion coefficients $\vec{a}^{\,(N)}$ of the scattered field we sought-after to the known expansion coefficients $\vec{b}$ of the primary incident field. But here we will take the other way which was already introduced when discussing the transformation character of the T-matrix in Sect. 2.2.3. (see especially the discussion concerning relations (2.24)–(2.32) in this section). As a result we get **one** equation from both transmission conditions (3.46) and (3.47) which can be treated as a modification of the Dirichlet condition related to the outer Dirichlet problem. However, this modified condition contains the real Dirichlet condition of the outer Dirichlet problem as a limiting case. For this we must first eliminate the unknown expansion coefficients $\vec{a}^{\,(N)}$ of the scattered field from the equation systems (1.62) and (1.63). Thus we get the relation

$$\vec{c}^{\,(N)^{tp}} = \mathbf{T}_{\psi} \cdot \vec{b}^{\,tp} \tag{3.48}$$

between the expansion coefficients of the internal and primary incident field. The quantity $\mathbf{T}_\psi$ therein is given by expression (2.29). Inserting (3.48) into (3.46) provides

$$\vec{\varphi}_0(\mathbf{x}) \cdot \vec{a}^{\,(N)\,tp} \;=\; \vec{\psi}(\mathbf{x}) \cdot \mathbf{T}_\psi \cdot \vec{b}^{\,tp} \;-\; \vec{\psi}_0(\mathbf{x}) \cdot \vec{b}^{\,tp}. \tag{3.49}$$

Next, we approximate the functions $\psi_i(\mathbf{x})$ at the scatterer surface by linear combinations of the functions $\psi_{0_i}(\mathbf{x})$ according to relation (2.31). The latter functions are also considered at the scatterer surface only. Thus, we obtain

$$\vec{\varphi}_0(\mathbf{x}) \cdot \vec{a}^{\,(N)\,tp} \;=\; -\,\vec{\psi}_0(\mathbf{x}) \cdot \left[\mathbf{E} \;-\; \mathbf{T}_{\psi_0/\psi} \cdot \mathbf{T}_\psi\right] \cdot \vec{b}^{\,tp} \tag{3.50}$$

or alternatively

$$\vec{\varphi}_0(\mathbf{x}) \cdot \vec{a}^{\,(N)\,tp} \;=\; -\,\vec{\psi}_0(\mathbf{x}) \cdot \vec{\tilde{b}}^{\,(N)\,tp} \tag{3.51}$$

with the new coefficients

$$\vec{\tilde{b}}^{\,(N)\,tp} \;=\; \left[\mathbf{E} \;-\; \mathbf{T}_{\psi_0/\psi} \cdot \mathbf{T}_\psi\right] \cdot \vec{b}^{\,tp}. \tag{3.52}$$

These new coefficients are dependent on the upper summation index N (they are not final any more!). They can be considered as expansion coefficients of a modified primary incident field at the scatterer surface. But this results in the modification

$$u_s(\mathbf{x}) \;=\; -\,\tilde{u}_{inc}(\mathbf{x})\,; \quad \mathbf{x} \in \partial\Gamma \tag{3.53}$$

of condition (1.10). That is, coefficients $\vec{\tilde{b}}^{\,(N)}$ are the expansion coefficients of the approximation of the modified field $\tilde{u}_{inc}$ at the scatterer surface. Equations (3.51) and (3.53) are thus a representation of the modified outer Dirichlet problem.

Second step:

For the Green function related to the outer Dirichlet problem we could derive approximation (3.32)/(3.33) in the foregoing section. Now, if replacing matrix $\mathbf{T}_{\partial\Gamma}$ in approximation (3.33) by matrix

$$\mathbf{T}^{(d)}_{\partial\Gamma} \;=\; \mathbf{T}_{\partial\Gamma} \cdot \left[\mathbf{E} \;-\; \mathbf{T}_{\psi_0/\psi} \cdot \mathbf{T}_\psi\right] \tag{3.54}$$

we obtain

$$G^{(d,N)}_{\Gamma_+}(\mathbf{x}, \mathbf{x}') \;=\; G_0(\mathbf{x}, \mathbf{x}') \;+\; G^{(d,N)}_s(\mathbf{x}, \mathbf{x}') \tag{3.55}$$

as an approximation of the Green function related to the outer transmission problem. The scattering contribution of this Green function is then given by

$$G^{(d,N)}_s(\mathbf{x}, \mathbf{x}') = \; -(ik_0) \sum_{i,k=0}^{N} \left[T^{(d)}_{\partial\Gamma}\right]_{i,k} \cdot \varphi_i(k_0, \mathbf{x}) \cdot \tilde{\varphi}_k(k_0, \mathbf{x}'). \tag{3.56}$$

The transformation matrix (3.54) was already derived in conjunction with equations (2.28) and (2.32). Obviously, if we choose $\mathbf{T}_\psi \equiv 0$, approximation (3.55) of the Green function related to the outer transmission problem becomes identical with the approximation of the Green function G_{Γ_+} related to the outer Dirichlet problem. Equation (3.55) in conjunction with (3.56) is moreover a solution of the inhomogeneous Helmholtz equation (2.279) subject to the radiation condition with respect to the variable $\mathbf{x}$. The prove of the fulfilment of boundary conditions (2.281) and (2.282) in the sense of this approximation will be shifted to Chap. 4.

Let us now consider the corresponding approximations of the dyadic Green functions.

3.4 The Dyadic Delta Distribution at the Scatterer Surface

The dyadic delta distribution $\mathbf{D}(\mathbf{x}-\mathbf{x}') = \mathbf{I}\delta(\mathbf{x}-\mathbf{x}')$ as the relevant inhomogeneity of the dyadic free-space Green function was already introduced in Sect. 2.6.3. In close analogy to (3.6) we are also able to define a corresponding dyadic delta distribution at the scatterer surface by the integral relation

$$\oint_{\partial\Gamma} \mathbf{D}_{\partial\Gamma}(\mathbf{x}'-\mathbf{x}) \cdot \vec{f}(\mathbf{x}')\, dS(\mathbf{x}') \;:=\; \vec{f}(\mathbf{x}); \quad \mathbf{x}, \mathbf{x}' \in \partial\Gamma. \tag{3.57}$$

But due to the boundary conditions (1.12) and (1.18) we are rather interested in a dyadic delta distribution for the special case of the tangential projections $\vec{f}^{\,\hat{n}}$ of the vector functions $\vec{f}$ at the surface $\partial\Gamma$. For our purposes it is therefore more convenient to define a dyadic delta distribution $\mathbf{D}_{\partial\mathbf{\Gamma}}^{(\hat{\mathbf{n}})}$ at the scatterer surface according to

$$\oint_{\partial\Gamma} \mathbf{D}_{\partial\mathbf{\Gamma}}^{(\hat{\mathbf{n}})}(\mathbf{x}'-\mathbf{x}) \cdot \vec{f}^{\,\hat{n}'}(\mathbf{x}')\, dS(\mathbf{x}') \;:=\; \vec{f}^{\,\hat{n}}(\mathbf{x}); \quad \mathbf{x}', \mathbf{x} \in \partial\mathbf{\Gamma}. \tag{3.58}$$

As already demonstrated in the scalar case we can approximate this specific dyadic delta distribution by a finite series expansion so that

$$\oint_{\partial\Gamma} \mathbf{D}_{\partial\mathbf{\Gamma}}^{(\hat{\mathbf{n}},\mathbf{N})}(\mathbf{x}'-\mathbf{x}) \cdot \vec{f}^{\,\hat{n}'}(\mathbf{x}')\, dS(\mathbf{x}') \;=\; \vec{f}^{\,(\hat{n},N)}(\mathbf{x}); \quad \mathbf{x}', \mathbf{x} \in \partial\Gamma \tag{3.59}$$

holds. To derive its approximation we go back to the results of Sect. 2.2. First we expand the tangential projections $\vec{f}^{\,\hat{n}}(\mathbf{x})$ of the vector functions $\vec{f}(\mathbf{x})$ at the scatterer surface into a finite series in terms of the vector functions $\vec{\varphi}_{i,\tau}^{\,\hat{n}}(\mathbf{x})$ according to (2.1). The expansion functions are not necessarily the radiating solutions of the vector-wave equation but they are assumed to be linearly independent at the scatterer surface. This provides

$$\vec{f}^{\,(\hat{n},N)}(\mathbf{x}) \;=\; \sum_{\tau=1}^{2} \sum_{i=0}^{N} b_{i,\tau}^{(N)} \cdot \vec{\varphi}_{i,\tau}^{\,\hat{n}}(\mathbf{x}); \quad \mathbf{x} \in \partial\Gamma \tag{3.60}$$

Please, note that the τ-summation cannot be neglected in the vector case. The expansion coefficients therein are again calculated from relation (2.14). With the definition (1.35) of the relevant scalar product we obtain the explicit expression

$$b_{i,\tau}^{(N)} = \sum_{\tau'=1}^{2} \sum_{j=0}^{N} [A_{\partial\Gamma}^{(g,\varphi)^{-1}}]_{i,j}^{\tau,\tau'} \cdot \oint_{\partial\Gamma} \vec{g}_{j,\tau'}^{\,*}(\mathbf{x}') \cdot \vec{f}^{\,\hat{n}'}(\mathbf{x}')\, dS(\mathbf{x}'). \tag{3.61}$$

Inserting these coefficients into (3.60), interchanging summation and integration, and comparing the result with (3.59) provides finally

$$\mathbf{D}_{\partial\mathbf{\Gamma}}^{(\hat{\mathbf{n}},\mathbf{N})}(\mathbf{x}' - \mathbf{x}) = \sum_{\tau,\tau'=1}^{2} \sum_{i,j=0}^{N} \left[A_{\partial\Gamma}^{(g,\varphi)^{-1}} \right]_{i,j}^{\tau,\tau'} \cdot \left\{ \vec{\varphi}_{i,\tau}^{\,\hat{n}}(\mathbf{x}) \odot \vec{g}_{j,\tau'}^{\,*}(\mathbf{x}') \right\} \tag{3.62}$$

as the appropriate approximation of the dyadic delta distribution (3.58).

The calculation of the elements of matrix $\mathbf{A}_{\partial\Gamma}^{(g,\varphi)}$ by use of (1.39) requires the calculation of the scalar product (1.35) of the weighting functions $\vec{g}_{j,\tau'}$ with the tangential projections $\vec{\varphi}_{i,\tau}^{\,\hat{n}}$ of the vector functions $\vec{\varphi}_{i,\tau}$. To distinguish the vector case from the scalar case in what follows and to avoid misunderstandings we will introduce an additional mark "$\hat{n}$" in the upper indices attached to the matrices if the tangential projections of vector functions are used. Mark "$\hat{n}$" is replaced by "$\hat{n}_-$" if the scatterer surface is considered to be the inner boundary surface of the outer region Γ_+. Instead of (3.62) we write therefore

$$\mathbf{D}_{\partial\mathbf{\Gamma}}^{(\hat{\mathbf{n}},\mathbf{N})}(\mathbf{x}' - \mathbf{x}) = \sum_{\tau,\tau'=1}^{2} \sum_{i,j=0}^{N} \left[A_{\partial\Gamma}^{(g,\varphi^{\hat{n}})^{-1}} \right]_{i,j}^{\tau,\tau'} \cdot \left\{ \vec{\varphi}_{i,\tau}^{\,\hat{n}}(\mathbf{x}) \odot \vec{g}_{j,\tau'}^{\,*}(\mathbf{x}') \right\}. \tag{3.63}$$

The dyadic product in (3.62) and (3.63) is a consequence of the definition (2.297) of a scalar product of a vector with a dyadic. In the above discussion this vector is given by the approximation $\vec{f}^{\,(\hat{n}',N)}(\mathbf{x}')$ according to (3.60).

3.5 The Dyadic Green Functions Related to the Vector-Wave Equation

3.5.1 The Outer Dirichlet Problem

Here too we want to show at the beginning that the expansion coefficients $a_{i,\tau}^{(N)}$ of approximation (1.21) for the scattered field $\vec{u}_s^{\,(N)}(\mathbf{x})$ which holds everywhere in the outer region Γ_+ are identical with the expansion coefficients $\alpha_{i,\tau}^{(N)}$ of the

corresponding approximation

$$\vec{u}_s^{\,(\hat{n}_-,N)}(\mathbf{x}) \;=\; \sum_{\tau=1}^{2}\sum_{i=0}^{N} \alpha_{i,\tau}^{(N)} \cdot \vec{\varphi}_{i,\tau}^{\,\hat{n}_-}(k_0,\mathbf{x})\;; \quad \mathbf{x}\in\partial\Gamma \tag{3.64}$$

at the scatterer surface calculated from the application of the continuity condition (1.29). This proof requires moreover that the radiating vector solutions (2.122)/(2.123) of the vector-wave equation and their tangential projections, respectively, are used as expansion functions in both of these approximations. First we use the vectorial form (2.316) of Green's theorem with the two vector functions $\vec{\Psi}(\mathbf{x}) = \vec{u}_s(\mathbf{x})$ and $\vec{\Phi}(\mathbf{x}) = \vec{\varphi}_{i,\tau}(k_0,\mathbf{x})$. Since $\vec{u}_s$ as well as $\vec{\varphi}_{i,\tau}$ are solutions of the homogeneous vector-wave equation, and since both vector functions are in correspondence with the radiation condition we get with identity

$$\vec{a}\cdot\left(\vec{b}\times\vec{c}\right) \;=\; \left(\vec{a}\times\vec{b}\right)\cdot\vec{c} \tag{3.65}$$

the equation

$$\oint_{\partial\Gamma}\Big\{\vec{\varphi}_{i,\tau}^{\,\hat{n}_-}(k_0,\mathbf{x})\cdot\left[\nabla\times\vec{u}_s(\mathbf{x})\right] - \vec{u}_s^{\,\hat{n}_-}(\mathbf{x})\cdot\left[\nabla\times\vec{\varphi}_{i,\tau}(k_0,\mathbf{x})\right]\Big\}\,dS(\mathbf{x}) \;=\; 0. \tag{3.66}$$

The tangential projections $\vec{\varphi}_{i,\tau}^{\,\hat{n}_-}$ are defined in (2.159). Next we replace $\vec{u}_s$ in the first term of the boundary integral on the left hand side by its approximation (1.21). As already mentioned in the scalar case, this is justified by the fact that the operation $\nabla\times\vec{u}_s$ must be performed first in Γ_+ before moving the argument $\mathbf{x}$ to the scatterer surface $\partial\Gamma$. But for the quantity $\vec{u}_s^{\,\hat{n}_-}(\mathbf{x})$ in the second term we can apply approximation (3.64). It follows

$$\sum_{\tau'=1}^{2}\sum_{j=0}^{N}\oint_{\partial\Gamma}\Big\{a_{j,\tau'}^{(N)}\cdot\vec{\varphi}_{i,\tau}^{\,\hat{n}_-}(k_0,\mathbf{x})\cdot\left[\nabla\times\vec{\varphi}_{j,\tau'}(k_0,\mathbf{x})\right] - \alpha_{j,\tau'}^{(N)}\cdot\vec{\varphi}_{j,\tau'}^{\,\hat{n}_-}(k_0,\mathbf{x})\cdot\left[\nabla\times\vec{\varphi}_{i,\tau}(k_0,\mathbf{x})\right]\Big\}\,dS(\mathbf{x}) \;=\; 0. \tag{3.67}$$

On the other hand, if using Green's theorem (2.316) with the two vector functions $\vec{\Psi}(\mathbf{x}) = \vec{\varphi}_{i,\tau}$ and $\vec{\Phi}(\mathbf{x}) = \vec{\varphi}_{j,\tau'}$ we obtain the identity

$$\oint_{\partial\Gamma}\vec{\varphi}_{j,\tau'}^{\,\hat{n}_-}(k_0,\mathbf{x})\cdot\left[\nabla\times\vec{\varphi}_{i,\tau}(k_0,\mathbf{x})\right] = \oint_{\partial\Gamma}\vec{\varphi}_{i,\tau}^{\,\hat{n}_-}(k_0,\mathbf{x})\cdot\left[\nabla\times\vec{\varphi}_{j,\tau'}(k_0,\mathbf{x})\right]dS(\mathbf{x}) \;=\; 0 \tag{3.68}$$

so that (3.67) can be rewritten into

$$\sum_{\tau'=1}^{2}\sum_{j=0}^{N}\left[a_{j,\tau'}^{(N)} - \alpha_{j,\tau'}^{(N)}\right]\cdot\oint_{\partial\Gamma}\vec{\varphi}_{i,\tau}^{\,\hat{n}_-}(k_0,\mathbf{x}) \cdot\left[\nabla\times\vec{\varphi}_{j,\tau'}(k_0,\mathbf{x})\right]dS(\mathbf{x}) = 0\, i=0,\ldots,N,\ \tau=1,2. \tag{3.69}$$

As in the scalar case we thus obtain

$$a_{j,\tau'}^{(N)} = \alpha_{j,\tau'}^{(N)} \tag{3.70}$$

if the matrix $\mathbf{M}$ is invertible. Its elements result from the boundary integral on the left-hand side of (3.69). For a certain geometry of the scatterer this can be proven numerically, as the case may be.

The cooking recipe for deriving the dyadic Green function related to the outer Dirichlet problem is as follows:

First step:

We expand the tangential projection of the primary incident field $\vec{u}_{inc}^{\,\hat{n}_-}$ at the scatterer surface according to (2.1) into a series in terms of the tangential projections $\vec{\psi}_{i,\tau}^{\,\hat{n}_-}(k_0,\mathbf{x})$ of the vector functions $\vec{\psi}_{i,\tau}(k_0,\mathbf{x})$. These could be the regular vector solutions of the vector-wave equation, for example, but not necessarily. The corresponding expansion coefficients $b_{i,\tau}^{(N)}$ are then calculated according to (2.14) and (2.15).

Second step:

Utilizing the transformation character (2.18) of the T-matrix (2.19) we accomplish the transition from the expansion functions $\vec{\psi}_{i,\tau}^{\,\hat{n}_-}(k_0,\mathbf{x})$ to the radiating vector solutions $\vec{\varphi}_{i,\tau}^{\,\hat{n}_-}(k_0,\mathbf{x})$ in the approximation of the tangential projection of the primary incident field at the scatterer surface. The new expansion coefficients $a_{i,\tau}^{(N)}$ are calculated by use of (2.23) from the old coefficients $b_{i,\tau}^{(N)}$. Due to the identical definitions (2.15) and (2.22) of both matrices $\mathbf{A}_{\partial\Gamma}^{(g,\psi_0^{\hat{n}_-})}$ and $\mathbf{B}_{\partial\Gamma}^{(g,\psi_0^{\hat{n}_-})}$ which appear in (2.14) and (2.19), from the continuity condition (1.29), from the above derived relation (3.70), and after interchanging integration and summation we get

$$\vec{u}_s^{\,(N)}(\mathbf{x}) = -\oint_{\partial\Gamma}\sum_{\tau,\tau'=1}^{2}\sum_{i,j=0}^{N}\left[A_{\partial\Gamma}^{(g,\varphi_0^{\hat{n}_-})^{-1}}\right]_{i,j}^{\tau,\tau'} \cdot\vec{g}_{j,\tau'}^{\,*}(\mathbf{x}')\cdot\vec{u}_{inc}^{\,\hat{n}_-}(\mathbf{x}')\,dS(\mathbf{x}')\cdot\vec{\varphi}_{i,\tau}(k_0,\mathbf{x}); \quad \mathbf{x}\in\Gamma_+,\ \mathbf{x}'\in\partial\Gamma \tag{3.71}$$

as an approximation of the scattered field u_s in the outer region Γ_+. This corresponds to (3.20) in Sect.3.3.1. As in the scalar case it holds also here that, once we have specified the primary incident field as well as the vectorial weighting functions

$\vec{g}_{j,\tau'}$, with (3.71) we have found an appropriate approximation of the outer Dirichlet problem related to the vector-wave equation.

Third step:

We use the vector-dyadic form (2.318) of Green's theorem with the two quantities $\Psi(\mathbf{x}) = \vec{u}_s(\mathbf{x})$ and $\mathbf{Q}(\mathbf{x}, \mathbf{x}') = \mathbf{G}_{\mathbf{\Gamma}_+}(\mathbf{x}, \mathbf{x}')$. $\vec{u}_s$ is a solution of the homogeneous vector-wave equation whereas G_{Γ_+} is a solution of the inhomogeneous equation (2.341). Both quantities obey additionally the radiation condition at S_∞. We get therefore

$$\vec{u}_s(\mathbf{x}') = -\oint_{\partial\Gamma} \hat{n}_- \cdot \left\{\vec{u}_s(\mathbf{x}) \times \left[\nabla_x \times \mathbf{G}_{\mathbf{\Gamma}_+}(\mathbf{x}, \mathbf{x}')\right]\right\} dS(\mathbf{x}). \tag{3.72}$$

From this it follows

$$\vec{u}_s(\mathbf{x}') = \oint_{\partial\Gamma} \left[\nabla_x \times \mathbf{G}_{\mathbf{\Gamma}_+}(\mathbf{x}, \mathbf{x}')\right]^{tp} \cdot \vec{u}_{inc}^{\hat{n}_-}(\mathbf{x})\, dS(\mathbf{x}) \tag{3.73}$$

with identities (2.309) and (2.310), and with the boundary condition (1.18). Let us interchange $\mathbf{x}$ and $\mathbf{x}'$ in this expression to denote the observation point with the unprimed variable, i.e., we write

$$\vec{u}_s(\mathbf{x}) = \oint_{\partial\Gamma} \left[\nabla_{x'} \times \mathbf{G}_{\mathbf{\Gamma}_+}(\mathbf{x}', \mathbf{x})\right]^{tp} \cdot \vec{u}_{inc}^{\hat{n}'_-}(\mathbf{x}')\, dS(\mathbf{x}'). \tag{3.74}$$

Now, with definition

$$\mathbf{G}_{\partial\mathbf{\Gamma}}(\mathbf{x}, \mathbf{x}') := \left[\nabla_{\mathbf{x}'} \times \mathbf{G}_{\mathbf{\Gamma}_+}(\mathbf{x}', \mathbf{x})\right]^{tp} \tag{3.75}$$

we introduce the dyadic surface Green function $\mathbf{G}_{\partial\mathbf{\Gamma}}$ related to $\mathbf{G}_{\mathbf{\Gamma}_+}$. Then, we write instead of (3.74)

$$\vec{u}_s(\mathbf{x}) = \oint_{\partial\mathbf{\Gamma}} \mathbf{G}_{\partial\Gamma}(\mathbf{x}, \mathbf{x}') \cdot \vec{u}_{inc}^{\hat{n}'_-}(\mathbf{x}')\, dS(\mathbf{x}'). \tag{3.76}$$

Comparing this expression with (3.71) provides

$$\mathbf{G}^{(\mathbf{N})}_{\partial\mathbf{\Gamma}}(\mathbf{x}, \mathbf{x}') = -\sum_{\tau,\tau'=1}^{2} \sum_{i,j=0}^{N} \left[A_{\partial\Gamma}^{(g,\varphi_0^{\hat{n}_-})^{-1}}\right]_{i,j}^{\tau,\tau'} \cdot \left\{\vec{\varphi}_{i,\tau}(k_0, \mathbf{x}) \odot \vec{g}^{\,*}_{j,\tau'}(\mathbf{x}')\right\}; \quad \mathbf{x} \in \Gamma_+,\ \mathbf{x}' \in \partial\mathbf{\Gamma} \tag{3.77}$$

as an approximation of the dyadic surface Green function.

Fourth step:

At first we want to derive Huygens' principle expressed solely in terms of Green functions. This can be achieved by employing the relevant dyadic-dyadic Green

theorem in the outer region. It interrelates the dyadic Green functions $\mathbf{G}_{\mathbf{\Gamma}_+}$ and $\mathbf{G}_{\partial\mathbf{\Gamma}}$. From this principle we are then able to derive the approximation of $\mathbf{G}_{\mathbf{\Gamma}_+}$ which is in correspondence with approximation (3.77). We use the two quantities

$$\mathbf{Q}(\bar{\mathbf{x}}, \mathbf{x}) = \mathbf{G}_{\mathbf{0}}(\bar{\mathbf{x}}, \mathbf{x}) \tag{3.78}$$

$$\mathbf{P}(\bar{\mathbf{x}}, \mathbf{x}') = \mathbf{G}_{\mathbf{\Gamma}_+}(\bar{\mathbf{x}}, \mathbf{x}') \tag{3.79}$$

in Green's theorem (2.319). Taking symmetry relation (2.329) into account we get

$$\begin{aligned}\mathbf{G}_{\mathbf{\Gamma}_+}(\mathbf{x}, \mathbf{x}') = \mathbf{G}_{\mathbf{0}}(\mathbf{x}, \mathbf{x}') \; + \oint_{\partial\Gamma} \left[\hat{\bar{n}}_- \times \mathbf{G}_{\mathbf{0}}(\bar{\mathbf{x}}, \mathbf{x})\right]^{tp} \\ \cdot \left[\nabla_{\bar{\mathbf{x}}} \times \mathbf{G}_{\mathbf{\Gamma}_+}(\bar{\mathbf{x}}, \mathbf{x}')\right] dS(\bar{\mathbf{x}}).\end{aligned} \tag{3.80}$$

This can be reformulated into

$$\begin{aligned}\mathbf{G}_{\mathbf{\Gamma}_+}(\mathbf{x}, \mathbf{x}') = \mathbf{G}_{\mathbf{0}}(\mathbf{x}, \mathbf{x}') \; + \oint_{\partial\Gamma} \left[\hat{\bar{n}}_- \times \mathbf{G}_{\mathbf{0}}(\bar{\mathbf{x}}, \mathbf{x})\right]^{tp} \\ \cdot \mathbf{G}^{\mathbf{tp}}_{\partial\mathbf{\Gamma}}(\mathbf{x}', \bar{\mathbf{x}})\, dS(\bar{\mathbf{x}})\end{aligned} \tag{3.81}$$

by use of definition (3.75) of the dyadic surface Green function. It can be shown that the following symmetry relation holds for the boundary integral on the right-hand side of (3.81):

$$\begin{aligned}\oint_{\partial\Gamma} \left\{\mathbf{G}_{\partial\mathbf{\Gamma}}(\mathbf{x}', \bar{\mathbf{x}}) \cdot \left[\hat{\bar{n}}_- \times \mathbf{G}_{\mathbf{0}}(\bar{\mathbf{x}}, \mathbf{x})\right]\right\}^{tp} dS(\bar{\mathbf{x}}) \\ = \oint_{\partial\Gamma} \mathbf{G}_{\partial\mathbf{\Gamma}}(\mathbf{x}, \bar{\mathbf{x}}) \cdot \left[\hat{\bar{n}}_- \times \mathbf{G}_{\mathbf{0}}(\bar{\mathbf{x}}, \mathbf{x}')\right] dS(\bar{\mathbf{x}}).\end{aligned} \tag{3.82}$$

This can be proven by use of identity (2.315) in conjunction with the symmetry relations (2.329) and (2.346). Then, Huygens' principle reads finally

$$\mathbf{G}_{\mathbf{\Gamma}_+}(\mathbf{x}, \mathbf{x}') \; = \; \mathbf{G}_{\mathbf{0}}(\mathbf{x}, \mathbf{x}') \; + \oint_{\partial\Gamma} \mathbf{G}_{\partial\mathbf{\Gamma}}(\mathbf{x}, \bar{\mathbf{x}}) \cdot \left[\hat{\bar{n}}_- \times \mathbf{G}_{\mathbf{0}}(\bar{\mathbf{x}}, \mathbf{x}')\right] dS(\bar{\mathbf{x}}) \tag{3.83}$$

if expressed solely in terms of dyadic Green functions.

Fifth step:

Utilizing approximation (3.77) in (3.83) and employing definition

$$\vec{\tilde{g}}^{\,*}_{j,\tau'}(\mathbf{x}') \; := \; \oint_{\partial\Gamma} \vec{g}^{\,*}_{j,\tau'}(\bar{\mathbf{x}}) \cdot \left[\hat{\bar{n}}_- \times \mathbf{G}_{\mathbf{0}}(\bar{\mathbf{x}}, \mathbf{x}')\right] dS(\bar{\mathbf{x}}) \tag{3.84}$$

results in the following expression:

$$\mathbf{G}^{(\mathbf{N})}_{\mathbf{\Gamma}_+}(\mathbf{x},\mathbf{x}') = \mathbf{G_0}(\mathbf{x},\mathbf{x}') - \sum_{\tau,\tau'=1}^{2}\sum_{i,j=0}^{N}\left[A^{(g,\varphi_0^{\hat{n}_-})^{-1}}_{\partial\Gamma}\right]^{\tau,\tau'}_{i,j} \cdot \left\{\vec{\varphi}_{i,\tau}(k_0,\mathbf{x}) \odot \vec{\tilde{g}}^{\,*}_{j,\tau'}(\mathbf{x}')\right\}. \tag{3.85}$$

The variable $\mathbf{x}'$ of the dyadic free-space Green function in (3.84) denotes the location of the source distribution of the primary incident field. As already done in the scalar case we assume that this source distribution is confined to an area which is located somewhere outside the smallest spherical surface circumscribing the scatterer. Moreover, since restricting our considerations to solenoidal fields only, we can replace $\mathbf{G_0}(\bar{\mathbf{x}},\mathbf{x}')$ in (3.84) by $\mathbf{G}^{<}_{\mathbf{t}}(\bar{\mathbf{x}},\mathbf{x}')$ according to (2.340). From this procedure we get

$$\vec{\tilde{g}}^{\,*}_{j,\tau'}(\mathbf{x}') = (ik_0)\cdot\sum_{\bar{\tau}=1}^{2}\sum_{k=0}^{N}\left[B^{(g,\psi_0^{\hat{n}_-})}_{\partial\Gamma}\right]^{\tau',\bar{\tau}}_{j,k}\cdot\vec{\tilde{\varphi}}_{k,\bar{\tau}}(k_0,\mathbf{x}') \tag{3.86}$$

with matrix elements $\left[B^{(g,\psi_0^{\hat{n}_-})}_{\partial\Gamma}\right]^{\tau',\bar{\tau}}_{j,k}$ given by the scalar product (2.22). The approximation of the dyadic Green function related to the outer Dirichlet problem reads therefore

$$\mathbf{G}^{(\mathbf{N})}_{\mathbf{\Gamma}_+}(\mathbf{x},\mathbf{x}') = \mathbf{G_0}(\mathbf{x},\mathbf{x}') + \mathbf{G}^{(\mathbf{N})}_{\mathbf{s}}(\mathbf{x},\mathbf{x}') \tag{3.87}$$

with

$$\mathbf{G}^{(\mathbf{N})}_{\mathbf{s}}(\mathbf{x},\mathbf{x}') = -(ik_0)\cdot\sum_{\tau,\bar{\tau}=1}^{2}\sum_{i,k=0}^{N}\left[T^{\hat{n}_-}_{\partial\Gamma}\right]^{\tau,\bar{\tau}}_{i,k} \cdot\left\{\vec{\varphi}_{i,\tau}(k_0,\mathbf{x})\odot\vec{\tilde{\varphi}}_{k,\bar{\tau}}(k_0,\mathbf{x}')\right\}. \tag{3.88}$$

$$\left[T^{\hat{n}_-}_{\partial\Gamma}\right]^{\tau,\bar{\tau}}_{i,k} = \sum_{\tau'=1}^{2}\sum_{j=0}^{N}\left[A^{(g,\varphi_0^{\hat{n}_-})^{-1}}_{\partial\Gamma}\right]^{\tau,\tau'}_{i,j}\cdot\left[B^{(g,\psi_0^{\hat{n}_-})}_{\partial\Gamma}\right]^{\tau',\bar{\tau}}_{j,k} \tag{3.89}$$

are again the elements of the transformation matrix (2.19). These elements differ only in the additional τ-summation and in the considered vector functions appearing in the relevant scalar product definitions. Approximation (3.88) is in agreement with the inhomogeneous equation (2.341) and the radiation condition with respect to $\mathbf{x}$. The question if it suffices the boundary condition (2.342) can be also answered in close analogy to the scalar case. From Huygens' principle (3.83) it becomes obvious that this boundary condition is fulfilled if relation

$$\hat{n}_-\times\mathbf{G}_{\partial\mathbf{\Gamma}}(\mathbf{x},\bar{\mathbf{x}}) = -\mathbf{D}^{\hat{\mathbf{n}}_-}_{\partial\mathbf{\Gamma}}(\bar{\mathbf{x}}-\mathbf{x}) \tag{3.90}$$

holds for $\mathbf{x} \in \partial\Gamma$, according to definition (3.58). Comparing (3.63) with (3.77) shows that this relation holds indeed for the approximations of $\mathbf{G}_{\partial\Gamma}$ and $\mathbf{D}_{\partial\Gamma}^{\hat{\mathbf{n}}-}$. Thus, we can state that boundary condition (3.342) is fulfilled in this approximate sense.

The derived approximations become again especially simple if a spherical scatterer is considered. If choosing the tangential projections of the regular vector solutions as weighting functions, and if taking the orthogonality relations (2.179) and (2.180) at the surface of a sphere with the radius $r = a$ into account we get the following expressions for the relevant matrix elements:

$$\left[A_{\partial\Gamma}^{(\psi_0^{\hat{n}-},\varphi_0^{\hat{n}-})^{-1}}\right]_{i,k}^{\tau,\tau'} = \delta_{\tau,\tau'}\delta_{i,k} \cdot \frac{1}{a^2} \cdot \frac{1}{d_{i,\tau}^{(\psi_0,\varphi_0)}} \tag{3.91}$$

and

$$\left[B_{\partial\Gamma}^{(\psi_0^{\hat{n}-},\psi_0^{\hat{n}-})}\right]_{i,k}^{\tau,\tau'} = \delta_{\tau,\tau'}\delta_{i,k} \cdot a^2 \cdot d_{i,\tau}^{(\psi_0,\psi_0)}. \tag{3.92}$$

The normalization constants therein are calculated from (2.183), (2.184), (2.187), and (2.188) with κ and κ' replaced by the parameter k_0. As a result, we obtain

$$\begin{aligned}\mathbf{G}_{\mathbf{\Gamma}_+}^{(\mathbf{N})}(\mathbf{x},\mathbf{x}') = \mathbf{G_0}(\mathbf{x},\mathbf{x}') - ik_0 \cdot \sum_{i=0}^{N} a_{i,1} \cdot \left\{\vec{\varphi}_{i,1}(k_0,\mathbf{x}) \odot \vec{\tilde{\varphi}}_{i,1}(k_0,\mathbf{x}')\right\} \\ + a_{i,2} \cdot \left\{\vec{\varphi}_{i,2}(k_0,\mathbf{x}) \odot \vec{\tilde{\varphi}}_{i,2}(k_0,\mathbf{x}')\right\}\end{aligned} \tag{3.93}$$

with coefficients

$$a_{i,1} = \frac{j_{n(i)}(k_0 a)}{h_{n(i)}^{(1)}(k_0 a)} \tag{3.94}$$

and

$$a_{i,2} = \frac{\frac{\partial}{\partial r}\left[r \cdot j_{n(i)}(k_0 r)\right]_{r=a}}{\frac{\partial}{\partial r}\left[r \cdot h_{n(i)}^{(1)}(k_0 r)\right]_{r=a}} \tag{3.95}$$

as the approximation of the dyadic Green function of the outer Dirichlet problem. The corresponding approximation of the dyadic surface Green function becomes

$$\begin{aligned}\mathbf{G}_{\partial\mathbf{\Gamma}}^{(\mathbf{N})}(\mathbf{x},\mathbf{x}') = -\sum_{i=0}^{N} \frac{1}{a^2\, d_{i,1}^{(\psi_0,\varphi_0)}} \cdot \left\{\vec{\varphi}_{i,1}(k_0,\mathbf{x}) \odot \left[\vec{\psi}_{i,1}^{\hat{n}-}(k_0,\mathbf{x}')\right]\right\}^* \\ + \frac{1}{a^2\, d_{i,2}^{(\psi_0,\varphi_0)}} \cdot \left\{\vec{\varphi}_{i,2}(k_0,\mathbf{x}') \odot \left[\vec{\psi}_{i,2}^{\hat{n}-}(k_0,\mathbf{x})\right]^*\right\}.\end{aligned} \tag{3.96}$$

As already demonstrated in the scalar case we can express the scattered field by the finite series expansion

$$\vec{u}_s^{\,(N)}(k_0 r, \theta, \phi) \;=\; -\sum_{\tau,\bar{\tau}=1}^{2}\sum_{i,k=0}^{N}\left[T_{\partial\Gamma}^{\hat{n}_-}\right]_{i,k}^{\tau,\bar{\tau}} \cdot b_{k,\bar{\tau}} \cdot \vec{\varphi}_{i,\tau}(k_0 r, \theta, \phi) \tag{3.97}$$

which results from the integral representation (2.348) and the scattering part (3.88) of $\mathbf{G}_{\mathbf{\Gamma}_+}^{(\mathbf{N})}$. In combination with the vector source (2.332) the coefficients $b_{k,1}$ and $b_{k,2}$ therein become identical with the coefficients specified in (2.236) and (2.237). These latter coefficients belong to the series expansion of a linearly polarized plane wave travelling along an arbitrary direction $\vec{k}_i$. For the proof of equality of these both sets of expansion coefficients we need the asymptotic behaviour (2.152) and (2.153) of the radiating vector solutions $\vec{\varphi}_{i,\tau}$ for large arguments as well as relations (2.136) and (2.137). The latter relations are a consequence of the unit vector $\vec{k}_i$ pointing from the source into the direction of the plane wave propagation. Because of (2.334) it causes the vector spherical harmonics with arguments $\vec{C}_{l,n}(\pi - \theta_i, \phi_i \pm \pi)$ and $\vec{B}_{l,n}(\pi - \theta_i, \phi_i \pm \pi)$. This proof shows us, moreover, that one can derive expansion (2.235) of the general case of a linearly polarized plane wave in a straightforward way by employing the expansion (2.340) of $\mathbf{G}_{\mathbf{t}}^{<}$ and the vector source (2.332) in the integral representation (2.331).

3.5.2 The Outer Transmission Problem

In Sect. 2.2.3 we have discussed the transformation character of the T-matrix by use of an abstract notation which is independent of whether the scalar or vectorial boundary value problems are considered. This allows us to adopt the approximation of the scalar Green function belonging to the outer transmission problem derived in Sect. 3.3.2 with only slight changes for the corresponding dyadic Green function. In place of the scalar expansion and weighting functions and their normal derivatives at the scatterer surface we apply simply the tangential projections of the corresponding vector functions as defined in (1.38), (1.61), and (1.54)–(1.59). The τ-summation must additionally be taken into account. Thus, we have for the approximation of the dyadic Green function related to the outer transmission problem

$$\mathbf{G}_{\mathbf{\Gamma}_+}^{(\mathbf{d},\mathbf{N})}(\mathbf{x}, \mathbf{x}') \;=\; \mathbf{G_0}(\mathbf{x}, \mathbf{x}') \;+\; \mathbf{G}_{\mathbf{s}}^{(\mathbf{d},\mathbf{N})}(\mathbf{x}, \mathbf{x}') \tag{3.98}$$

with its scattering part $\mathbf{G_s}$ given by

$$\begin{aligned}\mathbf{G}_{\mathbf{s}}^{(\mathbf{d},\mathbf{N})}(\mathbf{x}, \mathbf{x}') = -(ik_0) \cdot \sum_{\tau,\bar{\tau}=1}^{2}\sum_{i,k=0}^{N}\left[T_{\partial\Gamma}^{(\hat{n}_-,d)}\right]_{i,k}^{\tau,\bar{\tau}} \\ \cdot \left\{\vec{\varphi}_{i,\tau}(k_0, \mathbf{x}) \odot \vec{\tilde{\varphi}}_{k,\bar{\tau}}(k_0, \mathbf{x}')\right\}.\end{aligned} \tag{3.99}$$

For the T-matrix itself we obtain the expression

$$\mathbf{T}_{\partial\Gamma}^{(\hat{n}_-,d)} = \mathbf{T}_{\partial\Gamma}^{\hat{n}_-} \cdot \left[\mathbf{E} - \mathbf{T}_{\psi_0^{\hat{n}_-}/\psi^{\hat{n}_-}}^{\hat{n}_-} \cdot \mathbf{T}_{\psi^{\hat{n}_-}}^{\hat{n}_-} \right]. \tag{3.100}$$

This corresponds to (3.54) in the scalar case with the difference that all matrices are now (2×2)-block matrices, due to the additional τ-summation.

Chapter 4
Second Approach to the Green Functions: The Self-Consistent Way

4.1 Introduction

In Chap. 3 we have demonstrated that the scattering problems of our interest are solved approximately if knowing a finite series expansion of the primary incident field at the scatterer surface $\partial\Gamma$ in terms of the radiating eigensolutions of the Helmholtz and vector-wave equation, respectively. From this we could obtain an approximation of the scattered field everywhere in the outer region Γ_+ which is also given by a series expansion in terms of the radiating eigensolutions. Comparing this approximation with the integral representations resulting from the application of Green's theorems we could derive corresponding approximations for the scalar and dyadic surface Green functions $G_{\partial\Gamma}$ and $\mathbf{G}_{\partial\mathbf{\Gamma}}$. In the next step, by employing Huygens' principle formulated exclusively in terms of Green functions, we were able to derive the corresponding approximations of the actual Green functions G_{Γ_+} and $\mathbf{G}_{\mathbf{\Gamma}_+}$. In the course of these derivations, we had just one restriction concerning the location of the source generating the primary incident field. This source must be placed outside the smallest spherical surface circumscribing the scatterer.

In this chapter, we will now answer the question if it is possible to derive the approximations of the relevant Green functions without the fall-back to the approximation of the scattered field. Conversely and more naturally, the approximation of the scattered field should be a consequence of its integral representation in terms of these Green functions. The justification of such a question is due to the fact that the Green functions themselves are solutions of certain boundary value problems related to the inhomogeneous Helmholtz and vector-wave equation, respectively, with Dirac's delta distribution as inhomogeneity. The corresponding boundary conditions at the scatterer surface have been already formulated in Sects. 2.5.3 and 2.6.4. In the first part of this chapter, we will pursue this goal. The resulting formalism will be called "self-consistent Green function formalism" for obvious reasons.

We will show afterwards that those important properties of the T-matrix and the strongly related S-matrix like symmetry and unitarity are linked to specific properties of the Green functions. So far, these properties of the T- and S-matrix have been

T. Rother and M. Kahnert, *Electromagnetic Wave Scattering on Nonspherical Particles*, Springer Series in Optical Sciences 145, DOI: 10.1007/978-3-642-36745-8_4,

considered in the relevant literature as consequences of the physical principles of energy conservation and reciprocity which can be applied to the scattering processes under certain circumstances. But tracing back mathematical properties of mathematical quantities to physical experience seems somehow questionable. Therefore, we will demonstrate an alternative way to prove these properties.

4.2 The Scalar Green Functions Related to the Helmholtz Equation

4.2.1 The Outer Dirichlet Problem

In this section, we intend to derive approximation (3.32–3.34) of the scalar Green function G_{Γ_+} related to the outer Dirichlet problem on a direct way. For this purpose we introduce a new quantity, the so-called "interaction operator" $W_{\partial\Gamma_+}$. This interaction operator is solely determined at the scatterer surface and related to the Green function via the definition

$$G_{\Gamma_+}(\mathbf{x},\mathbf{x}') := G_0(\mathbf{x},\mathbf{x}') + \oint_{\partial\Gamma} G_0^{>}(\mathbf{x},\bar{\mathbf{x}}) \cdot W_{\partial\Gamma_+}(\bar{\mathbf{x}},\tilde{\mathbf{x}}) \cdot G_0(\tilde{\mathbf{x}},\mathbf{x}')\, dS(\bar{\mathbf{x}})\, dS(\tilde{\mathbf{x}}). \quad (4.1)$$

This definition can be considered as a modification of Huygens' principle (3.26) we derived already within the fourth step of Sect. 3.3.1. The first contribution on the right-hand side of (4.1) represents again the unperturbed problem. That is, the free-space Green function of the entire free space without any scatterer. The second term on the right-hand side describes the perturbation which is caused by adding a scatterer with a certain geometry and morphology to the free space. This additional structure results in an interaction of the primary (unperturbed) incident field with the scatterer surface thus generating the scattered field. Before continuing we should add the following remark: Mathematically seen it is not really correct to denote the quantity $W_{\partial\Gamma_+}$ with the word "operator". More precisely speaking, it is the kernel of a boundary integral operator which will be applied to the primary incident field $u_{inc}(\tilde{\mathbf{x}})$ at the scatterer surface, as we will see later on. But the notation "operator" for similar quantities is commonly used in the methodical and application oriented literature concerning electromagnetic wave scattering (see "Theory of Microwave Remote Sensing" and "Light Scattering by Nonspherical Particles: Theory, Measurement, and Applications" in the reference chapter, for example). Therefore, we will use it in this book, too, hoping that the more mathematically oriented reader will bend the rules.

Regarding the above given definition of the interaction operator the following more serious problem appears: The quantity $G_0^{>}(\mathbf{x},\bar{\mathbf{x}})$ in the second contribution on the right-hand side of (4.1) represents the infinite series expansion (2.276) of G_0

which is actually applicable only if the condition $|\mathbf{x}| > |\bar{\mathbf{x}}|$ holds for its arguments. Unfortunately, this condition is violated for observation points $\mathbf{x}$ located in the outer region Γ_+ but within the smallest spherical surface circumscribing the scatterer if a nonspherical scatterer geometry is considered (see Fig. 6.14). This problem is again strongly related to Rayleigh's hypothesis discussed in detail in Chap. 6. At this place, according to our pragmatic point of view concerning the convergence of all the series expansions employed in this book, we will treat $G_0^{>}(\mathbf{x}, \bar{\mathbf{x}})$ as an auxiliary quantity which obeys the radiation condition with respect to $\mathbf{x}$ as well as the homogeneous Helmholtz equation. This is obviously true without fail as long as expansion (2.276) is truncated at a finite number N, independent of whether this finite expansion approaches the free-space Green function correctly or not. Then the Green function G_{Γ_+} in (4.1) solves the corresponding inhomogeneous Helmholtz equation and obeys also the radiation condition with respect to $\mathbf{x}$. Moreover, by use of the interaction operator we are now able to make sure that G_{Γ_+} satisfies the homogeneous Dirichlet condition (2.280) at the scatterer surface in the approximate sense discussed in the foregoing chapter. This can be accomplished in the following way:

Let us move variable $\mathbf{x}$ to the scatterer surface $\partial\Gamma$. Applying (2.280) we get

$$\oint_{\partial\Gamma} G_0^{>}(\mathbf{x}, \bar{\mathbf{x}}) \cdot W_{\partial\Gamma_+}(\bar{\mathbf{x}}, \tilde{\mathbf{x}}) \cdot G_0^{<}(\tilde{\mathbf{x}}, \mathbf{x}')\, dS(\bar{\mathbf{x}}) dS(\tilde{\mathbf{x}}) = -G_0^{<}(\mathbf{x}, \mathbf{x}'), \mathbf{x} \in \partial\Gamma\,; \quad \mathbf{x}' \in \Gamma_+ \tag{4.2}$$

from definition (4.1). Here, we assumed again that the source point $\mathbf{x}'$ is located outside the smallest spherical surface circumscribing the scatterer. This gives us the justification to use $G_0^{<}(\mathbf{x}, \mathbf{x}')$ for both free-space Green functions G_0 on the right-hand side of (4.1). Next, if replacing $G_0^{>}$ and $G_0^{<}$ by the (now finite!) series expansions (2.277) and (2.278), then (4.2) reads

$$(ik_0)^2 \sum_{i,k=0}^{N} \oint_{\partial\Gamma} \varphi_i(k_0, \mathbf{x}) \cdot \tilde{\psi}_i(k_0, \bar{\mathbf{x}}) \cdot W_{\partial\Gamma_+}(\bar{\mathbf{x}}, \tilde{\mathbf{x}}) \cdot \psi_k(k_0, \tilde{\mathbf{x}}) \cdot \tilde{\varphi}_k(k_0, \mathbf{x}') dS(\bar{\mathbf{x}})\, dS(\tilde{\mathbf{x}}) = -(ik_0) \sum_{k=0}^{N} \psi_k(k_0, \mathbf{x}) \cdot \tilde{\varphi}_k(k_0, \mathbf{x}'). \tag{4.3}$$

The integral expression on the left-hand side defines the matrix elements

$$\left[W_{\partial\Gamma_+}\right]_{i,k} := (ik_0) \oint_{\partial\Gamma} \tilde{\psi}_i(k_0, \bar{\mathbf{x}}) \cdot W_{\partial\Gamma_+}(\bar{\mathbf{x}}, \tilde{\mathbf{x}}) \cdot \psi_k(k_0, \tilde{\mathbf{x}})\, dS(\bar{\mathbf{x}})\, dS(\tilde{\mathbf{x}}) \tag{4.4}$$

of the interaction operator. Thus, we may write instead of (4.3)

$$(ik_0)\sum_{i,k=0}^{N}\left[W_{\partial\Gamma_+}\right]_{i,k}\cdot\varphi_i(k_0,\mathbf{x})\cdot\tilde{\varphi}_k(k_0,\mathbf{x}')$$
$$=-(ik_0)\sum_{k=0}^{N}\psi_k(k_0,\mathbf{x})\cdot\tilde{\varphi}_k(k_0,\mathbf{x}'). \tag{4.5}$$

On the other hand, from (4.1) and with the finite series expansions (2.277) and (2.278) we get the approximation

$$G_{\Gamma_+}^{(N)}(\mathbf{x},\mathbf{x}')=G_0(\mathbf{x},\mathbf{x}')+(ik_0)\sum_{i,k=0}^{N}\left[W_{\partial\Gamma_+}\right]_{i,k}\cdot\varphi_i(k_0,\mathbf{x})\cdot\tilde{\varphi}_k(k_0,\mathbf{x}') \tag{4.6}$$

for the Green function G_{Γ_+} with so far unknown matrix elements $\left[W_{\partial\Gamma_+}\right]_{i,k}$. But now, by use of the transformation (2.17), let us switch over from the expansion functions $\psi_k(k_0,\mathbf{x})$ to the expansion functions $\varphi_i(k_0,\mathbf{x})$ on the right-hand side of (4.5). From this procedure we can infer the equality of both sides of (4.5) if the matrix elements of the interaction operator are given by

$$\left[W_{\partial\Gamma_+}\right]_{i,k}=-[\tilde{T}_{\partial\Gamma}]_{k,i}=-\{[\tilde{T}_{\partial\Gamma}]_{i,k}\}^{tp}=-[T_{\partial\Gamma}]_{i,k}. \tag{4.7}$$

Inserting this result into the approximation (4.6) of the Green function G_{Γ_+} we end up with

$$G_{\Gamma_+}^{(N)}(\mathbf{x},\mathbf{x}')=G_0(\mathbf{x},\mathbf{x}')-(ik_0)\sum_{i,k=0}^{N}[T_{\partial\Gamma}]_{i,k}\cdot\varphi_i(k_0,\mathbf{x})\cdot\tilde{\varphi}_k(k_0,\mathbf{x}');$$
$$\mathbf{x},\mathbf{x}'\in\Gamma_+\text{ and }|\mathbf{x}'|>|\mathbf{x}|\ \ \forall\,\mathbf{x}\in\partial\Gamma. \tag{4.8}$$

But this expression is obviously identical with approximation (3.32–3.34).

In Chap. 3 we derived this approximation from the corresponding approximation of the surface Green function $G_{\partial\Gamma}^{(N)}$. Now we can conversely derive the approximation of the surface Green function from approximation (4.8). For this we have to insert expression (2.19) or, alternatively, expression (3.34) into (4.8) and resolve the matrix $B_{\partial\Gamma}^{(g,\psi_0)}$ appearing therein by use of definition (2.22) as well as the relevant scalar product definition (1.34). Thus, we get from (4.8):

$$G_{\Gamma_+}^{(N)}(\mathbf{x},\mathbf{x}')=G_0(\mathbf{x},\mathbf{x}')-(ik_0)\oint_{\partial\Gamma}\sum_{i,j,k=0}^{N}[A_{\partial\Gamma}^{(g,\varphi_0)^{-1}}]_{i,j}$$
$$\cdot\,\varphi_i(k_0,\mathbf{x})\cdot g_j^*(\bar{\mathbf{x}})\cdot\psi_k(k_0,\bar{\mathbf{x}})\cdot\tilde{\varphi}_k(k_0,\mathbf{x}')\,dS(\bar{\mathbf{x}}). \tag{4.9}$$

Since $\mathbf{x}'$ belongs to the source located outside the smallest spherical surface circumscribing the scatterer we can perform the summation with respect to k. This is nothing

but the series expansion (2.278) of the free-space Green function. Instead of (4.9) we can therefore write

$$G_{\Gamma_+}^{(N)}(\mathbf{x},\mathbf{x}') = G_0(\mathbf{x},\mathbf{x}') - \oint_{\partial\Gamma} \sum_{i,j=0}^{N} [A_{\partial\Gamma}^{(g,\varphi_0)^{-1}}]_{i,j} \cdot \varphi_i(k_0,\mathbf{x}) \cdot g_j^*(\bar{\mathbf{x}}) \cdot G_0^<(\bar{\mathbf{x}},\mathbf{x}')\, dS(\bar{\mathbf{x}}). \tag{4.10}$$

Comparing this expression with Huygens' principle (3.26) provides finally

$$G_{\partial\Gamma}^{(N)}(\mathbf{x},\mathbf{x}') = -\sum_{i,j=0}^{N} \left[A_{\partial\Gamma}^{(g,\varphi_0)^{-1}}\right]_{i,j} \cdot \varphi_i(k_0,\mathbf{x}) \cdot g_j^*(\mathbf{x}') \quad \mathbf{x}' \in \partial\Gamma,\ \mathbf{x} \in \Gamma_+ \tag{4.11}$$

as the corresponding approximation of the surface Green function. This is identical with (3.24). Thus we have reached our initial goal to derive the approximations of the Green functions related to the outer Dirichlet problem without using a corresponding approximation of the scattered field.

4.2.2 The Outer Transmission Problem

In close analogy to (4.1) we introduce the interaction operator $W_{\partial\Gamma_+}^{(d)}$ related to the outer transmission problem via the definition

$$G_{\Gamma_+}^{(d)}(\mathbf{x},\mathbf{x}') := G_0(\mathbf{x},\mathbf{x}') + \oint_{\partial\Gamma} G_0^>(\mathbf{x},\bar{\mathbf{x}}) \cdot W_{\partial\Gamma_+}^{(d)}(\bar{\mathbf{x}},\tilde{\mathbf{x}}) G_0(\tilde{\mathbf{x}},\mathbf{x}')\, dS(\bar{\mathbf{x}})\, dS(\tilde{\mathbf{x}}). \tag{4.12}$$

But to derive the approximation of the Green function $G_{\Gamma_+}^{(d)}$ from this expression we have to introduce an additional interaction operator in conjunction with the auxiliary Green function $G^{(-/+)}$ defined in (2.283). The corresponding definition reads

$$G^{(-/+)}(\mathbf{x},\mathbf{x}') := \oint_{\partial\Gamma} G_{0_s}^<(\mathbf{x},\bar{\mathbf{x}}) W_{\partial\Gamma_-}^{(d)}(\bar{\mathbf{x}},\tilde{\mathbf{x}}) G_0(\tilde{\mathbf{x}},\mathbf{x}')\, dS(\bar{\mathbf{x}})\, dS(\tilde{\mathbf{x}}). \tag{4.13}$$

In contrast to (2.278) $G_{0_s}^<$ therein is given by the at first infinite expansion

$$G_{0_s}^<(\mathbf{x},\bar{\mathbf{x}}) = (ik) \cdot \sum_{i=0}^{\infty} \psi_i(k,\mathbf{x}) \cdot \tilde{\varphi}_i(k_0,\bar{\mathbf{x}}). \tag{4.14}$$

Please, note that k is occupied twice in what follows. First as an argument within the expansion functions ψ_i to characterize the scatterer physically, and second as a

summation index. With this definition and if restricting expansion (4.14) to a finite number of expansion terms we can see that the resulting approximation $G^{(-/+,N)}$ solves the homogeneous Helmholtz equation (2.283), as required. Moreover, it is regular everywhere inside the scatterer with respect to $\mathbf{x}$. The Green functions $G^{(d)}_{\Gamma_+}$ and $G^{(-/+)}$ may be then approximated by

$$G^{(d,N)}_{\Gamma_+}(\mathbf{x},\mathbf{x}') = G_0(\mathbf{x},\mathbf{x}') + (ik_0)\sum_{i,k=0}^{N}\left[W^{(d)}_{\partial\Gamma_+}\right]_{i,k}\cdot\varphi_i(k_0,\mathbf{x})\cdot\tilde{\varphi}_k(k_0,\mathbf{x}') \quad (4.15)$$

and

$$G^{(-/+,N)}(\mathbf{x},\mathbf{x}') = (ik_0)\sum_{i,k=0}^{N}\left[W^{(d)}_{\partial\Gamma_-}\right]_{i,k}\cdot\psi_i(k,\mathbf{x})\cdot\tilde{\varphi}_k(k_0,\mathbf{x}') \quad (4.16)$$

if using again the finite expansion (2.278) instead of $G_0(\tilde{\mathbf{x}},\mathbf{x}')$ in definitions (4.12) and (4.13). The corresponding matrix elements of the interaction operators are now defined according to

$$\left[W^{(d)}_{\partial\Gamma_+}\right]_{i,k} := (ik_0)\oint_{\partial\Gamma}\tilde{\psi}_i(k_0,\bar{\mathbf{x}})W^{(d)}_{\partial\Gamma_+}(\bar{\mathbf{x}},\tilde{\mathbf{x}})\psi_k(k_0,\tilde{\mathbf{x}})\,dS(\bar{\mathbf{x}})dS(\tilde{\mathbf{x}}) \quad (4.17)$$

and

$$\left[W^{(d)}_{\partial\Gamma_-}\right]_{i,k} := (ik)\oint_{\partial\Gamma}\tilde{\varphi}_i(k_0,\bar{\mathbf{x}})W^{(d)}_{\partial\Gamma_-}(\bar{\mathbf{x}},\tilde{\mathbf{x}})\psi_k(k_0,\tilde{\mathbf{x}})\,dS(\bar{\mathbf{x}})dS(\tilde{\mathbf{x}}). \quad (4.18)$$

From the transmission conditions (2.281–2.282) with respect to $\mathbf{x}$ we obtain the two equation systems

$$\vec{\varphi}(k_0,\mathbf{x})\cdot\mathbf{W}^{(\mathbf{d})}_{\partial\boldsymbol{\Gamma}_+} = \vec{\psi}(k,\mathbf{x})\cdot\mathbf{W}^{(\mathbf{d})}_{\partial\boldsymbol{\Gamma}_-} - \vec{\psi}(k_0,\mathbf{x})\cdot\mathbf{E} \quad (4.19)$$

and

$$\partial_{\hat{n}}\vec{\varphi}(k_0,\mathbf{x})\cdot\mathbf{W}^{(\mathbf{d})}_{\partial\boldsymbol{\Gamma}_+} = \partial_{\hat{n}}\vec{\psi}(k,\mathbf{x})\cdot\mathbf{W}^{(\mathbf{d})}_{\partial\boldsymbol{\Gamma}_-} - \partial_{\hat{n}}\vec{\psi}(k_0,\mathbf{x})\cdot\mathbf{E} \quad (4.20)$$

valid at the scatterer surface. Here, we used again the shorter matrix notation. In this notation we have the identity

$$\sum_{i,k}[A]_{i,k}\cdot f_i(\mathbf{x})\cdot g_k(\mathbf{x}') \equiv \vec{f}(\mathbf{x})\cdot\mathbf{A}\cdot\vec{g}(\mathbf{x}'), \quad (4.21)$$

for example. In deriving (4.19) and (4.20) we took into account that the functions $\tilde{\varphi}_i(k_0,\mathbf{x}')$ can be suppressed since appearing with identical arguments in each term

of the transmission conditions. Comparing (4.19) and (4.20) with (2.24) and (2.25) provides

$$-\mathbf{T}_{\varphi_0} = -\mathbf{T}_{\partial\Gamma}^{(d)} = \mathbf{W}_{\partial\boldsymbol{\Gamma}_+}^{(\mathbf{d})} \tag{4.22}$$

with $\mathbf{T}_{\partial\Gamma}^{(d)}$ given by (3.54), for example. In conjunction with (4.15) it becomes clear that the scalar Green function $G_{\Gamma_+}^{(d)}(\mathbf{x}, \mathbf{x}')$ of the outer transmission problem is then approximated by (3.55) and (3.56).

The way described just now to derive the approximations of the Green functions related to the outer Dirichlet and transmission problem is very similar to the way described already in Chap. 1 to approximate the scattered field by use of Rayleigh's method. The self-consistent formalism presented here is indeed nothing but the transfer of this method to Green functions. This becomes even more obvious if, instead of the definitions (4.1) or (4.12)/(4.13), we would have chosen the approximations (4.6) or (4.15)/(4.16) as a starting point for the respective derivation. That is because the definition of the matrix elements of the interaction operators are not really needed for the above described analysis. However, it was important for us to refer to the operator character of the Green functions and the corresponding interaction operators in conjunction with Huygens' principle already at this place.

4.3 The Dyadic Green Functions Related to the Vector-Wave Equation

4.3.1 The Outer Dirichlet Problem

The approximations of the dyadic Green functions can be derived in the same way with only slight modifications due to the dyadic and vector character of the relevant quantities. Assuming the source to be located somewhere outside the smallest spherical surface circumscribing the nonspherical scatterer we define the dyadic interaction operator $\mathbf{W}_{\partial\boldsymbol{\Gamma}_+}$ related to the outer Dirichlet problem of the vector-wave equation according to

$$\begin{aligned}\mathbf{G}_{\boldsymbol{\Gamma}_+}(\mathbf{x}, \mathbf{x}') := \mathbf{G}_{\mathbf{0}}(\mathbf{x}, \mathbf{x}') + \oint_{\partial\Gamma} \mathbf{G}_{\mathbf{t}}^{>}(\mathbf{x}, \bar{\mathbf{x}}) \cdot \mathbf{W}_{\partial\boldsymbol{\Gamma}_+}(\bar{\mathbf{x}}, \tilde{\mathbf{x}}) \\ \cdot \mathbf{G}_{\mathbf{t}}^{<}(\tilde{\mathbf{x}}, \mathbf{x}')\, dS(\bar{\mathbf{x}})\, dS(\tilde{\mathbf{x}}).\end{aligned} \tag{4.23}$$

$\mathbf{G}_{\boldsymbol{\Gamma}_+}$ solves the inhomogeneous vector-wave equation (2.341) and obeys the radiation condition (2.151) both with respect to $\mathbf{x}$. Employing the boundary condition (2.342) for all $\mathbf{x} \in \partial\Gamma$ results in the equation

$$\oint_{\partial\Gamma} \left[\hat{n}_- \times \mathbf{G}_{\mathbf{t}}^{>}(\mathbf{x},\bar{\mathbf{x}})\right] \cdot \mathbf{W}_{\partial\mathbf{\Gamma}_+}(\bar{\mathbf{x}},\tilde{\mathbf{x}}) \cdot \mathbf{G}_{\mathbf{t}}^{<}(\tilde{\mathbf{x}},\mathbf{x}')\, dS(\bar{\mathbf{x}})\, dS(\tilde{\mathbf{x}}) = -\left[\hat{n}_- \times \mathbf{G}_{\mathbf{t}}^{<}(\mathbf{x},\mathbf{x}')\right]; \quad \mathbf{x} \in \partial\Gamma; \quad \mathbf{x}' \in \Gamma_+. \tag{4.24}$$

Without any restriction for our scattering problems we can assume further that the interaction operator $\mathbf{W}_{\partial\mathbf{\Gamma}_+}$ is exclusively defined in the tangential planes at the scatterer surface with respect to its variables $\bar{\mathbf{x}}$ and $\tilde{\mathbf{x}}$. This is not really needed for the analysis in this section since we do not need an explicit expression for the interaction operator, as it happened already in the scalar case. But in Chap. 7, we will see that $\mathbf{W}_{\partial\mathbf{\Gamma}_+}$ is related to the induced surface current on an ideal metallic surface which exists only in the tangential plane at the scatterer surface. This indicates that we must restrict $\mathbf{W}_{\partial\mathbf{\Gamma}_+}$ to the tangential planes to ensure a unique solution of the scattering problem. Replacing $\mathbf{G}_t^{>}$ as well as $\mathbf{G}_{\mathbf{t}}^{<}$ by the respective (and now finite!) expansions (2.340) provides

$$-(ik_0) \sum_{\tau'=1}^{2} \sum_{k=0}^{N} \left\{ \vec{\psi}_{k,\tau'}^{\hat{n}_-}(k_0,\mathbf{x}) \odot \vec{\tilde{\psi}}_{k,\tau'}(k_0,\mathbf{x}') \right\} = (ik_0) \cdot \sum_{\tau=1}^{2} \sum_{i=0}^{N} \sum_{\tau'=1}^{2} \sum_{k=0}^{N} \left[W_{\partial\Gamma_+}\right]_{i,k}^{\tau,\tau'} \cdot \left\{ \vec{\varphi}_{i,\tau}^{\hat{n}_-}(k_0,\mathbf{x}) \odot \vec{\tilde{\varphi}}_{k,\tau'}(k_0,\mathbf{x}') \right\}. \tag{4.25}$$

The matrix elements are defined according to

$$\left[W_{\partial\Gamma_+}\right]_{i,k}^{\tau,\tau'} := (ik_0) \cdot \oint_{\partial\Gamma} \vec{\tilde{\psi}}_{i,\tau}(k_0,\bar{\mathbf{x}}) \cdot \mathbf{W}_{\partial\mathbf{\Gamma}_+}(\bar{\mathbf{x}},\tilde{\mathbf{x}}) \cdot \vec{\psi}_{k,\tau'}(k_0,\tilde{\mathbf{x}})\, \mathrm{d}S(\bar{\mathbf{x}})\, \mathrm{d}S(\tilde{\mathbf{x}}). \tag{4.26}$$

From (4.23) we obtain similarly

$$\mathbf{G}_{\mathbf{\Gamma}_+}^{(\mathbf{N})}(\mathbf{x},\mathbf{x}') = \mathbf{G_0}(\mathbf{x},\mathbf{x}') + (ik_0) \cdot \sum_{\tau=1}^{2} \sum_{i=0}^{N} \sum_{\tau'=1}^{2} \sum_{k=0}^{N} \left[W_{\partial\Gamma_+}\right]_{i,k}^{\tau,\tau'} \cdot \left\{ \vec{\varphi}_{i,\tau}(k_0,\mathbf{x}) \odot \vec{\tilde{\varphi}}_{k,\tau'}(k_0,\mathbf{x}') \right\} \tag{4.27}$$

as an approximation of the dyadic Green function $\mathbf{G}_{\mathbf{\Gamma}_+}$ which is again in correspondence with the inhomogeneous vector-wave equation and the radiation condition. Now, we are also able to determine the matrix elements of the interaction operator by expressing the tangential projections $\vec{\psi}_{k,\tau'}^{\hat{n}_-}(k_0,\mathbf{x})$ of the vectorial expansion functions $\vec{\psi}_{k,\tau'}(k_0,\mathbf{x})$ on the left-hand side of (4.25) according to the transformation

$$\vec{\psi}_{k,\tau'}^{\hat{n}_-}(k_0,\mathbf{x}) = \sum_{\tau=1}^{2} \sum_{i=0}^{N} \left[\tilde{T}_{\partial\Gamma}^{\hat{n}_-}\right]_{k,i}^{\tau',\tau} \cdot \vec{\varphi}_{i,\tau}^{\hat{n}_-}(k_0,\mathbf{x}) \tag{4.28}$$

by the tangential projections $\vec{\varphi}_{i,\tau}^{\,\hat{n}_-}(k_0,\mathbf{x})$ of the vectorial expansion functions $\vec{\varphi}_{i,\tau}(k_0,\mathbf{x})$ (please, note that (4.28) is nothing but the transformation (2.17) and (2.18) explicitly written for the vectorial case). The equal sign in (4.25) is obviously justified if we choose the matrix elements of the interaction operator according to

$$\left[W_{\partial\Gamma_+}\right]_{i,k}^{\tau,\tau'} = -\left[\tilde{T}_{\partial\Gamma}^{\hat{n}_-}\right]_{k,i}^{\tau',\tau} = -\left\{\left[\tilde{T}_{\partial\Gamma}^{\hat{n}_-}\right]_{i,k}^{\tau,\tau'}\right\}^{tp} = -\left[T_{\partial\Gamma}^{\hat{n}_-}\right]_{i,k}^{\tau,\tau'}. \tag{4.29}$$

The matrix elements $\left[T_{\partial\Gamma}^{\hat{n}_-}\right]_{i,k}^{\tau,\tau'}$ of the T-matrix $\mathbf{T}_{\partial\mathbf{\Gamma}}^{\hat{\mathbf{n}}_-}$ therein are now given by (3.89). Equation (4.27) becomes therefore identical with approximation (3.87)/(3.88).

4.3.2 The Outer Transmission Problem

$$\mathbf{G}_{\mathbf{\Gamma}_+}^{(\mathbf{d})}(\mathbf{x},\mathbf{x}') := \mathbf{G_0}(\mathbf{x},\mathbf{x}') + \oint_{\partial\Gamma} \mathbf{G}_{\mathbf{t}}^{>}(\mathbf{x},\bar{\mathbf{x}}) \cdot \mathbf{W}_{\partial\mathbf{\Gamma}_+}^{(\mathbf{d})}(\bar{\mathbf{x}},\tilde{\mathbf{x}}) \cdot \mathbf{G}_{\mathbf{t}}^{<}(\tilde{\mathbf{x}},\mathbf{x}')\, dS(\bar{\mathbf{x}})\, dS(\tilde{\mathbf{x}}) \tag{4.30}$$

is the definition of the dyadic interaction operator $\mathbf{W}_{\partial\mathbf{\Gamma}_+}^{(\mathbf{d})}$ which is equivalent to (4.23) in the scalar case. Here, we need also the additional operator $\mathbf{W}_{\partial\mathbf{\Gamma}_-}^{(\mathbf{d})}$ related to the auxiliary dyadic Green function $\mathbf{G}^{(-/+)}$. In close analogy to (4.13) we choose the definition

$$\mathbf{G}^{(-/+)}(\mathbf{x},\mathbf{x}') := \oint_{\partial\Gamma} \mathbf{G}_{\mathbf{t_s}}^{<}(\mathbf{x},\bar{\mathbf{x}}) \cdot \mathbf{W}_{\partial\mathbf{\Gamma}_-}^{(\mathbf{d})}(\bar{\mathbf{x}},\tilde{\mathbf{x}}) \cdot \mathbf{G}_{\mathbf{t}}^{<}(\tilde{\mathbf{x}},\mathbf{x}')\, dS(\bar{\mathbf{x}})\, dS(\tilde{\mathbf{x}}). \tag{4.31}$$

The quantity $\mathbf{G}_{t_s}^{<}$ therein is given by the expansion

$$\mathbf{G}_{t_s}^{<}(\mathbf{x},\bar{\mathbf{x}}) = (ik) \cdot \sum_{\tau=1}^{2} \sum_{i=0}^{\infty} \left\{\vec{\psi}_{i,\tau}(k,\mathbf{x}) \odot \vec{\tilde{\varphi}}_{i,\tau}(k_0,\bar{\mathbf{x}})\right\}. \tag{4.32}$$

With this expansion we can again ensure the regularity of $\mathbf{G}^{(-/+)}$ for every $\mathbf{x}$ inside Γ_- as well as the fulfilment of the homogeneous vector-wave equation (2.345) at least for a finite number of expansion terms in (4.32). Both of these interaction operators are again restricted to the tangential plane at the scatterer surface. Next, we replace $\mathbf{G}_t^{<}(\tilde{\mathbf{x}},\mathbf{x}')$ in (4.30) and (4.31) by the (again finite!) expansion (2.340). In conjunction with the two definitions

$$\left[W_{\partial\Gamma_+}^{(d)}\right]_{i,k}^{\tau,\tau'} := (ik_0) \oint_{\partial\Gamma} \vec{\tilde{\psi}}_{i,\tau}(k_0,\bar{\mathbf{x}}) \cdot \mathbf{W}_{\partial\mathbf{\Gamma}_+}^{(\mathbf{d})}(\bar{\mathbf{x}},\tilde{\mathbf{x}}) \cdot \vec{\psi}_{k,\tau'}(k_0,\tilde{\mathbf{x}})\, dS(\bar{\mathbf{x}})\, dS(\tilde{\mathbf{x}}) \tag{4.33}$$

and

$$\left[W^{(d)}_{\partial\Gamma_-}\right]^{\tau,\tau'}_{i,k} := (ik)\oint_{\partial\Gamma}\vec{\tilde{\varphi}}_{i,\tau}(k_0,\tilde{\mathbf{x}})\cdot\mathbf{W}^{(\mathbf{d})}_{\partial\boldsymbol{\Gamma}_-}(\tilde{\mathbf{x}},\tilde{\mathbf{x}})\cdot\vec{\psi}_{k,\tau'}(k_0,\tilde{\mathbf{x}})\,dS(\tilde{\mathbf{x}})dS(\tilde{\mathbf{x}}) \tag{4.34}$$

of the relevant matrix elements of the dyadic interaction operators $\mathbf{W}^{(\mathbf{d})}_{\partial\boldsymbol{\Gamma}_+}$ and $\mathbf{W}^{(\mathbf{d})}_{\partial\boldsymbol{\Gamma}_-}$ we get the approximations

$$\begin{aligned}\mathbf{G}^{(\mathbf{d},\mathbf{N})}_{\boldsymbol{\Gamma}_+}(\mathbf{x},\mathbf{x}') = \;& \mathbf{G_0}(\mathbf{x},\mathbf{x}') + (ik_0)\cdot\sum_{\tau=1}^{2}\sum_{i=0}^{N}\sum_{\tau'=1}^{2}\sum_{k=0}^{N}\left[W^{(d)}_{\partial\Gamma_+}\right]^{\tau,\tau'}_{i,k}\\ & \cdot\left\{\vec{\varphi}_{i,\tau}(k_0,\mathbf{x})\odot\vec{\tilde{\varphi}}_{k,\tau'}(k_0,\mathbf{x}')\right\}\end{aligned} \tag{4.35}$$

and

$$\mathbf{G}^{(-/+,N)}(\mathbf{x},\mathbf{x}') = (ik_0)\cdot\sum_{\tau=1}^{2}\sum_{i=0}^{N}\sum_{\tau'=1}^{2}\sum_{k=0}^{N}\left[W^{(d)}_{\partial\Gamma_-}\right]^{\tau,\tau'}_{i,k}\cdot\left\{\vec{\psi}_{i,\tau}(k,\mathbf{x})\odot\vec{\tilde{\varphi}}_{k,\tau'}(k_0,\mathbf{x}')\right\} \tag{4.36}$$

for the corresponding dyadic Green functions. Employing the transmission conditions (2.343) and (2.344) at the scatterer surface to these approximations results in the two equations (4.19) and (4.20) but appropriately modified due to the vector character of the expansion functions (i.e., the components of $\vec{\varphi}(k_0,\mathbf{x})$ in (4.19) are now vector functions by itself made up of the tangential projections of the corresponding vectorial expansion functions for $\tau=1$ and $\tau=2$). The matrices are now 2×2 block matrices as already discussed in Chap. 1. In analogy to (4.22) we have therefore

$$-\mathbf{T}^{(\hat{n}_-,d)}_{\partial\Gamma} = \mathbf{W}^{(\mathbf{d})}_{\partial\boldsymbol{\Gamma}_+}, \tag{4.37}$$

with $\mathbf{T}^{(\hat{n}_-,d)}_{\partial\Gamma}$ given by (3.100). Thus, we can state again the identity of approximation (4.35) with approximation (3.98)/(3.99).

Before dealing with the symmetry and unitarity properties we will summarize the approximations derived above for the Green functions related to the outer Dirichlet and transmission problem. The general expressions for the scalar Green functions may be written as

$$G^{(N)}_{\Gamma_+}(\mathbf{x},\mathbf{x}') = G_0(\mathbf{x},\mathbf{x}') + (ik_0)\sum_{i,k=0}^{N}[W]_{i,k}\cdot\varphi_i(k_0,\mathbf{x})\cdot\tilde{\varphi}_k(k_0,\mathbf{x}');\,\mathbf{x},\mathbf{x}'\in\Gamma_+. \tag{4.38}$$

The dyadic Green functions read

$$\mathbf{G}^{(\mathbf{N})}_{\mathbf{\Gamma}_+}(\mathbf{x},\mathbf{x}') = \mathbf{G_0}(\mathbf{x},\mathbf{x}') + (ik_0)\sum_{\tau,\tau'=1}^{2}\sum_{i,k=0}^{N}[W]^{\tau,\tau'}_{i,k} \cdot \left\{\vec{\varphi}_{i,\tau}(k_0,\mathbf{x}) \odot \vec{\tilde{\varphi}}_{k,\tau'}(k_0,\mathbf{x}')\right\}; \quad \mathbf{x},\mathbf{x}' \in \Gamma_+. \tag{4.39}$$

The matrix elements $[W]_{i,k}$ in the scalar approximation are the elements of the matrix

- $-\mathbf{T}_{\partial\Gamma}$ according to (3.34) if the outer Dirichlet problem of the scalar Helmholtz equation is considered. The corresponding Green function is then denoted with $G^{(N)}_{\Gamma_+}$.
- $-\mathbf{T}^{(d)}_{\partial\Gamma}$ according to (3.54) if the outer transmission problem of the scalar Helmholtz equation is considered. The corresponding Green function is then denoted with $G^{(d,N)}_{\Gamma_+}$.

The matrix elements $[W]^{\tau,\tau'}_{i,k}$ in the dyadic approximation are the elements of the matrix

- $-\mathbf{T}^{\hat{\mathbf{n}}_-}_{\partial\mathbf{\Gamma}}$ according to (3.89) if the outer Dirichlet problem of the vector-wave equation is considered. The corresponding Green function is then denoted with $\mathbf{G}^{(\mathbf{N})}_{\mathbf{\Gamma}_+}$.
- $-\mathbf{T}^{(\hat{\mathbf{n}}_-,\mathbf{d})}_{\partial\mathbf{\Gamma}}$ according to (3.100) if the outer transmission problem of the vector-wave equation is considered. The corresponding Green function is then denoted with $\mathbf{G}^{(\mathbf{d},\mathbf{N})}_{\mathbf{\Gamma}_+}$.

4.4 Symmetry and Unitarity

The T-matrices are the decisive elements of the approximate Green functions. At the same time, they are the most important quantities for solving the scattering problem. This can be considered to be the most essential results of Chap. 3 and of the foregoing sections of this chapter. Once we know the expansion coefficients of the primary incident field at the scatterer surface we are able to calculate the corresponding expansion coefficients of the scattered field via the T-matrix if the latter field is expanded in terms of the radiating eigensolutions of the Helmholtz or vector-wave equation.

However, the Green functions offer the possibility to prove certain important properties of the T-matrix and the strongly related "scattering matrix" (or "S-matrix", as it is also called). The S-matrix was originally and independently introduced by Wheeler and Heisenberg in quantum mechanics. Only later on it was utilized in the theory of electromagnetic wave scattering. The symmetry and unitarity properties of these matrices are of special importance in scattering theory since they can be related to the physical principles of reciprocity and energy conservation. In this context, it is quite

interesting that the fulfilment of these physical principles, which represent "merely" our physical experience gained in manifold experimental observations, are used to prove the symmetry and unitarity properties of the T- and S-matrices mathematically. This holds in the theory of electromagnetic wave scattering as well as in the quantum mechanical counterpart. Some of the relevant literature concerning this aspect is cited in the reference chapter. Such an approach of proving symmetry and unitarity seems very questionable for the following reason: Since energy conservation, for example, is solely an experience which is not mathematically revisable we had actually to infer that the unitarity of the S-matrix can never be proven. The evidence of symmetry and unitarity properties (among other properties) of mathematical structures like matrices should be therefore based only on mathematical considerations, independent of whether they can be linked to our physical experience or not. Only afterwards, i.e., once we know the mathematical conditions which will lead to a unitary S-matrix, we can think about linking this mathematical structure together with the relevant conditions to our physical experience of energy conservation in electromagnetic wave scattering. Moreover and regarding the field of electromagnetic wave scattering, the above mentioned "proofs" are usually restricted to the far-field region and to primary incident plane waves. This is essentially owed to the simplifications resulting from this special scenario. But this restriction is not justified from a physical point of view. Therefore, we want to demonstrate with the following two subsections how one can overcome these problems by employing Green functions.

4.4.1 Symmetry

To consider the symmetry property of the matrix elements of the interaction operators in the scalar case we write down (4.38) once again but with all indices and by taking the definition (2.85) into account:

$$G_{\Gamma_+}^{(N)}(\mathbf{x},\mathbf{x}') = G_0(\mathbf{x},\mathbf{x}') + (ik_0) \sum_{l,n;l',n'} (-1)^{l'} \cdot [W]_{l,n;l',n'} \cdot \varphi_{l,n}(k_0,\mathbf{x}) \cdot \varphi_{-l',n'}(k_0,\mathbf{x}'). \tag{4.40}$$

For the free-space Green function as well as the Green functions related to the outer Dirichlet and transmission problem we could derive in Chap. 2 the symmetry relations (2.245) and (2.284)/(2.285) by use of Green's theorem. From these symmetry relations and in conjunction with (4.40) we can infer the equality of the expressions

$$\sum_{l,n;l',n'} (-1)^{l'} \cdot [W]_{l,n;l'n'} \cdot \varphi_{l,n}(k_0,\mathbf{x}) \cdot \varphi_{-l',n'}(k_0,\mathbf{x}') = \sum_{l,n;l',n'} (-1)^{l'} \cdot [W]_{l,n;l',n'} \cdot \varphi_{l,n}(k_0,\mathbf{x}') \cdot \varphi_{-l',n'}(k_0,\mathbf{x}). \tag{4.41}$$

Let us now introduce a "nutritious" 1 in form of $(-1)^{l-l}$ on the right-hand side of this equation. Taking identity $(-1)^{-l} = (-1)^{l}$ into account we get for the right-hand side of (4.41)

$$RS = \sum_{l,n;l',n'} (-1)^{l+l'} \cdot [W]_{l,n;l',n'} \cdot (-1)^{l} \cdot \varphi_{l,n}(k_0, \mathbf{x}') \cdot \varphi_{-l',n'}(k_0, \mathbf{x}). \quad (4.42)$$

Then we interchange indices l, n and l', n' to get

$$RS = \sum_{l,n;l',n'} (-1)^{l+l'} \cdot [W]_{l',n';l,n} \cdot \varphi_{-l,n}(k_0, \mathbf{x}) \cdot (-1)^{l'} \cdot \varphi_{l',n'}(k_0, \mathbf{x}'). \quad (4.43)$$

Next, we replace index l by $-l$ and l' by $-l'$. Since the summation with respect to the azimuthal modes l runs from $-n$ to n (see (2.83), for example) this means only a rearranging of the original sum, i.e., identity

$$\sum_{n=0}^{n_{max}} \sum_{l=-n}^{n} a_{l,n} \cdot \varphi_{-l,n}(\mathbf{x}) = \sum_{n=0}^{n_{max}} \sum_{l=-n}^{n} a_{-l,n} \cdot \varphi_{l,n}(\mathbf{x}) \quad (4.44)$$

holds in general. But then we obtain from (4.43)

$$RS = \sum_{l,n;l',n'} (-1)^{l+l'} \cdot [W]_{-l',n';-l,n} \cdot \varphi_{l,n}(k_0, \mathbf{x}) \cdot (-1)^{l'} \cdot \varphi_{-l',n'}(k_0, \mathbf{x}'). \quad (4.45)$$

If comparing this expression with the left-hand side of (4.41) we obtain the following symmetry property for the matrix elements of the interaction operators related to the outer Dirichlet and transmission problem in the scalar case:

$$[W]_{l,n;l',n'} = (-1)^{l+l'} \cdot [W]_{-l',n';-l,n}\,. \quad (4.46)$$

This symmetry property is thus an obvious consequence of the symmetry relations derived for the Green functions if interchanging their arguments. It is moreover independent of the scatterer geometry and morphology, i.e., independent of whether we have an absorbing or nonabsorbing scatterer. For nonspherical scatterers (4.46) will be fulfilled only for infinitely large matrices, in general. But this offers the possibility to estimate the accuracy of a numerical calculated T-matrix in a certain application. The physical consequence of this symmetry together with its usage as a parameter to estimate the numerical accuracy of obtained scattering results will be discussed in Chap. 9. There is another aspect which should be mentioned here. In the older literature (in Waterman's original papers, for example) we can find instead of (4.46) the simpler symmetry relation

$$[W]_{l,n;l',n'} = [W]_{l',n';l,n}\,. \quad (4.47)$$

The difference to (4.46) is caused by the usage of different expressions for the spherical harmonics $Y_{l,n}$. Here, we used the complex function $e^{il\phi}$ with respect to the ϕ-dependence. But this function is in the literature sometimes replaced by the two sets of the real-valued $sinl\phi$ and $cosl\phi$ functions. The usage of the latter functions just produces the symmetry relation (4.47). In this case the azimuthal modes l are only represented by natural numbers.

In Chap. 8 of this book, it is demonstrated by employing group theoretical considerations in conjunction with the relevant Green functions as well as the related interaction operators that there exist an elegant and easy way to derive other symmetries of the matrix elements if the scatterer geometry exhibits a certain symmetry. And, moreover, it is demonstrated that exploiting those symmetry relations may result in a drastic simplification of the numerical effort and provides much more stable solution techniques. But such considerations are not within the scope of this section. Only one symmetry relation is of our special interest here. That is the symmetry relation resulting from a rotational symmetric scatterer geometry. It can be simply derived without falling back to group theoretical considerations. If we put the z-axis of the Cartesian coordinate system into the axis of rotation of the scatterer we get

$$[W]_{l,n;l',n'} = \delta_{l,l'} \cdot [W]_{l,n;l',n'} \,, \tag{4.48}$$

i.e., the matrix elements of the interaction operator (or the T-matrix, synonymously) become block-diagonal with respect to the azimuthal modes l and l'. This can be simply proven by utilizing the ϕ-independence of the resulting boundary integrals in the scalar product definition when calculating the T-matrix. The necessary ϕ-integration produces the Kronecker symbol $\delta_{l,l'}$ if the eigenfunctions of the scalar Helmholtz equation are chosen as weighting functions. It is not at least this possibility to take geometry dependent symmetry relations in a straightforward way into account which makes T-matrix methods very successful in many applications. This holds especially in remote sensing where we have to apply additional and time consuming orientation averaging procedures. We will become acquainted with such applications in the numerical simulations of Chap. 9.

We can proceed very similar in the case of the dyadic Green function (4.39). For the dyadic free-space Green function we still have the symmetry relation (2.329). But for the dyadic Green functions related to the outer Dirichlet and transmission problem we must now apply relation (2.346). The latter relation requires the equality of

$$\begin{aligned}
&\sum_{\tau,\tau'=1}^{2} \sum_{l,n;l',n'} (-1)^{l'} \cdot [W]^{\tau,\tau'}_{l,n;l'n'} \cdot \left\{ \vec{\varphi}_{l,n,\tau}(k_0, \mathbf{x}) \odot \vec{\varphi}_{-l',n',\tau'}(k_0, \mathbf{x}') \right\} \\
&= \sum_{\tau,\tau'=1}^{2} \sum_{l,n;l',n'} (-1)^{l'} \cdot [W]^{\tau,\tau'}_{l,n;l'n'} \cdot \left\{ \vec{\varphi}_{-l',n',\tau'}(k_0, \mathbf{x}) \odot \vec{\varphi}_{l,n,\tau}(k_0, \mathbf{x}') \right\} .
\end{aligned} \tag{4.49}$$

According to the three steps

- Insertion of $1 = (-1)^{l-l}$ on the right-hand side of (4.49)
- Interchanging n, l, τ and n', l', τ'
- Replacing l by $-l$ and l' by $-l'$

and after intercomparison with the left-hand side of (4.49) we obtain now the symmetry relation

$$[W]^{\tau,\tau'}_{l,n;l',n'} = (-1)^{l+l'} \cdot [W]^{\tau',\tau}_{-l',n';-l,n} \tag{4.50}$$

for the matrix elements of the dyadic interaction operators. And in the special case of rotational symmetric scatterer this simplifies to

$$[W]^{\tau,\tau'}_{l,n;l',n'} = \delta_{l,l'} \cdot [W]^{\tau,\tau'}_{l,n;l',n'} \,. \tag{4.51}$$

It should be mentioned again that (4.50) is independent of whether the scatterer is absorbing or nonabsorbing.

4.4.2 Unitarity

The relevant configuration for proving the unitarity property of the S-matrix is depicted in Fig. 4.1. The source of the primary incident field may be placed somewhere outside the outer boundary surface $\partial\Gamma_a$ enclosing the finite sub-volume $\tilde{\Gamma}$ of Γ. The scatterer surface represents the inner boundary surface of $\tilde{\Gamma}$. Furthermore, we assume that $|\mathbf{x}| < |\mathbf{x}'|$ holds for every $\mathbf{x} \in \partial\Gamma_a$. That is, the source of the pri-

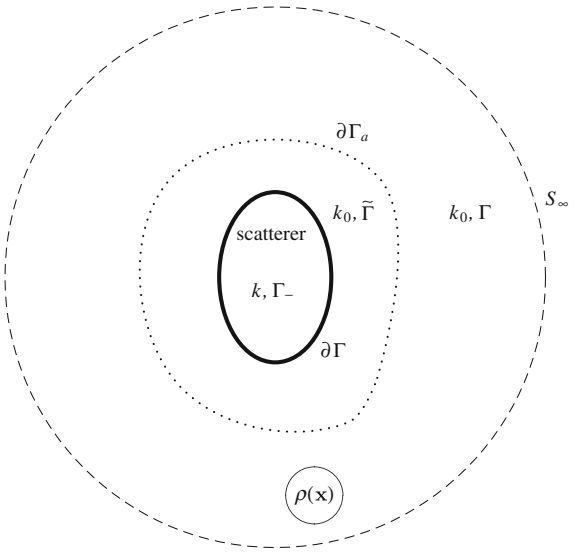

Fig. 4.1 The geometrical configuration to prove unitarity

mary incident field is located outside the smallest spherical surface circumscribing the volume $\tilde{\Gamma}$. This will allow us to use $G_0^<$ according to (2.278) or $\mathbf{G_t}^<$ according to (2.340) in the approximations of the Green functions $G_{\Gamma_+}(\mathbf{x},\mathbf{x}')$ and $\mathbf{G}_{\mathbf{\Gamma}_+}(\mathbf{x},\mathbf{x}')$, respectively, for every $\mathbf{x}\in\tilde{\Gamma}$. Let us denote the corresponding Green functions inside $\tilde{\Gamma}$ with $G^<_{\Gamma_+}(\mathbf{x},\mathbf{x}')$ and $\mathbf{G}^<_{\mathbf{\Gamma}_+}(\mathbf{x},\mathbf{x}')$. Thus, we write instead of approximations (4.38) and (4.39)

$$G^{(<,N)}_{\Gamma_+}(\mathbf{x},\mathbf{x}') = (ik_0)\cdot\sum_{i=0}^{N}\psi_i(k_0,\mathbf{x})\cdot\tilde{\varphi}_i(k_0,\mathbf{x}')+(ik_0)\sum_{i,k=0}^{N}[W]_{i,k}\cdot\varphi_i(k_0,\mathbf{x})\cdot\tilde{\varphi}_k(k_0,\mathbf{x}');\quad \mathbf{x}\in\tilde{\Gamma},\mathbf{x}'\in\Gamma_+ \tag{4.52}$$

and

$$\mathbf{G}^{(<,\mathbf{N})}_{\mathbf{\Gamma}_+}(\mathbf{x},\mathbf{x}') = (ik_0)\sum_{\tau=1}^{2}\sum_{i=0}^{N}\left\{\vec{\psi}_{i,\tau}(k_0,\mathbf{x})\odot\vec{\tilde{\varphi}}_{i,\tau}(k_0,\mathbf{x}')\right\} + (ik_0)\sum_{\tau,\tau'=1}^{2}\sum_{i,k=0}^{N}[W]^{\tau,\tau'}_{i,k}\cdot\left\{\vec{\varphi}_{i,\tau}(k_0,\mathbf{x})\odot\vec{\tilde{\varphi}}_{k,\tau'}(k_0,\mathbf{x}')\right\};\quad \mathbf{x}\in\tilde{\Gamma},\ \mathbf{x}'\in\Gamma_+\,. \tag{4.53}$$

Due to (2.82) and (2.162) these approximations can be rewritten into

$$G^{(<,N)}_{\Gamma_+}(\mathbf{x},\mathbf{x}') = (ik_0)\cdot\sum_{i,k=0}^{N}\frac{1}{2}\cdot\left\{\delta_{i,k}\cdot\chi_i(k_0,\mathbf{x})+[S]_{i,k}\cdot\varphi_i(k_0,\mathbf{x})\right\}\cdot\tilde{\varphi}_k(k_0,\mathbf{x}') \tag{4.54}$$

and

$$\mathbf{G}^{(<,\mathbf{N})}_{\mathbf{\Gamma}_+}(\mathbf{x},\mathbf{x}') = (ik_0)\sum_{\tau,\tau'=1}^{2}\sum_{i,k=0}^{N}\frac{1}{2}\cdot\left\{\delta_{i,k}\delta_{\tau,\tau'}\cdot\vec{\chi}_{i,\tau}(k_0,\mathbf{x})+[S]^{\tau,\tau'}_{i,k}\cdot\vec{\varphi}_{i,\tau}(k_0,\mathbf{x})\right\}\odot\vec{\tilde{\varphi}}_{k,\tau'}(k_0,\mathbf{x}'). \tag{4.55}$$

$$[S]_{i,k} = \delta_{i,k}+2\cdot[W]_{i,k} \tag{4.56}$$

and

$$[S]^{\tau,\tau'}_{i,k} = \delta_{i,k}\,\delta_{\tau,\tau'}+2\cdot[W]^{\tau,\tau'}_{i,k} \tag{4.57}$$

therein are the matrix elements of the respective S-matrix. Due to the initially formulated conventions we know that the Green function $G^<_{\Gamma_+}(\mathbf{x},\mathbf{x}')$ solves the

homogeneous Helmholtz equation with respect to $\mathbf{x}$ inside $\tilde{\mathbf{\Gamma}}$. Correspondingly, the dyadic Green function $\mathbf{G}^{<}_{\mathbf{\Gamma}_+}(\mathbf{x},\mathbf{x}')$ solves the homogeneous vector-wave equation in the same volume. To prove the unitarity of the S-matrix we need a further restriction. We assume that both parameters k_0 and k are pure real-valued quantities. Then we know that also the conjugate-complex Green functions are solutions of the homogeneous Helmholtz and vector-wave equation in $\tilde{\Gamma}$.

Let us first consider the scalar case. For this, we define the following functional at the boundary surface $\partial\Gamma_a$ with its outward directed unit normal vector $\hat{n}_a$:

$$\{f(\mathbf{x}), g(\mathbf{x})\}_{\partial\Gamma_a} := \oint_{\partial\Gamma_a} \left\{ \frac{\partial f^*(\mathbf{x})}{\partial \hat{n}_a} \cdot g(\mathbf{x}) - \frac{\partial g(\mathbf{x})}{\partial \hat{n}_a} \cdot f^*(\mathbf{x}) \right\} dS(\mathbf{x}). \tag{4.58}$$

The definition of this functional is obviously geared to the boundary integral of Green's theorem. Please, note that it is **not** a scalar product since it fulfils the relation

$$\{f(\mathbf{x}), g(\mathbf{x})\}_{\partial\Gamma_a} = -\{g(\mathbf{x}), f(\mathbf{x})\}^*_{\partial\Gamma_a}. \tag{4.59}$$

Now, we are able to show that

$$\left\{ G^{<}_{\Gamma_+}(\mathbf{x},\mathbf{x}'), G^{<}_{\Gamma_+}(\mathbf{x},\mathbf{x}') \right\}_{\partial\Gamma_a} = 0 \tag{4.60}$$

holds. The proof of this identity for the outer Dirichlet problem runs as follows: We apply Green's theorem (2.239) in volume $\tilde{\Gamma}$ with the two quantities $\Psi(\mathbf{x}) = \left[G^{<}_{\Gamma_+}(\mathbf{x},\mathbf{x}') \right]^*$ and $\Phi(\mathbf{x}) = G^{<}_{\Gamma_+}(\mathbf{x},\mathbf{x}')$. By use of the homogeneous Dirichlet condition which holds for both Green functions $\left[G^{<}_{\Gamma_+} \right]^*$ and $G^{<}_{\Gamma_+}$ if $\mathbf{x} \in \partial\Gamma$ (4.60) is obtained immediately. The proof for the outer transmission problem is again a little bit more complicate. As discussed earlier in Sect. 2.5.3 for the proof of the symmetry relation (2.285) we have to apply Green's theorem twice. First in $\tilde{\Gamma}$ with $\Psi(\mathbf{x}) = \left[G^{<}_{\Gamma_+}(\mathbf{x},\mathbf{x}') \right]^*$ and $\Phi(\mathbf{x}) = G^{<}_{\Gamma_+}(\mathbf{x},\mathbf{x}')$, and second in Γ_- with $\Psi(\mathbf{x}) = \left[G^{(-,+)}(\mathbf{x},\mathbf{x}') \right]^*$ and $\Phi(\mathbf{x}) = G^{(-,+)}(\mathbf{x},\mathbf{x}')$. Taking the transmission conditions at $\partial\Gamma$ into account which must be hold also for the conjugate-complex Green function we end up again with identity (4.60).

Beside (4.60) we need some more identities to prove the unitarity. Due to relations (2.80) and (2.81) we have for a real-valued parameter k_0

$$h^{(1)}_n(k_0 r) = \left[h^{(2)}_n(k_0 r) \right]^*. \tag{4.61}$$

This is the necessary precondition to prove the following identities which hold for the eigensolutions $\varphi_i(k_0,\mathbf{x})$ and $\chi_i(k_0,\mathbf{x})$ of the homogeneous Helmholtz equation:

$$\begin{aligned}\left\{\varphi_i(k_0,\mathbf{x}),\varphi_j(k_0,\mathbf{x})\right\}_{\partial\Gamma_a} &= \left\{\chi_i(k_0,\mathbf{x}),\chi_j(k_0,\mathbf{x})\right\}_{\partial\Gamma_a} \\ &= \left\{\chi_i(k_0,\mathbf{x}),\varphi_j(k_0,\mathbf{x})\right\}_{\partial\Gamma_a} = 0 \end{aligned} \tag{4.62}$$

for all $i \neq j$, and

$$\{\chi_i(k_0,\mathbf{x}),\varphi_i(k_0,\mathbf{x})\}_{\partial\Gamma_a} = \{\varphi_i(k_0,\mathbf{x}),\chi_i(k_0,\mathbf{x})\}_{\partial\Gamma_a} = 0 \tag{4.63}$$

as well as

$$\{\chi_i(k_0,\mathbf{x}),\chi_i(k_0,\mathbf{x})\}_{\partial\Gamma_a} = -\{\varphi_i(k_0,\mathbf{x}),\varphi_i(k_0,\mathbf{x})\}_{\partial\Gamma_a} = c \tag{4.64}$$

for all $i = 0,\ldots,N$. The constant c therein is a constant which does not depend on the index i. To derive (4.62) we apply Green's theorem (2.239) in the volume bounded by $\partial\Gamma_a$ and S_∞ with $\Psi(\mathbf{x}) = \varphi_i^*(k_0,\mathbf{x})$; $\Phi(\mathbf{x}) = \varphi_j(k_0,\mathbf{x})$, $\Psi(\mathbf{x}) = \chi_i^*(k_0,\mathbf{x})$; $\Phi(\mathbf{x}) = \chi_j(k_0,\mathbf{x})$, and $\Psi(\mathbf{x}) = \chi_i^*(k_0,\mathbf{x})$; $\Phi(\mathbf{x}) = \varphi_j(k_0,\mathbf{x})$, respectively, in conjunction with the orthogonality of these eigenfunctions at the spherical surface S_∞. For a real-valued k_0 we can moreover derive the general relation

$$\left\{f_i(k_0,\mathbf{x}),g_j(k_0,\mathbf{x})\right\}_{\partial\Gamma_a} = -\left\{f_i(k_0,\mathbf{x}),g_j(k_0,\mathbf{x})\right\}_{S_\infty}, \tag{4.65}$$

with f, g representing one of the above mentioned combinations of eigenfunctions used in conjunction with Green's theorem. Thus, we can see that the surface $\partial\Gamma_a$ must not be restricted to a spherical ones to get (4.62). It is sufficient that S_∞ is a spherical surface. Equation (4.63), on the other hand, is a direct consequence of (4.58) and (4.61). To show the validity of (4.64) we can choose the same way as for the proof of (4.62). But to show that the expression $\{\chi_i(k_0,\mathbf{x}),\chi_i(k_0,\mathbf{x})\}_{S_\infty}$ provides a constant in the far-field at S_∞ we have to consider the asymptotic behaviour (2.79) of the eigenfunctions $\chi_i(\mathbf{x})$. In doing so, we neglect all contributions running stronger against zero than $1/r$ (please, note that the normal derivative at S_∞ corresponds to the derivation with respect to the radial coordinate!). The explicit value of the constant c must not really be known for the proof of unitarity but it can of course be calculated with the mentioned procedure. All these calculations can be performed by the reader himself without greater problems. This will practice again the usage of Green's theorem.

Having gathered together all the necessary prerequisites it is now a relatively simple task to derive the unitarity property of the S-matrix. We insert approximation (4.54) into (4.60) (where we have to use different summation indices for $\left[G_{\Gamma_+}^{(<,N)}\right]^*$ and $G_{\Gamma_+}^{(<,N)}$, of course) to get

$$\left\{G_{\Gamma_+}^{(<,N)}(\mathbf{x},\mathbf{x}'),\, G_{\Gamma_+}^{(<,N)}(\mathbf{x},\mathbf{x}')\right\}_{\partial\Gamma_a}$$
$$= \frac{k_0^2}{4}\sum_{i,k,q=0}^{N}\{\chi_i(k_0,\mathbf{x}),\chi_i(k_0,\mathbf{x})\}_{\partial\Gamma_a}\cdot\left[\delta_{i,k}\cdot\delta_{i,q} - [S]_{i,k}^{*}\cdot[S]_{i,q}\right]$$
$$\cdot\,\tilde{\varphi}_k^{*}(k_0,\mathbf{x}')\cdot\tilde{\varphi}_q(k_0,\mathbf{x}') = 0. \tag{4.66}$$

This expression can be rewritten into

$$\left\{G_{\Gamma_+}^{(<,N)}(\mathbf{x},\mathbf{x}'),\, G_{\Gamma_+}^{(<,N)}(\mathbf{x},\mathbf{x}')\right\}_{\partial\Gamma_a}$$
$$= \frac{k_0^2}{4}\cdot c\cdot\left[<\vec{\tilde{\varphi}}|\vec{\tilde{\varphi}}> - <\vec{\tilde{\varphi}}_s|\vec{\tilde{\varphi}}_s>\right] = 0 \tag{4.67}$$

because of (4.64). $\vec{\tilde{\varphi}}$ therein represents the $(N+1)$-component vector $(\tilde{\varphi}_0(k_0,\mathbf{x}'),\ldots,\tilde{\varphi}_N(k_0,\mathbf{x}'))$ with fixed but arbitrary $\mathbf{x}'$. The vector $\vec{\tilde{\varphi}}_s(k_0,\mathbf{x}')$ is defined according to

$$\vec{\tilde{\varphi}}_s(k_0,\mathbf{x}') := \mathbf{S}\cdot\vec{\tilde{\varphi}}(k_0,\mathbf{x}') \tag{4.68}$$

via the S-matrix. $<\vec{f}(\mathbf{x}')\,|\,\vec{f}(\mathbf{x}')>$ denotes the conventional algebraic scalar product

$$<\vec{f}(\mathbf{x}')\,|\,\vec{f}(\mathbf{x}')> = \sum_{i=0}^{N} f_i^{*}(\mathbf{x}')\cdot f_i(\mathbf{x}')\,. \tag{4.69}$$

Because of

$$<\vec{\tilde{\varphi}}_s\,|\,\vec{\tilde{\varphi}}_s> = <\mathbf{S}\cdot\vec{\tilde{\varphi}}\,|\,\mathbf{S}\cdot\vec{\tilde{\varphi}}> = <\vec{\tilde{\varphi}}\,|\,\mathbf{S}^{\dagger}\cdot\mathbf{S}\cdot\vec{\tilde{\varphi}}> \tag{4.70}$$

($\mathbf{S}^{\dagger}$ denotes the transpose and conjugate-complex of the S-matrix) and by taking (4.67) into account we can thus infer the unitarity relation

$$\mathbf{S}^{\dagger}\cdot\mathbf{S} = \mathbf{E} \tag{4.71}$$

of the S-Matrix. It should be emphasized again that this unitarity relation is a consequence of real-valued parameters k_0 and k and the resulting identity (4.60). In the course of deriving this relation it was not necessary to put $\partial\Gamma_a$ into the far-field, as we could see. Due to (4.56) or

$$\mathbf{S} = \mathbf{E} + 2\cdot\mathbf{W} \tag{4.72}$$

if employing the matrix notation the unitarity relation of the S-matrix transforms into the relation

$$\mathbf{W}^{\dagger}\cdot\mathbf{W} = -\frac{1}{2}\cdot\left(\mathbf{W}^{\dagger}+\mathbf{W}\right) \tag{4.73}$$

of the matrix elements of the interaction operator.

The attentive reader may observed that we did not reached our initial goal in all aspects with the above given derivation of the unitarity property of the S-matrix. In what the problem precisely consists? We were searching for a way which does not requires any fall-back to a certain physical situation. But looking at Fig. 4.1 we have to state that this was not fully achieved because we had to restrict the location of the source of the primary incident field. Just to remember: it was placed outside the smallest spherical surface circumscribing $\tilde{\Gamma}$. This was a necessary condition to derive the essential identity (4.60). On the other hand and as discussed in Sect. 2.5, the decoupling of the primary source from the properties of the considered space is one of the essential advantages of Green functions. Therefore, we may expect that the S-matrix as a substantial part of the Green function should be always a unitary matrix as long as k_0 and k are nonabsorbing, independent of the location of the source. But then we can no longer apply identity (4.60). Interestingly, if looking at the outer Dirichlet problem, there exist another way to prove the unitarity of the S-matrix without any fall-back to the configuration depicted in Fig. 4.1. To demonstrate this let us define the following scalar product of the two at first arbitrary and $(N+1)$-component vector functions $\vec{u}(\mathbf{x})$ and $\vec{v}(\mathbf{x})$ at the scatterer surface:

$$(\vec{u}, \vec{v})_{\partial\Gamma} := \sum_{i=0}^{N} \oint_{\partial\Gamma} u_i^*(\mathbf{x}) \cdot v_i(\mathbf{x}) dS(\mathbf{x}). \tag{4.74}$$

If assuming again that the parameter k_0 is real-valued, and if using the incoming and radiating eigensolutions (2.58) and (2.59) of the Helmholtz equation it is straightforward to show in conjunction with (2.80) and (2.81) that

$$(\vec{\chi}_0, \vec{\chi}_0)_{\partial\Gamma} = (\vec{\varphi}_0, \vec{\varphi}_0)_{\partial\Gamma} \tag{4.75}$$

holds. The index "0" indicates that k_0 is used in the arguments of these functions. Utilizing the transformation character (2.18) of the T-matrix as well as relation (2.82) we get

$$\vec{\chi}_0^{\,tp} = -\mathbf{S}_{\partial\mathbf{\Gamma}}^{tp} \cdot \vec{\varphi}_0^{\,tp} \tag{4.76}$$

or

$$\vec{\chi}_0 = -\vec{\varphi}_0 \cdot \mathbf{S}_{\partial\mathbf{\Gamma}} \tag{4.77}$$

with $\mathbf{S}_{\partial\mathbf{\Gamma}}$ denoting the S-matrix related to the outer Dirichlet problem. Inserting this expression into (4.75) provides the identity

$$\left(\vec{\varphi}_0, \vec{\varphi}_0 \cdot \mathbf{S}_{\partial\mathbf{\Gamma}}^{\dagger} \cdot \mathbf{S}_{\partial\mathbf{\Gamma}}\right)_{\partial\Gamma} = (\vec{\varphi}_0, \vec{\varphi}_0)_{\partial\Gamma} \tag{4.78}$$

from which we can infer the unitarity property (4.71) of the S-matrix $\mathbf{S}_{\partial\mathbf{\Gamma}}$ for a real-valued parameter k_0 immediately. Because of (4.75) it seems to be sufficient for the proof of the unitarity of $\mathbf{S}_{\partial\mathbf{\Gamma}}$ that (4.77) holds in the sense of the weak convergence

(2.5) at the scatterer surface. Only for spherical surfaces we have the special situation that the equality sign in (4.76) and (4.77) holds already for every finite number of components of the vectors $\vec{\chi}_0$ and $\vec{\varphi}_0$, i.e., the unitarity of the S-matrix holds already for every finite matrix $\mathbf{S}_{\partial\mathbf{\Gamma}}$. Unfortunately, for the outer transmission problem we could not find a similar derivation of the unitarity of the related S-matrix, so far.

In close analogy to the way described just now, we are able to prove the unitarity of the S-matrix related to the dyadic Green functions. Assuming again real-valued parameters k_0 and k, and restricting again the situation to the configuration shown in Fig. 4.1 identity

$$\left\{\mathbf{G}^{<}_{\mathbf{\Gamma}_+}(\mathbf{x},\mathbf{x}'),\mathbf{G}^{<}_{\mathbf{\Gamma}_+}(\mathbf{x},\mathbf{x}')\right\}_{\partial\Gamma_a}=0 \tag{4.79}$$

can be derived by use of the dyadic-dyadic Green theorem (2.319). Expression $\{\mathbf{P},\mathbf{Q}\}_{\partial\Gamma_a}$ for the two dyadic quantities $\mathbf{P}$ and $\mathbf{Q}$ is now defined according to

$$\begin{aligned}\left\{\mathbf{P}(\mathbf{x},\mathbf{x}'),\mathbf{Q}(\mathbf{x},\mathbf{x}')\right\}_{\partial\Gamma_a} := \oint_{\partial\Gamma_a}\Big\{&\left[\hat{n}_a\times\mathbf{P}(\mathbf{x},\mathbf{x}')\right]^{*^{tp}}\cdot\left[\nabla_x\times\mathbf{Q}(\mathbf{x},\mathbf{x}')\right]\\&-\left[\nabla_x\times\mathbf{P}(\mathbf{x},\mathbf{x}')\right]^{*^{tp}}\cdot\left[\hat{n}_a\times\mathbf{Q}(\mathbf{x},\mathbf{x}')\right]\Big\}\,dS(\mathbf{x}).\end{aligned} \tag{4.80}$$

Moreover, we need the functional

$$\begin{aligned}\left\{\vec{\Psi}(\mathbf{x}),\vec{\Phi}(\mathbf{x})\right\}_{\partial\Gamma_a} := \oint_{\partial\Gamma_a}\Big\{&\left[\hat{n}_a\times\vec{\Psi}(\mathbf{x})\right]^{*}\cdot\left[\nabla_x\times\vec{\Phi}(\mathbf{x})\right]\\&-\left[\hat{n}_a\times\vec{\Phi}(\mathbf{x})\right]\cdot\left[\nabla_x\times\vec{\Psi}(\mathbf{x})\right]^{*}\Big\}\,dS(\mathbf{x})\end{aligned} \tag{4.81}$$

geared to the boundary integral of the vector-vector Green theorem (2.316). Then, we have the additional identities

$$\begin{aligned}\left\{\vec{\varphi}_{i,\tau}(k_0,\mathbf{x}),\vec{\varphi}_{j,\tau'}(k_0,\mathbf{x})\right\}_{\partial\Gamma_a} &= \left\{\vec{\chi}_{i,\tau}(k_0,\mathbf{x}),\vec{\chi}_{j,\tau'}(k_0,\mathbf{x})\right\}_{\partial\Gamma_a}\\&=\left\{\vec{\chi}_{i,\tau}(k_0,\mathbf{x}),\vec{\varphi}_{j,\tau'}(k_0,\mathbf{x})\right\}_{\partial\Gamma_a}=0\end{aligned} \tag{4.82}$$

for $i\neq j$ and $\tau\neq\tau'$, and

$$\left\{\vec{\chi}_{i,\tau}(k_0,\mathbf{x}),\vec{\varphi}_{i,\tau}(k_0,\mathbf{x})\right\}_{\partial\Gamma_a}=\left\{\vec{\varphi}_{i,\tau}(k_0,\mathbf{x}),\vec{\chi}_{i,\tau}(k_0,\mathbf{x})\right\}_{\partial\Gamma_a}=0 \tag{4.83}$$

as well as

$$\left\{\vec{\chi}_{i,\tau}(k_0,\mathbf{x}),\vec{\chi}_{i,\tau}(k_0,\mathbf{x})\right\}_{\partial\Gamma_a}=-\left\{\vec{\varphi}_{i,\tau}(k_0,\mathbf{x}),\vec{\varphi}_{i,\tau}(k_0,\mathbf{x})\right\}_{\partial\Gamma_a}=c \tag{4.84}$$

for all $i=0,\ldots,N$ and $\tau=1,2$. The proofs of these identities run along the same track as in the scalar case. We just have to apply the vector-vector Green theorem (2.316) in the region bounded by $\partial\Gamma_a$ and S_∞ to get the general relation

$$\left\{\vec{f}_{i,\tau}(k_0,\mathbf{x}),\vec{g}_{j,\tau'}(k_0,\mathbf{x})\right\}_{\partial\Gamma_a} = -\left\{\vec{f}_{i,\tau}(k_0,\mathbf{x}),\vec{g}_{j,\tau'}(k_0,\mathbf{x})\right\}_{S_\infty}, \tag{4.85}$$

which is the analogue of (4.65). Additionally, we have now to consider the asymptotic behaviour (2.152) and (2.153) instead of the corresponding scalar expressions. The constant c in (4.84) must again not even be known to prove the unitarity. Then, if using the approximations

$$\begin{aligned}\mathbf{G}^{(<,\mathbf{N})}_{\mathbf{\Gamma}_+}(\mathbf{x},\mathbf{x}') = (ik_0)\sum_{\kappa,\kappa'=1}^{2}\sum_{p,q=0}^{N}\frac{1}{2}\cdot\Big\{&\delta_{p,q}\delta_{\kappa,\kappa'}\cdot\vec{\chi}_{p,\kappa}(k_0,\mathbf{x})\\ &+[S]^{\kappa,\kappa'}_{p,q}\cdot\vec{\varphi}_{p,\kappa}(k_0,\mathbf{x})\Big\}\odot\vec{\tilde{\varphi}}_{q,\kappa'}(k_0,\mathbf{x}')\end{aligned} \tag{4.86}$$

and

$$\begin{aligned}\left[\mathbf{G}^{(<,\mathbf{N})}_{\mathbf{\Gamma}_+}(\mathbf{x},\mathbf{x}')\right]^{*tp} = (ik_0)\sum_{\tau,\tau'=1}^{2}\sum_{i,k=0}^{N}\frac{1}{2}\cdot\Big[&\delta_{i,k}\delta_{\tau,\tau'}\cdot\left\{\vec{\tilde{\varphi}}^{\,*}_{k,\tau'}(k_0,\mathbf{x}')\odot\vec{\chi}^{\,*}_{i,\tau}(k_0,\mathbf{x})\right\}\\ &+\left[S^*\right]^{\tau,\tau'}_{i,k}\cdot\left\{\vec{\tilde{\varphi}}^{\,*}_{k,\tau'}(k_0,\mathbf{x}')\odot\vec{\varphi}^{\,*}_{i,\tau}(k_0,\mathbf{x})\right\}\Big]\end{aligned} \tag{4.87}$$

in (4.79) we get from the identities (4.82)–(4.84)

$$\begin{aligned}&\left\{\mathbf{G}^{(<,\mathbf{N})}_{\mathbf{\Gamma}_+}(\mathbf{x},\mathbf{x}'),\mathbf{G}^{(<,\mathbf{N})}_{\mathbf{\Gamma}_+}(\mathbf{x},\mathbf{x}')\right\}_{\partial\Gamma_a}\\ &\quad=\frac{k_0^2}{4}\cdot\sum_{i,\tau}\left\{\vec{\chi}_{i,\tau}(k_0,\mathbf{x}),\vec{\chi}_{i,\tau}(k_0,\mathbf{x})\right\}_{\partial\Gamma_a}\\ &\qquad\cdot\Bigg[\sum_{\tau',k}\delta_{i,k}\delta_{\tau,\tau'}\cdot\vec{\tilde{\varphi}}^{\,*}_{k,\tau'}(k_0,\mathbf{x}')\odot\sum_{\kappa',q}\delta_{i,q}\delta_{\tau,\kappa'}\cdot\vec{\tilde{\varphi}}_{q,\kappa'}(k_0,\mathbf{x}')\\ &\qquad-\sum_{\tau',k}\left[S^*\right]^{\tau,\tau'}_{i,k}\cdot\vec{\tilde{\varphi}}_{k,\tau'}(k_0,\mathbf{x}')\odot\sum_{\kappa',q}[S]^{\tau,\kappa'}_{i,q}\cdot\vec{\tilde{\varphi}}_{q,\kappa'}(k_0,\mathbf{x}')\Bigg]=0.\end{aligned} \tag{4.88}$$

Because of (4.84) this can be transformed into

$$\begin{aligned}\frac{k_0^2}{4}\cdot c\cdot\sum_{k,\tau'}\Bigg[&\left\{\vec{\tilde{\varphi}}^{\,*}_{k,\tau'}(k_0,\mathbf{x}')\odot\vec{\tilde{\varphi}}_{k,\tau'}(k_0,\mathbf{x}')\right\}\\ &-\sum_{i,\tau,q,\kappa'}\left[S^*\right]^{\tau,\tau'}_{i,k}\cdot[S]^{\tau,\kappa'}_{i,q}\cdot\left\{\vec{\tilde{\varphi}}^{\,*}_{k,\tau'}(k_0,\mathbf{x}')\odot\vec{\tilde{\varphi}}_{q,\kappa'}(k_0,\mathbf{x}')\right\}\Bigg]=0.\end{aligned} \tag{4.89}$$

The expression inside the square brackets will vanish obviously if

$$\sum_{i,\tau} \left[S^*\right]_{i,k}^{\tau,\tau'} \cdot [S]_{i,q}^{\tau,\kappa'} \;=\; \delta_{k,q}\delta_{\tau',\kappa'} \tag{4.90}$$

holds. But this is again nothing but the unitarity relation (4.71) of the S-matrix in the dyadic case.

With the generalization

$$\left(\vec{V}^{\,\hat{n}_-}, \vec{U}^{\,\hat{n}_-}\right)_{\partial\Gamma} := \sum_{\tau=1}^{2}\sum_{i=0}^{N} \oint_{\partial\Gamma} \left[\vec{v}^{\,\hat{n}_-}\right]_{i,\tau}^{*}(\mathbf{x}) \cdot \vec{u}_{i,\tau}^{\,\hat{n}_-}(\mathbf{x})\, dS(\mathbf{x}) \tag{4.91}$$

of the scalar product introduced in (4.74) we can once again circumvent the problem with the physical configuration depicted in Fig. 4.1. That is, we are able to obtain the analogue of (4.75)–(4.78) for the S-matrix $\mathbf{S}_{\partial\mathbf{\Gamma}}$ of the outer Dirichlet problem for real-valued parameters k_0. As already done in (4.76), we can show by use of (2.162) that $\mathbf{S}_{\partial\mathbf{\Gamma}}$ transforms the radiating vector $\vec{\Phi}_0^{\,\hat{n}_-}$ into the incoming vector $\vec{\chi}_0^{\,\hat{n}_-}$ at the scatterer surface. Now, each component of these vectors represent the tangential projections of a three-dimensional vector at the scatterer surface, i.e., these vectors read

$$\begin{aligned}\vec{\Phi}_0^{\,\hat{n}_-}(k_0,\mathbf{x}) \;&=\; \big(\hat{n}_- \times \vec{\varphi}_{0,1}(k_0,\mathbf{x}), \ldots, \hat{n}_- \times \vec{\varphi}_{N,1}(k_0,\mathbf{x}),\\ &\qquad \hat{n}_- \times \vec{\varphi}_{0,2}(k_0,\mathbf{x}), \ldots, \hat{n}_- \times \vec{\varphi}_{N,2}(k_0,\mathbf{x})\big) \qquad (4.92)\\ \vec{\chi}_0^{\,\hat{n}_-}(k_0,\mathbf{x}) \;&=\; \big(\hat{n}_- \times \vec{\chi}_{0,1}(k_0,\mathbf{x}), \ldots, \hat{n}_- \times \vec{\chi}_{N,1}(k_0,\mathbf{x}),\\ &\qquad \hat{n}_- \times \vec{\chi}_{0,2}(k_0,\mathbf{x}), \ldots, \hat{n}_- \times \vec{\chi}_{N,2}(k_0,\mathbf{x})\big)\,. \qquad (4.93)\end{aligned}$$

In spherical coordinates we have

$$\left[\vec{v}^{\,\hat{n}_-}\right]_{i,\tau}^{*} \cdot \vec{u}_{i,\tau}^{\,\hat{n}_-} \;=\; \left[v^{\hat{n}_-}\right]_{i,\tau_r}^{*} \cdot u_{i,\tau_r}^{\hat{n}_-} + \left[v^{\hat{n}_-}\right]_{i,\tau_\theta}^{*} \cdot u_{i,\tau_\theta}^{\hat{n}_-} + \left[v^{\hat{n}_-}\right]_{i,\tau_\phi}^{*} \cdot u_{i,\tau_\phi}^{\hat{n}_-} \tag{4.94}$$

(with $i = 0, \ldots, N; \tau = 1, 2$) for the scalar product appearing in the boundary integral of (4.91).

Summarizing the results of the last two sections we want to state first that the symmetry relations valid for the Green functions if interchanging their arguments result in general symmetry relations of the matrix elements of the corresponding interaction operators. These symmetry relations are independent of the scatterer geometry. Moreover, they are independent of whether k_0 and k are real- or complex-valued parameters.

Second, for real-valued parameters k_0 and k we could derive the unitarity property of the S-matrices. These matrices are constituents of the Green functions of the outer Dirichlet and transmission problem. But for the general proof of unitarity we had to accept an additional restriction concerning the location of the source. Only if considering the outer Dirichlet problem we were able to overcome this restriction.

The same could not be accomplished for the outer transmission problem, so far. May be this will force some readers to search for a way!

Third, the symmetry property as well as the unitarity property holds for infinitely large matrices, in general. Therefore, we can use these properties within numerical procedures based on T-matrices to estimate the accuracy of a certain simulation, for example. But this is only possible as long as the relevant matrices do not exhibit these properties already at a finite size. The latter happens for any spherical scatterer, for example. Furthermore, in Waterman's original papers we can find a procedure to enforce the fulfilment of the unitarity property at finite T-matrices also for any other geometry (see the reference chapter for details). This procedure results in a more stable numerical algorithm, as demonstrated by Waterman. But then we lose the possibility to estimate the accuracy of the T-matrix by use of this property.

Chapter 5
Other Solution Methods

5.1 Introduction

In Chaps. 3 and 4 we became familiar with two different ways of approximating the Green functions related to the scattering problems by finite series expansions in terms of appropriate eigensolutions of the Helmholtz and vector-wave equation. Both of the described ways produce the same expressions. The thus approximated Green functions result in corresponding series expansions of the scattered field with expansion coefficients calculated via the T-matrix from the known expansion coefficients of the primary incident field at the scatterer surface. Demonstrating that the T-matrix is a decisive element of the relevant Green function and that some important properties of the T-matrix like symmetry and unitarity are related to corresponding properties of the Green function can be considered to be the most important results of these two chapters. But there still exist other solution methods for the scattering problem of our interest which have been derived historically from other principles and assumptions used in the foregoing two chapters. Surprisingly, this holds for the T-matrix method itself. It was originally developed by use of the so-called "Extended Boundary Condition". In this chapter we will therefore answer the question of how such methods fit into the developed Green function formalism, or, alternatively, how we have to change the formalism appropriately to end up with some other solution methods. Thereby, it is not our intention to provide a description of selected solution methods which is as complete as possible. In fact, we are more interested in demonstrating that some of the solution methods developed originally from other principles and assumptions can be mapped onto the Green function formalism, and that this formalism provides therefore a sound mathematical basis to analyse the advantages and disadvantages as well as the capabilities of different solution methods. The following considerations are mainly restricted to the scalar case. An exception from this is made when dealing with the so-called "Lippmann-Schwinger" equations which will be derived for the scalar as well as the dyadic Green functions and interaction operators at the end of this chapter.

T. Rother and M. Kahnert, *Electromagnetic Wave Scattering on Nonspherical Particles*, Springer Series in Optical Sciences 145, DOI: 10.1007/978-3-642-36745-8_5,

5.2 T-Matrix Methods

To begin with, let us consider the way originally used by Waterman to derive the T-matrix of the outer Dirichlet problem (and only this problem is of our interest here). The final result will be identical with that one derived in Chap. 3 or 4 if choosing the weighting functions in our approach appropriately. As already mentioned in the introduction Waterman employed the "Extended Boundary Condition" (EBC) to derive the T-matrix. The resulting method is sometimes also called "Null-Field method". This latter notation expresses quite good the essential nature of the EBC and the original objective Waterman intended to achieve with it. Only after a couple of years it became obvious that the methods discussed in Sects. 1.3.1 and 2.2.3 of this book provide the same results. Surprisingly, we have to state that, despite the discovery of the equivalence of Rayleigh's method described in Chap. 1 and Waterman's EBC method for deriving the T-matrix, we can find statements even in the recent literature which prefer the EBC method for it is assumed that this method does not suffer from Rayleigh's hypothesis underlying Rayleigh's method. To understand this point of view we will take a closer look at the EBC method. The problem of Rayleigh's hypothesis is shifted to the next chapter.

Another choice of weighting functions will lead us to a different solution technique known as "Point Matching methods" (PMM) or "Collocation methods". These methods have been used quite often for solving boundary value problems in the history and can be considered to be special realizations of the general T-matrix approach. Moreover, these methods play an essential role in the context of Rayleigh's hypothesis. But on the other hand, one can observe that the conventional PMM become of less importance nowadays because of their numerical instabilities and restricted range of applicability if more realistic scenarios are considered.

5.2.1 The Extended Boundary Condition Method

Before we will come to the methodical details we want to start with some historical considerations since it casts an interesting light on the roots of the EBC in electromagnetic wave scattering theory.

The first paper (to the best of our knowledge!) on the T-matrix method with the title "Matrix Formulation of Electromagnetic Scattering" was published by Waterman in IEEE in 1965 (for the details see the reference chapter). This paper is aimed to present a method which does not suffer from numerical instabilities at the internal eigenresonances if electromagnetic wave scattering on an ideal metallic scatterer is considered. This scattering problem corresponds mathematically to the outer Dirichlet problem. What was the reason for those numerical instabilities? In the literature one can find the hint (in J. J. H. Wang: "Generalized Moment Methods in Electromagnetics", 1991, Sect. 6.6, for example) that such a numerical instability (or resonance) has been observed first in the papers of Mei and Van Bladel ("Scattering by

Perfectly-Conducting Rectangular Cylinders"), and of Andreasen ("Comments on 'Scattering by Perfectly-Conducting Rectangular Cylinders"'). But reading these two papers we can state already a problem with this resonance phenomenon. It can be found **only** in the first cited paper of Mei and Van Bladel at a certain size parameter. In this paper the authors employed a conventional boundary integral equation method (this method will be explained in more detail in Sect. 5.4 of this chapter) to solve the electromagnetic wave scattering problem on an ideal metallic cylinder with a rectangular cross-section. The cited paper of Andreasen is just a comment to the paper of Mei and Van Bladel in which he advised the authors of the existence of a resonance in one of their figures. Moreover, he discussed therein that he used a comparable solution method which does not exhibit this resonance and that it is actually not awaited at this parameter. This comment was commented afterwards by Mei, in which he stated that, performing the calculations presented in their first paper once again, the resonance phenomenon disappeared and the obtained results became in good agreement with the results of Andreasen even for the critical parameter. Thus, there was no longer observed any resonance phenomenon. But since this time there is still an uncertain feeling among many authors concerning such resonances which is especially related to the following argumentation: The boundary integral equation method used by Mei and Van Bladel assumes that the tangential projections of the total magnetic field must vanish identically if approaching the surface of an ideal metallic scatterer from inside. This is, of course, not true for the tangential projections of the magnetic field of internal eigenresonances since producing an equivalent surface current at the inner boundary surface of the resonator. The usual physical understanding of what we call an ideal metallic resonator assumes now that there is no relation between the induced surface current which is equivalent to a possibly existing internal resonance and the induced surface current which is equivalent to a possibly existing scattered field outside the resonator. Or, in other words: The inner region of an ideal metallic resonator is totally decoupled from its outer region, i.e., there is no scattering experiment from outside which will allow us to analyse an internal eigenresonance. Concerning the resonance phenomenon it was then argued that the method used by Mei and Van Bladel as well as several other boundary integral equation methods are not able to distinguish between these two induced surface currents, and that this situation may produce numerical instabilities. This argumentation forced Waterman to replace the conventional boundary integral equation method by a method which seems to be able to avoid such resonance phenomena. To achieve this goal he introduced the EBC. By the way, the EBC was discovered independently of Waterman by Ewald and Oseen in the field of molecular optics. There it was called the "Extinction Theorem". Only later on it was discovered by Agarwal that both expressions are equivalent (see the book of Nieto-Vesperinas in Sect. 10.9 of the reference chapter). Let us now see how Waterman's approach works in detail if applying it to the Green function of the outer Dirichlet problem and if he really reached his initial goal with this method.

Beside the radiation condition we required additionally the fulfilment of boundary condition (2.280) at the scatterer surface for the scalar Green function G_{Γ_+} related to the outer Dirichlet problem. This condition was replaced by Waterman by the

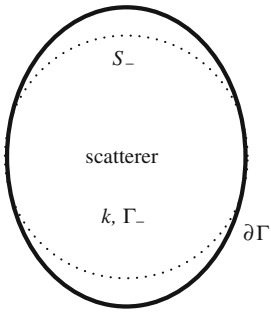

Fig. 5.1 S_- denotes the outer boundary surface of the subregion inside the scatterer to which the EBC is primarily applied

condition

$$G_{\Gamma_+}(\mathbf{x}, \mathbf{x}') = 0; \quad \mathbf{x} \in \Gamma_-; \ \mathbf{x}' \in \Gamma_+. \tag{5.1}$$

To avoid misunderstandings it should be mentioned that in the original paper of Waterman this was done for the total electric field and not for the scalar Green function. Condition (5.1) is obviously an extension of the former condition into the region Γ_- inside the scatterer. It is exactly the reason for calling this new condition the "Extended Boundary Condition". Waterman had demonstrated in his paper that the usually required vanishing of the tangential projections of the total electric field at the surface of an ideal metallic scatterer can be inferred from the vanishing of the electric field everywhere inside the scatterer. Since the magnetic field can be calculated by use of the "$\nabla\times$" operation if applied to the electric field the magnetic field it is also forced to vanish everywhere inside the scatterer. And this happens independent of whether there exist an internal resonance or not. According to Waterman, it is moreover sufficient to require that condition (5.1) is applied only to a subregion of Γ_-, for example to the region bounded by the spherical surface S_- (see Fig. 5.1). Using the procedure of continuing the field inside the subregion analytically he concluded the vanishing of this field everywhere inside the scatterer. But this procedure is described only verbal in his paper. This description ends with the remark that we "... assume, without further comment, that this analytic continuation procedure is valid". In the book of Doicu et al. already mentioned in Sect. 2.3.3 one can find a more precise mathematical justification for Waterman's assumption. So, let us also assume that it is correct. We place the source point $\mathbf{x}'$ outside the smallest spherical surface circumscribing the scatterer, as frequently done in the foregoing chapters. If the observation point is now placed somewhere in the subregion bounded by S_- we may write

$$G_{\Gamma_+}(\mathbf{x}, \mathbf{x}') := G_0^<(\mathbf{x}, \mathbf{x}') + \oint_{\partial\Gamma} G_0^<(\mathbf{x}, \bar{\mathbf{x}}) \cdot \tilde{W}_{\partial\Gamma}(\bar{\mathbf{x}}, \tilde{\mathbf{x}}) \cdot G_0^<(\tilde{\mathbf{x}}, \mathbf{x}')\, dS(\bar{\mathbf{x}})\, dS(\tilde{\mathbf{x}}) \tag{5.2}$$

as defining equation for the new interaction operator $\tilde{W}_{\partial\Gamma}$. It differs from definition (4.1) in using $G_0^<$ instead of $G_0^>$ in the boundary integral term on the right-hand side. Since $\mathbf{x}$ is somewhere inside S_- the usage of $G_0^<$, in contrast to the usage of $G_0^>$ in (4.1), is now justified without any doubt. Just to remember: $G_0^<$ solves the homogeneous Helmholtz equation and obeys the regularity requirement everywhere inside S_-. Combining (5.1) and (5.2) we get the integral equation

$$-G_0^<(\mathbf{x},\mathbf{x}') = \oint_{\partial\Gamma} G_0^<(\mathbf{x},\bar{\mathbf{x}}) \cdot \tilde{W}_{\partial\Gamma}(\bar{\mathbf{x}},\tilde{\mathbf{x}}) \cdot G_0^<(\tilde{\mathbf{x}},\mathbf{x}')\, dS(\bar{\mathbf{x}})\, dS(\tilde{\mathbf{x}}) \tag{5.3}$$

for observation points $\mathbf{x}$ inside S_-. This will allow us to determine the interaction operator $\tilde{W}_{\partial\Gamma}$. In Waterman's original paper there is used the induced surface current at the scatterer surface instead of the interaction operator introduced in (5.2). The interrelation between the induced surface current and the interaction operator will be clarified later on in Chap.7, as already mentioned in Sect. 4.3.1. Replacing $G_0^<$ by the (again finite!) approximation (2.278) (5.3) becomes

$$\begin{aligned} -(ik_0) \sum_{i=0}^{N} \psi_i(k_0,\mathbf{x}) \cdot \tilde{\varphi}_i(k_0,\mathbf{x}') \\ = (ik_0)^2 \sum_{i,k=0}^{N} \oint_{\partial\Gamma} \psi_i(k_0,\mathbf{x}) \cdot \tilde{\varphi}_i(k_0,\bar{\mathbf{x}}) \cdot \tilde{W}_{\partial\Gamma}(\bar{\mathbf{x}},\tilde{\mathbf{x}}) \cdot \psi_k(k_0,\tilde{\mathbf{x}}) \\ \cdot \tilde{\varphi}_k(k_0,\mathbf{x}')\, dS(\bar{\mathbf{x}})\, dS(\tilde{\mathbf{x}}). \end{aligned} \tag{5.4}$$

The equal sign is obviously justified if

$$(ik_0) \oint_{\partial\Gamma} \tilde{\varphi}_i(k_0,\bar{\mathbf{x}}) \cdot \tilde{W}_{\partial\Gamma}(\bar{\mathbf{x}},\tilde{\mathbf{x}}) \cdot \psi_k(k_0,\tilde{\mathbf{x}})\, dS(\bar{\mathbf{x}})\, dS(\tilde{\mathbf{x}}) = -\delta_{i,k} \tag{5.5}$$

holds. Next, we assume the following bilinear expansion for the interaction operator

$$\tilde{W}_{\partial\Gamma}(\bar{\mathbf{x}},\tilde{\mathbf{x}}) = (ik_0)^{-1} \sum_{\alpha,\beta=0}^{N} \left[\tilde{W}_{\partial\Gamma}\right]_{\alpha,\beta} \cdot g_\alpha(\bar{\mathbf{x}}) \cdot h_\beta(\tilde{\mathbf{x}}). \tag{5.6}$$

$g_\alpha(\bar{\mathbf{x}})$ and $h_\beta(\tilde{\mathbf{x}})$ therein are not yet specified but linearly independent expansion functions at the scatterer surface. Inserting this expansion into (5.5) provides

$$\sum_{\alpha,\beta=0}^{N} \oint_{\partial\Gamma} \tilde{\varphi}_i(k_0,\bar{\mathbf{x}}) \cdot \left[\tilde{W}_{\partial\Gamma}\right]_{\alpha,\beta} \cdot g_\alpha(\bar{\mathbf{x}}) \cdot h_\beta(\tilde{\mathbf{x}}) \cdot \psi_k(k_0,\tilde{\mathbf{x}})\, dS(\bar{\mathbf{x}})\, dS(\tilde{\mathbf{x}}) = -\delta_{i,k}. \tag{5.7}$$

with the definition of the matrix elements of the two matrices $\mathbf{A}_{\partial\Gamma}^{(\tilde{\varphi}_0^*,g)}$ and $\mathbf{B}_{\partial\Gamma}^{(h^*,\psi_0)}$ according to

$$\left[A_{\partial\Gamma}^{(\tilde{\varphi}_0^*,g)}\right]_{i,k} := \oint_{\partial\Gamma} \tilde{\varphi}_i(k_0,\bar{\mathbf{x}}) \cdot g_k(\bar{\mathbf{x}})\, dS(\bar{\mathbf{x}}) \tag{5.8}$$

and

$$\left[B_{\partial\Gamma}^{(h^*,\psi_0)}\right]_{i,k} := \oint_{\partial\Gamma} h_i(k_0,\tilde{\mathbf{x}}) \cdot \psi_k(k_0,\tilde{\mathbf{x}})\, dS(\tilde{\mathbf{x}}) \tag{5.9}$$

(please, note that this definition agrees with the scalar product definition (1.34) since we have used $h_i^*(k_0,\tilde{\mathbf{x}})$ in (5.9), for example, as weighting functions thus producing $h_i(k_0,\tilde{\mathbf{x}})$ in the boundary integral term!) we may write instead of (5.7) the matrix equation

$$\mathbf{A}_{\partial\Gamma}^{(\tilde{\varphi}_0^*,g)} \cdot \tilde{\mathbf{W}}_{\partial\Gamma} \cdot \mathbf{B}_{\partial\Gamma}^{(h^*,\psi_0)} \;=\; -\mathbf{E}. \tag{5.10}$$

From this, we get in a straightforward way the matrix equation

$$\tilde{\mathbf{W}}_{\partial\Gamma} = -\mathbf{A}_{\partial\Gamma}^{(\tilde{\varphi}_0^*,g)^{-1}} \cdot \mathbf{B}_{\partial\Gamma}^{(h^*,\psi_0)^{-1}} \tag{5.11}$$

to determine the expansion coefficients $\left[\tilde{W}_{\partial\Gamma}\right]_{\alpha,\beta}$ of the bilinear expansion of the interaction operator $\tilde{W}_{\partial\Gamma}$. Once we know approximation (5.6) we are able to present the corresponding approximation of the Green function $G_{\Gamma_+}(\mathbf{x},\mathbf{x}')$ for observation points $\mathbf{x}$ outside the smallest spherical surface circumscribing the scatterer (i.e., for observation points in Γ_+!). For these observation points we write instead of (5.2)

$$\begin{aligned} G_{\Gamma_+}(\mathbf{x},\mathbf{x}') &= G_0(\mathbf{x},\mathbf{x}') \\ &\quad + \oint_{\partial\Gamma} G_0^{>}(\mathbf{x},\bar{\mathbf{x}}) \cdot \tilde{W}_{\partial\Gamma}(\bar{\mathbf{x}},\tilde{\mathbf{x}}) \cdot G_0^{<}(\tilde{\mathbf{x}},\mathbf{x}')\, dS(\bar{\mathbf{x}})\, dS(\tilde{\mathbf{x}}), \end{aligned} \tag{5.12}$$

i.e., $G_0^{<}(\mathbf{x},\bar{\mathbf{x}})$ in the boundary integral term of (5.2) is now replaced without any problems by $G_0^{>}(\mathbf{x},\bar{\mathbf{x}})$. Utilizing the expansions of $G_0^{<}$ and $G_0^{>}$ as well as the bilinear expansion (5.6) we obtain

$$\begin{aligned} G_{\Gamma_+}^{(N)}(\mathbf{x},\mathbf{x}') &= G_0(\mathbf{x},\mathbf{x}') \\ &\quad + (ik_0) \cdot \sum_{i,k,\alpha,\beta=0}^{N} \oint_{\partial\Gamma} \varphi_i(k_0,\mathbf{x}) \cdot \tilde{\psi}_i(k_0,\bar{\mathbf{x}}) \left[\tilde{W}_{\partial\Gamma}\right]_{\alpha,\beta} \\ &\quad \cdot g_\alpha(\bar{\mathbf{x}}) \cdot h_\beta(\tilde{\mathbf{x}}) \cdot \psi_k(k_0,\tilde{\mathbf{x}}) \cdot \tilde{\varphi}_k(k_0,\mathbf{x}')\, dS(\bar{\mathbf{x}})\, dS(\tilde{\mathbf{x}}). \end{aligned} \tag{5.13}$$

This expression can be rewritten into

$$\begin{aligned} G_{\Gamma_+}^{(N)}(\mathbf{x},\mathbf{x}') &= G_0(\mathbf{x},\mathbf{x}') \\ &\quad + (ik_0) \cdot \sum_{i,k=0}^{N} \left[W_{\partial\Gamma_+}\right]_{i,k} \cdot \varphi_i(k_0,\mathbf{x}) \cdot \tilde{\varphi}_k(k_0,\mathbf{x}'). \end{aligned} \tag{5.14}$$

With the definitions

$$\left[C_{\partial\Gamma}^{(\tilde{\psi}_0^*,g)}\right]_{i,k} := \oint_{\partial\Gamma} \tilde{\psi}_i(k_0,\bar{\mathbf{x}}) \cdot g_k(\bar{\mathbf{x}})\, dS(\bar{\mathbf{x}}) \tag{5.15}$$

and

$$\left[D_{\partial\Gamma}^{(h^*,\psi_0)}\right]_{i,k} := \oint_{\partial\Gamma} h_i(k_0,\tilde{\mathbf{x}}) \cdot \psi_k(k_0,\tilde{\mathbf{x}})\, dS(\tilde{\mathbf{x}}) \tag{5.16}$$

of the elements of the matrices $\mathbf{C}_{\partial\Gamma}^{(\tilde{\psi}_0^*,g)}$ and $\mathbf{D}_{\partial\Gamma}^{(h^*,\psi_0)}$ we can calculate the new elements $\left[W_{\partial\Gamma_+}\right]_{i,k}$ in (5.14) from

$$\mathbf{W}_{\partial\Gamma_+} = -\mathbf{C}_{\partial\Gamma}^{(\tilde{\psi}_0^*,g)} \cdot \mathbf{A}_{\partial\Gamma}^{(\tilde{\varphi}_0^*,g)^{-1}} \cdot \mathbf{B}_{\partial\Gamma}^{(h^*,\psi_0)^{-1}} \cdot \mathbf{D}_{\partial\Gamma}^{(h^*,\psi_0)}. \tag{5.17}$$

But since both matrices $\mathbf{B}_{\partial\Gamma}^{(h^*,\psi_0)}$ and $\mathbf{D}_{\partial\Gamma}^{(h^*,\psi_0)}$ are obviously identical we end up with the simpler matrix equation

$$\mathbf{W}_{\partial\Gamma_+} = -\mathbf{C}_{\partial\Gamma}^{(\tilde{\psi}_0^*,g)} \cdot \mathbf{A}_{\partial\Gamma}^{(\tilde{\varphi}_0^*,g)^{-1}}. \tag{5.18}$$

This result agrees with that one obtained by Waterman in his 1965 paper (see Eqs. (7) and (14) therein!) if using the radiating eigensolutions $\varphi_\alpha(k_0,\bar{\mathbf{x}})$ and $\varphi_\beta(k_0,\tilde{\mathbf{x}})$ of the scalar Helmholtz equation as expansion functions $g_\alpha(\bar{\mathbf{x}})$ and $h_\beta(\tilde{\mathbf{x}})$ in the bilinear expansion (5.6). On the other hand, if choosing $\varphi_i^*(k_0,\mathbf{x})$ as weighting functions in (2.21) and (2.22), and if taking symmetry relation (4.46) additionally into account, then an intercomparison of (5.18) with (2.19) reveals the equality of both expressions. From this, we can infer the equality of approximation (5.14) and (4.8). Thus, we can state that, if choosing the expansion and weighting functions appropriately, the EBC method as well as Rayleigh's method may result in the same approximation of the Green function related to the outer Dirichlet problem.

Now, let us come back to the initially mentioned resonance phenomenon which was expected to be avoidable by use of the EBC. The above obtained result would then suggest that the same holds for the homogeneous Dirichlet condition valid solely at the scatterer surface. But looking at Sect. 3 of Waterman's 1965 paper shows us that this is not true. In this chapter, he discussed the corresponding eigenvalue problem of a nonspherical but ideal metallic resonator and its solution in terms of the appropriately modified EBC (see Eq. (17a) in this paper). The relevant matrix is identical with the matrix $\mathbf{C}_{\partial\Gamma}^{(\tilde{\psi}_0^*,g)}$ derived above. The values of k_0 for which its determinant becomes zero are the eigenvalues, i.e., the resonance frequencies of the problem. Fortunately, according to (5.18) for the scattering problem we just have to invert matrix $\mathbf{A}_{\partial\Gamma}^{(\tilde{\varphi}_0^*,g)}$, and not matrix $\mathbf{C}_{\partial\Gamma}^{(\tilde{\psi}_0^*,g)}$. Therefore, (5.18) will be not affected by a zero or nearly zero determinant of this matrix. But the situation changes if using the regular eigensolutions of the scalar Helmholtz equation instead of the radiating

ones in the bilinear expansion (5.6). This would correspond to choosing the regular eigensolutions as expansion functions for the induced surface current in Waterman's paper (see Eq. (6) therein). Then, we have to invert indeed even the critical matrix. But this will produce at least numerical problems near or at the eigenfrequencies, of course. Therefore, also if using the EBC to derive the T-matrix the occurrence of resonance phenomena depends strongly on the appropriate choice of expansion functions and can not be excluded from the beginning. That is exactly what was expressed more mathematically in Sect. 2.3.3 when considering the properties of the eigensolutions of Helmholtz's equation. There we pointed out that the regular eigensolutions are only linearly independent at the scatterer surface as long as k_0^2 is not an eigenvalue of the inner Dirichlet problem. Waterman has achieved his initial goal of avoiding resonances only by choosing the "correct" expansion functions, i.e., the radiating eigensolutions to approximate the induced surface current. But despite of this, with the EBC method he has offered a new solution technique for the scattering problem which became very successfully aftermath in many applications. We can therefore consider this 1965 paper as a milestone in the treatment of electromagnetic and acoustic wave scattering on nonspherical objects.

5.2.2 Point Matching Methods

This method is straightforward and very simple. Instead of (1.29) we can use the simpler boundary condition

$$\sum_{i=0}^{N} a_i^{(N)} \cdot \varphi_i(k_0, \mathbf{x}) = -\sum_{i=0}^{N} b_i \cdot \psi_i(k_0, \mathbf{x}); \quad \mathbf{x} \in \partial\Gamma \tag{5.19}$$

if the scalar outer Dirichlet problem is considered. But instead of this boundary condition we can also employ the transformation character of the T-matrix as a starting point. According to (2.17) we may write

$$\psi_i(k_0, \mathbf{x}) = \sum_{k=0}^{N} \left[\tilde{T}_{\partial\Gamma}\right]_{i,k} \cdot \varphi_k(k_0, \mathbf{x}); \quad i = 0, \ldots, N; \quad \mathbf{x} \in \partial\Gamma. \tag{5.20}$$

Both relations produces the same T-matrix, as already demonstrated in Chap. 1 and 2. For the conventional PMM it is simply required that both relations are fulfilled exactly only at $(N+1)$ selected points $\mathbf{x_j}$ $(j = 0, \ldots, N)$ at the scatterer surface $\partial\Gamma$. Then, we have the same number of matching points and unknown expansion coefficients $a_i^{(N)}$ in (5.19), for example. It is easy to see that this produces a T-matrix (2.19) of the size $(N+1) \times (N+1)$. The constituting matrices $\mathbf{A}_{\partial\Gamma}$ and $\mathbf{B}_{\partial\Gamma}$ are given by the values of the radiating and regular eigenfunctions at the selected surface points, i.e., by

$$[A_{\partial\Gamma}]_{i,j} = \varphi_j(k_0, \mathbf{x_i}) \tag{5.21}$$

$$[B_{\partial\Gamma}]_{i,j} = \psi_j(k_0, \mathbf{x_i}). \tag{5.22}$$

In accordance with (2.21) and (2.22) we obtain these matrix elements of the conventional PMM if choosing the scalar delta distribution at the scatterer surface defined in (3.6) as weighting functions,

$$g_i(\mathbf{x}) = \delta_{\partial\Gamma}(\mathbf{x} - \mathbf{x_i}); \quad i = 0, \ldots, N. \tag{5.23}$$

On the other hand, if considering the vectorial case of the outer Dirichlet problem we have to use

$$\vec{g}_{i,\tau}(\mathbf{x}) = \delta_{\partial\Gamma}(\mathbf{x} - \mathbf{x}_{\mathbf{i},\tau}) \cdot \hat{x}_1 + \delta_{\partial\Gamma}(\mathbf{x} - \mathbf{x}_{\mathbf{i},\tau}) \cdot \hat{x}_2 + \delta_{\partial\Gamma}(\mathbf{x} - \mathbf{x}_{\mathbf{i},\tau}) \cdot \hat{x}_3 \tag{5.24}$$

instead of (5.23) with $i = 0, \ldots, N$ and $\tau = 1, 2$. This produces again 2×2 block matrices, due to the additional τ-dependence.

The conventional PMM is not very stable and converges poorly even at the boundary surface but between the selected points, as it was experienced in many applications. But a slight change in the method results in drastic improvements. This change consists in choosing more matching points $\mathbf{x}_i$ along $\partial\Gamma$ than we have unknown expansion coefficients. The resulting overdetermined equation system is solved afterwards by employing a least-squares scheme. This can be done, for example, by use of the "Singular Value Decomposition" method. The thus modified conventional PMM is sometimes called the "generalized PMM".

5.3 The Method of Lines as a Special Finite-Difference Method

This section is concerned with a special Finite-Difference method. The method is called the "Method of Line" (MoL) for obvious reasons as we will see shortly. It was developed between 1950 and 1960 by Russian mathematicians, but sunk into oblivion until the advent of modern and powerful computers in science. Since 1980s it became of growing importance in several applications but especially in microwave technology and integrated optics. However, in all of these cases the application of the MoL was restricted to boundary value problems with boundary surfaces along constant coordinate lines in separable coordinate systems. Not till the beginning of the 1990s our group at the German Aerospace Center started with an upgrading of this method to the problem of light scattering on nonspherical particles in spherical coordinates as well as on infinitely extended cylinders with nonspherical cross-sections in cylindrical coordinates. Ultimately, these activities have led us to a new and more critical view on this special method and on the Finite-Difference methods in general. The reason for this rethinking will be explained in detail in this section. To anticipate the most important and somewhat provocative result: The Finite-Difference

methods are only a worsening of the Separation of Variables method and are not really advantageous if applied to the scattering problems discussed in this book. In what follows, we will show that there are tangible arguments supporting this opinion. But to avoid misunderstandings it should be emphasized that we do not want to claim that the Finite-Difference methods may produce wrong or incorrect results. They are, of course, a possible approach to solve the scattering problems of our interest. But these methods offer no evident advantages compared to other techniques. That these methods are widely used in the context of scattering, and that there still exist questionable point of views regarding the nature of this method are the essential reasons to include the MoL as a representative of the Finite-Difference methods in this book. Starting from a detailed discussion of the mathematical background, we will hopefully be able to provide a better understanding of the Finite-Difference methods thus supporting a more realistic estimate of their advantages and disadvantages in a certain application.

5.3.1 Discretization of the Scalar Helmholtz Equation and its Solution

Replacing the differential operator completely (conventional Finite-Difference methods) or partially (MoL) by appropriate difference schemes is the crucial step in all of the Finite-Difference techniques. In this way, the original partial differential equation will be substituted by a system of algebraic equations (conventional Finite-Difference methods) or a system of ordinary differential equations (MoL). So far, it is assumed that replacing the differential operator makes the essential methodical difference compared to those methods retaining the differential operator as it is but approximating the unknown function in terms of series expansions instead. The latter methods are sometimes called spectral methods. This at first glance simple concept in conjunction with the drastic improvements of our computational capabilities during the last decades are the main reasons for assuming the Finite-Difference methods to represent the most general and most easy to handle methods for solving scattering problems, for example. Appropriate arguments can be found frequently in recent papers and books. The preference of Finite-Difference methods is moreover supported by the fact that every solution technique is finally submitted to a certain discretization procedure if accomplished on a computer. But by use of the MoL, we will show now that such point of views deserve a correction. That is because, we can demonstrate that the original replacement of the differential operator can be transformed into an equivalent approximation of the unknown function in terms of a series expansion. In doing so, the MoL will lead us to specific expansion functions. We will demonstrate later that these expansion functions are nothing but a worsening of the known eigensolutions of the scalar Helmholtz equation in spherical coordinates discussed earlier in Sect. 2.3. The following considerations are restricted to axisymmetric scatterer geometries for simplicity.

Separating the ϕ-dependent part of the scalar Helmholtz equation (2.46) by use of the Fourier series

$$u(r, \theta, \phi) = \sum_l e^{il\phi} \cdot \tilde{u}^{(l)}(r, \theta), \tag{5.25}$$

results in the modified partial differential equation

$$\begin{aligned} &\left(\tilde{\nabla}^2 + k^2 r^2\right) \tilde{u}^{(l)}(r, \theta) = 0 \\ &\tilde{\nabla}^2 = \frac{\partial}{\partial r}\left(r^2 \frac{\partial}{\partial r}\right) + \frac{1}{\sin\theta} \frac{\partial}{\partial \theta}\left(\sin\theta \frac{\partial}{\partial \theta}\right) - \frac{l^2}{\sin^2\theta} \end{aligned} \tag{5.26}$$

for the unknown functions $\tilde{u}^{(l)}(r, \theta)$. Using this partial differential equation as a starting point is thus a consequence of the restriction to axisymmetric scatterers. Regarding the θ-dependence the functions $\tilde{u}^{(l)}(r, \theta)$ must obey conditions (2.68) and (2.69). To solve (5.26) by use of the MoL we replace all the derivatives with respect to θ by an equidistant discretization procedure within the interval $[0, \pi]$, i.e., we cover this interval with N_d radial lines starting from the origin. Please, note that the nonequidistant case is not of our interest here since providing no new insights. In contrast to the conventional Finite-Difference methods all derivatives with respect to the radial coordinate remain unaffected. Employing the discretization procedure with respect to θ we have to distinguish carefully the two cases with azimuthal modes $l = 0$ and $l \neq 0$. The two different discretization schemes are depicted in Figs. 5.2 and 5.3.

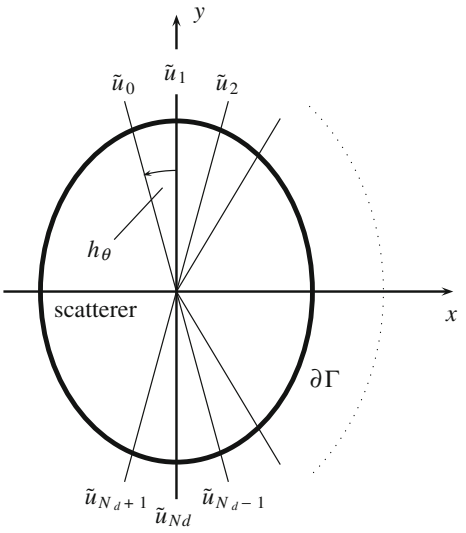

Fig. 5.2 Equidistant discretization procedure for $l = 0$ (homogeneous Neumann condition). We have $h_\theta = \pi/(N_d - 1)$; $\theta_i = (i-1)h_\theta$, and $i = 1, \ldots, N_d$

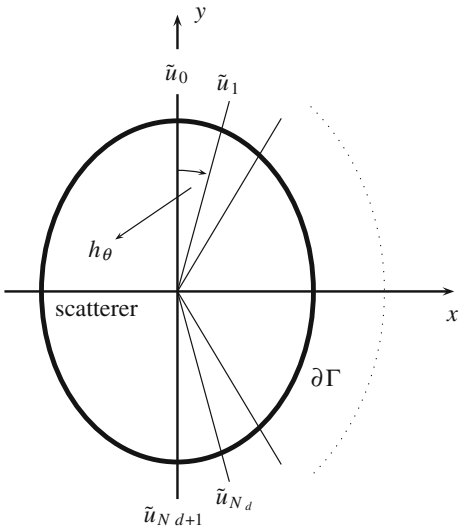

Fig. 5.3 Equidistant discretization procedure for $l \neq 0$ (homogeneous Dirichlet condition). We have $h_\theta = \pi/(N_d + 1)$; $\theta_i = i h_\theta$, and $i = 1, \ldots, N_d$

Obviously, at $\theta = 0, \pi$ the homogeneous Neumann condition is fulfilled only approximately whereas the homogeneous Dirichlet condition is reproduced exactly by use of this discretization procedure. We are now interested on the radial dependent solutions of (5.26) along the discretization lines. We assume further that each possible discretization line crosses the boundary surface of the scatterer only once. This is called a star-shaped scatterer geometry. All first derivatives with respect to θ may be replaced by an appropriate left-hand (subscript ls), right-hand (subscript rs), or central (subscript zt) discretization operator according to

$$\frac{\partial}{\partial\theta} \Rightarrow \frac{1}{h_\theta}\mathbf{D}_{ls}^{(\alpha)}, \quad \frac{1}{h_\theta}\mathbf{D}_{rs}^{(\alpha)}, \quad \text{or} \quad \frac{1}{h_\theta}\mathbf{D}_{zt}^{(\alpha)} \tag{5.27}$$

with superscript α denoting whether the homogeneous Neumann condition (NC) or the homogeneous Dirichlet condition (DC) is fulfilled at $\theta = 0, \pi$. These discretization operators are nothing but square matrices of the size $N_d \times N_d$. They read

$$\mathbf{D}_{ls}^{(\alpha)} = \begin{pmatrix} l_1 & 0 & 0 & 0 & \ldots & \ldots & 0 \\ -1 & 1 & 0 & 0 & 0 & \ldots & 0 \\ 0 & -1 & 1 & 0 & 0 & \ldots & 0 \\ \vdots & \vdots & \vdots & \vdots & \vdots & \vdots & \vdots \\ 0 & \ldots & \ldots & 0 & -1 & 1 & 0 \\ 0 & \ldots & \ldots & \ldots & 0 & l_2 & l_3 \end{pmatrix} \tag{5.28}$$

$$\mathbf{D}_{rs}^{(\alpha)} = \begin{pmatrix} r_1 & r_2 & 0 & 0 & \dots & \dots & 0 \\ 0 & -1 & 1 & 0 & 0 & \dots & 0 \\ 0 & 0 & -1 & 1 & 0 & \dots & 0 \\ \vdots & \vdots & \vdots & \vdots & \vdots & \vdots & \vdots \\ 0 & \dots & \dots & 0 & 0 & -1 & 1 \\ 0 & \dots & \dots & \dots & 0 & 0 & r_3 \end{pmatrix} \tag{5.29}$$

$$\mathbf{D}_{zt}^{(\alpha)} = \begin{pmatrix} 0 & c_1 & 0 & 0 & \dots & \dots & 0 \\ -1 & 0 & 1 & 0 & 0 & \dots & 0 \\ 0 & -1 & 0 & 1 & 0 & \dots & 0 \\ \vdots & \vdots & \vdots & \vdots & \vdots & \vdots & \vdots \\ 0 & \dots & \dots & 0 & -1 & 0 & 1 \\ 0 & \dots & \dots & \dots & 0 & c_2 & 0 \end{pmatrix}. \tag{5.30}$$

In dependence on the boundary condition at $\theta = 0, \pi$ the constants in these matrices are given by

–	l_1	l_2	l_3	r_1	r_2	r_3	c_1	c_2
NC	0	0	0	0	0	0	0	0
DC	1	−1	1	−1	1	−1	1	−1

The second derivative with respect to θ is replaced by the discretization operator

$$\frac{\partial^2}{\partial\theta^2} \Rightarrow \frac{1}{{h_\theta}^2}\,\mathbf{D}_z^{(\alpha)}. \tag{5.31}$$

This operator can be calculated from the Taylor expansion

$$\tilde{u}^{(l)}(r, \theta_{i\pm1}) = \tilde{u}^{(l)}(r, \theta_i) \pm \frac{h_\theta}{1!}\left(\frac{\partial\tilde{u}^{(l)}}{\partial\theta}\right)_{\theta_i} \pm \frac{h_\theta^2}{2!}\left(\frac{\partial^2\tilde{u}^{(l)}}{\partial\theta^2}\right)_{\theta_i} \pm \cdots \tag{5.32}$$

of the function $\tilde{u}^{(l)}(r, \theta)$ of (5.25) at a fixed angle θ_i. Employing the Taylor series up to the second order results in

$$\left(\frac{\partial^2\tilde{u}^{(l)}}{\partial\theta^2}\right)_{\theta_i} = \frac{1}{{h_\theta}^2} \cdot \left(\tilde{u}^{(l)}(r, \theta_{i-1}) - 2 \cdot \tilde{u}^{(l)}(r, \theta_i) + \tilde{u}^{(l)}(r, \theta_{i+1})\right). \tag{5.33}$$

The corresponding discretization operator thus becomes

$$\mathbf{D}_z^{(\alpha)} = \begin{pmatrix} 2 & z_1 & 0 & 0 & \dots & \dots & 0 \\ -1 & 2 & -1 & 0 & 0 & \dots & 0 \\ 0 & -1 & 2 & -1 & 0 & \dots & 0 \\ \vdots & \vdots & \vdots & \vdots & \vdots & \vdots & \vdots \\ 0 & \dots & \dots & 0 & -1 & 2 & -1 \\ 0 & \dots & \dots & \dots & 0 & z_2 & 2 \end{pmatrix} \tag{5.34}$$

with constants

–	z_1	z_2
NC	-2	-2
DC	-1	-1

Next, we apply these discretization operators to (5.26). In this way, we obtain the following system of coupled ordinary differential equations for the radial dependent functions $\tilde{u}^{(l)}(r, \theta_i)$ on the discretization lines:

$$\left\{ h_\theta^2 \left[\frac{d}{dr} \left(r^2 \frac{d}{dr} \right) + k^2 r^2 \right] \cdot \mathbf{E} - \mathbf{P}^{(l)} \right\} \cdot \mid \tilde{u}^{(l)}(r) >= \mid 0 > . \tag{5.35}$$

Taking the two different cases $l = 0$ and $l \neq 0$ into account, and because of

$$\mathbf{P}^{(0)} = \mathbf{D}_z^{(NC)} - diag(\kappa) \cdot \mathbf{D}_{rs}^{(NC)} \tag{5.36}$$

and

$$\mathbf{P}^{(l)} = \mathbf{D}_z^{(DC)} - diag(\kappa) \cdot \mathbf{D}_{rs}^{(DC)} + diag(\gamma^{(l)}) \tag{5.37}$$

we get for the matrices $\mathbf{P}^{(l)}$ the expressions

$$\mathbf{P}^{(0)} = \begin{pmatrix} 2 & -2 & 0 & 0 & \dots & \dots & 0 \\ -1 & (2+\kappa_2) & -(1+\kappa_2) & 0 & 0 & \dots & 0 \\ 0 & -1 & (2+\kappa_3) & -(1+\kappa_3) & 0 & \dots & 0 \\ \vdots & \vdots & \vdots & \vdots & \vdots & \vdots & \vdots \\ 0 & \dots & \dots & 0 & -1 & (2+\kappa_{Nd-1}) & -(1+\kappa_{Nd-1}) \\ 0 & \dots & \dots & \dots & 0 & -2 & 2 \end{pmatrix} \tag{5.38}$$

and

$$\mathbf{P}^{(l)} = \begin{pmatrix} (2+\kappa_1 & -(1+\kappa_1) & 0 & 0 & \dots & \dots & 0 \\ +\gamma_1^{(l)}) & & & & & & \\ -1 & (2+\kappa_2 & -(1+\kappa_2) & 0 & 0 & \dots & 0 \\ & +\gamma_2^{(l)}) & & & & & \\ 0 & -1 & (2+\kappa_3 & -(1+\kappa_3) & 0 & \dots & 0 \\ & & +\gamma_3^{(l)}) & & & & \\ \vdots & \vdots & \vdots & \vdots & \vdots & \vdots & \vdots \\ 0 & 0 & \dots & 0 & -1 & (2+\kappa_{Nd-1} & -(1+ \\ & & & & & +\gamma_{Nd-1}^{(l)}) & \kappa_{Nd-1}) \\ 0 & 0 & \dots & \dots & 0 & -1 & (2+ \\ & & & & & & \kappa_{Nd}+\gamma_{Nd}^{(l)}) \end{pmatrix} \tag{5.39}$$

$\gamma_i^{(l)}$ and κ_i therein are given by

$$\gamma_i^{(l)} = \frac{h_\theta^2 l^2}{\sin^2 \theta_i} \tag{5.40}$$

$$\kappa_i = h_\theta \cdot \cot \theta_i . \tag{5.41}$$

$\mathbf{E}$ is the unit matrix and h_θ denotes the equidistant discretization angle. The N_d-dimensional "ket" vector $|\, \tilde{u}^{(l)}(r) >$ is the transpose of the row vector with the radial dependent functions $\tilde{u}^{(l)}(r, \theta_i)$ as its components, i.e.,

$$|\, \tilde{u}^{(l)}(r) > = \left(\tilde{u}^{(l)}(r, \theta_1), \dots, \tilde{u}^{(l)}(r, \theta_{Nd},) \right)^{tp} . \tag{5.42}$$

This corresponds to the definition (1.24) introduced in Chap. 1.

The derived system of coupled but ordinary differential equations seems to offer no essential advantages compared to the original partial differential equation, at first glance. But it can be shown that both the tridiagonal coupling matrices (5.38) and (5.39) may be transformed into diagonal matrices thus resulting in a decoupling of the system of ordinary differential equations. This is a consequence of the special form of (5.38) and (5.39) since every nonsymmetric but tridiagonal matrix

$$\mathbf{P}^{(l)}_{unsym.} = \begin{pmatrix} \alpha_1 & -\beta_2 & 0 & 0 & \dots & \dots & 0 \\ -\gamma_2 & \alpha_2 & -\beta_3 & 0 & 0 & \dots & 0 \\ 0 & -\gamma_3 & \alpha_3 & -\beta_4 & 0 & \dots & 0 \\ \vdots & \vdots & \vdots & \vdots & \vdots & \vdots & \vdots \\ 0 & \dots & \dots & 0 & -\gamma_{Nd-1} & \alpha_{Nd-1} & -\beta_{Nd} \\ 0 & \dots & \dots & \dots & 0 & -\gamma_{Nd} & \alpha_{Nd} \end{pmatrix}, \tag{5.43}$$

with $\gamma_i \cdot \beta_i > 0$ may be brought into a symmetric form by use of an similarity transformation . This is achieved by

$$\mathbf{P}^{(l)}_{sym.} = \mathbf{Z}^{(l)^{-1}} \cdot \mathbf{P}^{(l)}_{unsym.} \cdot \mathbf{Z}^{(l)}. \tag{5.44}$$

$$\left[z^{(l)}\right]_{1,1} = 1, \quad \text{and} \quad \left[z^{(l)}\right]_{i,i} = \left(\frac{\gamma_2 \cdot \ldots \cdot \gamma_i}{\beta_2 \cdot \ldots \cdot \beta_i}\right)^{1/2} \tag{5.45}$$

are the elements of the diagonal transformation matrix $\mathbf{Z}^{(l)}$. The resulting elements of matrix (5.44) read

$$\left[p^{(l)}_{sym.}\right]_{i,i} = \alpha_i; \qquad \left[p^{(l)}_{sym.}\right]_{i,i+1} = \left[p^{(l)}_{sym.}\right]_{i+1,i} = -\left(\beta_{i+1} \cdot \gamma_{i+1}\right)^{1/2}. \tag{5.46}$$

By applying a principal axis transformation to this symmetric matrix we are able to transform it into a diagonal matrix. For this, we have to consider the eigenvalue problem

$$\left(\mathbf{P}^{(l)}_{sym.} - \lambda^{(l)}_i \cdot \mathbf{E}\right) \cdot \vec{x}^{\,(l)}_i = \vec{0} \tag{5.47}$$

which must be solved for each azimuthal mode l independently. The resulting eigenvectors $\vec{x}^{\,(l)}_i$ form the columns of the required transformation matrix $\mathbf{H}^{(l)}$. Unfortunately, problem (5.47) can be solved only numerically in spherical coordinates. Fortunately, this solution provides no essential difficulties and can be performed with numerical standard methods. It is, however, not necessary to solve this problem numerically, as we will see shortly. But for a moment let us assume that we have solved the problem successfully. Then we are able to accomplish the decoupling of the system (5.35). For this, we define the transformed solution vector according to

$$|\,\tilde{u}^{(l)}(r)\,> = \mathbf{Tr}^{(l)^{-1}} \cdot |\,\tilde{u}^{(l)}(r)\,> \tag{5.48}$$

with

$$\mathbf{Tr}^{(l)} = \mathbf{Z}^{(l)} \cdot \mathbf{H}^{(l)} \tag{5.49}$$

$$\mathbf{Tr}^{(l)^{-1}} = \mathbf{H}^{(l)^{-1}} \cdot \mathbf{Z}^{(l)^{-1}} \tag{5.50}$$

being the overall transformation matrix of the diagonalization. This matrix is characterized by its property

$$\mathbf{Tr}^{(l)^{-1}} \cdot \mathbf{Tr}^{(l)} = \mathbf{Tr}^{(l)} \cdot \mathbf{Tr}^{(l)^{-1}} = \mathbf{E}. \tag{5.51}$$

Inserting the unit matrix $\mathbf{E} = \mathbf{Tr}^{(l)} \cdot \mathbf{Tr}^{(l)^{-1}}$ in between the expressions $\mathbf{P}^{(l)}$ and $|\,\tilde{u}^{(l)}(r)\,>$ of (5.35), multiplying the resulting equation with $\mathbf{Tr}^{(l)^{-1}}$ afterwards, taking the property

$$\mathbf{Tr}^{(l)^{-1}} \cdot \mathbf{P}^{(l)} \cdot \mathbf{Tr}^{(l)} = diag(\lambda^{(l)}) \tag{5.52}$$

into account, and, finally, substituting

$$\rho = k \cdot r \tag{5.53}$$

and

$$\bar{u}_i^{(l)}(\rho) = \frac{1}{\sqrt{\rho}} \cdot B_i^{(l)}(\rho) \tag{5.54}$$

provides the following ordinary differential equation for each of the component of the transformed and according to (5.54) substituted solution vector $|\, \bar{u}^{(l)}(\rho) >$:

$$\frac{d^2 B_i^{(l)}(\rho)}{d\rho^2} + \frac{1}{\rho} \cdot \frac{d B_i^{(l)}(\rho)}{d\rho} + \left[1 - \frac{\nu_i^{(l)^2}}{\rho^2} \right] \cdot B_i^{(l)}(\rho) = 0. \tag{5.55}$$

Here we have

$$\nu_i^{(l)^2} = \frac{\lambda_i^{(l)}}{h_\theta^2} + \frac{1}{4}, \quad i = 1, \ldots, N_d. \tag{5.56}$$

Equation (5.55) is nothing but Bessel's ordinary differential equation. Its solution was already discussed in Chap. 2. Therefore, if the radiation condition (2.76) must additionally be taken into account, we obtain

$$\bar{u}_i^{(l)}(\rho) = c_{l,i}^{(N_d)} \cdot \frac{H_{\nu_i^{(l)}}^{(1)}(\rho)}{\sqrt{\rho}} \tag{5.57}$$

as the general solution for each component of $|\, \bar{u}^{(l)}(\rho) >$. If the regularity is required we have on the other hand

$$\bar{u}_i^{(l)}(\rho) = c_{l,i}^{(N_d)} \cdot \frac{J_{\nu_i^{(l)}}(\rho)}{\sqrt{\rho}} \tag{5.58}$$

with unknown coefficients $c_{l,i}^{(N_d)}$ in both cases. The difference to the solutions given in (2.65) and (2.66) consists in the order of the Bessel and Hankel functions. In (5.57) and (5.58) these orders are defined via the eigenvalues of the eigenvalue problem (5.47) according to relation (5.56). Having determined the formal solution of the discretized Helmholtz equation in the transformed region we have to go back to the original region. This can be accomplished with the inverse of (5.48), i.e., by

$$|\, \tilde{u}^{(l)}(\rho) >= \mathbf{Tr}^{(l)} \cdot |\, \bar{u}^{(l)}(\rho) > . \tag{5.59}$$

Thus, we get for the general solution of the discretized Helmholtz equation (5.26) in the intersection points of the discretization lines with the scatterer surface $\partial\Gamma$

$$| u_{l,n}(\rho_i, \phi) >= c_{l,n}^{(N_d)} \cdot | \tilde{x}_{l,n} >= c_{l,n}^{(N_d)} \cdot e^{il\phi} \cdot \mathbf{U}_n^{(l)} \cdot \vec{x}_n^{(l)}. \tag{5.60}$$

$\mathbf{U}_n^{(l)}$ therein are diagonal matrices with elements

$$\left[U_n^{(l)}\right]_{i,i} = \frac{Z_{\nu_n^{(l)}}(\rho_i)}{\sqrt{\rho_i}}, \quad i = 1, \ldots, N_d, \tag{5.61}$$

and $Z_{\nu_n^{(l)}}$ are Bessel's functions $J_{\nu_n^{(l)}}$ or Hankel's functions of first kind $H^{(1)}_{\nu_n^{(l)}}$, depending on whether the regularity requirement or the radiation condition must be additionally fulfilled. Expression $\rho_i = k \cdot r_i$ denotes the the respective argument at the intersection point of the considered discretization line with the scatterer surface according to (5.53). The N_d-dimensional vectors $| \tilde{x}_{l,n} >$ are the eigenvectors $\vec{x}_n^{(l)}$ of the eigenvalue problem (5.47) but modified by the term $e^{il\phi} \cdot \mathbf{U}_n^{(l)}$. Note moreover that i in $e^{il\phi}$ represents the imaginary unit and not the summation index. The best way to convince oneself that (5.60) is indeed a consequence of Eq. (5.59) is to write down explicitly the inverse transformation for two discretization lines only. In doing so the transformation matrix $\mathbf{Tr}^{(l)}$ with eigenvectors $\vec{x}_n^{(l)}$ as its columns can considered to be a known quantity.

The following statement is the most important result of the procedure described just now: Vector $| u(\rho_i, \phi) >$ with a finite number of components defined at the intersection points of the discretization lines with the scatterer surface $\partial\Gamma$ can be represented by a finite series in terms of the eigenvectors $| \tilde{x}_{l,n} >$ given in (5.60) according to

$$| u(\rho_i, \phi) >= \sum_l \sum_{n=1}^{N} c_{l,n}^{(N)} \cdot | \tilde{x}_{l,n} >, \quad N \leq N_d. \tag{5.62}$$

The unknown expansion coefficients $c_{l,n}^{(N)}$ can be determined afterwards by applying the Rayleigh method described in Chap. 1. The modified eigenvectors $| \tilde{x}_{l,n} >$, in contrast to the original eigenvectors $\vec{x}_n^{(l)}$ of the eigenvalue problem (5.47), are not orthogonal, in general. Their orthogonality holds only if the scatter surface is a spherical one, due to the resulting constancy of the arguments ρ_i.

5.3.2 *The Limiting Behaviour of the Method of Lines*

What are the consequences of (5.62) for the conceptual interpretation of the MoL? This is what we try to find out in this subsection. The most remarkable aspect of (5.62) is the fact that it transforms the initial discretization of the differential operator of

Helmholtz's equation into an equivalent approximation of the unknown solution in terms of a finite series expansion. But that is exactly what is known from all the spectral methods, including the Separation of Variables method. Thus, the following question arises: What are the differences between the eigensolutions of the Helmholtz equation discussed in Sect. 2.3.1 and the eigenvectors $\vec{x}_n^{(l)}$ of the eigenvalue problem (5.47) we have to solve if employing the MoL? On the one hand, both eigensolutions differ in the order of the Bessel functions and Hankel functions of the first kind. Applying the Separation of Variables method these orders are given by semi-integer numbers (see Sect. 2.3.1). In the MoL the orders are calculated from the eigenvalues according to (5.56). At first glance, these orders are not even semi-integer numbers. On the other hand, both eigensolutions differ in the θ-dependence of the eigenvectors. In the Separation of Variables method this dependency is expressed by the associated Legendre polynomials. In the MoL we have the N_d-dimensional and orthogonal eigenvectors $\vec{x}_n^{(l)}$ instead. These are the only differences! Thus, we are faced with a strange situation. Both approaches the Separation of Variables method and the MoL result in an expansion of a continuously varying function $| f >$ with respect to θ at $\partial\Gamma$ or a discrete function $| f >$ defined at the intersection points θ_i along $\partial\Gamma$ into the corresponding eigenvectors of the respective method. At least for a spherical scatterer surface we may expect from both expansions that they will approximate the continuously varying or discrete function $| f >$ at this surface in the sense of the criteria discussed in Sect. 2.2.1, for example, if the relevant parameters are chosen appropriately. But then the above mentioned differences should disappear since both methods claim to solve the eigenvalue problems of Helmholtz's equation without further approximations. And this is what we can indeed demonstrate if going back to the eigenvalue problem (5.47). It determines the essential elements of the MoL, the orders of the components of the discrete expansion vectors and the expansion vectors itself. An "appropriate choice of the relevant parameters" means an increase of the number N_d of discretization lines within the interval $[0, \pi]$. We have therefore to prove if the relations

$$\lim_{N_d \to \infty} \vec{x}_n^{(l)} = P_n^l \tag{5.63}$$

$$\lim_{N_d \to \infty} \nu_n^{(l)} = n + \frac{1}{2} \tag{5.64}$$

hold for the eigenvectors and eigenvalues of the MoL. A numerical treatment of (5.47) in spherical coordinates reveals the correctness of these relations. For each arbitrary number N_d we obtain already eigenvectors $\vec{x}_n^{(l)}$ which agree by all but a constant factor with the associated Legendre polynomials P_n^l calculated at the discrete points θ_i. This factor is a consequence of the different normalization used in each of the methods. In the MoL, the normalization of the finite-dimensional eigenvectors is usually performed according to

$$< x_m^{(l)} \mid x_n^{(l)} >= \delta_{m,n}. \tag{5.65}$$

The Separation of Variables method employs (2.70), on the other hand. Unfortunately, the proof of (5.64) is not as simple. The dependence of the orders $\nu_n^{(l)}$ on the azimuthal modes l is one obvious difference. Remember: (5.47) must be solved independently for every azimuthal mode l! But such a dependence can also be generated in (2.83) and (2.84) if reordering the summation with respect to l and n,

$$\sum_{n=0}^{\infty} \sum_{l=-n}^{n} \cdots = \sum_{l} \sum_{n=|l|}^{\infty} \cdots ; \quad l = 0, \pm 1, \pm 2, \cdots . \tag{5.66}$$

To prove (5.64) numerically we fix mode l to a certain integer number and consider the dependence of the resulting orders $\nu_n^{(l)}$ on the number N_d of discretization lines. It bears out that for an increasing N_d the orders are represented better and better by the sequences

$$|l| + \frac{1}{2}, \ |l| + 1 + \frac{1}{2}, \ |l| + 2 + \frac{1}{2}, \cdots . \tag{5.67}$$

Thus, we can approve (5.64) at least numerically. But it is somehow unsatisfactory to rest on a pure numerical treatment. Therefore, we will deal with the equivalent two-dimensional problem in Cartesian coordinates which allows for an analytical treatment.

We look at the solution $f(x, y)$ of the two-dimensional Helmholtz equation

$$\left(\frac{\partial^2}{\partial x^2} + \frac{\partial^2}{\partial y^2} \right) f(x, y) + k^2 f(x, y) = 0 \tag{5.68}$$

subject to the homogeneous Dirichlet conditions

$$f(0, y) = f(a, y) = 0 \tag{5.69}$$

at $x = 0, a$. The boundary conditions with respect to the variable y can be ignored. We apply the MoL to (5.68) by performing an equidistant discretization with respect to x which is in accordance with (5.69). The corresponding discretization scheme is depicted in Fig. 5.4. This procedure provides us with the following analytical expressions of the eigenvalues and eigenvectors:

$$\vec{x}_i = sin\left(\frac{ij\pi}{N_d + 1} \right) = sin\left(\frac{i\pi}{a} j h_x \right), \quad i, j = 1, \cdots, N_d \tag{5.70}$$

$$\lambda_i = \frac{4}{h_x^2} \cdot sin^2 \left[\frac{i\pi}{2(N_d + 1)} \right], \quad h_x = \frac{a}{N_d + 1}. \tag{5.71}$$

The derivation of these expressions is omitted here. It is a not to difficult exercise for the reader. In contrast to what happens in spherical coordinates the discretization procedure results directly into a symmetric and tridiagonal coupling matrix, i.e., there is no need to perform the similarity transformation (5.44). The lazy reader is

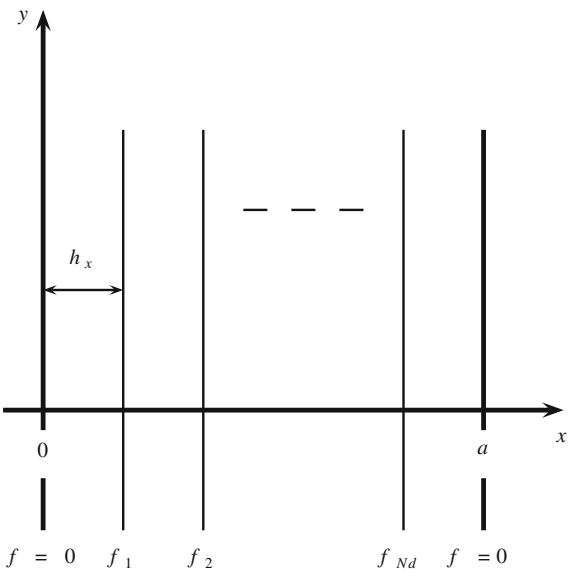

Fig. 5.4 Equidistant discretization scheme applied to the two-dimensional homogeneous Dirichlet problem of Helmholtz's equation in Cartesian coordinates

referred to the book of Pregla and Pascher cited in the reference chapter. Among others, he can find therein the derivation of the above given expressions. With (5.70) and (5.71) we know the decisive elements of the MoL. On the other hand, if applying the separation ansatz $f(x, y) = Y(y) \cdot X(x)$, we obtain the expressions

$$X_n(x) = sin\left(\frac{n\pi}{a}x\right) \tag{5.72}$$

and

$$k_n^2 = \left(\frac{n\pi}{a}\right)^2 \tag{5.73}$$

for the x-dependent eigenvectors and eigenvalues of the Separation of Variables method. It becomes obvious that (5.72) is identical with (5.70) at the N_d discrete points $x_j = j \cdot h_x$. To check the equality of the eigenvalues (5.73) and (5.71) in the limiting case of an infinite number of discretization lines we expand the sine function in (5.71) into a Taylor series. The linear term of this expansion just provides $\lambda_i = \left(\frac{i\pi}{a}\right)^2$. All higher order contributions vanish with an increasing N_d. This confirms our result obtained only numerically in spherical coordinates. It is exactly this behaviour which forced us to make the provocative statement at the beginning of this section that the MoL turns out to be just a worsening of the Separation of Variables method, and that it provides no additional advantages compared to spectral methods.

But, in the light of the considerations performed above, we must also state that the MoL, if applied to scattering problems in open domains, offers two essential advantages compared to the conventional Finite-Difference methods. The scattering

solution requires the fulfilment of the nonlocal radiation condition (2.76) at infinity, as frequently employed in the chapters before. Even this condition is difficult to handle within the conventional Finite-Difference methods. This happens because these methods are based on an additional discretization of the radial coordinate. To accomplish this discretization the outer region Γ_+ must be necessarily restricted to a finite domain with respect to the radius. As a consequence, the nonlocal radiation condition has to be replaced by so-called "Absorbing Boundary Conditions" (ABCs) which are introduced at a certain finite (i.e., local!) distance from the scatterer. The appropriate choice of these ABCs has a major impact on the stability and accuracy of the solution. It may also happen that spurious solutions occur, as observed in several applications. This requires an additional numerical effort to filter out the correct solution by controlling energy conservation, for example. The MoL is free of this problem since solving (5.55) in agreement with the nonlocal radiation condition. Another advantage of the MoL compared to the conventional Finite-Difference methods consists in the analytical solution of (5.55). Of course, it would be also possible to solve (5.55) by a discretization procedure with respect to the r-dependence, as the conventional Finite-Difference methods will do. But, beside the problem with the radiation condition, this would result in an additional worsening of the diagonal matrices $\mathbf{U}_n^{(l)}$. Moreover, each new orientation of the scatterer in the incident field is a new scattering problem within the Finite-Difference methods thus making orientation averaging a much more cumbersome task than with T-matrix methods. In Chap. 7 of the book "Light Scattering by Nonspherical Particles" (see Sect. 10.9 for details) there is described a Finite-Difference-Time-Domain method by Yang and Liou. An intercomparison of the results obtained with this method if applied to a spherical scatterer with the results of Mie's theory is depicted in Fig. 2 on page 187 of this contribution. A maximum of 10 % difference between both phase functions can be already observed at a comparable small size parameter of $k_0 a = 15$. This difference becomes even larger if looking at the elements of the phase matrix (the quantities "phase function" and "phase matrix" are introduced in Chap. 7 of this book!). These are the reasons which cast the application of the conventional Finite-Difference methods into doubt, at least if applied to the scattering problems in open domains considered in this book, and if a more complex scatterer geometry than that of a sphere or scattering at higher size parameters is considered.

For completeness we will finally generalize the results obtained in Chaps. 3 and 4 of this book in such a way that they hold also for the MoL. This can be simply performed by employing again the "bra" and "ket" symbols already introduced in Chap. 1. $G_{\partial\Gamma}^{(N)}$, for example, may be represented in this generalized form by

$$G_{\partial\Gamma}^{(N)}(\mathbf{x},\mathbf{x}') = -\sum_{i,j=0}^{N} \left[A_{\partial\Gamma}^{(g,\varphi_0)^{-1}}\right]_{i,j} \cdot \mid \varphi_i(k_0,\mathbf{x}) >< g_j(k_0,\mathbf{x}') \mid$$
$$\mathbf{x}' \in \partial\Gamma,\ \mathbf{x} \in \Gamma_+. \tag{5.74}$$

$G^{(N)}_{\Gamma_+}$ reads correspondingly

$$G^{(N)}_{\Gamma_+}(\mathbf{x},\mathbf{x}') = G_0(\mathbf{x},\mathbf{x}') - (ik_0)\sum_{i,k=0}^{N}[T_{\partial\Gamma}]_{i,k}\cdot|\,\varphi_i(k_0,\mathbf{x})><\tilde{\varphi}^*_k(k_0,\mathbf{x}')\,| \quad \mathbf{x},\mathbf{x}'\in\Gamma_+. \tag{5.75}$$

The solution of the outer Dirichlet problem may be then written according to

$$|\,u_t(\mathbf{x})>=G_{\Gamma_+}(\mathbf{x},\mathbf{x}')\,|\,\rho(\mathbf{x}')> \tag{5.76}$$

or

$$|\,u_s(\mathbf{x})>=G_{\partial\Gamma}(\mathbf{x},\mathbf{x}')\,|\,u_{inc}(\mathbf{x}')>, \tag{5.77}$$

respectively. If the MoL is used this solution is given only at N_d discrete points along an arbitrary curvature in Γ_+. The free-space Green function in (5.75) may be discretized to fit into the MoL. $[T_{\partial\Gamma}]_{i,k}$ are still the elements of the T-matrix belonging to the outer Dirichlet and transmission problem. If they will be also calculated consequently by use of the MoL the discrete expansion vectors $|\,\tilde{x}_{l,n}>$ must be used instead of the continuously varying eigenvectors, and the scalar product (1.34) must be replaced by (1.36). Expression $<\tilde{\varphi}^*_k(k_0,\mathbf{x}')\,|\,\rho(\mathbf{x}')>$ resulting from (5.75) and (5.76) represents the volume integral

$$<\tilde{\varphi}^*_k(k_0,\mathbf{x}')\,|\,\rho(\mathbf{x}')>=\int_{\Gamma_+}\tilde{\varphi}_k(k_0,\mathbf{x}')\cdot\rho(\mathbf{x}')\,dV(\mathbf{x}') \tag{5.78}$$

performed over the source region in Γ_+. Within the MoL the integration with respect to θ has to be replaced by a corresponding summation over the discretization angles, of course.

5.4 Integral Equation Methods

Boundary integral equation methods and volume integral equation methods are two other solution techniques which are frequently applied for solving scattering problems. They are essentially based on the equivalence principle which states that a field outside a finite scattering volume Γ_- may be considered as the result of an equivalent surface current at the surface of this volume or an equivalent volume current inside this volume. These equivalent currents are the unknown quantities in the

integral equation methods which have to be determined. That is in contrast to all the methods considered so far, which take the scattered field for the unknown quantity. Once the scattered field is known the induced surface or volume currents can be calculated afterwards, of course. We will come back to this interrelation between induced currents and fields in Chap. 7 in conjunction with the physical background of electromagnetic wave scattering. Here we just want to state the different point of views underlying the methods considered so far and the integral equation methods we will discuss now. More generally speaking, regarding the Trinity of physics, "cause", "action", and "interaction", this difference represents our experience that the result of an interaction can be interpreted as a new cause (in our case an induced surface current, for example) producing the same action (the scattered field). That is exactly the physical content of Huygens' principle we expressed already in terms of Green functions.

It is not our intention here to provide a complete description of the different integral equation methods. We included several books and papers in the reference chapter dealing with these methods in much more detail. The main focus in what follows is on the problem of how one can come from the picture of Green functions and interaction operators developed so far to the integral equation methods. The boundary integral equations are discussed in conjunction with the scalar outer Dirichlet and transmission problem whereas the volume integral equations are restricted to the scalar case of the outer transmission problem. All derivations can be similarly performed for the dyadic case if using the corresponding dyadic and vector forms of Green's theorem. But in the dyadic case there appears an additional difficulty resulting from the stronger singularity of the dyadic free-space Green function—sometimes a not even simple undertaking in numerical procedures. In such cases, it may be of benefit not to take the integral equations which results in a straightforward way from the homogeneous Dirichlet condition but to use those one which are expressed in terms of the induced surface current, for example. These equations exhibit a weaker singularity, due to the operation mentioned already in (2.335). This will also be discussed in detail in Chap. 7 of this book when dealing with the scattering problem of an ideal metallic obstacle. Avoiding the confrontation with the strong singularity of the dyadic free-space Green function represents one of the advantages of the T-matrix methods which should not be underestimated.

This chapter will be finalized with deriving the so-called "Lippmann-Schwinger equations". Since these integral equations are an ideal starting point for iterative solutions of the scattering problem, they deserve a mention in this chapter. They will be derived in both scalar and dyadic form. The latter especially because of the fact that the lowest order iteration appears to be not affected by the strong singularity of the dyadic free-space Green function. Deriving the Lippmann-Schwinger equations for the dyadic Green function and the dyadic interaction operator demonstrates moreover how one can translate the scalar derivations discussed beforehand into the dyadic notation.

5.4.1 Boundary Integral Equation Method Related to the Outer Dirichlet Problem

To obtain the boundary integral equation for the interaction operator related to the outer Dirichlet problem we have to perform a slight but important change in definition (4.1). We replace the quantity $G_0^>$ used in this definition by the full free-space Green function G_0, i.e., instead of (4.1) we use the definition

$$G_{\Gamma_+}(\mathbf{x},\mathbf{x}') := G_0(\mathbf{x},\mathbf{x}') + \oint_{\partial\Gamma} G_0(\mathbf{x},\bar{\mathbf{x}}) \cdot \hat{W}_{\partial\Gamma_+}(\bar{\mathbf{x}},\tilde{\mathbf{x}}) \cdot G_0(\tilde{\mathbf{x}},\mathbf{x}')\, dS(\bar{\mathbf{x}})\, dS(\tilde{\mathbf{x}}). \tag{5.79}$$

To distinguish the interaction operators introduced by the different definitions we will mark the new interaction operator in (5.79) with a "hat". The Green function G_{Γ_+} defined according to (5.79) is also a solution of the inhomogeneous Helmholtz equation subject to the radiation condition with respect to $\mathbf{x}$. We can then use the additionally required homogeneous Dirichlet condition at the scatterer surface to determine the interaction operator $\hat{W}_{\partial\Gamma_+}$, as already done in Chap. 4. For this, we have to move $\mathbf{x}$ toward the scatterer surface. But this procedure forces us now to take the singularity of $G_0(\mathbf{x},\bar{\mathbf{x}})$ at the surface point $\mathbf{x} = \bar{\mathbf{x}}$ seriously into account. Please, remember: In contrast to $G_0(\mathbf{x},\bar{\mathbf{x}})$ used in (5.79) the quantity $G_0^>(\mathbf{x},\bar{\mathbf{x}})$ used in (4.1) was assumed to obey generally the homogeneous Helmholtz equation also if $\mathbf{x} \in \partial\Gamma$. The integral expression

$$\oint_{\partial\Gamma} G_0(\mathbf{x},\bar{\mathbf{x}}) \cdot f(\bar{\mathbf{x}})\, dS(\bar{\mathbf{x}}); \quad \mathbf{x},\bar{\mathbf{x}} \in \partial\Gamma \tag{5.80}$$

represents therefore an improper integral, due to the singularity of $G_0(\mathbf{x},\bar{\mathbf{x}})$ at the surface point $\mathbf{x} = \bar{\mathbf{x}}$. To calculate the boundary integral (5.80) we exclude at first a small surface element $\partial\Gamma_\delta$ which encloses the singular point. The improper integral is convergent if there exists a finite value of the sum of the integrals

$$\int_{\partial\Gamma - \partial\Gamma_\delta} G_0(\mathbf{x},\bar{\mathbf{x}}) \cdot f(\bar{\mathbf{x}})\, dS(\bar{\mathbf{x}}) + \int_{\partial\Gamma_\delta} G_0(\mathbf{x},\bar{\mathbf{x}}) \cdot f(\bar{\mathbf{x}})\, dS(\bar{\mathbf{x}}) \tag{5.81}$$

in the limiting case $\lim \partial\Gamma_\delta \to 0$. Even if it is not quite exact from a mathematical point of view it is common practice to denote the limiting value of the first integral of expression (5.81) as "principal value",

$$p.v. \oint_{\partial\Gamma} G_0(\mathbf{x},\bar{\mathbf{x}}) \cdot f(\bar{\mathbf{x}})\, dS(\bar{\mathbf{x}}) := \lim_{\partial\Gamma_\delta \to 0} \int_{\partial\Gamma - \partial\Gamma_\delta} G_0(\mathbf{x},\bar{\mathbf{x}}) \cdot f(\bar{\mathbf{x}})\, dS(\bar{\mathbf{x}}), \tag{5.82}$$

and that is the way we will use it, too. It can be moreover shown that for any sufficiently smooth function $f(\bar{\mathbf{x}})$ with no singularities along $\partial\Gamma$

$$\lim_{\partial\Gamma_\delta \to 0} \int_{\partial\Gamma_\delta} G_0(\mathbf{x}, \bar{\mathbf{x}}) \cdot f(\bar{\mathbf{x}})\, dS(\bar{\mathbf{x}}) \to 0 \tag{5.83}$$

holds. Thus we have

$$\oint_{\partial\Gamma} G_0(\mathbf{x}, \bar{\mathbf{x}}) \cdot f(\bar{\mathbf{x}})\, dS(\bar{\mathbf{x}}) = p.v. \oint_{\partial\Gamma} G_0(\mathbf{x}, \bar{\mathbf{x}}) \cdot f(\bar{\mathbf{x}})\, dS(\bar{\mathbf{x}}) \tag{5.84}$$

if $\mathbf{x}, \bar{\mathbf{x}} \in \partial\Gamma$. To prove (5.83), let us consider the boundary integral

$$\int_{\partial\Gamma_\delta} G_0(\mathbf{x}, \bar{\mathbf{x}}) \cdot f(\bar{\mathbf{x}})\, dS(\bar{\mathbf{x}}) \tag{5.85}$$

with $\partial\Gamma_\delta$ being a very small but finite surface patch enclosing the singular point. Correspondingly, we can replace the analytical expression (2.261) of the free-space Green function $G_0(\mathbf{x}, \bar{\mathbf{x}})$ by its static approximation

$$G_0(\mathbf{x}, \bar{\mathbf{x}}) \approx \frac{1}{4\pi|\mathbf{x} - \bar{\mathbf{x}}|}. \tag{5.86}$$

$\partial\Gamma_\delta$ can be assumed w.l.o.g. to be a surface patch with a circular boundary, and with the z-axis of the coordinate system running through the centre of the boundary circle. This holds even if the scatterer surface is a nonspherical ones (compare Fig. 5.5). The observation point $\mathbf{x}$ is placed into the centre of the circle in distance a from the origin of the coordinate system. $|\mathbf{x}| = |\bar{\mathbf{x}}| = a$ is assumed to be constant across the small

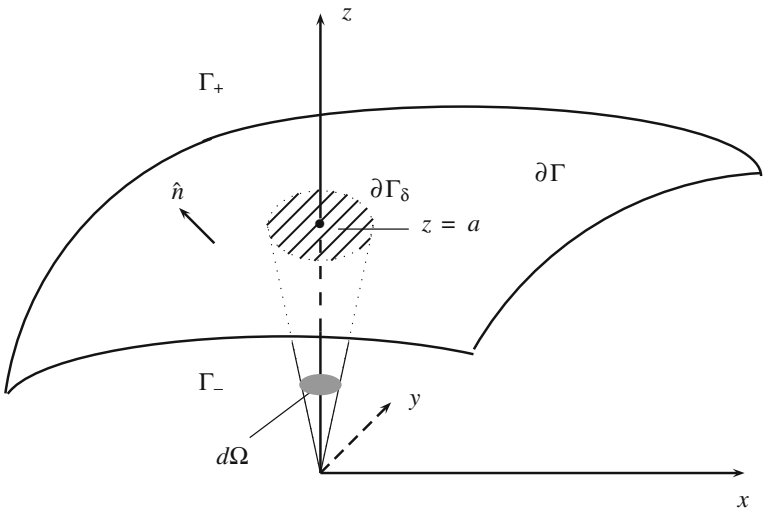

Fig. 5.5 Geometrical configuration to calculate the boundary integrals (5.85) and (5.107)

surface patch $\partial\Gamma_\delta$. In conjunction with (2.51), because of approximation

$$|\mathbf{x} - \bar{\mathbf{x}}| \;\approx\; a \cdot \sin\bar{\theta} \tag{5.87}$$

for every $\bar{\mathbf{x}} \in \partial\Gamma_\delta$, and due to the factor 2π which results from the $\bar{\phi}$-integration we obtain in spherical coordinates

$$\int_{\partial\Gamma_\delta} \frac{f(\bar{\mathbf{x}})}{4\pi|\mathbf{x} - \bar{\mathbf{x}}|}\, dS(\bar{\mathbf{x}}) \approx \frac{f(a)}{2} \cdot a \cdot \int_0^{\bar{\theta}_\delta} d\bar{\theta}. \tag{5.88}$$

In deriving (5.88) it was moreover assumed that the sufficiently smooth function $f(\bar{\mathbf{x}})$ can be replaced by its value in point $(r = a, \theta = 0°, \phi = 0°)$ everywhere across the small surface patch. Thus we have finally

$$\int_{\partial\Gamma_\delta} \frac{f(\bar{\mathbf{x}})}{4\pi|\mathbf{x} - \bar{\mathbf{x}}|}\, dS(\bar{\mathbf{x}}) \approx \frac{f(a)}{2} \cdot a \cdot \bar{\theta}_\delta. \tag{5.89}$$

If $\bar{\theta}_\delta$ tends to zero this expression vanishes indeed. But in the numerical realization of the boundary integral equation method it may be of some benefit to take the contribution from the second integral term in (5.81) into account. It is reported in several papers (see the paper of Fikioris and Magoulas cited in Sect. 10.6, for example) that this may lead to an improved stability and accuracy of the numerical procedure. Otherwise, one has to cover the scatterer surface with a very fine surface mesh to obtain accurate results which may increase the numerical effort drastically.

Now, we are prepared to move the observation point in expression (5.79) towards the surface. Applying the homogeneous Dirichlet condition we get the integral equation

$$\begin{aligned} -G_0(\mathbf{x}, \mathbf{x}') = p.v. \oint_{\partial\Gamma} & G_0(\mathbf{x}, \bar{\mathbf{x}}) \cdot \hat{W}_{\partial\Gamma_+}(\bar{\mathbf{x}}, \tilde{\mathbf{x}}) \cdot G_0(\tilde{\mathbf{x}}, \mathbf{x}')\, dS(\bar{\mathbf{x}})\, dS(\tilde{\mathbf{x}}); \\ & \mathbf{x} \in \partial\Gamma \end{aligned} \tag{5.90}$$

to calculate the interaction operator $\hat{W}_{\partial\Gamma_+}(\bar{\mathbf{x}}, \tilde{\mathbf{x}})$. The principal value symbol therein corresponds to the integration with respect to the variable $\bar{\mathbf{x}}$. Let us now consider one possible way to calculate $\hat{W}_{\partial\Gamma_+}(\bar{\mathbf{x}}, \tilde{\mathbf{x}})$ in more detail. The interaction operator may be approximated by the bilinear expansion

$$\hat{W}_{\partial\Gamma_+}(\bar{\mathbf{x}}, \tilde{\mathbf{x}}) = -\sum_{k,l=0}^{N} \left[\hat{W}_{\partial\Gamma_+}\right]_{k,l} \cdot \varphi_k(k_0, \bar{\mathbf{x}}) \cdot \varphi_l(k_0, \tilde{\mathbf{x}}); \quad \bar{\mathbf{x}}, \tilde{\mathbf{x}} \in \partial\Gamma \tag{5.91}$$

in terms of the radiating eigensolutions of Helmholtz's equation. Both the free-space Green functions $G_0(\mathbf{x}, \mathbf{x}')$ and $G_0(\tilde{\mathbf{x}}, \mathbf{x}')$ in (5.90) can be replaced without any problems by the series expansion (2.278) since the source point $\mathbf{x}'$ is still located

outside the smallest sphere circumscribing the scatterer. This results into the equation

$$\sum_{j=0}^{N} \psi_j(k_0, \mathbf{x}) \cdot \tilde{\varphi}_j(k_0, \mathbf{x}') = \sum_{j,k,l=0}^{N} p.v. \oint_{\partial\Gamma} G_0(\mathbf{x}, \bar{\mathbf{x}}) \cdot \left[\hat{W}_{\partial\Gamma_+}\right]_{k,l} \cdot \varphi_k(k_0, \bar{\mathbf{x}}) \cdot \varphi_l(k_0, \tilde{\mathbf{x}}) \cdot \psi_j(k_0, \tilde{\mathbf{x}}) \cdot \tilde{\varphi}_j(k_0, \mathbf{x}')\, dS(\bar{\mathbf{x}})\, dS(\tilde{\mathbf{x}}); \quad \mathbf{x} \in \partial\Gamma. \tag{5.92}$$

Since the functions $\tilde{\varphi}_j(k_0, \mathbf{x}')$ form a linearly independent system in Γ_+ we get the equation

$$\psi_j(k_0, \mathbf{x}) = \sum_{k,l=0}^{N} p.v. \oint_{\partial\Gamma} G_0(\mathbf{x}, \bar{\mathbf{x}}) \cdot \left[\hat{W}_{\partial\Gamma_+}\right]_{k,l} \cdot \varphi_k(k_0, \bar{\mathbf{x}}) \cdot \varphi_l(k_0, \tilde{\mathbf{x}}) \cdot \psi_j(k_0, \tilde{\mathbf{x}})\, dS(\bar{\mathbf{x}})\, dS(\tilde{\mathbf{x}}); \quad \mathbf{x} \in \partial\Gamma; \ j = 0, \cdots, N \tag{5.93}$$

to determine the unknown elements $\left[\hat{W}_{\partial\Gamma_+}\right]_{k,l}$ in the bilinear expansion (5.91). For this we integrate both sides of this equation according to

$$\oint_{\partial\Gamma} g_i^*(\mathbf{x}) \cdots\, dS(\mathbf{x}); \quad i = 0, \cdots, N \tag{5.94}$$

with respect to $\mathbf{x}$. $g_i(\mathbf{x})$ therein are again yet not specified weighting functions. In doing so, we obtain the matrix equation

$$\mathbf{A}_{\partial\Gamma}^{(g,\psi_0)} = \mathbf{B}_{\partial\Gamma}^{(g,G_0\,\varphi_0)} \cdot \hat{\mathbf{W}}_{\partial\Gamma_+} \cdot \mathbf{C}_{\partial\Gamma}^{(\varphi_0^*,\psi_0)} \tag{5.95}$$

with matrix elements defined by the integral expressions

$$\left[A_{\partial\Gamma}^{(g,\psi_0)}\right]_{i,j} := \oint_{\partial\Gamma} g_i^*(\mathbf{x}) \cdot \psi_j(k_0, \mathbf{x})\, dS(\mathbf{x}) \tag{5.96}$$

$$\left[B_{\partial\Gamma}^{(g,G_0\,\varphi_0)}\right]_{i,j} := p.v. \oint_{\partial\Gamma} g_i^*(\mathbf{x}) \cdot G_0(\mathbf{x}, \bar{\mathbf{x}}) \cdot \varphi_j(k_0, \bar{\mathbf{x}})\, dS(\mathbf{x})\, dS(\bar{\mathbf{x}}) \tag{5.97}$$

$$\left[C_{\partial\Gamma}^{(\varphi_0^*,\psi_0)}\right]_{i,j} := \oint_{\partial\Gamma} \varphi_i(k_0, \tilde{\mathbf{x}}) \cdot \psi_j(k_0, \tilde{\mathbf{x}})\, dS(\tilde{\mathbf{x}}). \tag{5.98}$$

Thus we have finally

$$\hat{\mathbf{W}}_{\partial\Gamma_+} = \mathbf{B}_{\partial\Gamma}^{(g,G_0\,\varphi_0)^{-1}} \cdot \mathbf{A}_{\partial\Gamma}^{(g,\psi_0)} \cdot \mathbf{C}_{\partial\Gamma}^{(\varphi_0^*,\psi_0)^{-1}} \tag{5.99}$$

to calculate the elements $\left[\hat{W}_{\partial\Gamma_+}\right]_{k,l}$. This expression becomes especially simple if $g_i(\mathbf{x}) = \varphi_i^*(k_0, \mathbf{x})$ are chosen as weighting functions. Then

$$\mathbf{A}_{\partial\Gamma}^{(\varphi_0^*,\psi_0)} \cdot \mathbf{C}_{\partial\Gamma}^{(\varphi_0^*,\psi_0)^{-1}} = \mathbf{E} \tag{5.100}$$

holds and we have

$$\hat{\mathbf{W}}_{\partial\Gamma_+} = \mathbf{B}_{\partial\Gamma}^{(\varphi_0^*,G_0\,\varphi_0)^{-1}}. \tag{5.101}$$

If we now insert the elements $\left[\hat{W}_{\partial\Gamma_+}\right]_{k,l}$ into the bilinear expansion (5.91), and, moreover, this expansion into equation (5.79) we are able to calculate the Green function related to the outer Dirichlet problem at any observation point $\mathbf{x} \in \Gamma_+$. This raises the following question: What is the interrelation between the approximation of this Green function derived in Chaps. 3 and 4, respectively, in conjunction with the T-matrix and the approximation derived just now? Since, this question is strongly related to Rayleigh's hypothesis, we will shift it to the next chapter.

The way described above to derive the boundary integral equation related to the outer Dirichlet problem is not the usual way one can find in the relevant literature. It is more customary not to introduce an interaction operator but to employ the induced surface current as the unknown quantity. However, this at first glance not very important aspect has the consequence that the boundary integral equation methods are considered to be inappropriate if a certain scattering problem requires orientation averaging. This is because each new orientation of the scatterer in the primary incident field produces a new induced surface current, i.e., the induced surface current exhibits a crucial link to the primary incident field. This situation can be avoided if choosing the interaction operator as the unknown quantity in the boundary integral equation, as described above. To see this, we have to reveal the relation between the interaction operator and the induced surface current. Inserting (5.79) into (2.286) provides

$$u_t(\mathbf{x}) = u_{inc}(\mathbf{x}) + \oint_{\partial\Gamma} G_0(\mathbf{x}, \bar{\mathbf{x}}) \cdot \hat{W}_{\partial\Gamma_+}(\bar{\mathbf{x}}, \tilde{\mathbf{x}}) \cdot u_{inc}(\tilde{\mathbf{x}})\, dS(\bar{\mathbf{x}})\, dS(\tilde{\mathbf{x}}) \tag{5.102}$$

for the total field in the outer region Γ_+ if taking (2.271) into account (u_0 in (2.271) is just the primary incident field!). If defining the induced surface current $J_{\partial\Gamma}$ according to

$$J_{\partial\Gamma}(\bar{\mathbf{x}}) := \oint_{\partial\Gamma} \hat{W}_{\partial\Gamma_+}(\bar{\mathbf{x}}, \tilde{\mathbf{x}}) \cdot u_{inc}(\tilde{\mathbf{x}})\, dS(\tilde{\mathbf{x}}) \tag{5.103}$$

(5.102) may be rewritten into

$$u_t(\mathbf{x}) = u_{inc}(\mathbf{x}) + \oint_{\partial\Gamma} G_0(\mathbf{x}, \bar{\mathbf{x}}) \cdot J_{\partial\Gamma}(\bar{\mathbf{x}})\, dS(\bar{\mathbf{x}}). \tag{5.104}$$

Now, we can move again $\mathbf{x}$ in this equation toward the scatterer surface by taking the homogeneous Dirichlet condition into account. In this way we end up with the

known boundary integral equation

$$-u_{inc}(\mathbf{x}) = p.v. \oint_{\partial\Gamma} G_0(\mathbf{x}, \bar{\mathbf{x}}) \cdot J_{\partial\Gamma}(\bar{\mathbf{x}})\, dS(\bar{\mathbf{x}}); \quad \mathbf{x} \in \partial\Gamma \tag{5.105}$$

which allows us to calculate the unknown surface current related to the outer Dirichlet problem. It may be expanded, for example, in terms of the radiating solutions at the scatterer surface (but for the surface current we use a single expansion, and not a bilinear expansion, of course). The unknown expansion coefficients can be determined in the way described just now for the interaction operator. As it becomes obvious from definition (5.103) each new direction of incidence of the primary field results in a new surface current although the interaction operator is still the same. The decoupling of the primary incident field and the interaction operator is therefore an advantage of the latter quantity, and its practical implications should not be underestimated.

5.4.2 *Boundary Integral Equation Method Related to the Outer Transmission Problem*

To derive the corresponding boundary integral equations related to the outer transmission problem we have to deal first with the improper integral

$$\oint_{\partial\Gamma} \frac{\partial G_0(\mathbf{x}, \bar{\mathbf{x}})}{\partial \hat{n}_-} \cdot f(\bar{\mathbf{x}})\, dS(\bar{\mathbf{x}}); \quad \mathbf{x}, \bar{\mathbf{x}} \in \partial\Gamma. \tag{5.106}$$

This expression appears if $\mathbf{x}$ approaches point ($z = a$, $\theta = 0°$, $\phi = 0°$) of the surface patch $\partial\Gamma_\delta$. We have moreover to distinguish whether $\mathbf{x}$ approaches this point from the outer region Γ_+ or from the inner region Γ_- (see again Fig. 5.5). Equation (5.106) is a consequence of the transmission condition (2.282). As already done in the former subsection we replace the free-space Green function G_0 by the static approximation (5.86), and the function $f(\bar{\mathbf{x}})$ by its value $f(a)$ across the small surface patch $\partial\Gamma_\delta$. In this way, we obtain the approximate expression

$$\int_{\partial\Gamma_\delta} \frac{\partial G_0(\mathbf{x}, \bar{\mathbf{x}})}{\partial \hat{n}_-} \cdot f(\bar{\mathbf{x}})\, dS(\bar{\mathbf{x}}) \approx \frac{f(a)}{4\pi} \cdot \int_{\partial\Gamma_\delta} \frac{1}{\partial \hat{n}_-} \frac{1}{|\mathbf{x} - \bar{\mathbf{x}}|}\, dS(\bar{\mathbf{x}}). \tag{5.107}$$

The remaining integral on the right-hand side is nothing but the solid angle subtended by the surface element $dS(\bar{\mathbf{x}})$ (which is an infinitesimal part of $\partial\Gamma_\delta$) as seen from points $a \pm \epsilon$, respectively. Then, if we let $\epsilon \to 0$, this integral becomes simply $\pm 2\pi$. This value is independent of the form of $\partial\Gamma_\delta$. The positive sign applies if approaching point $r = a$ from region Γ_+, and the negative sign applies if coming from inside the scatterer. The improper integral (5.106) may be therefore represented by

$$\oint_{\partial\Gamma} \frac{\partial G_0(\mathbf{x},\bar{\mathbf{x}})}{\partial \hat{n}_-} \cdot f(\bar{\mathbf{x}})\, dS(\bar{\mathbf{x}}) = \pm\frac{f(\mathbf{x})}{2} + p.v. \oint_{\partial\Gamma} \frac{\partial G_0(\mathbf{x},\bar{\mathbf{x}})}{\partial \hat{n}_-} \cdot f(\bar{\mathbf{x}})\, dS(\bar{\mathbf{x}}) \tag{5.108}$$

with the principal value according to (5.82), and $\mathbf{x}$ located at the outer side (this corresponds to the positive sign!) or inner side (this corresponds to the negative sign!) of the scatterer surface. Now, we can derive the relevant boundary integral equations related to the outer transmission problem.

In close analogy to (5.79) of the outer Dirichlet problem we first introduce the two interaction operators $\hat{W}^{(d)}_{\partial\Gamma_+}$ and $\hat{W}^{(d)}_{\partial\Gamma_-}$ needed for the outer transmission problem by the definitions

$$G^{(d)}_{\Gamma_+}(\mathbf{x},\mathbf{x}') := G_0(\mathbf{x},\mathbf{x}') + \oint_{\partial\Gamma} G_0(\mathbf{x},\bar{\mathbf{x}})\, \hat{W}^{(d)}_{\partial\Gamma_+}(\bar{\mathbf{x}},\tilde{\mathbf{x}})\, G_0(\tilde{\mathbf{x}},\mathbf{x}')\, dS(\bar{\mathbf{x}})\, dS(\tilde{\mathbf{x}}) \tag{5.109}$$

and

$$G^{(-/+)}(\mathbf{x},\mathbf{x}') := \oint_{\partial\Gamma} G_{0_s}(\mathbf{x},\bar{\mathbf{x}})\, \hat{W}^{(d)}_{\partial\Gamma_-}(\bar{\mathbf{x}},\tilde{\mathbf{x}})\, G_0(\tilde{\mathbf{x}},\mathbf{x}')\, dS(\bar{\mathbf{x}})\, dS(\tilde{\mathbf{x}}). \tag{5.110}$$

These definitions differ again from the definitions (4.12) and (4.13) in using $G_0(\mathbf{x},\bar{\mathbf{x}})$ and $G_{0_s}(\mathbf{x},\bar{\mathbf{x}})$ instead of $G_0^{>}(\mathbf{x},\bar{\mathbf{x}})$ and $G_{0_s}^{<}(\mathbf{x},\bar{\mathbf{x}})$. If the observation point $\mathbf{x}$ approaches the scatterer surface $\partial\Gamma$ then the transmission conditions (2.281) and (2.282) as well as relations (5.84) and (5.108) result in the two boundary integral equations

$$\begin{aligned} G_0(\mathbf{x},\mathbf{x}') + p.v. \oint_{\partial\Gamma} G_0(\mathbf{x},\bar{\mathbf{x}})\, \hat{W}^{(d)}_{\partial\Gamma_+}(\bar{\mathbf{x}},\tilde{\mathbf{x}})\, G_0(\tilde{\mathbf{x}},\mathbf{x}')\, dS(\bar{\mathbf{x}})\, dS(\tilde{\mathbf{x}}) \\ = p.v. \oint_{\partial\Gamma} G_{0_s}(\mathbf{x},\bar{\mathbf{x}})\, \hat{W}^{(d)}_{\partial\Gamma_-}(\bar{\mathbf{x}},\tilde{\mathbf{x}})\, G_0(\tilde{\mathbf{x}},\mathbf{x}')\, dS(\bar{\mathbf{x}})\, dS(\tilde{\mathbf{x}}) \end{aligned} \tag{5.111}$$

and

$$\begin{aligned} \partial_{\hat{n}_-} G_0(\mathbf{x},\mathbf{x}') + \frac{1}{2}\cdot \oint_{\partial\Gamma} \hat{W}^{(d)}_{\partial\Gamma_+}(\mathbf{x},\tilde{\mathbf{x}})\, G_0(\tilde{\mathbf{x}},\mathbf{x}')\, dS(\tilde{\mathbf{x}}) \\ + p.v. \oint_{\partial\Gamma} \partial_{\hat{n}_-} G_0(\mathbf{x},\bar{\mathbf{x}})\, \hat{W}^{(d)}_{\partial\Gamma_+}(\bar{\mathbf{x}},\tilde{\mathbf{x}})\, G_0(\tilde{\mathbf{x}},\mathbf{x}')\, dS(\bar{\mathbf{x}})\, dS(\tilde{\mathbf{x}}) \\ = -\frac{1}{2}\cdot \oint_{\partial\Gamma} \hat{W}^{(d)}_{\partial\Gamma_-}(\mathbf{x},\tilde{\mathbf{x}})\, G_0(\tilde{\mathbf{x}},\mathbf{x}')\, dS(\tilde{\mathbf{x}}) \\ + p.v. \oint_{\partial\Gamma} \partial_{\hat{n}_-} G_{0_s}(\mathbf{x},\bar{\mathbf{x}})\, \hat{W}^{(d)}_{\partial\Gamma_-}(\bar{\mathbf{x}},\tilde{\mathbf{x}})\, G_0(\tilde{\mathbf{x}},\mathbf{x}')\, dS(\bar{\mathbf{x}})\, dS(\tilde{\mathbf{x}}). \end{aligned} \tag{5.112}$$

Here, we used the abbreviation

$$\partial_{\hat{n}_-} G(\mathbf{x},\mathbf{x}') := \hat{n}_- \cdot \nabla_{\mathbf{x}} G(\mathbf{x},\mathbf{x}'). \tag{5.113}$$

If employing again a bilinear expansion for both interaction operators $\hat{W}^{(d)}_{\partial\Gamma_+}$ and $\hat{W}^{(d)}_{\partial\Gamma_-}$ we can proceed exactly in the same way as already done in the case of the outer Dirichlet problem. But now we have two equations from which we can determine $\hat{W}^{(d)}_{\partial\Gamma_+}$ needed to calculate $G^{(d)}_{\Gamma_+}$. Once we know $G^{(d)}_{\Gamma_+}$ we can calculate the total field outside the scatterer. Moreover, with the definitions

$$J^{(+)}_{\partial\Gamma}(\bar{\mathbf{x}}) := \oint_{\partial\Gamma} \hat{W}^{(d)}_{\partial\Gamma_+}(\bar{\mathbf{x}}, \tilde{\mathbf{x}}) \cdot u_{inc}(\tilde{\mathbf{x}})\, dS(\tilde{\mathbf{x}}) \tag{5.114}$$

and

$$J^{(-)}_{\partial\Gamma}(\bar{\mathbf{x}}) := \oint_{\partial\Gamma} \hat{W}^{(d)}_{\partial\Gamma_-}(\bar{\mathbf{x}}, \tilde{\mathbf{x}}) \cdot u_{inc}(\tilde{\mathbf{x}})\, dS(\tilde{\mathbf{x}}) \tag{5.115}$$

we are again able to derive the conventional boundary integral equations of the outer transmission problem. For this we have to multiply (5.111) and (5.112) with the source distribution $\rho(\mathbf{x}')$ (where it is again assumed that $\rho(\mathbf{x}')$ is located somewhere outside the smallest sphere circumscribing the scatterer) and have to integrate over Γ_+. Thus, we get the boundary integral equations

$$\begin{aligned} u_{inc}(\mathbf{x}) + p.v. \oint_{\partial\Gamma} G_0(\mathbf{x}, \bar{\mathbf{x}})\, J^{(+)}_{\partial\Gamma}(\bar{\mathbf{x}})\, dS(\bar{\mathbf{x}}) \\ = p.v. \oint_{\partial\Gamma} G_{0_s}(\mathbf{x}, \bar{\mathbf{x}})\, J^{(-)}_{\partial\Gamma}(\bar{\mathbf{x}})\, dS(\bar{\mathbf{x}}) \end{aligned} \tag{5.116}$$

and

$$\begin{aligned} \partial_{\hat{n}_-} u_{inc}(\mathbf{x}) + \frac{1}{2} \cdot J^{(+)}_{\partial\Gamma}(\mathbf{x}) + p.v. \oint_{\partial\Gamma} \partial_{\hat{n}_-} G_0(\mathbf{x}, \bar{\mathbf{x}})\, J^{(+)}_{\partial\Gamma}(\bar{\mathbf{x}})\, dS(\bar{\mathbf{x}}) \\ = -\frac{1}{2} \cdot J^{(-)}_{\partial\Gamma}(\mathbf{x}) + p.v. \oint_{\partial\Gamma} \partial_{\hat{n}_-} G_{0_s}(\mathbf{x}, \bar{\mathbf{x}})\, J^{(-)}_{\partial\Gamma}(\bar{\mathbf{x}})\, dS(\bar{\mathbf{x}}), \end{aligned} \tag{5.117}$$

from which we can calculate the two induced surface currents $J^{(+)}_{\partial\Gamma}$ and $J^{(-)}_{\partial\Gamma}$. But for the scattered field u_s in Γ_+ we need only the surface current $J^{(+)}_{\partial\Gamma}$.

5.4.3 *Volume Integral Equation Method Related to the Outer Transmission Problem*

Alternatively, we can solve the outer transmission problem by appropriate volume integral equations. To derive these equations we have to juggle again with Green's theorem (2.239). We apply it with the two quantities

$$\Psi(\mathbf{x}) = G^{(d)}_{\Gamma_+}(\mathbf{x}, \mathbf{x}'); \quad \mathbf{x}, \mathbf{x}' \in \Gamma_+ \tag{5.118}$$

$$\Phi(\mathbf{x}) = G_0(\mathbf{x}, \mathbf{x}''); \quad \mathbf{x} \in \Gamma_+. \tag{5.119}$$

Concerning the location of the source point $\mathbf{x}''$ we have to distinguish two cases. The source point may be located either in the outer region Γ_+ (case 1a) or somewhere inside Γ_- (case 1b). In the former case, the free-space Green function G_0 solves the inhomogeneous Helmholtz equation (2.241) in Γ_+. But in the latter case, it is a solution of the homogeneous Helmholtz equation within Γ_+. From Green's theorem it follows for each of these cases:

case 1a:

$$G^{(d)}_{\Gamma_+}(\mathbf{x}'', \mathbf{x}') = G_0(\mathbf{x}', \mathbf{x}'') + \oint_{\partial\Gamma} \left[G_0(\mathbf{x}, \mathbf{x}'') \cdot \frac{\partial G^{(d)}_{\Gamma_+}(\mathbf{x}, \mathbf{x}')}{\partial \hat{n}_-} - G^{(d)}_{\Gamma_+}(\mathbf{x}, \mathbf{x}') \cdot \frac{\partial G_0(\mathbf{x}, \mathbf{x}'')}{\partial \hat{n}_-} \right] dS(\mathbf{x}). \tag{5.120}$$

case 1b:

$$G_0(\mathbf{x}'', \mathbf{x}') = -\oint_{\partial\Gamma} \left[G_0(\mathbf{x}'', \mathbf{x}) \cdot \frac{\partial G^{(d)}_{\Gamma_+}(\mathbf{x}, \mathbf{x}')}{\partial \hat{n}_-} - G^{(d)}_{\Gamma_+}(\mathbf{x}, \mathbf{x}') \cdot \frac{\partial G_0(\mathbf{x}'', \mathbf{x})}{\partial \hat{n}_-} \right] dS(\mathbf{x}). \tag{5.121}$$

In the next step we apply Green's theorem with the two quantities

$$\Psi(\mathbf{x}) = G^{(-/+)}(\mathbf{x}, \mathbf{x}'); \quad \mathbf{x} \in \Gamma_-; \ \mathbf{x}' \in \Gamma_+ \tag{5.122}$$

$$\Phi(\mathbf{x}) = G_0(\mathbf{x}, \mathbf{x}''); \quad \mathbf{x} \in \Gamma_- \tag{5.123}$$

inside the scatterer. Here we have again to distinguish the two cases $\mathbf{x}'' \in \Gamma_+$ (case 2a) and $\mathbf{x}'' \in \Gamma_-$ (case 2b). $G^{(-/+)}$ solves the homogeneous Helmholtz equation (2.283) in both cases. This results into

case 2a:

$$\kappa_d^2 \int_{\Gamma_-} G_0(\mathbf{x}, \mathbf{x}'') \cdot G^{(-/+)}(\mathbf{x}, \mathbf{x}')\, dV(\mathbf{x}) = \oint_{\partial\Gamma} \left[G_0(\mathbf{x}, \mathbf{x}'') \cdot \frac{\partial G^{(-/+)}(\mathbf{x}, \mathbf{x}')}{\partial \hat{n}_-} - G^{(-/+)}(\mathbf{x}, \mathbf{x}') \cdot \frac{\partial G_0(\mathbf{x}, \mathbf{x}'')}{\partial \hat{n}_-} \right] dS(\mathbf{x}). \tag{5.124}$$

case 2b:

$$-G^{(-/+)}(\mathbf{x}'',\mathbf{x}')+\kappa_d^2\int_{\Gamma_-}G_0(\mathbf{x},\mathbf{x}'')\cdot G^{(-/+)}(\mathbf{x},\mathbf{x}')\,dV(\mathbf{x})$$
$$=\oint_{\partial\Gamma}\left[G_0(\mathbf{x},\mathbf{x}'')\cdot\frac{\partial G^{(-/+)}(\mathbf{x},\mathbf{x}')}{\partial\hat{n}_-}-G^{(-/+)}(\mathbf{x},\mathbf{x}')\cdot\frac{\partial G_0(\mathbf{x},\mathbf{x}'')}{\partial\hat{n}_-}\right]dS(\mathbf{x}). \tag{5.125}$$

κ_d^2 therein is given by

$$\kappa_d^2=k^2-k_0^2. \tag{5.126}$$

Next, we combine the two cases 1a and 2a as well as 1b and 2b. The results are

$$G_{\Gamma_+}^{(d)}(\mathbf{x},\mathbf{x}')=G_0(\mathbf{x},\mathbf{x}')+\kappa_d^2\int_{\Gamma_-}G_0(\mathbf{x},\bar{\mathbf{x}})\cdot G^{(-/+)}(\bar{\mathbf{x}},\mathbf{x}')\,dV(\bar{\mathbf{x}})$$
$$\mathbf{x},\mathbf{x}'\in\Gamma_+ \tag{5.127}$$

and

$$G^{(-/+)}(\mathbf{x},\mathbf{x}')=G_0(\mathbf{x},\mathbf{x}')+\kappa_d^2\int_{\Gamma_-}G_0(\mathbf{x},\bar{\mathbf{x}})\cdot G^{(-/+)}(\bar{\mathbf{x}},\mathbf{x}')\,dV(\bar{\mathbf{x}})$$
$$\mathbf{x}'\in\Gamma_+,\mathbf{x}\in\Gamma_-. \tag{5.128}$$

In deriving these two equations we have to take the transmission conditions (2.281)/(2.282) into account, to rename $\mathbf{x}$ as $\bar{\mathbf{x}}$ and $\mathbf{x}''$ as $\mathbf{x}$, and to consider the symmetry relation (2.245) of G_0. These are the relevant volume integral equations we were looking for. Once we have calculated $G^{(-/+)}(\mathbf{x},\mathbf{x}')$ from (5.128) (if using again a bilinear expansion for this Green function, for example) we are then able to calculate $G_{\Gamma_+}^{(d)}(\mathbf{x},\mathbf{x}')$ from (5.127). In the process of solving (5.128) the singularity of G_0 at point $\mathbf{x}=\bar{\mathbf{x}}$ inside the scatterer deserves some attention. But due to the weak singularity of the scalar free-space Green function this is not too difficult. The integration may be performed in the sense of the principal value discussed in the context of the boundary integral equations. We just have to exclude a small volume element Γ_δ enclosing the singular point from the integration,

$$G^{(-/+)}(\mathbf{x},\mathbf{x}')=G_0(\mathbf{x},\mathbf{x}')$$
$$+\lim_{\Gamma_\delta\to 0}\kappa_d^2\int_{\Gamma_--\Gamma_\delta}G_0(\mathbf{x},\bar{\mathbf{x}})\cdot G^{(-/+)}(\bar{\mathbf{x}},\mathbf{x}')\,dV(\bar{\mathbf{x}});$$
$$\mathbf{x}'\in\Gamma_+\ ,\ \mathbf{x}\in\Gamma_-. \tag{5.129}$$

with the definition

$$G^{(d)}_{\Gamma_+}(\mathbf{x},\mathbf{x}') := G_0(\mathbf{x},\mathbf{x}') + \int_{\Gamma_-} G_0(\mathbf{x},\bar{\mathbf{x}})\, \hat{W}^{(d)}_{\Gamma_-}(\bar{\mathbf{x}},\tilde{\mathbf{x}})\, G_0(\tilde{\mathbf{x}},\mathbf{x}')\, dV(\bar{\mathbf{x}})\, dV(\tilde{\mathbf{x}}) \tag{5.130}$$

of the corresponding interaction operator $\hat{W}^{(d)}_{\Gamma_-}$ (which describes now the interaction of the primary incident field with the whole scattering volume!) we obtain after intercomparison with (5.127) the relation

$$\kappa_d^2\, G^{(-/+)}(\bar{\mathbf{x}},\mathbf{x}') = \int_{\Gamma_-} \hat{W}^{(d)}_{\Gamma_-}(\bar{\mathbf{x}},\tilde{\mathbf{x}}) \cdot G_0(\tilde{\mathbf{x}},\mathbf{x}')\, dV(\tilde{\mathbf{x}}). \tag{5.131}$$

The following statement seems to be appropriate at this point: It seems as if the difference of definition (5.130) compared to the definition (4.12) used in Sect. 4.2.2 to solve the outer transmission problem consists not only in the replacement of $G_0^>$ by the full free-space Green function G_0 but also by performing a volume integration over the scatterer volume instead of the boundary integration over its surface. However, the usage of the definitions

$$G^{(d)}_{\Gamma_+}(\mathbf{x},\mathbf{x}') := G_0(\mathbf{x},\mathbf{x}') + \int_{\Gamma_-} G_0^>(\mathbf{x},\bar{\mathbf{x}}) \cdot W^{(d)}_{\Gamma_+}(\bar{\mathbf{x}},\tilde{\mathbf{x}}) \cdot G_0(\tilde{\mathbf{x}},\mathbf{x}')\, dV(\bar{\mathbf{x}})\, dV(\tilde{\mathbf{x}}) \tag{5.132}$$

and

$$G^{(-/+)}(\mathbf{x},\mathbf{x}') := \int_{\Gamma_-} G_{0_s}^<(\mathbf{x},\bar{\mathbf{x}})\, W^{(d)}_{\Gamma_-}(\bar{\mathbf{x}},\tilde{\mathbf{x}})\, G_0(\tilde{\mathbf{x}},\mathbf{x}')\, dV(\bar{\mathbf{x}})\, dV(\tilde{\mathbf{x}}) \tag{5.133}$$

instead of definitions (4.12) and (4.13) would not change the result obtained in Sect. 4.2.2. That is because the change of the definitions affects only the corresponding definitions (4.17) and (4.18) of the matrix elements of the relevant interaction operators. This change would therefore result into

$$\left[W^{(d)}_{\Gamma_+}\right]_{i,k} := (ik_0) \int_{\Gamma_-} \tilde{\psi}_i(k_0,\bar{\mathbf{x}})\, W^{(d)}_{\Gamma_+}(\bar{\mathbf{x}},\tilde{\mathbf{x}})\, \psi_k(k_0,\tilde{\mathbf{x}})\, dV(\bar{\mathbf{x}})\, dV(\tilde{\mathbf{x}}) \tag{5.134}$$

and

$$\left[W^{(d)}_{\Gamma_-}\right]_{i,k} := (ik) \int_{\Gamma_-} \tilde{\varphi}_i(k_0,\bar{\mathbf{x}})\, W^{(d)}_{\Gamma_-}(\bar{\mathbf{x}},\tilde{\mathbf{x}})\, \psi_k(k_0,\tilde{\mathbf{x}})\, dV(\bar{\mathbf{x}})\, dV(\tilde{\mathbf{x}}). \tag{5.135}$$

It is then not difficult to convince oneself that expression (4.22) derived in Sect. 4.2.2 holds also for the new matrix elements $\left[W^{(d)}_{\Gamma_+}\right]_{i,k}$.

If we now replace $G^{(-/+)}$ on the left-hand side of Eq. (5.131) by expression (5.128) and apply again (5.131) afterwards we end up with the volume integral equation

$$\hat{W}^{(d)}_{\Gamma_-}(\bar{\mathbf{x}},\tilde{\mathbf{x}}) = \kappa_d^2 \cdot \left[\delta(\bar{\mathbf{x}}-\tilde{\mathbf{x}}) + \int_{\Gamma_-} G_0(\bar{\mathbf{x}},\hat{\mathbf{x}}) \cdot \hat{W}^{(d)}_{\Gamma_-}(\hat{\mathbf{x}},\tilde{\mathbf{x}})\, dV(\hat{\mathbf{x}})\right] \tag{5.136}$$

of the interaction operator $\hat{W}^{(d)}_{\Gamma_-}$ which is equivalent to (5.128). This type of equation is called a "Lippmann-Schwinger" equation. They are of our interest in the next section. But we can also define the equivalent volume current inside the scatterer via the definition

$$J_{\Gamma_-}(\mathbf{x}) := \int_{\Gamma_-} \hat{W}^{(d)}_{\Gamma_-}(\mathbf{x},\tilde{\mathbf{x}}) \cdot u_{inc}(\tilde{\mathbf{x}})\, dV(\tilde{\mathbf{x}}). \tag{5.137}$$

Then, the total field outside the scatterer reads because of (2.286) and (5.130)

$$u_t(\mathbf{x}) = u_{inc}(\mathbf{x}) + \int_{\Gamma_-} G_0(\mathbf{x},\bar{\mathbf{x}}) \cdot J_{\Gamma_-}(\bar{\mathbf{x}})\, dV(\bar{\mathbf{x}}). \tag{5.138}$$

If we multiply (5.136) with the primary incident field u_{inc} and integrate the resulting equation over the volume of the scatterer subsequently we get the known volume integral equation

$$J_{\Gamma_-}(\mathbf{x}) = \kappa_d^2 \cdot \left[u_{inc}(\mathbf{x}) + \int_{\Gamma_-} G_0(\mathbf{x},\bar{\mathbf{x}}) \cdot J_{\Gamma_-}(\bar{\mathbf{x}})\, dV(\bar{\mathbf{x}})\right] \tag{5.139}$$

from which we can calculate the equivalent volume current inside the scatterer.

5.5 Lippmann-Schwinger Equations

5.5.1 The Scalar Problem

Equation (5.130) provides already an appropriate starting point to solve the outer transmission problem iteratively. Its lowest order iteration is of course given by

$$\left[G^{(d)}_{\Gamma_+}(\mathbf{x},\mathbf{x}')\right]^{(0)} = G_0(\mathbf{x},\mathbf{x}') \tag{5.140}$$

and represents nothing but the unperturbed problem, i.e., the Green function in the absence of any scatterer. The first iteration which takes the existence of a scatterer into account can then be calculated from the lowest order iteration

$$\left[\hat{W}^{(d)}_{\Gamma_-}(\bar{\mathbf{x}},\tilde{\mathbf{x}})\right]^{(1)} = \kappa_d^2\, \delta(\bar{\mathbf{x}}-\tilde{\mathbf{x}}) \tag{5.141}$$

of the Lippmann-Schwinger equation (5.136) of the related interaction operator. The result is

$$\left[G_{\Gamma_+}^{(d)}(\mathbf{x},\mathbf{x}')\right]^{(1)} = G_0(\mathbf{x},\mathbf{x}') + \kappa_d^2 \cdot \int_{\Gamma_-} G_0(\mathbf{x},\bar{\mathbf{x}}) \cdot G_0(\bar{\mathbf{x}},\mathbf{x}')\, dV(\bar{\mathbf{x}}). \quad (5.142)$$

The corresponding iteration of the Green function $G^{(-/+)}$ becomes

$$\left[G^{(-/+)}(\mathbf{x},\mathbf{x}')\right]^{(1)} = G_0(\mathbf{x},\mathbf{x}') \quad (5.143)$$

because of (5.131). This iteration procedure can be continued indefinitely. At all higher iterations we have to consider carefully the singularity of the free-space Green function in the integral terms. But then it becomes questionable whether higher order iterations are of benefit compared with the non-iterative solution of (5.136). In most of its applications the iteration procedure is therefore restricted to the first iteration (5.142), or at most to the second one. The required transmission conditions are obviously not fulfilled in these cases. Therefore, using the iterative solutions makes only sense if the scatterer affects only slightly the unperturbed problem. What exactly do we mean by "slightly" depends "strongly" on the problem under consideration and cannot be defined in advance.

We are now interested to derive the Lippmann-Schwinger equations of the Green function and the interaction operator related to the outer Dirichlet problem. For this we have to go back to (3.27) which reads in more detail

$$G_{\Gamma_+}(\mathbf{x},\mathbf{x}') = G_0(\mathbf{x},\mathbf{x}') + \oint_{\partial\Gamma} G_0(\mathbf{x},\bar{\mathbf{x}}) \cdot \hat{\bar{n}}_- \cdot \nabla_{\bar{x}}\, G_{\Gamma_+}(\bar{\mathbf{x}},\mathbf{x}')\, dS(\bar{\mathbf{x}}), \quad (5.144)$$

if making use of the symmetry relation (2.245) and the definition (3.22) of the surface Green function related to G_{Γ_+}. It should be emphasized that the homogeneous Dirichlet condition (2.280) at the scatterer surface was already incorporated in deriving (3.27). Now, if employing the scalar delta distribution at the scatterer surface defined in (3.6), we can "inflate" (5.144) identical into

$$G_{\Gamma_+}(\mathbf{x},\mathbf{x}') = G_0(\mathbf{x},\mathbf{x}') + \oint_{\partial\Gamma} G_0(\mathbf{x},\bar{\mathbf{x}}) \cdot \delta_{\partial\Gamma}(\tilde{\mathbf{x}}-\bar{\mathbf{x}}) \cdot \hat{\tilde{n}}_- \cdot \nabla_{\tilde{x}}\, G_{\Gamma_+}(\tilde{\mathbf{x}},\mathbf{x}')\, dS(\tilde{\mathbf{x}})\, dS(\bar{\mathbf{x}}). \quad (5.145)$$

with the definition of the operator

$$U_{\partial\Gamma}(\bar{\mathbf{x}},\tilde{\mathbf{x}}) := \delta_{\partial\Gamma}(\tilde{\mathbf{x}}-\bar{\mathbf{x}}) \cdot \hat{\tilde{n}}_- \cdot \nabla_{\tilde{x}} \quad (5.146)$$

we can thus write

$$G_{\Gamma_+}(\mathbf{x},\mathbf{x}') = G_0(\mathbf{x},\mathbf{x}') + \oint_{\partial\Gamma} G_0(\mathbf{x},\bar{\mathbf{x}}) \cdot U_{\partial\Gamma}(\bar{\mathbf{x}},\tilde{\mathbf{x}}) \cdot G_{\Gamma_+}(\tilde{\mathbf{x}},\mathbf{x}')\, dS(\tilde{\mathbf{x}})\, dS(\bar{\mathbf{x}}) \tag{5.147}$$

instead of (3.27). Please, note that the product $U_{\partial\Gamma} \cdot G_{\Gamma_+}$ on the right-hand side of this equation does not mean the conventional product of two functions but the application of the operator $U_{\partial\Gamma}$ to the function which follows this operator (G_{Γ_+} in our case). As a consequence, we can not change its position under the integral sign. The shortened operator notation of (5.147) reads

$$G_{\Gamma_+}(\mathbf{x},\mathbf{x}') = G_0(\mathbf{x},\mathbf{x}') + G_0(\mathbf{x},\bar{\mathbf{x}}) \circ U_{\partial\Gamma}(\bar{\mathbf{x}},\tilde{\mathbf{x}}) \circ G_{\Gamma_+}(\tilde{\mathbf{x}},\mathbf{x}') \tag{5.148}$$

where we have to integrate according to $\oint_{\partial\Gamma} \cdots dS$ over variables which appear twice. Equation (5.147) or (5.148) represents the Lippmann-Schwinger equation of the Green function G_{Γ_+} related to the outer Dirichlet problem. Its lowest order iteration (the unperturbed problem) is again given by

$$G^{(0)}_{\Gamma_+}(\mathbf{x},\mathbf{x}') = G_0(\mathbf{x},\mathbf{x}'). \tag{5.149}$$

Its next iteration

$$G^{(1)}_{\Gamma_+}(\mathbf{x},\mathbf{x}') = G_0(\mathbf{x},\mathbf{x}') + G_0(\mathbf{x},\bar{\mathbf{x}}) \circ U_{\partial\Gamma}(\bar{\mathbf{x}},\tilde{\mathbf{x}}) \circ G_0(\tilde{\mathbf{x}},\mathbf{x}') \tag{5.150}$$

or, more precisely,

$$\begin{aligned} G^{(1)}_{\Gamma_+}(\mathbf{x},\mathbf{x}') &= G_0(\mathbf{x},\mathbf{x}') \\ &\quad + \oint_{\partial\Gamma} G_0(\mathbf{x},\bar{\mathbf{x}}) \cdot U_{\partial\Gamma}(\bar{\mathbf{x}},\tilde{\mathbf{x}}) \cdot G_0(\tilde{\mathbf{x}},\mathbf{x}')\, dS(\tilde{\mathbf{x}})\, dS(\bar{\mathbf{x}}) \\ &= G_0(\mathbf{x},\mathbf{x}') + \oint_{\partial\Gamma} G_0(\mathbf{x},\bar{\mathbf{x}}) \cdot \hat{\bar{n}}_- \cdot \nabla_{\bar{x}}\, G_0(\bar{\mathbf{x}},\mathbf{x}')\, dS(\bar{\mathbf{x}}) \end{aligned} \tag{5.151}$$

considers already the existence of the scatterer. Here it holds also that all higher iterations become affected by the singularity of the free-space Green function. This can be easily seen if replacing G_{Γ_+} on the right-hand side of (5.148) by its iteration (5.150)/(5.151).

To derive the equivalent Lippmann-Schwinger equation of the interaction operator we remember the definition (5.79) which reads in operator notation

$$G_{\Gamma_+}(\mathbf{x},\mathbf{x}') := G_0(\mathbf{x},\mathbf{x}') + G_0(\mathbf{x},\bar{\mathbf{x}}) \circ \hat{W}_{\partial\Gamma_+}(\bar{\mathbf{x}},\tilde{\mathbf{x}}) \circ G_0(\tilde{\mathbf{x}},\mathbf{x}'). \tag{5.152}$$

Comparing this with expression (5.148) provides

$$G_0(\mathbf{x},\bar{\mathbf{x}})\circ U_{\partial\Gamma}(\bar{\mathbf{x}},\tilde{\mathbf{x}})\circ G_{\Gamma_+}(\tilde{\mathbf{x}},\mathbf{x}') = G_0(\mathbf{x},\bar{\mathbf{x}})\circ \hat{W}_{\partial\Gamma_+}(\bar{\mathbf{x}},\tilde{\mathbf{x}})\circ G_0(\tilde{\mathbf{x}},\mathbf{x}'). \quad (5.153)$$

Replacing G_{Γ_+} on the left-hand side again by its definition (5.152) provides the Lippmann-Schwinger equation

$$\hat{W}_{\partial\Gamma_+}(\mathbf{x},\mathbf{x}') = U_{\partial\Gamma}(\mathbf{x},\mathbf{x}') + U_{\partial\Gamma}(\mathbf{x},\bar{\mathbf{x}})\circ G_0(\bar{\mathbf{x}},\tilde{\mathbf{x}})\circ \hat{W}_{\partial\Gamma_+}(\tilde{\mathbf{x}},\mathbf{x}') \quad (5.154)$$

of the interaction operator related to the outer Dirichlet problem we were looking for. If its lowest order iteration

$$\hat{W}^{(1)}_{\partial\Gamma_+}(\mathbf{x},\mathbf{x}') = U_{\partial\Gamma}(\mathbf{x},\mathbf{x}'). \quad (5.155)$$

is inserted into (5.152) we obtain again the first iteration (5.151) of the Green function.

5.5.2 The Dyadic Problem

We proceed in close analogy to the scalar case but with the difference that we have to apply now the dyadic-dyadic Green theorem (2.319) in the respective regions. Let us start with the outer transmission problem. From the application of (2.319) in Γ_+ with the two dyadics

$$\mathbf{Q}(\mathbf{x},\mathbf{x}'') = \mathbf{G_0}(\mathbf{x},\mathbf{x}''); \quad \mathbf{x}\in\Gamma_+ \quad (5.156)$$

$$\mathbf{P}(\mathbf{x},\mathbf{x}') = \mathbf{G}^{(\mathbf{d})}_{\mathbf{\Gamma}_+}(\mathbf{x},\mathbf{x}'); \quad \mathbf{x},\mathbf{x}'\in\Gamma_+ \quad (5.157)$$

where we have again to distinguish between the two cases $\mathbf{x}''\in\Gamma_+$ (case 1a) and $\mathbf{x}''\in\Gamma_-$ (case 1b), and, on the other hand, from the application in Γ_- with the two dyadics

$$\mathbf{Q}(\mathbf{x},\mathbf{x}'') = \mathbf{G_0}(\mathbf{x},\mathbf{x}''); \quad \mathbf{x}\in\Gamma_+ \quad (5.158)$$

$$\mathbf{P}(\mathbf{x},\mathbf{x}') = \mathbf{G}^{(-/+)}(\mathbf{x},\mathbf{x}'); \quad \mathbf{x}\in\Gamma_-\,,\ \mathbf{x}'\in\Gamma_+ \quad (5.159)$$

and $\mathbf{x}''\in\Gamma_+$ (case 2a) or $\mathbf{x}''\in\Gamma_-$ (case 2b) we obtain from the transmission conditions (2.343) and (2.344) the two equations

$$\mathbf{G}^{(\mathbf{d})}_{\mathbf{\Gamma}_+}(\mathbf{x},\mathbf{x}') = \mathbf{G_0}(\mathbf{x},\mathbf{x}') + \kappa_d^2\int_{\mathbf{\Gamma}_-}\mathbf{G_0}(\mathbf{x},\bar{\mathbf{x}})\cdot\mathbf{G}^{(-/+)}(\bar{\mathbf{x}},\mathbf{x}')\,dV(\bar{\mathbf{x}})$$
$$\mathbf{x},\mathbf{x}'\in\Gamma_+ \quad (5.160)$$

and

$$\mathbf{G}^{(-/+)}(\mathbf{x},\mathbf{x}') = \mathbf{G_0}(\mathbf{x},\mathbf{x}') + \kappa_d^2 \int_{\mathbf{\Gamma}_-} \mathbf{G_0}(\mathbf{x},\bar{\mathbf{x}}) \cdot \mathbf{G}^{(-/+)}(\bar{\mathbf{x}},\mathbf{x}')\, dV(\bar{\mathbf{x}})$$
$$\mathbf{x}' \in \Gamma_+, \mathbf{x} \in \Gamma_-. \tag{5.161}$$

This is the dyadic analogue to the scalar case. The interim results are omitted here because the derivation runs along the same track as in the scalar case. With the definition

$$\mathbf{G}^{(\mathbf{d})}_{\mathbf{\Gamma}_+}(\mathbf{x},\mathbf{x}') := \mathbf{G_0}(\mathbf{x},\mathbf{x}') + \int_{\mathbf{\Gamma}_-} \mathbf{G_0}(\mathbf{x},\bar{\mathbf{x}})\, \hat{\mathbf{W}}^{(d)}_{\mathbf{\Gamma}_-}(\bar{\mathbf{x}},\tilde{\mathbf{x}})\, \mathbf{G_0}(\tilde{\mathbf{x}},\mathbf{x}')\, dV(\bar{\mathbf{x}})\, dV(\tilde{\mathbf{x}}) \tag{5.162}$$

we thus obtain

$$\hat{\mathbf{W}}^{(d)}_{\mathbf{\Gamma}_-}(\bar{\mathbf{x}},\tilde{\mathbf{x}}) = \kappa_d^2 \cdot \left[\mathbf{I}\delta(\bar{\mathbf{x}}-\tilde{\mathbf{x}}) + \int_{\mathbf{\Gamma}_-} \mathbf{G_0}(\bar{\mathbf{x}},\hat{\mathbf{x}}) \cdot \hat{\mathbf{W}}^{(d)}_{\mathbf{\Gamma}_-}(\hat{\mathbf{x}},\tilde{\mathbf{x}})\, dV(\hat{\mathbf{x}}) \right] \tag{5.163}$$

as the Lippmann-Schwinger equation of the dyadic interaction operator of the outer transmission problem. It is the analogue of the scalar equation (5.136). Its lowest order iteration, if inserted into (5.162), provides again the first iteration of $\mathbf{G}_{\mathbf{\Gamma}_+}(\mathbf{x},\mathbf{x}')$ which takes the existence of the scatterer into account. All higher iterations have to consider carefully the (now strong!) singularity of $\mathbf{G_0}$ inside the scatterer.

The treatment of the outer Dirichlet problem in the dyadic case is also quite similar to the scalar case. By use of (2.329) and identity (2.312) we can rewrite (3.80) into

$$\mathbf{G}_{\mathbf{\Gamma}_+}(\mathbf{x},\mathbf{x}') = \mathbf{G_0}(\mathbf{x},\mathbf{x}') - \oint_{\partial\Gamma} \mathbf{G_0}(\mathbf{x},\bar{\mathbf{x}}) \cdot \left[\hat{\bar{n}}_- \times \nabla_{\bar{\mathbf{x}}} \times \mathbf{G}_{\mathbf{\Gamma}_+}(\bar{\mathbf{x}},\mathbf{x}') \right] dS(\bar{\mathbf{x}}). \tag{5.164}$$

The dyadic delta distribution at the scatterer surface introduced in (3.58) allows us to define the operator

$$\mathbf{U}^{(\hat{\tilde{\mathbf{n}}})}_{\partial\mathbf{\Gamma}}(\bar{\mathbf{x}},\tilde{\mathbf{x}}) := -\mathbf{D}^{(\hat{\tilde{\mathbf{n}}})}_{\partial\mathbf{\Gamma}}(\tilde{\mathbf{x}}-\bar{\mathbf{x}}) \cdot \left[\hat{\tilde{n}} \times \nabla_{\tilde{x}} \times \right] \mathbf{I}, \tag{5.165}$$

so that

$$\oint_{\partial\Gamma} \mathbf{U}^{(\hat{\tilde{\mathbf{n}}}_-)}_{\partial\mathbf{\Gamma}}(\bar{\mathbf{x}},\tilde{\mathbf{x}}) \cdot \mathbf{G}_{\mathbf{\Gamma}_+}(\tilde{\mathbf{x}},\mathbf{x}')\, dS(\tilde{\mathbf{x}}) = -\hat{\bar{n}}_- \times \nabla_{\bar{\mathbf{x}}} \times \mathbf{G}_{\mathbf{\Gamma}_+}(\bar{\mathbf{x}},\mathbf{x}') \tag{5.166}$$

holds. Thus, we can rewrite (5.164) into

$$\mathbf{G}_{\mathbf{\Gamma}_+}(\mathbf{x},\mathbf{x}') = \mathbf{G}_{\mathbf{0}}(\mathbf{x},\mathbf{x}') + \oint_{\partial\Gamma} \mathbf{G}_{\mathbf{0}}(\mathbf{x},\bar{\mathbf{x}}) \cdot \mathbf{U}_{\partial\mathbf{\Gamma}}^{(\hat{\bar{\mathbf{n}}}_-)}(\bar{\mathbf{x}},\tilde{\mathbf{x}}) \cdot \mathbf{G}_{\mathbf{\Gamma}_+}(\tilde{\mathbf{x}},\mathbf{x}')\, dS(\tilde{\mathbf{x}})\, dS(\bar{\mathbf{x}}), \quad (5.167)$$

or, if employing the more simple operator notation,

$$\mathbf{G}_{\mathbf{\Gamma}_+}(\mathbf{x},\mathbf{x}') = \mathbf{G}_{\mathbf{0}}(\mathbf{x},\mathbf{x}') + \mathbf{G}_{\mathbf{0}}(\mathbf{x},\bar{\mathbf{x}}) \circ \mathbf{U}_{\partial\mathbf{\Gamma}}^{(\hat{\bar{\mathbf{n}}}_-)}(\bar{\mathbf{x}},\tilde{\mathbf{x}}) \circ \mathbf{G}_{\mathbf{\Gamma}_+}(\tilde{\mathbf{x}},\mathbf{x}'). \quad (5.168)$$

This represents already the Lippmann-Schwinger equation of the outer Dirichlet problem in the dyadic case. The first two iterations are given by

$$\mathbf{G}_{\mathbf{\Gamma}_+}^{(\mathbf{0})}(\mathbf{x},\mathbf{x}') = \mathbf{G}_{\mathbf{0}}(\mathbf{x},\mathbf{x}') \quad (5.169)$$

(this is the unperturbed problem) and

$$\mathbf{G}_{\mathbf{\Gamma}_+}^{(\mathbf{1})}(\mathbf{x},\mathbf{x}') = \mathbf{G}_{\mathbf{0}}(\mathbf{x},\mathbf{x}') + \mathbf{G}_{\mathbf{0}}(\mathbf{x},\bar{\mathbf{x}}) \circ \mathbf{U}_{\partial\mathbf{\Gamma}}^{(\hat{\bar{\mathbf{n}}}_-)}(\bar{\mathbf{x}},\tilde{\mathbf{x}}) \circ \mathbf{G}_{\mathbf{0}}(\tilde{\mathbf{x}},\mathbf{x}') \quad (5.170)$$

or, in more detail,

$$\begin{aligned}\mathbf{G}_{\mathbf{\Gamma}_+}^{(1)}(\mathbf{x},\mathbf{x}') &= \mathbf{G}_{\mathbf{0}}(\mathbf{x},\mathbf{x}') \\ &\quad + \oint_{\partial\Gamma} \mathbf{G}_{\mathbf{0}}(\mathbf{x},\bar{\mathbf{x}}) \cdot \mathbf{U}_{\partial\mathbf{\Gamma}}^{(\hat{\bar{\mathbf{n}}}_-)}(\bar{\mathbf{x}},\tilde{\mathbf{x}}) \cdot \mathbf{G}_{\mathbf{0}}(\tilde{\mathbf{x}},\mathbf{x}')\, dS(\tilde{\mathbf{x}})\, dS(\bar{\mathbf{x}}) \\ &= \mathbf{G}_{\mathbf{0}}(\mathbf{x},\mathbf{x}') - \oint_{\partial\Gamma} \mathbf{G}_{\mathbf{0}}(\mathbf{x},\bar{\mathbf{x}}) \cdot \left[\hat{\bar{n}}_- \times \nabla_{\bar{\mathbf{x}}} \times \mathbf{G}_{\mathbf{0}}(\bar{\mathbf{x}},\mathbf{x}')\right] dS(\bar{\mathbf{x}}) \quad (5.171)\end{aligned}$$

(this is the first deviation from the unperturbed problem). These two iterations avoid the strong singularity of $\mathbf{G}_{\mathbf{0}}$. The equivalent Lippmann-Schwinger equation of the dyadic interaction operator can be obtained from the defining equation

$$\mathbf{G}_{\mathbf{\Gamma}_+}(\mathbf{x},\mathbf{x}') := \mathbf{G}_{\mathbf{0}}(\mathbf{x},\mathbf{x}') + \oint_{\partial\Gamma} \mathbf{G}_{\mathbf{0}}(\mathbf{x},\bar{\mathbf{x}}) \cdot \hat{\mathbf{W}}_{\partial\Gamma_+}(\bar{\mathbf{x}},\tilde{\mathbf{x}}) \cdot \mathbf{G}_{\mathbf{0}}(\tilde{\mathbf{x}},\mathbf{x}')\, dS(\bar{\mathbf{x}})\, dS(\tilde{\mathbf{x}}), \quad (5.172)$$

the dyadic analogue of (4.23). This reads in operator notation

$$\mathbf{G}_{\mathbf{\Gamma}_+}(\mathbf{x},\mathbf{x}') := \mathbf{G}_{\mathbf{0}}(\mathbf{x},\mathbf{x}') + \mathbf{G}_{\mathbf{0}}(\mathbf{x},\bar{\mathbf{x}}) \circ \hat{\mathbf{W}}_{\partial\Gamma_+}(\bar{\mathbf{x}},\tilde{\mathbf{x}}) \circ \mathbf{G}_{\mathbf{0}}(\tilde{\mathbf{x}},\mathbf{x}'). \quad (5.173)$$

From this equation and after intercomparison with (5.168) we get finally the Lippmann-Schwinger equation

$$\hat{\mathbf{W}}_{\partial\mathbf{\Gamma}_+}(\mathbf{x},\mathbf{x}') = \mathbf{U}_{\partial\mathbf{\Gamma}}^{(\hat{\bar{\mathbf{n}}}_-)}(\mathbf{x},\mathbf{x}') + \mathbf{U}_{\partial\mathbf{\Gamma}}^{(\hat{\bar{\mathbf{n}}}_-)}(\mathbf{x},\bar{\mathbf{x}}) \circ \mathbf{G}_{\mathbf{0}}(\bar{\mathbf{x}},\tilde{\mathbf{x}}) \circ \hat{\mathbf{W}}_{\partial\mathbf{\Gamma}_+}(\tilde{\mathbf{x}},\mathbf{x}') \quad (5.174)$$

of the dyadic interaction operator related to the outer Dirichlet problem. Its lowest order iteration, if inserted into (5.171), just provides the first iteration (5.171) of the corresponding dyadic Green function.

At the end of this chapter, we will once again emphasize the difference between the integral equation methods discussed above and the approach considered in Chap. 4 which results into the T-matrix methods. Both classes of methods can be obtained by starting from the representation of the Green functions related to the scattering problems by appropriate interaction operators. The defining equations of the interaction operators can be considered to be expressions of Huygens' principle. To derive the T-matrices the auxiliary functions $G_0^>$ or $\mathbf{G}_\mathbf{t}^>$, depending on whether the scalar or dyadic case is considered, must be employed in the respective defining equations. These functions are solutions of the homogeneous Helmholtz or vector-wave equation. The Green functions represented in this way solve the corresponding inhomogeneous Helmholtz or vector-wave equation subject to the radiation condition with respect to the observation point. From the additional conditions the Green functions have to fulfil at the scatterer surface we are then able to derive explicit expressions for the T-matrices. Thereby, it is of no importance whether the interaction operators are introduced via a boundary or volume integral. This affects only the definition of the corresponding matrix elements, as demonstrated above for the outer transmission problem. On the other hand, to derive the boundary or volume integral equations we have to replace the auxiliary functions $G_0^>$ or $\mathbf{G}_\mathbf{t}^>$ in the defining equations of the interaction operators by the full free-space Green functions G_0 or $\mathbf{G_0}$. But these functions are singular at the boundary surface or inside the scatterer thus resulting in singular boundary or volume integral equations for the interaction operators itself as well as for the strongly related induced surface or volume currents. These singularities must be considered seriously in every numerical procedure. One essential advantage of the T-matrices is the fact that these are not affected by such singularities. But in contrast to the singular boundary or volume integral equation methods the T-matrix methods are faced with the problem of Rayleigh's hypothesis.

Chapter 6
The Rayleigh Hypothesis

6.1 Introduction

Frequently alluded in the foregoing chapters, we will now deal in more detail with the problem of Rayleigh's hypothesis. In 1907, Lord Rayleigh published a paper on the dynamic theory of gratings, as mentioned earlier in Chap. 1. In this paper he presented a rigorous approach for solving plane wave scattering on periodic surfaces in Cartesian coordinates (see Fig. 6.1). Those gratings are of importance in many different fields of physics and in engineering. They are used as dispersive elements in grating spectrographs, for example. In his paper, Rayleigh used a series expansion of the scattered wave in terms of outgoing plane waves only, i.e., in terms of waves which move only away from the grating. He determined the unknown expansion coefficients afterwards by application of the boundary conditions at the periodic surface appropriately, as discussed in Chap. 1. For the special case of a perpendicularly incident plane wave on a sinusoidal but perfectly conducting surface, he derived an equation system which is at first independent of the groove depth. But Rayleigh approximated this system afterwards to allow for an iterative solution for shallow grooves.

There were no essential arguments against Rayleigh's approach until 1953, when Lippmann published a short note (see Sect. 10.7 in the reference chapter) in which he intuitively criticized the usage of solely outgoing plane waves in the representation of the scattered field in the grooves (in space point $\mathbf{r_1}$ in Fig. 6.1, for example). Lippmann argued that in the grooves one has to consider also waves which move toward the surface resulting from surface current elements above the points of observation according to Huygens' principle. This paper can be considered as the hour of birth of the so-called "Rayleigh hypothesis" or "Rayleigh assumption", as the problem was called in the manifold discussions and treatments of subsequent papers. Especially, the papers of Petit and Cadilhac, Burrows, and Millar (see Sect. 10.7 in the reference chapter for details) constituted the next and most essential milestones in this discussion and are cited very often in this context, even in recent publications. Petit and Cadilhac presented a mathematical proof of the untenability of Rayleigh's

T. Rother and M. Kahnert, *Electromagnetic Wave Scattering on Nonspherical Particles*, Springer Series in Optical Sciences 145, DOI: 10.1007/978-3-642-36745-8_6,

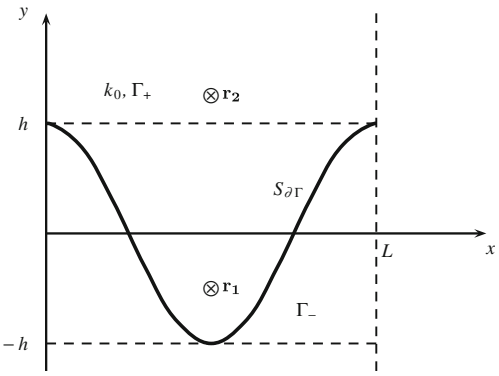

Fig. 6.1 Geometry of a sinusoidal grating. The boundary surface $S_{\partial\Gamma}$ is given by $y = R(x) = h \cos px$. In Rayleigh's approach, solely outgoing plane waves have been considered for the scattered wave everywhere above the surface. According to Lippmann's argumentation, this is correct only for points above $y = h$ (point $\mathbf{r_2}$, for example). For all points below $y = h$ (point $\mathbf{r_1}$, for example) one has to consider also incoming waves

assumption if the product of the amplitude h and the inverse of period L of the grating exceeds a certain value (more precisely: if $h \cdot p > 0.448$ with $p = 2\pi/L$). But there was a numerical development in parallel with seemingly contradictory results. Using Rayleigh's original approach, there have been developed certain numerical methods which were able to produce reliable scattering results even if $h \cdot p$ exceeds the theoretical limit of 0.448 (see the cited tutorial of Petit in Sect. 10.7, for example). Moreover, Burrows stated in his paper that Rayleigh's approach can be considered to be applicable without any restriction in a generalized sense. The term "generalized sense" is related to the fulfilment of the boundary conditions at the scatterer surface. Unfortunately, it was not precisely defined by Burrows. But the most detailed treatment was given in the papers by Millar. There, we can find a proof of the correctness of Rayleigh's approach if $h \cdot p < 0.448$. This proof was later on simplified and applied to other periodic surfaces as well as to two-dimensional problems (scattering of plane waves on cylindrical structures with noncircular cross-sections, for example) by van den Berg, Fokkema, DeSanto, and Keller. The discovered limit for the validity of Rayleigh's hypothesis is used very often in the literature to justify the restriction of numerical methods but especially that of conventional Point Matching. Beside this proof, Millar's papers contain additional proofs of the completeness of the outgoing plane waves on the surface of the sinusoidal grating (in the space $L_2(\partial\Gamma)$), and of the general possibility to apply a least-squares approach to the boundary condition. This least-squares approach results in a uniformly convergent series expansion of the scattered field in terms of only outgoing plane waves everywhere outside the grating and independent of whether Rayleigh's assumption is fulfilled or not. Especially, this last aspect provides an explanation of the above mentioned contradictory results obtained with those numerical methods which fit into a least-squares approach. However, in other papers we can find the statement that convergent results beyond the

theoretical groove depth limit can be obtained only for the far-field quantities (see the cited book of Loewen and Popov in Sect. 10.7, Chap. 10, therein). This seems to contradict the least-squares proof of Millar. And what happens with the methods which does not fit into a least-squares approach? Some of those methods are also able to produce reliable and stable results beyond the theoretical groove depth limit. Surprisingly, as we will show here, this happens especially for Rayleigh's original approach for which the limit was claimed to hold. Thus, the two questions arise: What does "Rayleigh's hypothesis" really means, and what Rayleigh really did in his 1907 paper? Regarding the first question we will see that there exist different interpretations. Here, we are not able to cite and discuss all the published literature dealing with Rayleigh's hypothesis and its influence on the usefulness or worthlessness of a certain numerical methodology for solving scattering problems on structures which are not appropriate for the separation of variables method. But if one winnows the literature one gets the feeling "that the problem has perhaps been papered over rather than resolved", as Wiscombe and Mugnai stated when discussing the influence of Rayleigh's hypothesis on Waterman's T-matrix approach (see the NASA Reference Publication of Wiscombe and Mugnai in Sect. 10.4).

This somehow muddled situation forced us to treat Rayleigh's original problem (the problem of a p-polarized plane wave perpendicularly incident on an ideal metallic and sinusoidal grating) once again by three different numerical approaches even in the grooves up to the boundary surface, and beyond. This special scattering problem can be related to the homogeneous Dirichlet problem of the scalar Helmholtz equation. Two of the methods we intend to apply are T-matrix methods for which it is not generally clear to date whether they can be used for near-field calculations or not. There are different answers in the literature. Those near-field computations become of importance if one is interested in analysing the scattering behaviour of more than one scatterer located nearby, for example. The first T-matrix method we apply to the scattering problem is just Rayleigh's original approach. This is to demonstrate that he used not a least-squares approach but a set of smooth weighting functions to fulfil the boundary condition somehow in between a least-squares approach and pointwise. The second T-matrix approach, we apply to solve the problem is a least-squares approach. It differs from Rayleigh's approach only in the choice of the weighting functions. Thus, we can clearly demonstrate that the choice of the weighting functions has a major impact on the stability and reliability of the results—a fact which is well-known to practitioners, of course. Finally, we solve the problem by a boundary integral equation method as described in Chap. 5. This method is considered to be generally not influenced by Rayleigh's hypothesis. This approach is therefore in agreement with Lippmann's requirement to take not only outgoing but also incoming plane waves into account. Interestingly, it turns out that all three methods produce the same results even in the grooves. They are moreover applicable above the groove depth limit of $h \cdot p = 0.448$. These results are our justification to perform the numerical simulations presented in Chap. 9 solely by use of a T-matrix method. It is also to demonstrate with the following considerations that the problem of Rayleigh's hypothesis can be mapped onto the two different ways of defining the interaction operators. That is, the definitions (4.1) and (5.79) seem to be equivalent, at least for

Rayleigh's original scattering problem. But the following explanations can be also considered as a short summary of the Chaps. 1, 4, and 5 in the context of Rayleigh's original scattering problem.

6.2 Plane Wave Scattering on Periodic Gratings

In the following two subsections we will present two different formulations of the scattering problem of a p-polarized plane wave perpendicularly incident on a sinusoidal and perfectly conducting surface. This emphasizes once again the equivalence of the formalisms developed in Chaps. 1 and 4 of this book. The general T-matrix approach is derived later by use of the Green's function formalism. Regarding this T-matrix approach, three different types of weighting functions will be discussed. These weighting functions result in the conventional point matching method mentioned in Sect. 5.2.2, in Rayleigh's original approach, and, finally, in a least-squares approach with respect to the fulfilment of the required boundary condition. The two last-mentioned methods are implemented numerically and applied to Rayleigh's original problem. The next subsection is concerned with a discussion of the different understandings of what Rayleigh's hypothesis means. Starting from Lippmann's argumentation the corresponding boundary integral equation approach is developed in the last subsection. It is also implemented numerically and applied to Rayleigh's original problem.

6.2.1 Conventional Formulation of the Scattering Problem

The scattering configuration is depicted in Fig. 6.2. The scattering problem of a p-polarized plane wave perpendicularly incident from above on a sinusoidal and perfectly conducting surface can be related to the following Dirichlet problem of the homogeneous Helmholtz equation: We are seeking for a solution $u_t(\mathbf{r})$ of Helmholtz's equation

$$\nabla^2 u_t(\mathbf{r}) + k_0^2 u_t(\mathbf{r}) = 0 \tag{6.1}$$

in region Γ_+ above the surface. Here, we have

$$\nabla^2 = \frac{\partial^2}{\partial x^2} + \frac{\partial^2}{\partial y^2}. \tag{6.2}$$

Vector $\mathbf{r}$ represents the two-dimensional vector (x, y). The assumed time dependence $exp(-i\omega t)$ is suppressed throughout the considerations. The open region Γ_+ above the periodic surface $S_{\partial\Gamma}$ is characterized by the free-space wave number k_0 (please, note that in contrast to the notation $\partial\Gamma$ used for the closed surface in the three-dimensional case we are now using the notation $S_{\partial\Gamma}$ for the periodic surface!). Along

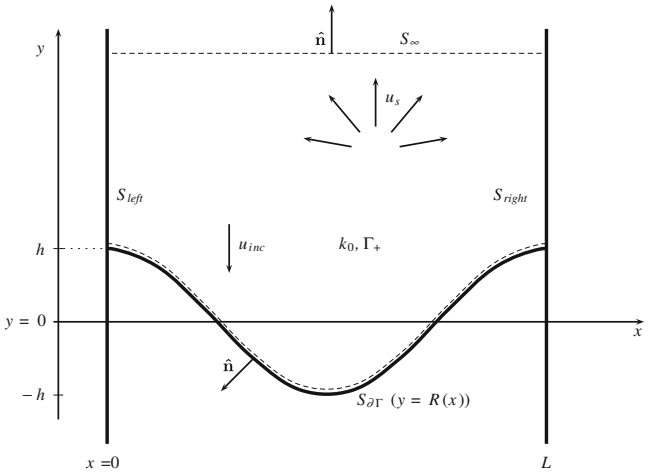

Fig. 6.2 Scattering geometry of a sinusoidal grating

the periodic surface we have to fulfil the homogeneous Dirichlet condition

$$u_t(x, R(x)) = 0. \tag{6.3}$$

Due to the linearity of Maxwell's equations, we can represent the total field $u_t(\mathbf{r})$ as a superposition of the incident and scattered field u_{inc} and u_s,

$$u_t(\mathbf{r}) = u_{inc}(\mathbf{r}) + u_s(\mathbf{r}). \tag{6.4}$$

$$u_{inc}(\mathbf{r}) = e^{-ik_0 y} \tag{6.5}$$

is the given plane wave perpendicularly incident from above the periodic surface. This plane wave is obviously a solution of the homogeneous Helmholtz equation (6.1). Furthermore, due to the periodicity of the problem, we require the fulfilment of condition

$$u_t(0, y) = u_t(L, y) \tag{6.6}$$

with respect to x. Thus, we can approximate $u_t(\mathbf{r})$ by

$$u_t^{(N)}(\mathbf{r}) = u_{inc}(\mathbf{r}) + u_s^{(N)}(\mathbf{r}) = u_{inc}(\mathbf{r}) + \sum_{n=-N}^{N} u_n(y) \cdot e^{ik_{xn}x} \tag{6.7}$$

with

$$k_{xn} = np; \quad p = \frac{2\pi}{L}. \tag{6.8}$$

We need an additional condition in order to specify $u_n(y)$ in the series expansion of the scattered field. This is the one-dimensional, non-local radiation condition

$$\lim_{y\to\infty}\left(\frac{\partial u_n(y)}{\partial y} - ik_{yn}u_n(y)\right) = 0 \tag{6.9}$$

which must hold at S_∞. The discrete values of k_{yn} are defined according to

$$k_{yn} = \begin{cases} \sqrt{k_0^2 - k_{xn}^2}\ ; \text{ if } k_0^2 > k_{xn}^2 \\ i\sqrt{k_{xn}^2 - k_0^2}\ ; \text{ if } k_{xn}^2 > k_0^2. \end{cases} \tag{6.10}$$

This radiation condition is fulfilled by every outgoing plane wave

$$u_n(y) = a_n \cdot e^{ik_{yn}y} \tag{6.11}$$

with constant a_n. But it is **not** fulfilled by the total field $u_t(\mathbf{r})$ since the incident plane wave (6.5) obviously violates this condition. This is similar to what we already know from the three-dimensional case. Inserting (6.11) into the series expansion of the scattered field in (6.7) provides the approximation

$$u_s^{(N)}(x, y) = \sum_{n=-N}^{N} a_n^{(N)} \cdot e^{i(k_{xn}x + k_{yn}y)}. \tag{6.12}$$

This is a representation in terms of outgoing plane waves only which should be applicable at least for every $y > h$. Since the boundary surface $S_{\partial\Gamma}$ is given by the even function

$$y = R(x) = h\cos px, \tag{6.13}$$

and since we consider a perpendicular incidence of the plane wave $a_n^{(N)} = a_{-n}^{(N)}$ holds, i.e., the scattered modes are symmetric with respect to the y-axis (compare Fig. 6.2). Thus, we can rewrite representation (6.12) as follows:

$$\begin{aligned} u_s^{(N)}(x, y) &= \sum_{n=0}^{N} a_n^{(N)} \cdot e^{i(k_{xn}x + k_{yn}y)} + \sum_{n=1}^{N} a_n^{(N)} e^{i(-k_{xn}x + k_{yn}y)} \\ &= \sum_{n=0}^{N} a_n^{(N)} \cdot \epsilon_n \cdot \cos k_{xn}x \cdot e^{ik_{yn}y}. \end{aligned} \tag{6.14}$$

Here, we have $\epsilon_n = 1$ if $n = 0$, and $\epsilon_n = 2$ if $n > 0$. It is exactly this representation which was used by Rayleigh in his 1907 paper. Before discussing the different methods to calculate the unknown coefficients $a_n^{(N)}$, we will now formulate the problem again by applying Green functions.

6.2.2 Formulation in Terms of Green Functions

In contrast to (6.1), we ask now for the solution of the inhomogeneous Helmholtz equation

$$\nabla^2 u_t(\mathbf{r}) + k_0^2 u_t(\mathbf{r}) = -\rho(\mathbf{r}) \tag{6.15}$$

subject to the Dirichlet condition (6.3), the periodicity condition (6.6), and the radiation condition (6.9). $\rho(\mathbf{r})$ is the source which generates the primary incident field u_{inc}, i.e., u_{inc} is a solution of

$$\nabla^2 u_{inc}(\mathbf{r}) + k_0^2 u_{inc}(\mathbf{r}) = -\rho(\mathbf{r}). \tag{6.16}$$

The necessity of introducing a local source is a consequence of the cause and action concept of Green's functions. We will now express the incident field u_{inc} as well as the total field u_t by use of appropriate Green functions.

At first we are interested in representing the incident plane wave by the free-space Green function. It should be emphasized that for the scattering problem under consideration the free-space Green function depends on the direction of incidence of the plane wave. This is a consequence of the restriction to a space with only periodic functions which applies to the fields as well as to the sources. All ongoing discussions and representations of G_0 are therefore restricted to perpendicular incidence only! Let us now see how we can generate the plane wave (6.5) perpendicularly incident on the periodic boundary (6.13). For this, we introduce the free-space Green function by the defining equation

$$\nabla_{\mathbf{r}}^2 G_0(\mathbf{r}, \mathbf{r}') + k_0^2 G_0(\mathbf{r}, \mathbf{r}') = -\delta(\mathbf{r} - \mathbf{r}'). \tag{6.17}$$

This Green's function is related to the whole space $\Gamma = \Gamma_+ \cup \Gamma_-$ without the grating (i.e., the unperturbed problem). But we require additionally the fulfilment of the periodicity condition

$$G_0(0, y; \mathbf{r}') = G_0(L, y; \mathbf{r}') \tag{6.18}$$

with respect to x. Due to this condition, we can expand G_0 into the Fourier series

$$G_0(\mathbf{r}, \mathbf{r}') = \sum_{n=-\infty}^{\infty} G_n(y, \mathbf{r}') \cdot e^{ik_{xn}x}. \tag{6.19}$$

The $G_n(y, \mathbf{r}')$ have to fulfil the radiation condition

$$\lim_{|y| \to \infty} \left(\frac{\partial G_n(y, \mathbf{r}')}{\partial |y|} - ik_{yn} G_n(y, \mathbf{r}') \right) = 0 \tag{6.20}$$

which holds at S_∞ as well as at $S_{-\infty}$. In the literature one can find several expressions for this free-space Green function (for an overview, see the paper of Linton cited in

Sect. 10.7). Here, we want to employ the expression

$$G_0(\mathbf{r},\mathbf{r}') \;=\; \frac{i}{2L}\cdot\sum_{n=0}^{\infty}\frac{\epsilon_n}{k_{yn}}\cos k_{xn}(x-x')\,e^{ik_{yn}|y-y'|}. \tag{6.21}$$

Please, note that the $e^{ik_{xn}x}$ term in (6.19) has been resolved into the term $\cos k_{xn}(x-x')$ thus restricting the sum over n to run from 0 to ∞. The values of ϵ_n are defined as in (6.14). This representation of G_0 does not explicitly shows the expected logarithmic singularity at $\mathbf{r}=\mathbf{r}'$ (in contrast to the $1/r$ singularity in the three-dimensional case!). But it is obviously divergent in this point. An alternative representation is given by

$$G_0(\mathbf{r},\mathbf{r}') \;=\; -\frac{i}{4}\cdot\sum_{n=-\infty}^{\infty}H_0^{(1)}(k_0 r_n)\;\;;\;r_n\;=\;\sqrt{(x-x'-nL)^2+(y-y')^2} \tag{6.22}$$

which exhibits more clearly the logarithmic singularity since $H_0^{(1)}$ is the Hankel function of first kind and zero order. But now it becomes more complicate to prove the fulfilment of the radiation condition (6.20). However, it should be already mentioned at this point that both representations provide identical scattering results. The free-space Green function exhibits the symmetry

$$G_0(\mathbf{r},\mathbf{r}') \;=\; G_0(\mathbf{r}',\mathbf{r}) \tag{6.23}$$

which can be clearly seen from (6.21). The general proof follows from the application of Green's theorem (2.240) in $\Gamma=\Gamma_+\cup\Gamma_-$ with

$$\Psi(\mathbf{r}) = G_0(\mathbf{r},\mathbf{r}') \tag{6.24}$$
$$\Phi(\mathbf{r}) = G_0(\mathbf{r},\mathbf{r}''), \tag{6.25}$$

and in conjunction with the radiation condition (6.20) and periodicity condition (6.18). The closed boundary S of Γ consists of the parts S_{right}, S_{left}, S_∞, and $S_{-\infty}$ (see Fig. 6.3). On the other hand, if we choose

$$\Psi(\mathbf{r}) = G_0(\mathbf{r},\mathbf{r}') \tag{6.26}$$
$$\Phi(\mathbf{r}) = u_{inc}(\mathbf{r}), \tag{6.27}$$

in Green's theorem we get

$$u_{inc}(\mathbf{r}) \;=\; \int_\Gamma G_0(\mathbf{r},\mathbf{r}')\cdot\rho(\mathbf{r}')\,dV(\mathbf{r}') \tag{6.28}$$

if taking the symmetry (6.23) and (6.16) and (6.17) into account. The radiation condition (6.20) holds therefore also for u_{inc}. Then, it is straightforward to show that

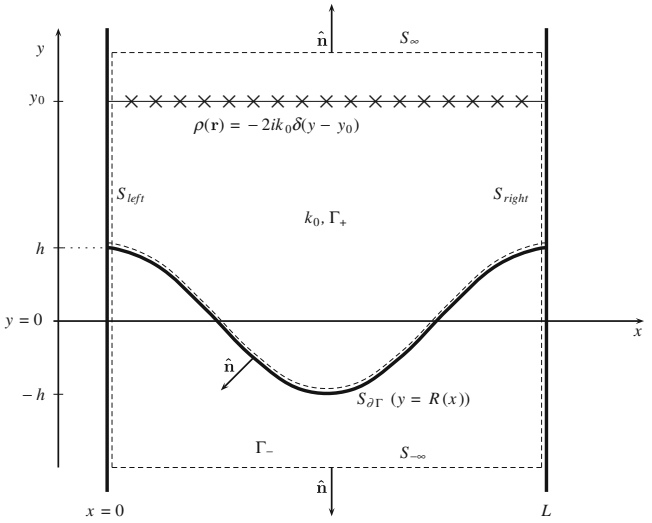

Fig. 6.3 Scattering geometry of a sinusoidal grating with the source distribution generating the primary incident plane wave

the source distribution

$$\rho(\mathbf{r}) \;=\; -2ik_0\delta(y-y_0) \;=\; -2ik_0\cdot\cos k_{x0}x\cdot\delta(y-y_0) \tag{6.29}$$

in conjunction with expression (6.21) generates the incident field

$$u_{inc}(\mathbf{r}) \;=\; e^{ik_0|y-y_0|}. \tag{6.30}$$

If we locate y_0 somewhere in Γ_+ but such that $y_0 > h$, and if we choose w.l.o.g.

$$e^{ik_0y_0} \;=\; 1 \tag{6.31}$$

we generate exactly the incident field (6.5) below y_0 needed for our discussion (see Fig. 6.3). But representation (6.21) can be simplified further. Due to the considered surface (6.13) it is sufficient to take only the even part

$$\widetilde{G}_0(\mathbf{r},\mathbf{r}') \;=\; \frac{i}{2L}\cdot\sum_{n=0}^{\infty}\frac{\epsilon_n}{k_{yn}}\cos k_{xn}x\,\cos k_{xn}x'\,e^{ik_{yn}|y-y'|} \tag{6.32}$$

of G_0 with respect to x into account. This expression can be decomposed into

$$\widetilde{G}_0(\mathbf{r},\mathbf{r}') \;=\; \begin{cases} \widetilde{G}_0^{>}(\mathbf{r},\mathbf{r}') & ;\; y>y' \\ \widetilde{G}_0^{<}(\mathbf{r},\mathbf{r}') & ;\; y<y' \end{cases} \tag{6.33}$$

with

$$\widetilde{G}_0^{>}(\mathbf{r},\mathbf{r}') = \frac{i}{2L}\cdot\sum_{n=0}^{\infty}\widetilde{\phi}_n(\mathbf{r})\cdot\widetilde{\psi}_n(\mathbf{r}') \tag{6.34}$$

$$\widetilde{G}_0^{<}(\mathbf{r},\mathbf{r}') = \frac{i}{2L}\cdot\sum_{n=0}^{\infty}\widetilde{\psi}_n(\mathbf{r})\cdot\widetilde{\phi}_n(\mathbf{r}'). \tag{6.35}$$

The expansion functions therein are given by

$$\widetilde{\phi}_n(\mathbf{r}) = \sqrt{\frac{\epsilon_n}{k_{yn}}}\cdot\phi_n(\mathbf{r}) \tag{6.36}$$

$$\phi_n(\mathbf{r}) = \cos k_{xn}x\ e^{ik_{yn}y} \tag{6.37}$$

$$\widetilde{\psi}_n(\mathbf{r}) = \sqrt{\frac{\epsilon_n}{k_{yn}}}\cdot\psi_n(\mathbf{r}) \tag{6.38}$$

$$\psi_n(\mathbf{r}) = \cos k_{xn}x\ e^{-ik_{yn}y}. \tag{6.39}$$

This even part of G_0, together with the source distribution (6.29), produces the same incident field (6.5) below y_0.

The Green function which is related to the considered scattering problem in Γ_+ is also a solution of the inhomogeneous Helmholtz equation

$$\nabla_{\mathbf{r}}^2\, G_{\Gamma_+}(\mathbf{r},\mathbf{r}') \ + \ k_0^2\, G_{\Gamma_+}(\mathbf{r},\mathbf{r}') \ = \ -\,\delta(\mathbf{r}-\mathbf{r}'). \tag{6.40}$$

Γ_+ is enclosed by S_{right}, S_{left}, S_∞, and $S_{\partial\Gamma}$. We require again the fulfilment of the periodicity condition

$$G_{\Gamma_+}(0,y;\mathbf{r}') \ = \ G_{\Gamma_+}(L,y;\mathbf{r}') \tag{6.41}$$

with respect to x as well as the radiation condition (6.9) if $y\to\infty$. But in contrast to the free-space Green's function we have the additional homogeneous Dirichlet condition

$$G_{\Gamma_+}(x,R(x);\mathbf{r}') \ = \ 0 \tag{6.42}$$

which must hold on the surface of the grating. G_{Γ_+} obeys the symmetry relation we already know from G_0, i.e.,

$$G_{\Gamma_+}(\mathbf{r},\mathbf{r}') \ = \ G_{\Gamma_+}(\mathbf{r}',\mathbf{r}). \tag{6.43}$$

This symmetry relation as well as the integral representation

$$u_t(\mathbf{r}) \ = \ \int_{\Gamma_+} G_{\Gamma_+}(\mathbf{r},\mathbf{r}')\cdot\rho(\mathbf{r}')\,dV(\mathbf{r}') \tag{6.44}$$

are again consequences of Green's theorem but now applied in Γ_+. Next, we introduce the interaction operator $W_{S_{\partial\Gamma}}$ by the definition

$$G_{\Gamma_+}(\mathbf{r},\mathbf{r}') \;:=\; \widetilde{G}_0(\mathbf{r},\mathbf{r}') \;+\; \int_{S_{\partial\Gamma}} \widetilde{G}_0(\mathbf{r},\hat{\mathbf{r}})\cdot W_{S_{\partial\Gamma}}(\hat{\mathbf{r}},\tilde{\mathbf{r}})\cdot \widetilde{G}_0(\tilde{\mathbf{r}},\mathbf{r}')\,dS(\hat{\mathbf{r}})\,dS(\tilde{\mathbf{r}}). \tag{6.45}$$

Please, note that in Cartesian coordinates the unit normal vector on the surface $S_{\partial\Gamma}$ of the grating reads

$$\hat{\mathbf{n}} \;=\; \frac{\hat{\mathbf{e}}_{\mathbf{x}}\cdot R'(x) \;-\; \hat{\mathbf{e}}_{\mathbf{y}}}{\sqrt{1+[R'(x)]^2}} \tag{6.46}$$

with $R'(x) = dR(x)/dx$. The surface element dS in the surface integral on the right-hand side of (6.45) is given by

$$dS(\mathbf{r}) \;=\; \sqrt{1+[R'(x)]^2}\,dx \;=\; S(x)\,dx. \tag{6.47}$$

If we restrict the variable y_0 to the region in Γ_+ for which $y_0 > h$ holds (this corresponds to the location of the source outside the smallest sphere circumscribing the scatterer we have frequently mentioned in the three-dimensional case) we can replace $\widetilde{G}_0(\mathbf{r},\mathbf{r}')$ and $\widetilde{G}_0(\tilde{\mathbf{r}},\mathbf{r}')$ in (6.45) by $\widetilde{G}_0^<$, i.e., we have

$$G_{\Gamma_+}(\mathbf{r},\mathbf{r}') \;=\; \widetilde{G}_0^<(\mathbf{r},\mathbf{r}') \;+\; \int_{S_{\partial\Gamma}} \widetilde{G}_0(\mathbf{r},\hat{\mathbf{r}})\cdot W_{S_{\partial\Gamma}}(\hat{\mathbf{r}},\tilde{\mathbf{r}})\cdot \widetilde{G}_0^<(\tilde{\mathbf{r}},\mathbf{r}')\,dS(\hat{\mathbf{r}})\,dS(\tilde{\mathbf{r}}). \tag{6.48}$$

If we further restrict the variable y to the region in Γ_+ for which $y_0 > y > h$ holds we can furthermore replace $\widetilde{G}_0(\mathbf{r},\hat{\mathbf{r}})$ in the surface integral of (6.45) by $\widetilde{G}_0^>(\mathbf{r},\hat{\mathbf{r}})$. Thus, we may write finally

$$G_{\Gamma_+}(\mathbf{r},\mathbf{r}') \;=\; \widetilde{G}_0^<(\mathbf{r},\mathbf{r}') \;+\; \int_{S_{\partial\Gamma}} \widetilde{G}_0^>(\mathbf{r},\hat{\mathbf{r}})\cdot W_{S_{\partial\Gamma}}(\hat{\mathbf{r}},\tilde{\mathbf{r}})\cdot \widetilde{G}_0^<(\tilde{\mathbf{r}},\mathbf{r}')\,dS(\hat{\mathbf{r}})\,dS(\tilde{\mathbf{r}}). \tag{6.49}$$

If using expansions (6.34) and (6.35) but now truncated at a finite number N, and if defining the matrix elements of the interaction operator according to

$$\left[W_{S_{\partial\Gamma}}\right]_{n,n'} \;:=\; \frac{i}{2L}\cdot \int_{S_{\partial\Gamma}} \widetilde{\psi}_n(\hat{x},R(\hat{x}))\cdot W_{S_{\partial\Gamma}}(\hat{\mathbf{r}},\tilde{\mathbf{r}})\cdot \widetilde{\psi}_{n'}(\tilde{x},R(\tilde{x}))\,dS(\hat{\mathbf{r}})dS(\tilde{\mathbf{r}}) \tag{6.50}$$

we get as an approximation of G_{Γ_+}

$$G_{\Gamma_+}^{(N)}(\mathbf{r},\mathbf{r}') \;=\; \widetilde{G}_0^{<}(\mathbf{r},\mathbf{r}') \;+\; \frac{i}{2L}\cdot\sum_{n,n'=0}^{N}\left[W_{S_{\partial\Gamma}}\right]_{n,n'}\cdot\widetilde{\phi}_n(\mathbf{r})\cdot\widetilde{\phi}_{n'}(\mathbf{r}') \tag{6.51}$$

valid at first in the region with $y_0 > y > h$. It is a representation in terms of only outgoing plane waves. Inserting this expression together with the source distribution (6.29) into (6.44) provides the corresponding representation

$$u_t(\mathbf{r}) \;=\; u_{inc} \;+\; \sqrt{k_0}\cdot\sum_{n=0}^{N}\sqrt{\frac{\epsilon_n}{k_{yn}}}\cdot\left[W_{S_{\partial\Gamma}}\right]_{n,0}\cdot\phi_n(\mathbf{r}) \tag{6.52}$$

of the total field which holds also at first in the region $h < y < y_0$. The second part on the right-hand side of this equation represents the scattered field. If comparing this expression with (6.14) we get

$$a_n^{(N)} \;=\; \sqrt{\frac{k_0}{k_{yn}\,\epsilon_n}}\cdot\left[W_{S_{\partial\Gamma}}\right]_{n,0} \tag{6.53}$$

as the relation between the expansion coefficients in Rayleigh's representation and the matrix elements of the interaction operator. Thus, we can state that in region $h < y < y_0$ representation (6.49) or approximation (6.51) of the Green's function related to our scattering problem is equivalent to the conventional representation of the total field with the scattered part given by (6.14). But the question how to determine the unknown expansion coefficients or the matrix elements (6.50) of the interaction operator, respectively, is still open. This will be considered now.

6.2.3 T-Matrix Solution

The essential step to determine the unknown coefficients is the following assumption which dates back to Rayleigh:

- **Representation** (6.14) **holds not only for** $y > h$ **but also for all values of** y **within the grooves and at the surface of the grating.**

To determine the matrix elements of the interaction operator we formulate the equivalent assumption for the Green function related to the scattering problem:

- **Representation**

$$\begin{aligned} G_{\Gamma_+}^{R}(\mathbf{r},\mathbf{r}') \;=\; & \widetilde{G}_0^{<}(\mathbf{r},\mathbf{r}') \\ & +\int_{S_{\partial\Gamma}} \widetilde{G}_0^{>}(\mathbf{r},\hat{\mathbf{r}})\cdot W_{S_{\partial\Gamma}}^{R}(\hat{\mathbf{r}},\tilde{\mathbf{r}})\cdot\widetilde{G}_0^{<}(\tilde{\mathbf{r}},\mathbf{r}')\,dS(\hat{\mathbf{r}})\,dS(\tilde{\mathbf{r}}) \end{aligned} \tag{6.54}$$

or, equivalently, approximation (6.51) holds not only for $y > h$ but also for all values of y within the grooves and at the surface of the grating.

Please, note that the Green function as well as the matrix elements (6.50) of the interaction operator are marked with the upper letter "R" to distinguish the resulting approach from the approach on the basis of Lippmann's argumentation we will consider later on. We will call both assumptions "Rayleigh's assumption". They allow us to apply the additional Dirichlet conditions (6.3) or (6.42), respectively, to determine the unknown quantities. The matrix elements of the interaction operator can thus be determined in the following way:

Applying (6.42) to (6.51) provides the equation

$$\sum_{n'=0}^{N} \widetilde{\psi}_{n'}(x, R(x)) \cdot \widetilde{\phi}_{n'}(\mathbf{r}') \;=\; - \sum_{n,n'=0}^{N} \widetilde{\phi}_{n}(x, R(x)) \cdot \left[W^{R}_{S_{\partial\Gamma}} \right]_{n,n'} \cdot \widetilde{\phi}_{n'}(\mathbf{r}'). \quad (6.55)$$

if using the (now finite!) expansion (6.35) to approximate also $\widetilde{G}_0^{<}(\mathbf{r}, \mathbf{r}')$ in equation (6.51). Next, we ask for the transformation matrix $\widetilde{T}_{\partial\Gamma}$ which allows us to express the expansion functions $\widetilde{\psi}_{n'}(x, R(x))$ by the expansion functions $\widetilde{\phi}_{n}(x, R(x))$ on the surface $y = R(x)$ of the grating according to

$$\widetilde{\psi}_{n'}(x, R(x)) \;=\; \sum_{n=0}^{N} \left[\widetilde{T}_{S_{\partial\Gamma}} \right]_{n',n} \widetilde{\phi}_{n}(x, R(x)) \quad (6.56)$$

where the equal sign holds only for a plane interface $R(x) = const$ (see also the corresponding discussion in Sect. 2.2.3 regarding the validity of (2.17)!). If we insert this relation into (6.55) we obtain after intercomparison

$$\left[W^{R}_{S_{\partial\Gamma}} \right]_{n,n'} \;=\; - \left[T_{S_{\partial\Gamma}} \right]_{n,n'} \;=\; - \left[\widetilde{T}_{S_{\partial\Gamma}} \right]^{tp}_{n,n'} . \quad (6.57)$$

In close analogy to (2.19) the T-matrix $\mathbf{T}_{S_{\partial\Gamma}}$ can now be calculated according to

$$\mathbf{T}_{S_{\partial\Gamma}} \;=\; \mathbf{A}^{-1}_{S_{\partial\Gamma}} \cdot \mathbf{B}_{S_{\partial\Gamma}} \quad (6.58)$$

from the two matrices $\mathbf{A}_{S_{\partial\Gamma}}$ and $\mathbf{B}_{S_{\partial\Gamma}}$. Their elements are defined by the scalar products

$$\left[A_{S_{\partial\Gamma}} \right]_{n,m} := < w_n(\mathbf{r}) | \, \widetilde{\phi}_m(\mathbf{r}) > \quad (6.59)$$

$$\left[B_{S_{\partial\Gamma}} \right]_{n,m} := < w_n(\mathbf{r}) | \, \widetilde{\psi}_m(\mathbf{r}) > \quad (6.60)$$

of the expansion functions $\widetilde{\phi}_m(\mathbf{r})$ and $\widetilde{\psi}_m(\mathbf{r})$ with the yet not specified weighting functions $w_n(\mathbf{r})$. The scalar product itself is defined via the integral

$$< w_n(\mathbf{r})|\, f_m(\mathbf{r}) > := \frac{1}{L} \cdot \int_0^L w_n^*(x, R(x)) \cdot f_m(x, R(x))\, dx. \tag{6.61}$$

As it can be seen from (6.53) it is sufficient to know only the first column of the matrix $\mathbf{W}^R_{\partial\Gamma}$, i.e., we have only to calculate

$$\left[T_{S_{\partial\Gamma}}\right]_{n,0} = \sum_{m=0}^{N} \left[A^{-1}_{S_{\partial\Gamma}}\right]_{n,m} \left[B_{S_{\partial\Gamma}}\right]_{m,0}. \tag{6.62}$$

Due to our special scattering surface, the weighting functions can be also restricted to even functions with respect to x. Three types of weighting functions are of our special interest here:

Let

$$w_n(\mathbf{r}) = L \cdot \delta(x - x_n) \tag{6.63}$$

with x_n being $N + 1$ points within the interval $[0, L)$ or $(0, L]$ (note that due to the periodicity condition matching points $x = 0$ **and** $x = L$ are not allowed!). These weighting functions result in the conventional Point Matching technique discussed earlier in Sect. 5.2.2. It is characterized by the same number of matching points and unknown expansion coefficients. Especially this technique was the starting point of a controversial discussion by Bates and Millar and of Millar's detailed analysis of Rayleigh's hypothesis. As discussed earlier, this method is not very stable and provides accurate results only for shallow gratings. But as also discussed, a drastic improvement can be achieved if the number of matching points exceeds the number of unknowns in series expansion (6.14).

If we choose

$$w_n(\mathbf{r}) = \cos k_{xn} x \tag{6.64}$$

as weighting functions, and, furthermore, if we take the integral representation

$$\frac{1}{2\pi} \cdot \int_0^{2\pi} e^{i(ny - z\cos y)} dy = e^{-i\,(n\pi)/2} \cdot J_n(z) \tag{6.65}$$

of Bessel's functions $J_n(z)$ into account we get from the scalar products (6.59) and (6.60) the analytical expressions

$$\begin{aligned}\left[A_{S_{\partial\Gamma}}\right]_{m,n} = \frac{1}{2}\sqrt{\frac{\epsilon_n}{k_{yn}}} \Big\{ & e^{i(m+n)\frac{\pi}{2}} \cdot J_{m+n}(hk_{yn}) \\ & + e^{i(m-n)\frac{\pi}{2}} \cdot J_{m-n}(hk_{yn}) \Big\}\end{aligned} \tag{6.66}$$

$$\begin{aligned}\left[B_{S_{\partial\Gamma}}\right]_{m,n} = \frac{1}{2}\sqrt{\frac{\epsilon_n}{k_{yn}}} \Big\{ & e^{-i(m+n)\frac{\pi}{2}} \cdot J_{m+n}(hk_{yn}) \\ & + e^{-i(m-n)\frac{\pi}{2}} \cdot J_{m-n}(hk_{yn}) \Big\}\end{aligned} \tag{6.67}$$

as the relevant matrix elements. Albeit of our more compact notation this agrees exactly with the equation system derived by Rayleigh in his original 1907 paper (see (28–34) therein). It should be mentioned that Rayleigh applied the Jacobi-Anger formula instead of integral representation (6.65) to derive this equation system. It was resolved by Rayleigh under the assumption of shallow gratings. This allowed him to derive explicit expressions for the expansion coefficients. But we have to state also that these weighting functions does not belong to a least-squares scheme.

A least-squares scheme results from the weighting functions

$$w_n(\mathbf{r}) \;=\; \widetilde{\phi}_n(x,\, R(x)) \tag{6.68}$$

with $\widetilde{\phi}_n$ according to (6.36). We are again able to perform the scalar product in (6.59) and (6.60) analytically. The matrix elements read in this case

$$\begin{aligned}\left[A_{S_{\partial\Gamma}}\right]_{m,n} \;&=\; \frac{1}{2}\sqrt{\frac{\epsilon_n\epsilon_m}{k_{yn}k_{ym}}}\;\Big\{e^{i(m+n)\frac{\pi}{2}}\cdot J_{m+n}(h(k_{yn}-k_{ym}^*)) \\ &\quad + e^{i(m-n)\frac{\pi}{2}}\cdot J_{m-n}(h(k_{yn}-k_{ym}^*))\Big\} \qquad (6.69)\\ \left[B_{S_{\partial\Gamma}}\right]_{m,n} \;&=\; \frac{1}{2}\sqrt{\frac{\epsilon_n\epsilon_m}{k_{yn}k_{ym}}}\;\Big\{e^{-i(m+n)\frac{\pi}{2}}\cdot J_{m+n}(h(k_{yn}+k_{ym}^*)) \\ &\quad + e^{-i(m-n)\frac{\pi}{2}}\cdot J_{m-n}(h(k_{yn}+k_{ym}^*))\Big\}. \qquad (6.70)\end{aligned}$$

The numerical implications of the different weighting functions will be discussed shortly. But beforehand, we will deal with the two different understandings of Rayleigh's hypothesis according to Petit, Cadilhac, and Millar, and to Lippmann.

6.2.4 *Rayleigh's Hypothesis According to Petit, Cadilhac, and Millar*

Millar started his papers from the following representation of the scattered field:

$$u_s(x,\, y) \;=\; \sum_{n=-\infty}^{\infty} a_n \cdot e^{i(k_{xn}x - k_{yn}y)}. \tag{6.71}$$

It differs from representation (6.12) by assuming an infinite expansion with final expansion coefficients. By application of Green's theorem (2.240) in a subdomain of Γ_+ bounded by S_{left}, S_{right}, $S_{\partial\Gamma}$, and the constant line $h < y \leq const. < y_0$ with the two quantities

$$\Psi(\mathbf{r}) = u_s(\mathbf{r}) \tag{6.72}$$

$$\Phi(\mathbf{r}) = e^{-i(k_{xn}x - k_{yn}y)} \tag{6.73}$$

Millar could relate the final coefficients to the boundary integral

$$a_n = \frac{i}{2k_{yn}L} \cdot \int_{S_{\partial\Gamma}} \left[u_s(\mathbf{r}) \frac{\partial}{\partial \hat{n}} - \frac{\partial u_s(\mathbf{r})}{\partial \hat{n}} \right] \cdot e^{i(k_{xn}x - k_{yn}y)} \, dS(\mathbf{r}). \tag{6.74}$$

This expression contains the known scattered field u_s (it is identical with the primary incident field except for the sign, due to the required Dirichlet condition) and its unknown normal derivative at the boundary surface $S_{\partial\Gamma}$. But it should be mentioned that the unknown normal derivative $\partial u_s(\mathbf{r})/\partial \hat{n}$ of the scattered field is related via a boundary integral equation to the known scattered field u_s, and vice versa. That is, if the normal derivative of the scattered field would be the known quantity then the scattered field is related via a boundary integral equation to this known quantity. These boundary integral relations between u_s and $\partial u_s(\mathbf{r})/\partial \hat{n}$ at the boundary surface expresses the fact that only one quantity must be fixed at this surface to make the boundary value problem uniquely solvable (mathematically seen, this corresponds to the Dirichlet and von Neumann problem each of which can be solved uniquely). This important aspect together with its implications is discussed in detail in the contribution of Hoenl, Maue, and Westsphal cited in Sect. 10.6. Equation (6.74) represents therefore a quite formal relation. Rayleigh's hypothesis according to the understanding of Petit, Cadilhac, and Millar can be defined as follows (and if we talk about Rayleigh's hypothesis in the ongoing discussion of this subsection this definition is tacitly meant!):

- It is the assumption that expansion (6.71) with coefficients (6.74) is a valid representation of u_s not only in $y > h$ but in every point of Γ_+ and especially on the surface $R(x)$. Thus the Dirchlet condition (6.3) provides

$$e^{-ik_0 R(x)} = -\sum_{n=-\infty}^{\infty} a_n \cdot e^{i(k_{xn}x - k_{yn}R(x))}, \tag{6.75}$$

  which is assumed further to hold **in every point** of this surface.

This understanding of Rayleigh's hypothesis can be found in the papers of Millar, for example. It targeted obviously at conventional point matching methods. According to the above discussion, it is of course somehow questionable to denote this understanding with "Rayleigh's hypothesis" since Rayleigh never used the conventional point matching method nor he assumed final expansion coefficients according to (6.74). Some misunderstandings in the recent literature may result from this confusing designation. However, for practitioners operating with the conventional point matching methods the analysis of Petit, Cadilhac, and Millar is of some importance. Petit and Cadilhac found a counter example, i.e., a point on the surface which violates boundary condition (6.75). They could show in an elegant way that in $x = L/2$ condition (6.75) is violated if $h \cdot p > 0.448$. Millar, on the other hand, could show by inspection of the singularities of the scattered field that Rayleigh's hypothesis as formulated above holds for $h \cdot p < 0.448$. Thus, $h \cdot p = 0.448$ can be considered to

be an upper limit of the applicability of conventional point matching methods even though they rarely reach this value in practical calculations since running into stability problems before. Excluding such critical surface points in the corresponding procedure would be therefore of little benefit. This is the reason why conventional point matching methods are nowadays of less importance. But the requirement that boundary condition (6.75) must hold in every point on the surface is questionable also from a more physical point of view. Sommerfeld stated in his book "Partial Differential Equations in Physics" (see Sect. 10.2) that "*in mathematical lectures on Fourier series emphasis is usually put on the concept of arbitrary functions, on its continuity properties and its singularities. This point of view becomes immaterial in the physical applications. For, the initial boundary values of functions ... must always be taken as smoothed mean values, just as the partial differential equations in which they enter arise from a statistical averaging of much more complicated elementary laws. Hence we are concerned with relatively simple idealized functions and with their approximation with ... "Method of Least Squares". We shall see that it opens a simple and rigorous approach not only to Fourier series but to all other series expansions of mathematical physics ... in eigenfunctions*".

This physical point of view is reflected in Millar's proof that an understanding of boundary condition (6.75) in a least-squares sense, i.e.,

$$e^{-ik_0 R(x)} \;=\; -\sum_{n=-N}^{N} a_n^{(N)} \cdot e^{i(k_{xn}x - k_{yn}R(x))} \;=\; -\,u_s^{(N)}(R(x)) \tag{6.76}$$

with coefficients $a_n^{(N)}$ calculated by minimizing the least-squares norm

$$\sqrt{< u_{inc}(R(x)) \,+\, u_s^{(N)}(R(x)) \,|\, u_{inc}(R(x)) \,+\, u_s^{(N)}(R(x)) >} \tag{6.77}$$

is generally not influenced by Rayleigh's hypothesis and results in a representation of the scattered field everywhere above $y = R(x)$ which converges uniformly against the exact solution. The relevant scalar product $< g(\mathbf{x}) \mid f(\mathbf{x}) >$ is defined in (6.61). T-matrix methods which are based on the third choice (6.68) of weighting functions as well as generalized point matching methods are therefore not in conflict with Rayleigh's hypothesis. Rayleigh's original approach is somewhere in between conventional point matching and least-squares methods and provide also stable results beyond the found limit of Petit, Cadilhac, and Millar. But as we will demonstrate in our numerical analysis, the region of stable and convergent results depends strongly on the choice of weighting functions. And it is also known from many practical applications that a least-squares approach is not necessarily the best one.

In this context, it should be mentioned that one can find in the more mathematically oriented literature the following abstract definition of Rayleigh's hypothesis (see the paper of Kleinman, Roach, and Stroem cited in Sect. 10.2, for example):

- If the outgoing plane wave functions form a Schauder basis in $L_2(\partial\Gamma)$ Rayleigh's hypothesis is said to be satisfied. An infinite set of functions f_n form a Schauder

basis if there is a unique set of final coefficients a_n such that any function u on the surface of the grating can be approximated by

$$u = \sum_{n=0}^{\infty} a_n \cdot f_n. \tag{6.78}$$

What does it means from a more practical point of view? If the expansion functions form a Schauder basis we would then be able to apply the T-matrix approach with least-squares weighting functions up to an infinite truncation parameter N, i.e., we would then be able to perform the necessary inversion of the infinite matrix $\mathbf{A}_{\partial\Gamma}$ in (6.62), for example. But this definition is of less importance for practitioners since one can find no clear answer whether the outgoing plane wave functions form a Schauder basis on a sinusoidal surface or not. And if they do this would be of little help since every numerical procedure is based always on a finite numerical accuracy and on a finite series expansion.

6.2.5 *Rayleigh's Hypothesis According to Lippmann, and a Corresponding Boundary Integral Solution*

Lippmann's criticism on Rayleigh's approach is much more intuitive and traceable for practitioners since it is based on the clear physical picture of Huygens' principle, at first glance (see Fig. 6.4). It is therefore employed very often as a justification for the supposed advantage of boundary integral equation methods. It can be formulated as follows:

- For observation points above the line $y = h$ Lippmann agrees with Rayleigh's representation of the scattered field as a series expansion in terms of outgoing waves only. But for observation points below $y = h$ there exist surface current

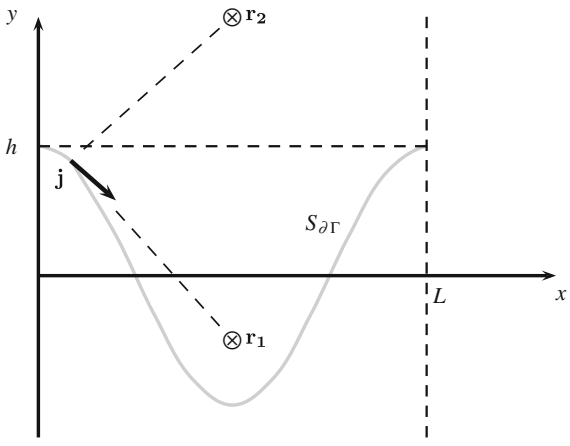

Fig. 6.4 Lippmann's criticism on Rayleigh's approach is based on the assumption that in point r_1 waves must be taken into account which move toward the surface of the grating. According to Huygens' principle, these waves stem from surface current elements j above r_1

elements located above the observation point. These elements are generating waves which move toward the surface of the grating. Ignoring those waves will result in an incomplete representation of the scattered field in such regions, but especially at the surface of the grating.

If we speak about Rayleigh's hypothesis in this subsection we have this understanding of Lippmann in mind. It is not easy to withstand his argumentation. Regarding our developed Green function formalism it means that representations (6.54) and (6.51) are not allowed in the grooves of the grating. Or, in other words, replacing $\widetilde{G}_0(\mathbf{r}, \hat{\mathbf{r}})$ in the surface integral of (6.48) by $\widetilde{G}_0^{>}(\mathbf{r}, \hat{\mathbf{r}})$ is not allowed for points in the grooves up to the surface $R(x)$. This point of view seems to be even more supported by the fact that according to (6.33) series expansion (6.34) is a valid representation of the free-space Green function in (6.54) only if $y > \hat{y}$. But this replacement was the essential step to derive the T-matrices. We should therefore not be able to present a correct solution of the scattered field in the region in question by use of a T-matrix method. Fortunately, beside his pure criticism, Lippmann provided a loophole. Using the full free-space Green function, i.e., employing equation (6.48) instead of (6.49) in the grooves up to the surface, will not suffer from his criticism. This results in the boundary integral equation discussed in Chap. 5. How does the corresponding solution scheme looks like? In contrast to (6.54) we start from the defining equation

$$G^L_{\Gamma_+}(\mathbf{r}, \mathbf{r}') \;:=\; \widetilde{G}_0^{<}(\mathbf{r}, \mathbf{r}') \;+\; \int_{S_{\partial\Gamma}} \widetilde{G}_0(\mathbf{r}, \hat{\mathbf{r}}) \cdot W^L_{S_{\partial\Gamma}}(\hat{\mathbf{r}}, \tilde{\mathbf{r}}) \cdot \widetilde{G}_0^{<}(\tilde{\mathbf{r}}, \mathbf{r}')\, dS(\hat{\mathbf{r}})\, dS(\tilde{\mathbf{r}}) \tag{6.79}$$

of the unknown interaction operator $W^L_{S_{\partial\Gamma}}$ (please, note that the upper letter "L" denotes the "Lippmann approach"!). This interaction operator can be approximated by the bilinear expansion

$$W^L_{S_{\partial\Gamma}}(\hat{\mathbf{r}}, \tilde{\mathbf{r}}) \;=\; \frac{i}{2L} \cdot \sum_{n,n'=0}^{N} \chi_n(\hat{\mathbf{r}}) \cdot \left[\Omega^L_{S_{\partial\Gamma}}\right]_{n,n'} \cdot \chi^*_{n'}(\tilde{\mathbf{r}}); \quad \hat{\mathbf{r}}, \tilde{\mathbf{r}} \in S_{\partial\Gamma} \tag{6.80}$$

with expansion functions $\chi_n(x, R(x))$ given by

$$\chi_n(x, R(x)) \;=\; \frac{\widetilde{\phi}_n(x, R(x))}{S(x)}. \tag{6.81}$$

The denominator $S(x)$ is defined in Eq. (6.47). If we insert this bilinear expansion together with series expansion (6.35) (which is now again assumed to be finite!) into (6.79) we get from the Dirichlet condition (6.42)

$$-\sum_{m'=0}^{N} \widetilde{\psi}_{m'}(x, R(x)) \cdot \widetilde{\phi}_{m'}(\mathbf{r}') = \left(\frac{i}{2L}\right) \sum_{n,n',m'=0}^{N} \int_{S_{\partial\Gamma}} \widetilde{G}_0(x, R(x); \hat{\mathbf{r}}) \cdot \frac{\widetilde{\phi}_n(\hat{\mathbf{r}})}{S(\hat{\mathbf{r}})} \cdot \left[\Omega^L_{S_{\partial\Gamma}}\right]_{n,n'} \cdot \frac{\widetilde{\phi}^*_{n'}(\tilde{\mathbf{r}})}{S(\tilde{\mathbf{r}})} \cdot \widetilde{\psi}_{m'}(\tilde{\mathbf{r}})\, dS(\hat{\mathbf{r}})\, dS(\tilde{\mathbf{r}}) \cdot \widetilde{\phi}_{m'}(\mathbf{r}')$$

$$= \frac{i}{2} \cdot \sum_{n,n',m'=0}^{N} \int_0^L \widetilde{G}_0(x, R(x); \hat{x}, R(\hat{x})) \cdot \tilde{\phi}_n(\hat{x}, R(\hat{x}))\, d\hat{x}$$
$$\cdot \left[\Omega^L_{S_{\partial\Gamma}}\right]_{n,n'} \cdot \left[B^{(\tilde{\phi},\tilde{\psi})}_{S_{\partial\Gamma}}\right]_{n',m'} \cdot \widetilde{\phi}_{m'}(\mathbf{r}'). \tag{6.82}$$

The matrix elements $\left[B^{(\tilde{\phi},\tilde{\psi})}_{S_{\partial\Gamma}}\right]_{n',m'}$ are defined according to (6.60)/(6.61) (note that the used weighting and expansion functions can be taken from the superscript brackets "$(\tilde{\phi}, \tilde{\psi})$" attached to the matrix). Next, we multiply this equation with $\widetilde{\phi}^*_m(x, R(x))$ and integrate over x. This provides

$$\sum_{m'} \left[B^{(\tilde{\phi},\tilde{\psi})}_{S_{\partial\Gamma}}\right]_{m,m'} \cdot \widetilde{\phi}_{m'}(\mathbf{r}')$$
$$= -\frac{i}{2} \sum_{n,n',m'} \left[\widetilde{G}^{(\tilde{\phi},\tilde{\phi})}_{S_{\partial\Gamma}}\right]_{m,n} \cdot \left[\Omega^L_{S_{\partial\Gamma}}\right]_{n,n'} \cdot \left[B^{(\tilde{\phi},\tilde{\psi})}_{S_{\partial\Gamma}}\right]_{n',m'} \cdot \widetilde{\phi}_{m'}(\mathbf{r}') \tag{6.83}$$

with

$$\left[\widetilde{G}^{(\tilde{\phi},\tilde{\phi})}_{S_{\partial\Gamma}}\right]_{m,n} = \frac{1}{L} \int_0^L \tilde{\phi}^*_m(x, R(x)) \cdot \widetilde{G}_0(x, R(x); \hat{x}, R(\hat{x})) \cdot \tilde{\phi}_n(\hat{x}, R(\hat{x}))\, dx\, d\hat{x}. \tag{6.84}$$

As already mentioned, the calculation of this integral provides no numerical difficulties, independent of whether representation (6.32) or (6.22) is used. Thus, we have finally the equation system (in matrix notation)

$$\mathbf{B}^{(\tilde{\phi},\tilde{\psi})}_{S_{\partial\Gamma}} = -\frac{i}{2} \cdot \widetilde{\mathbf{G}}^{(\tilde{\phi},\tilde{\phi})}_{S_{\partial\Gamma}} \cdot \mathbf{\Omega}^L_{S_{\partial\Gamma}} \cdot \mathbf{B}^{(\tilde{\phi},\tilde{\psi})}_{S_{\partial\Gamma}} \tag{6.85}$$

from which we can determine $\mathbf{\Omega}^L_{S_{\partial\Gamma}}$ according to

$$\mathbf{\Omega}^L_{S_{\partial\Gamma}} = 2\,i \left[\widetilde{\mathbf{G}}^{(\tilde{\phi},\tilde{\phi})}_{S_{\partial\Gamma}}\right]^{-1}. \tag{6.86}$$

$$G^L_{\Gamma_+}(\mathbf{r}, \mathbf{r}') = \widetilde{G}^{<}_0(\mathbf{r}, \mathbf{r}') - \frac{i}{2L} \sum_{n,n',m'=0}^{N}$$
$$\int_0^L \widetilde{G}_0(\mathbf{r}, \hat{\mathbf{r}}) \cdot \tilde{\phi}_n(\hat{\mathbf{r}})\, d\hat{x} \cdot \left[\widetilde{G}^{(\tilde{\phi},\tilde{\phi})^{-1}}_{S_{\partial\Gamma}}\right]_{n,n'} \cdot \left[B^{(\tilde{\phi},\tilde{\psi})}_{S_{\partial\Gamma}}\right]_{n',m'} \cdot \widetilde{\phi}_{m'}(\mathbf{r}') \tag{6.87}$$

and

$$u_s(\mathbf{r}) \;=\; -\sqrt{k_0}\sum_{n,n'=0}^{N}\int_0^L \widetilde{G}_0(\mathbf{r},\hat{\mathbf{r}})\cdot\tilde{\phi}_n(\hat{\mathbf{r}})\,d\hat{x}\cdot\left[\widetilde{G}_{S_{\partial\Gamma}}^{(\tilde{\phi},\tilde{\phi})^{-1}}\right]_{n,n'}\cdot\left[B_{S_{\partial\Gamma}}^{(\tilde{\phi},\tilde{\psi})}\right]_{n',0} \tag{6.88}$$

are the corresponding approximations of the Green's function and of the scattered field in Γ_+ we are interested in.

According to Lippmann's argumentation, there should be a difference between representation (6.14) with coefficients calculated according to (6.53) or (6.62), and representation (6.88) of the scattered field especially within the grooves of the grating. If this really happens will be discussed now.

6.3 Numerical Near-Field Analysis

The goals of the numerical considerations are the following:

- It will be demonstrated that there is **no difference** in the numerical results between the T-matrix approaches with weighting functions according to (6.64) and (6.68), and the approach (6.88) based on Lippmann's argumentation even in the grooves of the grating, and even beyond the found groove depth limit of $h \cdot p = 0.448$.
- It will be demonstrated that Rayleigh's original approach with weighting functions which does not fit into a least-squares scheme is able to produce accurate and stable results even in the grooves also if $h \cdot p$ exceeds the value of $h \cdot p = 0.448$. The obtained results agree with those of the boundary integral equation approach based on Lippmann's argumentation.
- It will be demonstrated that the solution based on (6.88) does not provide an analytical solution at the surface of the grating. This is what is expected since the normal derivative of the electric field exhibits a jump at the surface which is related to the induced surface current. Below the surface, the scattered field cancels the primary incident plane wave, as it should be. The T-matrix approach, on the other hand, results in a representation which is continuous across the surface but becomes divergent somewhere below it. But this divergent behaviour is meaningless for practical applications since the corresponding representation of the scattered field makes sense only above the grating as well as on its surface.

For these purposes, we have plotted the scattered field data obtained with the different approaches along the two lines depicted in Fig. 6.5 as well as along the surface of the grating. The latter was done to demonstrate the accuracy of the fulfilment of the boundary condition. The truncation parameter N and the number of expansion terms used in the approximation of the free-space Green's function in all of the performed calculations were chosen according to the requirement that the relative error of this boundary condition does not exceeds 1% along the whole surface. Concerning the boundary integral equation approach we have to fix additionally the accuracy of the surface integration which must be performed numerically, and the

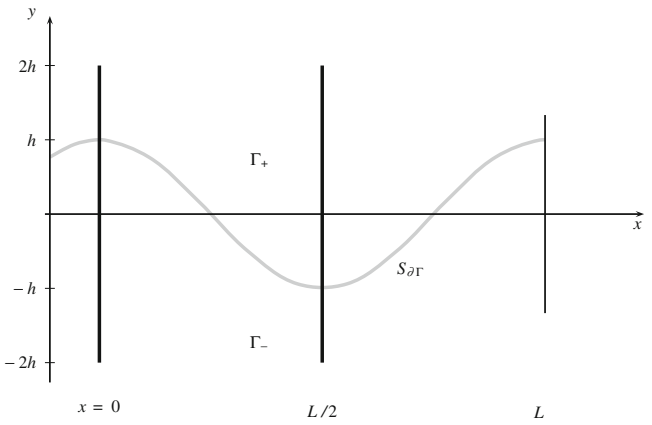

Fig. 6.5 The scattered field is plotted along the line $x = 0$ in Figs. 6.6, 6.9, and 6.12, and along the line $x = L/2$ in Figs. 6.7, 6.10, and 6.13. To verify the boundary condition the scattered field is additionally plotted along the boundary surface $S_{\partial\Gamma}$ in Figs. 6.8 and 6.11

number of expansion terms used in the representation of the full free-space Green's function $\widetilde{G}_0$. To calculate (6.84) we used a two-dimensional Gauss-Kronrod formula with a step width ensuring a relative error less than 10^{-3}. The same was done to calculate the scattered field according to (6.88) but with an one-dimensional Gauss-Kronrod formula. The number of expansion terms in the representation of $\widetilde{G}_0$ was the most sensitive parameter in these calculations. If $h \cdot p = 0.51$ was chosen it became necessary to take 200 expansion terms into account. $h \cdot p = 0.942$ required about 300 expansion terms to achieve the above mentioned accuracy of the boundary condition. A standard NAG routine was used for the necessary matrix inversion. All calculations have been performed within double precision accuracy.

All relevant parameters used in the calculations can be taken from the figure captions. Figures 6.6–6.8 demonstrate the excellent agreement between the results of Rayleigh's original approach (this corresponds to the T-matrix method with weighting functions according to (6.64)!) and the boundary integral equation method even if $h \cdot p$ exceeds the limit of 0.448 ($h \cdot p = 0.51$ in the considered case). Moreover, it can be clearly seen that the result of the boundary integral equation approach cancels the incident plane wave in Γ_-. The T-matrix results behave continuous when crossing the surface of the grating but become divergent below. In the partial figures (a) and (b) there are respectively plotted the real and imaginary parts of the different fields. The same grating was also analysed with the T-matrix approach corresponding to the least squares method (LSM), i.e., with weighting functions according to (6.68). These results were not plotted in Figs. 6.6–6.8 since differences are hardly to see. But it should be mentioned that the LSM-results have been obtained with a truncation parameter of $N = 10$. In contrast to this, $N = 18$ was needed in Rayleigh's original approach. If a grating with $h \cdot p = 0.942$ is considered no convergence could be achieved with Rayleigh's original approach but with the LSM. The results of the

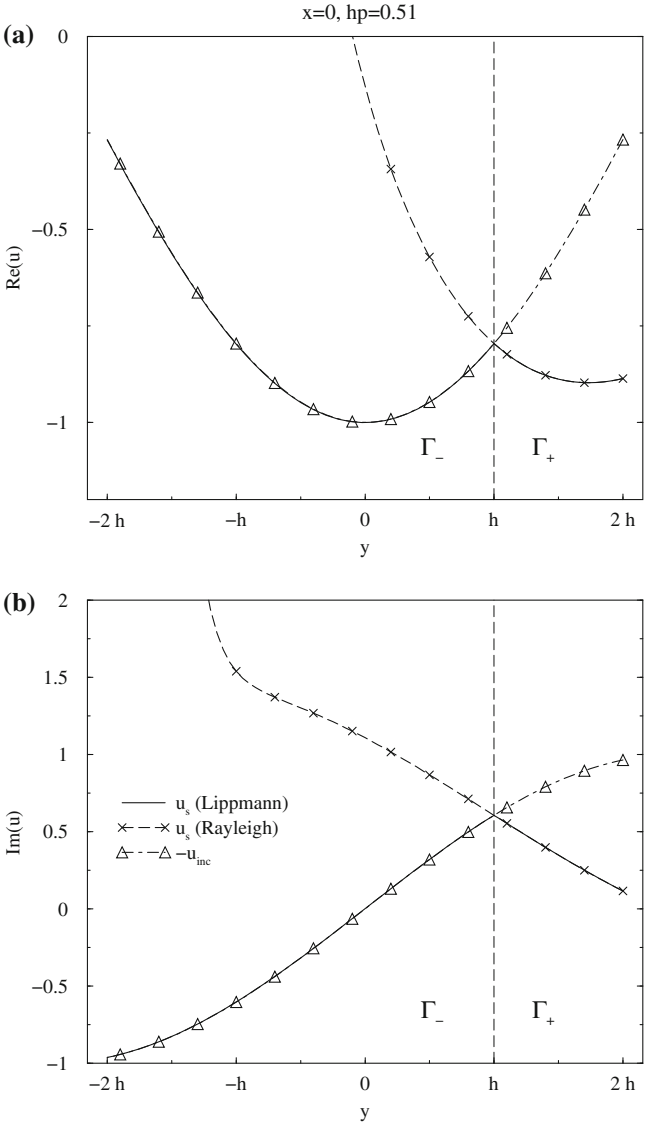

Fig. 6.6 Fields $u_s(x, y)$ and $-u_{inc}(x, y)$ (real part in **a**, imaginary part in **b**) for $h \cdot p = 0.51$ ($k_0 = 1$, $L = 8$ and $h = 0.65$) along the line $x = 0$. For the Lippmann approximation of u_s (*solid line*) $N = 10$, and for the Rayleigh approximation (*dashed line with crosses*) $N = 18$ was used. $-u_{inc}$ (*dot-dashed line with triangles*) is also plotted for comparison

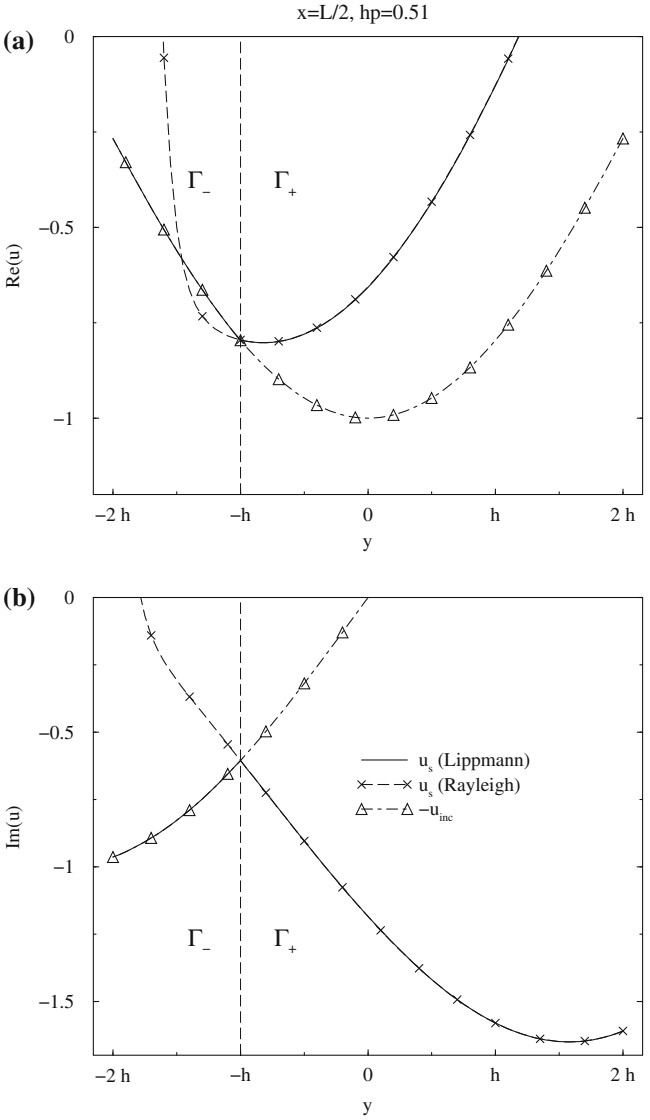

Fig. 6.7 Fields $u_s(x, y)$ and $-u_{inc}(x, y)$ (real part in **a**, imaginary part in **b**) for $h \cdot p = 0.51$ along the line $x = L/2$. The same parameters as in Fig. 6.6 are used

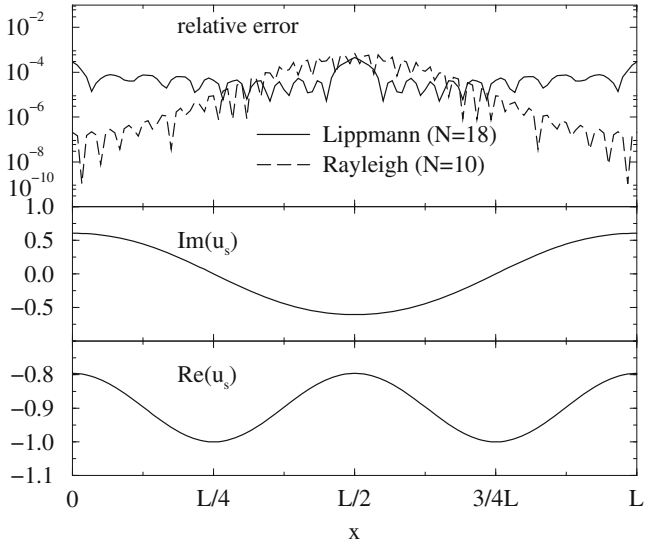

Fig. 6.8 Lippmann's and Rayleigh's approximation of the scattering field $u_s(x, R(x))$ for $h \cdot p = 0.51$ along the surface $S_{\partial\Gamma}$ (parameters: see Fig. 6.6). The relative error is calculated according to $|u_s(x, R(x)) + u_{inc}(x, R(x)|/|u_{inc}(x, R(x)|$

latter method are plotted in Figs. 6.9, 6.10 and 6.11 against the results obtained with the boundary integral equation method. We can state again an excellent agreement even if this grating exceeds the groove depth limit more then twice. In Figs. 6.12 and 6.13, it is shown that the series expansion of the scattered field based on the LSM seems to diverge in Γ_- but at different locations along the lines $x = 0$ and $x = L/2$. It should be also mentioned that it is more difficult to achieve convergence in the near-field than for the scattering quantities in the far-field. $h \cdot p = 0.942$ was the upper limit we were able to treat within double precision accuracy for the earlier mentioned criterion of the fulfilment of the Dirichlet boundary condition.

6.4 Summary

At the end of this chapter, we want to summarize its main results. Two different approaches were considered to solve the scattering problem of a p-polarized plane wave perpendicularly incident on an ideal metallic and periodic grating. One of this approach is the T-matrix approach based on Huygens' principle in the form of (6.54). This approach was numerically accomplished with two different types of weighting functions belonging to Rayleigh's original solution scheme and to a least-squares scheme. The other approach starts from Huygens' principle according to (6.79) and results in a conventional boundary integral equation. Even if the usage of (6.54)

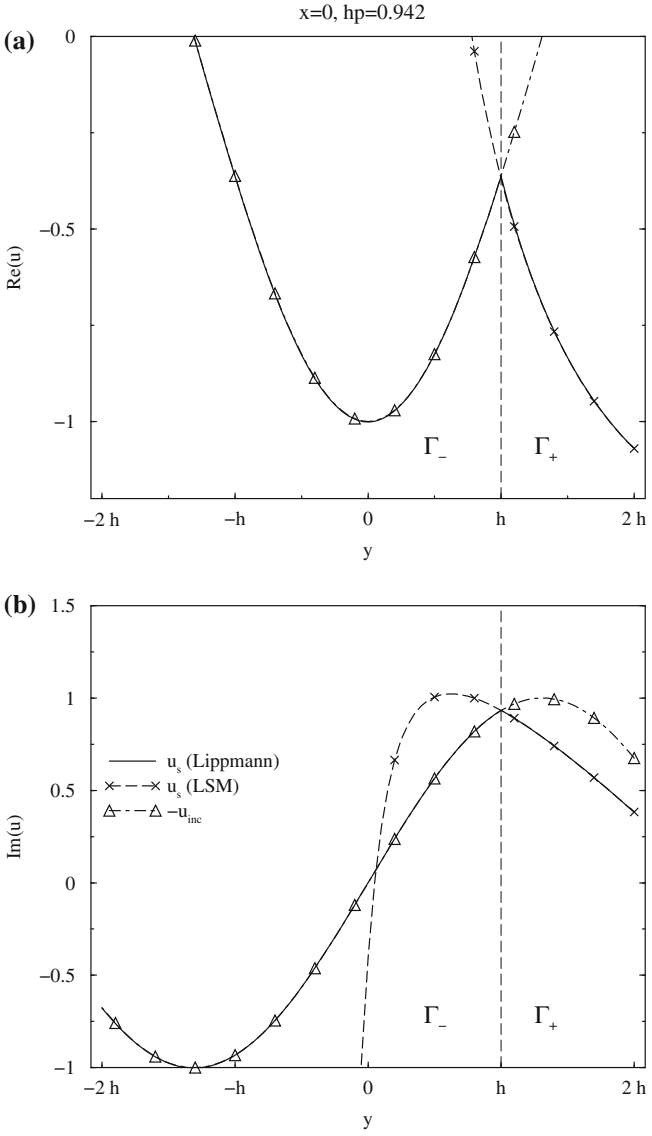

Fig. 6.9 Fields $u_s(x, y)$ and $-u_{inc}(x, y)$ (real part in **a**, imaginary part in **b**) for $h \cdot p = 0.942$ ($k_0 = 1$, $L = 8$ and $h = 1.2$) along the line $x = 0$. For the Lippmann approximation of u_s (*solid line*) $N = 12$, and for the least-squares approximation (*dashed line with crosses*) $N = 18$ was used. $-u_{inc}$ (*dot-dashed line with triangles*) is also plotted for comparison

especially in the grooves of the grating appears incomplete and has to be replaced by expression (6.79) according to Lippmann's point of view it turned out that the results of both approaches agree very well even in the near-field up to the boundary surface

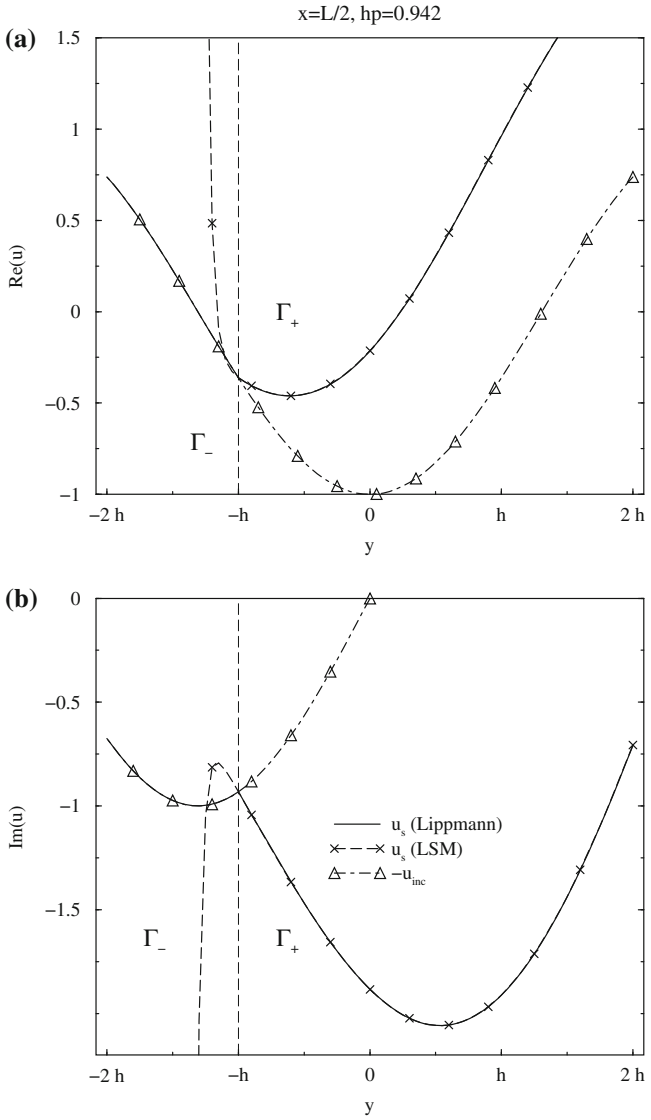

Fig. 6.10 Fields $u_s(x, y)$ and $-u_{inc}(x, y)$ (real part in **a**, imaginary part in **b**) for $h \cdot p = 0.942$ along the line $x = L/2$. The same parameters as in Fig. 6.9 are used

of the grating. This holds also for gratings which exceed the found groove depth limit of $h \cdot p = 0.448$. This limit represents essentially a limit of the applicability of conventional point matching methods. It was moreover shown that Rayleigh's original approach is not a conventional point matching method, as it was and is still assumed in several papers. The obtained results are our numerical justification for

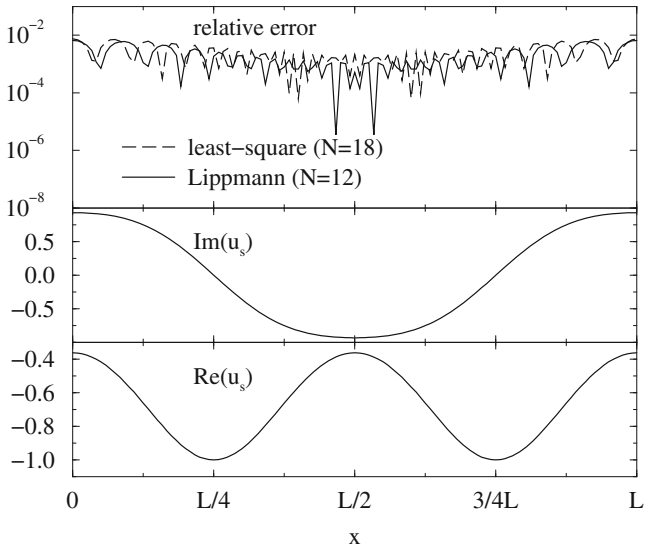

Fig. 6.11 Lippmann's and Rayleigh's approximation of the scattering field $u_s(x, R(x))$ for $h \cdot p = 0.942$ along the surface $S_{\partial\Gamma}$ (parameters: see Fig. 6.9). The relative error is calculated according to $|u_s(x, R(x)) + u_{inc}(x, R(x)|/|u_{inc}(x, R(x)|$

looking at (6.54) and (6.79) as two equivalent starting points for solving scattering problems not only in the far-field but also in the near-field.

Regarding Rayleigh's hypothesis in conjunction with the scattering problem of three-dimensional objects in spherical coordinates the region of interest is bounded by the scatterer surface and the smallest spherical surface circumscribing the scatterer (see Fig. 6.14). According to Lippmann's argumentation, if expanding the scattered field in observation point x_1, for example, one has to take not only the radiating eigensolutions (2.58) or (2.112)/(2.123) into account but also the incoming eigensolutions (2.59) or (2.124)/(2.125). If we are interested to calculate the relevant Green functions of a three-dimensional, ideal metallic scatterer this means that we have to start with (5.79) or (5.172) instead of (4.1) or (4.23). However, in view of the above obtained results we may expect that both starting points are also equivalent in spherical coordinates. But the numerical proof of this assumption is still outstanding, to the best of our knowledge. Wouldn't it be a nice Ph.D. work? There is another aspect of importance in this context. In the literature dealing with the T-matrix approach one can find the statement that the EBC-based T-matrix is not affected by Rayleigh's hypothesis. This assumption is based on the fact that the scattered field is not needed in the critical region, as it can be seen from our discussion of the EBCM in Sect. 5.2.1. And outside the smallest spherical surface circumscribing the scatterer there is consensus that the expansion of the scattered field in terms of radiating eigenfunctions only is correct. But this point of view clearly excludes the usage of the T-matrix methods from calculating the scattered field inside the critical region. According to

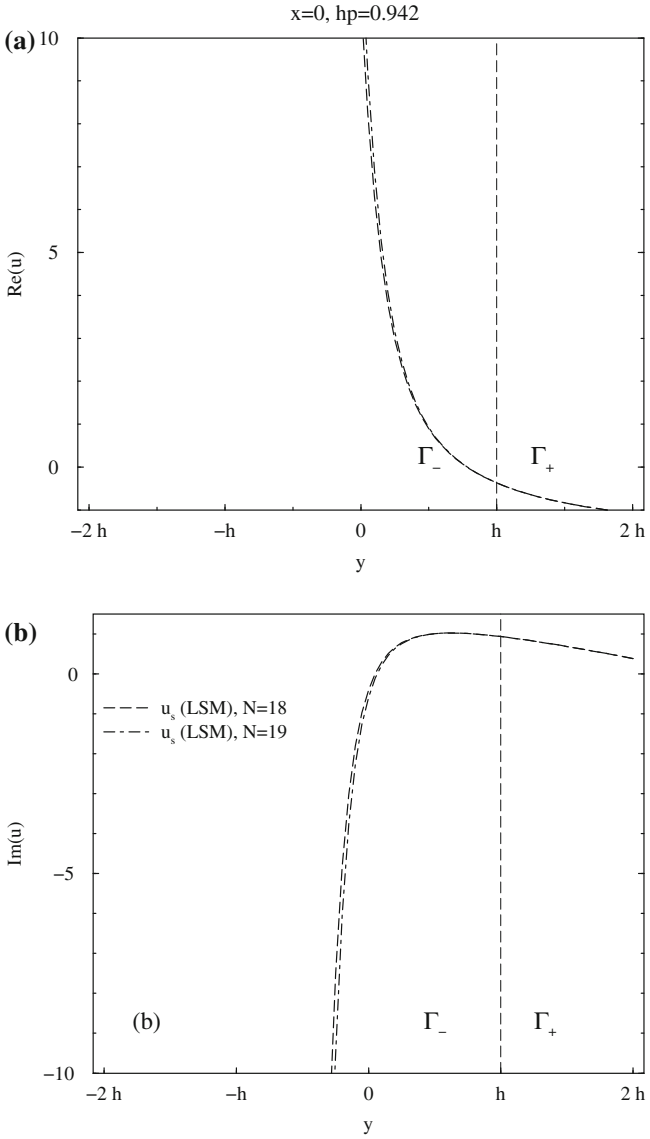

Fig. 6.12 Least-square approximations of u_s at $h \cdot p = 0.942$ (see Fig. 6.9 for details) for two consecutive truncation parameters N along the line $x = 0$ (N = 18-*dashed*, N = 19 *dot-dashed*)

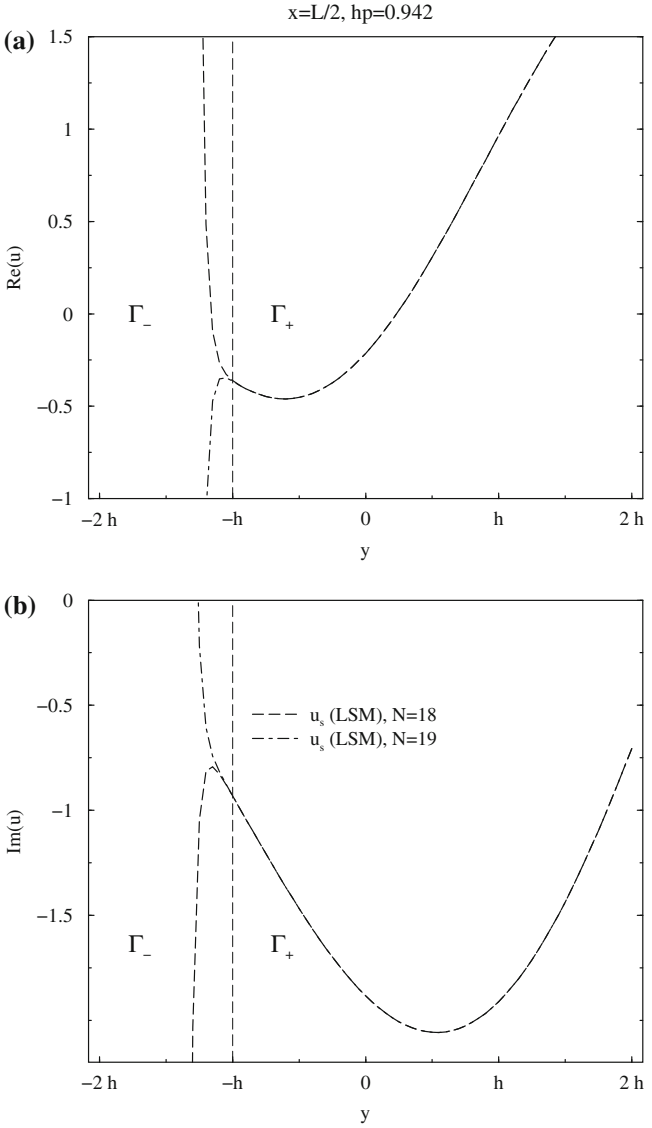

Fig. 6.13 Least-square approximations of u_s at $h \cdot p = 0.942$ (see Fig. 6.9 for details) for two consecutive truncation parameters N along the line $x = L/2$ (N = 18 *dashed*, N = 19-*dot-dashed*)

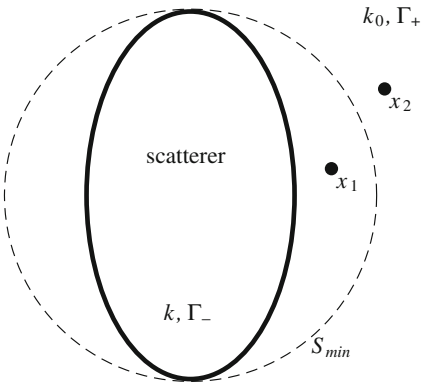

Fig. 6.14 Regarding the problem of Rayleigh's hypothesis in spherical coordinates the outer region bounded by the scatterer surface and the smallest spherical surface S_{min} circumscribing the scatterer is the region of interest

this understanding, it can only be applied to the region outside the smallest spherical surface circumscribing the scatterer. But then the EBC method is after all affected by Rayleigh's hypothesis since this hypothesis restricts its range of applicability. In contrast to this assumption the obtained results of this chapter indicate that one can generally apply the T-matrix methods everywhere in Γ_+, the critical region included.

Chapter 7
Physical Basics of Electromagnetic Wave Scattering

7.1 Introduction

In all the foregoing chapters, we have tacitly assumed that the scalar Helmholtz and the vector wave equation are the partial differential equations underlying the scattering problems. In Sect. 7.2 we will provide the justification for this assumption for electromagnetic wave scattering. Starting from Maxwell's equations, we will discuss the physical constraints resulting in these partial differential equations. This includes a short course in conventional Mie Theory as formulated by Debye. By use of definition (5.79) we will moreover derive a boundary integral equation to calculate the induced surface current at the surface of a three-dimensional, ideal metallic scatterer. This boundary integral equation is already known in the literature. As already mentioned in Sect. 5.4, this equation avoids the strong singularity of the free-space Green function appearing in (5.105) if the dyadic case is considered. It is demonstrated later how one can transfer this solution scheme to calculate the corresponding Green functions.

The next section is concerned with the definition of selected scattering quantities we will use in the numerical simulations of Chap. 9. Starting from an appropriate representation of the fields the scattering quantities will be derived. They form the essential link between theory and experiment. In this section, we pursue the goal to emphasize the importance and implications of the far-field region and the plane wave as the primary incident field in the theory of electromagnetic wave scattering as well as in the related experiments. Using a plane wave as the primary incident field allow us to winnow the scattering problem from the more general diffraction problem . The latter considers any primary incident field generated from a source $\vec{\rho}(\mathbf{x})$ which is located somewhere in Γ_+ but within a finite distance from the scatterer. Moreover, it does not ask exclusively for the scattered field in the far-field region.

The scalability of the scattering problem is the content of the last section. "Scalability" expresses the fact that the scattering properties of a given object are only dependent on the ratio of a certain parameter characterizing its geometry (the radius of the volume equivalent sphere, for example) and the wavelength of the primary

T. Rother and M. Kahnert, *Electromagnetic Wave Scattering on Nonspherical Particles*, Springer Series in Optical Sciences 145, DOI: 10.1007/978-3-642-36745-8_7,

incident plane wave. This behaviour will allow us to define the so-called "size parameter". This parameter can be of some benefit. It provides an appropriate scaling parameter, for example, if one is interested in establishing a scattering database. Such a database of precalculated scattering quantities will be presented in Chap. 9. The scalability is moreover the underlying principle of the microwave analogue to light scattering measurements.

This chapter could have been placed at the beginning of this book as a physical motivation. Placing the more mathematical and methodical aspects prior to the physical aspects of electromagnetic wave scattering to emphasize the generalizability of the former also to other problems was the authors' reason which opposes this choice. Such other problems are the electromagnetic resonance problem indicated in Sect. 5.2.1, for example. The solution of the Schroedinger equation related to a constant potential inside a finite region with an infinitely large potential barrier at its boundary is another example from Quantum Mechanics. Similar problems in other physical disciplines can be found in the two volumes of Morse and Feshbach cited in Sect. 10.3. It should also be mentioned that the Green's function formalism developed in Chap. 4 is not only restricted to the Helmholtz or vector wave equation. It can be generalized to other linear partial differential equations as well.

7.2 The Electromagnetic Scattering Problems

Maxwell's equations together with the required boundary conditions are our starting point. Here, we are especially interested in studying the physical situations which can be related to the outer Dirichlet and transmission problem introduced in Chap. 1. In what follows, we will discuss two equivalent ways to derive the governing equations of the electromagnetic fields. One way leads directly to the vector wave equation. The other way employs the so-called "Debye potentials". It ends up with two scalar Helmholtz equations for each of the potentials. The latter way is the usual way one can find in the literature to represent the conventional Mie theory for plane wave scattering on spherical particles.

7.2.1 Maxwell's Equations and Boundary Conditions

Let us begin with some general remarks which are of importance for a better understanding of the different but equivalent pictures used in classical Electrodynamics to describe a problem, and for certain discussions concerning the relation between theory and experiment. Maxwell's equations present a set of pure phenomenological equations to describe the behaviour of the electromagnetic fields in a certain region. The electromagnetic fields as well as the regions in which the fields exist are considered to be continuously varying quantities. The material properties of the regions (the dielectric properties in our case) must be given, and cannot be derived

within Electrodynamics itself. Determining such material properties requires, in fact, a recourse to a microscopical theory like Quantum Statistics or the more classical oscillator models like the Lorentz model. For example, there is an important relation between the real and imaginary part of the dielectric constant known as the Kramers-Kronig relation. It can be derived from the causality principle and the fluctuation-dissipation theorem of statistical mechanics. This relation has to be taken into account if one wants to infer the dielectric properties of a scatterer from scattering measurements. The reader who is interested in such aspects is referred to the book of Bohren and Huffman cited in Sect. 10.9. There, he can find a detailed and exciting representation of how to get the optical constants which are of importance in electromagnetic wave scattering. Moreover, classical Electrodynamics says nothing about the nature of the primary sources generating the electromagnetic fields. Even if the sources are usually named with "free charges" or "impressed currents" questions concerning their nature must be shifted to Particle Physics. In other words, Maxwell's equations are "just" a description of the action (the fields) but not of the causes (the sources). But that is what we can find in other physical theories as well. On the other hand, there exist "induced sources" (the "induced surface current" introduced in Chap. 5, for example) which are equivalent quantities to the considered fields. The relation between the induced sources and the fields are governed by interaction principles like Huygens' principle. Those principles express our experience that we can describe the result of an interaction with a certain object by replacing this object by appropriate "induced sources". This point of view was already the staring point for the derivation of the boundary and volume integral equations in Chap. 5.

To narrow down the physical situation to become treatable by the Helmholtz or vector wave equation we have to make the following assumptions :

- We consider only the steady-state of scattering with an assumed time dependence of $e^{-i\omega t}$. According to this choice of time dependence we have

$$\vec{E} \;=\; \vec{E}_0 \cdot e^{i(k_0 z - \omega t)} \tag{7.1}$$

as a representation of a plane wave travelling along the positive z-axis.

$$\omega \;=\; \frac{2\pi}{T} \;=\; 2\pi\nu \tag{7.2}$$

denotes the angular frequency, and k_0 is the wave number in vacuum. Characterizing the absorptivity of the scatterer by a complex refractive index n with a positive imaginary part, i.e. by

$$n \;=\; n_r \;+\; i n_i; \quad n_i \geq 0 \tag{7.3}$$

is a further consequence of the chosen time dependence. A nonabsorbing material is thus characterized by $n_i = 0$. The relation between the refractive index and the permittivity is given by

$$n \;=\; \sqrt{\epsilon}. \tag{7.4}$$

The time dependence $e^{-i\omega t}$ will be suppressed throughout the ongoing derivations. This term can be added to the final result, but it is of no importance for the definition of the scattering quantities since these are related to the intensities of the fields. It should be mentioned that a time dependence of $e^{+i\omega t}$ is sometimes used in the literature. In this case, we have to choose $n_i \leq 0$ for an absorbing material! This may cause some confusion especially if the time dependence is not clearly indicated.

- We consider electromagnetic wave scattering only on single, homogeneous and isotropic scatterers with no impressed sources inside. The magnetic permeability μ_0 is that of vacuum. The open region Γ_+ outside the scattering particle is that of a free-space characterized by ϵ_0—the permittivity of vacuum.
- As frequently mentioned in the foregoing chapters, we place the impressed source $\vec{\rho}(\mathbf{x})$ of the primary incident field generally outside the smallest spherical surface circumscribing the scatterer. To treat the special plane wave scattering problem we have to impose a further restriction on the location of this source, as we will see shortly. There is also the possibility to ignore the source and to consider the incident plane wave as an a priory given quantity. The latter possibility expresses the fact that the plane wave is a solution of the homogeneous Helmholtz or vector wave equation, as already mentioned at the end of Sect. 3.3.1.
- We consider only weak electromagnetic fields, i.e., the fields inside the scatterer do not change its dielectric properties. Concerning the more general diffraction problem it is also assumed that the scattered field has no influence on the primary source generating the primary incident field.

Provided that these assumptions hold Maxwell's equations can be reduced to

$$\nabla \times \vec{E}(\mathbf{x}) = i\omega \vec{B}(\mathbf{x}) \tag{7.5}$$

$$\nabla \times \vec{H}(\mathbf{x}) = -\, i\omega \vec{D}(\mathbf{x}) \;+\; \vec{\rho}(\mathbf{x}) \tag{7.6}$$

$$\nabla \cdot \vec{D}(\mathbf{x}) = 0 \tag{7.7}$$

$$\nabla \cdot \vec{B}(\mathbf{x}) = 0. \tag{7.8}$$

These equations must be supplemented with the two constitutive relations

$$\vec{D}(\mathbf{x}) = \epsilon\, \vec{E}(\mathbf{x}) \;=\; \epsilon_0\, \epsilon_r\, \vec{E}(\mathbf{x}) \tag{7.9}$$

$$\vec{B}(\mathbf{x}) = \mu_0\, \vec{H}(\mathbf{x}). \tag{7.10}$$

$\vec{E}$ and $\vec{H}$ are the electric and magnetic field in units of $[V/m]$ and $[A/m]$. $\vec{D}$ and $\vec{B}$ are the electric displacement and the magnetic flux density. For the absolute permittivity and magnetic permeability of vacuum we have in SI units

$$\epsilon_0 \;=\; \frac{10^7}{4\pi c_0^2} \quad \left[\frac{As}{Vm}\right] \tag{7.11}$$

$$\mu_0 \;=\; 4\pi \cdot 10^{-7} \quad \left[\frac{Vs}{Am}\right] \tag{7.12}$$

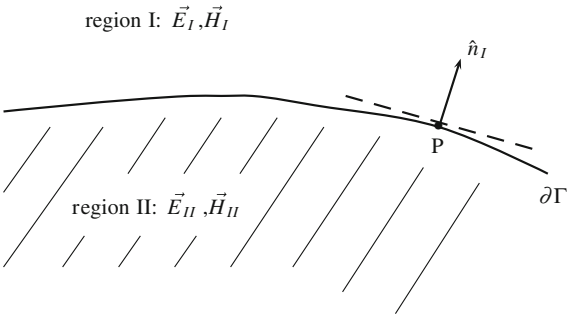

Fig. 7.1 Behaviour of the tangential field components at the boundary layer $\partial\Gamma$ between two regions with different dielectric properties

with c_0 being the vacuum speed of light. The wave number k_0 in (7.1) is related to the wavelength λ by

$$k_0 = \sqrt{\omega^2 \cdot \epsilon_0 \cdot \mu_0} = \frac{(2\pi)}{\lambda}. \tag{7.13}$$

Beside the Maxwell equations and the constitutive relations we need to know the behaviour of the field components across the boundary layer between two regions with different dielectric properties (see Fig. 7.1). These boundary conditions are also formulated on the basis of our experimental experience with electromagnetic fields. They cannot be derived within Electrodynamics even if the integral formulation of Maxwell's equations creates this impression (see the detailed discussion of this aspect in the book of Tai cited in Sect. 10.3). Here, we are especially interested in the following two cases:

1. Region II consists of an ideal metallic material. In this case we have

$$\hat{n}_I \times \vec{E}_I(\mathbf{x}) = 0; \quad \mathbf{x} \in \partial\Gamma, \tag{7.14}$$

i.e., the tangential components of the electric field become zero at the boundary layer $\partial\Gamma$. $\hat{n}_I$ is the unit normal vector pointing into region I. This is the sufficient boundary condition to treat the scattering problem on an ideal metallic object. It is thus related to the outer Dirichlet problem. Once the electric field is known we can calculate the magnetic field from (7.5) and (7.10). Contrary to the electric field, the tangential components of the magnetic field do not vanish at the boundary layer $\partial\Gamma$. The jump of these components at this surface provides the induced surface current $\vec{J}_{\partial\Gamma}$. Thus, we have

$$\hat{n}_I \times \vec{H}_I(\mathbf{x}) = \vec{J}_{\partial\Gamma}(\mathbf{x}); \quad \mathbf{x} \in \partial\Gamma, \tag{7.15}$$

as the relevant boundary condition of the tangential components of the magnetic field. But it should be emphasized again that in view of the sufficient boundary condition (7.14) $\vec{H}_I$ and $\vec{J}_{\partial\Gamma}$ are secondary quantities, i.e., they can be calculated from the known electric field. However, choosing condition (7.15) as the basic

condition represents another picture to describe scattering on an ideal metallic object. It will be considered in more detail in the next subsection. $\vec{J}_{\partial\Gamma}$ is the unknown quantity in this picture which can be calculated from boundary integral equations similar to those derived in Chap. 5. This is just one example of the different representations of one and the same problem which result into different solution schemes.

2. Regions I and II consist of two different dielectric materials. In this case, we have

$$\hat{n}_I \times \left[\vec{E}_I(\mathbf{x}) - \vec{E}_{II}(\mathbf{x})\right] = 0; \quad \mathbf{x} \in \partial\Gamma \tag{7.16}$$

$$\hat{n}_I \times \left[\vec{H}_I(\mathbf{x}) - \vec{H}_{II}(\mathbf{x})\right] = 0; \quad \mathbf{x} \in \partial\Gamma\ , \tag{7.17}$$

i.e., the tangential components of the electric and magnetic field must behave continuously across the boundary layer. Taking Maxwell's equations (7.5) and (7.10) into account we may write instead of (7.17)

$$\hat{n}_I \times \left[\nabla \times \vec{E}_I(\mathbf{x}) - \nabla \times \vec{E}_{II}(\mathbf{x})\right] = 0; \quad \mathbf{x} \in \partial\Gamma. \tag{7.18}$$

The dielectric scattering problem is therefore related to the outer transmission problem. "Outer" problem because the primary source is located somewhere outside the scatterer, according to our initial assumptions.

Maxwell's equations (7.5–7.10) are not independent of each other. That is, there is no need to determine all the 12 components of the $\vec{E}$-, $\vec{H}$-, $\vec{D}$-, and $\vec{B}$-fields. Due to the constitutive relations (7.9) and (7.10) there remain at first only the 6 unknown components of the $\vec{E}$- and $\vec{H}$-field, for example. But because of relations (7.5) and (7.6) there is also a relation between the $\vec{E}$- and $\vec{H}$-field. Thus, we have to calculate only the 3 components of the $\vec{E}$- or the $\vec{H}$-field. Furthermore, since the scattered field is free of sources, we need to know only 2 components of the scattered electric field, due to relation (7.7). Thus, there remain finally 2 unknown field components we have to determine to solve the scattering problem. Two possible approaches will be considered in the next two subsections. By the way, the necessity to determine 2 unknown components to solve the electromagnetic scattering problem is also reflected in the additional τ-summation $\sum_{\tau=1}^{2}$ used in the foregoing chapters if the vectorial or dyadic problem was considered.

7.2.2 Vector Wave Equations of the Electromagnetic Fields

The vector wave equations for the electric as well as the magnetic field can be derived in a straightforward way by applying the *curl* operation ($\nabla\times$) to either of Maxwell's equations (7.5) and (7.6), and in conjunction with the constitutive relations (7.9) and (7.10). In doing so, we obtain immediately

$$\nabla \times \nabla \times \vec{E}(\mathbf{x}) \;=\; i\omega\mu_0\, \nabla \times \vec{H}(\mathbf{x}) \;=\; i\omega\mu_0 \left[-i\omega\epsilon_0\, \vec{E}(\mathbf{x})\right] \;+\; i\omega\mu_0\, \vec{\rho}(\mathbf{x}) \tag{7.19}$$

for the electric field. Applying (7.13) this equation becomes

$$\nabla \times \nabla \times \vec{E}(\mathbf{x}) \;-\; k_0^2\, \vec{E}(\mathbf{x}) \;=\; i\omega\mu_0\, \vec{\rho}(\mathbf{x}). \tag{7.20}$$

The corresponding vector wave equation for the magnetic field reads

$$\nabla \times \nabla \times \vec{H}(\mathbf{x}) \;-\; k_0^2\, \vec{H}(\mathbf{x}) \;=\; \nabla \times \vec{\rho}(\mathbf{x}). \tag{7.21}$$

Both equations differ only in the inhomogeneity on the right-hand side. The general expression (2.232) of a plane wave as well as the special plane wave given by (2.198) are solutions of the homogeneous vector wave equation (7.20). In Sect. 2.6.3, in conjunction with (2.332), we could see on the other hand that a certain choice of the primary source $\vec{\rho}(\mathbf{x}')$ is also able to generate a plane wave at the location of the scatterer.

What do we know already about the possibilities to solve the vector wave equation?

From (2.348), with $\mathbf{G}_{\mathbf{\Gamma}_+}$ according to (4.27), and with the matrix elements (4.29) we are able to calculate the total electric field outside an ideal metallic scatterer within the T-matrix approach, for example. On the other hand, representation (2.349), $\mathbf{G}^{(\mathbf{d})}_{\mathbf{\Gamma}_+}$ according to (4.35), and matrix elements (4.37) are needed to calculate the total electric field outside a dielectric scatterer within the T-matrix approach. Explicit expressions for T-matrix of an ideal metallic scatterer (or, equivalently, the matrix elements of the corresponding interaction operator $\mathbf{W}_{\partial\mathbf{\Gamma}_+}$) could be derived from Huygens' principle (5.172) and the boundary condition (7.14) of the electric field. The two tangential components of the scattered electric field at the scatterer surface are therefore the two unknown and independent components in this solution scheme. Once we know these two components all other field components can be calculated later not only at the scatterer surface but everywhere outside the scatterer, as we have already demonstrated in Chap. 3. We can do the same, in principle, with Huygens' principle (5.172) which provides us with a boundary integral equation for the electric field. This way was described in Sect. 5.4.1 for the scalar case of the outer Dirichlet problem. However, in the vectorial case we have to take the stronger singularity of the dyadic free-space Green function into account . Hence, using boundary condition (7.15) of the magnetic field as the basic condition instead of condition (7.14) will be the better choice. Then the induced surface current $\vec{J}_{\partial\Gamma}$ becomes the unknown quantity. To demonstrate that this will indeed ease the treatment of the stronger singularity let us consider the solution of the vectorial scattering problem on an ideal metallic object in terms of boundary integral equations.

We start from representation (5.172) of the Green function $\mathbf{G}_{\mathbf{\Gamma}_+}$ subject to the boundary condition (2.342). Then, we may write for the total electric field

$$\vec{E}_t(\mathbf{x}) = \int_{\Gamma_+} \mathbf{G}_{\mathbf{\Gamma}_+}(\mathbf{x},\mathbf{x}') \cdot \vec{\rho}(\mathbf{x}')\, dV(\mathbf{x}')$$
$$= \vec{E}_{inc}(\mathbf{x}) + \oint_{\partial\Gamma} \mathbf{G_0}(\mathbf{x},\bar{\mathbf{x}}) \cdot \widehat{\mathbf{W}}_{\partial\mathbf{\Gamma}_+}(\bar{\mathbf{x}},\tilde{\mathbf{x}}) \cdot \vec{E}_{inc}(\tilde{\mathbf{x}})\, dS(\bar{\mathbf{x}})\, dS(\tilde{\mathbf{x}}). \quad (7.22)$$

Here,

$$\vec{E}_{inc}(\mathbf{x}) = \int_{\Gamma_+} \mathbf{G_0}(\mathbf{x},\mathbf{x}') \cdot \vec{\rho}(\mathbf{x}')\, dV(\mathbf{x}') \quad (7.23)$$

represents the primary incident field generated by the given source $\vec{\rho}(\mathbf{x}')$. By use of (7.5), if applied to (7.22), we obtain for the corresponding magnetic field

$$\vec{H}_t(\mathbf{x}) = \vec{H}_{inc}(\mathbf{x}) - \frac{i}{\omega\mu_0} \cdot \nabla_{\mathbf{x}} \times \oint_{\partial\Gamma} \mathbf{G_0}(\mathbf{x},\bar{\mathbf{x}}) \cdot \widehat{\mathbf{W}}_{\partial\mathbf{\Gamma}_+}(\bar{\mathbf{x}},\tilde{\mathbf{x}}) \cdot \vec{E}_{inc}(\tilde{\mathbf{x}})\, dS(\bar{\mathbf{x}})\, dS(\tilde{\mathbf{x}}). \quad (7.24)$$

The induced surface current is introduced via the definition

$$\vec{J}_{\partial\Gamma}(\bar{\mathbf{x}}) := -\frac{i}{\omega\mu_0} \cdot \oint_{\partial\Gamma} \widehat{\mathbf{W}}_{\partial\mathbf{\Gamma}_+}(\bar{\mathbf{x}},\tilde{\mathbf{x}}) \cdot \vec{E}_{inc}(\tilde{\mathbf{x}})\, dS(\tilde{\mathbf{x}}). \quad (7.25)$$

Since the interaction operator $\widehat{\mathbf{W}}_{\partial\mathbf{\Gamma}_+}$ was defined to exist only in the tangential plane at the scatterer surface (see Chap. 4) the same holds for the induced surface current. The latter differs from definition (5.103) used in the scalar case by the prefactor $-i/(\omega\mu_0)$. This prefactor ensures that the surface current $\vec{J}_{\partial\Gamma}$ is equipped with the correct unit of $[A/m]$. Now, in terms of the induced surface current (7.24) becomes

$$\vec{H}_t(\mathbf{x}) = \vec{H}_{inc}(\mathbf{x}) + \nabla_{\mathbf{x}} \times \oint_{\partial\Gamma} \mathbf{G_0}(\mathbf{x},\bar{\mathbf{x}}) \cdot \vec{J}_{\partial\Gamma}(\bar{\mathbf{x}})\, dS(\bar{\mathbf{x}}). \quad (7.26)$$

By use of relation (2.335) this expression can be rewritten into

$$\vec{H}_t(\mathbf{x}) = \vec{H}_{inc}(\mathbf{x}) - \oint_{\partial\Gamma} \vec{J}_{\partial\Gamma}(\bar{\mathbf{x}}) \times \nabla_{\mathbf{x}} G_0(\mathbf{x},\bar{\mathbf{x}})\, dS(\bar{\mathbf{x}}). \quad (7.27)$$

In the next step, coming from region I (regarding the scattering problem this corresponds to the outer region Γ_+!), we move the observation point $\mathbf{x}$ toward the boundary surface. The resulting expression is then projected onto the tangential plane at the scatterer surface by vectorial multiplication of both sides with $\hat{n}_I \times$. Thus, we obtain

$$\hat{n}_I \times \vec{H}_t(\mathbf{x}) = \hat{n}_I \times \vec{H}_{inc}(\mathbf{x}) - \hat{n}_I \times \oint_{\partial\Gamma} \vec{J}_{\partial\Gamma}(\bar{\mathbf{x}}) \times \nabla_{\mathbf{x}} G_0(\mathbf{x},\bar{\mathbf{x}})\, dS(\bar{\mathbf{x}}). \quad (7.28)$$

The second contribution on the right-hand side of this equation contains the singularity at point $\mathbf{x} = \bar{\mathbf{x}}$. Please, note also that the unit normal vector $\hat{n}_I$ applies to the variable $\mathbf{x}$ located at the scatterer surface. To treat the singularity we make use of identity

$$\hat{n} \times (\vec{a} \times \vec{b}) \;=\; (\hat{n} \cdot \vec{b})\vec{a} \;-\; (\hat{n} \cdot \vec{a})\vec{b}. \tag{7.29}$$

Applying it to (7.28) results into

$$\begin{aligned} \hat{n}_I \times \vec{H}_t(\mathbf{x}) = \hat{n}_I \times \vec{H}_{inc}(\mathbf{x}) - \oint_{\partial\Gamma} \frac{\partial G_0(\mathbf{x}, \bar{\mathbf{x}})}{\partial \hat{n}_I} \cdot \vec{J}_{\partial\Gamma}(\bar{\mathbf{x}})\, dS(\bar{\mathbf{x}}) \\ + \oint_{\partial\Gamma} \left[\hat{n}_I \cdot \vec{J}_{\partial\Gamma}(\bar{\mathbf{x}})\right] \cdot \nabla_{\mathbf{x}} G_0(\mathbf{x}, \bar{\mathbf{x}})\, dS(\bar{\mathbf{x}}). \end{aligned} \tag{7.30}$$

Both boundary integrals on the right-hand side can be decomposed by use of (5.81) into two parts with respect to the two surface areas "$\partial\Gamma - \partial\Gamma_\delta$" and "$\partial\Gamma_\delta$". Regarding $\partial\Gamma_\delta$ (please, have in mind that this boundary surface element encloses the singularity!) the unit normal vector $\hat{n}_I$ can be considered to be perpendicularly oriented with respect to the induced surface current element existing on this small boundary surface element. This is justified by the fact that we can replace $\vec{J}_{\partial\Gamma}(\bar{\mathbf{x}})$ approximately by $\vec{J}_{\partial\Gamma}(\mathbf{x})$ since both variables $\mathbf{x}$ and $\bar{\mathbf{x}}$ are elements of $\partial\Gamma_\delta$. Hence, expression

$$\oint_{\partial\Gamma_\delta} \left[\hat{n}_I \cdot \vec{J}_{\partial\Gamma}(\bar{\mathbf{x}})\right] \cdot \nabla_{\mathbf{x}} G_0(\mathbf{x}, \bar{\mathbf{x}})\, dS(\bar{\mathbf{x}}) \tag{7.31}$$

becomes zero, and only the part

$$\oint_{\partial\Gamma_\delta} \frac{\partial G_0(\mathbf{x}, \bar{\mathbf{x}})}{\partial \hat{n}_I} \cdot \vec{J}_{\partial\Gamma}(\bar{\mathbf{x}})\, dS(\bar{\mathbf{x}}) \tag{7.32}$$

remains. But its contribution can be calculated along the way described in Sect. 5.4.2. In doing so we have only to take into account that, in contrast to (5.106), $\hat{n}_I = -\hat{n}_-$ holds now for the unit normal vector $\hat{n}_I$. Due to this difference $\pm f(\mathbf{x})/2$ on the right-hand side of (5.108) must be simply replaced by $\mp\vec{J}_{\partial\Gamma}(\mathbf{x})/2$. Thus, if $\mathbf{x}$ approaches the scatterer surface from outside, we get

$$\begin{aligned} \hat{n}_I \times \vec{H}_t(\mathbf{x}) = \hat{n}_I \times \vec{H}_{inc}(\mathbf{x}) \;+\; \frac{\vec{J}_{\partial\Gamma}(\mathbf{x})}{2} - p.v. \oint_{\partial\Gamma} \frac{\partial G_0(\mathbf{x}, \bar{\mathbf{x}})}{\partial \hat{n}_I} \cdot \vec{J}_{\partial\Gamma}(\bar{\mathbf{x}})\, dS(\bar{\mathbf{x}}) \\ + \oint_{\partial\Gamma} \left[\hat{n}_I \cdot \vec{J}_{\partial\Gamma}(\bar{\mathbf{x}})\right] \cdot \nabla_{\mathbf{x}} G_0(\mathbf{x}, \bar{\mathbf{x}})\, dS(\bar{\mathbf{x}}) \end{aligned} \tag{7.33}$$

or, in view of (7.29),

$$\hat{n}_I \times \vec{H}_I(\mathbf{x}) = \hat{n}_I \times \vec{H}_{inc}(\mathbf{x}) + \frac{\vec{J}_{\partial\Gamma}(\mathbf{x})}{2} - p.v. \left[\hat{n}_I \times \oint_{\partial\Gamma} \vec{J}_{\partial\Gamma}(\bar{\mathbf{x}}) \times \nabla_{\mathbf{x}} G_0(\mathbf{x}, \bar{\mathbf{x}})\, dS(\bar{\mathbf{x}}) \right]. \quad (7.34)$$

"$p.v.$" denotes again the principal value according to (5.82). Since the magnetic field has to obey the (now basic) boundary condition (7.15) we end up with the boundary integral equation

$$\frac{\vec{J}_{\partial\Gamma}(\mathbf{x})}{2} + p.v. \left[\hat{n}_I \times \oint_{\partial\Gamma} \vec{J}_{\partial\Gamma}(\bar{\mathbf{x}}) \times \nabla_{\mathbf{x}} G_0(\mathbf{x}, \bar{\mathbf{x}})\, dS(\bar{\mathbf{x}}) \right] = \hat{n}_I \times \vec{H}_{inc}(\mathbf{x}) \quad (7.35)$$

which allows us to determine the induced surface current $\vec{J}_{\partial\Gamma}$. This equation is often employed in the literature to solve the scattering problem on ideal metallic objects. The last step comprises an important aspect we will not suppress. To come from (7.34) to (7.35) it is tacitly assumed that the induced surface current in boundary condition (7.15) is identical with the induced surface current in definition (7.25). However, one may get the impression that this latter definition is introduced seemingly at random. But this is not the case. In the book of Hoenl, Maue and Westphal mentioned earlier in Sect. 5.4.2 one can find the proof for (7.35) being the correct boundary integral equation. So, what does this mean? If the induced surface current resulting from this equation is used to calculate the total magnetic field outside the scatterer according to relation (7.27), and, moreover, if the scattered electric field is then calculated by use of Maxwell's equation (7.6), we end up with a total electric field outside the scatterer which is in correspondence with boundary condition (7.14). The electromagnetic fields which result from $\vec{J}_{\partial\Gamma}$ of Eq. (7.35) are therefore in correspondence with Maxwell's equations as well as with the required boundary conditions. This is our justification for choosing the definition (7.25). The reader who may be interested in this proof is referred to the book of Hoenl, Maue and Westphal (see Sect. 10.6). It should also be noted that the scattering problem on dielectric objects can be solved in a similar way as described just now. Beside the induced surface current $\vec{J}_{\partial\Gamma}$ it is then necessary to introduce a second surface current $\vec{K}_{\partial\Gamma}$ governed by a boundary integral equation similar to (7.35). Details can again be found in the book of Hoenl, Maue, and Westphal.

The derivation of the boundary integral equation demonstrated above opens an alternative way to derive the dyadic Green function related to the outer Dirichlet problem. We will therefore conclude this subsection with a recourse to the Green function formalism of Chap. 4. Of course, once we have found a solution of (7.35) it would be possible by use of definition (7.25) to determine the interaction operator in terms of a bilinear expansion, for example. Due to (5.172) we are then able to calculate the Green function $\mathbf{G}_{\mathbf{\Gamma}_+}$. But there exist a more elegant way as we will see now. We introduce a "magnetic Green function" $\mathbf{G}^{(\mathbf{h})}_{\mathbf{\Gamma}_+}$ according to the definition

$$\mathbf{G}^{(\mathbf{h})}_{\mathbf{\Gamma}_+}(\mathbf{x}, \mathbf{x}') := \nabla_{\mathbf{x}} \times \mathbf{G}_{\mathbf{\Gamma}_+} \quad (7.36)$$

with $\mathbf{G}_{\mathbf{\Gamma}_+}$ being the Green function related to the outer Dirichlet problem, i.e., the Green function which is a solution of (2.341) subject to the boundary condition (2.342). $\mathbf{G}_{\mathbf{\Gamma}_+}$ is represented by (5.172) with the so far unknown interaction operator $\widehat{\mathbf{W}}_{\partial\mathbf{\Gamma}_+}$. From (2.341) and (7.36) it then follows that $\mathbf{G}^{(\mathbf{h})}_{\mathbf{\Gamma}_+}$ is a solution of equation

$$\left[\nabla_{\mathbf{x}} \times \nabla_{\mathbf{x}} \times - k_0^2\right] \mathbf{G}^{(\mathbf{h})}_{\mathbf{\Gamma}_+}(\mathbf{x}, \mathbf{x}') \;=\; \nabla_{\mathbf{x}} \times \mathbf{I}\delta(\mathbf{x} - \mathbf{x}'). \tag{7.37}$$

Based on relation (2.335) we may further define the "dyadic magnetic free-space Green function" $\mathbf{G}^{(\mathbf{h})}_{\mathbf{0}}$ according to

$$\mathbf{G}^{(\mathbf{h})}_{\mathbf{0}}(\mathbf{x}, \mathbf{x}') \;:=\; \nabla_{\mathbf{x}} \times \mathbf{G}_{\mathbf{0}}(\mathbf{x}, \mathbf{x}') \;=\; \nabla_{\mathbf{x}} G_0(\mathbf{x}, \mathbf{x}') \times \mathbf{I}. \tag{7.38}$$

Thus we get

$$\mathbf{G}^{(\mathbf{h})}_{\mathbf{\Gamma}_+}(\mathbf{x}, \mathbf{x}') = \mathbf{G}^{(\mathbf{h})}_{\mathbf{0}}(\mathbf{x}, \mathbf{x}') + \oint_{\partial\Gamma} \mathbf{G}^{(\mathbf{h})}_{\mathbf{0}}(\mathbf{x}, \bar{\mathbf{x}}) \cdot \widehat{\mathbf{W}}_{\partial\mathbf{\Gamma}_+}(\bar{\mathbf{x}}, \tilde{\mathbf{x}}) \cdot \mathbf{G}_{\mathbf{0}}(\tilde{\mathbf{x}}, \mathbf{x}')\, dS(\bar{\mathbf{x}})\, dS(\tilde{\mathbf{x}}). \tag{7.39}$$

Making use of Maxwell's equation (7.5) as well as of (7.22) and (7.23), we are then able to calculate the magnetic fields from the integral representations

$$\vec{H}_t(\mathbf{x}) \;=\; \frac{1}{i\omega\mu_0} \cdot \int_{\Gamma_+} \mathbf{G}^{(\mathbf{h})}_{\mathbf{\Gamma}_+}(\mathbf{x}, \mathbf{x}') \cdot \vec{\rho}(\mathbf{x}')\, dV(\mathbf{x}') \tag{7.40}$$

and

$$\vec{H}_{inc}(\mathbf{x}) \;=\; \frac{1}{i\omega\mu_0} \cdot \int_{\Gamma_+} \mathbf{G}^{(\mathbf{h})}_{\mathbf{0}}(\mathbf{x}, \mathbf{x}') \cdot \vec{\rho}(\mathbf{x}')\, dV(\mathbf{x}'). \tag{7.41}$$

Next, we impose the inhomogeneous Dirichlet condition

$$\hat{n}_I \times \mathbf{G}^{(\mathbf{h})}_{\mathbf{\Gamma}_+}(\mathbf{x}, \mathbf{x}') \;=\; \oint_{\partial\Gamma} \widehat{\mathbf{W}}_{\partial\mathbf{\Gamma}_+}(\mathbf{x}, \tilde{\mathbf{x}}) \cdot \mathbf{G}_{\mathbf{0}}(\tilde{\mathbf{x}}, \mathbf{x}')\, dS(\tilde{\mathbf{x}}) \tag{7.42}$$

which applies to $\mathbf{G}^{(\mathbf{h})}_{\mathbf{\Gamma}_+}$ if the observation point $\mathbf{x}$ is placed at the scatterer surface. We can also look upon this condition as an inhomogeneous Neumann condition which applies to $\mathbf{G}_{\mathbf{\Gamma}_+}$. It is then straightforward to see that the boundary integral equation

$$\begin{aligned} &\frac{1}{2} \cdot \oint_{\partial\Gamma} \widehat{\mathbf{W}}_{\partial\mathbf{\Gamma}_+}(\mathbf{x}, \tilde{\mathbf{x}}) \cdot \mathbf{G}_{\mathbf{0}}(\tilde{\mathbf{x}}, \mathbf{x}')\, dS(\tilde{\mathbf{x}}) \\ &\quad - p.v. \left[\hat{n}_I \times \oint_{\partial\Gamma} \mathbf{G}^{(\mathbf{h})}_{\mathbf{0}}(\mathbf{x}, \bar{\mathbf{x}}) \cdot \widehat{\mathbf{W}}_{\partial\mathbf{\Gamma}_+}(\bar{\mathbf{x}}, \tilde{\mathbf{x}}) \cdot \mathbf{G}_{\mathbf{0}}(\tilde{\mathbf{x}}, \mathbf{x}')\, dS(\bar{\mathbf{x}})\, dS(\tilde{\mathbf{x}})\right] \\ &= \hat{n}_I \times \mathbf{G}^{(\mathbf{h})}_{\mathbf{0}}(\mathbf{x}, \mathbf{x}') \end{aligned} \tag{7.43}$$

is the equivalent equation to (7.35) for the interaction operator. Once the interaction operator is known we can calculate $\mathbf{G}^{(\mathbf{h})}_{\mathbf{\Gamma}_+}$ from (7.39). To reverse (7.36) we just have to apply the *curl* operation to this equation. Taking (2.341) into account provides

$$\mathbf{G}_{\mathbf{\Gamma}_+}(\mathbf{x},\mathbf{x}') \;=\; \frac{1}{k_0^2}\cdot\nabla_{\mathbf{x}}\times\mathbf{G}^{(\mathbf{h})}_{\mathbf{\Gamma}_+}(\mathbf{x},\mathbf{x}') \;-\; \frac{1}{k_0^2}\cdot\mathbf{I}\delta(\mathbf{x}-\mathbf{x}'). \tag{7.44}$$

It obeys the homogeneous Dirichlet condition at the scatterer surface. In view of (7.42), the above given consideration makes clear that it is sufficient for the solution of the vector wave equation related to electromagnetic wave scattering problem on an ideal metallic object to impose either the homogeneous Dirichlet condition or the inhomogeneous Neumann condition. But it indicates further that using the Green function $\mathbf{G}^{(\mathbf{h})}_{\mathbf{\Gamma}_+}$ to solve the scattering problem on ideal metallic objects in terms of boundary integral equations ease the treatment of the strong singularity of the dyadic free-space Green function which appears if $\mathbf{G}_{\mathbf{\Gamma}_+}$, and if the homogeneous Dirichlet condition is used instead.

7.2.3 Helmholtz Equation of the Debye Potentials and Mie Theory

There exist an alternative way to the vector wave equation which consists in the decomposition of an electromagnetic field into transverse electric (TE) and transverse magnetic (TM) parts. Each of this part can be calculated from a scalar potential, the so-called "Debye potential". These potentials are named for Debye who first invented and applied these scalar functions to calculate the light pressure on spherical particles within Mie's theory (see the citation in Sect. 10.1). The Debye potentials are solutions of the scalar Helmholtz equation. This approach makes it even more obvious that Maxwell's equations can be reduced to the solution of two scalar equations for two independent scalar functions only.

To derive the Helmholtz equation for the Debye potentials the TE- and TM parts of an electromagnetic field are defined at first by use of two vector potentials $\vec{F}_p$ and $\vec{A}_p$ according to

$$\vec{E}^{\,(TE)}(\mathbf{x}) := \nabla\times\vec{F}_p(\mathbf{x}) \tag{7.45}$$

$$\vec{H}^{\,(TM)}(\mathbf{x}) := \nabla\times\vec{A}_p(\mathbf{x}). \tag{7.46}$$

Why we call these parts transverse electric and transverse magnetic parts will become clear later on. Due to the identity $\nabla\cdot(\nabla\times\vec{V})\equiv 0$ these definitions are obviously in accordance with the required solenoidality (7.7) and (7.8) for the electric and magnetic field. Applying Maxwell's equations (7.5) and (7.6) we get

$$\vec{H}^{(TE)}(\mathbf{x}) = -\frac{i}{\omega\mu_0} \cdot \nabla \times \nabla \times \vec{F}_p(\mathbf{x}) \tag{7.47}$$

$$\vec{E}^{(TM)}(\mathbf{x}) = \frac{i}{\omega\epsilon} \cdot \nabla \times \nabla \times \vec{A}_p(\mathbf{x}) \tag{7.48}$$

for the respective parts $\vec{E}^{(TM)}$ and $\vec{H}^{(TE)}$. The complete electric and magnetic field can then be represented by the sum of its two parts, i.e., by

$$\vec{H}(\mathbf{x}) = \nabla \times \vec{A}_p(\mathbf{x}) \; - \; \frac{i}{\omega\mu_0} \cdot \nabla \times \nabla \times \vec{F}_p(\mathbf{x}) \tag{7.49}$$

$$\vec{E}(\mathbf{x}) = \nabla \times \vec{F}_p(\mathbf{x}) \; + \; \frac{i}{\omega\epsilon} \cdot \nabla \times \nabla \times \vec{A}_p(\mathbf{x}). \tag{7.50}$$

This decomposition holds of course for each of the fields (internal, scattered, primary incident) we have to consider within a certain scattering problem. But because of identity $\nabla \times (\nabla\Phi) \equiv 0$ the vector potentials $\vec{A}_p$ and $\vec{F}_p$ are arbitrary to the extent that the gradient of some scalar function can be added. That is, choosing the potentials

$$\vec{A}_p'(\mathbf{x}) = \vec{A}_p(\mathbf{x}) \; - \; \frac{i}{\omega\mu_0} \nabla\Phi_p(\mathbf{x}) \tag{7.51}$$

$$\vec{F}_p'(\mathbf{x}) = \vec{F}_p(\mathbf{x}) \; + \; \frac{i}{\omega\epsilon} \nabla\Psi_p(\mathbf{x}) \tag{7.52}$$

will result into the same relations (7.49) and (7.50). The vector potentials can be fixed by use of a procedure called "Lorentz gauge" . There exist also other possibilities but we will restrict our further considerations to this one. Applying Maxwell's equation (7.5) to the TM-component of the electric field provides

$$\vec{E}^{(TM)}(\mathbf{x}) \; = \; i\omega\mu_0 \cdot \vec{A}_p(\mathbf{x}) \; + \; \nabla\Phi_p(\mathbf{x}). \tag{7.53}$$

From Eq. (7.48) we get moreover

$$\nabla \times \nabla \times \vec{A}_p(\mathbf{x}) \; - k^2 \cdot \vec{A}_p(\mathbf{x}) \; = \; -i\omega\epsilon \cdot \nabla\Phi_p(\mathbf{x}) \tag{7.54}$$

with $k^2 = \omega^2\epsilon\mu_0$. By use of the Lorentz condition

$$-\, i\omega\epsilon \cdot \Phi_p(\mathbf{x}) \; = \; \nabla \cdot \vec{A}_p(\mathbf{x}) \; , \tag{7.55}$$

and if employing identity $\nabla \times \nabla \times \vec{V} = \nabla\nabla \cdot \vec{V} - \nabla^2\vec{V}$ we end up with the vectorial form of the homogeneous Helmholtz equation

$$\nabla^2 \vec{A}_p(\mathbf{x}) \; + k^2 \, \vec{A}_p(\mathbf{x}) \; = \; \vec{0} \tag{7.56}$$

for the vector potential $\vec{A}_p$. If looking at the TE-component of the magnetic field we can proceed in a similar way to derive the vectorial form of the homogeneous

Helmholtz equation

$$\nabla^2 \vec{F}_p(\mathbf{x}) + k^2 \vec{F}_p(\mathbf{x}) = \vec{0} \tag{7.57}$$

for the vector potential $\vec{F}_p$. The scalar Debye potentials Π_e and Π_m are now introduced by the following ansatz for the vector potentials in spherical coordinates:

$$\vec{A}_p(\mathbf{x}) = \hat{r}\,(r \cdot \Pi_e(\mathbf{x})); \quad \vec{F}_p(\mathbf{x}) \equiv \vec{0} \tag{7.58}$$

$$\vec{F}_p(\mathbf{x}) = \hat{r}\,(r \cdot \Pi_m(\mathbf{x})); \quad \vec{A}_p(\mathbf{x}) \equiv \vec{0}. \tag{7.59}$$

With this ansatz, i.e., with assuming that both vector potentials have only a radial component, we can accomplish the decomposition of the electric and magnetic field into transverse electric and transverse magnetic parts with respect to the radial direction. This can be seen if we insert (7.58) and (7.59) into (7.49) and (7.50). We obtain for the components of the electric field

$$E_r(r,\theta,\phi) = \frac{i}{\omega\epsilon}\left[\frac{\partial^2(r \cdot \Pi_e(r,\theta,\phi))}{\partial r^2} + k^2 r\,\Pi_e(r,\theta,\phi)\right] \tag{7.60}$$

$$E_\theta(r,\theta,\phi) = \frac{i}{\omega\epsilon}\frac{1}{r} \cdot \frac{\partial^2(r \cdot \Pi_e(r,\theta,\phi))}{\partial r \partial\theta} + \frac{1}{\sin\theta} \cdot \frac{\partial \Pi_m(r,\theta,\phi)}{\partial\phi} \tag{7.61}$$

$$E_\phi(r,\theta,\phi) = \frac{i}{\omega\epsilon}\frac{1}{r\sin\theta} \cdot \frac{\partial^2(r \cdot \Pi_e(r,\theta,\phi))}{\partial r \partial\phi} - \frac{\partial \Pi_m(r,\theta,\phi)}{\partial\theta}. \tag{7.62}$$

$$H_r(r,\theta,\phi) = -\frac{i}{\omega\mu_0}\left[\frac{\partial^2(r \cdot \Pi_m(r,\theta,\phi))}{\partial r^2} + k^2 r\,\Pi_m(r,\theta,\phi)\right] \tag{7.63}$$

$$H_\theta(r,\theta,\phi) = -\frac{i}{\omega\mu_0}\frac{1}{r} \cdot \frac{\partial^2(r \cdot \Pi_m(r,\theta,\phi))}{\partial r \partial\theta} + \frac{1}{\sin\theta} \cdot \frac{\partial \Pi_e(r,\theta,\phi)}{\partial\phi} \tag{7.64}$$

$$H_\phi(r,\theta,\phi) = -\frac{i}{\omega\mu_0}\frac{1}{r\sin\theta} \cdot \frac{\partial^2(r \cdot \Pi_m(r,\theta,\phi))}{\partial r \partial\phi} - \frac{\partial \Pi_e(r,\theta,\phi)}{\partial\theta} \tag{7.65}$$

are the corresponding components of the magnetic field. If we choose $\Pi_e \neq 0$ and $\Pi_m = 0$ according to (7.58) then we can see from (7.63)-(7.65) that there remains indeed only a transverse magnetic field with respect to the radial direction. That is, there is no radial component of the magnetic field. Otherwise, if choosing $\Pi_m \neq 0$ and $\Pi_e = 0$ according to (7.59) we have only a transverse electric field with respect to the radial direction, as it can be seen from (7.60)–(7.62). From (7.58)/(7.59) and the vectorial Helmholtz equations (7.56)/(7.57) it follows moreover that both Debye potentials Π_e and Π_m are now solutions of the scalar homogeneous Helmholtz equation

$$\nabla^2 \Pi_{e/m} + k^2 \Pi_{e/m} = 0. \tag{7.66}$$

At first glance this approach appears more cumbersome than the vector wave equation approach. But its advantage shows up if we consider the limiting case of plane wave scattering on spherical objects. In this case (and only in this!) we are able to transform the continuity conditions of the tangential field components at the spherical surface into corresponding and independent conditions of the Debye potentials. Since for every spherical surface the components E_θ and E_ϕ of the electric field are already the tangential components we obtain from (7.14), (7.61), and (7.62) for an ideal metallic sphere with radius $r = a$ the alternative boundary conditions

$$\frac{\partial(r \cdot \Pi_e^s(r,\theta,\phi))}{\partial r} = -\frac{\partial(r \cdot \Pi_e^{inc}(r,\theta,\phi))}{\partial r} \tag{7.67}$$

$$\Pi_m^s(a,\theta,\phi) = -\Pi_m^{inc}(a,\theta,\phi) \tag{7.68}$$

of the Debye potentials. The superscripts "s" and "inc" attached to the potentials shall indicate whether they belong to the scattered or incident field. The boundary conditions for a dielectric sphere with radius $r = a$ read on the other hand

$$\frac{\partial(r \cdot \Pi_m^s(r,\theta,\phi))}{\partial r} + \frac{\partial(r \cdot \Pi_m^{inc}(r,\theta,\phi))}{\partial r} = \frac{\partial(r \cdot \Pi_m^{int}(r,\theta,\phi))}{\partial r} \tag{7.69}$$

$$\frac{\partial(r \cdot \Pi_e^s(r,\theta,\phi))}{\partial r} + \frac{\partial(r \cdot \Pi_e^{inc}(r,\theta,\phi))}{\partial r} = \frac{\epsilon_0}{\epsilon} \cdot \frac{\partial(r \cdot \Pi_e^{int}(r,\theta,\phi))}{\partial r} \tag{7.70}$$

$$\Pi_m^s(a,\theta,\phi) + \Pi_m^{inc}(a,\theta,\phi) = \Pi_m^{int}(a,\theta,\phi) \tag{7.71}$$

$$\Pi_e^s(a,\theta,\phi) + \Pi_e^{inc}(a,\theta,\phi) = \Pi_e^{int}(a,\theta,\phi). \tag{7.72}$$

$\Pi_{e/m}^{int}$ are the Debye potentials of the internal field. Of course, $\Pi_{e/m}^s$ of the scattered field must additionally obey the radiation condition (2.76) at infinity whereas the regularity condition inside the scatterer applies to the potentials $\Pi_{e/m}^{int}$. To solve the plane wave scattering problem on an ideal metallic or dielectric sphere we need furthermore explicit expressions for the Debye potentials related to the incident plane wave since the latter is the given quantity. Such expressions can be derived from a representation of the incident plane wave similar to (7.60)–(7.65). Due to the spherical symmetry of the scatterer it is sufficient to consider only the plane wave

$$\vec{E}_{inc}(r,\theta,\phi) = \hat{x} \cdot E_0 \cdot e^{ik_0 r \cos\theta} \tag{7.73}$$

polarized with respect to the $\hat{x}$-direction. Its radial component follows from Table 2.1 and reads

$$E_r^{inc}(r,\theta,\phi) = E_0 \cdot \sin\theta \cdot \cos\phi \cdot e^{ik_0 r \cos\theta}. \tag{7.74}$$

This radial component is a function of Π_e^{inc} only, according to (7.60). But then we should be able to derive an explicit expression for this potential from an appropriate representation of the radial component. This representation can be obtained if inserting the expansion coefficients (2.229) (and only these coefficients are needed for

the radial component because of (2.127) and (2.131)!) into approximation (2.201). Having in mind that the contribution of $l = \pm 1$ provides $e^{i\phi} + e^{-i\phi} = 2\cos\phi$ we get

$$E_0 \cdot \sin\theta \cdot \cos\phi \cdot e^{ik_0 r\cos\theta} \;=\; -\,\frac{E_0\cos\phi}{k_0 r} \cdot \sum_{n=1}^{\infty} i^{n-1}(2n+1)\, j_n(k_0 r)\, P_n^1(\cos\theta) \tag{7.75}$$

as an approximation of the radial component E_r^{inc}. This expression deserves some care if it is compared to equivalent expressions given in the literature. According to the remark concerning the term $(-1)^l$ we added subsequent to (2.73) there will be a positive sign on the right-hand side of (7.75) if this term is neglected. That's what was done in the book "Principles of Optics" of Born and Wolf, for example (see Eq. (46) on page 642 therein). Choosing the Debye potential Π_e^{inc} according to

$$\Pi_e^{inc}(r,\theta,\phi) \;=\; \frac{k_0}{\omega\mu_0} \cdot E_0 \cdot \cos\phi \cdot \sum_{n=1}^{\infty} i^n \frac{(2n+1)}{n(n+1)}\, j_n(k_0 r)\, P_n^1(\cos\theta) \tag{7.76}$$

is then in correspondence with (7.60) and (7.75) as one can simply prove by insertion and by taking Bessel's differential equation (2.54) into account. We can derive an explicit expression for the Debye potential Π_m^{inc} in exactly the same way from the radial component of the magnetic field assigned to the electric field (7.73). This magnetic field can be calculated from Maxwell's equation (7.5). We get

$$\vec{H}_{inc}(r,\theta,\phi) \;=\; \hat{y} \cdot \sqrt{\frac{\epsilon_0}{\mu_0}} \cdot E_0 \cdot e^{ik_0 r\cos\theta}. \tag{7.77}$$

After transformation into spherical coordinates, and if approximating its radial part again by use of a series expansion similar to (7.75) reveals that

$$\Pi_m^{inc}(r,\theta,\phi) \;=\; -\,E_0 \cdot \sin\phi \cdot \sum_{n=1}^{\infty} i^n \frac{(2n+1)}{n(n+1)}\, j_n(k_0 r)\, P_n^1(\cos\theta) \tag{7.78}$$

is the appropriate expression of the potential Π_m^{inc}. The potentials (7.76) and (7.78) are moreover solutions of the scalar and homogeneous Helmholtz equation. Thus, we have found the representation of the incident plane wave in terms of Debye potentials we where looking for. The derived expressions of Π_m^{inc} and Π_e^{inc} suggest the following ansatz for the potentials related to the internal and scattered fields:

$$\Pi_e^s(r,\theta,\phi) = \frac{k_0}{\omega\mu_0} \cdot E_0 \cdot \cos\phi \cdot \sum_{n=1}^{\infty} a_n h_n^{(1)}(k_0 r) P_n^1(\cos\theta) \tag{7.79}$$

$$\Pi_m^s(r,\theta,\phi) = -E_0 \cdot \sin\phi \cdot \sum_{n=1}^{\infty} b_n h_n^{(1)}(k_0 r) P_n^1(\cos\theta) \tag{7.80}$$

$$\Pi_e^{int}(r,\theta,\phi) = \frac{k}{\omega\mu_0} \cdot E_0 \cdot \cos\phi \cdot \sum_{n=1}^{\infty} c_n j_n(kr) P_n^1(\cos\theta) \tag{7.81}$$

$$\Pi_m^{int}(r,\theta,\phi) = -E_0 \cdot \sin\phi \cdot \sum_{n=1}^{\infty} d_n j_n(kr) P_n^1(\cos\theta). \tag{7.82}$$

The unknown expansion coefficients a_n, b_n, c_n, and d_n can now be determined by applying the boundary conditions (7.67) and (7.68) or conditions (7.69)–(7.72), respectively. If the ideal metallic sphere with radius $r = a$ is considered we obtain

$$a_n = -i^n \frac{2n+1}{n(n+1)} \cdot \frac{\frac{\partial}{\partial r}\left[r \cdot j_n(k_0 r)\right]_{r=a}}{\frac{\partial}{\partial r}\left[r \cdot h_n^{(1)}(k_0 r)\right]_{r=a}} \tag{7.83}$$

$$b_n = -i^n \frac{2n+1}{n(n+1)} \cdot \frac{j_n(k_0 a)}{h_n^{(1)}(k_0 a)} \tag{7.84}$$

for the expansion coefficients of the Debye potentials related to the scattered field. For the scattering coefficients of a dielectric sphere with radius $r = a$ we have on the other hand

$$a_n = i^n \frac{2n+1}{n(n+1)} \cdot \frac{\epsilon_0 j_n^{(0)}\left[j_n^{(s)}\right]' - \epsilon j_n^{(s)}\left[j_n^{(0)}\right]'}{\epsilon j_n^{(s)}[h_n]' - \epsilon_0 h_n\left[j_n^{(s)}\right]'} \tag{7.85}$$

$$b_n = i^n \frac{2n+1}{n(n+1)} \cdot \frac{j_n^{(0)}\left[j_n^{(s)}\right]' - j_n^{(s)}\left[j_n^{(0)}\right]'}{j_n^{(s)}[h_n]' - h_n\left[j_n^{(s)}\right]'} \tag{7.86}$$

with

$$j_n^{(0)} = j_n(k_0 a) \tag{7.87}$$

$$j_n^{(s)} = j_n(ka) \tag{7.88}$$

$$h_n = h_n^{(1)}(k_0 a) \tag{7.89}$$

$$\left[j_n^{(0)}\right]' = \frac{\partial}{\partial r}\left[r \cdot j_n(k_0 r)\right]_{r=a} \tag{7.90}$$

$$\left[j_n^{(s)}\right]' = \frac{\partial}{\partial r}\left[r \cdot j_n(kr)\right]_{r=a} \tag{7.91}$$

$$[h_n]' = \frac{\partial}{\partial r}\left[r \cdot h_n^{(1)}(k_0 r)\right]_{r=a}. \tag{7.92}$$

Please, note that all coefficients are final! Once we know the coefficients we know the Debye potentials, and, moreover, by use of (7.60) - (7.65) we are able to calculate all components of the scattered electromagnetic field. This is the classical Mie theory for plane wave scattering on spherical objects formulated in terms of Debye potentials.

The same results for spherical scatterer could have been obtained, of course, if using the vector wave equation. But the reduction of the boundary conditions of the fields to those of the Debye potentials facilitates the derivation of the expansion coefficients considerably. However, this advantage is lost if we are interested in plane wave scattering on nonspherical particles since the θ- and ϕ-components of the electromagnetic fields are no longer the tangential components. In this case we have to express the Debye potentials by the more general approximations

$$\Pi_e^s(r,\theta,\phi) = \frac{k_0}{\omega\mu_0} \cdot E_0 \cdot \sum_{n=1}^{N} \sum_{l=-n}^{n} a_{l,n}^{(N)} h_n^{(1)}(k_0 r) P_n^l(\cos\theta) \cdot e^{il\phi} \tag{7.93}$$

$$\Pi_m^s(r,\theta,\phi) = E_0 \cdot \sum_{n=1}^{N} \sum_{l=-n}^{n} b_{l,n}^{(N)} h_n^{(1)}(k_0 r) P_n^l(\cos\theta) \cdot e^{il\phi} \tag{7.94}$$

$$\Pi_e^{int}(r,\theta,\phi) = \frac{k}{\omega\mu_0} \cdot E_0 \cdot \sum_{n=1}^{N} \sum_{l=-n}^{n} c_{l,n}^{(N)} j_n(kr) P_n^l(\cos\theta) \cdot e^{il\phi} \tag{7.95}$$

$$\Pi_m^{int}(r,\theta,\phi) = E_0 \cdot \sum_{n=1}^{N} \sum_{l=-n}^{n} d_{l,n}^{(N)} j_n(kr) P_n^l(\cos\theta) \cdot e^{il\phi} \tag{7.96}$$

with non-final expansion coefficients. Now, they can be used only as an intermediate step in the solution scheme, for there are no equivalent boundary conditions for the potentials. Employing (7.93)–(7.96) we have to calculate the electromagnetic field components in the next step. The resulting expressions contain the unknown and non-final expansion coefficients which can be determined afterwards by applying the relevant boundary conditions of the tangential field components. However, it can be shown by a tedious analysis that the expressions resulting from this procedure are identical with expressions (2.163) and (2.164) of Chap. 3 we employed already in conjunction with the vector wave equation. Thus, we may state that for nonspherical scatterers the Debye potential approach would be just a detour. Only in the context of the Method of Lines discussed in Chap. 5 it would be of some benefit since the θ-dependent functions $P_n^l(\cos\theta)$ in (7.93)–(7.96) can be replaced by the algebraic eigenvectors of the Method of Lines obtained from the scalar Helmholtz equation. But the discussed disadvantages of this special Finite-Difference technique still remain.

On the other hand, if we leave the spherical coordinate system then there are still scattering configurations for which the Debye potential approach offers benefits. That is exactly what happened in Chap. 6. There we have tacitly assumed that the

scattering problem of a plane wave perpendicularly incident from above on a periodic grating can be decomposed in Cartesian coordinates into two separate problems, each of which is related to the scalar Helmholtz equation. In Chap. 6, we have considered only one of these problems—the p-polarized plane wave. The same is possible in cylindrical coordinates, for example, if considering the scattering problem of an infinitely extended cylinder with a nonspherical cross-section and for perpendicular incidence of the plane wave with respect to the cylindrical axis. In this case, we are also able to perform a decomposition of the electromagnetic field into transverse electric and transverse magnetic parts with respect to the coordinate related to the cylindrical axis. This will allow us to benefit from all the advantages of the scalar Green's function formalism like the weaker singularity of the scalar free-space Green function.

7.3 The Far-Field and the Scattering Quantities

In this section, we want to take a closer look at the definitions and calculations of physical quantities which can be related to real measurements. Scattering measurements are performed in the far-field of the scatterer, as already discussed in the introduction of the first chapter. This makes it necessary to consider the behaviour of the electromagnetic fields in the nonlocal far-field region. Starting point for the following investigations is the general representation

$$\mathbf{G}_{\mathbf{\Gamma}_+}(\mathbf{x},\mathbf{x}') = \mathbf{G}_{\mathbf{0}}(\mathbf{x},\mathbf{x}') + \oint_{\partial\Gamma} \mathbf{G}_{\mathbf{0}}(\mathbf{x},\bar{\mathbf{x}}) \cdot \mathbf{W}(\bar{\mathbf{x}},\tilde{\mathbf{x}}) \cdot \mathbf{G}_{\mathbf{0}}(\tilde{\mathbf{x}},\mathbf{x}')\, dS(\bar{\mathbf{x}})\, dS(\tilde{\mathbf{x}}) \tag{7.97}$$

of the Green function related to a certain scattering problem. That is, for the ideal metallic scatterer we have to replace $\mathbf{W}(\bar{\mathbf{x}},\tilde{\mathbf{x}})$ by the interaction operator $\mathbf{W}_{\partial\mathbf{\Gamma}_+}(\bar{\mathbf{x}},\tilde{\mathbf{x}})$ according to definition (4.23). For the dielectric scatterer the interaction operator $\mathbf{W}^{(\mathbf{d})}_{\partial\mathbf{\Gamma}_+}(\bar{\mathbf{x}},\tilde{\mathbf{x}})$ according to definition (4.30) must be used. The auxiliary dyadic functions $\mathbf{G}_{\mathbf{t}}^{>}$ and $\mathbf{G}_{\mathbf{t}}^{<}$ appearing in these definitions can be replaced without any problems by the full dyadic free-space Green function $\mathbf{G}_{\mathbf{0}}$ since both variables $\mathbf{x}$ and $\mathbf{x}'$ are now outside the smallest sphere circumscribing the scatterer. Employing the analytical expression (2.321) for the dyadic free-space Green function it is no longer necessary to distinguish between $\mathbf{G}_{\mathbf{t}}^{>}$ and $\mathbf{G}_{\mathbf{t}}^{<}$.

Concerning the definitions of the scattering quantities in the far-field region we have generally to distinguish between angular dependent (differential) and total scattering quantities for a scatterer in a fixed orientation. But in many applications (in technical diagnostics as well as in remote sensing, for example) this orientation is not known or, as it also happens frequently, the measurement volume contains many but different oriented particles. Especially the latter situation makes it necessary to introduce orientation averaged scattering quantities. The following considerations

are moreover restricted to those scattering quantities which are of our interest in the numerical simulations presented in Chap. 9.

7.3.1 The Far-Field

The general scattering configuration was already depicted in Fig. 1.2. The nonlocal far-field is represented in this figure by the spherical surface S_∞. The term "nonlocal" is mathematically expressed by the limiting behaviour $\lim_{|\mathbf{x}|\to\infty}$ of a given physical quantity depending on $\mathbf{x}$. However, this term gets its practical importance from our experimental experience that it can be applied within a sufficient accuracy already at a finite (local!) distance from the scatterer.

According to the discussion in Chap. 2, we know that the dyadic free-space Green function $\mathbf{G_0}(\mathbf{x}, \mathbf{x}')$ is a solution of the inhomogeneous vector wave equation (2.320) subject to the radiation condition (1.20) in the far-field with respect to the variable $\mathbf{x}$. Its analytical expression is given by Eq. (2.321). The primary field generated by the impressed source distribution (2.332) can then be calculated from the volume integral representation (2.331). To generate a plane wave at the scatter position (i.e., near the origin of the coordinate system) we have to apply the additional condition (2.333) to the source distribution. This condition allows us to use the asymptotic expression (2.327) of the dyadic free-space Green function. But placing this primary source distribution only far away from the scatterer is not sufficient to define the scattering quantities in the far-field appropriately. For this we have to assume moreover that the primary plane wave exists not only at the location of the scatterer but also in the far-field S_∞, where it interferes with the scattered field generated by the interaction of the primary incident plane wave with the scatterer. The superposition of the primary incident and scattered field is reflected in the second term on the right-hand side of (7.97). This additional assumption is now related to the following problem (see also the discussion at the end of Sect. 3.3.1): The general plane wave (2.232) is a solution of the **homogeneous** vector wave equation and finite everywhere in the free space. In contrast to a primary incident field generated by a real source and thus represented by the volume integral relation (2.331) the radiation condition does **not** apply to a plane wave. From this point of view the plane wave concept contradicts the Green function concept of cause and action, since the latter necessarily requires a source to have an action! To unite the plane wave model even in the far-field with the Green function concept (i.e. with representation (7.97)!) we are forced to introduce a second and enlarged far-field (let us call it the XXL far-field S_{XXL}) which is placed in the far-field of the primary far-field at S_∞ (i.e., behind Γ_+), what ever this means mathematically. There we have to place the source (2.332) of the primary incident plane wave. Then, we get indeed a plane wave from (7.97) also in the primary far-field S_∞. Employing this somehow strange construction leaves the reader with an ambivalent feeling. Alternatively, we can assume the a priori existence of a plane wave without any sources ("smoke without fire") which is not really a more reasonable point of view. This problem is discussed here to demonstrate the strange

character of the physical plane wave model. The following considerations rest upon the concept of a second far-field S_{XXL} to stay with Eq. (7.97).

Let us now deal with the plane wave in more detail.

$$\vec{E}_{inc}(\mathbf{x}) \;=\; \vec{E}_0 \cdot e^{i\mathbf{k}_i \cdot \mathbf{x}} \;=\; \vec{E}_0 \cdot e^{ik_0 \cdot |\mathbf{x}| \cdot \hat{n}_i \cdot \hat{n}_s} \tag{7.98}$$

is a solution of the homogeneous vector wave equation

$$\left(\nabla \times \nabla \times - \, k_0^2\right) \vec{E}_{inc}(\mathbf{x}) \;=\; \vec{0} \tag{7.99}$$

in Γ_+, as already mentioned above. $\hat{n}_i$ and $\hat{n}_s$ are the unit vectors pointing into the direction of propagation of the plane wave and into the direction of the observation point. They have to be distinguished from the unit normal vector $\hat{n}$ and $\hat{n}_-$ related to the boundary surfaces. Maxwell's equations (7.5)–(7.8) thus become for a plane wave

$$\mathbf{k}_i \times \vec{E}_{inc}(\mathbf{x}) = \omega \mu_0 \vec{H}_{inc}(\mathbf{x}) \tag{7.100}$$

$$\mathbf{k}_i \times \vec{H}_{inc}(\mathbf{x}) = -\, \omega \epsilon_0 \vec{E}_{inc}(\mathbf{x}) \tag{7.101}$$

$$\mathbf{k}_i \cdot \vec{E}_{inc}(\mathbf{x}) = 0 \tag{7.102}$$

$$\mathbf{k}_i \cdot \vec{H}_{inc}(\mathbf{x}) = 0. \tag{7.103}$$

From these (7.99) follows immediately. But we can see moreover that $\vec{E}_0$ and $\vec{H}_0$ are orthogonal to each other and are both perpendicular to $\mathbf{k}_i$. The plane surface normal to $\mathbf{k}_i$ is defined by $\mathbf{k}_i \cdot \mathbf{x} = const.$. These are some important properties of a plane wave.

In the far-field at S_∞ the plane wave enjoys an interesting representation. In (7.98) there appears the term $e^{ik_0 \cdot |\mathbf{x}| \cdot \hat{n}_i \cdot \hat{n}_s}$. This expression can be rewritten in terms of incoming and outgoing spherical waves according to

$$e^{ik_0 \cdot |\mathbf{x}| \cdot \hat{n}_i \cdot \hat{n}_s} \;=\; \frac{2\pi i}{k_0} \cdot \left[\delta(\hat{n}_i + \hat{n}_s) \, \frac{e^{-ik_0|\mathbf{x}|}}{|\mathbf{x}|} \;-\; \delta(\hat{n}_i - \hat{n}_s) \, \frac{e^{ik_0|\mathbf{x}|}}{|\mathbf{x}|} \right] \tag{7.104}$$

with

$$\delta(\hat{n}_i \pm \hat{n}_s) \;=\; \delta(\cos\theta_i \pm \cos\theta_s) \cdot \delta(\phi_i \pm \phi_s). \tag{7.105}$$

This decomposition can be derived from expansion (2.117) in a straightforward way if taking the asymptotic behaviour (2.77) of $j_n(k_0 r)$, the completeness relation (2.64) of the spherical harmonics as well as symmetry relation (2.63) into account (for the necessity of using this symmetry relation see the remark following (3.45)!). The plane wave (7.98) can be therefore represented in the far-field by

$$\vec{E}_{inc}(\mathbf{x}) \;=\; \frac{2\pi i}{k_0} \cdot \vec{E}_0 \cdot \left[\delta(\hat{n}_i + \hat{n}_s) \, \frac{e^{-ik_0|\mathbf{x}|}}{|\mathbf{x}|} \;-\; \delta(\hat{n}_i - \hat{n}_s) \, \frac{e^{ik_0|\mathbf{x}|}}{|\mathbf{x}|} \right]. \tag{7.106}$$

Obviously, if looking into the propagation direction of the plane wave (i.e. if $\hat{n}_s = \hat{n}_i$) we are not able to distinguish between an outgoing spherical wave and the plane wave. But the more important aspect of (7.106) becomes clear if we consider the representation of the total field resulting from (2.348) and (2.349), respectively, in conjunction with the dyadic Green function (7.97). It should be emphasized once again that in dependence on the chosen interaction operator (7.97) summarizes the two scattering problems of an ideal metallic and dielectric scatterer. The subsequent discussions are therefore valid for both types of scatterers until the interaction operator is explicitly specified.

From the source (2.332) and the asymptotic behaviour (2.327) of $\mathbf{G_0}$ (due to our S_{XXL} construction this asymptotic behaviour can be used for observation points in the far-field, too!) we obtain from the first part of the right-hand side of (7.97) just the above discussed plane wave (7.106) as the primary incident field. The scattered field follows from the second term on the right-hand side of (7.97). Using again the asymptotic expression (2.327) results in

$$\vec{E}_s(\mathbf{x}) \;=\; \mathbf{A}(\hat{n}_s, \hat{n}_i) \cdot \vec{E}_0 \cdot \frac{e^{ik_0|\mathbf{x}|}}{|\mathbf{x}|} \tag{7.107}$$

with the dyadic scattering amplitude $\mathbf{A}(\hat{n}_s, \hat{n}_i)$ given by

$$\mathbf{A}(\hat{n}_s, \hat{n}_i) \;=\; \frac{1}{4\pi} \cdot \oint_{\partial\Gamma} \mathbf{I}_t^{(\hat{n}_s)} \cdot e^{-ik_0 \hat{n}_s \bar{\mathbf{x}}} \cdot \mathbf{W}(\bar{\mathbf{x}}, \tilde{\mathbf{x}}) \cdot \mathbf{I}_t^{(\hat{n}_i)} \cdot e^{ik_0 \hat{n}_i \tilde{\mathbf{x}}} \, dS(\bar{\mathbf{x}}) \, dS(\tilde{\mathbf{x}}). \tag{7.108}$$

Because of

$$\mathbf{I}_t^{(\hat{n}_s)} = \hat{\theta}_s \odot \hat{\theta}_s \;+\; \hat{\phi}_s \odot \hat{\phi}_s \tag{7.109}$$

$$\mathbf{I}_t^{(\hat{n}_i)} = \hat{\theta}_i \odot \hat{\theta}_i \;+\; \hat{\phi}_i \odot \hat{\phi}_i \tag{7.110}$$

the relation

$$\hat{n}_s \cdot \mathbf{A}(\hat{n}_s, \hat{n}_i) \;=\; \mathbf{A}(\hat{n}_s, \hat{n}_i) \cdot \hat{n}_i \;=\; \vec{0} \tag{7.111}$$

holds. Superposition of the plane wave with the scattered field provides the total field

$$\begin{aligned} \vec{E}_t(\mathbf{x}) = \frac{2\pi i}{k_0} \cdot \vec{E}_0 \cdot \Bigg[\delta(\hat{n}_i + \hat{n}_s) \frac{e^{-ik_0|\mathbf{x}|}}{|\mathbf{x}|} \;-\; \delta(\hat{n}_i - \hat{n}_s) \frac{e^{ik_0|\mathbf{x}|}}{|\mathbf{x}|} \Bigg] \\ + \mathbf{A}(\hat{n}_s, \hat{n}_i) \cdot \vec{E}_0 \cdot \frac{e^{ik_0|\mathbf{x}|}}{|\mathbf{x}|} \end{aligned} \tag{7.112}$$

in the far-field region S_∞. We can recognize from this expression that each sensor not looking into the direction of incidence of the plane wave (i.e. for which $\hat{n}_s \neq \hat{n}_i$ holds) registers only the scattered field.

But a sensor looking into the forward direction (i.e., if $\hat{n}_s = \hat{n}_i$) registers the superposition of the primary incident plane wave with the scattered field (see Fig. 7.2).

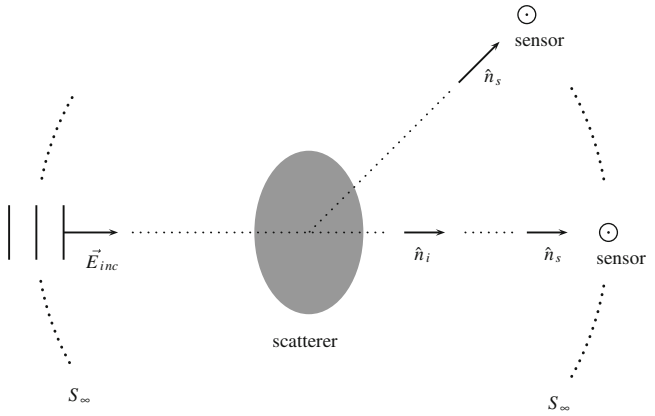

Fig. 7.2 Scattering measurements in the far-field. Only if $\hat{n}_s = \hat{n}_i$ the sensor registers the superposition of the primary incident field with the scattered field

On the other hand, if we had assumed a primary field generated from a source located within a finite distance from the scatterer (this corresponds to the general radiation problem in Electrodynamics) then we could only see the interference of two outgoing spherical waves (the one from the primary source, and the other from the scatterer) in any direction $\hat{n}_s$ in the far-field region at S_∞. It is exactly the former behaviour of being able to distinguish between the primary incident and scattered field if $\hat{n}_s \neq \hat{n}_i$ which makes the plane wave especially suited for scattering experiments and their interpretations. But let us emphasize again that the usefulness of the models "plane wave" and "far-field" is justified only by our experimental experience. Conversely, every interpretation of experimental data in terms of quantities defined within the scattering theory requires that the measurements are performed in agreement with the assumptions underlying the models "plane wave" and "far-field". But this is sometimes a tedious task and may require again some experience.

Equation (7.112) can be split into incoming and outgoing spherical waves according to

$$\vec{E}_t(\mathbf{x}) \;=\; \vec{F}_1(\hat{n}_s)\cdot\frac{e^{-ik_0|\mathbf{x}|}}{|\mathbf{x}|} \;+\; \vec{F}_2(\hat{n}_s)\cdot\frac{e^{ik_0|\mathbf{x}|}}{|\mathbf{x}|} \tag{7.113}$$

with the amplitude vectors

$$\vec{F}_1(\hat{n}_s) = \frac{2\pi i}{k_0}\cdot\delta(\hat{n}_i+\hat{n}_s)\cdot\mathbf{I}_t^{(\hat{n}_i)}\cdot\vec{E}_0 \tag{7.114}$$

$$\vec{F}_2(\hat{n}_s) = -\frac{2\pi i}{k_0}\cdot\mathbf{S}(\hat{n}_s,\hat{n}_i)\cdot\vec{E}_0 \tag{7.115}$$

and the dyadic far-field scattering function

$$\mathbf{S}(\hat{n}_s, \hat{n}_i) \;:=\; \frac{ik_0}{2\pi} \cdot \mathbf{A}(\hat{n}_s, \hat{n}_i) \;+\; \delta(\hat{n}_i - \hat{n}_s) \cdot \mathbf{I}_t^{(\hat{n}_i)}. \tag{7.116}$$

This function can now be used as the kernel of the so-called "dyadic far-field scattering operator" $\hat{\mathbf{S}}$. This operator allows us to map an at first arbitrary but transverse far-field vector $\vec{f}(\hat{n})$ into the transverse far-field vector $\vec{g}(\hat{n})$. That is, we have

$$\hat{\mathbf{S}} : \vec{f} \to \vec{g} \tag{7.117}$$

with

$$\vec{g}(\hat{\hat{n}}) \;:=\; \oint\!\!\!\!\!\!\int_{S_\infty} \mathbf{S}(\hat{\hat{n}}, \hat{n}) \cdot \vec{f}(\hat{n})\, d\hat{n}. \tag{7.118}$$

"$\oint\!\!\!\!\!\!\int_{S_\infty} \cdots\, d\hat{n}$" denotes the integral

$$\int_0^{2\pi} \int_0^{\pi} \cdots \sin\theta\, d\theta\, d\phi. \tag{7.119}$$

From this definition and the resulting relation

$$\vec{F}_2(\hat{n}_s) \;=\; \oint\!\!\!\!\!\!\int_{S_\infty} \mathbf{S}(\hat{n}_s, \hat{n}) \cdot \left[-\vec{F}_1(-\hat{n}) \right] d\hat{n} \tag{7.120}$$

we can see that the operator $\hat{\mathbf{S}}$ transforms the amplitude vector $\vec{F}_1(-\hat{n})$ of the incoming wave into the amplitude vector $\vec{F}_2(\hat{n}_s)$ of the outgoing wave. The dyadic scattering amplitude as well as the dyadic far-field scattering function obey the symmetry relations

$$\mathbf{A}(\hat{n}_s, \hat{n}_i) \;=\; \mathbf{A}^{tp}(-\hat{n}_i, -\hat{n}_s) \tag{7.121}$$

and

$$\mathbf{S}(\hat{n}_s, \hat{n}_i) \;=\; \mathbf{S}^{tp}(-\hat{n}_i, -\hat{n}_s). \tag{7.122}$$

The former relation is a consequence of the symmetry relations (2.329) and (2.346)/(2.347). Equation (7.122) then follows from (7.116).

The matrix representation of the dyadic far-field scattering operator $\hat{\mathbf{S}}$ is defined by

$$[S]_{l,n;l',n'}^{\tau,\tau'} \;:=\; \oint\!\!\!\!\!\!\int_{S_\infty} \vec{Y}_{l,n,\tau}^{\,*}(\hat{n}_s) \cdot \mathbf{S}(\hat{n}_s, \hat{n}_i) \cdot \vec{Y}_{l',n',\tau'}(\hat{n}_i)\, d\hat{n}_s\, d\hat{n}_i. \tag{7.123}$$

Index τ takes the two values 1 and 2. The transverse vector functions $\vec{Y}_{l,n,\tau}$ therein are related to the vector spherical harmonics given in (2.128) and (2.129) by

$$\vec{Y}_{l,n,1}(\hat{n}) := i^n \cdot \gamma_{l,n} \cdot \vec{C}_{l,n}(\theta, \phi) \tag{7.124}$$

$$\vec{Y}_{l,n,2}(\hat{n}) := i^{(n-1)} \cdot \gamma_{l,n} \cdot \vec{B}_{l,n}(\theta, \phi). \tag{7.125}$$

Due to the orthogonality relations (2.138) and (2.139) they form an orthonormal system at S_∞, i.e., they obey the relations

$$\oint_{S_\infty} \vec{Y}^*_{l,n,1}(\hat{n}) \cdot \vec{Y}_{l',n',1}(\hat{n})\, d\hat{n} = \delta_{l,l'}\, \delta_{n,n'} \tag{7.126}$$

$$\oint_{S_\infty} \vec{Y}^*_{l,n,2}(\hat{n}) \cdot \vec{Y}_{l',n',2}(\hat{n})\, d\hat{n} = \delta_{l,l'}\, \delta_{n,n'} \tag{7.127}$$

and

$$\oint_{S_\infty} \vec{Y}^*_{l,n,1}(\hat{n}) \cdot \vec{Y}_{l',n',2}(\hat{n})\, d\hat{n} \;=\; \oint_{S_\infty} \vec{Y}^*_{l,n,2}(\hat{n}) \cdot \vec{Y}_{l',n',1}(\hat{n})\, d\hat{n} \;=\; 0. \tag{7.128}$$

The second contribution on the right-hand side of (7.116) provides therefore the matrix elements

$$\delta_{\tau,\tau'}\, \delta_{l,l'}\, \delta_{n,n'}. \tag{7.129}$$

To determine the matrix elements of the first contribution on the right-hand side of (7.116) we have to go back to (7.108). First we note that the expression $\mathbf{I}_t^{(\hat{n}_i)} \cdot e^{ik_0\hat{n}_i\tilde{\mathbf{x}}}$ is nothing but the plane wave (2.232) if multiplied with the polarization vector $\vec{E}_0$. But for such a plane wave we know already an expansion given by (2.235)–(2.237). From this and relations (2.134) and (2.135) it follows that $\mathbf{I}_t^{(\hat{n}_i)} \cdot e^{ik_0\hat{n}_i\tilde{\mathbf{x}}}$ may be expanded, too, according to

$$\mathbf{I}_t^{(\hat{n}_i)} \cdot e^{ik_0\hat{n}_i\tilde{\mathbf{x}}} \;=\; 4\pi \cdot \sum_{\tau=1}^{2} \sum_{n=0}^{\infty} \sum_{l=-n}^{n} \vec{\psi}_{l,n,\tau}(k_0\tilde{r}, \tilde{\theta}, \tilde{\phi}) \odot \vec{Y}^*_{l,n,\tau}(\hat{n}_i). \tag{7.130}$$

In deriving this expansion one has to take advantage of the fact that this dyadic quantity is symmetric according to definition (2.295). Expansion

$$\mathbf{I}_t^{(\hat{n}_s)} \cdot e^{-ik_0\hat{n}_s\bar{\mathbf{x}}} \;=\; 4\pi \cdot \sum_{\tau=1}^{2} \sum_{n=0}^{\infty} \sum_{l=-n}^{n} \vec{Y}_{l,n,\tau}(\hat{n}_s) \odot \vec{\psi}^*_{l,n,\tau}(k_0\bar{r}, \bar{\theta}, \bar{\phi}) \tag{7.131}$$

for the other dyadic quantity $\mathbf{I}_t^{(\hat{n}_s)} \cdot e^{-ik_0\hat{n}_s\bar{\mathbf{x}}}$ in (7.108) can be derived in close analogy. Now, if using both expansions in expression (7.108) of the dyadic scattering amplitude, we obtain in conjunction with (7.123) and (2.161) the following matrix elements related to the first term on the right-hand side of (7.116):

$$\begin{aligned} &\frac{ik_0}{2\pi} \cdot \oint_{S_\infty} \vec{Y}^*_{l,n,\tau}(\hat{n}_s) \cdot \mathbf{A}(\hat{n}_s, \hat{n}_i) \cdot \vec{Y}_{l',n',\tau'}(\hat{n}_i)\, d\hat{n}_s\, d\hat{n}_i \\ &= 2\,(ik_0) \oint_{\partial\Gamma} \vec{\tilde{\psi}}_{l,n,\tau}(k_0, \bar{\mathbf{x}}) \cdot \mathbf{W}(\bar{\mathbf{x}}, \tilde{\mathbf{x}}) \cdot \vec{\psi}_{l',n',\tau'}(k_0, \tilde{\mathbf{x}})\, dS(\bar{\mathbf{x}})\, dS(\tilde{\mathbf{x}})\,. \end{aligned} \tag{7.132}$$

But the integral on the right-hand side of this expression is identical with definitions (4.26) and (4.33) of the matrix elements of the interaction operators related to the ideal metallic and dielectric scatterer. The matrix elements of the dyadic far-field scattering operator can therefore be expressed by

$$[S]^{\tau,\tau'}_{l,n;l',n'} \;=\; \delta_{\tau,\tau'}\,\delta_{l,l'}\,\delta_{n,n'} \;+\; 2\cdot[W]^{\tau,\tau'}_{l,n;l',n'}\,, \tag{7.133}$$

or, in matrix notation,

$$\mathbf{S} \;=\; \mathbf{E} \;+\; 2\cdot\mathbf{W}. \tag{7.134}$$

This is a remarkable result since this expression is identical with expression (4.57) we derived already in Sect. 4.4.2 in the context of the proof of unitarity of the S-matrix . Thus, we have derived the interesting result that the matrix elements of the S-matrix introduced in Sect. 4.4.2 are identical with the matrix elements of the dyadic far-field scattering operator $\hat{\mathbf{S}}$. In this context, let us bring to mind that the S-matrix was formally introduced without any relation to the dyadic far-field scattering operator introduced above. But since we have already proven the unitarity of the S-matrix if nonabsorbing scatterers are considered we can now come to the conclusion that the same property applies to the matrix elements of the dyadic far-field scattering operator. The unitarity relation reads in operator notation

$$\oint_{S_\infty} \mathbf{S}^{\dagger}(\hat{n},\hat{n}')\cdot\mathbf{S}(\hat{n},\hat{n}'')\,d\hat{n} = \oint_{S_\infty} \mathbf{S}^{*}(\hat{n}',\hat{n})\cdot\mathbf{S}(\hat{n},\hat{n}'')\,d\hat{n} = \mathbf{I}_t^{(\hat{n}')}\cdot\delta(\hat{n}'-\hat{n}''). \tag{7.135}$$

The functional (4.81), if applied to the total field $\vec{E}_t$ in the far-field region at S_∞ (i.e., if the boundary integral over $\partial\Gamma_a$ is replaced by the boundary integral over S_∞!), provides the identity

$$\left\{\vec{E}_t(\mathbf{x}),\,\vec{E}_t(\mathbf{x})\right\}_{S_\infty} \;=\; 0 \tag{7.136}$$

for nonabsorbing scatterers, due to our S_{XXL} construction (please, note that in performing the necessary *curl* operation all contributions can be neglected that tend to zero stronger than $1/r$!). Employing (7.113), (7.120), and (7.135) we can thus infer the equality of the scalar products

$$<\vec{F}_2(\hat{n})\,|\,\vec{F}_2(\hat{n})>_{S_\infty} \;=\; <\vec{F}_1(\hat{n})\,|\,\vec{F}_1(\hat{n})>_{S_\infty} \tag{7.137}$$

of the transverse amplitude vectors with the scalar product defined by

$$<\vec{g}(\hat{n})\,|\,\vec{f}(\hat{n})>_{S_\infty} := \oint_{S_\infty} \vec{g}^{\,*}(\hat{n})\cdot\vec{f}(\hat{n})\,d\hat{n}. \tag{7.138}$$

A further consequence of the unitarity relation (7.135) and (7.116) is the relation

$$\oint_{S_\infty} \mathbf{A}^\dagger(\hat{n},\hat{n}') \cdot \mathbf{A}(\hat{n},\hat{n}'')\, d\hat{n} = \frac{2\pi}{ik_0} \cdot \Big[\mathbf{A}(\hat{n}',\hat{n}'') - \mathbf{A}^\dagger(\hat{n}'',\hat{n}')\Big] = \frac{2\pi}{ik_0} \cdot \Big[\mathbf{A}(\hat{n}',\hat{n}'') - \mathbf{A}^{*^{tp}}(\hat{n}'',\hat{n}')\Big] \quad (7.139)$$

which holds for the dyadic scattering amplitude. It is called the "generalized optical theorem". The more familiar form of this theorem can be derived in the following way: Let us assume that $\vec{p}$ is some constant vector. Next, we apply a scalar multiplication with this vector from left and right of (7.139). If $\hat{n}' = \hat{n}''$ is chosen, and with definition

$$\vec{A}_p(\hat{n},\hat{n}') := \mathbf{A}(\hat{n},\hat{n}') \cdot \vec{p}\ , \quad (7.140)$$

we get from (7.139) the conventional optical theorem

$$\oint_{S_\infty} \vec{A}_p^*(\hat{n},\hat{n}') \cdot \vec{A}_p(\hat{n},\hat{n}')\, d\hat{n} = \frac{4\pi}{k_0} \cdot \mathrm{Im}\Big[\vec{p} \cdot \vec{A}_p(\hat{n}',\hat{n}')\Big]. \quad (7.141)$$

This optical theorem becomes of special importance if $\vec{p}$ is a unit vector in the direction of polarization of the primary incident plane wave since it results in an easy calculation of the extinction cross-section. This is one of the scattering quantities of our interest which will be introduced in the next subsection.

Another important quantity is the time-averaged Poynting vector. It can be calculated from the real part of the complex Poynting vector according to

$$< \vec{P}(\mathbf{x}) >_t = \frac{1}{2} \cdot \mathrm{Re}\Big[\vec{E}(\mathbf{x}) \times \vec{H}^*(\mathbf{x})\Big] \quad (7.142)$$

and is given in units of $\Big[\text{energy}/(\text{area} \times \text{time})\Big]$. For the plane wave

$$\vec{E}(\mathbf{x}) = \vec{E}_0 \cdot e^{i\, k_0\, |\mathbf{x}|\, \hat{n}_i \cdot \hat{n}_s} \quad (7.143)$$

we obtain in conjunction with (7.11)–(7.13), (7.100), (7.102), and identity

$$\vec{a} \times (\vec{b} \times \vec{c}) = \vec{b}\,(\vec{a} \cdot \vec{c}) - \vec{c}\,(\vec{a} \cdot \vec{b}) \quad (7.144)$$

the time averaged Poynting vector

$$< \vec{P}(\mathbf{x}) >_t = \frac{1}{2}\sqrt{\frac{\epsilon_0}{\mu_0}}\, |\vec{E}_0|^2 \cdot \hat{n}_i. \quad (7.145)$$

It is pointing into the direction of propagation of the plane wave. And how does the time averaged Poynting vector for the total field

$$\vec{E}_t(\mathbf{r}) \;=\; \vec{F}_1(\hat{n}_s)\cdot\frac{e^{-ik_0 r}}{r} \;+\; \vec{F}_2(\hat{n}_s)\cdot\frac{e^{ik_0 r}}{r} \tag{7.146}$$

in the far-field region looks like (note that $\mathbf{x}$ and $|\mathbf{x}|$ in (7.113) was simply replaced by $\mathbf{r}$ and r)? From (7.5), (7.10), and identity

$$\nabla\times(U\cdot\vec{u}) \;=\; U\cdot\nabla\times\vec{u} \;+\; \nabla U\times\vec{u} \tag{7.147}$$

we obtain for the corresponding total magnetic field

$$\vec{H}_t(\mathbf{r}) \;=\; -\sqrt{\frac{\epsilon_0}{\mu_0}}\cdot\left[\hat{r}\times\vec{F}_1(\hat{n}_s)\cdot\frac{e^{-ik_0 r}}{r} \;-\; \hat{r}\times\vec{F}_2(\hat{n}_s)\cdot\frac{e^{ik_0 r}}{r}\right] \tag{7.148}$$

if again neglecting contributions which tend to zero stronger than $1/r$. Then it follows

$$<\vec{P}(\mathbf{r})>_t \;=\; -\frac{1}{2\,r^2}\sqrt{\frac{\epsilon_0}{\mu_0}}\left[|\vec{F}_1(\hat{n}_s)|^2 \;-\; |\vec{F}_2(\hat{n}_s)|^2\right]\cdot\hat{r} \tag{7.149}$$

as the time averaged Poynting vector of the total field in the far-field region. It is pointing into the radial direction. Let us next calculate the boundary integral

$$\lim_{r\to\infty}\oint_{S_r} <\vec{P}(\mathbf{r})>_t\cdot\hat{r}\,dS \tag{7.150}$$

over the spherical surface S_r, and for $<\vec{P}(\mathbf{r})>_t$ according to (7.149) if r tends to infinity. Taking (2.52), (7.119) as well as (7.137) into account we obtain

$$\oint_{S_\infty}\left[|\vec{F}_1(\hat{n}_s)|^2 \;-\; |\vec{F}_2(\hat{n}_s)|^2\right]d\hat{n}_s \;=\; 0. \tag{7.151}$$

Since we can look upon the boundary integral (7.150) as the net flux of energy per time through the spherical surface S_r (7.151) can be taken as an expression of energy conservation for plane wave scattering on nonabsorbing scatterers in the far-field. In this way we can link the physical experience of "energy conservation" to the unitarity property of the dyadic far-field scattering operator which was proven independently of this experience before.

7.3.2 Definition of Scattering Quantities

Now, we intend to introduce the scattering quantities in a concise manner. We restrict our considerations to those quantities which are of importance in the numerical simulations we will present in Chap. 9. Those readers who are interested in other scattering quantities and in a more detailed treatment of the physical background

like the importance of the Stokes vector to characterize the state of polarisation of the fields are referred to the literature cited especially in Sect. 10.9.

Representation (7.107) of the scattered field in the far-field region serves as a starting point for the definitions of scattering quantities. Let us consider at first the general case resulting from (2.232) as the primary incident plane wave. Then the scattered field (7.107) becomes

$$\vec{E}_s(\mathbf{r}) \;=\; \mathbf{A}(\theta_s, \phi_s; \theta_i, \phi_i) \cdot \left(\hat{\theta}_i \cdot E^{inc}_{\theta_i} \;+\; \hat{\phi}_i \cdot E^{inc}_{\phi_i} \right) \cdot \frac{e^{ik_0 r}}{r}. \tag{7.152}$$

Its components with respect to θ_s and ϕ_s can be obtained from scalar multiplication of (7.152) from left with the unit vectors $\hat{\theta}_s$ and $\hat{\phi}_s$, respectively. Summarizing the components into a column vector we thus get

$$\begin{aligned} \begin{pmatrix} E^s_{\theta_s} \\ E^s_{\phi_s} \end{pmatrix} &= \frac{e^{ik_o r}}{r} \cdot \mathbf{F} \cdot \begin{pmatrix} E^{inc}_{\theta_i} \\ E^{inc}_{\phi_i} \end{pmatrix} \\ &= \frac{e^{ik_o r}}{r} \cdot \begin{pmatrix} F_{\theta\theta}\,(\theta_s, \phi_s; \theta_i, \phi_i) & F_{\theta\phi}\,(\theta_s, \phi_s; \theta_i, \phi_i) \\ F_{\phi\theta}\,(\theta_s, \phi_s; \theta_i, \phi_i) & F_{\phi\phi}\,(\theta_s, \phi_s; \theta_i, \phi_i) \end{pmatrix} \cdot \begin{pmatrix} E^{inc}_{\theta_i} \\ E^{inc}_{\phi_i} \end{pmatrix} \end{aligned} \tag{7.153}$$

as relation between the θ and ϕ components of the primary incident plane wave and the scattered wave. Matrix $\mathbf{F}$ is called the "scattering amplitude matrix" or "amplitude matrix". Its elements are calculated from the dyadic scattering amplitude according to

$$F_{\alpha\beta}\,(\theta_s, \phi_s; \theta_i, \phi_i) \;=\; \hat{\alpha}_s \cdot \mathbf{A}(\theta_s, \phi_s; \theta_i, \phi_i) \cdot \hat{\beta}_i \quad \text{with } \alpha, \beta \;=\; \theta, \phi. \tag{7.154}$$

A more detailed and numerical favorable expression can be obtained if one uses the expansions (7.130) and (7.131) of the dyadics $\mathbf{I}_t^{(\hat{n}_i)} \cdot e^{ik_0 \hat{n}_i \tilde{\mathbf{x}}}$ and $\mathbf{I}_t^{(\hat{n}_s)} \cdot e^{-ik_0 \hat{n}_s \bar{\mathbf{x}}}$ in (7.108). Then (7.154) becomes

$$\begin{aligned} F_{\alpha\beta}\,(\theta_s, \phi_s; \theta_i, \phi_i) = 4\pi \sum_{\tau,\tau'=1}^{2} \sum_{l,n;l'n'} & \left[\hat{\alpha} \cdot \vec{Y}_{l,n,\tau}(\theta_s, \phi_s) \right] \\ \cdot \oint_{\partial\Gamma} \vec{\psi}^{*}_{l,n,\tau}(k_0, \bar{\mathbf{x}}) \cdot \mathbf{W}(\bar{\mathbf{x}}, \tilde{\mathbf{x}}) \cdot \vec{\psi}_{l',n',\tau'}(k_0, \tilde{\mathbf{x}})\, dS(\bar{\mathbf{x}})\, dS(\tilde{\mathbf{x}}) & \\ \cdot \left[\vec{Y}_{l',n',\tau'}(\theta_i, \phi_i) \cdot \hat{\beta} \right] & \end{aligned} \tag{7.155}$$

or

$$F_{\alpha\beta}(\theta_s, \phi_s; \theta_i, \phi_i) = \frac{4\pi}{ik_0} \sum_{\tau,\tau'=1}^{2} \sum_{l,n;l'n'} \left[\hat{\alpha} \cdot \vec{Y}_{l,n,\tau}(\theta_s, \phi_s)\right] \cdot [W]^{\tau,\tau'}_{l,n;l',n'} \cdot \left[\vec{Y}_{l',n',\tau'}(\theta_i, \phi_i) \cdot \hat{\beta}\right] \tag{7.156}$$

if taking the definition of the matrix elements $[W]^{\tau,\tau'}_{l,n;l',n'}$ of the interaction operator into account. These elements of the scattering amplitude matrix are the decisive elements to define the scattering quantities. But for this we must have in mind that in scattering experiments intensities rather than fields are measured. For this purpose we impose the so-called "Stokes vector" of a certain field

$$\vec{E} \;=\; \hat{\theta} \cdot E_\theta \;+\; \hat{\phi} \cdot E_\phi \;, \tag{7.157}$$

by

$$\mathbf{I} \;:=\; \begin{pmatrix} I \\ Q \\ U \\ V \end{pmatrix} \;=\; \frac{1}{2}\sqrt{\frac{\epsilon_0}{\mu_0}} \cdot \begin{pmatrix} E_\theta E_\theta^* + E_\phi E_\phi^* \\ E_\theta E_\theta^* - E_\phi E_\phi^* \\ 2\mathrm{Re}\left[E_\theta E_\phi^*\right] \\ 2\mathrm{Im}\left[E_\theta E_\phi^*\right] \end{pmatrix} . \tag{7.158}$$

This vector contains only real-valued quantities and describes the polarization state of the field. Please, note that there exist other definitions of the Stokes vector in the literature. The first Stokes parameter I represents the intensity of the field $\vec{E}$. From (7.153) we get the relation

$$\mathbf{I}_s \;=\; \frac{1}{r^2} \cdot \mathbf{Z}(\theta_s, \phi_s; \theta_i, \phi_i) \cdot \mathbf{I}_{inc} \tag{7.159}$$

between the Stokes vector of the primary incident and scattered field. $\mathbf{Z}$ therein denotes the "Stokes matrix". Its elements are related to the elements of the scattering amplitude matrix as follows:

$$Z_{11} = \frac{1}{2} \cdot \left(|F_{\theta\theta}|^2 + |F_{\theta\phi}|^2 + |F_{\phi\theta}|^2 + |F_{\phi\phi}|^2\right) \tag{7.160}$$

$$Z_{12} = \frac{1}{2} \cdot \left(|F_{\theta\theta}|^2 - |F_{\theta\phi}|^2 + |F_{\phi\theta}|^2 - |F_{\phi\phi}|^2\right) \tag{7.161}$$

$$Z_{13} = \mathrm{Re}\left(F_{\theta\phi}F_{\theta\theta}^* + F_{\phi\phi}F_{\theta\phi}^*\right) \tag{7.162}$$

$$Z_{14} = \mathrm{Im}\left(F_{\theta\phi}F_{\theta\theta}^* + F_{\phi\phi}F_{\theta\phi}^*\right) \tag{7.163}$$

$$Z_{21} = \frac{1}{2} \cdot \left(|F_{\theta\theta}|^2 + |F_{\theta\phi}|^2 - |F_{\phi\theta}|^2 - |F_{\phi\phi}|^2\right) \tag{7.164}$$

$$Z_{22} = \frac{1}{2} \cdot \left(|F_{\theta\theta}|^2 - |F_{\theta\phi}|^2 - |F_{\phi\theta}|^2 + |F_{\phi\phi}|^2\right) \tag{7.165}$$

$$Z_{23} = \mathrm{Re}\left(F_{\theta\phi}F^*_{\theta\theta} - F_{\phi\phi}F^*_{\phi\theta}\right) \tag{7.166}$$

$$Z_{24} = \mathrm{Im}\left(F_{\theta\phi}F^*_{\theta\theta} - F_{\phi\phi}F^*_{\phi\theta}\right) \tag{7.167}$$

$$Z_{31} = \mathrm{Re}\left(F_{\phi\theta}F^*_{\theta\theta} + F_{\phi\phi}F^*_{\theta\phi}\right) \tag{7.168}$$

$$Z_{32} = \mathrm{Re}\left(F_{\phi\theta}F^*_{\theta\theta} - F_{\phi\phi}F^*_{\theta\phi}\right) \tag{7.169}$$

$$Z_{33} = \mathrm{Re}\left(F_{\phi\phi}F^*_{\theta\theta} + F_{\phi\theta}F^*_{\theta\phi}\right) \tag{7.170}$$

$$Z_{34} = \mathrm{Im}\left(F_{\phi\phi}F^*_{\theta\theta} - F_{\phi\theta}F^*_{\theta\phi}\right) \tag{7.171}$$

$$Z_{41} = -\mathrm{Im}\left(F_{\phi\theta}F^*_{\theta\theta} + F_{\phi\phi}F^*_{\theta\phi}\right) \tag{7.172}$$

$$Z_{42} = -\mathrm{Im}\left(F_{\phi\theta}F^*_{\theta\theta} - F_{\phi\phi}F^*_{\theta\phi}\right) \tag{7.173}$$

$$Z_{43} = -\mathrm{Im}\left(F_{\phi\phi}F^*_{\theta\theta} + F_{\phi\theta}F^*_{\theta\phi}\right) \tag{7.174}$$

$$Z_{44} = \mathrm{Re}\left(F_{\phi\phi}F^*_{\theta\theta} - F_{\phi\theta}F^*_{\theta\phi}\right). \tag{7.175}$$

For the ongoing considerations we restrict the primary incident plane wave to the special case (2.232) with $\theta_i = \phi_i = 0^o$ and $E_{\phi_i} = 0, E_{\theta_i} = E_0 = 1$ or $E_{\phi_i} = E_0 = 1, E_{\theta_i} = 0$ depending on whether the incident plane wave is polarized with respect to the x- or y-axis with amplitude E_0 normalized to unity. Since the directional vectors $\hat{n}_i$ and $\hat{n}_s$ set up the scattering planes these are given in this special case by cuts along the lines of longitudes of the sphere with radius S_∞ (see Fig. 7.3). It is common in electromagnetic wave scattering to replace the unit vectors $\hat{\theta}$ and $\hat{\phi}$ by the horizontal ($\hat{h}$) and vertical ($\hat{v}$) unit vector with respect to the scattering planes. Due to the fixing of the angles θ_i and ϕ_i of the incident plane wave the elements of the scattering amplitude matrix are only functions of the scattering angles θ_s and ϕ_s. Equation (7.156) can therefore be reduced to

$$F_{\alpha\beta}(\theta_s, \phi_s) = \frac{4\pi}{ik_0} \sum_{\tau,\tau'=1}^{2} \sum_{l,n;l'n'} \left[\hat{\alpha} \cdot \vec{Y}_{l,n,\tau}(\theta_s, \phi_s)\right] \cdot [W]^{\tau,\tau'}_{l,n;l',n'} \cdot \left[\vec{Y}_{l',n',\tau'}(\theta_i = 0^o, \phi_i = 0^o) \cdot \hat{\beta}\right]; \quad \alpha, \beta = h, v. \tag{7.176}$$

Moreover, because of (2.141) and (2.142) only the contributions $\left[\vec{Y}_{l',n',\tau'}(\theta_i = 0^o, \phi_i = 0^o) \cdot \hat{\beta}\right]$ with $l' = \pm 1$ are non-zero. The coordinate system whose z-axis agrees with the direction of propagation of the incident plane wave is usually called the "laboratory system". Of course, the matrix elements

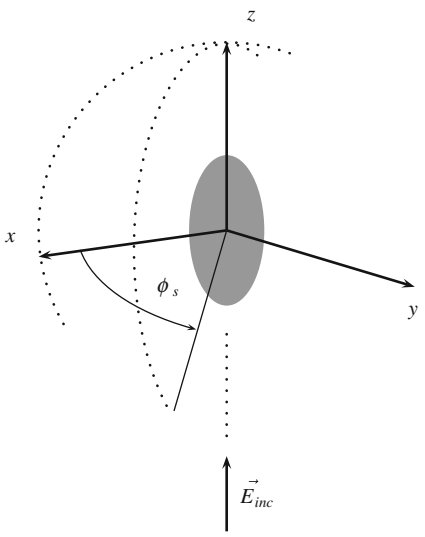

Fig. 7.3 Cuts along the lines of longitudes of the sphere with radius S_∞ are the scattering planes if the primary incident plane wave is travelling along the z-axis

$$[W(L)]_{l,n;l',n'}^{\tau,\tau'} = (ik_0) \cdot \oint_{\partial\Gamma} \vec{\psi}_{l,n,\tau}^{*}(k_0, \bar{\mathbf{x}}_L) \cdot \mathbf{W}(\bar{\mathbf{x}}_L, \tilde{\mathbf{x}}_L) \cdot \vec{\psi}_{l',n',\tau'}(k_0, \tilde{\mathbf{x}}_L)\, dS(\bar{\mathbf{x}}_L)\, dS(\tilde{\mathbf{x}}_L) \tag{7.177}$$

in (7.156) must be calculated in this laboratory system. Both vector functions $\vec{\psi}_{l,n,\tau}^{*}(k_0, \bar{\mathbf{x}}_L)$ and $\vec{\psi}_{l',n',\tau'}(k_0, \tilde{\mathbf{x}}_L)$ contain the surface geometry of the scatterer expressed in the coordinates $\bar{\mathbf{x}}_L$ and $\tilde{\mathbf{x}}_L$ of the laboratory system, too. These matrix elements are therefore denoted with $[W(L)]_{l,n;l',n'}^{\tau,\tau'}$. On the other hand, introducing a particle frame which accounts for possible symmetries of the scatterer geometry would possibly allow a more simple description of the scatterer surface. This applies to the considerations in Chap. 8 as well as to the rotationally symmetric scatterers we intend to analyse in Chap. 9. The laboratory system can be transformed by the three Eulerian angles (α, β, γ) of rotation into the particle frame, as already described in Sect. 2.4.2. Regarding rotationally symmetric scatterers we place the z-axis of the particle frame into the axis of symmetry. However, the question arises if it is possible to calculate the matrix elements of the interaction operator at first within the simpler particle frame and to transform these results into the laboratory frame afterwards? This is indeed possible, and it is one of the essential advantages of the T-matrix approach, as demonstrated in many applications by Mishchenko (see the book of Mishchenko, Travis, and Lacis cited in Sect. 10.9). To derive the transformation equation for the matrix elements of the interaction operator we have to go back to the transformation behaviour of the vectorial eigensolutions discussed in Sect. 2.4.2. By use of (2.195) we may write instead of (7.177) if expressed in the new coordinates $\bar{\mathbf{x}}_K$ and $\tilde{\mathbf{x}}_K$ of the particle frame and the Eulerian angles (α, β, γ):

$$[W(L)]^{\tau,\tau'}_{l,n;l',n'} = (ik_0) \cdot \sum_{l_1=-n}^{n} \sum_{l_2=-n'}^{n'} \left[D^{(n)}_{l_1,l}(-\gamma,-\beta,-\alpha) \right]^* \cdot \oint_{\partial\Gamma} \vec{\psi}^*_{l_1,n,\tau}(k_0,\bar{\mathbf{x}}_K) \cdot \mathbf{W}(\bar{\mathbf{x}}_K,\tilde{\mathbf{x}}_K) \cdot \vec{\psi}_{l_2,n',\tau'}(k_0,\tilde{\mathbf{x}}_K)\, dS(\bar{\mathbf{x}}_K)\, dS(\tilde{\mathbf{x}}_K) \cdot D^{(n')}_{l_2,l'}(-\gamma,-\beta,-\alpha). \tag{7.178}$$

But the boundary integrals are just the matrix elements of the interaction operator in the particle frame, i.e., we get

$$[W(L)]^{\tau,\tau'}_{l,n;l',n'} = \sum_{l_1=-n}^{n} \sum_{l_2=-n'}^{n'} \left[D^{(n)}_{l_1,l}(-\gamma,-\beta,-\alpha) \right]^* \cdot [W(K)]^{\tau,\tau'}_{l_1,n;l_2,n'} \cdot D^{(n')}_{l_2,l'}(-\gamma,-\beta,-\alpha). \tag{7.179}$$

Interchanging the summation indices l_1 and l in $D^{(n)}_{l_1,l}$ and taking relation (2.194) as well as relation (2.192) into account results finally into the transformation equation

$$[W(L)]^{\tau,\tau'}_{l,n;l',n'} = \sum_{l_1=-n}^{n} \sum_{l_2=-n'}^{n'} D^{(n)}_{l,l_1}(\alpha,\beta,\gamma) \cdot [W(K)]^{\tau,\tau'}_{l_1,n;l_2,n'} \cdot D^{(n')}_{l_2,l'}(-\gamma,-\beta,-\alpha). \tag{7.180}$$

Different orientations of one and the same scatterer with respect to the primary incident plane wave (i.e., in the laboratory frame) are thus expressed by different Eulerian angles, but, most important, the calculation of the matrix elements must be performed **only once** within the particle frame. It is especially this behaviour which bears drastic improvements if orientation averaging becomes necessary. Now, we are prepared to define some scattering quantities.

Let us start with the total extinction (σ^{ext}_α) , scattering (σ^{s}_α), and absorption cross-sections (σ^{abs}_α). These total quantities are calculated from the elements of the scattering amplitude matrix according to

$$\sigma^{ext}_\alpha := \tfrac{4\pi}{k_0} \cdot \mathrm{Im}\left[F_{\alpha\alpha}(\theta_s = 0^o, \phi_s = 0^o) \right], \tag{7.181}$$

$$\sigma^{s}_\alpha := \int_0^{2\pi} \int_0^{\pi} \left[|F_{\alpha\alpha}(\theta_s,\phi_s)|^2 + |F_{\beta\alpha}(\theta_s,\phi_s)|^2 \right] \sin\theta_s \, d\theta_s \, d\phi_s, \tag{7.182}$$

and

$$\sigma^{abs}_\alpha := \sigma^{ext}_\alpha - \sigma^{s}_\alpha. \tag{7.183}$$

Subindex α corresponds to the state of polarization of the primary incident plane wave with respect to the considered scattering plane. It will be restricted to the x-z-plane in all the subsequent considerations as well as in the numerical simulations presented in

Chap. 9. These cross-sections are functions of the Eulerian angles (α, β, γ) of rotation which are used to characterize the orientation of the scatterer in the laboratory frame, as already mentioned. Due to the conventional optical theorem (7.141), and because of (7.151) and (7.152)

$$\sigma_{\alpha}^{ext} = \sigma_{\alpha}^{s} \tag{7.184}$$

holds for nonabsorbing scatterers. If these cross-sections are normalized to a characteristic cross-section then we speak of the corresponding dimensionless "efficiencies" (i.e., extinction $(\tilde{\sigma}_{\alpha}^{ext})$, scattering $(\tilde{\sigma}_{\alpha}^{s})$, and absorption efficiency $(\tilde{\sigma}_{\alpha}^{abs})$). The characteristic cross-section of a spherical particle with radius $r = a$ is just its circular cross-section πa^2.

The differential polarimetric scattering cross-sections with respect to the x-z-plane are defined according to

$$\frac{d\sigma_{\beta\alpha}(\theta_s, \phi_s = 0^o/180^o)}{d\Omega_s} := |F_{\beta\alpha}\left(\theta_s, \phi_s = 0^o/180^o\right)|^2 \tag{7.185}$$

with $F_{\beta\alpha}$ calculated again by use of (7.176). $d\Omega_s = \sin\theta_s \, d\theta_s \, d\phi_s$ denotes the differential solid angle. These differential cross sections characterize the amount of energy of the primary incident wave of polarization $\hat{\alpha}$ scattered into a certain direction $d\Omega_s$ with polarization $\hat{\beta}$. In more detail, these are the 4 differential cross-sections

$$\begin{aligned} &\frac{d\sigma_{hh}(\theta_s, \phi_s = 0^o/180^o)}{d\Omega_s}, \quad \frac{d\sigma_{vv}(\theta_s, \phi_s = 0^o/180^o)}{d\Omega_s}, \\ &\frac{d\sigma_{hv}(\theta_s, \phi_s = 0^o/180^o)}{d\Omega_s}, \quad \frac{d\sigma_{vh}(\theta_s, \phi_s = 0^o/180^o)}{d\Omega_s}. \end{aligned} \tag{7.186}$$

These quantities can be measured with two additional polarisers in the scattering plane, one for the primary incident plane wave and one for the scattered field. They are also functions of the Eulerian angles (α, β, γ). $\theta_s = 0^o$ denotes forward scattering, and $\theta_s = 180^o$ backscattering. Please, note also that ϕ_s takes on only the two values 0^o or 180^o depending on whether θ_s are given in the first and fourth or second and third quadrant of the x-z-plane.

$$\frac{d\sigma_h}{d\Omega_s} = \frac{d\sigma_{hh}}{d\Omega_s} + \frac{d\sigma_{vh}}{d\Omega_s} \tag{7.187}$$

and

$$\frac{d\sigma_v}{d\Omega_s} = \frac{d\sigma_{vv}}{d\Omega_s} + \frac{d\sigma_{hv}}{d\Omega_s} \tag{7.188}$$

are the unpolarized differential scattering cross-sections for an incident plane wave which is horizontally or vertically polarized.

Orientation averaged scattering quantities are also of our interest in Chap. 9. But all simulations will be restricted to the most simple case of randomly oriented par-

ticles. Then the angular dependent scattering behaviour becomes identical in each meridional cut, i.e., it is again sufficient to restrict the considerations to the x-z-plane.

$$< \mathcal{M} > = \frac{1}{8\pi^2} \cdot \int_0^{2\pi} d\alpha \int_0^{\pi} d\beta \sin\beta \int_0^{2\pi} d\gamma \, \mathcal{M}(\alpha, \beta, \gamma) \tag{7.189}$$

is the orientation averaged value of the scattering quantity $\mathcal{M}$. The prefactor $1/8\pi^2$ results from the normalization of the random distribution function to unity. The orientation averaged Stokes matrix $< \mathbf{Z} >$ is called the "phase matrix", and its orientation averaged element $< Z_{11} >$ is the so-called "phase function". This element, if normalized to unity, provides the likelihood that a photon travelling originally along the z-axis of the laboratory system will be scattered into the direction of $d\Omega_s$. $< Z_{11} >$ is therefore an important source function in radiative transfer theory.

7.4 Scalability of the Scattering Problem

At the end of this chapter, we will discuss the possibility to scale the scattering problem. This allow us to introduce the important "size parameter". This parameter expresses the ratio of a certain characteristic dimension of the scatterer to the wavelength of the incident plane wave. In the literature one can find very often the statement that "*this numerical approach can be applied up to a size parameter of* ...", i.e., it is an important parameter to determine the range of applicability of a certain solution method. But this parameter can also be used as a scaling parameter for databases, like that one discussed in Chap. 9.

The far-field scattering quantities are calculated from the elements of the dyadic scattering amplitude matrix, as we could see in the foregoing section. However, to calculate the dyadic scattering matrix requires knowledge about the elements of the T-matrix (interaction operator) in the particle frame. The geometry of the scatterer is contained in these latter elements. To discuss the scalability property let us therefore go back to the transformation character of the T-matrix. Equations (2.18) and (2.24)/(2.25) are the relevant relations. They express the general transformation behaviour of the different eigenfunctions at the scatterer surface and hold for the scalar and dyadic case as well. A characteristic property of all the eigenfunctions at the scatterer surface is their dependence on "$k_0 \cdot r$" or "$k \cdot r$" only, depending on whether we are outside (k_0) or inside (k) the scatterer. That is, the scatterer geometry contributes only via the arguments

$$k_0 \cdot r(\theta, \phi) \quad \text{and} \quad k \cdot r(\theta, \phi) \; = \; \sqrt{\epsilon_r} \cdot k_0 \cdot r(\theta, \phi) \tag{7.190}$$

to expressions (2.18) and (2.24)/(2.25) with $r(\theta, \phi)$ being the parameter representation of the scatterer surface according to (2.48). ϵ_r is the dielectric constant of the scatterer (see Sect. 7.2.1). This has the following implication: Whenever we consider

"similar scatterer geometries"

$$r'(\theta, \phi) \; = \; s \cdot r(\theta, \phi) \tag{7.191}$$

with "s" being some constant parameter, and an incident plane wave with the wavelength

$$k_0' \; = \; \frac{1}{s} \cdot k_0 \tag{7.192}$$

we end up with identical T-matrix elements. This follows obviously from the identities

$$k_0 \cdot r(\theta, \phi) = k_0' \cdot r'(\theta, \phi) \tag{7.193}$$

$$k \cdot r(\theta, \phi) = k' \cdot r'(\theta, \phi) \tag{7.194}$$

which hold if the dielectric constant of the scatterer remains unchanged. How can we use this property to scale the scattering problem? To answer this question let us consider three rotationally symmetric scatterer geometries which are of special importance in Chap. 9.

$$r(\theta) \; = \; r_K \cdot \left[p \cdot \cos\theta \; + \; \left(1 \; - \; p^2 \cdot \sin^2\theta \right)^{1/2} \right] \tag{7.195}$$

with

$$p \; = \; \frac{\epsilon}{r_K} \tag{7.196}$$

is the parameter representation of a sphere with radius $r = r_K$ shifted by ϵ along the z-axis from its origin. Let us now consider a second sphere shifted by

$$\epsilon' \; = \; s \cdot \epsilon \tag{7.197}$$

and with the new radius

$$r_K' \; = \; s \cdot r_K . \tag{7.198}$$

This second shifted sphere exhibits the same scattering behaviour at wavenumber k_0' as the first shifted sphere at wavenumber k_0. "$k_0 \cdot r_K$" would thus be an appropriate size and scaling parameter for this geometry.

As another example let us consider a spheroidal particle with the z-axis of the particle frame being identical with its axis of revolution. The boundary surface may be described by

$$r(\theta) \; = \; a \cdot \left[\cos^2\theta \; + \; \left(\frac{a}{b} \right)^2 \cdot \sin^2\theta \right]^{-1/2} . \tag{7.199}$$

"a" denotes the semi-axis along the z-axis, and "b" denotes the second semi-axis. The aspect ratio is given by

$$av = \frac{a}{b}. \tag{7.200}$$

$av < 1$ and $av > 1$ are the aspect ratios of oblate and prolate spheroids, respectively. $av = 1$ is just the sphere with radius $r = a$.

$$a' = s \cdot a \tag{7.201}$$

$$b' = s \cdot b \tag{7.202}$$

is a similar spheroid, i.e., it has the same aspect ratio as the former ones. Its scattering behaviour at wavenumber k_0' is identical with the scattering behaviour of the former spheroid at wavenumber k_0. "$k_0 \cdot a$" would be therefore an appropriate size and scaling parameter. "$k_0 \cdot r_{eqv}$" with "r_{eqv}" being the radius of the volume equivalent sphere is another possibility of a size parameter we will use in Chap. 9. Semi-axis a, aspect ratio av, and r_{eqv} are related among each other via equation

$$a = r_{eqv} \cdot \sqrt{(av)^2}. \tag{7.203}$$

Chebyshev particles are another kind of particles which are of our interest in Chap. 9.

$$r(\theta) = r_K \cdot (1 + \epsilon \cdot \cos n \cdot \theta) \tag{7.204}$$

is the corresponding parameter representation of its surface. "r_K" denotes the radius of the underlying sphere, "ϵ" is the deformation parameter, and "n" represents the order of the Chebyshev particle. The limiting case of a spherical particle with radius $r = r_K$ results obviously from $\epsilon = 0$. The z-axis of the particle frame is again the axis of revolution. A similar Chebyshev particle is given by

$$r_K' = s \cdot r_K \tag{7.205}$$

but for fixed values of ϵ and n. "$k_0 \cdot r_K$" as well as "$k_0 \cdot r_{eqv}$" would be again appropriate size and scaling parameters. But the calculation of the radius of the volume equivalent sphere "r_{eqv}" is now a little bit more complicate.

Chapter 8
Scattering on Particles with Discrete Symmetries

8.1 Introduction

Particles in nature are found in countless different shapes, and we have little hope of computing optical properties of ensembles of particles by accounting for each and every individual geometry. Instead, we are often forced to solve the electromagnetic scattering problem by introducing approximations appropriate to describing the main physical and morphological features of the particles and their impact on the scattered field. In many applications we can achieve great simplifications by invoking symmetry assumptions about the particle geometry. Solutions with symmetry are particularly useful for numerical applications, since they help to substantially expedite numerical computations and to increase the stability of numerical algorithms.

The heretofore developed Green functions formalism provides a powerful starting point for discussing symmetries in boundary value problems. The following considerations will therefore serve as an illustration of how to apply this formalism in theoretical studies. We will first investigate in quite general terms how symmetries of the scattering object manifest themselves as symmetry relations of the interaction operator. From the symmetries of the interaction operatorwe will obtain the corresponding symmetry relations of the Green functionand of the T-matrix. We will then discuss in some detail how to exploit the symmetry relations in the T-matrix formalism by using the specific basis of the eigensolutions of the wave equation in spherical coordinates.

8.1.1 Symmetry Relations

Geometric symmetry is a concept that is, in essence, rather easy to grasp, since it strongly appeals to our intuition. The main problem is usually to develop an adequate mathematical language for bringing our intuitive pictures into a more explicit and directly applicable form. In this section we will get quite far in our investigation of

T. Rother and M. Kahnert, *Electromagnetic Wave Scattering on Nonspherical Particles*, Springer Series in Optical Sciences 145, DOI: 10.1007/978-3-642-36745-8_8,

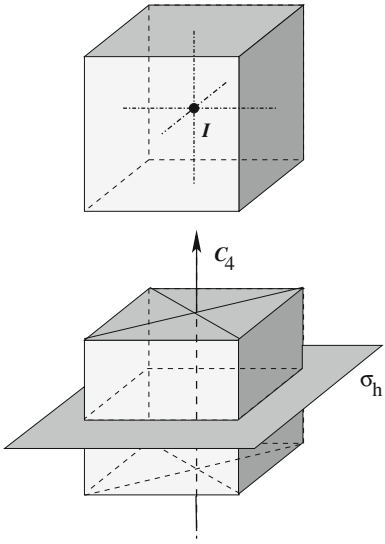

Fig. 8.1 Examples of symmetry elements of a cube

symmetries in boundary value problems just by relying on our geometric intuition and on the results derived in the previous chapters. The symmetry relations we derive will be rather general. In Sect. 8.2 we bring the symmetry relations into a more explicit form by choosing a specific set of basis functions. A more formal mathematical development will follow in Sects. 8.3 and 8.4.

Consider, as a first example, a cube as shown in Fig. 8.1. This geometrical object is invariant under various coordinate transformations. For instance, if we perform an inversion of all spatial coordinates by mirroring all points of the cube through the point I at the geometrical centre, then the resulting object is indistinguishable from the original object. Similarly, if we consider a rotation axis C_4 that passes through the centre of the cube and intercepts two opposite faces at a right angle, then a rotation about this axis by an angle $2\pi n/4$ (where n is an integer) brings the object into a new orientation indistinguishable from the original one. The same is true if we mirror all points through a reflection plane σ_h as indicated in the figure. Such coordinate transformations, as spatial inversions, rotations, reflections, or combined rotation-reflections, are called *symmetry operations*. The associated geometrical entities that describe the symmetries of the object of interest, such as mirror points, rotation axes, or mirror planes, are called *symmetry elements*. Let us now turn to electromagnetic scattering and investigate how geometric symmetries of the scattering object manifest themselves in our boundary value problems.

The Outer Dirichlet Problem

We start by considering the scalar case. The interaction operator $W_{\partial\Gamma_+}(\bar{\mathbf{x}}, \tilde{\mathbf{x}})$ defined in Eq. (4.1) describes the interaction of the unperturbed incident field with the

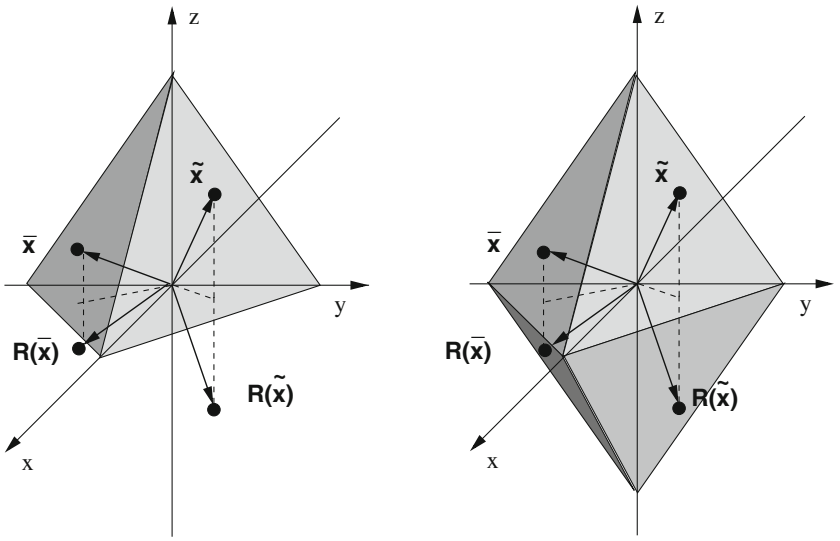

Fig. 8.2 Two objects that are not invariant (*left panel*) and invariant (*right panel*) under reflection in the xy-plane

surface of the scattering object, and the generation of the scattered field. According to the remarks following Eq. (4.1), $W_{\partial\Gamma_+}$ is dependent on the scatterer's geometry. Symmetries of the boundary surface therefore have to manifest themselves in $W_{\partial\Gamma_+}$.

Now consider a coordinate transformation $\mathbf{R}$ that transforms a position vector $\mathbf{x}$ in a fixed coordinate system into a new vector $\mathbf{R}(\mathbf{x})$. As a specific example, consider a Cartesian coordinate system, in which $\mathbf{x} = (x, y, z)$, and let $\mathbf{R}$ represent a reflection in the xy-plane, i.e. $\mathbf{R}(x, y, z) = (x, y, -z)$. If the geometry of the scatterer is invariant under the coordinate transformation $\mathbf{R}$, then the scatterer's interaction with the incident field has to be invariant too. This means that the interaction operator should satisfy the symmetry relation

$$W_{\partial\Gamma_+}(\mathbf{R}(\bar{\mathbf{x}}), \mathbf{R}(\tilde{\mathbf{x}})) = W_{\partial\Gamma_+}(\bar{\mathbf{x}}, \tilde{\mathbf{x}}) \quad \forall\, \bar{\mathbf{x}}, \tilde{\mathbf{x}} \in \partial\Gamma. \tag{8.1}$$

As an illustration, consider Fig. 8.2. The points $\bar{\mathbf{x}}$ and $\tilde{\mathbf{x}}$ lie on the boundary surface $\partial\Gamma$. If the object is not invariant under a reflection in the xy-plane, as that depicted in the left panel, then the reflected points $\mathbf{R}(\bar{\mathbf{x}})$ and $\mathbf{R}(\tilde{\mathbf{x}})$ lie, in general, not on $\partial\Gamma$, so $W_{\partial\Gamma_+}(\mathbf{R}(\bar{\mathbf{x}}), \mathbf{R}(\tilde{\mathbf{x}}))$ is not even defined in this case. However, if $\mathbf{R}$ is a symmetry operation of the scattering object, as in the right panel of Fig. 8.2, then $W_{\partial\Gamma_+}(\mathbf{R}(\bar{\mathbf{x}}), \mathbf{R}(\tilde{\mathbf{x}}))$ is well defined and should be invariant under the symmetry operation $\mathbf{R}$.

Equation 8.1 is our basic symmetry postulate, which we have introduced based on a plausibility argument. We can gain further confidence in this postulate by investigating its consequences for the Green function, and by interpreting the results physically. The strategy is to substitute Eq. (8.1) into Eq. (4.1) in order to obtain the

corresponding symmetry relation of the Green function G_{Γ_+} related to the outer Dirichlet problem. Before we can proceed with this plan, we have to make three essential remarks.

First we note that if $\mathbf{R}$ represents a symmetry of $\partial\Gamma$, then it has to be surjective on $\partial\Gamma$. This is a fancy way of saying that each point on the boundary surface is mapped by $\mathbf{R}$ onto a new point on the boundary surface. More concisely

$$\forall \bar{\mathbf{x}} \in \partial\Gamma \quad \exists \bar{\mathbf{x}}' \in \partial\Gamma; \quad \mathbf{R}(\bar{\mathbf{x}}) = \bar{\mathbf{x}}'. \tag{8.2}$$

Second we note that if $\mathbf{R}$ represents a symmetry of $\partial\Gamma$, then the surface element $dS(\bar{\mathbf{x}})$ has to be invariant under $\mathbf{R}$, i.e.

$$dS\left(\mathbf{R}(\bar{\mathbf{x}})\right) = dS\left(\bar{\mathbf{x}}\right). \tag{8.3}$$

The third remark refers to the symmetry properties of the free-space Green function G_0. The kind of operations we are interested in are symmetry operations of objects of finite extent. Such operations include rotation and reflection operations and combinations thereof. (As we will see later, the inversion operation discussed in conjunction with Fig. 8.1 is a special case of a rotation-reflection operation.) The free-space Green function is only subject to the radiation condition (1.19), not to any conditions defined on the boundary surface $\partial\Gamma$. Since free space is homogeneous and isotropic, G_0 is invariant under any rotation and reflection operation (and, in fact, even under translations), i.e.

$$G_0(\mathbf{R}(\mathbf{x}), \mathbf{R}(\mathbf{x}_0)) = G_0(\mathbf{x}, \mathbf{x}_0) \quad \forall\, \mathbf{x}, \mathbf{x}_0 \in \Gamma_+. \tag{8.4}$$

Rotations and reflection are represented by orthogonal transformations, which leave the norm of a vector unchanged. More formally speaking, the symmetry groups we are interested in are subgroups of the orthogonal group $\mathcal{O}(3)$. Thus if $|\mathbf{x}| > |\mathbf{x}_0|$, then $|\mathbf{R}(\mathbf{x})| > |\mathbf{R}(\mathbf{x}_0)|$. So the relation (8.4) even holds for the Green function $G_0^>$ defined in Eq. (2.276), i.e.

$$G_0^>(\mathbf{R}(\mathbf{x}), \mathbf{R}(\mathbf{x}_0)) = G_0^>(\mathbf{x}, \mathbf{x}_0) \quad |\mathbf{x}| > |\mathbf{x}_0|. \tag{8.5}$$

Now we are well prepared for investigating the symmetry properties of the Green function G_{Γ_+}. From Eq. (4.1) we obtain

$$\begin{aligned} G_{\Gamma_+}(\mathbf{x}, \mathbf{x}_0) &= G_0(\mathbf{x}, \mathbf{x}_0) \\ &\quad + \oint_{\partial\Gamma} G_0^>(\mathbf{x}, \bar{\mathbf{x}}) \cdot W_{\partial\Gamma_+}(\bar{\mathbf{x}}, \tilde{\mathbf{x}}) \cdot G_0(\tilde{\mathbf{x}}, \mathbf{x}_0)\, dS(\bar{\mathbf{x}})\, dS(\tilde{\mathbf{x}}) \\ &= G_0(\mathbf{R}(\mathbf{x}), \mathbf{R}(\mathbf{x}_0)) \; + \oint_{\partial\Gamma} G_0^>(\mathbf{R}(\mathbf{x}), \mathbf{R}(\bar{\mathbf{x}})) \cdot W_{\partial\Gamma_+}(\mathbf{R}(\bar{\mathbf{x}}), \mathbf{R}(\tilde{\mathbf{x}})) \\ &\quad \cdot G_0(\mathbf{R}(\tilde{\mathbf{x}}), \mathbf{R}(\mathbf{x}_0))\, dS(\mathbf{R}(\bar{\mathbf{x}}))\, dS(\mathbf{R}(\tilde{\mathbf{x}})) \end{aligned}$$

$$
\begin{aligned}
&= G_0(\mathbf{R}(\mathbf{x}), \mathbf{R}(\mathbf{x}_0)) \\
&\quad + \oint_{\partial\Gamma} G_0^{>}(\mathbf{R}(\mathbf{x}), \bar{\mathbf{x}}') \cdot W_{\partial\Gamma_+}(\bar{\mathbf{x}}', \tilde{\mathbf{x}}') \cdot G_0(\tilde{\mathbf{x}}', \mathbf{R}(\mathbf{x}_0))\, dS(\bar{\mathbf{x}}')\, dS(\tilde{\mathbf{x}}') \\
&= G_{\Gamma_+}(\mathbf{R}(\mathbf{x}), \mathbf{R}(\mathbf{x}_0)).
\end{aligned} \tag{8.6}
$$

In the second line we used the symmetry relations (8.1) and (8.3–8.5), and in the third line we used the surjectivity of $\mathbf{R}$ given in Eq. (8.2). So by using the interrelation of the Green function and the interaction operator, we have obtained a symmetry relation for G_{Γ_+} from the postulated symmetry relation of $W_{\partial\Gamma_+}$. Now let's see how we can understand this result physically.

The Green function $G_{\Gamma_+}(\mathbf{x}, \mathbf{x_0})$ belonging to the outer Dirichlet problem can be interpreted as the field at $\mathbf{x} \in \Gamma_+$ generated by a unit point source at $\mathbf{x_0} \in \Gamma_+$, subject to the radiation condition (1.19) and to the homogeneous Dirichlet condition (2.280). This can be seen either directly in Eq. (2.279), or by substituting in Eq. (2.286) the unit point source $\rho(\mathbf{x}') = \delta(\mathbf{x}' - \mathbf{x_0})$. We want to understand what happens to the Green function if we perform a coordinate transformation of the scattering object. As an example, let us consider a boundary surface such as that shown in the upper left panel of Fig. 8.3, and let us denote the Green function that solves the corresponding outer Dirichlet problem by $G^{(1)}_{\Gamma_+}(\mathbf{x}, \mathbf{x_0})$. Now we perform a reflection of the scatterer in the xy-plane, as shown in the upper right panel of Fig. 8.3. We now have a different boundary surface $\partial\Gamma$, hence a different boundary condition (2.280), and therefore a different Green function $G^{(2)}_{\Gamma_+}(\mathbf{x}, \mathbf{x_0})$ that solves the outer Dirichlet problem. It is clear that, in general, $G^{(1)}_{\Gamma_+}(\mathbf{x}, \mathbf{x_0}) \neq G^{(2)}_{\Gamma_+}(\mathbf{x}, \mathbf{x_0})$.

An alternative way to look at this is to leave the scattering object fixed and, instead, perform a corresponding coordinate transformation $\mathbf{R}$ of both the source point and the observation point. We can see in the middle panels of Fig. 8.3 that this picture is equivalent to that in which we transform the particle and keep the source and observation points fixed. However, since we do not alter the particle geometry in this picture, we are dealing with one and the same boundary value problem, hence with one and the same Green function G_{Γ_+}. So instead of comparing different Green functions $G^{(1)}_{\Gamma_+}$ and $G^{(2)}_{\Gamma_+}$ at the same argument $(\mathbf{x}, \mathbf{x_0})$, we now compare the same Green function G_{Γ_+} at different arguments $(\mathbf{x}, \mathbf{x_0})$ and $(\mathbf{R}(\mathbf{x}), \mathbf{R}(\mathbf{x_0}))$. By the same argument as in the case depicted in the upper panels of Fig. 8.3, we have, in general, $G_{\Gamma_+}(\mathbf{x}, \mathbf{x_0}) \neq G_{\Gamma_+}(\mathbf{R}(\mathbf{x}), \mathbf{R}(\mathbf{x_0}))$.

Now let's consider the case in which the xy-plane is a symmetry element of the scattering object. In that case, reflection of the scattering object in the xy-plane produces a geometry indistinguishable from the original one. Consequently, $G^{(1)}_{\Gamma_+}(\mathbf{x}, \mathbf{x_0}) = G^{(2)}_{\Gamma_+}(\mathbf{x}, \mathbf{x_0})$ for all $\mathbf{x}, \mathbf{x_0} \in \Gamma_+$. Alternatively, we can again keep the scattering objet fixed and reflect the source and observation points in the xy-plane, as shown in the lower panels of Fig. 8.3. Due to the symmetry of the scattering object we now have

$$
G_{\Gamma_+}(\mathbf{R}(\mathbf{x}), \mathbf{R}(\mathbf{x_0})) = G_{\Gamma_+}(\mathbf{x}, \mathbf{x_0}) \quad \forall\, \mathbf{x}, \mathbf{x_0} \in \Gamma_+. \tag{8.7}
$$

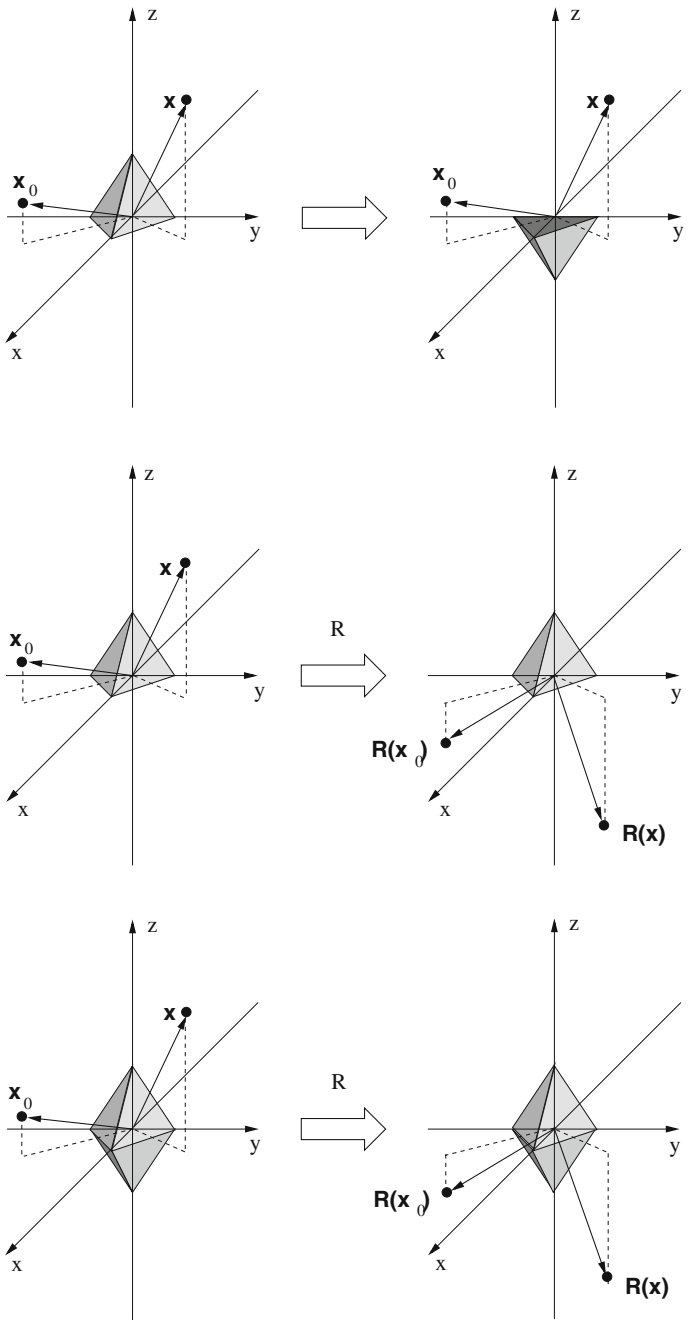

Fig. 8.3 Reflection of an object in the xy-plane (*top*); reflection of the source and observation points in the xy-plane in the presence of an asymmetric (*middle*) and symmetric object (*bottom*)

So we see that physical arguments lead us to the same manifest symmetry relation of G_{Γ_+} as that we obtained in Eq. (8.6) from the corresponding symmetry relation of the interaction operator. The symmetry relation given in (8.7) holds for any coordinate transformation $\mathbf{R}$ that corresponds to a symmetry operation of the scattering object.

The next step is to investigate the symmetries of the T-matrix. To this end, we have to consider the matrix elements of the interaction operator given in (4.4), which contain the expansion functions ψ_i. Up to now we have represented the effect of a symmetry transformation by a linear, orthogonal transformation $\mathbf{R}$ operating on the elements of a three-dimensional vector space. To investigate the effect of a symmetry transformation on the T-matrix, we now have to discuss, at least in rather general terms, how a symmetry transformation affects the functions ψ_i. In Eq. (2.189) we saw, as a specific example, how the vectorial eigensolutions transform under general rotations. The rotations are represented in the function space by linear matrices containing as components the Wigner D-functions. According to Eq. (2.194), the matrix representations are unitary. More generally, any symmetry transformation can be represented in the space of the functions ψ_i by a unitary matrix $\mathbf{V}$, such that

$$\psi_i(k_0, \mathbf{R}(\mathbf{x})) = \sum_{j=0}^{N} V_{i,j}\psi_j(k_0, \mathbf{x}), \tag{8.8}$$

and

$$\psi_i(k_0, \mathbf{R}^{-1}(\mathbf{x})) = \sum_{j=0}^{N} [V^\dagger]_{i,j}\psi_j(k_0, \mathbf{x}). \tag{8.9}$$

The analogy to Eqs. (2.189) and (2.193) is manifest. Relabelling $V^* = U$, we can write

$$\psi_i(k_0, \mathbf{R}^{-1}(\mathbf{x})) = \sum_{j=0}^{N} \psi_j(k_0, \mathbf{x})U_{j,i}. \tag{8.10}$$

Since k_0 is real, we can use (2.88) and obtain, in conjunction with the unitarity of $\mathbf{U}$,

$$\tilde{\psi}_i(k_0, \mathbf{R}^{-1}(\mathbf{x})) = \sum_{j=0}^{N} [U^{-1}]_{i,j}\tilde{\psi}_j(k_0, \mathbf{x}). \tag{8.11}$$

Now we can substitute the symmetry relation of the interaction operator (8.1) into the equation for the matrix elements of the interaction operator (4.4). This gives

$$\begin{aligned}\left[W_{\partial\Gamma_+}\right]_{i,k} &= (ik_0)\oint_{\partial\Gamma} \tilde{\psi}_i(k_0, \bar{\mathbf{x}}) \cdot W_{\partial\Gamma_+}(\bar{\mathbf{x}}, \tilde{\mathbf{x}}) \cdot \psi_k(k_0, \tilde{\mathbf{x}})\, dS(\bar{\mathbf{x}})\, dS(\tilde{\mathbf{x}}) \\ &= (ik_0)\oint_{\partial\Gamma} \tilde{\psi}_i(k_0, \bar{\mathbf{x}}) \cdot W_{\partial\Gamma_+}(\mathbf{R}(\bar{\mathbf{x}}), \mathbf{R}(\tilde{\mathbf{x}})) \cdot \psi_k(k_0, \tilde{\mathbf{x}})\, dS(\bar{\mathbf{x}})\, dS(\tilde{\mathbf{x}}).\end{aligned} \tag{8.12}$$

Here we substitute $\bar{\mathbf{x}}' = \mathbf{R}(\bar{\mathbf{x}})$ and $\tilde{\mathbf{x}}' = \mathbf{R}(\tilde{\mathbf{x}})$, and obtain

$$\left[W_{\partial\Gamma_+}\right]_{i,k} = (ik_0) \oint_{\partial\Gamma} \tilde{\psi}_i(k_0, \mathbf{R}^{-1}(\bar{\mathbf{x}}')) \cdot W_{\partial\Gamma_+}(\bar{\mathbf{x}}', \tilde{\mathbf{x}}') \cdot \psi_k(k_0, \mathbf{R}^{-1}(\tilde{\mathbf{x}}')) \cdot dS(\mathbf{R}^{-1}(\bar{\mathbf{x}}'))\, dS(\mathbf{R}^{-1}(\tilde{\mathbf{x}}')). \tag{8.13}$$

Since $\mathbf{R}^{-1}$ represents a symmetry operation of the boundary surface, relation (8.3) implies that $dS(\mathbf{R}^{-1}(\bar{\mathbf{x}}')) = dS(\bar{\mathbf{x}}')$. Using Eqs. (8.10) and (8.11), we obtain

$$\begin{aligned}\left[W_{\partial\Gamma_+}\right]_{i,k} &= (ik_0) \sum_{j,l=0}^{N} [U^{-1}]_{i,j} \\ &\quad \cdot \left\{ \oint_{\partial\Gamma} \tilde{\psi}_j(k_0, \bar{\mathbf{x}}') \cdot W_{\partial\Gamma_+}(\bar{\mathbf{x}}', \tilde{\mathbf{x}}') \cdot \psi_l(k_0, \tilde{\mathbf{x}}') dS(\bar{\mathbf{x}}')\, dS(\tilde{\mathbf{x}}') \right\} \cdot U_{l,k} \\ &= \sum_{j,l=0}^{N} [U^{-1}]_{i,j} \cdot \left[W_{\partial\Gamma_+}\right]_{j,l} \cdot U_{l,k}. \end{aligned} \tag{8.14}$$

In the last line we have again used (4.4). According to Eq. (4.7) the relation we have just obtained also holds for the T-matrix elements. So in compact matrix notation we finally have

$$\mathbf{T}_{\partial\mathbf{\Gamma}} = \mathbf{U}^{-1} \cdot \mathbf{T}_{\partial\mathbf{\Gamma}} \cdot \mathbf{U}, \tag{8.15}$$

or, equivalently,

$$[\mathbf{U}, \mathbf{T}_{\partial\mathbf{\Gamma}}] = \mathbf{0}, \tag{8.16}$$

where $[\mathbf{U}, \mathbf{T}_{\partial\mathbf{\Gamma}}] = \mathbf{U} \cdot \mathbf{T}_{\partial\mathbf{\Gamma}} - \mathbf{T}_{\partial\mathbf{\Gamma}} \cdot \mathbf{U}$ denotes the commutator of the two matrices $\mathbf{U}$ and $\mathbf{T}_{\partial\mathbf{\Gamma}}$, and where $\mathbf{0}$ represents the null-matrix. This can again be compared to relation (7.180) for rotationally symmetric objects.

The symmetry relation for the T-matrix is manifest. Equation (8.15) states that the T-matrix of the scattering object is invariant under any unitary transformation $\mathbf{U}$ that represents a symmetry operation of the scatterer. Note the formal analogy between the commutation relation (8.16) and the familiar commutation relation in quantum mechanics $[\hat{U}, \hat{H}] = 0$, where $\hat{H}$ represents the Hamiltonian operator. These commutation relations are associated with conservation laws for the generators of the unitary operators $\hat{U}$. A conserved quantity is a quantity that does not change in a dynamic process, where the dynamics of the system is described by the Hamiltonian. By contrast, we are considering a boundary value problem for a stationary amplitude distribution, as we explained in Sect. 7.2. So the commutation relation for the T-matrix must not be confused with symmetry relations in dynamic processes. Rather, it can be interpreted as an invariance of the solution to the outer Dirichlet problem under spatial coordinate transformations $\mathbf{U}$ that represent geometric symmetries of the boundary surface.

The generalisation of the previous findings to the outer Dirichlet problem of the vector-wave equation is straightforward. By the same reasoning as in the scalar problem, we start by postulating the symmetry relation of the dyadic interaction operator:

$$\mathbf{W}_{\partial\mathbf{\Gamma}_+}(\mathbf{R}(\mathbf{x}), \mathbf{R}(\mathbf{x_0})) = \mathbf{W}_{\partial\mathbf{\Gamma}_+}(\mathbf{x}, \mathbf{x_0}) \quad \forall\, \mathbf{x}, \mathbf{x_0} \in \partial\Gamma. \tag{8.17}$$

In complete analogy to the scalar case, substitution of the relation (8.17) into Eq. (4.23) results in a manifest symmetry relation of the dyadic Green function:

$$\mathbf{G}_{\mathbf{\Gamma}_+}(\mathbf{R}(\mathbf{x}), \mathbf{R}(\mathbf{x_0})) = \mathbf{G}_{\mathbf{\Gamma}_+}(\mathbf{x}, \mathbf{x_0}) \quad \forall\, \mathbf{x}, \mathbf{x_0} \in \Gamma_+. \tag{8.18}$$

The main difference between the definition of the matrix elements of the scalar and dyadic interaction operators in (4.4) and (4.26) is the extra τ-index. So in our previous derivations, we have to replace Eqs. (8.10) and (8.11) by

$$\vec{\psi}_{i,\tau}(k_0, \mathbf{R}^{-1}(\mathbf{x})) = \sum_{\sigma=1}^{2} \sum_{j=0}^{N} \vec{\psi}_{j,\sigma}(k_0, \mathbf{x}) U_{j,i}^{\sigma,\tau} \tag{8.19}$$

and

$$\vec{\tilde{\psi}}_{i,\tau}(k_0, \mathbf{R}^{-1}(\mathbf{x})) = \sum_{\sigma=1}^{2} \sum_{j=0}^{N} [U^{-1}]_{i,j}^{\tau,\sigma} \vec{\tilde{\psi}}_{j,\sigma}(k_0, \mathbf{x}), \tag{8.20}$$

respectively. Following the same procedure as in the scalar case, we arrive at

$$\left[W_{\partial\Gamma_+}\right]_{i,k}^{\tau,\tau'} = \sum_{\sigma,\sigma'=1}^{2} \sum_{j,l=0}^{N} [U^{-1}]_{i,j}^{\tau,\sigma} \cdot \left[W_{\partial\Gamma_+}\right]_{j,l}^{\sigma,\sigma'} \cdot U_{l,k}^{\sigma',\tau'}. \tag{8.21}$$

In compact matrix notation, this implies for the T-matrix

$$[\mathbf{U}, \mathbf{T}_{\partial\mathbf{\Gamma}}] = \mathbf{0}, \tag{8.22}$$

where both $\mathbf{U}$ and $\mathbf{T}_{\partial\mathbf{\Gamma}}$ now have extra indices τ, τ'.

The Outer Transmission Problem

In the outer Dirichlet problem we considered ideal metallic scatterers that are impenetrable for the electromagnetic field. In that case the symmetries of the boundary value problem were entirely determined by the geometric symmetries of the boundary surface $\partial\Gamma$. By contrast, in the outer transmission problem we are dealing with dielectric scatterers. Now the solution does not only depend on the geometry of the boundary surface, but also on the interior structure within Γ_-. Physically, this means that, e.g. inhomogeneities in the material properties of the scattering object can break the

symmetries of the object's boundary surface. But throughout this book we assume that the interior region Γ_- is homogeneous and isotropic with a constant wave number k. In such case, the symmetries of the problem are, again, fully defined by the symmetries of $\partial\Gamma$.

We start by considering the scalar case. If $\mathbf{R}$ represents a coordinate transformation that corresponds to a symmetry operation of the scatterer, then, by the same reasoning as in the Dirichlet case, we now postulate the two symmetry relations

$$W^{(d)}_{\partial\Gamma_+}(\mathbf{R}(\bar{\mathbf{x}}), \mathbf{R}(\tilde{\mathbf{x}})) = W^{(d)}_{\partial\Gamma_+}(\bar{\mathbf{x}}, \tilde{\mathbf{x}}) \quad \forall\, \bar{\mathbf{x}}, \tilde{\mathbf{x}} \in \partial\Gamma, \tag{8.23}$$

$$W^{(d)}_{\partial\Gamma_-}(\mathbf{R}(\bar{\mathbf{x}}), \mathbf{R}(\tilde{\mathbf{x}})) = W^{(d)}_{\partial\Gamma_-}(\bar{\mathbf{x}}, \tilde{\mathbf{x}}) \quad \forall\, \bar{\mathbf{x}}, \tilde{\mathbf{x}} \in \partial\Gamma. \tag{8.24}$$

Using these in Eqs. (4.12) and (4.13), we obtain, in complete analogy to the outer Dirichlet problem, the symmetry relations for the dielectric and auxiliary Green functions, i.e.

$$G^{(d)}_{\Gamma_+}(\mathbf{R}(\mathbf{x}), \mathbf{R}(\mathbf{x_0})) = G^{(d)}_{\Gamma_+}(\mathbf{x}, \mathbf{x_0}) \quad \forall\, \mathbf{x}, \mathbf{x_0} \in \Gamma_+, \tag{8.25}$$

$$G^{(-/+)}(\mathbf{R}(\mathbf{x}), \mathbf{R}(\mathbf{x_0})) = G^{(-/+)}(\mathbf{x}, \mathbf{x_0}) \quad \forall\, \mathbf{x} \in \Gamma_-,\ \forall\, \mathbf{x_0} \in \Gamma_+. \tag{8.26}$$

From (8.23), the defining equations of the matrix elements (4.17) and (4.18), the transformation of the vector functions (8.19) and (8.20), and by using Eq. (4.22), we derive the commutation relations of the T-matrix

$$\left[\mathbf{U}, \mathbf{T}^{(d)}_{\partial\Gamma}\right] = \mathbf{0}. \tag{8.27}$$

The generalization to the dyadic case is straightforward. We start with the symmetry relations

$$\mathbf{W}^{(\mathbf{d})}_{\partial\boldsymbol{\Gamma}_+}(\mathbf{R}(\bar{\mathbf{x}}), \mathbf{R}(\tilde{\mathbf{x}})) = \mathbf{W}^{(\mathbf{d})}_{\partial\boldsymbol{\Gamma}_+}(\bar{\mathbf{x}}, \tilde{\mathbf{x}}) \quad \forall\, \bar{\mathbf{x}}, \tilde{\mathbf{x}} \in \partial\Gamma, \tag{8.28}$$

$$\mathbf{W}^{(\mathbf{d})}_{\partial\boldsymbol{\Gamma}_-}(\mathbf{R}(\bar{\mathbf{x}}), \mathbf{R}(\tilde{\mathbf{x}})) = \mathbf{W}^{(\mathbf{d})}_{\partial\boldsymbol{\Gamma}_-}(\bar{\mathbf{x}}, \tilde{\mathbf{x}}) \quad \forall\, \bar{\mathbf{x}}, \tilde{\mathbf{x}} \in \partial\Gamma. \tag{8.29}$$

From Eqs. (4.30) and (4.31), we obtain the corresponding symmetry relations of the dyadic Green functions

$$\mathbf{G}^{(\mathbf{d})}_{\boldsymbol{\Gamma}_+}(\mathbf{R}(\mathbf{x}), \mathbf{R}(\mathbf{x_0})) = \mathbf{G}^{(\mathbf{d})}_{\boldsymbol{\Gamma}_+}(\mathbf{x}, \mathbf{x_0}) \quad \forall\, \mathbf{x}, \mathbf{x_0} \in \Gamma_+, \tag{8.30}$$

$$\mathbf{G}^{(-/+)}(\mathbf{R}(\mathbf{x}), \mathbf{R}(\mathbf{x_0})) = \mathbf{G}^{(-/+)}(\mathbf{x}, \mathbf{x_0}) \quad \forall\, \mathbf{x} \in \Gamma_-,\ \forall\, \mathbf{x_0} \in \Gamma_+. \tag{8.31}$$

Equations (8.28), (4.33), (4.34), and (4.37) in conjunction with (8.19) and (8.20) leads to the symmetry relation of the T-matrix belonging to the outer vectorial transmission problem

$$\left[\mathbf{U}, \mathbf{T}^{(\hat{\mathbf{n}}_-, \mathbf{d})}_{\partial\boldsymbol{\Gamma}}\right] = \mathbf{0}. \tag{8.32}$$

8.2 Explicit Commutation Relations of the T-matrix

The commutation relations of the T-matrix, such as those given in Eq. (8.32), are rather general and formal. To bring them into an explicit and readily applicable form, we need to obtain explicit expressions for the unitary matrices **U**. According to Eq. (8.19), this means that we need to make an explicit choice for the expansion functions $\vec{\psi}_{i,\tau}$ and investigate the transformation of those functions under various symmetry operations. Throughout the rest of this chapter, we will restrict ourselves to the dyadic problem and choose as expansion functions the vectorial eigenfunctions of the vector-wave equation in spherical coordinates, which are given in Eqs. (2.120–2.133).

8.2.1 Unitary Representations of Symmetry Operations

8.2.1.1 Proper Rotations

We have already learned how the vectorial eigensolutions transform under a general rotation by the Euler angles (α, β, γ). The transformation has been given in Eq. (2.189), which is of the general form of Eq. (8.9). (Note that Eq. (2.189) describes a passive transformation of the coordinate basis, which corresponds to an active rotation $\mathbf{R}^{-1}$ of the position vectors of the source and observations points.) By setting $V^* = U$, we brought Eq. (8.9) into the form of Eq. (8.10). Thus we have

$$\begin{aligned} U^{\tau,\tau'}_{n,l,n',l'}(\alpha,\beta,\gamma) &= \delta_{n,n'}\delta_{\tau,\tau'}\left[D^*\right]^{(n)}_{l',l}(\alpha,\beta,\gamma) \\ &= \delta_{n,n'}\delta_{\tau,\tau'}\exp(-il\alpha)\cdot d^{(n)}_{l',l}(\beta)\cdot\exp(-il'\gamma), \end{aligned} \tag{8.33}$$

where we have used Eq. (2.190) and the fact that the Wigner d-functions are real.

In practice it is a great advantage to choose the orientation of the coordinate system in accordance with the symmetries of the problem. For instance, the scatterer shown in Fig. 8.4 has a symmetry axis through the mid-points of the triangular top- and bottom faces. We denote the abstract symmetry operation associated with this axis by C_3. In general, an operation labeled by C_N denotes a rotation by and angle $2\pi/N$ about the z-axis. In addition, the scatterer in Fig. 8.4 has three C_2-axes perpendicular to the C_3-axis and passing through the geometrical centre of the prism. Such operations are known as dihedral symmetry operations. We label these by $C_2^{\prime(j)}$, where, in this case, $j = 0, 1, 2$. In this example we would choose our coordinate system such that the z-axis coincides with the main C_3-axis, and the x-axis coincides with the $C_2^{\prime(0)}$-axis.

We readily obtain a unitary representations for a C_N-rotation about the z-axis by setting in Eq. (8.33) $\alpha = 2\pi/N$ and $\beta = \gamma = 0$. This gives

$$U^{\tau,\tau'}_{n,l,n',l'}(C_N) = \delta_{n,n'}\delta_{l,l'}\delta_{\tau,\tau'}\exp\left(-i\frac{2\pi l}{N}\right). \tag{8.34}$$

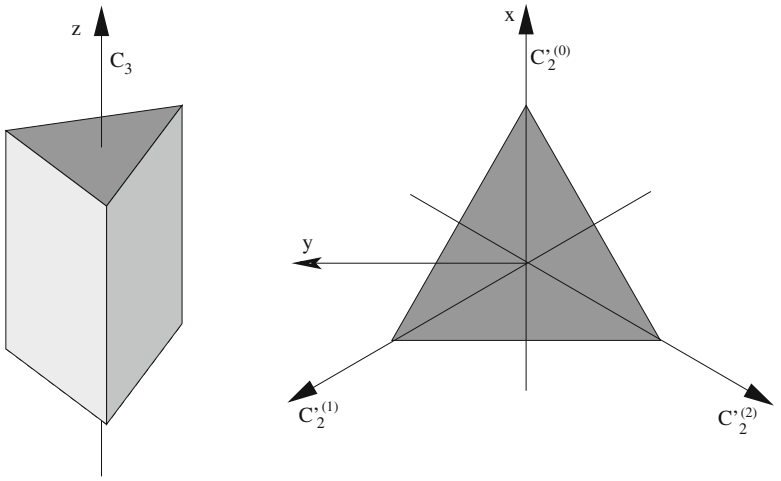

Fig. 8.4 Examples of rotational symmetries of a triangular prism with equilateral *top* and *bottom* faces

We can obtain another symmetry operation by applying the rotation C_3 twice, (which we denote by C_3^2). More generally, if the scatterer has C_N-symmetry, then it also has C_N^j-symmetry, where $j = 1, \ldots, N-1$. The corresponding unitary representation is

$$U^{\tau,\tau'}_{n,l,n',l'}(C_N^j) = \delta_{n,n'}\delta_{l,l'}\delta_{\tau,\tau'} \exp\left(-i\frac{2\pi jl}{N}\right). \tag{8.35}$$

For obtaining a representation of the $C_2^{\prime(j)}$ symmetries we need to work a little harder. We start by noting that a rotation $C_2^{\prime y}$ by an angle $2\pi/2 = \pi$ about the y-axis can be represented with the help of Eq. (8.33) by setting $\beta = \pi$ and $\alpha = \gamma = 0$. The Wigner d-functions have the property $d^{(n)}_{l,l'}(\pi) = \delta_{l,-l'}(-1)^{n+l}$; this can be shown directly from Eq. (2.191). So

$$U^{\tau,\tau'}_{n,l,n',l'}(C_2^{\prime y}) = \delta_{n,n'}\delta_{l,-l'}\delta_{\tau,\tau'}(-1)^{n+l}. \tag{8.36}$$

The rotation $C_2^{\prime(0)}$ about the x-axis can now be constructed in three steps as illustrated in Fig. 8.5. First, we perform an active rotation of the object about the z-axis by an angle $2\pi/4$, denoted by C_4. Next, we rotate the object about the y-axis by an angle π, denoted by $C_2^{\prime y}$. Finally, we perform a rotation about the z-axis by an angle $-2\pi/4$, denoted by C_4^{-1}. So we reduce the problem of performing the $C_2^{\prime(0)}$ rotation to the already solved problems of performing $C_2^{\prime y}$ and C_N rotations, which we write symbolically

$$C_2^{\prime(0)} = C_4^{-1} \circ C_2^{\prime y} \circ C_4. \tag{8.37}$$

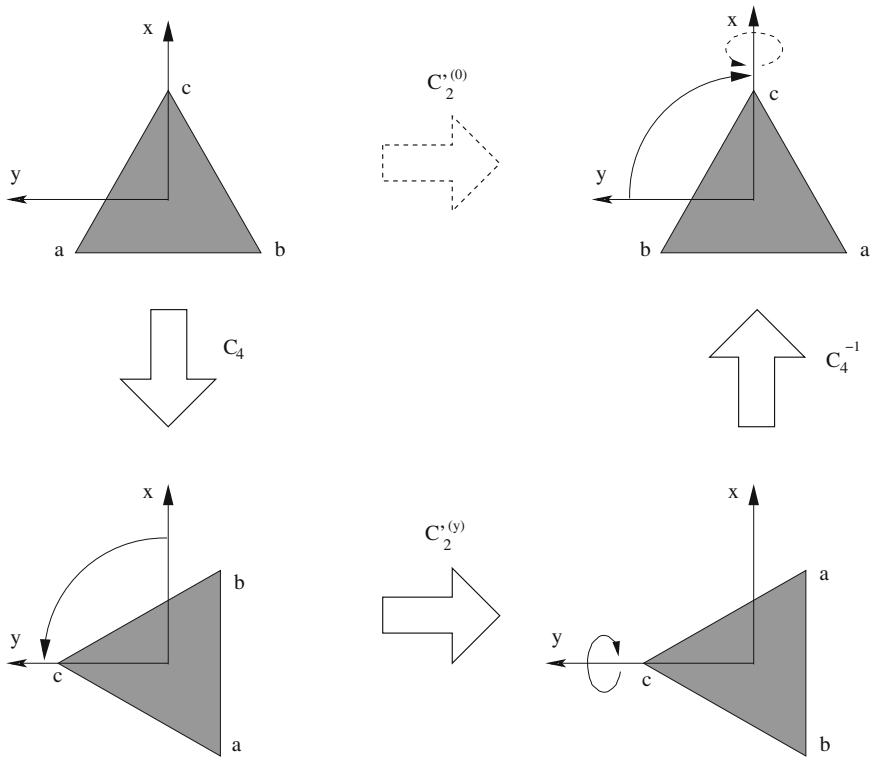

Fig. 8.5 Decomposition of the $C_2^{\prime(0)}$ rotation

Note that the rightmost operation is applied first. In terms of our unitary representations, we obtain

$$\mathbf{U}(C_2^{\prime(0)}) = \mathbf{U}(C_4^{-1}) \cdot \mathbf{U}(C_2^{\prime y}) \cdot \mathbf{U}(C_4). \tag{8.38}$$

Using Eqs. (8.34) and (8.35), we obtain

$$\begin{aligned} U^{\tau,\tau'}_{n,l,n',l'}(C_2^{\prime(0)}) &= \delta_{n,n'}\delta_{l,-l'}\delta_{\tau,\tau'}(-1)^{n+l}\exp\left(-i\frac{2\pi(l'-l)}{4}\right) \\ &= \delta_{n,n'}\delta_{l,-l'}\delta_{\tau,\tau'}(-1)^{n}. \end{aligned} \tag{8.39}$$

The strategy of deriving representations for symmetry operations by decomposing them into operations for which we already have obtained representations is extremely useful. We can apply this method to obtain representations for the rotations $C_2^{\prime(1)}$ and $C_2^{\prime(2)}$ in Fig. 8.4. The decompositions are

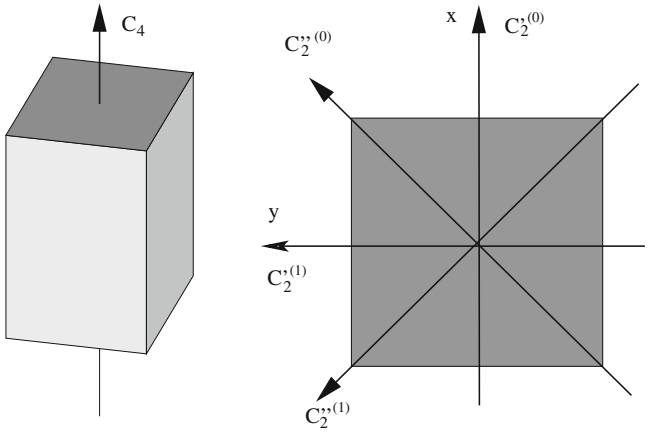

Fig. 8.6 Examples of rotational symmetries of a rectangular prism

$$C_2'^{(1)} = C_3 \circ C_2'^{(0)} \circ C_3^{-1} \tag{8.40}$$

$$C_2'^{(2)} = C_3^2 \circ C_2'^{(0)} \circ C_3^{-2}. \tag{8.41}$$

More generally, let's assume we have an object with C_N-symmetry and with dihedral symmetries $C_2'^{(j)}$, where the angle between two neighbouring dihedral axes j and $(j+1)$ is $2\pi/N$. Then

$$C_2'^{(j)} = C_N^j \circ C_2'^{(0)} \circ C_N^{-j}. \tag{8.42}$$

From Eqs. (8.35) and (8.39) we derive

$$U^{\tau,\tau'}_{n,l,n',l'}(C_2'^{(j)}) = \delta_{n,n'}\delta_{l,-l'}\delta_{\tau,\tau'}(-1)^n \exp\left(-i\frac{4\pi jl}{N}\right). \tag{8.43}$$

The example given in Fig. 8.4 suggests that if a particle has, in addition to a C_N symmetry, dihedral symmetry, then there are N dihedral symmetry axes, and the angle between any two neighbouring dihedral axes is $2\pi/N$. However, this holds only for odd N. In Fig. 8.6 we see an example for a rectangular prism, which has C_4-symmetry and four dihedral symmetry axes. These consist of two groups labeled by $C_2'^{(j)}$ and $C_2''^{(j)}$, where $j = 0, 1$. Within each of these two groups, the angle between neighbouring angles is $2\pi/4$, but the angle between, e.g., the $C_2'^{(0)}$ and $C_2''^{(0)}$-axes is $2\pi/8$.

In general, if an object has a C_N-axis with even N, and if there are, in addition, dihedral axes perpendicular to this axis, then there exist, in total, N dihedral symmetries $C_2'^{(j)}$ and $C_2''^{(j)}$ with $j = 0, \ldots, N/2-1$. The angle between any two neighbouring axes within each group is $2\pi/N$, and the angle between the $C_2'^{(0)}$ and the $C_2''^{(0)}$

axes is $2\pi/(2N)$. The unitary representations of the $C_2^{\prime(j)}$-symmetries are, as before, given by (8.43). To obtain the corresponding representations of the $C_2^{\prime\prime(j)}$-symmetries we first note that

$$C_2^{\prime\prime(0)} = C_{2N} \circ C_2^{\prime(0)} \circ C_{2N}^{-1}, \tag{8.44}$$

$$C_2^{\prime\prime(j)} = C_N^{j} \circ C_2^{\prime\prime(0)} \circ C_N^{-j}. \tag{8.45}$$

Using Eqs. (8.35) and (8.43) gives

$$U^{\tau,\tau'}_{n,l,n',l'}(C_2^{\prime\prime(j)}) = \delta_{n,n'}\delta_{l,-l'}\delta_{\tau,\tau'}(-1)^n \exp\left(-i\frac{4\pi(j+1/2)l}{N}\right). \tag{8.46}$$

The examples given thus far should be sufficient to illustrate the procedure for deriving representations for rotational symmetry operations. Note that an object can have more than one N-fold rotational symmetry with $N \geq 3$. For instance, a tetrahedron has four C_3-axes, a cube and an octahedron have four C_3- and three C_4-axes.

Reflections

We now turn to the question how the vectorial eigensolutions transform under reflection operations. Consider first an arbitrary vector field $\vec{\Psi}(\mathbf{r})$, where $\mathbf{r} = (r, \theta, \phi)$ is a position vector in a fixed spherical coordinate system, and where $\vec{\Psi} = (\Psi_r, \Psi_\theta, \Psi_\phi)$ is, at each position $\mathbf{r}$, given in a *local* spherical coordinate system $\{\hat{r}, \hat{\theta}, \hat{\phi}\}$. This is illustrated in Fig. 8.7. Now let us apply a reflection in the xy-plane to the entire vector field. This operation is denoted by σ_h, where σ derives from the German word "Spiegelsymmetrie" for reflection symmetry, and where the subscript h indicates a "horizontal" reflection plane. Under this operation the position vector $\mathbf{r}$ is transformed into $\mathbf{r}' = (r, \pi - \theta, \phi)$. The vector field is transformed into a new field $\vec{\Psi}'$, which is now, at each position $\mathbf{r}'$, specified in a new local spherical coordinate system $\{\hat{r}', \hat{\theta}', \hat{\phi}'\}$. As illustrated in Fig. 8.7, the components Ψ_r and Ψ_ϕ remain unaffected by the reflection operation, while Ψ_θ switches its sign. So

$$\begin{pmatrix} \Psi'_r(r', \theta', \phi') \\ \Psi'_\theta(r', \theta', \phi') \\ \Psi'_\phi(r', \theta', \phi') \end{pmatrix} = \begin{pmatrix} \Psi_r(r, \pi - \theta, \phi) \\ -\Psi_\theta(r, \pi - \theta, \phi) \\ \Psi_\phi(r, \pi - \theta, \phi) \end{pmatrix}. \tag{8.47}$$

This is valid for an arbitrary vector field $\vec{\Psi}$. Let us now substitute into the general relation (8.47) the vector spherical harmonics given in Eqs. (2.127–2.129). For $\theta' = \pi - \theta$ we get from (2.72) and (2.73) the relations

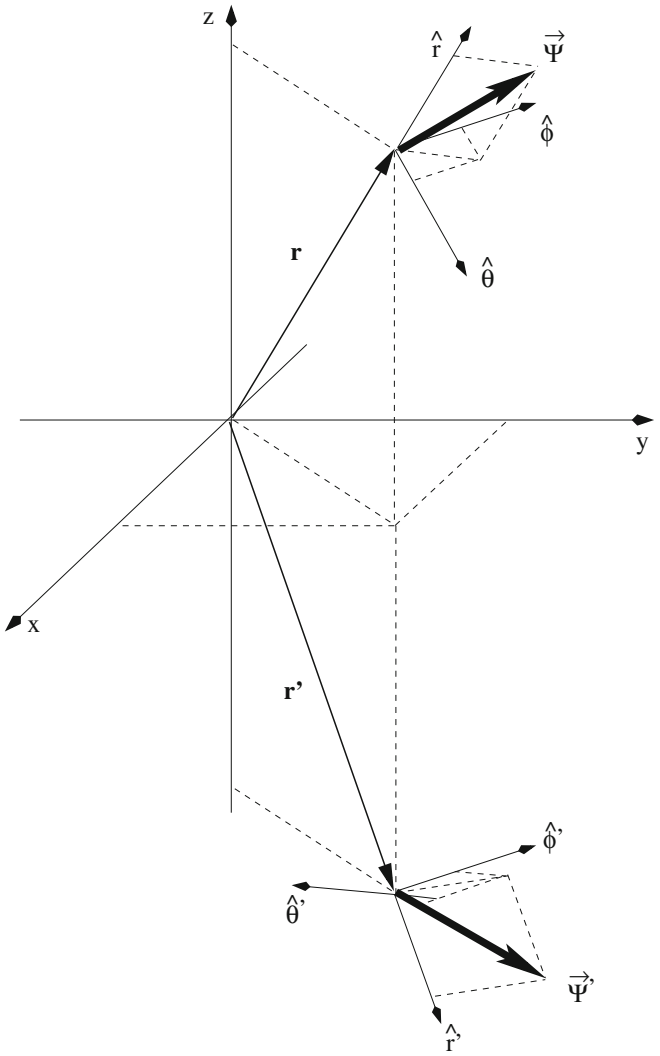

Fig. 8.7 Transformation of a vector field under σ_h reflection

$$P_n^l(\cos\theta') = (-1)^{n+l} P_n^l(\cos\theta) \tag{8.48}$$

$$\frac{dP_n^l(\cos\theta')}{d\theta'} = -(-1)^{n+l} \frac{dP_n^l(\cos\theta)}{d\theta} \tag{8.49}$$

$$\sin\theta' = \sin\theta. \tag{8.50}$$

Using those in conjunction with Eqs. (2.127–2.129) and (8.47), we obtain

$$\vec{P}'_{l,n}(\theta', \phi') = (-1)^{n+l} \vec{P}_{l,n}(\theta, \phi) \tag{8.51}$$

$$\vec{C}'_{l,n}(\theta', \phi') = -(-1)^{n+l} \vec{C}_{l,n}(\theta, \phi) \tag{8.52}$$

$$\vec{B}'_{l,n}(\theta', \phi') = (-1)^{n+l} \vec{B}_{l,n}(\theta, \phi). \tag{8.53}$$

Substitution of these relations into the equations for the regular vectorial eigensolutions (2.130) and (2.131) gives

$$\vec{\psi}'_{l,n,1}(r', \theta', \phi') = -(-1)^{n+l} \vec{\psi}_{l,n,1}(r, \theta, \phi) \tag{8.54}$$

$$\vec{\psi}'_{l,n,2}(r', \theta', \phi') = (-1)^{n+l} \vec{\psi}_{l,n,2}(r, \theta, \phi) \tag{8.55}$$

or, in more compact notation,

$$\vec{\psi}'_{l,n,\tau}(r', \theta', \phi') = (-1)^{n+l+\tau} \vec{\psi}_{l,n,\tau}(r, \theta, \phi). \tag{8.56}$$

In complete analogy, we obtain for the radiating eigensolutions

$$\vec{\varphi}'_{l,n,\tau}(r', \theta', \phi') = (-1)^{n+l+\tau} \vec{\varphi}_{l,n,\tau}(r, \theta, \phi). \tag{8.57}$$

The unitary representation for the σ_h operation is therefore given by

$$U^{\tau,\tau'}_{n,l,n',l'}(\sigma_h) = \delta_{n,n'} \delta_{l,l'} \delta_{\tau,\tau'} (-1)^{n+l+\tau}. \tag{8.58}$$

Reflections with respect to a plane containing the main C_N-axis are denoted by $\sigma_v^{(j)}$, where the subscript v stands for "vertical". In the example shown in Fig. 8.8, $j = 0, 1, 2$. We label these symmetry operations such that the $\sigma_v^{(0)}$-plane coincides with the xz-plane. The problem of finding unitary representations for the $\sigma_v^{(j)}$ operations can again be reduced by decomposing these operations into other operations for which we already know the unitary representations.

Figure 8.9 illustrates that we can write

$$\sigma_v^{(0)} = C_2'^{(0)} \circ \sigma_h. \tag{8.59}$$

Accordingly, we have

$$\mathbf{U}(\sigma_v^{(0)}) = \mathbf{U}(C_2'^{(0)}) \cdot \mathbf{U}(\sigma_h). \tag{8.60}$$

Together with Eqs. (8.39) and (8.58) we obtain

$$U^{\tau,\tau'}_{n,l,n',l'}(\sigma_v^{(0)}) = \delta_{n,n'} \delta_{l,-l'} \delta_{\tau,\tau'} (-1)^{l+\tau}. \tag{8.61}$$

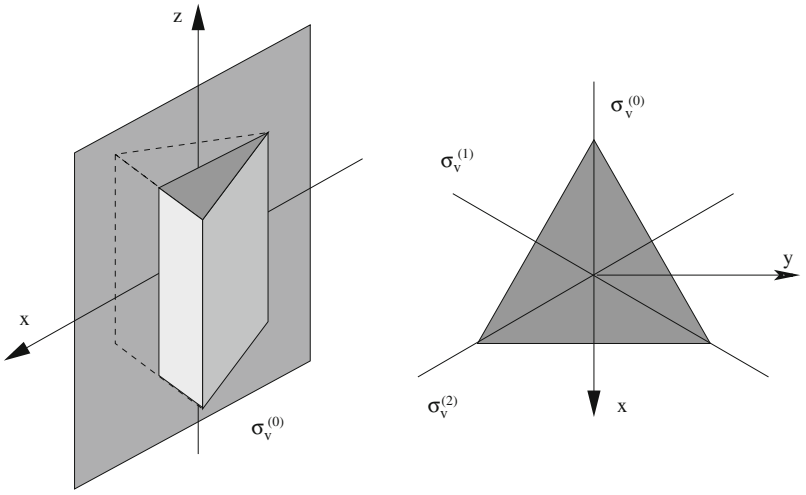

Fig. 8.8 Examples of σ_v reflection symmetries

By inspecting Fig. 8.8 (right), we can see that a $\sigma_v^{(j)}$ reflection can be performed by first rotating the object by and angle $-2\pi j/N$ about the z-axis, then performing a $\sigma_v^{(0)}$ reflection, and then rotating the object back by an angle $2\pi j/N$ about the z-axis. Thus

$$\sigma_v^{(j)} = C_N^j \circ \sigma_v^{(0)} \circ C_N^{-j}, \tag{8.62}$$

where, as usual, the rightmost operation is performed first. Together with Eqs. (8.35) and (8.61) we derive

$$U^{\tau,\tau'}_{n,l,n',l'}(\sigma_v^{(j)}) = \delta_{n,n'}\delta_{l,-l'}\delta_{\tau,\tau'}(-1)^{l+\tau} \exp\left(-i\frac{4\pi jl}{N}\right). \tag{8.63}$$

Vertical reflection planes that contain a C_N axis of even order N fall into two groups, as illustrated in Fig. 8.10. There are $N/2$ reflections $\sigma_v^{(j)}$ and $N/2$ reflections $\sigma_d^{(j)}$. The angle between neighbouring reflection planes within each group is $2\pi/N$, while the angle between, e.g. the $\sigma_v^{(0)}$ and $\sigma_d^{(0)}$ planes is $2\pi/(2N)$. Note the analogy to the dihedral symmetries $C_2^{\prime(j)}$ and $C_2^{\prime\prime(j)}$. We can again reduce the derivation of the representations by noting that

$$\sigma_d^{(0)} = C_{2N} \circ \sigma_v^{(0)} \circ C_{2N}^{-1}, \tag{8.64}$$

and

$$\sigma_d^{(j)} = C_N^j \circ \sigma_d^{(0)} \circ C_N^{-j}, \tag{8.65}$$

which gives

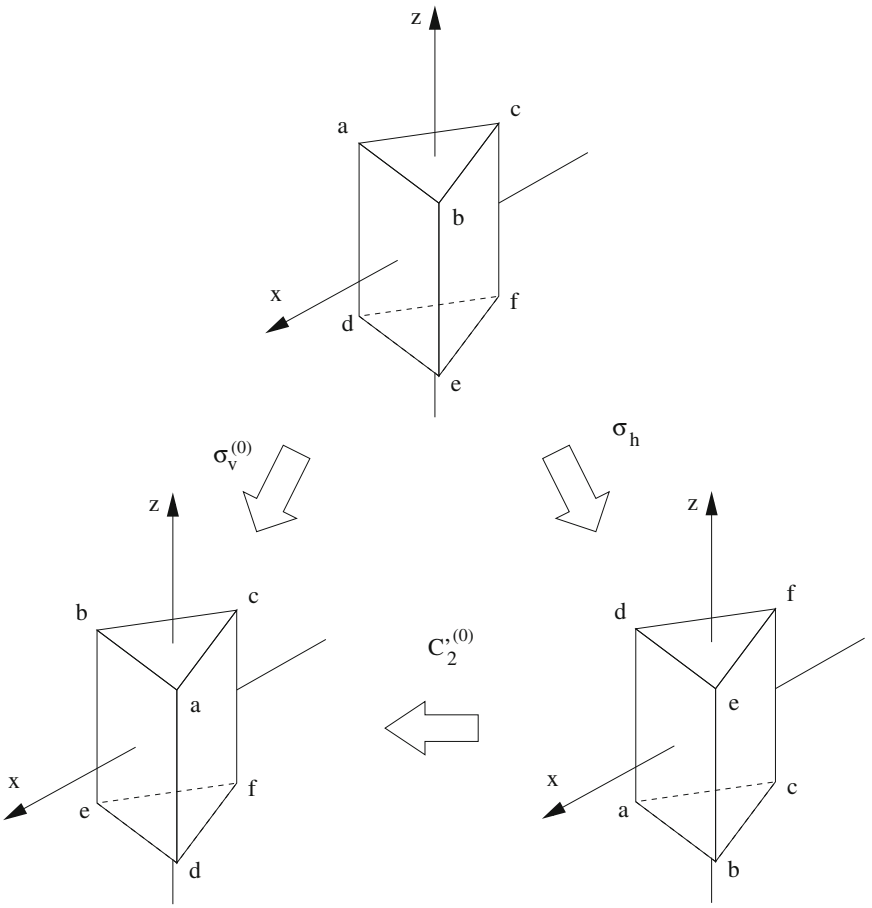

Fig. 8.9 Illustration of the relation $\sigma_v^{(0)} = C_2^{\prime(0)} \circ \sigma_h$

$$U^{\tau,\tau'}_{n,l,n',l'}(\sigma_d^{(j)}) = \delta_{n,n'}\delta_{l,-l'}\delta_{\tau,\tau'}(-1)^{l+\tau}\exp\left(-i\frac{4\pi(j+1/2)l}{N}\right). \tag{8.66}$$

Rotation-Reflections

Figure 8.11 shows a trigonal antiprism. This object has neither a rotational nor a horizontal reflection symmetry. However, the combination $S_6 = C_6 \circ \sigma_h$ of a rotation C_6 about the z-axis and a reflection σ_h in the xy-plane is a symmetry operation of the object. Also, the operations $S_6^{(3)} = C_6^3 \circ \sigma_h$ and $S_6^{(5)} = C_6^5 \circ \sigma_h$ are symmetry operations. By inspection of Fig. 8.11 it is easy to see that $S_6^{(3)}$ is identical with the inversion operation I that inverts all spatial coordinates. Note that objects such as

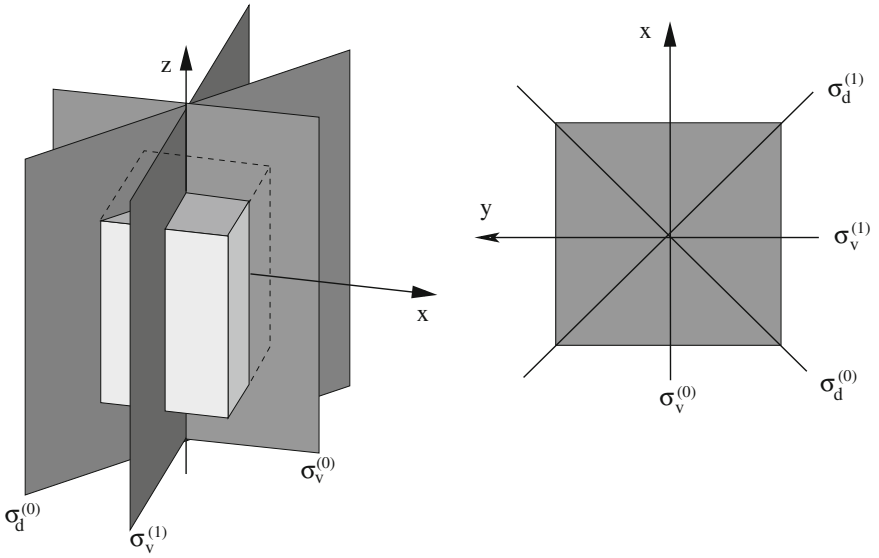

Fig. 8.10 Reflection symmetries σ_v and σ_d

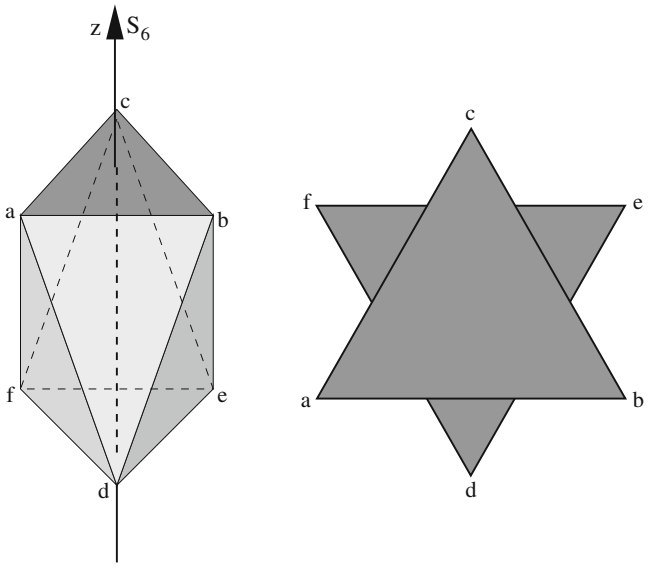

Fig. 8.11 Rotation-reflection symmetry $S_6 = C_6 \circ \sigma_h$

regular prisms can also have rotation-reflection symmetries with even superscripts. For instance, the triangular prism shown in Fig. 8.8 has S_3 and $S_3^{(2)} = C_3^2 \circ \sigma_h$ symmetry.

In general, we have $S_N^{(j)} = C_N^j \circ \sigma_h$. By use of Eqs. (8.35) and (8.58), we obtain the unitary representation

$$U^{\tau,\tau'}_{n,l,n',l'}(S_N^{(j)}) = \delta_{n,n'}\delta_{l,l'}\delta_{\tau,\tau'}(-1)^{n+l+\tau}\exp\left(-i\frac{2\pi jl}{N}\right). \tag{8.67}$$

Identity

We don't give away too much if we mention already now that the set of all symmetry operations forms a group. Any group must contain an identity element E. The representation of the identity element is trivially given by $U^{\tau,\tau'}_{n,l,n',l'}(E) = \delta_{n,n'}\delta_{l,l'}\delta_{\tau,\tau'}$.

8.2.2 Commutation Relations

It is now a simple task to substitute the representations derived above into the commutation relation (8.32). As an example, consider C_N symmetry. By use of Eq. (8.34), the commutation relation for the T-matrix becomes

$$\left[T_{\partial\Gamma}^{(\hat{n}_-,d)}\right]^{\tau,\tau'}_{n,l,n',l'} = \left[T_{\partial\Gamma}^{(\hat{n}_-,d)}\right]^{\tau,\tau'}_{n,l,n',l'} \cdot \exp\left(-i\frac{2\pi(l-l')}{N}\right), \tag{8.68}$$

or, equivalently,

$$\left[T_{\partial\Gamma}^{(\hat{n}_-,d)}\right]^{\tau,\tau'}_{n,l,n',l'} = 0 \qquad \text{unless} \quad |l-l'| = 0, N, 2N, \ldots \tag{8.69}$$

This commutation relation reduces the number of T-matrix elements we need to compute by a factor of N. Alternatively, we can use this relation to test the correctness of numerical computations. Note that in the limiting case $N \to \infty$, we obtain the commutation relation for C_∞, i.e. axial symmetry

$$\left[T_{\partial\Gamma}^{(\hat{n}_-,d)}\right]^{\tau,\tau'}_{n,l,n',l'} = \delta_{l,l'}\left[T_{\partial\Gamma}^{(\hat{n}_-,d)}\right]^{\tau,\tau'}_{n,l,n',l}, \tag{8.70}$$

so the T-matrix is diagonal in the index l.

The commutation relation for σ_h-symmetry is obtained by substituting Eq. (8.58) into Eq. (8.32). This gives

$$\left[T_{\partial\Gamma}^{(\hat{n}_-,d)}\right]^{\tau,\tau'}_{n,l,n',l'} = \left[T_{\partial\Gamma}^{(\hat{n}_-,d)}\right]^{\tau,\tau'}_{n,l,n',l'} \cdot (-1)^{n+l+\tau+n'+l'+\tau'}, \tag{8.71}$$

or

$$\left[T_{\partial\Gamma}^{(\hat{n}_-,d)}\right]^{\tau,\tau'}_{n,l,n',l'} = 0 \qquad \text{unless} \quad (n+l+\tau+n'+l'+\tau') \quad \text{even}. \tag{8.72}$$

This commutation relation reduces the number of nonzero T-matrix elements by a factor of 2.

Similarly, we can substitute Eq. (8.39) into Eq. (8.32) to obtain the commutation relation for dihedral symmetry:

$$\left[T_{\partial\Gamma}^{(\hat{n}_-,d)}\right]_{n,l,n',l'}^{\tau,\tau'} = \left[T_{\partial\Gamma}^{(\hat{n}_-,d)}\right]_{n,-l,n',-l'}^{\tau,\tau'} \cdot (-1)^{n+n'}. \tag{8.73}$$

This relation reduces the number of independent T-matrix elements by a factor of 2.

As a test, we can also investigate the special case of spherical symmetry. For spherically symmetric particles the T-matrix has to be invariant under any rotation. In particular, it has to be invariant under a rotation about the y-axis by an arbitrary angle β. By setting $\alpha = \gamma = 0$ in Eq. (8.33), the commutation relation reads

$$\left[T_{\partial\Gamma}^{(\hat{n}_-,d)}\right]_{n,l,n',l'}^{\tau,\tau'} = \delta_{l,l'} \sum_{l_1=-n}^{n} d_{l,l_1}^{(n)}(-\beta) \left[T_{\partial\Gamma}^{(\hat{n}_-,d)}\right]_{n,l_1,n',l_1}^{\tau,\tau'}, d_{l_1,l'}^{(n')}(\beta), \tag{8.74}$$

where we have exploited the commutation relation (8.70) for rotational symmetry about the z-axis. The Wigner d-functions have the properties

$$d_{l,l_1}^{(n)}(-\beta) = d_{l_1,l}^{(n)}(\beta) \tag{8.75}$$

and

$$\int_0^\pi \mathrm{d}\beta \sin\beta \; d_{l,l'}^{(n)}(\beta) \; d_{l,l'}^{(n')}(\beta) = \frac{2}{2n+1}\delta_{n,n'}. \tag{8.76}$$

Thus integration of Eq. (8.74) over β yields

$$\pi \left[T_{\partial\Gamma}^{(\hat{n}_-,d)}\right]_{n,l,n',l'}^{\tau,\tau'} = \delta_{l,l'} \; \delta_{n,n'} \; \frac{1}{2n+1} \sum_{l_1=-n}^{n} \left[T_{\partial\Gamma}^{(\hat{n}_-,d)}\right]_{n,l_1,n,l_1}^{\tau,\tau'}. \tag{8.77}$$

A spherically symmetric particle also has σ_h symmetry. Owing to the diagonality in the indices n and l, Eq. (8.72) reduces to

$$\left[T_{\partial\Gamma}^{(\hat{n}_-,d)}\right]_{n,l,n,l}^{\tau,\tau'} = 0 \qquad \text{unless} \quad (\tau+\tau') \quad \text{even}. \tag{8.78}$$

Since τ and τ' only take on the values 1 or 2, this means that the T-matrix is also diagonal in τ. Thus we have

$$\left[T_{\partial\Gamma}^{(\hat{n}_-,d)}\right]_{n,l,n',l'}^{\tau,\tau'} = \delta_{l,l'} \; \delta_{n,n'} \; \delta_{\tau,\tau'} \; T_n^{\tau} \tag{8.79}$$

where we have defined

$$T_n^\tau = \frac{1}{\pi(2n+1)} \sum_{l_1=-n}^{n} \left[T_{\partial\Gamma}^{(\hat{n}_-,d)} \right]_{n,l_1,n,l_1}^{\tau,\tau}. \tag{8.80}$$

So for spherically symmetric particles the T-matrix is diagonal in all its indices, and the matrix elements only depend on n and τ. This agrees with what we found earlier in Eqs. (3.91) and (3.92) for the A- and B-matrices.

Note that in practice we often compute the T-matrix via Eq. (3.89). The matrices $\mathbf{A}_{\partial\Gamma}^{(g,\varphi_0^{\hat{n}_-})^{-1}}$ and $\mathbf{B}_{\partial\Gamma}^{(g,\psi_0^{\hat{n}_-})}$ appearing in this equation are defined according to Eqs. (2.21) and (2.22) as integrals over the boundary surface. These matrices have the same symmetry structure as the T-matrix, i.e. they satisfy the same commutation relations.

8.2.3 Simplification of Scalar Products

The fact that the matrices $\mathbf{A}_{\partial\Gamma}^{(g,\varphi_0^{\hat{n}_-})}$ and $\mathbf{B}_{\partial\Gamma}^{(g,\psi_0^{\hat{n}_-})}$ as well as the inverse of $\mathbf{A}_{\partial\Gamma}^{(g,\varphi_0^{\hat{n}_-})}$ have the same symmetry properties as the T-matrix can be further exploited in practical computations. We illustrate this for the matrix $\mathbf{A}_{\partial\Gamma}^{(g,\varphi_0^{\hat{n}_-})}$ and for the case of C_N symmetry. To be specific, we choose in Eq. (2.21) as weighting functions

$$\boldsymbol{g}_{l,n,\tau}(\mathbf{x}) = \vec{\psi}_{l,n,\tau}^{\hat{n}_-}(k_0, \mathbf{x}), \quad \mathbf{x} \in \partial\Gamma \tag{8.81}$$

and substitute the definition of the scalar product (1.35). This gives

$$\left[A_{\partial\Gamma}^{(\psi^{\hat{n}_-},\varphi_0^{\hat{n}_-})} \right]_{l,n,l',n'}^{\tau,\tau'} = \oint_{\partial\Gamma} \vec{\psi}_{l,n,\tau}^{\hat{n}_-*}(k_0, \mathbf{x}) \cdot \vec{\varphi}_{l',n',\tau'}^{\hat{n}_-}(k_0, \mathbf{x}) \mathrm{d}S(\mathbf{x}). \tag{8.82}$$

The functions in the integrand are explicitly defined in Eqs. (2.126–2.133), (2.158) and (2.159). Inspection of these equations shows that the azimuthal dependency of the integrand in Eq. (8.82) is given by $\exp(-\mathrm{i}(l-l')\phi)$. However, for C_N symmetry the matrix $\mathbf{A}_{\partial\Gamma}^{(g,\varphi_0^{\hat{n}_-})}$ satisfies a commutation relation of the form of Eq. (8.69). So the matrix only has non-zero elements for $(l-l') = mN$, where m is an integer. This implies that

$$\exp\left(\mathrm{i}(l-l')\left(\phi + \frac{2\pi}{N}\right)\right) = \exp\left(\mathrm{i}(l-l')\phi\right) \exp\left(\mathrm{i}2\pi m\right) = \exp\left(\mathrm{i}(l-l')\phi\right). \tag{8.83}$$

Also, the surface element is invariant under a C_N rotation, so $\mathrm{d}S(\theta, \phi + 2\pi/N) = \mathrm{d}S(\theta, \phi)$. The azimuthal integral appearing in Eq. (8.82) can therefore be simplified according to

$$\int_0^{2\pi} \mathrm{d}\phi \cdots = N \int_0^{2\pi/N} \mathrm{d}\phi \cdots . \tag{8.84}$$

Similar considerations for σ_h symmetry in conjunction with the commutation relation (8.72) leads to a reduction in the polar integration range according to

$$\int_0^{\pi} \mathrm{d}\theta \cdots = 2 \int_0^{\pi/2} \mathrm{d}\theta \cdots . \tag{8.85}$$

Exploitation of C_2 or σ_v symmetry is a bit more tricky and involves a few case distinctions. It turns out that the azimuthal integration range can be further reduced by a factor of 2. A more detailed account of exploiting the commutation relations in the explicit evaluation of the matrices $\mathbf{A}_{\partial\Gamma}^{(g,\varphi_0^{\hat{n}-})}$ and $\mathbf{B}_{\partial\Gamma}^{(g,\psi_0^{\hat{n}-})}$ can be found in a paper by Kahnert et al. (Appl. Opt. 40, 3110–3123, 2001) cited in the reference chapter. Figure 8.12 illustrates the total reduction in integration area that can be achieved for a hexagonal prism. The area over which the surface integral has to be evaluated is only 1/24th of the total surface area. The rest of the integral is given by symmetry! The same argument applies to the process of numerical orientation averaging too, as it becomes necessary in remote sensing applications, for example. This reduction is the combined effect of exploiting C_6-symmetry (contributing a factor of 6), σ_h-symmetry

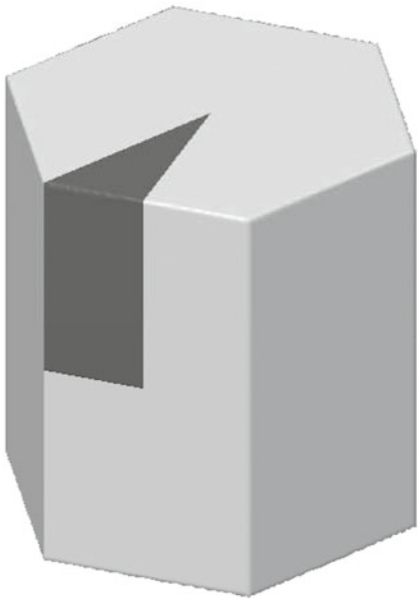

Fig. 8.12 Evaluation of integrals over the boundary surface as that given in Eq. (8.82) can be reduced to a fraction of the boundary surface as indicated by the *dark-shaded area* in the figure. This reduction is achieved by exploiting the commutation relations in conjunction with the properties of the vectorial eigensolutions

(contributing a factor of 2), and $C_2^{(0)}$-symmetry (contributing a factor of 2). Why can we not exploit the other symmetry elements of the prism? The answer to this question will become clear in the following section, in which we will approach symmetries from a more formal point of view.

8.3 Symmetry Groups

The proper mathematical framework for studying symmetries is group theory. We will here discuss only the most essential elements of group theory to the extent needed for exploiting symmetries in electromagnetic scattering problems.

8.3.1 Groups and Generators

A group $(\mathcal{G}, \circ)$ is a set $\mathcal{G}$ together with an operation $\circ : \mathcal{G} \times \mathcal{G} \to \mathcal{G}$ with $(g_1, g_2) \mapsto g_1 \circ g_2$ that has the following properties.

$$\exists\, E \in \mathcal{G}; \quad g \circ E = E \circ g = g \qquad \forall\, g \in \mathcal{G}, \tag{8.86}$$

$$\forall\, g \in \mathcal{G} \quad \exists\, g^{-1} \in \mathcal{G}; \quad g \circ g^{-1} = g^{-1} \circ g = E \tag{8.87}$$

$$g_1 \circ (g_2 \circ g_3) = (g_1 \circ g_2) \circ g_3 \qquad \forall\, g_1, g_2, g_3 \in \mathcal{G}. \tag{8.88}$$

The group operation satisfies closure, i.e.

$$g_1 \circ g_2 \in \mathcal{G} \qquad \forall\, g_1, g_2 \in \mathcal{G}. \tag{8.89}$$

The number of elements M_o in a finite group $\mathcal{G}$ is called the *order of the group*.

As an example, consider the trigonal pyramid shown in Fig. 8.13. The symmetry group to which this object belongs is denoted by $\mathcal{C}_{3v}$. It consists of the elements

$$\mathcal{C}_{3v} = \left\{ E, C_3, C_3^2, \sigma_v^{(0)}, \sigma_v^{(1)}, \sigma_v^{(2)} \right\}. \tag{8.90}$$

Multiplication of different group elements by the binary operation "$\circ$" can be presented in the form of a group multiplication table, as shown in Table 8.1. The table shows the resulting group elements g_3 obtained by multiplying any two elements g_1 and g_2, i.e. $g_3 = g_1 \circ g_2$. As usual, the rightmost element g_2 is applied first. In the table we find g_3 under the column-element g_2 and the row-element g_1. For example, looking into the column $\sigma_v^{(0)}$ and the row C_3, we see that $\sigma_v^{(2)} = C_3 \circ \sigma_v^{(0)}$. Note that the group is non-Abelian. For instance, $\sigma_v^{(0)} \circ C_3 \neq C_3 \circ \sigma_v^{(0)}$. A closer look at the table also shows that the group properties (8.86–8.88) are satisfied.

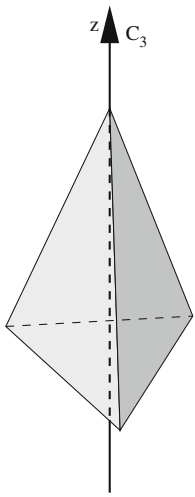

Fig. 8.13 Trigonal prism belonging to the symmetry group $\mathcal{C}_{3v}$

Table 8.1 Multiplication table for the group $\mathcal{C}_{3v}$

	E	C_3	C_3^2	$\sigma_v^{(0)}$	$\sigma_v^{(1)}$	$\sigma_v^{(2)}$
E	E	C_3	C_3^2	$\sigma_v^{(0)}$	$\sigma_v^{(1)}$	$\sigma_v^{(2)}$
C_3	C_3	C_3^2	E	$\sigma_v^{(2)}$	$\sigma_v^{(0)}$	$\sigma_v^{(1)}$
C_3^2	C_3^2	E	C_3	$\sigma_v^{(1)}$	$\sigma_v^{(2)}$	$\sigma_v^{(0)}$
$\sigma_v^{(0)}$	$\sigma_v^{(0)}$	$\sigma_v^{(1)}$	$\sigma_v^{(2)}$	E	C_3	C_3^2
$\sigma_v^{(1)}$	$\sigma_v^{(1)}$	$\sigma_v^{(2)}$	$\sigma_v^{(0)}$	C_3^2	E	C_3
$\sigma_v^{(2)}$	$\sigma_v^{(2)}$	$\sigma_v^{(0)}$	$\sigma_v^{(1)}$	C_3	C_3^2	E

The groups that describe the symmetries of finite objects, such as particles in electromagnetic scattering or molecules in chemical physics, all have one thing in common. There is one point in space that is left unaltered by all symmetry operations. In other words, these groups do not contain any translations, because translations cannot be symmetry operations of finite objects. For this reason, these kinds of symmetry groups are called point groups. All point groups are subgroups of the orthogonal group $\mathcal{O}(3)$.

There is another interesting fact we can learn from Table 8.1. If we take only the elements C_3 and $\sigma_v^{(0)}$ and consider all possible products of these elements, then we find

$$C_3^2 = C_3 \circ C_3 \tag{8.91}$$

$$E = \sigma_v^{(0)} \circ \sigma_v^{(0)} \tag{8.92}$$

$$\sigma_v^{(1)} = \sigma_v^{(0)} \circ C_3 \tag{8.93}$$

$$\sigma_v^{(2)} = C_3 \circ \sigma_v^{(0)}. \tag{8.94}$$

So all other group elements can be generated from these two elements. C_3 and $\sigma_v^{(0)}$ are therefore called the generators of the group $\mathcal{C}_{3v}$. Note that this choice is not unique. We could also choose any two elements C_3^j and $\sigma_v^{(k)}$ with $j = 1$ or 2 and $k = 0$, 1, or 2. Note also that in our example of the $\mathcal{C}_{3v}$ group it was sufficient to form products involving only two factors of generators in order to produce all other group elements. In other groups generating all group elements may require products of the generators involving more than just two factors.

The concept of group generators is essential in conjunction with the commutation relations of the T-matrix. Consider three group elements $g_1, g_2, g_3 \in \mathcal{G}$ and the corresponding unitary representations $\mathbf{U}_i = \mathbf{U}(g_i)$. Let us further assume that $g_3 = g_1 \circ g_2$, so that $\mathbf{U}_3 = \mathbf{U}_1 \cdot \mathbf{U}_2$. The commutation relations for g_1- and g_2-symmetry are

$$\mathbf{U}_1 \cdot \mathbf{T}_{\partial\mathbf{\Gamma}}^{(\hat{\mathbf{n}}_-,\mathbf{d})} \cdot \mathbf{U}_1^{-1} = \mathbf{T}_{\partial\mathbf{\Gamma}}^{(\hat{\mathbf{n}}_-,\mathbf{d})} \tag{8.95}$$

$$\mathbf{U}_2 \cdot \mathbf{T}_{\partial\mathbf{\Gamma}}^{(\hat{\mathbf{n}}_-,\mathbf{d})} \cdot \mathbf{U}_2^{-1} = \mathbf{T}_{\partial\mathbf{\Gamma}}^{(\hat{\mathbf{n}}_-,\mathbf{d})}. \tag{8.96}$$

By multiplying the second relation from the left with $\mathbf{U}_1$ and from the right with $\mathbf{U}_1^{-1}$, and by exploiting the first relation, we obtain

$$\mathbf{U}_1 \cdot \mathbf{U}_2 \cdot \mathbf{T}_{\partial\mathbf{\Gamma}}^{(\hat{\mathbf{n}}_-,\mathbf{d})} \cdot \mathbf{U}_2^{-1} \cdot \mathbf{U}_1^{-1} = \mathbf{T}_{\partial\mathbf{\Gamma}}^{(\hat{\mathbf{n}}_-,\mathbf{d})}. \tag{8.97}$$

However, since $\mathbf{U}_3 = \mathbf{U}_1 \cdot \mathbf{U}_2$, this is just the commutation relation for g_3-symmetry,

$$\mathbf{U}_3 \cdot \mathbf{T}_{\partial\mathbf{\Gamma}}^{(\hat{\mathbf{n}}_-,\mathbf{d})} \cdot \mathbf{U}_3^{-1} = \mathbf{T}_{\partial\mathbf{\Gamma}}^{(\hat{\mathbf{n}}_-,\mathbf{d})}. \tag{8.98}$$

So the commutation relation belonging to g_3-symmetry is *not* an independent symmetry relation of the T-matrix. It can be derived from the commutation relations belonging to g_1- and g_2-symmetry. This followed directly from $g_3 = g_1 \circ g_2$. Consequently, only the generators of a symmetry group provide us with independent commutation relations, since all other group elements can be obtained by forming products of generators. Now we can understand the reduction of the surface integration area discussed in the previous section. In the example of the hexagonal prism we only exploited the group elements C_6, σ_h, and $C_2'^{(0)}$, and we claimed that no further reduction of the integration surface is possible. This is because these three elements are the generators of the corresponding symmetry group (which is known as the prismatic symmetry group $\mathcal{D}_{6h}$). So only the C_6, σ_h, and $C_2'^{(0)}$ symmetries provide us with independent commutation relations.

At this point the reader may wonder why we went through the painstaking efforts of deriving so many unitary representations in the previous sections, if it now turns out that we only need a handful of them for any given symmetry group. The reason will become apparent later when we introduce the concept of irreducible representations.

So how much computation time can we save by exploiting the commutation relations? Consider, as an example, the group $\mathcal{C}_{3v}$ with its two generators C_3 and $\sigma_v^{(0)}$. According to our remarks following Eqs. (8.69) and (8.72), C_3-symmetry reduces

the number of T-matrix elements by a factor of 3, while $\sigma_v^{(0)}$ saves us a factor of 2, which makes a factor of 6 in total. In addition, we can save another factor of 6 in the numerical evaluation of the matrices $\mathbf{A}_{\partial\Gamma}^{(g,\varphi_0^{\hat{n}_-})}$ and $\mathbf{B}_{\partial\Gamma}^{(g,\psi_0^{\hat{n}_-})}$ owing to the reduction of the integration domain. So in total we can save a factor of 6^2. In case of the symmetry group $\mathcal{D}_{6h}$ of the hexagonal prism, we save a factor of 24^2. In either case this is just equal to the square of the order of the group M_o^2. This observation holds in general: For any given finite point-group, the commutation relations reduce the number of nonzero, independent elements of the matrices $\mathbf{A}_{\partial\Gamma}^{(g,\varphi_0^{\hat{n}_-})}$, $\mathbf{B}_{\partial\Gamma}^{(g,\psi_0^{\hat{n}_-})}$ and $\mathbf{T}_{\partial\mathbf{\Gamma}}^{(\hat{\mathbf{n}}_-,\mathbf{d})}$ by a factor of M_o, and they reduce the integration domain in the numerical evaluation of the matrices $\mathbf{A}_{\partial\Gamma}^{(g,\varphi_0^{\hat{n}_-})}$ and $\mathbf{B}_{\partial\Gamma}^{(g,\psi_0^{\hat{n}_-})}$ by another factor of M_o, resulting in a total reduction by M_o^2. We will see shortly that there are more ways in which we can exploit symmetries to cut down computational efforts.

8.3.2 Conjugate Elements and Classes

Consider, as an example, the elements $\sigma_v^{(k)} \in \mathcal{C}_{3v}$, $k = 0, 1, 2$. By use of Table 8.1, we can see that

$$\sigma_v^{(1)} = \left[C_3^2\right]^{-1} \circ \sigma_v^{(0)} \circ C_3^2 \tag{8.99}$$

$$\sigma_v^{(2)} = C_3^{-1} \circ \sigma_v^{(0)} \circ C_3, \tag{8.100}$$

where $C_3^{-1} = C_3^2$ and $\left[C_3^2\right]^{-1} = C_3$. In general, two group elements $g_1, g_2 \in \mathcal{G}$ are called conjugate to each other if there exists an element $h \in \mathcal{G}$ such that

$$g_1 = h^{-1} \circ g_2 \circ h. \tag{8.101}$$

Conjugacy defines a relation among group elements, which we will abbreviate by $g_1 \sim g_2$. The reader is encouraged to verify that this relation is reflexive, symmetric, and transitive, i.e.

$$g \sim g \qquad \forall g \in \mathcal{G} \tag{8.102}$$

$$g_1 \sim g_2 \Rightarrow g_2 \sim g_1 \qquad \forall g_1, g_2 \in \mathcal{G} \tag{8.103}$$

$$g_1 \sim g_2 \text{ and } g_2 \sim g_3 \Rightarrow g_1 \sim g_3 \qquad \forall g_1, g_2, g_3 \in \mathcal{G}. \tag{8.104}$$

Relations that have the properties (8.102–8.104) are known as equivalence relations. For example, equality "=" is an equivalence relation. On the other hand, the order relation "$\leq$" is not an equivalence relation, since it is only reflexive and transitive, but not symmetric.

An equivalence class $[g_0]_\sim$ is defined as the set of all group elements that are related to g_0 by the equivalence relation $\sim$, i.e.

$$[g_0]_\sim := \{g \in \mathcal{G} \,|\, g \sim g_0\}. \tag{8.105}$$

g_0 is called a representative of the equivalence class $[g_0]_\sim$. In group theory the equivalence classes defined by the conjugacy relation are called conjugacy classes, or just classes. For example, the group $\mathcal{C}_{3h}$ contains the three classes

$$[E]_\sim = \{E\} \tag{8.106}$$

$$[C_3]_\sim = \left\{C_3, C_3^2\right\} \tag{8.107}$$

$$\left[\sigma_v^{(0)}\right]_\sim = \left\{\sigma_v^{(0)}, \sigma_v^{(1)}, \sigma_v^{(2)}\right\}. \tag{8.108}$$

The significance of structuring the group into classes will become clearer in the context of representations.

8.3.3 Linear Representations of a Group

Let's return to our example of the group $\mathcal{C}_{3v}$. We have an intuitive idea about what each abstract element in this group does. For instance, the transformation C_3 is a rotation about the vertical axis by an angle $2\pi/3$. In practice, we want to apply the fairly abstract concept of such a rotation to specific objects, such as a position vector (x, y, z) in Cartesian coordinates, or to a vectorial eigenfunction $\vec{\psi}_{l,n,\tau}$ of the vector-wave equation. Such objects are elements of vector spaces. So we need to represent our group elements as operators acting on the elements of a given vector space. For example, in three-dimensional Cartesian coordinates, the abstract group element C_3 can be represented by the regular (3×3) matrix

$$\mathbf{R}(C_3) = \begin{pmatrix} \cos(2\pi/3) & \sin(2\pi/3) & 0 \\ -\sin(2\pi/3) & \cos(2\pi/3) & 0 \\ 0 & 0 & 1 \end{pmatrix}. \tag{8.109}$$

In the function space of the eigenfunctions $\vec{\psi}_{l,n,\tau}$, C_3 can be represented by a unitary matrix with elements

$$U^{\tau,\tau'}_{n,l,n',l'}(C_3) = \delta_{n,n'}\delta_{l,l'}\delta_{\tau,\tau'} \exp\left(-i\frac{2\pi l}{3}\right). \tag{8.110}$$

These two expressions represent one and the same abstract group element in two different vector spaces.

We have repeatedly and tacitly assumed that the representation matrices $\mathbf{U}$ have the property $\mathbf{U}(g_1 \circ g_2) = \mathbf{U}(g_1) \cdot \mathbf{U}(g_2)$— see, e.g., Eqs. (8.59) and (8.60). This is, indeed, a defining property of representations. So a linear representation can, in somewhat simplified terms, be thought of a map

$$\mathbf{D} : \mathcal{G} \longrightarrow \mathcal{M}_n, \ g \mapsto \mathbf{D}(g) \tag{8.111}$$

with

$$\mathbf{D}(g_1 \circ g_2) = \mathbf{D}(g_1) \cdot \mathbf{D}(g_2), \tag{8.112}$$

where $\mathcal{M}_n$ is the set of regular $(n \times n)$ matrices. *In somewhat more general terms for the mathematically inclined reader: A representation of a group in an n-dimensional vector space V is a map $D : \mathcal{G} \to GL(n)$, where $GL(n)$ is the general linear group in n dimensions. The latter is the equivalence class of invertible linear transformations mapping from V to V (automorphisms), where the equivalence relation is given by group isomorphy.* The regularity requirement means that the matrices are invertible. This makes sense, because group property (8.87) implies that

$$\mathbf{D}(E) = \mathbf{D}(g \circ g^{-1}) = \mathbf{D}(g) \cdot \mathbf{D}(g^{-1}), \tag{8.113}$$

while group property (8.86) implies

$$\mathbf{D}(g) = \mathbf{D}(E \circ g) = \mathbf{D}(E) \cdot \mathbf{D}(g). \tag{8.114}$$

The second equation shows that $\mathbf{D}(E)$ is the unit element in $\mathcal{M}_n$. Therefore, the first equation suggests that

$$\mathbf{D}(g^{-1}) = \mathbf{D}^{-1}(g). \tag{8.115}$$

8.4 Irreducible Representations

The unitary representations we derived in Sect. 8.2.1 are valid in the specific expansion basis of the vectorial eigensolutions of the vector-wave equation. It turns out that there is an even smarter choice of basis functions in which we obtain representations of the group that are better adapted to the symmetries of the problem. These are known as the irreducible representations of the group. Before we venture into a more formal treatment of irreducible representations, let us first consider a simple example to motivate what we want to achieve.

8.4.1 Motivation

Let's assume that our scatterer belongs to the symmetry group $\mathcal{C}_3 = \{E, C_3, C_3^2\}$, which contains three elements. Each element is in a class by itself, so the group has three classes. This group is actually a subgroup of the group $\mathcal{C}_{3v}$. The group $\mathcal{C}_3$ has only one generator, C_3, so there is only one independent commutation relation of the T-matrix. The matrices $\mathbf{A}_{\partial\Gamma}^{(g,\varphi_0^{\hat{n}_-})}$ and $\mathbf{B}_{\partial\Gamma}^{(g,\psi_0^{\hat{n}_-})}$ employed for computing the T-matrix in Eq. (3.89) satisfy the same commutation relation as the T-matrix. Thus, according to Eq. (8.69), we have

$$\left[A_{\partial\Gamma}^{(g,\varphi_0^{\hat{n}_-})}\right]_{n,l,n',l'}^{\tau,\tau'} = 0 \qquad \text{unless} \quad |l - l'| = 0, 3, 6, \ldots \tag{8.116}$$

The symmetry structure of the matrix is schematically shown in Fig. 8.14 (left panel). In this example $l_{cut} = 4$. The black and white squares represent block-matrices each belonging to a distinct pair of indices l, l'. Each square contains matrix elements with different indices n, n', τ, τ'. The white squares represent those block-matrices that are zero due to symmetry. The black squares contain, in general, non-zero matrix elements.

After re-arranging the columns and rows as shown in the right panel of Fig. 8.14 we obtain a matrix $\tilde{\mathbf{A}}_{\partial\Gamma}^{(g,\varphi_0^{\hat{n}_-})}$ with block-diagonal structure. This re-arrangement is achieved by a transformation

$$\tilde{\mathbf{A}}_{\partial\Gamma}^{(g,\varphi_0^{\hat{n}_-})} = \mathbf{P} \cdot \mathbf{A}_{\partial\Gamma}^{(g,\varphi_0^{\hat{n}_-})} \cdot \mathbf{P}^{-1}. \tag{8.117}$$

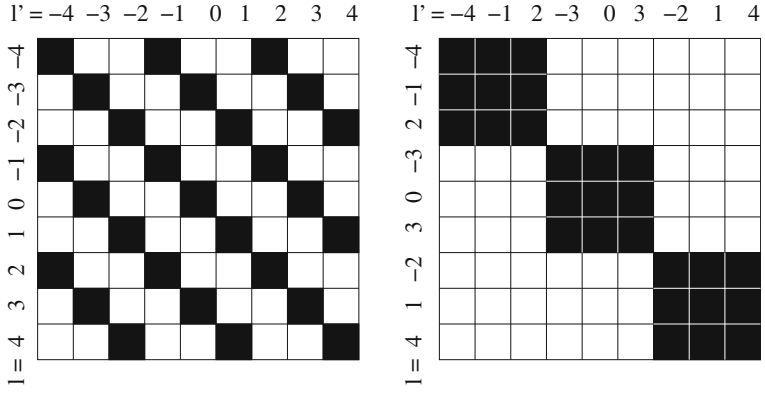

Fig. 8.14 C_3 symmetry structure of the matrices $\mathbf{T}_{\partial\Gamma}^{(\hat{n}_-,d)}$, $\mathbf{A}_{\partial\Gamma}^{(g,\varphi_0^{\hat{n}_-})}$ and $\mathbf{B}_{\partial\Gamma}^{(g,\psi_0^{\hat{n}_-})}$ (*left*), and the same matrix after re-ordering of the rows and columns (*right*)

In our example the transformation matrix is given by

$$\mathbf{P} = \begin{pmatrix} 0&1&0&0&0&0&0&0&0 \\ 0&0&0&0&1&0&0&0&0 \\ 0&0&0&0&0&0&0&1&0 \\ 1&0&0&0&0&0&0&0&0 \\ 0&0&0&1&0&0&0&0&0 \\ 0&0&0&0&0&0&1&0&0 \\ 0&0&1&0&0&0&0&0&0 \\ 0&0&0&0&0&1&0&0&0 \\ 0&0&0&0&0&0&0&0&1 \end{pmatrix} \tag{8.118}$$

and

$$\mathbf{P}^{-1} = \begin{pmatrix} 0&0&0&1&0&0&0&0&0 \\ 1&0&0&0&0&0&0&0&0 \\ 0&0&0&0&0&0&1&0&0 \\ 0&0&0&0&1&0&0&0&0 \\ 0&1&0&0&0&0&0&0&0 \\ 0&0&0&0&0&0&0&1&0 \\ 0&0&0&0&0&1&0&0&0 \\ 0&0&1&0&0&0&0&0&0 \\ 0&0&0&0&0&0&0&0&1 \end{pmatrix}, \tag{8.119}$$

where each 1-element actually represents a unit block-matrix. (Remember that each square in Fig. 8.14) represents a block-matrix with elements $\left[A_{\partial\Gamma}^{(g,\varphi_0^{\hat{n}-})}\right]_{l_0,n,l_0',n'}^{\tau,\tau'}$ with fixed l_0, l_0'.

It is precisely this block-diagonal matrix structure that we want to obtain. Why is this structure so advantageous? Recall that the computation of the T-matrix by use of Eq. (3.89) involves inversion of the matrix $\mathbf{A}_{\partial\Gamma}^{(g,\varphi_0^{\hat{n}-})}$. Matrix inversions can run into numerical ill-conditioning problems. The block-diagonalisation reduces the problem of inverting one large matrix to the problem of inverting three smaller matrices, which reduces potential ill-conditioning problems. Further, in a numerical inversion of a matrix such as that in the left panel of Fig. 8.14 we perform a large number of unnecessary numerical operations involving zero-elements. Inversion of each of the three block-matrices in the right panel of Fig. 8.14 by-passes such operations, thus saving computation time.

The example of the $\mathcal{C}_3$ symmetry group was rather simple. We could pretty much guess the necessary re-arrangement of columns and rows in the left matrix of Fig. 8.14 in order to bring it into the block-diagonal form on the right hand side of the figure. In more complex symmetry groups this will be considerably less trivial. Also, the block-diagonalisation will, in general, not be achieved by a simple permutation of rows and columns. Rather, it will require a general transformation, which involves both permutations and linear combinations of different columns and rows. We now

want to develop an automatic procedure for constructing the transformation matrix **P** for an arbitrary point group. To this end we now need to introduce the concept of irreducible representations.

8.4.2 Basic Definitions

Let $(\mathcal{G}, \circ)$ be a group, and $\mathbf{D} : \mathcal{G} \to \mathcal{M}_n$ with $g \mapsto \mathbf{D}(g) = \mathbf{D}_g$ be a representation of the group, where the elements of $\mathcal{M}_n$ are, as we know, regular $(n \times n)$ matrices operating on the elements of an n-dimensional vector space V_n. Let further $T_m \subset V_n$ be a subspace of V_n, where $m \leq n$. T_m is called an *invariant subspace* of V_n if

$$\mathbf{D}_g \cdot \vec{x} \in T_m \quad \forall g \in \mathcal{G} \quad \forall \vec{x} \in T_m. \tag{8.120}$$

In other words, operating with any of the represented group elements $\mathbf{D}_g$ on the elements of T_m does not lead us out of the subspace T_m.

Every vector space contains two trivial invariant subspaces, namely, $\{\vec{0}\}$ and V_n with dimensions 0 and n, respectively (where $\vec{0}$ denotes the null vector). We will only be interested in proper invariant subspaces with $0 < m < n$. The representation **D** is called a *reducible representation*, if the vector space V_n contains a proper invariant subspace.

Let's first see what reducibility implies for the structure of the matrices $\mathbf{D}_g$. To this end, let us assume that we can "decompose" our vector space V_n into invariant subspaces $T^{(1)}_{m_1}, \ldots, T^{(r)}_{m_r}$ with dimensions $m_1, \ldots, m_r$ such that

$$\sum_{\mu=1}^{r} m_\mu = n \tag{8.121}$$

$$V_n = \bigcup_{\mu=1}^{r} T^{(\mu)}_{m_\mu} \tag{8.122}$$

$$T^{(\mu)}_{m_\mu} \cap T^{(\nu)}_{m_\nu} = \{\vec{0}\} \quad \text{for } \mu \neq \nu. \tag{8.123}$$

Let us further choose a set of basis vectors $\vec{f}^{(\mu)}_1, \ldots, \vec{f}^{(\mu)}_{m_\mu}$ in each invariant subspace $T^{(\mu)}_{m_\mu}$. The union of all basis vectors is then a basis of the entire vector space V_n.

How do the matrices $\mathbf{D}_g$ look in this particular basis? To answer this question, we consider what happens if we multiply any of the represented group elements $\mathbf{D}_g$ with a vector

$$\vec{x} = \sum_{j=1}^{m_1} x^{(1)}_j \vec{f}^{(1)}_j \in T^{(1)}_{m_1}. \tag{8.124}$$

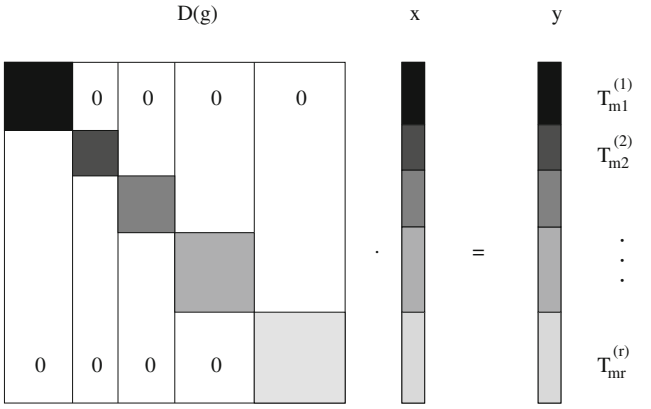

Fig. 8.15 Block-diagonal structure of the matrix $\mathbf{D}(g)$ in the basis of the invariant subspaces

We know that the resulting vector $\vec{y} = \mathbf{D}_g \cdot \vec{x}$ also has to be an element of $T^{(1)}_{m_1}$ (because $T^{(1)}_{m_1}$ is, by assumption, and invariant subspace). So both $\vec{x}$ and $\vec{y}$ have components $x^{(\mu)}_j = y^{(\mu)}_j = 0$ for $\mu \neq 1$. This means that the structure of the matrix $\mathbf{D}_g$ has to be such that it does not have any non-zero components $[D_g]^{\mu,1}_{j,k}$ for $\mu \neq 1$, because such components would couple to the non-zero components $x^{(1)}_k$ and produce non-zero components $y^{(\mu)}_j$ with $\mu \neq 1$, in contradiction to the invariance of the subspace $T^{(1)}_{m_1}$.

The situation is shown schematically in Fig. 8.15. In columns 1 to m_1, only the elements in the first 1 to m_1 rows can be nonzero. In a similar way, we can operate with $\mathbf{D}(g)$ on a vector

$$\vec{x} = \sum_{j=1}^{m_1} x^{(2)}_j \vec{f}^{(2)}_j \in T^{(2)}_{m_1} \tag{8.125}$$

and use the fact that $\vec{y} = \mathbf{D}_g \cdot \vec{x}$ has to be an element of $T^{(2)}_{m_1}$. This implies that in columns $m_1 + 1$ to $m_1 + m_2$, only the elements of $\mathbf{D}(g)$ in rows $m_1 + 1$ to $m_1 + m_2$ can be non-zero. Continuing this kind of argument for all invariant subspaces, we finally conclude that the matrix $\mathbf{D}_g$ must be block-diagonal. So the block-diagonal structure is a consequence of the fact that we chose a basis $\vec{f}^{(1)}_1, \ldots, \vec{f}^{(r)}_{m_r}$ such that each subset $\vec{f}^{(\mu)}_1, \ldots, \vec{f}^{(\mu)}_{m_\mu}$ is a basis of the μth invariant subspace. In any other basis, the matrix $\mathbf{D}_g$ will, in general, not be block-diagonal.

We denote the μth block-matrix by $\mathbf{D}^{(\mu)}_g$, so

$$\mathbf{D}_g = \begin{pmatrix} \mathbf{D}^{(1)}_g & & & \\ & \mathbf{D}^{(2)}_g & & \\ & & \ddots & \\ & & & \mathbf{D}^{(r)}_g \end{pmatrix} = \bigoplus_{\mu=1}^{r} \mathbf{D}^{(\mu)}_g, \tag{8.126}$$

where the symbolic notation "$\bigoplus$" denotes the direct sum of the block-matrices to form a block-diagonal matrix. Each block-matrix $\mathbf{D}_g^{(\mu)}$ is a representation of the group $\mathcal{G}$ in the vectorspace $T_{m_\mu}^{(\mu)}$, i.e.

$$\mathbf{D}^{(\mu)} : \mathcal{G} \longrightarrow \mathcal{M}_{m_\mu} \quad \text{with} \quad g \mapsto \mathbf{D}^{(\mu)}(g) = \mathbf{D}_g^{(\mu)}. \tag{8.127}$$

We are interested in breaking down the representation $\mathbf{D}$ in the vector space V_n into as small block-matrices as possible, i.e. into block matrices that cannot be reduced to any smaller block-matrices. $\mathbf{D}^{(\mu)}$ is called an *irreducible representation*, of the group $\mathcal{G}$ in the vector space $T_{m_\mu}^{(\mu)}$, if $T_{m_\mu}^{(\mu)}$ does not possess any proper invariant subspaces.

As a simple example, we consider the unitary representation for C_3-symmetry, $\mathbf{D} = \mathbf{U}(C_3)$ given in Eq. (8.34). We explicitly write out the representation matrix for $l_{cut} = 4$:

$$\mathbf{U}(C_3) = \text{diag}\Big[(u^{-4}), (u^{-3}), (u^{-2}), (u^{-1}), (u^0), (u^1), (u^2), (u^3), (u^4)\Big], \tag{8.128}$$

where $u := \exp(-2\pi i/3)$, and (u^l) is a diagonal matrix with elements $(u^l)_{n,n'}^{\tau,\tau'} = \delta_{n,n'}$ $\delta_{\tau,\tau'}\, u^l$. For this case we have already given the transformation that transforms into the irreducible basis in Eqs. (8.118) and (8.119), although we have not yet discussed how to derive the transformation matrix. Application of this transformation to $\mathbf{U}(C_3)$ gives

$$\begin{aligned}\mathbf{P} \cdot \mathbf{U}(C_3) \cdot \mathbf{P}^{-1} &= \text{diag}\Big[(u^0), (u^0), (u^0), (u^{-1}), (u^{-1}), (u^{-1}), (u^1), (u^1), (u^1)\Big] \\ &= \text{diag}\big[(1), (1), (1), (u^*), (u^*), (u^*), (u), (u), (u)\big].\end{aligned} \tag{8.129}$$

So we see a few interesting things here. First, we have three irreducible representations, and second, each irreducible representation can occur several times along the matrix diagonal. The reduction of a reducible representation given in Eq. (8.126) should therefore be written, more generally, as

$$\mathbf{D}_g = \bigoplus_{\mu=1}^{r} \alpha_\mu \mathbf{D}_g^{(\mu)}, \tag{8.130}$$

where the cardinal numbers α_μ denote how many times the μth irreducible representation $\mathbf{D}_g^{(\mu)}$ occurs in the reduction of the reducible representations $\mathbf{D}_g$. In fact, each of the matrices (u^l) in Eq. (8.129) is a diagonal matrix with elements u^l along its diagonal. If the matrix (u^l) has dimension n_l, then the element u^l occurs $3n_l$ times along the diagonal of $\mathbf{P} \cdot \mathbf{U}(C_3) \cdot \mathbf{P}^{-1}$. So the irreducible representations are, in this case, (1×1) matrices with a single element u^l ($l = 0, -1, 1$), and $\alpha_i = 3n_i$. The attentive reader may have noticed that the $\mathcal{C}_3$ group has exactly as many

irreducible representations as classes. This is, in fact, generally true for any symmetry group.

Finding the irreducible representations means to block-diagonalise the representation $\mathbf{D}$. This is achieved by choosing a proper basis of the vector space. As we will see, this choice of basis will automatically block-diagonalise any matrix that commutes with $\mathbf{D}$. If we return to the specific problem of electromagnetic scattering by particles with geometrical symmetries, then the goal is now to block-diagonalise the unitary representations $\mathbf{U}(g)$. This will lead to a block-diagonalisation of all matrices that commute with $\mathbf{U}(g)$, such as $\mathbf{A}_{\partial\Gamma}^{(g,\hat{\varphi}_0^{\hat{n}_-})}$, $\mathbf{B}_{\partial\Gamma}^{(g,\hat{\psi}_0^{\hat{n}_-})}$, and $\mathbf{T}_{\partial\Gamma}^{(\hat{n}_-,d)}$. The block-diagonalisation of $\mathbf{A}_{\partial\Gamma}^{(g,\hat{\varphi}_0^{\hat{n}_-})}$ is the desired pre-conditioning that alleviates ill-conditioning problems in the numerical inversion of $\mathbf{A}_{\partial\Gamma}^{(g,\hat{\varphi}_0^{\hat{n}_-})}$. The block-diagonalisation of the representation is achieved, as we have seen, by making a proper choice of the basis. The basis has to be such that it subdivides the entire vector space into invariant subspaces. The strategy is therefore to find the invariant subspaces. More specifically, we will construct projection operators $\tilde{\mathbf{P}}^{(\mu)}$ that project into the μth invariant subspace, i.e.

$$\tilde{\mathbf{P}}^{(\mu)} \cdot \vec{x} \in T_{m_\mu}^{(\mu)} \quad \forall \vec{x} \in V_n, \quad \mu = 1, \ldots, r. \tag{8.131}$$

To this end, we first have to learn a bit more about group theory.

The trace of the μth irreducible representation of group element g

$$\chi^{(\mu)}(g) := Tr\mathbf{D}^{(\mu)}(g) \tag{8.132}$$

is called the *character*, of $\mathbf{D}^{(\mu)}(g)$. In the above example of $g = C_3$ and $\mathcal{G} = \mathcal{C}_3$, we can see in Eq. (8.129) that $\chi^{(1)}(C_3) = u^0 = 1$, $\chi^{(2)}(C_3) = u^* = \exp(2\pi i/3)$, and $\chi^{(3)}(C_3) = u = \exp(-2\pi i/3)$.

All group elements within the same class have the same characters, as we can see as follows. If g_1 and g_2 belong to the same class, then there exists an element $h \in \mathcal{G}$ such that $g_1 = h^{-1} \circ g_2 \circ h$—see Eq. (8.101). Using Eq. (8.112), we obtain $\mathbf{D}_{g_1}^{(\mu)} = [\mathbf{D}_h^{(\mu)}]^{-1} \cdot \mathbf{D}_{g_2}^{(\mu)} \cdot \mathbf{D}_h^{(\mu)}$. Taking the trace and using the facts that arguments under the trace can be permuted, we obtain

$$\chi^{(\mu)}(g_1) = Tr\mathbf{D}_{g_1}^{(\mu)} = Tr\left\{[\mathbf{D}_h^{(\mu)}]^{-1} \cdot \mathbf{D}_h^{(\mu)} \cdot \mathbf{D}_{g_2}^{(\mu)}\right\} = \chi^{(\mu)}(g_2). \tag{8.133}$$

In the example given above, we calculated the characters $\chi^{(\mu)}(C_3)$ for the $\mathcal{C}_3$ group after transforming the reducible representations by use of the transformation $\mathbf{P}$. This was, of course, "cheating", because in practice we do not know the transformation $\mathbf{P}$. On the contrary, the transformation matrix $\mathbf{P}$ is what we want to construct. There exist group theoretical methods for computing the irreducible characters without prior knowledge of the irreducible representations or the invariant subspaces. The details of the mathematical theory are beyond the scope of this book. However, for

Table 8.2 Character table for the group $\mathcal{C}_3$, where $u = \exp(-2\pi i/3)$

E	C_3	C_3^2
1	1	1
1	u^*	u
1	u	u^*

many point-groups the characters can be found tabulated in the literature. There also exist group theoretical software packages for computing the characters of general groups (e.g. the Groups Algorithms and Programming package, http://www.gap-system.org). Table 8.2 shows, as an example, the character table for the group $\mathcal{C}_3$. The column headings show one representative of each class. In this example, each class contains only one group element. The three rows contain the characters for the three irreducible representations. For instance, the character $\chi^{(2)}(C_3^2)$ can be found in the second row and the third column.

The characters are the essential ingredient we will need to construct the projection operators $\tilde{\mathbf{P}}^{(\mu)}$ that project into the μth invariant subspace. However, there is one more thing we will need for proving the projection property (8.131), namely, an important group theoretical theorem that we will give here without proof.

8.4.3 The Great Orthogonality Theorem

Let $(\mathcal{G}, \circ)$ be a group of order M_o, and let $\mathbf{D}^{(\mu)} : \mathcal{G} \to \mathcal{M}_{m_\mu}$ denote the irreducible representation of the group in the μth invariant subspace $T_{m_\mu}^{(\mu)}$ of dimension m_μ. Then

$$\sum_{g\in\mathcal{G}} D_{i,l}^{(\mu)}(g)\, D_{j,m}^{(\nu)*}(g) = \frac{M_o}{m_\mu}\delta_{\mu,\nu}\,\delta_{i,j}\,\delta_{l,m}. \tag{8.134}$$

The summation is carried out over all group elements. In this formulation of the theorem we have assumed, without loss of generality, that the representations $\mathbf{D}^{(\mu)}$ are unitary, so that $\mathbf{D}^{(\nu)}(g^{-1}) = \mathbf{D}^{(\nu)-1}(g) = \mathbf{D}^{(\nu)\dagger}(g)$.

8.4.4 Projection Operators into the Invariant Subspaces

Now we have everything in place to formulate an automatic block-diagonalisation procedure. The first step is to construct operators that project an arbitrary vector into the μth invariant subspace. We claim that the matrix with components

$$\tilde{P}_{i,j}^{(\mu)} := \sum_{g\in\mathcal{G}} \chi^{(\mu)*}(g)\, D_{i,j}(g) \tag{8.135}$$

has the property (8.131), where $D_{i,j}(g)$ are just the matrix elements of the reducible representations.

To keep things simple, let us prove the projection property for the case that each irreducible representation occurs only once in the reducible one, so we can set in Eq. (8.130) $\alpha_\mu = 1$ for all $\mu = 1, \ldots, r$. The more general case with $\alpha_\mu \geq 1$ only clutters up the notation, but it does not provide us with any new conceptual insights. The basis vectors of V_n in which the reducible representations $\mathbf{D}(g)$ are defined are denoted by $\vec{\psi}_1, \ldots, \vec{\psi}_n$. In the electromagnetic scattering problem, these are just the known vectorial eigensolutions of the vector-wave equation. The basis functions of the μth invariant subspace are denoted by $\vec{f}_1^{(\mu)}, \ldots, \vec{f}_{m_\mu}^{(\mu)}$. Although we do not know these vectors, we know that they exist, and that there has to exist a transformation from the irreducible to the reducible basis in the form

$$\vec{\psi}_k = \sum_{\nu=1}^{r} \sum_{i=1}^{m_\nu} \vec{f}_i^{(\nu)} a_{i,k}^{(\nu)}, \quad k = 1, \ldots, n, \tag{8.136}$$

as well as a transformation from the reducible to the irreducible basis

$$\vec{f}_j^{(\mu)} = \sum_{k=1}^{n} \vec{\psi}_k b_{k,j}^{(\mu)}, \quad j = 1, \ldots, m_\mu, \quad \mu = 1, \ldots, r. \tag{8.137}$$

Substitution of (8.136) into (8.137) gives

$$\sum_{k=1}^{n} a_{i,k}^{(\nu)} b_{k,j}^{(\mu)} = \delta_{i,j}\delta_{\mu,\nu}. \tag{8.138}$$

With these transformation matrices, we can formally transform the irreducible to the reducible matrix representations. The reducible representations describe the action of a group element g in the reducible basis. According to Eq. (8.19), the basis functions $\vec{\psi}_i$ transform as

$$\vec{\psi}_j(\mathbf{R}_g^{-1}(\mathbf{x})) = \sum_{i=1}^{n} \vec{\psi}_i(\mathbf{x}) D_{i,j}(g), \quad j = 1, \ldots, n. \tag{8.139}$$

Likewise, the irreducible representations transform the irreducible basis vectors in each of the invariant subspaces according to

$$\vec{f}_q^{(\mu)}(\mathbf{R}_g^{-1}(\mathbf{x})) = \sum_{p=1}^{m_\mu} \vec{f}_p^{(\mu)}(\mathbf{x}) D_{p,q}^{(\mu)}(g), \quad \mu = 1, \ldots, r, \quad q = 1, \ldots, m_\mu. \tag{8.140}$$

We substitute Eq. (8.137) into (8.140), multiply with $a_{q,j}^{(\mu)}$ on both sides, and sum over μ and q, which gives

$$\sum_{\mu=1}^{r}\sum_{q=1}^{m_\mu}\vec{f}_q^{(\mu)}(\mathbf{R}_g^{-1}(\mathbf{x}))a_{q,j}^{(\mu)}=\sum_{\mu=1}^{r}\sum_{p,q=1}^{m_\mu}\sum_{i=1}^{n}\vec{\psi}_i(\mathbf{x})b_{i,p}^{(\mu)}D_{p,q}^{(\mu)}(g)a_{q,j}^{(\mu)}. \tag{8.141}$$

According to Eq. (8.136), the lhs is just $\vec{\psi}_j(\mathbf{R}_g^{-1}(\mathbf{x}))$. Thus, comparison with Eq. (8.139) gives

$$D_{i,j}(g)=\sum_{\mu=1}^{r}\sum_{p,q=1}^{m_\mu}b_{i,p}^{(\mu)}D_{p,q}^{(\mu)}(g)a_{q,j}^{(\mu)}\quad\forall g\in\mathcal{G}. \tag{8.142}$$

Equation (8.142) can now be used to express the operator $\tilde{P}_{i,j}^{(\mu)}$ defined in Eq. (8.135) in terms of the transformation matrices **a** and **b**. Using the definition of the characters $\chi(g)=\sum_{l=1}^{m_\mu}D_{l,l}^{(\mu)}(g)$, Eq. (8.135) becomes

$$\begin{aligned}\tilde{P}_{i,j}^{(\mu)}&=\sum_{g\in\mathcal{G}}\sum_{l=1}^{m_\mu}D_{l,l}^{(\mu)*}(g)\,D_{i,j}(g)\\&=\sum_{\nu=1}^{r}\sum_{p,q=1}^{m_\nu}\sum_{l=1}^{m_\mu}b_{i,p}^{(\nu)}a_{q,j}^{(\nu)}\sum_{g\in\mathcal{G}}D_{l,l}^{(\mu)*}(g)\,D_{p,q}^{(\nu)}(g)\\&=\frac{M_o}{m_\mu}\sum_{l=1}^{m_\mu}b_{i,l}^{(\mu)}a_{l,j}^{(\mu)}.\end{aligned} \tag{8.143}$$

In the last line, we have exploited the Great Orthogonality Theorem (8.134). Application of $\tilde{\mathbf{P}}^{(\mu)}$ to an arbitrary vector $\sum_j\vec{\psi}_jx_j$ gives

$$\begin{aligned}\sum_{i,j=1}^{n}\vec{\psi}_i\tilde{P}_{i,j}^{(\mu)}x_j&=\frac{M_o}{m_\mu}\sum_{i,j=1}^{n}\sum_{l=1}^{m_\mu}\vec{\psi}_ib_{i,l}^{(\mu)}a_{l,j}^{(\mu)}x_j\\&=\frac{M_o}{m_\mu}\sum_{j=1}^{n}\sum_{l=1}^{m_\mu}\vec{f}_l^{(\mu)}a_{l,j}^{(\mu)}x_j\;\in T_{m_\mu}^{(\mu)},\end{aligned} \tag{8.144}$$

which proves the projection property of $\tilde{\mathbf{P}}^{(\mu)}$. In the last line we made use of Eq. (8.137).

As already mentioned, the characters can be assumed to be known a priori for any given point-group. No prior knowledge of the irreducible representations or the invariant subspaces is needed to determine the characters. So the definition of the projectors in Eq. (8.135) contains only known quantities. Note that the construction of the projectors requires knowledge of the reducible representations $\mathbf{D}(g)$ for *all* group elements $g\in\mathcal{G}$, not just for the generators! This is the reason why we took the effort to derive a large number of unitary representations in Sect. 8.2.1, even

though only the generators of each group provide us with independent commutation relations.

8.4.5 Construction of the Basis Transformation from the Reducible to the Irreducible Basis

We have learnt how to project into the irreducible invariant subspaces. This allows us to construct the desired transformation from the reducible to the irreducible basis. We first discuss a rather intuitive method for constructing the transformation into the irreducible basis, followed by a more systematic method.

Note first that the sum of $\tilde{\mathbf{P}}^{(\mu)}$ over all μ is a map from V_n to V_n. This can be seen by summing Eq. (8.144) over all μ:

$$\sum_{i,j=1}^{n} \vec{\psi}_i \left(\sum_{\mu=1}^{r} \tilde{P}_{i,j}^{(\mu)} \right) x_j = \sum_{\mu=1}^{r} \frac{M_o}{m_\mu} \sum_{j=1}^{n} \sum_{l=1}^{m_\mu} \vec{f}_l^{(\mu)} a_{l,j}^{(\mu)} x_j \in \bigcup_{\mu=1}^{r} T_{m_\mu}^{(\mu)} = V_n, \tag{8.145}$$

so $(\sum_{\mu=1}^{r} \tilde{\mathbf{P}}^{(\mu)}) : V_n \to V_n$. This is not surprising. Each $\tilde{\mathbf{P}}^{(\mu)}$ projects into the μth invariant subspace, which has dimension m_μ. So the dimension of the range of $\tilde{\mathbf{P}}^{(\mu)}$ is m_μ. But according to Eq. (8.121), the sum over all m_μ is the dimension of the vector space, and the intersection of two invariant subspaces has zero dimension. Thus, we expect that the sum over all $\tilde{\mathbf{P}}^{(\mu)}$ has a range of dimension n, so it has to be a map from V_n into V_n.

To construct the transformation from the reducible to the irreducible basis we want to construct a map from V_n into V_n by somehow combining all projectors $\tilde{\mathbf{P}}^{(\mu)}$ into one matrix. To this end, we will do some permutations of the rows in each $\tilde{\mathbf{P}}^{(\mu)}$ prior to summation of the projectors. To illustrate this, let us return once more to the specific example of the $\mathcal{C}_3$ group considered in Sects. 8.4.1 and 8.4.2.

We write Eq. (8.128) in the form

$$\mathbf{U}(C_3) = \mathrm{diag}\left[(u^*), (1), (u), (u^*), (1), (u), (u^*), (1), (u)\right], \tag{8.146}$$

and similarly

$$\mathbf{U}(C_3^2) = \mathrm{diag}\left[(u), (1), (u^*), (u), (1), (u^*), (u), (1), (u^*)\right]. \tag{8.147}$$

The representation of the unit element E is just the unit matrix. By use of the character Table 8.2 and the definition of the projection matrices given in (8.135) it is straight forward to derive

$$\tilde{\mathbf{P}}^{(1)} = 3 \times \begin{pmatrix} 0&0&0&0&0&0&0&0&0 \\ 0&1&0&0&0&0&0&0&0 \\ 0&0&0&0&0&0&0&0&0 \\ 0&0&0&0&0&0&0&0&0 \\ 0&0&0&0&1&0&0&0&0 \\ 0&0&0&0&0&0&0&0&0 \\ 0&0&0&0&0&0&0&0&0 \\ 0&0&0&0&0&0&0&1&0 \\ 0&0&0&0&0&0&0&0&0 \end{pmatrix}. \tag{8.148}$$

$$\tilde{\mathbf{P}}^{(2)} = 3 \times \begin{pmatrix} 1&0&0&0&0&0&0&0&0 \\ 0&0&0&0&0&0&0&0&0 \\ 0&0&0&0&0&0&0&0&0 \\ 0&0&0&1&0&0&0&0&0 \\ 0&0&0&0&0&0&0&0&0 \\ 0&0&0&0&0&0&0&0&0 \\ 0&0&0&0&0&0&1&0&0 \\ 0&0&0&0&0&0&0&0&0 \\ 0&0&0&0&0&0&0&0&0 \end{pmatrix}. \tag{8.149}$$

$$\tilde{\mathbf{P}}^{(3)} = 3 \times \begin{pmatrix} 0&0&0&0&0&0&0&0&0 \\ 0&0&0&0&0&0&0&0&0 \\ 0&0&1&0&0&0&0&0&0 \\ 0&0&0&0&0&0&0&0&0 \\ 0&0&0&0&0&0&0&0&0 \\ 0&0&0&0&0&1&0&0&0 \\ 0&0&0&0&0&0&0&0&0 \\ 0&0&0&0&0&0&0&0&0 \\ 0&0&0&0&0&0&0&0&1 \end{pmatrix}. \tag{8.150}$$

The reader is encouraged to check this. The overall factor of 3 is not important for the projection property and can be omitted. Now let's permute the matrix rows such that the three linearly independent row vectors of $\tilde{\mathbf{P}}^{(1)}$ are collected in rows 1–3, the three linearly independent row vectors of $\tilde{\mathbf{P}}^{(2)}$ end up in rows 4–6, and the linearly independent row vectors of $\tilde{\mathbf{P}}^{(3)}$ are in rows 7–9. This permutation of row vectors just corresponds to a re-labelling of the elements of our reducible basis. Then we add up the three projectors. The result is just the matrix $\mathbf{P}$ given in Eq. (8.118). This is the desired matrix that transforms from the reducible to the irreducible basis, which block-diagonalises the representation matrices $\mathbf{D}_g$ according to Eq. (8.126) (or, more generally, Eq. (8.130)).

In summary, we have the following recipe to block-diagonalise the representation matrices.

1. For a given point group, compute the unitary reducible representations of *all* elements in the group in the chosen basis (e.g. in the basis of vectorial eigensolutions of the vector-wave equation).

2. Find the character table for the given point group. If unavailable, compute the characters with a linear algebra software package, such as Groups Algorithms and Programming (http://www.gap-system.org).
3. Using Eq. (8.135) compute the projectors $\tilde{\mathbf{P}}^{(\mu)}$ for each irreducible invariant subspace $T^{(\mu)}_{m_\mu}$, $\mu = 1, \ldots, r$.
4. Each projector has m_μ linearly independent row vectors. Construct the transformation matrix $\mathbf{P}$ such that its first m_1 row vectors are the linearly independent vectors of $\tilde{\mathbf{P}}^{(1)}$, the following m_2 row vectors are the linearly independent vectors of $\tilde{\mathbf{P}}^{(2)}$, etc.
5. Compute the inverse $\mathbf{P}^{-1}$.

Now the reduction of the reducible representations can be performed according to

$$\mathbf{P} \cdot \mathbf{D}_g \cdot \mathbf{P}^{-1} = \bigoplus_{\mu=1}^{r} \alpha_\mu \mathbf{D}^{(\mu)}_g \quad \forall g \in \mathcal{G}. \tag{8.151}$$

However, it is not the reduction of $\mathbf{D}_g$ that we are interested in. Rather, we want to reduce the matrix $\mathbf{A}^{(g,\varphi_0^{\hat{n}-})}_{\partial\Gamma}$ according to Eq. (8.117). So it remains to be shown that the transformation $\mathbf{P}$ that reduces $\mathbf{D}_g$ also reduces $\mathbf{A}^{(g,\varphi_0^{\hat{n}-})}_{\partial\Gamma}$. More generally, we claim that any matrix $\mathbf{Q}$ that commutes with $\mathbf{D}_g$ has the same block-diagonal structure as $\mathbf{D}_g$ in the irreducible basis. As before, we limit the proof to the case $\alpha_\mu = 1$ for $\mu = 1, \ldots, r$. So in the irreducible basis, $\mathbf{D}_g$ is a block-diagonal matrix of the form

$$\mathbf{D}_g = \begin{pmatrix} \mathbf{D}^{(1)}_g & & \\ & \ddots & \\ & & \mathbf{D}^{(r)}_g \end{pmatrix}. \tag{8.152}$$

We write the matrix $\mathbf{Q}$ in the form

$$\mathbf{Q} = \begin{pmatrix} \mathbf{Q}^{(1,1)} & \cdots & \mathbf{Q}^{(1,r)} \\ \vdots & & \vdots \\ \mathbf{Q}^{(r,1)} & \cdots & \mathbf{Q}^{(r,r)} \end{pmatrix}. \tag{8.153}$$

In other words, we label the elements of $\mathbf{Q}$ so that we split up the matrix into block matrices $\mathbf{Q}^{(\mu,\nu)}$ with components $Q^{(\mu,\nu)}_{i,j}$, $i = 1, \ldots, m_\mu$, $j = 1, \ldots, m_\nu$. Then the commutation relations

$$\mathbf{D}_g \cdot \mathbf{Q} = \mathbf{Q} \cdot \mathbf{D}_g \tag{8.154}$$

can be split into block-components

$$\mathbf{D}^{(\mu)}_g \cdot \mathbf{Q}^{(\mu,\nu)} = \mathbf{Q}^{(\mu,\nu)} \cdot \mathbf{D}^{(\nu)}_g, \quad \mu, \nu = 1, \ldots, r, \tag{8.155}$$

where we have exploited the fact that $\mathbf{D}_g$ is block-diagonal in the irreducible basis. More explicitly, the last equation reads

$$\sum_{p=1}^{m_\mu} D_{i,p}^{(\mu)}(g)\, Q_{p,j}^{(\mu,\nu)} = \sum_{q=1}^{m_\nu} Q_{i,q}^{(\mu,\nu)}\, D_{q,j}^{(\nu)}(g), \qquad (8.156)$$
$$\mu,\nu = 1,\ldots,r, \quad i = 1,\ldots,m_\mu, \quad j = 1,\ldots,n_\nu.$$

The commutation relation holds for all $g \in \mathcal{G}$. So we can multiply both sides by $\chi^{(\mu)*}(g) = \sum_l D_{l,l}^{(\mu)*}(g)$ and sum over all $g \in \mathcal{G}$:

$$\sum_{p,l=1}^{m_\mu} \left(\sum_{g\in\mathcal{G}} D_{l,l}^{(\mu)*}(g) D_{i,p}^{(\mu)}(g) \right) Q_{p,j}^{(\mu,\nu)} = \sum_{q=1}^{m_\nu} \sum_{l=1}^{m_\mu} Q_{i,q}^{(\mu,\nu)} \left(\sum_{g\in\mathcal{G}} D_{l,l}^{(\mu)*}(g) D_{q,j}^{(\nu)}(g) \right) \qquad (8.157)$$

Now we apply the Great Orthogonality Theorem (8.134) to the expressions in parentheses and obtain

$$Q_{i,j}^{(\mu,\nu)} = \delta_{\mu,\nu}\, Q_{i,j}^{(\mu,\nu)}. \qquad (8.158)$$

So if $\mathbf{D}_g$ is in the irreducible basis, and if $\mathbf{Q}$ commutes with $\mathbf{D}_g$ for all $g \in \mathcal{G}$, then $\mathbf{Q}$ necessarily has the same block-diagonal structure as $\mathbf{D}_g$, Q.E.D.

In summary, we have developed a general recipe for constructing a transformation matrix $\mathbf{P}$ for arbitrary symmetry groups. Applying this transformation to the matrix $\mathbf{A}_{\partial\Gamma}^{(g,\varphi_0^{\hat{n}-})}$ according to Eq. (8.117) pre-conditions the matrix by bringing it into block-diagonal form. The number of block-matrices is equal to the number of irreducible representations, thus to the number of classes in the symmetry group. This pre-conditioning greatly alleviates problems in the numerical inversion of $\mathbf{A}_{\partial\Gamma}^{(g,\varphi_0^{\hat{n}-})}$, and it can reduce computation time.

The method for constructing the transformation matrix from the projectors is conceptually rather simple. It is based on identifying a set of linearly independent row vectors for each projector, and collecting those row vectors into the transformation matrix. In practice, this method is easy to implement and numerically expedient. However, it also has its weaknesses. If two row vectors $\mathbf{x}$ and $\mathbf{y}$ are linearly independent, then there exists a constant C such that $x_i - C\, y_i = 0$ for all vector components i. Numerically, one needs to check if this criterion is fulfilled within a pre-defined precision. For inappropriate choices of that precision the algorithm may not identify the correct number of linearly independent row vectors. In practice, such problems are rarely encountered for low-order symmetry groups, but they become more common for high-order symmetry groups. In such cases, a more systematic way to construct the transformation into the irreducible basis is based on performing a singular value decomposition (SVD) of the projectors according to

$$\tilde{\mathbf{P}}^{(\mu)} = \mathbf{U}^{(\mu)} \cdot \Sigma^{(\mu)} \cdot \mathbf{V}^{(\mu)^\dagger}. \qquad (8.159)$$

Here $\Sigma^{(\mu)}$ is a diagonal matrix containing the singular values, while $\mathbf{U}^{(\mu)}$ and $\mathbf{V}^{(\mu)}$ are matrices that contain the left and right singular vectors, respectively. Since the projector $\tilde{\mathbf{P}}^{(\mu)}$ projects into the μth invariant subspace of dimension m_μ, the dimension of the range of $\tilde{\mathbf{P}}^{(\mu)}$ is equal to m_μ. Thus the SVD of $\tilde{\mathbf{P}}^{(\mu)}$ has m_μ non-zero singular values $\sigma_1^{(\mu)}, \sigma_2^{(\mu)}, \ldots, \sigma_{m_\mu}^{(\mu)}$. Let $\mathbf{v}_1^{(\mu)\dagger}, \ldots, \mathbf{v}_{m_\mu}^{(\mu)\dagger}$ denote the right singular row vectors belonging to the non-zero singular values. Then we can collect those singular vectors from each projector into a square matrix

$$\mathbf{P} = \begin{pmatrix} \mathbf{v}_1^{(1)\dagger} \\ \vdots \\ \mathbf{v}_{m_1}^{(1)\dagger} \\ \mathbf{v}_1^{(2)\dagger} \\ \vdots \\ \mathbf{v}_{m_2}^{(2)\dagger} \\ \vdots \\ \mathbf{v}_1^{(r)\dagger} \\ \vdots \\ \mathbf{v}_{m_r}^{(r)\dagger} \end{pmatrix}. \tag{8.160}$$

Alternatively, we can collect from each projector the left singular column vectors $\mathbf{u}_1^{(\mu)}, \ldots, \mathbf{u}_{m_\mu}^{(\mu)}$ belonging to the non-zero singular values into a square matrix

$$\mathbf{P} := \left(\mathbf{u}_1^{(1)}, \ldots, \mathbf{u}_{m_1}^{(1)}, \mathbf{u}_1^{(2)}, \ldots, \mathbf{u}_{m_2}^{(2)}, \ldots, \mathbf{u}_1^{(r)}, \ldots, \mathbf{u}_{m_r}^{(r)} \right). \tag{8.161}$$

Either method yields a transformation matrix into the irreducible basis. Recall that, according to Eq. (8.117), we also need the inverse of $\mathbf{P}$. This is trivial to compute. Since both $\mathbf{U}^{(\mu)}$ and $\mathbf{V}^{(\mu)}$ are unitary matrices, so is $\mathbf{P}$. Thus, $\mathbf{P}^{-1} = \mathbf{P}^\dagger$. In practice, the SVD method is very stable, but it can be more time consuming than the direct method we discussed, depending on the order of the symmetry group.

Note that the dimension m_μ of the invariant subspace T_μ is known a priori. It can be shown that the number of times an irreducible representation occurs in a reducible one, α_μ, is given by

$$\alpha_\mu = M_o^{-1} \sum_{i=1}^{r} M_i \chi^{\text{red}}(g_i) \chi^{(\mu)*}(g_i). \tag{8.162}$$

Here M_i is the number of group elements in the ith class, and g_i denotes a representative of the ith class. The reducible characters χ^{red} can be directly computed by taking the trace of the reducible representations given in Chap. 8.2.1. Then the dimension m_μ of the invariant subspace T_μ is given by

$$m_\mu = \alpha_\mu \chi^{(\mu)}(E), \tag{8.163}$$

where the trace of the irreducible representation of the unit element, $\chi^{(\mu)}(E)$, is simply the dimension of the μth irreducible representation. A priori knowledge of the cardinal numbers m_μ can be used to check the correctness of the computation of $\mathbf{P}$. When constructing $\mathbf{P}$ by collecting row vectors of the projectors, the algorithm has to identify exactly m_μ linearly independent row vectors in the projector $\tilde{\mathbf{P}}^{(\mu)}$. When using SVD, only the first m_μ singular values must be non-zero. Numerically, this means that the ratio of the singular values $\sigma_{m_\mu+1}/\sigma_{m_\mu}$ must be very small.

Let us now look back at our procedure for block-diagonalising the matrix $\mathbf{A}_{\partial\Gamma}^{(g,\varphi_0^{\hat{n}-})}$ prior to inverting it. The attentive reader may object that Eq. (8.117) involves products of large matrices, which may introduce additional computation time requirements. However, the matrix $\mathbf{P}$ turns out to be highly sparse. We saw this in the example given in Eq. (8.118). But we can also understand this, more generally, from Eq. (8.135) by recalling that the matrix $\mathbf{P}$ is constructed from the projectors, and by noting that the projectors are constructed from the reducible representations. Those, in turn, are highly sparse matrices, as we saw in Sect. 8.2.1. Thus, the matrix products in Eq. (8.117) involve very few non-zero matrix elements; therefore these operations require very little computation time. One may also try to exploit the sparsity of the projectors by using SVD algorithms tailored to large, sparse matrices.

As mentioned earlier, the block-diagonalisation can save a lot of computation time in the inversion of $\mathbf{A}_{\partial\Gamma}^{(g,\varphi_0^{\hat{n}-})}$. Without block-diagonalisation, the numerical inversion will require a large number of unnecessary operations involving matrix elements that are zero or dependent on other matrix elements due to symmetry. After block-diagonalisation, the matrix inversion becomes more expedient. Depending on the order of the symmetry group and the numerical method employed for constructing the transformation matrix $\mathbf{P}$, the extra time required for the group theoretical computations may even be less than the computation time one saves in the inversion of $\mathbf{A}_{\partial\Gamma}^{(g,\varphi_0^{\hat{n}-})}$. Thus the use of group theory can increase the numerical stability, while at the same time reducing computation time. By contrast, standard procedures for increasing the stability of matrix inversions, such as an increase of floating point precision, always come at the price of considerably longer computation times.

At the end of this chapter, one final remark is in order. Throughout this chapter we have illustrated symmetries by showing pictures of regular polyhedrons. It is essential to understand that our treatment of symmetries was completely general and by no means limited to polyhedral geometries. Figure 8.16 shows, as an example, four objects with rather different geometries. The upper left object is a regular polyhedral prism with hexagonal cross section. Polyhedra are composed of plane faces. By contrast, the upper right object has a curved convex boundary. The lower left object has a non-convex boundary perturbed by a small-scale surface roughness. The lower right object is an aggregate that is not even singly connected. All four objects will have very different optical properties and T-matrices. However, all objects belong to the same prismatic symmetry group $\mathcal{D}_{6h}$ of order 24. So the T-matrices of all four

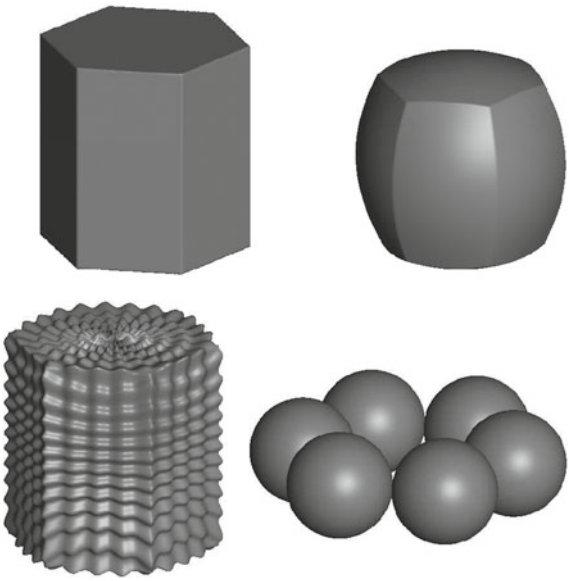

Fig. 8.16 Examples of objects belonging to the $\mathcal{D}_{6h}$ point group

objects will display exactly the same symmetry structure given by the commutation relations. Only one out of 24 T-matrix elements will be a non-zero, independent element. In the irreducible basis, the T-matrix of each of these objects consists of twelve block matrices, since the $\mathcal{D}_{6h}$ has twelve classes. So the discussions and results in this chapter are not limited to specific geometries, but apply to a wide variety of morphologies classified by their geometric symmetries and corresponding point groups.

With the end of this chapter we have reached the end of our methodical considerations. In the next chapter, we will see three special T-matrix approaches in action, i.e, we will present selective numerical examples for electromagnetic plane wave scattering on nonchemical objects. We will become acquainted with the most significant differences in the scattering behaviour of spherical and nonspherical particles which are of importance in several applications as well as with the underlying T-matrix approaches.

Chapter 9
Numerical Simulations of Scattering Experiments

9.1 Introduction

In this chapter we will become acquainted with some scattering properties, which are characteristic for nonspherical particles, in general. A special numerical implementation of a T-matrix method in Cartesian coordinates was already discussed in Chap. 6 in conjunction with Rayleigh's hypothesis. It was applied there, not to calculate the scattering quantities in the far-field but to obtain the scattered near-field generated by a plane wave perpendicularly incident on an ideal metallic and periodic grating. Now, we intend to present the far-field scattering properties of single nonspherical but rotationally symmetric scatterers in spherical coordinates. This will be accomplished again by applying a T-matrix method. The restriction to rotationally symmetric particles results in important numerical simplifications, due to the symmetry relation (4.51) and the independence of the orientation of the Eulerian angle γ. However, to demonstrate the numerical advantages resulting from the considerations of the preceding chapter we abandon the restriction to rotationally symmetric geometries in Sect. 9.3.

Regarding spherical particles (i.e., Mie theory) there exist already a large number of different numerical methods whose correctness, efficiency, and reliability have been proven in many applications. But regarding nonspherical particles, the situation is much more complicate. The numerical effort increases considerably, and deriving the necessary convergence criteria becomes a much more complex task. The latter depends strongly on the chosen method and requires a lot of experience and a detailed knowledge of its methodical background. Applying a certain method to a new nonspherical scatterer geometry is therefore always a new adventure. Most experience have been gained over the last decades with rotationally symmetric particles like spheroids, Chebyshev particles, and finite but circular cylinders. This is the reason for restricting the following simulations essentially to these geometries. The program *mieschka* we will present in this chapter, can be applied to other rotationally symmetric geometries, as well. But then, there are possibly only a few or even no results from other methods to compare to. In this situation, one has to throw a critical

T. Rother and M. Kahnert, *Electromagnetic Wave Scattering on Nonspherical Particles*, Springer Series in Optical Sciences 145, DOI: 10.1007/978-3-642-36745-8_9,

look upon the outcome of *mieschka*, and more reasonable tests from a physical point of view may have to be taken into consideration. Program *Tsym* allows the user to overcome the restriction to rotationally symmetric particles. Its usage is described at the end of this chapter.

The following section is concerned with selective numerical simulations. To demonstrate essential differences in the scattering behaviour of spherical and non-spherical particles as well as to show the capabilities of the program *mieschka* are the essential goals of this section.

9.2 Numerical Simulations with *mieschka*

In the introduction of Chap. 1, in Fig. 1.1, we have shown the scattering efficiency of a nonabsorbing sphere for an increasing size parameter. Now we are more interested in the scattering behaviour at a fixed size parameter but for rotationally symmetric particles in fixed and random orientations.

All the following results are generated with the program *mieschka*. The necessary numerical operations like the calculation of the boundary integrals, the calculation of the expansion and weighting functions, the matrix inversion, etc. are all performed within double precision accuracy. The Eulerian angles (α, β, γ) are denoted in *mieschka* with $(\phi_p, \theta_p, \psi_p)$. Due to the mentioned restriction to rotationally symmetric geometries, we have fixed the Eulerian angle ψ_p to $\psi_p = 180°$. This value was chosen for intercomparison with the program of Barber and Hill (see the cited literature in Sect. 10.4). The orientation of the scatterer in the laboratory frame is therefore completely described by the two Eulerian angles θ_p and ϕ_p. The convergence parameters n_{cut} and l_{cut} mentioned in the captions are described in detail in Sect. 9.4.1. It must also be emphasized that all the differential polarimetric scattering cross-sections presented in the next subsection are calculated at a fixed frequency of $f = 47.71\,\text{GHz}$, and that they are multiplied with k_0^2 to become dimensionless.

9.2.1 Single Particles in Fixed Orientations

Let us start with rotationally symmetric particles in fixed orientations. The most simple particle which is moreover independent of the orientation is the spherical particle with its centre at the origin of the laboratory system. Therefore, we will first present the differential polarimetric scattering cross-sections of an absorbing and nonabsorbing sphere for size parameters in the Rayleigh and resonance region. On account of the propagation of the primary incident plane wave along the z-axis of the laboratory system, only the two azimuthal modes $l = \pm 1$ are of relevance for the calculation of the T-matrix elements. Thus, there is no need to consider the convergence parameter l_{cut} for spherical particles.

These results of the centred spheres are used afterwards to discuss the importance of the sphere which is off-centre shifted along the z-axis to validate the T-matrix methods. Next, we look at the differential polarimetric scattering cross-sections of selected spheroids.

The reciprocity property of a prolate spheroid as a consequence of the symmetry property of the matrix elements of the interaction operator discussed in Sect. 4.4.1 is of our interest in the last subsection.

Differential Polarimetric Scattering Cross-Sections of Spheres

The differential polarimetric scattering cross-sections of a nonabsorbing sphere with radius $r = 0.1\,\text{mm}$ (at the frequency of 47.71 GHz of the primary incident plane wave this corresponds to a size parameter of $k_0 r = 0.1$!) are shown in Fig. 9.1. This size parameter belongs to the Rayleigh region as one can see from the typical dipole scattering behaviour. The vanishing of the contribution of the hh-polarisation at a scattering angle of 90° is typical of this region and responsible for the blue sky polarization of the primarily unpolarized sun light at the same angle (counted from the sun). This effect can be observed in nature with a simple polariser if there are clear sky conditions. Since the sphere was assumed to be nonabsorbing, the scattering and extinction cross-sections are identical.

In Fig. 9.2 the corresponding differential scattering cross-sections of an absorbing sphere with the same real part of the refractive index and at the same size parameter are

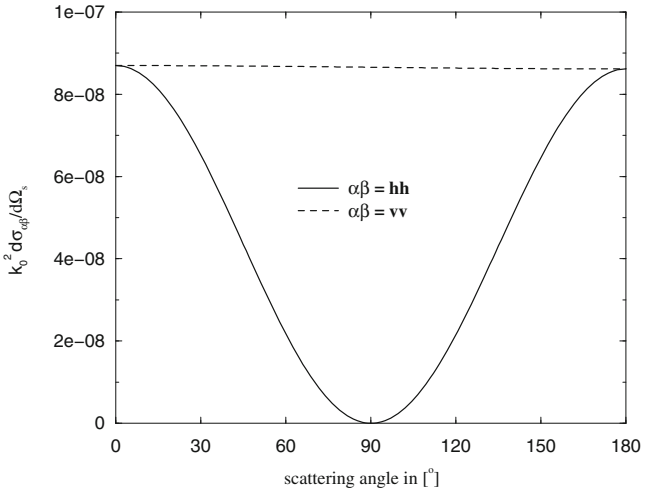

Fig. 9.1 Differential polarimetric scattering cross-sections of a nonabsorbing sphere with a refractive index of $n = 1.5$. Other parameters are: size parameter $k_0 r = 0.1$. Scattering and extinction cross-sections: $\sigma_h^{ext} = \sigma_v^{ext} = \sigma_h^s = \sigma_v^s = 7.25E-07\,\text{mm}^2$. Convergence parameters: $n_{cut} = 3$, $l = \pm 1$

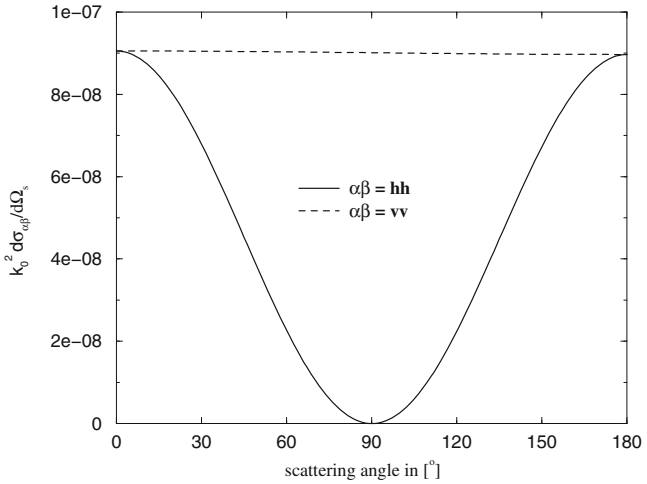

Fig. 9.2 Differential polarimetric scattering cross-sections of an absorbing sphere with a refractive index of $n = 1.5 + 0.1i$. Other parameters as in Fig. 9.1. Scattering and extinction cross-sections: $\sigma_h^s = \sigma_v^s = 7.55E-07\,\mathrm{mm}^2$, $\sigma_h^{ext} = \sigma_v^{ext} = 6.302E-04\,\mathrm{mm}^2$. Convergence parameters: $n_{cut} = 3$, $l = \pm 1$

depicted. There are nearly no differences in the differential scattering cross-sections between the nonabsorbing and absorbing sphere. But the (integral) extinction and absorption cross-sections are, of course, different since energy conservation does not apply to the absorbing sphere.

The differences in the differential scattering cross-sections between nonabsorbing and absorbing spheres become more obvious at higher size parameters as can be seen from Figs. 9.3 and 9.4. In these two figures a size parameter of $k_0 r = 10$ was chosen (this corresponds to a sphere radius of $r = 10$ mm at the frequency of 47.71 GHz). The resonances of the absorbing sphere are less pronounced, and the differential scattering-cross-sections at scattering angles of $\theta_s \in [30°, 180°]$ are clearly below the corresponding values of the nonabsorbing sphere. Moreover, to achieve the same accuracy the absorbing sphere requires a higher value of the convergence parameter n_{cut} than the nonabsorbing sphere.

There is one essential difference between the scattering behaviour of spheres and nonspherical particles. The off-diagonal elements of the scattering amplitude matrix (7.176) of spherical particles are zero, in general (i.e., $F_{hv} = F_{vh} \equiv 0$!). Therefore, the corresponding differential polarimetric scattering cross-sections are also zero. Regarding nonspherical particles this behaviour can be observed only for special geometries and in specific orientations. This happens, for example, if we consider rotationally symmetric particles with their symmetry axis located in the scattering plane. In this case we have mirror symmetry with respect to the scattering plane.

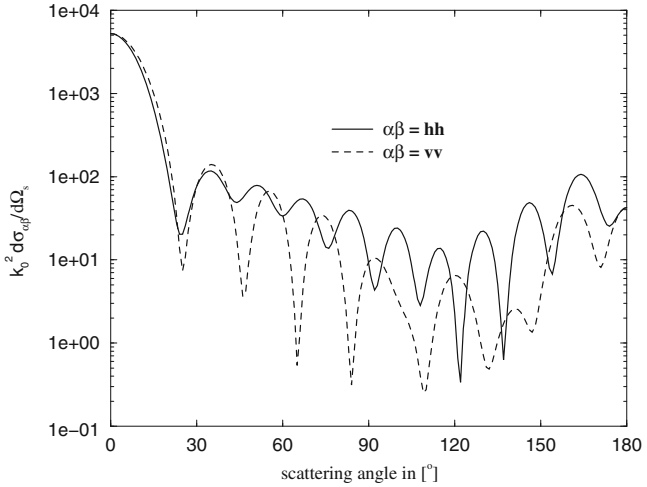

Fig. 9.3 Differential polarimetric scattering cross-sections of a nonabsorbing sphere with a refractive index of $n = 1.5$. Other parameters are: size parameter $k_0 r = 10$. Scattering and extinction cross-sections: $\sigma_h^{ext} = \sigma_v^{ext} = \sigma_h^s = \sigma_v^s = 9.056E+02\,\mathrm{mm}^2$. Convergence parameters: $n_{cut} = 15$, $l = \pm 1$

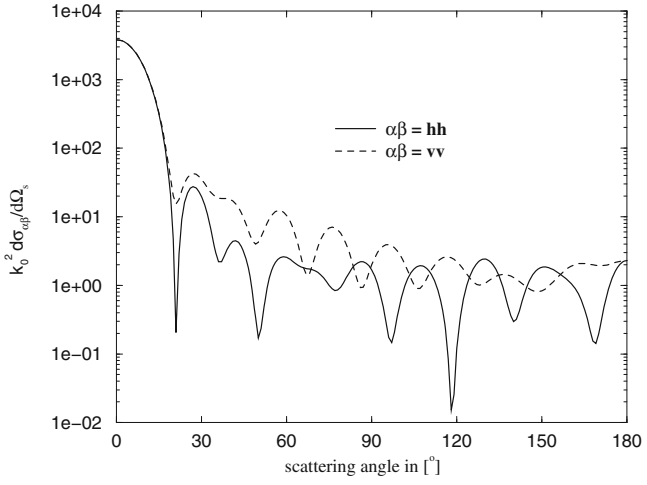

Fig. 9.4 Differential polarimetric scattering cross-sections of an absorbing sphere with a refractive index of $n = 1.5 + 0.1i$. Other parameters as in Fig. 9.3. Scattering and extinction cross-sections: $\sigma_h^s = \sigma_v^s = 3.88E+02\,\mathrm{mm}^2$, $\sigma_h^{ext} = \sigma_v^{ext} = 7.73E+02\,\mathrm{mm}^2$. Convergence parameters: $n_{cut} = 18$, $l = \pm 1$

Differential Polarimetric Scattering Cross-Sections of Shifted Spheres

How can we use the presented results of spherical particles with their centre located in the origin of the laboratory system, to validate the T-matrix approach underlying our *mieschka* program? Simply by shifting these spheres off-centre along the z-axis of the laboratory system. The corresponding parameter representation of the surface in the laboratory system is then given by (7.195). The interesting aspect of this shift is the following: Mathematically seen, it transforms the simple spherical boundary surface into a nonspherical surface with all the resulting implications for the calculation of the T-matrix elements. But from a physical point of view, the far-field scattering quantities are still these one of the centred spheres. That's due to the fact that this shift appears only as a phase term in the far-field and is washed out when calculating intensities. An intercomparison of the results presented in Figs. 9.3 and 9.5 as well as in Figs. 9.4 and 9.6 reveals at least the numerical correctness of this expected behaviour (its mathematical proof is a little bit more tedious). However, the results for the shifted spheres are obtained with higher values of n_{cut}. To calculate the differential polarimetric scattering cross-sections depicted in Figs. 9.5 and 9.6 the Eulerian angles $\theta_p = 0°$ and $\phi_p = 0°$ have been chosen. That is, the symmetry axis of the shifted sphere and the z-axis of the laboratory system are identical. For this orientation of the shifted spheres, we have to consider again only the azimuthal modes $l = \pm 1$. This restriction does not apply if we choose an orientation of the shifted sphere given by the Eulerian angles $\theta_p = \phi_p = 45°$. In this case we need values of $n_{cut} = 22$ and $l_{cut} = 10$ to achieve convergence and agreement with the results of the centred spheres.

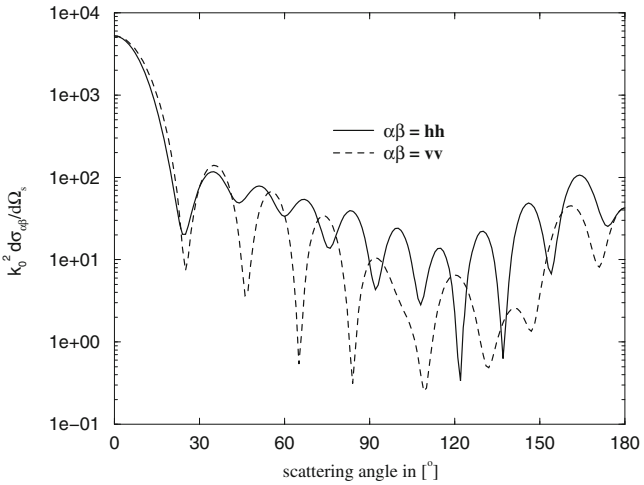

Fig. 9.5 Differential polarimetric scattering cross-sections of a shifted nonabsorbing sphere with a refractive index of $n = 1.5$. Other parameters are: size parameter $k_0 r_K = 10$, $\epsilon = 3\,\text{mm}$. Scattering and extinction cross-sections: $\sigma_h^{ext} = \sigma_v^{ext} = \sigma_h^s = \sigma_v^s = 9.056E + 02\,\text{mm}^2$. Convergence parameters: $n_{cut} = 22$, $l = \pm 1$

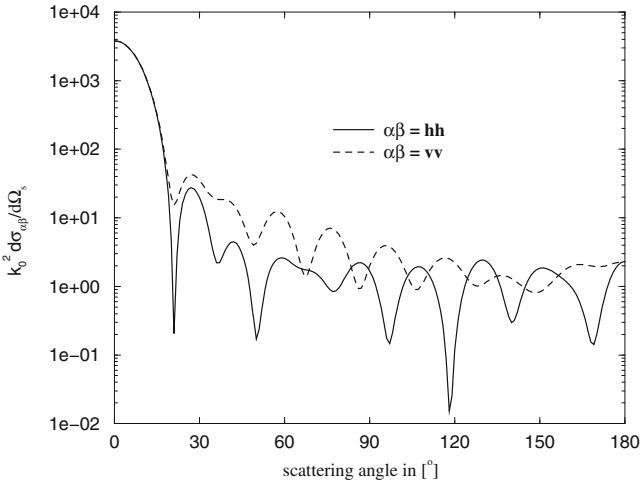

Fig. 9.6 Differential polarimetric scattering cross-sections of a shifted absorbing sphere with a refractive index of $n = 1.5 + 0.1i$. Other parameters are: size parameter $k_0 r_K = 10$, $\epsilon = 3\,\text{mm}$. Scattering and extinction cross-sections: $\sigma_h^s = \sigma_v^s = 3.88E + 02\,\text{mm}^2$, $\sigma_h^{ext} = \sigma_v^{ext} = 7.73E + 02\,\text{mm}^2$. Convergence parameters: $n_{cut} = 25$, $l = \pm 1$

Differential Polarimetric Scattering Cross-Sections of Spheroids

Let us now consider the spheroidal particle as an actual nonspherical geometry. Figures 9.7 and 9.8 reveal again the typical scattering behaviour of the Rayleigh region. It is moreover nearly independent of whether the nonabsorbing or absorbing spheroid is analysed. The size parameter of the volume equivalent sphere was chosen to agree with that of the spherical particle considered in Figs. 9.1 and 9.2. Increasing the size parameter of the volume equivalent sphere up to $k_0 \cdot r_{eqv} = 10$ (this corresponds to the size parameter used in Figs. 9.3 and 9.4 for spherical particles) results in the typical resonance structures. But, even if the size parameter is comparable we need a higher value of n_{cut} for the spheroidal particles to achieve convergence.

In Figs. 9.7, 9.8, 9.9, and 9.10 the orientation of the spheroid was chosen such that the incident plane wave propagates along the axis of revolution. Only the azimuthal modes $l = \pm 1$ are needed in this case, as already mentioned. Another consequence of this orientation is the mirror symmetry of the differential polarimetric scattering cross-sections with respect to the z-axis. The next example is therefore concerned with a spheroid tilted about 45° in the scattering plane, i.e., with Eulerian angles given by $(\theta_p, \phi_p) = (45°, 0°)$. In this case, the above mentioned mirror symmetry gets lost, as can be seen from Fig. 9.11. The integral scattering and extinction cross-sections also become dependent on the polarization of the primary incident plane wave. Moreover, beside the parameter n_{cut}, we have additionally to check convergence with respect to the number l_{cut} of azimuthal modes. But the off-diagonal elements F_{hv} and F_{vh} of the scattering amplitude matrix are still zero in this orientation. These

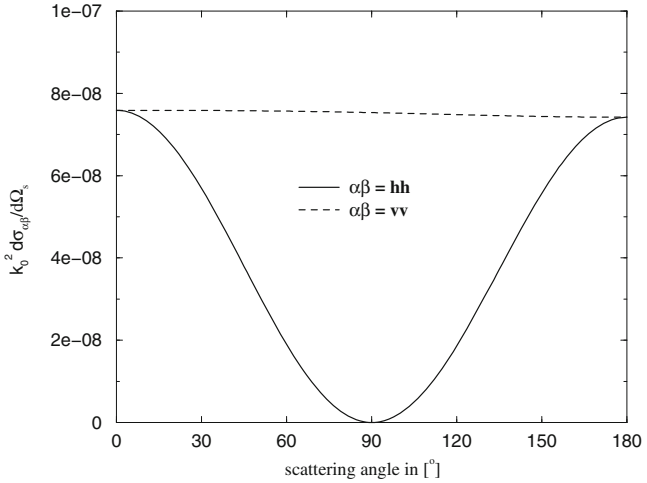

Fig. 9.7 Differential polarimetric scattering cross-sections of a nonabsorbing spheroid with a refractive index of $n = 1.5$. Other parameters are: size parameter $k_0 \cdot r_{eqv} = 0.1$, aspect ratio $av = 2$, orientation $(\theta_p, \phi_p) = (0°, 0°)$. Scattering and extinction cross-sections: $\sigma_h^{ext} = \sigma_v^{ext} = \sigma_h^s = \sigma_v^s = 6.301E - 07\,\mathrm{mm}^2$. Convergence parameters: $n_{cut} = 3$, $l = \pm 1$

elements become nonzero if we choose the Eulerian angles $(\theta_p, \phi_p) = (45°, 45°)$. Figures 9.12 and 9.13 show the resulting differential cross-sections $k_0^2 \cdot d\sigma_{hh}/d\Omega_s$, $k_0^2 \cdot d\sigma_{vh}/d\Omega_s$, $k_0^2 \cdot d\sigma_{vv}/d\Omega_s$, and $k_0^2 \cdot d\sigma_{hv}/d\Omega_s$.

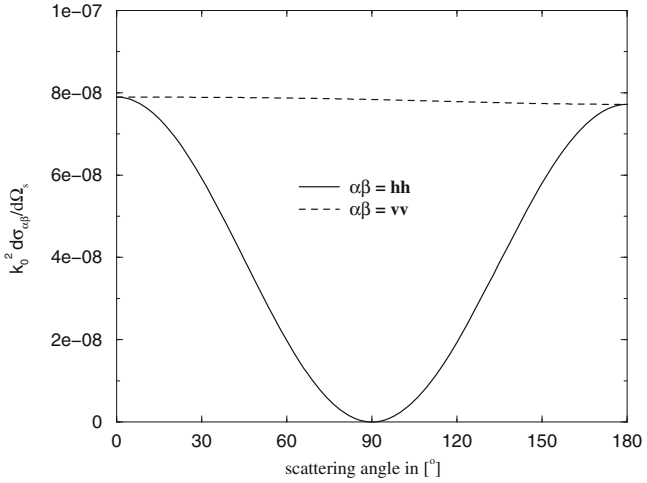

Fig. 9.8 Differential polarimetric scattering cross-sections of an absorbing spheroid with a refractive index of $n = 1.5 + 0.1i$. Other parameters as in Fig. 9.7. Scattering and extinction cross-sections: $\sigma_h^s = \sigma_v^s = 6.555E - 07\,\mathrm{mm}^2$, $\sigma_h^{ext} = \sigma_v^{ext} = 5.494E - 04\,\mathrm{mm}^2$. Convergence parameters: $n_{cut} = 3$, $l = \pm 1$

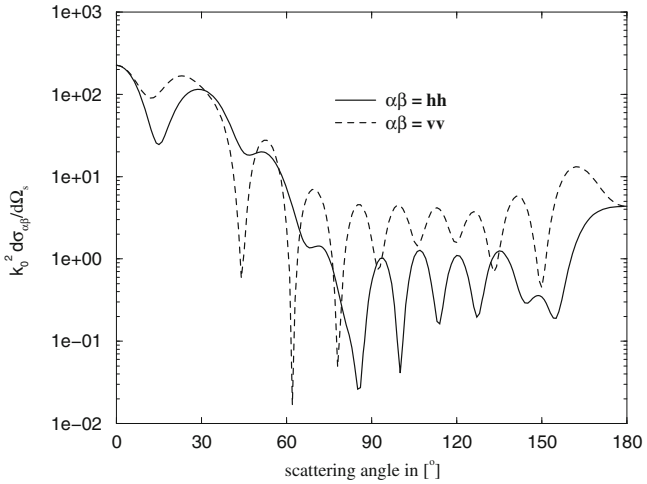

Fig. 9.9 Differential polarimetric scattering cross-sections of a nonabsorbing spheroid with a refractive index of $n = 1.5$. Other parameters are: size parameter $k_0 \cdot r_{eqv} = 10$, aspect ratio $av = 2$, orientation $(\theta_p, \phi_p) = (0°, 0°)$. Scattering and extinction cross-sections: $\sigma_h^{ext} = \sigma_v^{ext} = \sigma_h^s = \sigma_v^s = 1.88E + 02\,\mathrm{mm}^2$. Convergence parameters: $n_{cut} = 28$, $l = \pm 1$

Reciprocity

The symmetry relations of the Green functions when interchanging their arguments, and the resulting symmetry relations of the matrix elements of the related

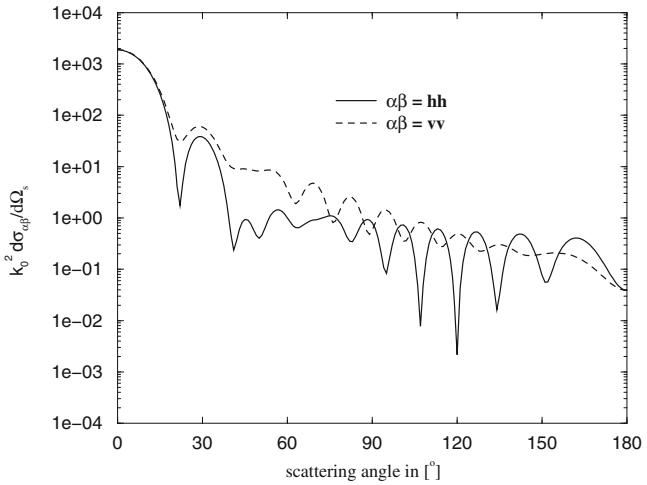

Fig. 9.10 Differential polarimetric scattering cross-sections of an absorbing spheroid with a refractive index of $n = 1.5+0.1i$. Other parameters as in Fig. 9.9. Scattering and extinction cross-sections: $\sigma_h^s = \sigma_v^s = 2.5468E + 02\,\mathrm{mm}^2$, $\sigma_h^{ext} = \sigma_v^{ext} = 5.346E + 02\,\mathrm{mm}^2$. Convergence parameters: $n_{cut} = 28$, $l = \pm 1$

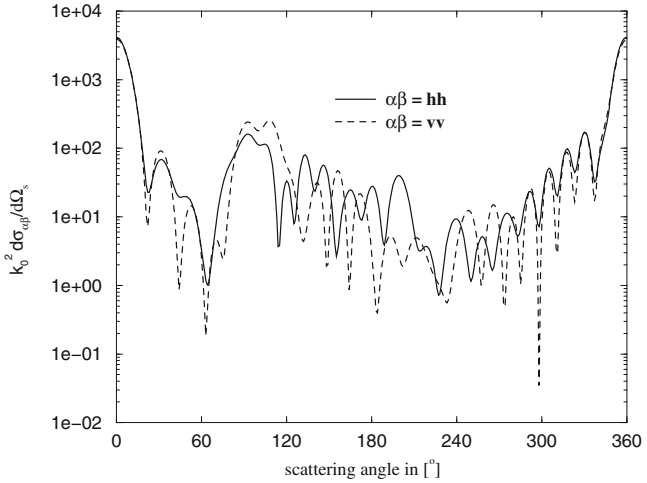

Fig. 9.11 Differential polarimetric scattering cross-sections of a nonabsorbing spheroid with a refractive index of $n = 1.5$. Orientation: $(\theta_p, \phi_p) = (45°, 0°)$. Other parameters as in Fig. 9.9. Scattering and extinction cross-sections: $\sigma_v^{ext} = \sigma_v^s = 7.704E + 02\,\text{mm}^2$, $\sigma_h^{ext} = \sigma_h^s = 8.018E + 02\,\text{mm}^2$. Convergence parameters: $n_{cut} = 28$, $l_{cut} = 18$

interaction operators have been studied in detail in Chap. 4. There, we mentioned already, that these symmetry relations result in an observable physical property called "reciprocity". Reciprocity states that we can interchange in a certain scattering

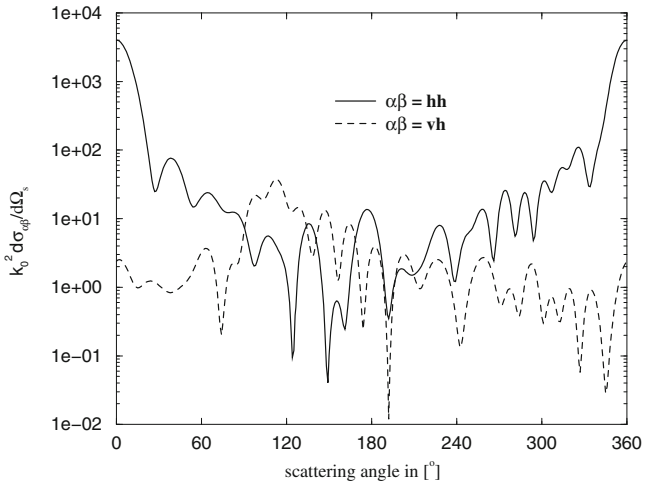

Fig. 9.12 Differential polarimetric scattering cross-sections of a nonabsorbing spheroid with a refractive index of $n = 1.5$. Orientation: $(\theta_p, \phi_p) = (45°, 45°)$. Other parameters as in Fig. 9.9. Scattering and extinction cross-sections: $\sigma_v^{ext} = \sigma_v^s = \sigma_h^{ext} = \sigma_h^s = 7.861E + 02\,\text{mm}^2$. Convergence parameters: $n_{cut} = 31$, $l_{cut} = 18$

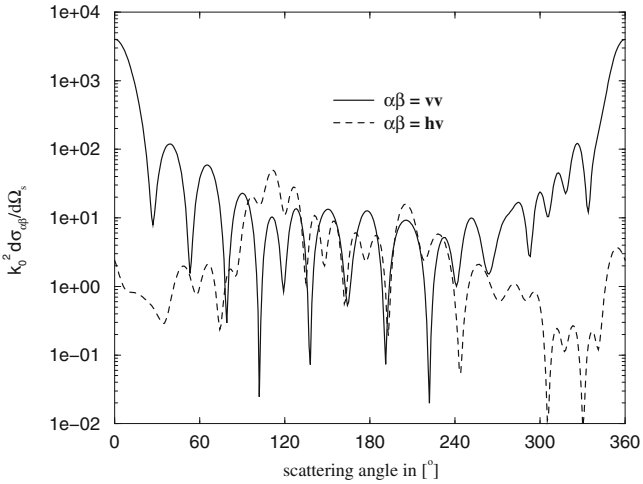

Fig. 9.13 Differential polarimetric scattering cross-sections of a nonabsorbing spheroid. All parameters and integral cross-sections as in Fig. 9.12

experiment the source location of the primary incident field (i.e., the direction of its incidence) and the observation point without changing the final result. What does this mean for our simulations? This can be explained most simply by looking at the backscattering results at $\theta_s = 180°$. If reciprocity is fulfilled, then we may expect that for any scatterer (not necessarily a rotationally symmetric ones) the vertically polarized differential scattering cross-section at $\theta_s = 180°$ produced by a horizontally polarized incident plane wave becomes identical with the horizontally polarized differential scattering cross-section at the same scattering angle produced by a vertically polarized incident plane wave, i.e., relation

$$\frac{d\sigma_{hv}(\theta_s = 180°)}{d\Omega_s} = \frac{d\sigma_{vh}(\theta_s = 180°)}{d\Omega_s} \tag{9.1}$$

should hold independent of the orientation.

To prove this reciprocity behaviour numerically, let us consider again the differential scattering cross-section of the spheroid, which was already analysed in Fig. 9.9. We choose two different orientations given by the two sets $(\theta_p, \phi_p) = (45°, 45°)$ and $(\theta_p, \phi_p) = (60°, 30°)$ of Eulerian angles. Figures 9.14 and 9.15 show a zoom into the backscattering region of interest. The numbers above the boxes are the numerical values of the corresponding differential cross-sections at $\theta_s = 180°$. They agree very well as one can see from the figures and also from the data generated by *mieschka* (a detailed description of the output data can be found in Sect. 8.3.2). The interested reader may prove by himself that the same holds for other orientations. In this way, he can become acquainted with program *mieschka*.

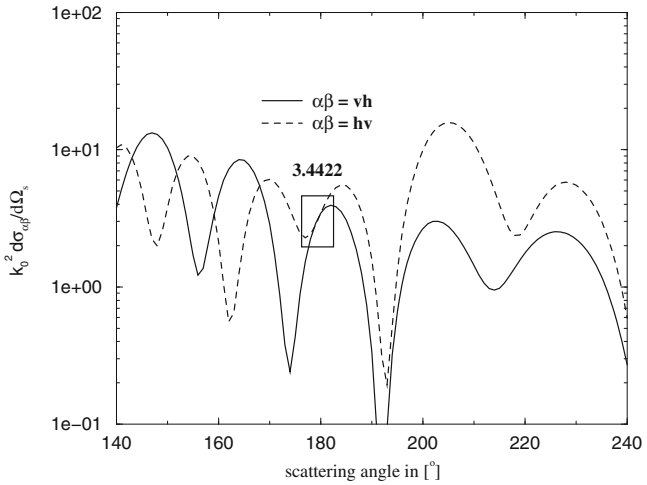

Fig. 9.14 Differential polarimetric scattering cross-sections of a nonabsorbing spheroid. Refractive index and orientation as in Fig. 9.12. Convergence parameters: $n_{cut} = 31$, $l_{cut} = 18$

Moreover in Chap. 4, we mentioned that the symmetry relations of the matrix elements of the interaction operators hold only for infinitely large matrices, in general. Since reciprocity is a consequence of these symmetry relations, one may expect the same behaviour for this property. But it does not apply to the reciprocity in the backscattering direction. In this special situation, reciprocity is already fulfilled at

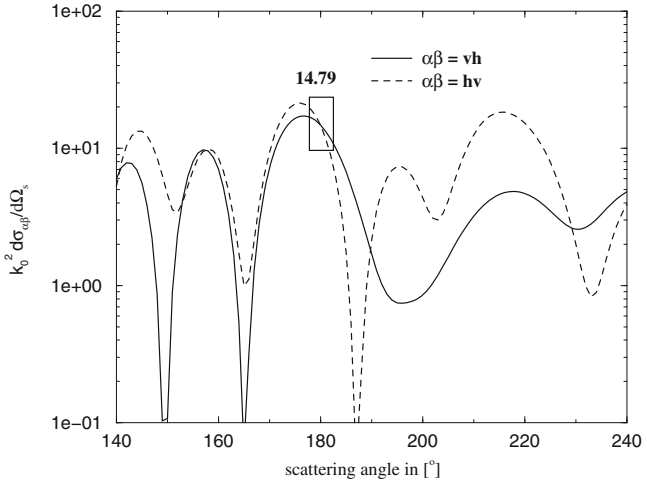

Fig. 9.15 Differential polarimetric scattering cross-sections of a nonabsorbing spheroid. Refractive index as in Fig. 9.12. Orientation $(\theta_p, \phi_p) = (60°, 30°)$. Convergence parameters: $n_{cut} = 31$, $l_{cut} = 18$

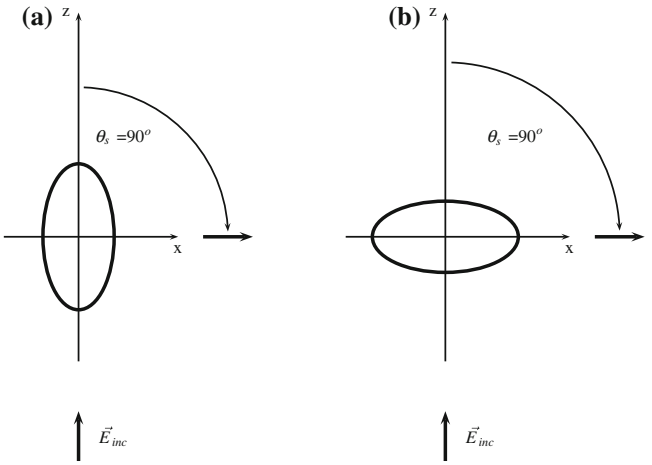

Fig. 9.16 Two measurement configurations to prove the dependence of the reciprocity on the convergence. At a scattering angle of $\theta_s = 90°$ reciprocity should result into the same results for the hh- and vv-polarized differential scattering cross-sections. **a** ($\theta_p = 0°, \phi_p = 0°$); **b** ($\theta_p = 90°, \phi_p = 0°$)

any approximation and independent of whether convergence has been achieved or not. But if we look at the two experimental configurations shown in Fig. 9.16 we can clearly observe this dependence on the size of the T-matrix or, better, on the convergence behaviour of the approximate solution. Therefore, these two configurations provide us with one possibility to estimate the accuracy of a certain scattering approximation, according to our pragmatic position concerning the convergence behaviour we have formulated in Sect. 2.2.1. The relevant differential scattering cross-sections are represented in Figs. 9.17 and 9.18 for a size parameter of $k_0 \cdot r_{eqv} = 5$, and in Figs. 9.19 and 9.20 for a size parameter of $k_0 \cdot r_{eqv} = 20$. The numerical values at the scattering angle of $\theta_s = 90°$ are given in the captions. In both cases we have analysed a prolate spheroid with an aspect ratio of $av = 1.5$. From the obtained results we can also see that reciprocity holds for nonabsorbing as well as absorbing particles. On the other hand, if we lower the convergence parameter to $n_{cut} = 38$ and $l_{cut} = 15$ instead of $n_{cut} = 41$ and $l_{cut} = 21$ for measurement configuration (b) and for the spheroid analysed in Figs. 9.19 and 9.20 we get the values $d\sigma_{hh}(\theta_s = 90°)/d\Omega_s = 0.475$ and $d\sigma_{vv}(\theta_s = 90°)/d\Omega_s = 6.53$, i.e., we get a stronger deviation from the results of measurement configuration (a). This confirms the expected dependence of reciprocity from the convergence behaviour.

The spheroidal particle of Fig. 9.16 exhibits a mirror symmetry with respect to the x-axis. If this particle is replaced by a particle with no such symmetry (by the Chebyshev particle of Fig. 9.28, for example), then we have to compare $d\sigma_{hh}(\theta_s = 90°)/d\Omega_s$ and $d\sigma_{vv}(\theta_s = 90°)/d\Omega_s$ of the orientation used in configuration (a) with $d\sigma_{hh}(\theta_s = 270°)/d\Omega_s$ and $d\sigma_{vv}(\theta_s = 270°)/d\Omega_s$ of the orientation used in configuration (b), of course.

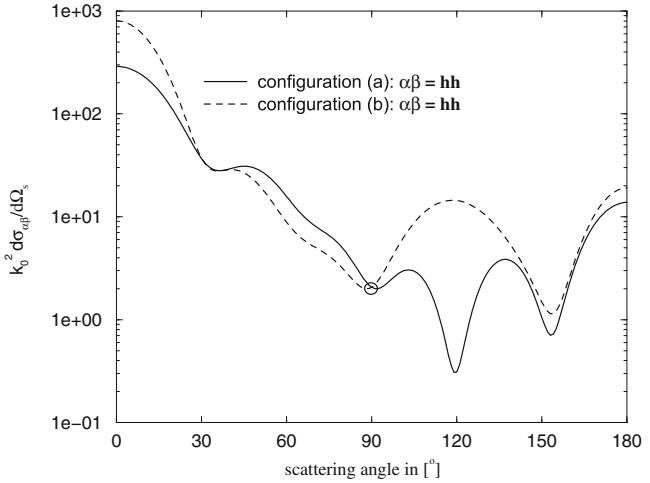

Fig. 9.17 Differential polarimetric scattering cross-sections (hh-polarization) of a nonabsorbing spheroid with a refractive index of $n = 1.5$. Other parameters are: size parameter $k_0 \cdot r_{eqv} = 5$, aspect ratio $av = 1.5$. Numerical values of the scattering cross-sections at $\theta_s = 90°$ (values in the *circle*), and convergence parameters: **a** $d\sigma_{hh}/d\Omega_s = 2.063$, $n_{cut} = 14$, $l = \pm 1$; **b** $d\sigma_{hh}/d\Omega_s = 2.068$, $n_{cut} = 14$, $l_{cut} = 7$

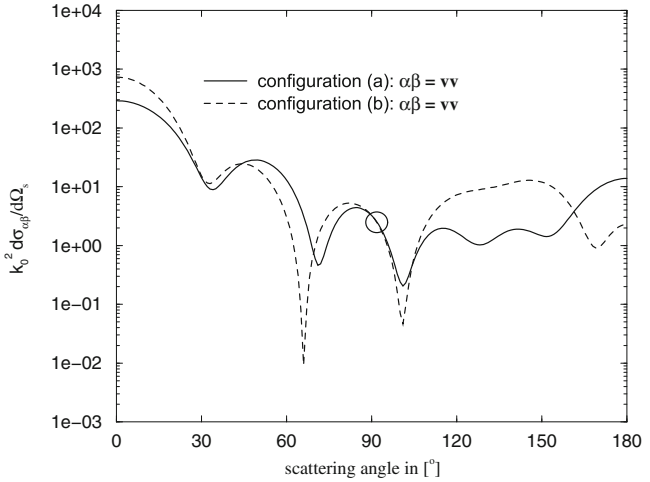

Fig. 9.18 Differential polarimetric scattering cross-sections (vv-polarization) of a nonabsorbing spheroid with a refractive index of $n = 1.5$. Other parameters are: size parameter $k_0 \cdot r_{eqv} = 5$, aspect ratio $av = 1.5$. Numerical values of the scattering cross-sections at $\theta_s = 90°$ (values in the *circle*), and convergence parameters: **a** $d\sigma_{vv}/d\Omega_s = 3.226$, $n_{cut} = 14$, $l = \pm 1$; **b** $d\sigma_{vv}/d\Omega_s = 3.228$, $n_{cut} = 14$, $l_{cut} = 7$

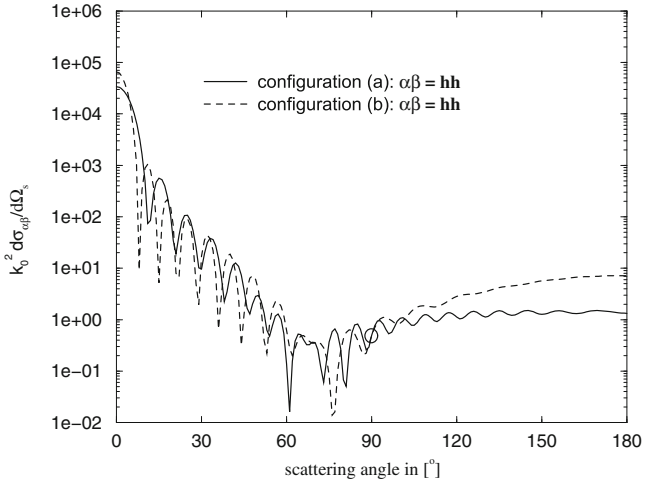

Fig. 9.19 Differential polarimetric scattering cross-sections (hh-polarization) of an absorbing spheroid with a refractive index of $n = 1.5 + 0.1i$. Other parameters are: size parameter $k_0 \cdot r_{eqv} = 20$, aspect ratio $av = 1.5$. Numerical values of the scattering cross-sections at $\theta_s = 90°$ (values in the *circle*), and convergence parameters: **a** $d\sigma_{hh}/d\Omega_s = 0.497$, $n_{cut} = 38$, $l = \pm 1$; **b** $d\sigma_{hh}/d\Omega_s = 0.497$, $n_{cut} = 41$, $l_{cut} = 21$

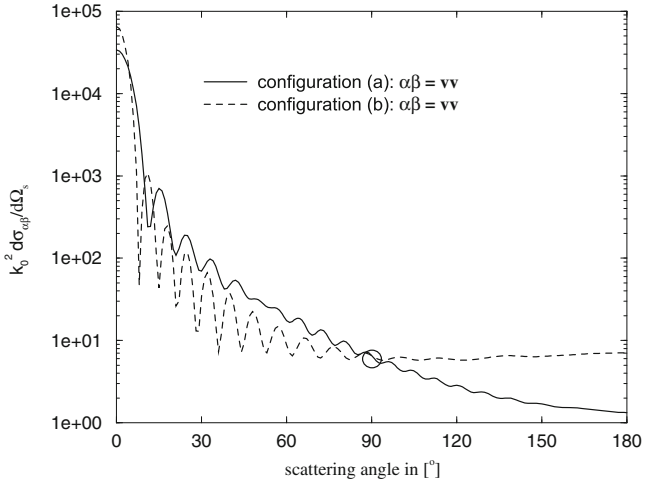

Fig. 9.20 Differential polarimetric scattering cross-sections (vv-polarization) of an absorbing spheroid with a refractive index of $n = 1.5 + 0.1i$. Other parameters are: size parameter $k_0 \cdot r_{eqv} = 20$, aspect ratio $av = 1.5$. Numerical values of the scattering cross-sections at $\theta_s = 90°$ (values in the *circle*), and convergence parameters: **a** $d\sigma_{vv}/d\Omega_s = 6.583$, $n_{cut} = 38$, $l = \pm 1$; **b** $d\sigma_{vv}/d\Omega_s = 6.583$, $n_{cut} = 41$, $l_{cut} = 21$

9.2.2 Single Particles in Random Orientation

In some situations we know the geometry, dielectric property, and orientation of the scatterer with respect to the primary incident plane wave very well in advance. This happens, for example, in specific microwave analogue to light scattering measurements. The appearance of the cross-polarization contributions (hv- and vh-polarization) in the differential scattering cross-sections in certain fixed orientations can be considered to be the most important difference in the scattering behaviour of spherical and nonspherical particles. One example of employing this difference with benefit is the detection of the backscattering depolarization with modern LIDAR measurements to discriminate between spherical and nonspherical particles in clouds. But more often we are faced with the situation that geometry, material properties, and orientation are not known. On the contrary, even scattering experiments are often designed to determine these unknown quantities. In this section we will therefore study the influence of orientation averaging on the scattering behaviour of different rotationally symmetric particles. The geometry and dielectric properties of the scatterer are again assumed to be known. The following simulations are moreover restricted to randomly oriented particles. The phase function $< Z_{11} >$ (i.e., the Z_{11} element of the Stokes matrix if orientation averaged according to (7.189)!) of selected spherical and nonspherical particles will be discussed first. Afterwards, we will present all elements of the phase matrix. These elements are particularly sensitive to the scatterer geometry.

Comparison of the Phase Functions of Spheres and Spheroids

In the Rayleigh region at lower size parameters, we get a "quite boring phase function" (QBPF), i.e., there are hardly any pronounced structures or differences in the phase functions to see between the spherical and spheroidal scatterer as well as between absorbing and nonabsorbing dielectric properties. This can be confirmed by looking upon the Figs. 9.21 and 9.22. The Rayleigh phase function is, therefore, not of particular interest if we try to determine geometry and/or permittivity of unknown objects from scattering measurements.

A totally different result is obtained if one compares phase functions belonging to size parameters in the resonance region. The normalized phase functions of the nonabsorbing sphere and the spheroid we have already considered in Figs. 9.3 and 9.9 are depicted in Fig. 9.23. A remarkable difference is the less pronounced ripple structure of the spheroid's phase function. This can be simply explained by the fact that, regarding the spherical geometry, the position and strength of the resonances remain unchanged for different orientations. This does not apply to the spheroid. Each new orientation of the spheroid provides a phase function with resonances differing in strength and location. Performing orientation averaging results therefore in a remarkably smoother phase function. On the other hand, increasing the absorptivity of the scatterer results in less differences in the phase functions and in a much

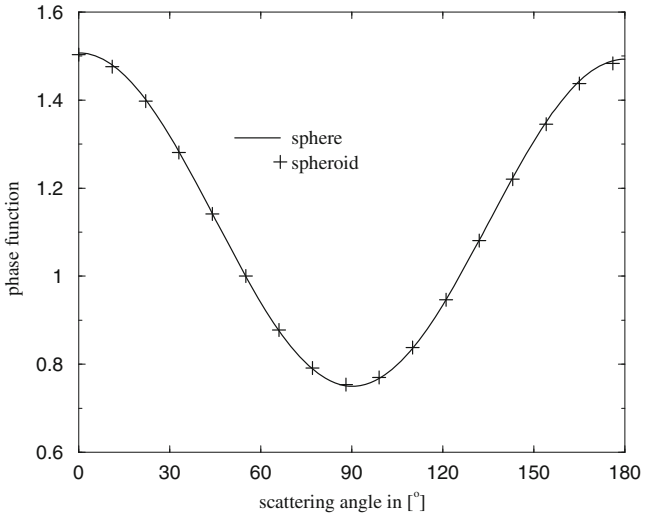

Fig. 9.21 Normalized phase function of the nonabsorbing sphere of Fig. 9.1, and of the nonabsorbing spheroid of Fig. 9.7. Convergence parameters related to the spheroid: $n_{cut} = 6$, $l_{cut} = 2$

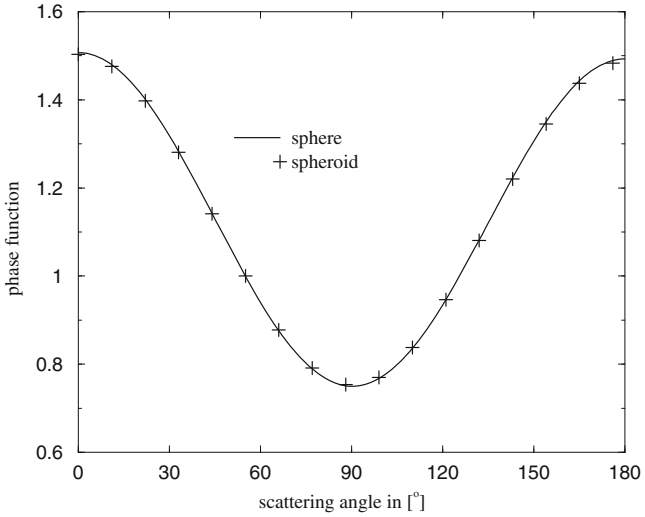

Fig. 9.22 Normalized phase function of the absorbing sphere of Fig. 9.2, and of the absorbing spheroid of Fig. 9.8. Convergence parameters related to the spheroid: $n_{cut} = 6$, $l_{cut} = 2$

smoother behaviour in the backscattering region $\theta_s > 90°$, as one can see from the Figs. 9.24 and 9.25. Only in the forward scattering region we can still observe more or less pronounced resonances.

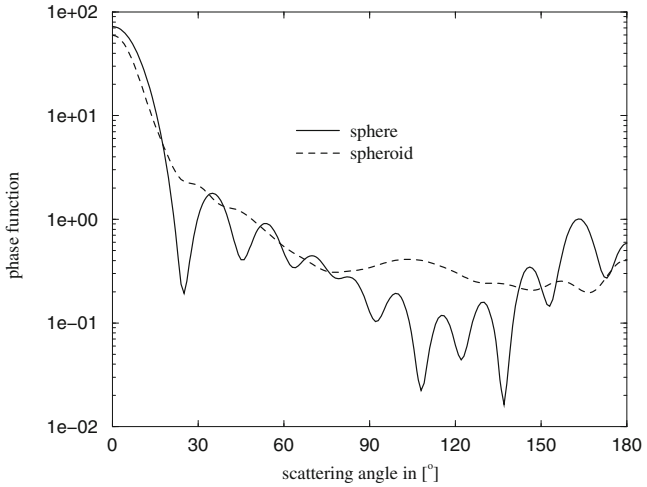

Fig. 9.23 Normalized phase function of the nonabsorbing sphere of Fig. 9.3, and of the nonabsorbing spheroid of Fig. 9.9. Convergence parameters of the spheroid: $n_{cut} = 28$, $l_{cut} = 12$

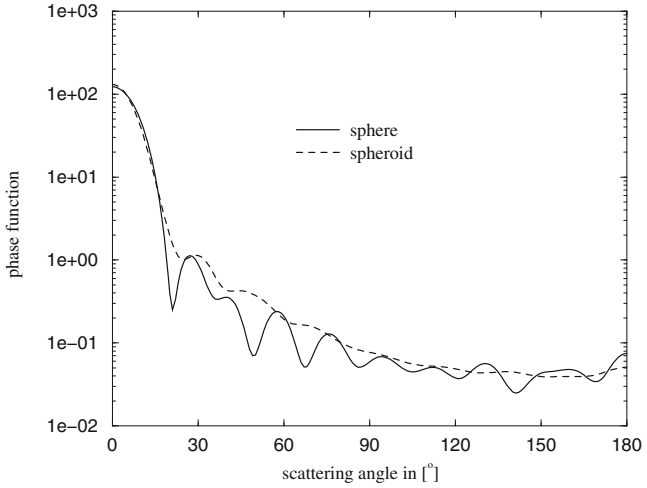

Fig. 9.24 Normalized phase function of the absorbing sphere of Fig. 9.4, and of the absorbing spheroid of Fig. 9.10. Convergence parameters related to the spheroid: $n_{cut} = 28$, $l_{cut} = 11$

Comparison of the Phase Functions of Spheres and Finitely Extended Circular Cylinders

Next, let us compare the scattering behaviour of a sphere and a finitely extended circular cylinder. Figures 9.26 and 9.27 show again the normalized phase functions of both geometries for nonabsorbing as well as absorbing dielectric properties. The

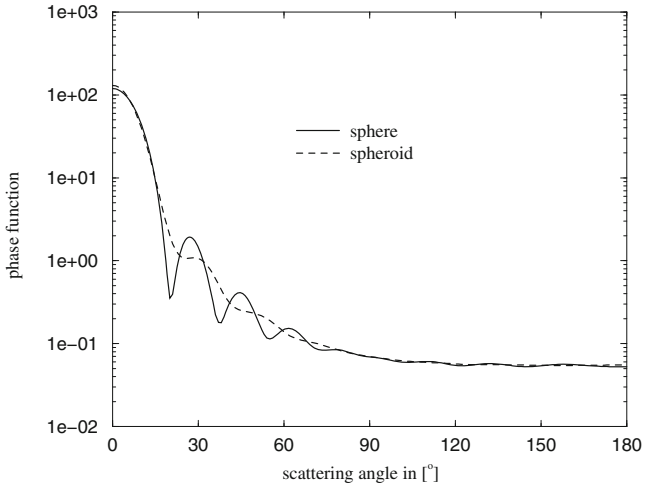

Fig. 9.25 Normalized phase function of the same particles as in Fig. 9.24 but with a refractive index of $n = 1.5 + 0.4i$. Convergence parameters related to the spheroid: $n_{cut} = 28$, $l_{cut} = 11$

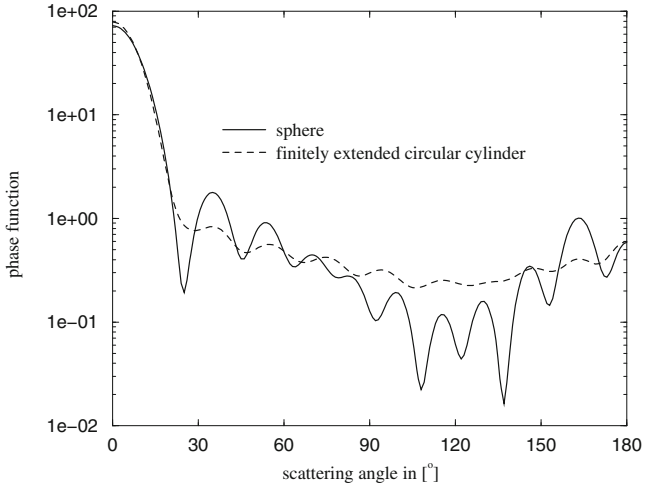

Fig. 9.26 Normalized phase function of the nonabsorbing sphere of Fig. 9.3, and of a nonabsorbing, finitely extended circular cylinder with the same refractive index as the sphere. Parameters of the cylinder: radius of its circular cross-section $r = 8.737\,\text{mm}$, cylinder height $H = 17.474\,\text{mm}$. Convergence parameters related to the cylinder: $n_{cut} = 25$, $l_{cut} = 11$

radius of the circular cross-section of the finitely extended cylinder was chosen to fit into the size parameter of the sphere, i.e., the radius of $r = 8.737\,\text{mm}$ just provides $k_0 \cdot r_{eqv} = 10$. The differences are again most obvious in the nonabsorbing case.

Now, let us take a closer look on Figs. 9.23 and 9.26. Besides the differently pronounced resonance structure we may observe another remarkable difference between

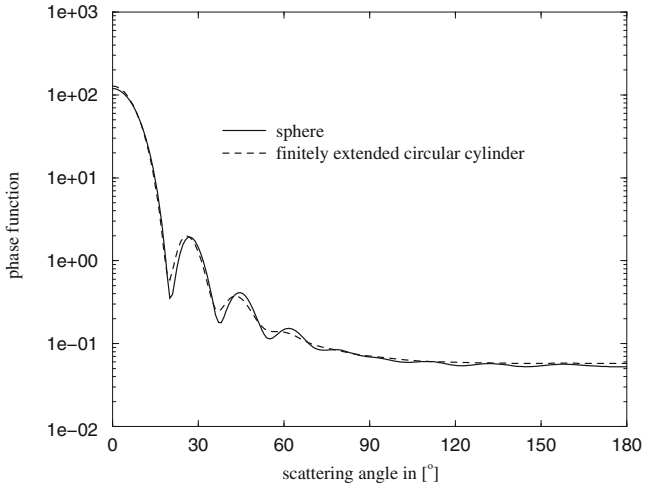

Fig. 9.27 Normalized phase function of an absorbing sphere and an absorbing, finitely extended circular cylinder both with a refractive index of $n = 1.5 + 0.4i$. Other parameters as in Fig. 9.26. Convergence parameters related to the cylinder: $n_{cut} = 28$, $l_{cut} = 12$

the phase functions of a spherical and a nonspherical particle. For nonspherical particles (at least for the spheroid and the finitely extended circular cylinder) we may state an enhancement of the phase function in the backscattering region around $\theta_s \in [80°, 140°]$. However, this holds only for nonabsorbing or weakly absorbing particles. The enhanced side scattering effect disappears with increasing absorptivity.

Comparison of the Phase Functions of a Sphere and a Chebyshev Particle

These basic differences in the phase functions of a spherical and a nonspherical particle can be again confirmed by comparing a sphere with a Chebyshev particle. The geometry of the Chebyshev particle used in our simulations is shown in Fig. 9.28. The order $n = 3$ was chosen to abandon the mirror symmetry with respect to the x-y-plane in the particle frame of the nonspherical particles considered so far. In Fig. 9.29 we can observe once more the typical side scattering enhancement for the

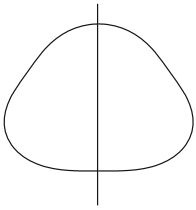

Fig. 9.28 Geometry of a Chebyshev particle. Parameters: order of the Chebyshev polynomial $n = 3$, radius of the underlying sphere $r_k = 10\,\text{mm}$, deformation parameter $\epsilon = 0.1$

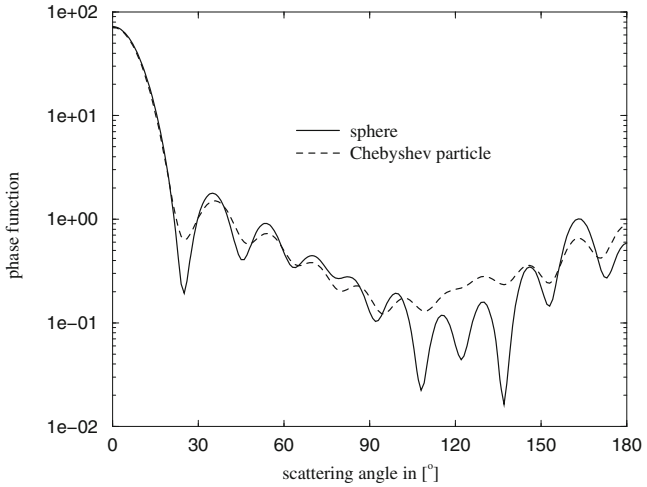

Fig. 9.29 Normalized phase function of the nonabsorbing sphere of Fig. 9.3, and of the nonabsorbing Chebyshev particle of Fig. 9.28 with the same refractive index as the sphere. Convergence parameters related to the Chebyshev particle: $n_{cut} = 19$, $l_{cut} = 13$

nonabsorbing Chebyshev particle. But increasing the absorptivity again results in less pronounced differences (see Fig. 9.30).

Chebyshev particles play an important role in remote sensing of water clouds to model the geometry of raindrops. They have been intensively studied by Wiscombe

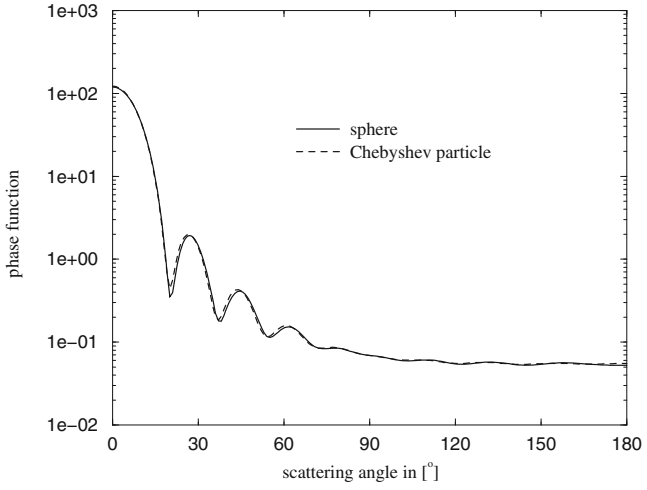

Fig. 9.30 Normalized phase function of the absorbing sphere of Fig. 9.4, and of the absorbing Chebyshev particle of Fig. 9.28 both with a refractive index of $n = 1.5 + 0.4i$. Convergence parameters related to the Chebyshev particle: $n_{cut} = 19$, $l_{cut} = 13$

and Mugnai by employing a T-matrix approach (see the corresponding citation in the reference chapter). Moreover, Chebyshev particles especially of higher order can be used to estimate the influence of a small-scale surface roughness on electromagnetic wave scattering as will be demonstrated in Sect. 9.3.

Phase Matrices

We will now present all phase matrix elements of the geometries analysed above. But these simulations are restricted to nonabsorbing scatterers, and to the size parameter of $k_0 \cdot r_{eqv} = 10$. All the simulated phase matrices exhibit the block structure

$$< \mathbf{Z} > = \begin{pmatrix} < Z_{11} > & < Z_{12} > & 0 & 0 \\ < Z_{12} > & < Z_{22} > & 0 & 0 \\ 0 & 0 & < Z_{33} > & < Z_{34} > \\ 0 & 0 & - < Z_{34} > & < Z_{44} > \end{pmatrix}. \tag{9.2}$$

But due to the additional symmetry relations

$$\begin{aligned} < Z_{21} > &= < Z_{12} > \\ < Z_{43} > &= - < Z_{34} > \end{aligned} \tag{9.3}$$

we have only six independent elements. The accuracy of the fulfilment of these symmetry relations provide another possibility to estimate the accuracy of the approximate solution. It should also be noted that the matrix elements of the phase matrix are usually normalized to the Element $< Z_{11} >$, i.e., $< Z_{\alpha\beta} > / < Z_{11} >$ instead of $< Z_{\alpha\beta} >$ are presented in the figures. The only exception is the element $< Z_{11} >$ itself.

Comparing Figs. 9.33, 9.34, 9.35, 9.36, 9.37, and 9.38 with Figs. 9.31 and 9.32 reveals another basic difference in the scattering behaviour between spherical and nonspherical particles. For spherical particles, beside the symmetry relations (9.3), we have the additional equality of the elements

$$\begin{aligned} < Z_{11} > &= < Z_{22} > \\ < Z_{33} > &= < Z_{44} > . \end{aligned} \tag{9.4}$$

This equality does not apply to nonspherical scatterers. That (9.4) holds for spherical particles can indeed be generally proven (see the book of Mishchenko and Hovenier cited in Sect. 10.9). Furthermore, we may observe again the less pronounced resonance structure in all phase matrix elements of nonspherical particles. This can, of course, be explained in the same way as discussed already in conjunction with the phase function.

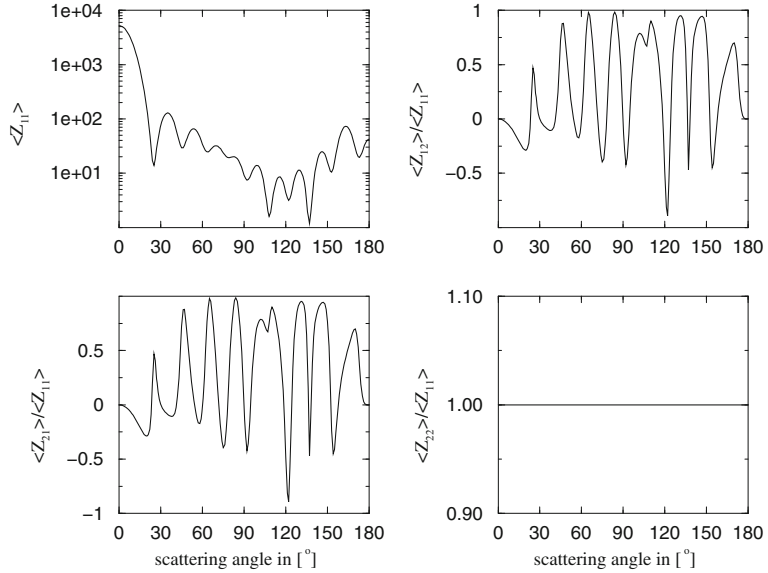

Fig. 9.31 Upper block of the phase matrix of the nonabsorbing sphere analysed in Fig. 9.3

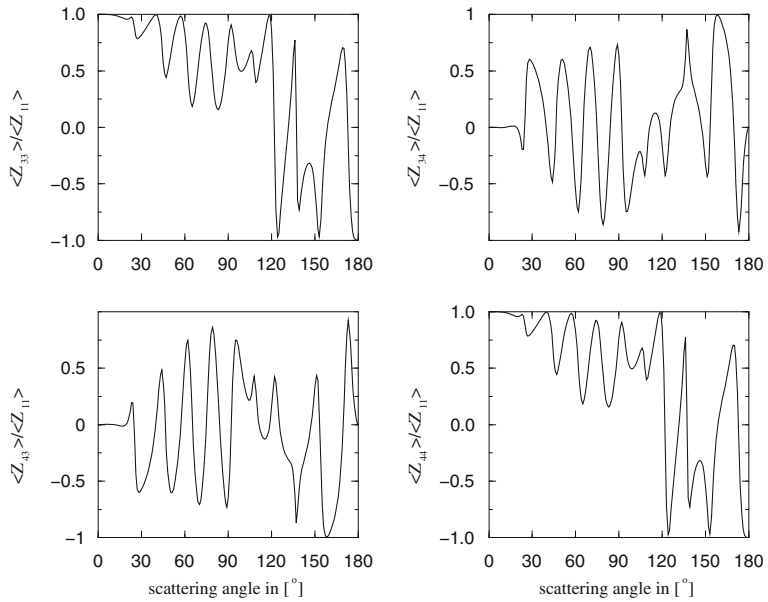

Fig. 9.32 Lower block of the phase matrix of the nonabsorbing sphere analysed in Fig. 9.3

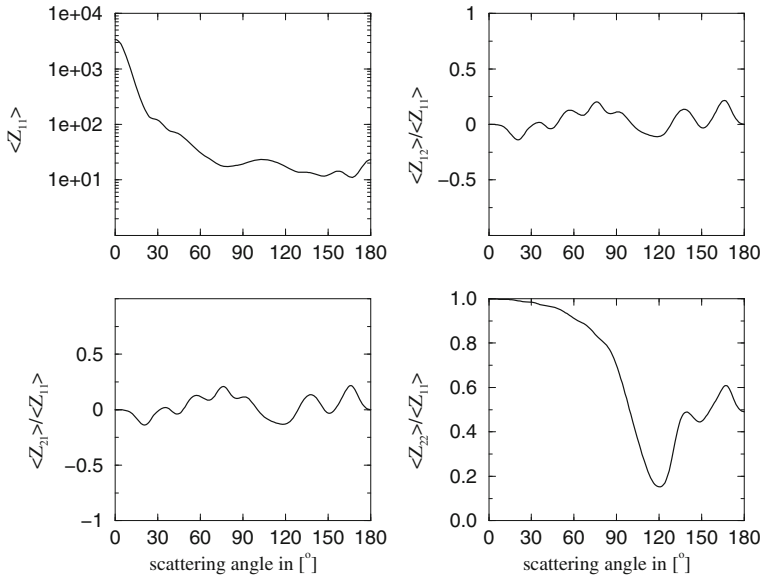

Fig. 9.33 Upper block of the phase matrix of the nonabsorbing spheroid analysed in Fig. 9.9

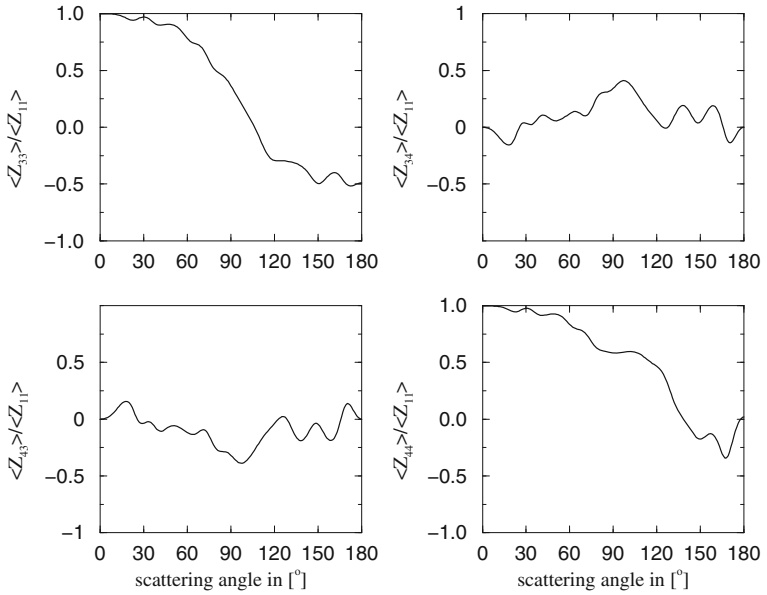

Fig. 9.34 Lower block of the phase matrix of the nonabsorbing spheroid analysed in Fig. 9.9

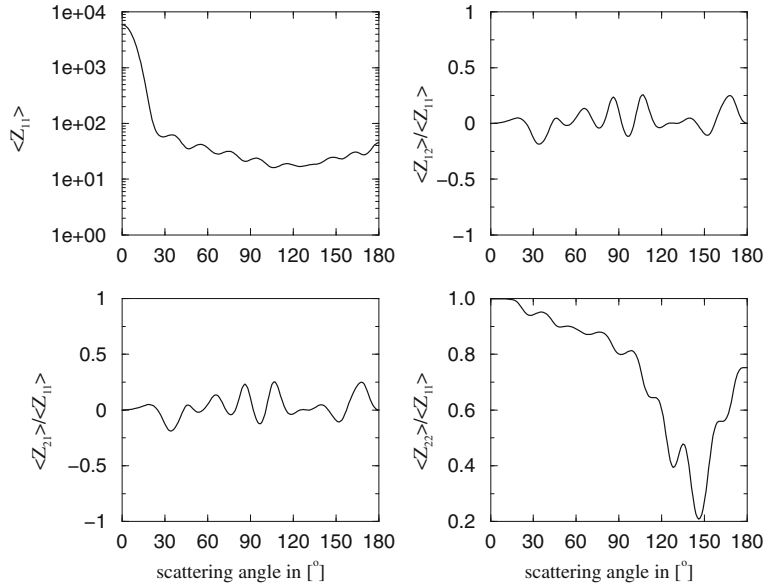

Fig. 9.35 Upper block of the phase matrix of the nonabsorbing, finitely extended circular cylinder analysed in Fig. 9.26

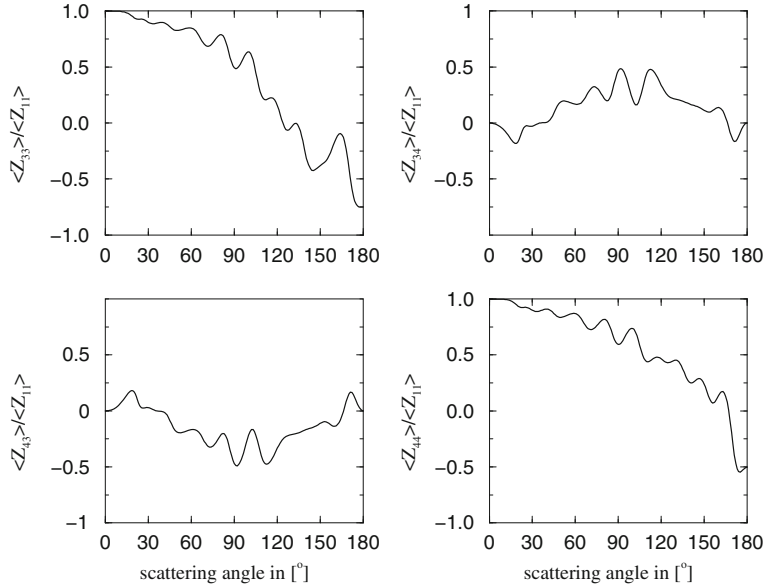

Fig. 9.36 Lower block of the phase matrix of the nonabsorbing, finitely extended circular cylinder analysed in Fig. 9.26

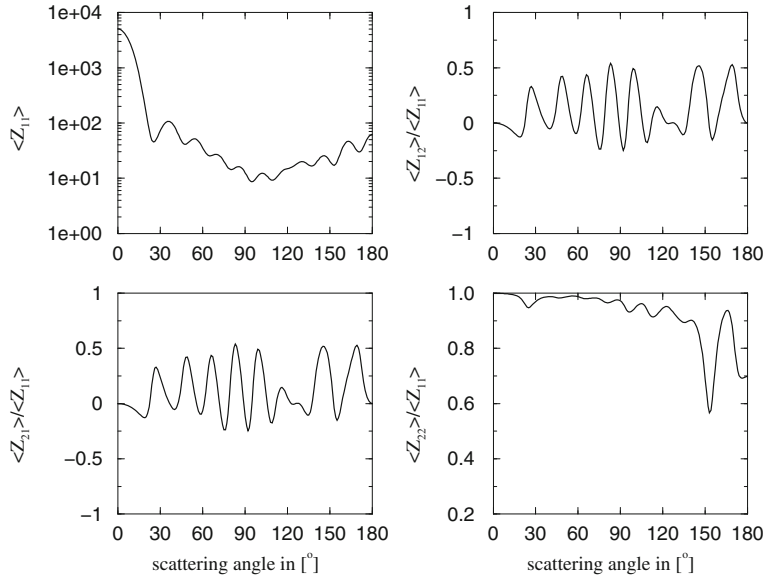

Fig. 9.37 Upper block of the phase matrix of the nonabsorbing Chebyshev particle of Fig. 9.28

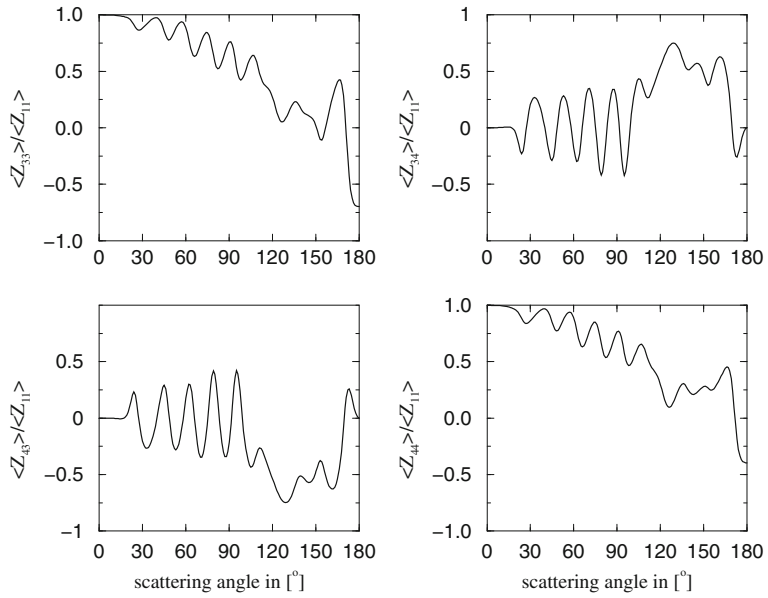

Fig. 9.38 Lower block of the phase matrix of the nonabsorbing Chebyshev particle of Fig. 9.28

9.2.3 Database for Spheroidal Particles and Size Averaging

In remote sensing we are usually faced with the situation that the scattering signal from a certain volume element of our interest (which comes from a certain height of the atmosphere, for example) are caused by an ensemble of particles rather than a single particle. Such ensembles of particles are characterized by different geometries, sizes, and dielectric properties, in general. If these particles are sufficiently far from each other we may speak of independent scattering within the considered volume element. This condition can be met in many remote sensing applications. Let us moreover assume that the particles are randomly oriented in the considered measurement volume. Fixing their dielectric properties and the geometry then requires only size averaging over randomly oriented particles to analyse the measured scattering signal. This subsection is concerned with this aspect. However, particles of different sizes like spheres with different radii cover a certain size parameter region even if their scattering behaviour is considered at a fixed measurement wavelength. Size averaging then requires the calculation of the scattering behaviour at several size parameters. Regarding nonspherical particles this can become a very time-consuming task. Having a database with pre-calculated scattering data would therefore be of some benefit to perform corresponding simulations. Such a database for spheroidal particles is included in our software package. Before presenting an example of size averaged phase functions of spheres and spheroids, let us first take a quick look on the database itself. More detailed information about the parameter ranges, the chosen accuracy, and the resolution with respect to size parameter and scattering angle can be found in the document "scatdb.pdf" which is part of the software package.

Database for Spheroidal Particles

All the necessary calculations have been performed with the program *mieschka*, too. The parameters which are required to fix the relative errors in the convergence strategy used in *mieschka* (for details see Sect. 9.4) are shown in Table 9.1. These parameters ensure a high accuracy of all scattering quantities in the size parameter region covered by the database.

Regarding aspect ratio and complex refractive index the grid presented in Table 9.2 was used. The upper limit of the considered size parameter region is given by $kr_{eqv(v)} = 40$. The chosen resolution of $\Delta kr_{eqv(v)} = 0.2$ with respect to the size parameter allows for an interpolation between two adjacent data sets within a sufficient accuracy for most applications (for details see the document "scatdb.pdf" of the software package).

The two different resolutions with respect to the scattering angle can be taken from Table 9.3. Due to the more pronounced resonance structure of the phase function at higher size parameters, it became necessary to introduce two different size parameter regions each with its own angular resolution.

Table 9.1 Parameters used to fix the relative errors required for the convergence strategy of *mieschka*

Parameter	Value
`rel_err`	0.05/0.02 respectively
`rel_err_int`	0.001
`rel_err_pm`	0.05

Table 9.2 Aspect ratios and refractive indices for which the scattering data have been precalculated

$\Re(n)$	1.33	1.4	1.5	1.6	1.7	1.8	
$\Im(n)$	0	0.001	0.005	0.01	0.03	0.05	0.1
av	0.67	0.77	0.87	1.0	1.15	1.3	1.5

Table 9.3 Resolution with respect to the scattering angle in dependence on the considered size parameter interval

Size parameter	0°–10°	10°–173°	173°–180°
0–20	0.75°	2.5°	0.75°
20–40	0.5°	1.5°	0.5°

The following scattering quantities have been calculated within these parameter regions:

- Normalized phase function in the angular region [0°, 180°]
- Extinction efficiency (orientation averaged)
- Scattering efficiency (orientation averaged)
- Absorption efficiency (orientation averaged)
- Single scattering albedo (orientation averaged)
- Back scattering efficiency (orientation averaged)
- Asymmetry parameter.

The total amount of pre-calculated scattering data sets is therefore 58.800! This will allow precise simulations in the covered size parameter region.

Size Averaged Phase Functions

Due to the above mentioned amount of data sets, it would be very desirable to have an interface between this database and the users needs. For this purpose, we have developed the interface db_surf which is also included in the software package. It is described in detail in the document "usermanual.pdf". Among others, this interface contains a log-normal size distribution of the radius (the radius of the volume

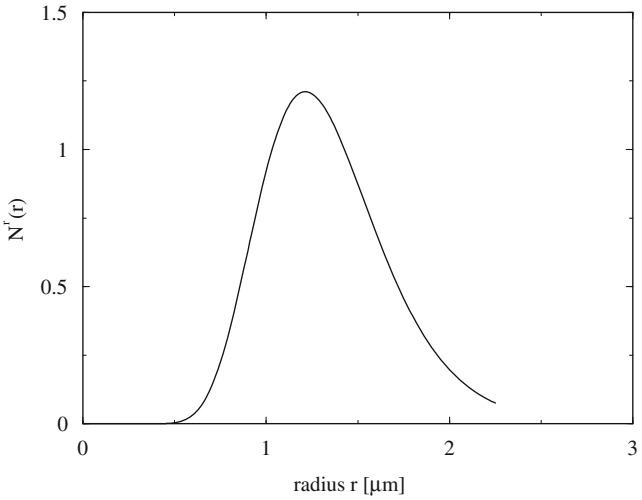

Fig. 9.39 Log-normal size distribution with parameters $r_1 = 1.3\,\mu\text{m}$ and $\sigma_1 = 1.3\,\mu\text{m}$

equivalent sphere, for example) given by

$$N^r(r) = r^{-1} \exp\left[-\frac{(\ln r - \ln r_1)^2}{2\ln^2 \sigma_1}\right] \tag{9.5}$$

as one of three pre-defined size distributions to perform size averaging. r_1 and σ_1 are the two parameters which can be specified in an interactive way by the user.

Now, with this interface, it becomes a comparatively simple task to answer the question whether there are differences in the phase functions for spherical and spheroidal particles if both types of particles are averaged independently with respect to size using the log-normal distribution depicted in Fig. 9.39. The result can be seen from Fig. 9.40. Regarding the distribution with respect to the aspect ratio (which is interactively requested by the user interface) the same number of particles were used for all aspect ratios available in the database. Due to the normalization, this number can be set to 1. The remarkable difference of an increased side scattering around $\theta_s = 135°$ of the spheroidal particles compared to spherical ones (see also the foregoing phase function simulations!) still remains in the size averaged phase functions.

9.2.4 Morphology Dependent Resonances

Another interesting effect which is highly sensitive to the morphology of the considered particle (and which provides therefore a good touchstone for the accuracy of the achieved results) is the existence of so-called "morphology dependent resonances"

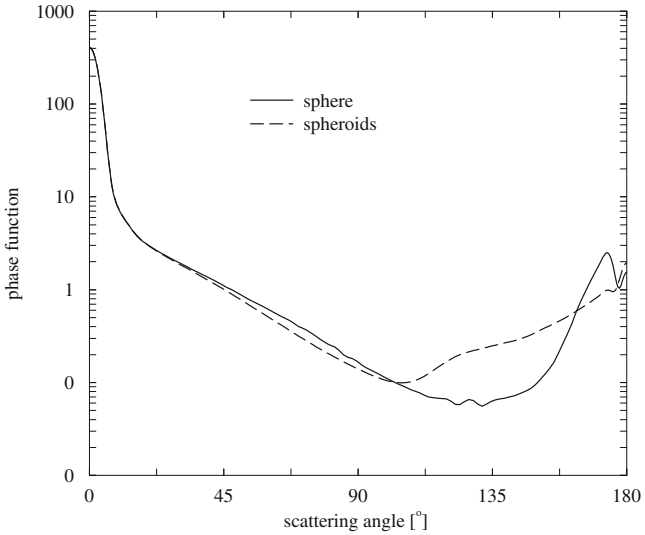

Fig. 9.40 Size averaged phase function for spheres and spheroids at a wavelength of $\lambda = 0.355\,\mu\text{m}$, a refractive index of $n = 1.6$, and an integration step size of 0.01 with respect to the size distribution. Please, note that the phase function for spheroids contains no spheres!

(MDR's). This effect can not only be observed in several scattering quantities if scanning the size parameter with an appropriate resolution but also in fluorescence and Raman spectra, for example. Here, we will only use the extinction efficiency to demonstrate this effect. MDR's become important for size parameters in the resonance region, and if the refractive index of the particle exceeds that of its environment. The book of Barber and Chang (see the reference chapter in Sect. 10.9) provides a detailed overview of the theoretical background as well as a detailed discussion of several applications of this effect. In this subsection, we intend to demonstrate only the capability of *mieschka* to reveal this effect adequately not only for spheres but also for nonspherical particles. A Chebyshev particle of order 45 with two different deformation parameters and a spheroidal particle with two different aspect ratios are used as nonspherical particles. It should be emphasized that we have to choose a much higher resolution with respect to the size parameter than that provided with the data base for spheroidal particles ($\Delta kr_{eqv(v)} = 0.2$, as explained in the foregoing subsection) as well as the resolution used to generate Fig. 1.1.

First, let's have a look at the MDR's of a spherical particle with three different refractive indices, and for size parameters in the region $kr \in [17, 18]$. A resolution of $\Delta kr = 0.01$ was used for the calculations. The results are depicted in Fig. 9.41. The Lorentzian line shapes of the three pronounced resonances in the considered size parameter region can be clearly observed. The solid line, that belongs to the sphere with a nonabsorbing refractive index of $n = 1.4$, is in excellent agreement with the result presented in Fig. 3 in the book of Barber and Chang (see Chap. 3.3 therein). Increasing the absorptivity results in a lowering and broadening of the line shape,

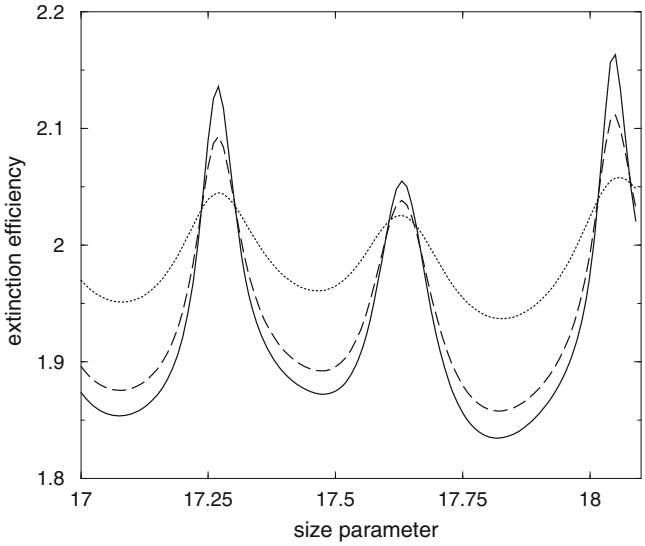

Fig. 9.41 Morphology dependent resonances of a sphere with three different refractive indices: $n = 1.4$ (*solid line*), $n = 1.4 + 0.001i$ (*dashed line*), and $n = 1.4 + 0.005i$ (*dotted line*)

as one may expect. But the location of the maxima remain unchanged. However, Fig. 9.42 reveals the shift of the resonances of a nonabsorbing sphere if changing the real part of the refractive index slightly. Regarding spheres, the MDR's can be related to the complex zeros of the denominators in Eqs. (7.85) and (7.86), i.e., to the poles of the TE- and TM-modes of the Debye potentials.

Next, let's see the influence of a Chebyshev polynomial of order $n_o = 45$ with two different deformation parameters, if superimposed to the regular boundary surface of the above considered spherical particle according to (7.204). Now, we have $kr_K \in [17, 18]$. The incident plane wave is assumed to travel along the axis of symmetry. The resulting MDR's are presented in Fig. 9.43. The solid line (spherical particle) is identical with that one of Fig. 9.41. There can be observed a shift of the MDR's to higher size parameters for an increasing deformation parameter.

Finally, Fig. 9.44 shows the results for an oblate and prolate spheroidal particle in the size parameter region $kr_{eqv(v)} \in [6.45, 6.8]$. For the calculation we used again a resolution of $\Delta kr_{eqv(v)} = 0.01$. Moreover, the result of the corresponding spherical particle (solid line) with the same refractive index of $n = 2.0$ is shown. Going from oblate to prolate spheroidal particles reveals again a shift of the resonance lines towards higher size parameters.

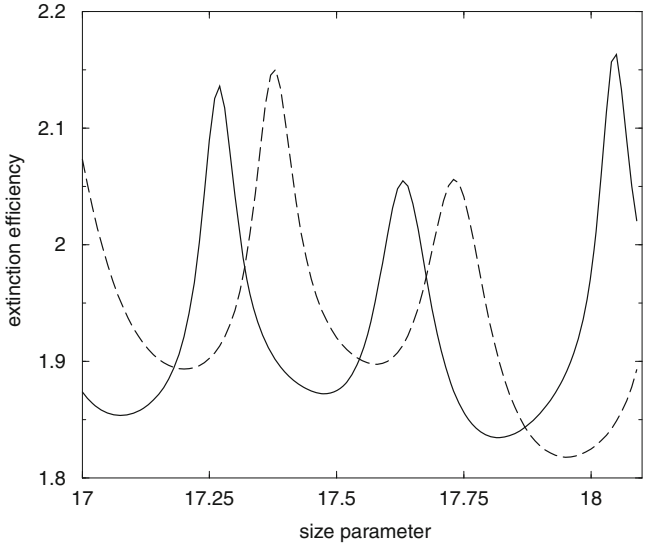

Fig. 9.42 Morphology dependent resonances of a nonabsorbing sphere with two different refractive indices: $n = 1.4$ (*solid line*), $n = 1.39$ (*dashed line*)

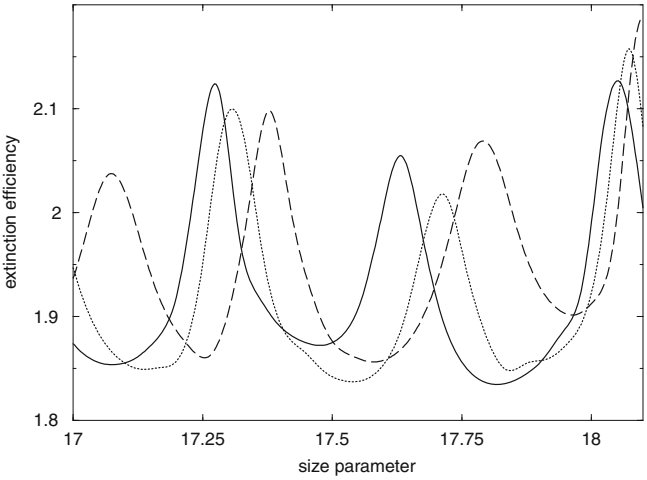

Fig. 9.43 Morphology dependent resonances of Chebyshev particles with a refractive index of $n = 1.4$. Order of the Chebyshev polynomial $n = 45$. Deformation parameters: $\epsilon = 0$ (*solid line*), $\epsilon = 0.03$ (*dotted line*), $\epsilon = 0.05$ (*dashed line*). Orientation of the Chebyshev particle ($\theta_p = 0°, \phi_p = 0°$)

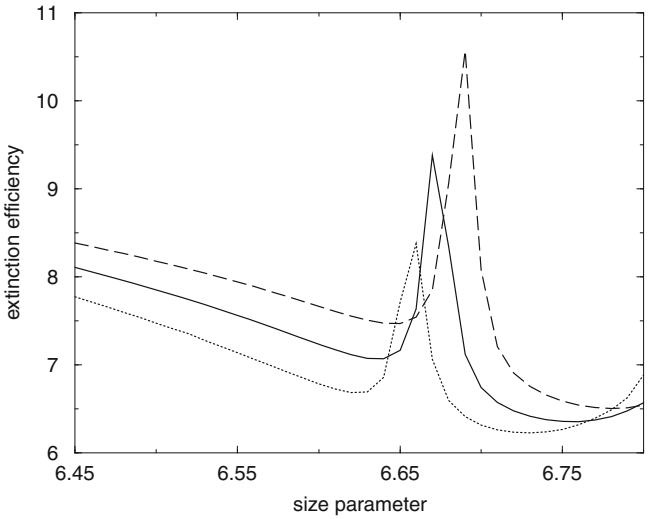

Fig. 9.44 Morphology dependent resonances of spheroidal particles with a refractive index of $n = 2.0$. Aspect ratios: $av = 0.985$ (*dotted line*), $av = 1.0$ (*solid line*), $av = 1.015$ (*dashed line*)

9.3 High-Order Chebyshev Particles

Departures from spherical shape can manifest themselves on different size scales. A rather subtle morphological feature is small-scale surface roughness. By that we mean a perturbation of the particle's boundary surface with a perturbation amplitude and perturbation length scale that is much smaller than both the size of the particle and the wavelength of light. For instance, mineral aerosols in the terrestrial or Martian atmospheres, as well as dust particles in the interplanetary and interstellar medium often have rough surfaces. Another example are ice cloud particles with rimed surfaces.

A simple model for a particle with a perturbed boundary surface is a Chebyshev particle given by the surface parameterization (7.204). This is an axisymmetric particle, i.e., r is only dependent on the polar coordinate θ. We therefore refer to this particle as a "2D" Chebyshev particle. A corresponding "3D" model is given by the parameterization

$$r(\theta, \phi) = r_K[1 + \epsilon \cos(n\theta)\cos(n\phi)]. \tag{9.6}$$

Figure 9.45 shows a 2D (left) and 3D (right) Chebyshev particle. The perturbing Chebyshev polynomial has a "wavelength" $\Lambda = 2\pi r_K/n$ on the surface of the sphere, and the perturbation amplitude is $|\epsilon| r_K$. Small-scale surface roughness can be mimicked by choosing ϵ sufficiently small, and n sufficiently large. Typically, when starting from small values of n, the optical properties initially change as the Chebyshev order is increased; but eventually, the optical properties converge, and any further increase in the Chebyshev order has no more effect on the optical properties.

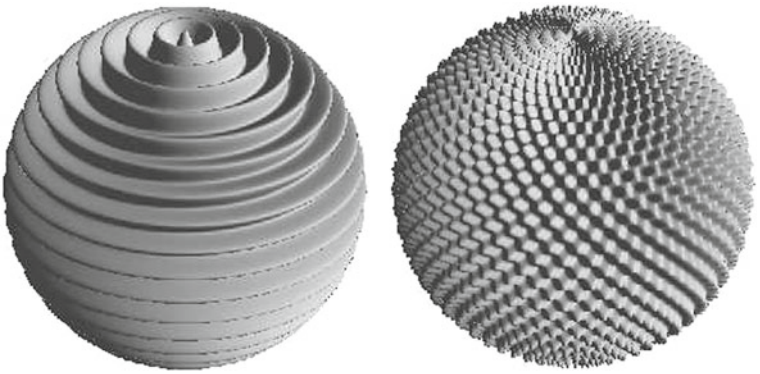

Fig. 9.45 Chebyshev particles with 2D (*left*) and 3D (*right*) surface perturbations; the Chebyshev order is $n = 40$, and deformation parameter is $\epsilon = 0.05$

In the computations shown below, convergence was reached when $2\pi r_K/n < \lambda/4$, where λ denotes the wavelength of light.

T-matrix computations for high-order Chebyshev particles can be plagued by ill-conditioning problems, especially for large size parameters. Therefore, before presenting some actual computations for Chebyshev particles, we first discuss a perturbation approach that has been geared to computing the T-matrix of particles with small-scale surface roughness.

9.3.1 Perturbation Approach of the T-Matrix

From Eqs. (4.37) and (5.18) we see that the extended boundary condition method computes the T-matrix from two matrices $\mathbf{C}$ and $\mathbf{A}$ according to

$$\mathbf{T} = \mathbf{C} \cdot \mathbf{A}^{-1}. \tag{9.7}$$

For simplicity, we have now omitted all subscripts and superscripts on the matrices. Moreover, in deriving (5.18) we restricted the consideration to the outer Dirichlet problem of the scalar Helmholtz equation. But it can be shown (see Schmidt et al.: "The equivalence of applying the Extended Boundary Condition and the continuity conditions for solving electromagnetic scattering problems" in Opt. Com. 1998, for example) that the corresponding expression (1.71) for the outer transmission problem of the vector-wave-equation can be also converted into (9.7). The matrix inversion involved in this equation can become ill-conditioned in numerical computations, thus introducing numerical errors. In practice, this limits the range of size parameters for which accurate computational results can be obtained. Ill-conditioning problems associated with this matrix inversion tend to become more severe for particles deviating significantly from spherical shape, for particles composed of optically

hard or strongly absorbing material, as well as for particles with small-scale surface perturbations.

Our goal is to find a way to circumvent the potentially ill-conditioned inversion of the matrix $\mathbf{A}$ in Eq. (9.7). Suppose we compute the two matrices $\mathbf{C}$ and $\mathbf{A}$ of a particle with a perturbed boundary surface, such as a Chebyshev particle, as well as the A-matrix of the corresponding unperturbed geometry, which we denote by $\mathbf{A}_0$. We formally introduce the difference $\Delta\mathbf{A} = \mathbf{A} - \mathbf{A}_0$, so that Eq. (9.7) can be brought into the form

$$\mathbf{T} \cdot (\mathbf{A}_0 + \Delta\mathbf{A}) = \mathbf{C}. \tag{9.8}$$

Subtraction of $\mathbf{T} \cdot \Delta\mathbf{A}$ followed by multiplication by $\mathbf{A}_0^{-1}$ from the right yields

$$\mathbf{T} = (\mathbf{C} - \mathbf{T} \cdot \Delta\mathbf{A}) \cdot \mathbf{A}_0^{-1}. \tag{9.9}$$

This T-matrix equation is mathematically equivalent to the original equation (9.7). However, it is very different from a numerical point of view. Equation (9.9) only involves the inversion of the matrix $\mathbf{A}_0$ of the unperturbed geometry, which is numerically much more well-conditioned than the inversion of $\mathbf{A}$. In fact, if the unperturbed geometry is a sphere, such as in the case of Chebyshev particles, then the A-matrix has the symmetry property given in Eq. (8.80), i.e., it is a diagonal matrix. The inversion of a diagonal matrix is trivial, so the ill-conditioning problem of the matrix inversion has been entirely eliminated. The price we have to pay for that is that Eq. (9.9) is only an implicit equation for the T-matrix. In fact, we see certain parallels to the Lippmann-Schwinger equation given, e.g., in Eq. (5.148), in which the quantity of interest appears both on the left and right hand side of the equation. We can therefore apply the same iterative approach as in Sect. 5.5 to solving Eq. (9.9).

A lowest-order estimate $\mathbf{T}^{(0)}$ of the T-matrix can be obtained by setting $\mathbf{T} = \mathbf{0}$ on the rhs of Eq. (9.9). Subsequently, $\mathbf{T}^{(0)}$ can be substituted into the rhs to obtain an improved estimate $\mathbf{T}^{(1)}$. That, in turn, can be substituted into the rhs to obtain a second-order estimate $\mathbf{T}^{(2)}$, etc. So, the iterative solution method based on Eq. (9.9) is given by

$$\mathbf{T}^{(0)} = \mathbf{C} \cdot \mathbf{A}_0^{-1} \tag{9.10}$$

$$\mathbf{T}^{(n)} = (\mathbf{C} - \mathbf{T}^{(n-1)} \cdot \Delta\mathbf{A}) \cdot \mathbf{A}_0^{-1}. \tag{9.11}$$

Equation (9.10) provides a starting value, and Eq. (9.11) defines the iteration procedure for computing the T-matrix. It is important to emphasize that this iterative method is by no means limited to Chebyshev particles. It can be applied as long as the iteration converges, and provided that the inversion of the matrix $\mathbf{A}_0$ is numerically more stable than the inversion of $\mathbf{A}$.

9.3.2 Results

The iterative method given in Eqs. (9.10) and (9.11) has been implemented into the program *Tsym*, which is a T-matrix program for non-axisymmetric particles. The *Tsym* program is described in Sect. 9.5. As an illustration of the method we perform calculations for 3D Chebyshev particles with an index of refraction of $n = 3 + 0.1i$, which is typical for hematite at visible wavelengths (neglecting birefringence). The deformation parameter and Chebyshev order are chosen such that $|\epsilon| r_K/\lambda = 0.11$, and $\Lambda = 2\pi r_K/n \leq \lambda/4$ (please, discriminate between the refractive index n and the order n of the Chebyshev polonomial!).

Figure 9.46 shows the phase matrix elements $< Z_{11} >$ (left column) and $- < Z_{12} > / < Z_{11} >$ (right column) for a size parameter of $x = 10$ (top row) and $x = 60$ (bottom row), with x defined according to $x := k_0 \cdot r_K$. For both size parameters the phase function of unperturbed spheres (dashed line) displays less forward scattering and significantly more side- and backscattering than 3D Chebyshev particles (solid line) of comparable size. Oscillations in the phase function as well as in $- < Z_{12} > / < Z_{11} >$ are found at similar scattering angles for both particle geometries; however, the amplitude of the oscillations is significantly higher for high-order Chebyshev particles than for unperturbed spheres.

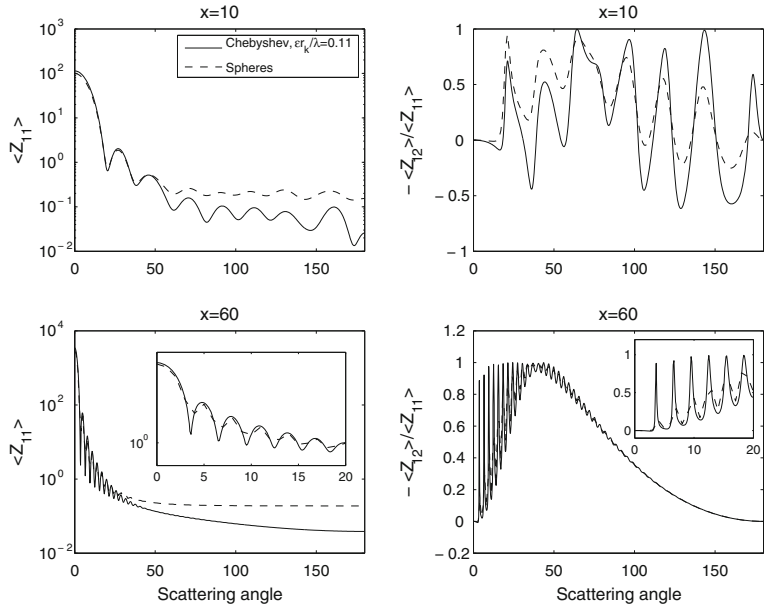

Fig. 9.46 Phase matrix elements computed for 3D Chebyshev particles (*solid line*) and unperturbed spheres (*dashed line*) with an index of refraction of $n = 3 + 0.1i$, and with size parameters 10 (*top row*) and 60 (*bottom row*)

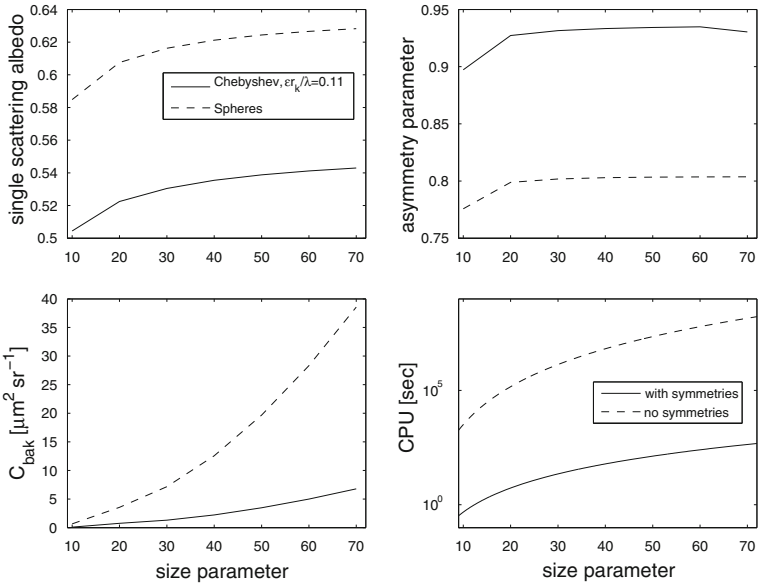

Fig. 9.47 Comparison of optical properties ω, g, and C_{bak} for spheres and Chebyshev particles as in Fig. 9.46, as well as computation time with and without the use of symmetries

Figure 9.47 shows corresponding results for the single-scattering albedo ω (top left), asymmetry parameter g (top right), and backscattering cross section C_{bak} (bottom left) as functions of the size parameter. These quantities are defined as follows.

$$g := \frac{1}{2}\int_{-1}^{1} p(\Theta)\cos\Theta \,\mathrm{d}(\cos(\Theta)) \tag{9.12}$$

$$\omega := \frac{C_{\text{sca}}}{C_{\text{ext}}} \tag{9.13}$$

$$C_{\text{bak}} := \frac{1}{4\pi}\cdot p(180^\circ), \tag{9.14}$$

where $p =< Z_{11} >$ denotes the phase function (see (7.189), and the consecutive remark). The asymmetry parameter is the first Legendre moment of the phase function; it is a measure for the partitioning between scattering in the forward and backward hemispheres. C_{ext} and C_{sca} denote the extinction and total scattering cross sections, respectively. Thus, ω expresses the ratio of scattering to total extinction. C_{bak} is the cross section for unpolarized incident radiation scattered in the exact backward direction. It is important for Lidar measurements of the backscattering coefficient. The latter is proportional to C_{bak} and to the particle number density. The figure shows that in comparison to smooth spheres, high-order Chebyshev particles predict significantly lower values of ω (i.e. less scattering in relation to absorption) and higher values of g (i.e., on average, more forward in relation to

backscattering). An atmosphere containing such particles with small-scale surface roughness would therefore give rise to a higher transmittance and a lower absorptance, thus less radiative cooling as compared to size-equivalent spheres with the same dielectric properties. Further, spheres yield values of C_{bak} that are, depending on the particle size, up to five times higher than those computed for Chebyshev particles. Neglecting roughness effects in the interpretation of Lidar measurements would introduce correspondingly high errors in the retrieved number densities of particles.

While the differences observed in this test case are rather dramatic, it is important to note that the importance of small-scale surface roughness can strongly depend on the physical parameters of the particles. The optical properties of particles composed of optically hard materials (i.e., with high values of the real part of the refractive index) are expected to be more sensitive to the presence of small-scale surface perturbations than those of optically soft particles. The same is true for particles with high absorption cross sections, since the optical properties of particles are strongly influenced by internal resonances inside the particle. As the resonances are quenched in highly absorbing particles, the relative importance of small-scale surface perturbations increases.

The computations presented here have been based on the iterative T-matrix approach according to Eqs. (9.10) and (9.11). The iteration in Eq. (9.11) has been carried out to sixth order. The reciprocity condition was used to ensure the accuracy of the results. Further, the group theoretical methods discussed in Chap. 8 have been implemented in *Tsym*. The bottom right panel in Fig. 9.47 shows the CPU time used for the computations as a function of size parameter (solid line), as well as theoretical values for the CPU-time that would have been required for these calculations if symmetries had not been exploited. For the smallest sizes ($x = 10$), the use of symmetries reduces the computation time to 0.5 s. Without the use of symmetries theoretical estimates based on the number of extra numerical operations predict that the program would run for 1.25 h. An actual run of *Tsym* with symmetries switched off confirms this. For the largest particles considered here ($x = 70$), the use of group theory reduces CPU time to 7.35 min. Without group theory, the program would have run for 4.5 years! This clearly illustrates that group theory can profoundly reduce the required computational resources. In cases such as that considered here, computations for larger size parameters are practically not possible without exploiting symmetries.

9.4 Description of Program *mieschka*

In what follows, we intend to provide a detailed insight into the special T-matrix approach, called *mieschka*, underlying the numerical simulations presented in the second section of this chapter. Program *mieschka*—a wordplay which contains the surname of Gustav Mie but which is also used in Russian to denote the bear, a strong and perennial animal—has overcome a nearly 10 years history of ongoing developments. It saw the light of day as the first numerical implementation of the Method of Lines considered in Chap. 5 and evolved through several phases to a

full-grown T-matrix approach with several capabilities. It was recently used in the German Aerospace Center to establish an extensive database for remote sensing applications. But it was also frequently used in university education via the "DLR Virtual Laboratory". The latter is an Internet platform, which was designed and developed especially to allow for online access to scientific software (details can be found in the corresponding paper cited in Sect. 10.11).

While developing *mieschka* over the years, most of our effort was spent to put it into practice and to develop an appropriate convergence strategy. This is of some importance since the convergence behaviour of nonspherical particles is quite complex and depends strongly on the considered scattering configuration, as already mentioned. All tests have been performed essentially on spheroids, Chebyshev particles, and finitely extended circular cylinders. For these geometries, there exist already a number of independent calculations to compare with. Today, *mieschka* presents a versatile and suitable program to perform scattering simulations on rotationally symmetric as well as spherical particles both in fixed and random orientations, which do not have to fear the competition of other programs.

9.4.1 Convergence Strategy Used in mieschka

A Quick Look at the Numerical Background

Equations (7.176), (7.180), and the symmetry relation (4.51) constitute the numerical background to solve the electromagnetic wave scattering problem on rotationally symmetric, dielectric particles. To calculate the matrix elements of the interaction operator (or T-matrix, respectively) we use expression (1.71) with matrices defined according to (1.64)–(1.69). In every numerical calculation we have to truncate the n, n'-summation in (7.176) at a certain finite number. In *mieschka* this is accomplished as follows: First, we replace the summation

$$\sum_{\tau=1}^{2} \sum_{n=0}^{\infty} \sum_{l=-n}^{n} \cdots \tag{9.15}$$

by

$$\sum_{\tau=1}^{2} \sum_{n=0}^{n_{cut}} \sum_{l=-n}^{n} \cdots \tag{9.16}$$

with n_{cut} being the upper truncation parameter of the summation with respect to n. The summation with respect to n' is truncated at the same parameter n_{cut} to end up with square matrices. Regarding the summation with respect to the azimuthal modes l' in the laboratory frame we have to take only the two values $l' = \pm 1$ into account, according to our remark following (7.176). But instead of (9.16) we use the

summation

$$\sum_{\tau=1}^{2} \sum_{l=-l_{cut}}^{l_{cut}} \sum_{n=|l|}^{n_{cut}} \cdots \tag{9.17}$$

which becomes identical with (9.16) only if $l_{cut} = n_{cut}$. The justification of introducing a second truncation parameter l_{cut} is supported by our numerical experience that l_{cut} can be chosen much smaller than n_{cut} in most of the simulations. This can be confirmed by looking at the convergence parameters given in the captions of the figures presented in Sect. 9.2. Using (9.17) instead of (9.16) results, therefore, in less computational effort regarding computing time and storage requirements. Thus, the elements (7.176) of the scattering amplitude matrix are calculated according to

$$\begin{aligned} F_{\alpha\beta}(\theta_s, \phi_s) = \frac{4\pi}{ik_0} \sum_{\tau,\tau'=1}^{2} \sum_{l=-l_{cut}}^{l_{cut}} \sum_{n=|l|}^{n_{cut}} \sum_{l'=-l_{cut}}^{l_{cut}} \sum_{n'=|l'|}^{n_{cut}} (\delta_{1,l'} + \delta_{-1,l'}) \\ \cdot [\hat{\alpha} \cdot \vec{Y}_{l,n,\tau}(\theta_s, \phi_s)] \cdot [W(L)]^{\tau,\tau'}_{l,n;l',n'} \cdot [\vec{Y}_{l',n',\tau'}(\theta_i = 0°, \phi_i = 0°) \cdot \hat{\beta}]; \\ \alpha, \beta = h, v \end{aligned} \tag{9.18}$$

in *mieschka*. We assume further that the calculation of $\mathbf{W}(K)$ in the particle frame requires a number of azimuthal modes l_1 which is identical with the number of azimuthal modes l we choose in the laboratory frame to calculate $\mathbf{W}(L)$. Due to symmetry relation (4.51) matrix $\mathbf{W}(K)$ in Eq. (7.180) becomes block-diagonal with respect to the azimuthal modes l_1 and l_2 in the particle frame. Thus, we have instead of (7.180) the simpler expression

$$[W(L)]^{\tau,\tau'}_{l,n;l',n'} = \sum_{l_1=-l_{cut}}^{l_{cut}} D^{(n)}_{l,l_1}(\alpha, \beta, \gamma) \cdot [W(K)]^{\tau,\tau'}_{l_1,n;l_1,n'} \cdot D^{(n')}_{l_1,l'}(-\gamma, -\beta, -\alpha). \tag{9.19}$$

Calculating the matrix elements of the interaction operator in the particle frame requires the calculation of boundary surface integrals containing different combinations of regular and outgoing eigensolutions with appropriate weighting functions, as discussed in Chaps. 1 and 2. Consequently, the stability and the convergence behaviour of the approximate solutions obtained with *mieschka* as well as with other T-matrix approaches are essentially dependent on

- The appropriate choice of the weighting functions $\vec{g}_{j,\tau'}(\mathbf{x})$ and $\vec{h}_{j,\tau'}(\mathbf{x})$ to calculate the matrices (1.64)–(1.69).
- The accuracy of the surface integration.
- The accuracy and stability of the matrix inversion which becomes necessary to calculate the T-matrix according to (1.71).
- The appropriate determination of the convergence parameter (truncation parameter) n_{cut} and l_{cut} to fix the number of terms used in the relevant series expansions.
- The accuracy of the orientation averaging process.

Regarding these aspects *mieschka* is equipped with a convergence strategy that runs automatically on user's request. This strategy is based on the experience of Wiscombe and Mugnai, and Barber and Hill (for details see the corresponding publications cited in Sect. 10.4) and was tested and developed further for our own purposes. On the one hand, such an automatic convergence procedure releases the user from performing his own convergence analysis. On the other hand, this advantage is gained with additional computation time. The experienced user has therefore the possibility to fix most of the necessary parameters appropriately in advance to speed up the program. But this requires some experience with its behaviour and should not be done at the very beginning. Now, let us see how does the automatic convergence strategy looks like.

Automatic Convergence Strategy

In all the simulations we have performed so far with *mieschka* convergent and most stable results have been obtained with the weighting functions

$$\vec{g}_{j,\tau'}(\mathbf{x}) \;=\; \left[\vec{\psi}^{\hat{n}_-}_{j,\tau'}(k_0,\mathbf{x})\right]^*; \quad \mathbf{x}\in\partial\Gamma \tag{9.20}$$

and

$$\vec{h}_{j,\tau'}(\mathbf{x}) \;=\; \left[\hat{n}_-\times\nabla\times\vec{\psi}_{j,\tau'}(k_0,\mathbf{x})\right]^*; \quad \mathbf{x}\in\partial\Gamma. \tag{9.21}$$

$\vec{\psi}_{j,\tau'}(k_0,\mathbf{x})$ are the regular eigensolutions of the vector wave equation defined in (2.120) and (2.121). This experience was gained by other authors of T-matrix approaches, too. These weighting functions are therefore chosen as standard weighting functions in program *mieschka*. But the experienced user has the possibility to choose from some other, predefined weighting functions.

The surface integration is performed, by default, by use of a Gauss-Konrod quadrature with automatic step size control. For this, we have to fix the relative integration error rel_err_int. Its predefined default value is given by $rel\_err\_int = 0.001$.

All necessary matrix inversions are performed by use of a LU-factorization procedure taken from the NAG-Fortran90 library. This subroutine is called *nag_gen_lin_sol*. It generates warnings if the matrix becomes ill-conditioned. But these warnings can be ignored if the run of program *mieschka* ends successfully.

Regarding orientation averaging, there are two possibilities within *mieschka*. On the one hand, the necessary integration in (7.189) with respect to the Eulerian angles can be performed numerically by employing again a Gauss-Konrod quadrature. But this is often a time consuming process which can be drastically simplified especially for rotationally symmetric particles in random orientation by employing an analytical orientation averaging procedure. This procedure was used in a consequent way by Mishchenko. Moreover, he proved its usefulness in manyfold applications. The analytical procedure is based on an expansion of the Stokes matrix elements into a series of the "Wigner d-functions" introduced in Sect. 2.4.2. The details can be found

in the book of Mishchenko, Travis, and Lacis cited in Sect. 10.9. At first glance, the analytical orientation averaging process looks pretty complicate since it requires the additional calculation of the Clebsch-Gordan coefficients. But it proves to be much faster than the numerical orientation averaging process especially for rotationally symmetric particles in random orientation.

To determine the convergence parameters n_{cut} and l_{cut} we have to distinguish whether the particle is in fixed or random orientation.

1. Particle in fixed orientation, i.e., ϕ_p and θ_p are set to certain values:
   (a) The Eulerian angles are fixed to $\phi_p = \theta_p = 0°$, and only the azimuthal mode $l = 1$ is considered, at first. The polarimetric differential scattering cross-sections $d\sigma_{hh}/d\Omega_s$ and $d\sigma_{vv}/d\Omega_s$ are calculated for increasing values of n_{cut} afterwards, and in steps of 1° within the interval $\theta_s \in [0°, 180°]$ of the scattering plane. At each step of n_{cut} these cross-sections are compared to those of the former step at all scattering angles. If the relative error of two successive calculations is equal to or less than rel_err at 80 % of the scattering angles, the last value of n_{cut} is taken as the convergence parameter. The default value of rel_err is $rel\_err = 0.05$. The restriction to 80 % of all scattering angles avoids exaggerate accuracy requirements in the grooves and spikes of the differential cross-sections. This procedure is similar to the one used by Wiscombe and Mugnai, and by Barber and Hill.
   (b) ϕ_p and θ_p are now set to the given values. l_{cut} is determined afterwards in the same way as described above for n_{cut}.

2. Particle in random orientation, and if orientation averaging is performed numerically:
   (a) n_{cut} is determined as in 1(a).
   (b) Employing a 3-point Gauss-Konrod rule to perform the integration with respect to both Eulerian angles ϕ_p and θ_p we calculate all elements of the phase matrix for increasing values of l_{cut}, and in steps of 1° within the interval $\theta_s \in [0°, 180°]$ of the scattering plane. Please, note that these elements are **not** the real and final elements of the phase matrix since orientation averaging is at first performed only with nine different sets of Eulerian angles! Therefore, we will call this phase matrix the "effective phase matrix $< \mathbf{Z}^{(eff)} >$." If the relative error of two successive calculations is equal to or less than rel_err for each element of the effective phase matrix and at each scattering angle (not at 80 %, now!) the last value of l_{cut} is taken as the convergence parameter. This procedure can be optionally restricted to the element $< Z_{11}^{(eff)} >$ of the phase matrix, i.e., to the phase function only.
   (c) In this last step the precalculated values of n_{cut} and l_{cut} are used in conjunction with a 15-point Gauss-Konrod quadrature with automatic step size control to perform orientation averaging with respect to ϕ_p and θ_p. This process is stopped if the relative integration error is equal to or less than rel_err_pm for each element of the phase matrix, and at each scattering angle. The default value of rel_err_pm is $rel\_err\_pm = 0.05$.

3. Particle in random orientation, and if orientation averaging is performed analytically:
   (a) n_{cut} is determined as in 1(a).
   (b) l_{cut} is determined as in 2(b). In this step, one can optionally replace the effective phase matrix by the analytically averaged phase matrix. But using the effective phase matrix saves computing time.
   (c) The precalculated values of n_{cut} and l_{cut} are then used to perform analytical orientation averaging.

As already mentioned, those users who are not familiar with the program and with the scattering behaviour of nonspherical particles should use the automatic convergence procedure with the default values as well as the default procedures given above. This will guarantee accurate and reliable results if *mieschka* ends successfully. However, there are several applications where the default values determining the accuracy can be weakened. For example, convergence in the very forward region can be obtained with lower values of n_{cut} and l_{cut} than in the backward region. Program *mieschka* provides, therefore, the possibility to change the default values as well as some of the standard routines like quadrature rules, for example. The experienced user will thus be able to match the program to his own requirements. According to this goal *mieschka* can be used in different operation modi and with different options which will be described in the following subsections.

9.4.2 Functionality and Usage of mieschka

Modes of Operation

Regarding the convergence strategy, the user has the possibility to choose between the two modes "automatic convergence strategy" and "user defined convergence parameters". In the latter case, all convergence parameters and all the required error limits must be defined by the user himself. Moreover, in this mode, he has to apply his own criteria to estimate the accuracy and reliability of the results obtained with *mieschka*.

There are two other modes of operation regarding the organization of the input. These two modes can be combined with the two modes concerning the convergence strategy. One way to generate all the necessary input data for a certain run of *mieschka* is the interactive input. But there is also the possibility to run *mieschka* with a prepared input file. This last possibility enables the usage of *mieschka* as a subroutine in a user program, for example. A valid input file can be generated from the file *commented_initialization_file.eng* that comes along with the software package. It is recommended to rename the copied input file and to copy it into another directory like the actual working directory, for example. But the interactive input mode comes along with some restrictions which can be partially revoked by use of

corresponding options or by employing an initialization file (for the latter possibility see the subsection **Environmental parameter**). The restrictions are the following:

- All calculations are performed at equidistant scattering angles θ_s in steps of 1°.
- Only the weighting functions (9.20) and (9.21) are used.
- Placing fixed sensors with a finite aperture in the scattering plane is not possible.
- All integrations are performed by use of a Gauss-Konrod quadrature rule.
- All physical units are fixed. The frequency of the primary incident plane wave is fixed to 47.71 GHz. This is not a restriction, due to the scalability of the scattering process. Lengths are fixed to mm. The above mentioned frequency is chosen in such a way that a sphere with radius $r = 1$ mm results in a size parameter of $k_0 \cdot r = 1$, i.e., the radius in [mm] is identical with the size parameter. This fixing of the units can be revoked by the interactive usage of *mieschka* with the option **−v**.
- Only the automatic convergence strategy is allowed. This restriction can be revoked by the interactive usage of *mieschka* with the option **−u**.

Options

The generic command to run *mieschka* is

```
mieschka [options]
```

Please, have in mind that the used options may overwrite the parameters fixed in a possibly existing initialization or input file. The following options are possible:

- `no option`
  The necessary input parameters required for a *mieschka* run will be specified in an interactive way. The result files are written into the actual working directory. **{mieschka}** is used as their base name (see also the subsection **Result files**).
- `[-f]` **{file}**
  {file} is the name of a valid input file. It may also contain a valid path. Using this option, the input parameters are provided via the specified input file. The base name of the result files is set to **{file}**, suppressing a possibly existing '.inp' extension.
- `-o` **{name}**
  The base name of the result files is set to **{name}**.
- `-v`
  "verbose" option. The user gets several additional information:
  - The convergence behaviour is displayed online while *mieschka* is running.
  - *mieschka* generates files containing all used input parameters of a program run (see also the subsection **Result files**).
  - *mieschka* generates several files to analyse the convergence behaviour subsequent to a program run (see also the subsection **Result files**).

- `-i`
  Option of interactive input (equivalent to `no option`).
- `-h`
  Help option. *mieschka* provides short information about all possible options, but it is not running.
- `-V`
  mieschka provides the version number of the program, but it is not running.
- `-p`
  Plot option. At the end of a program run the differential scattering cross-sections or the phase functions (depending on whether a particle in fixed or random orientation is considered) are plotted automatically. This option requires the correct installation of the tools *xmgr* or *xmgrace* of ACE/gr.
- `-d`
  This option overwrites the DISPLAY variable to plot the results into a specified display.
- `-u`
  This option allows for the user driven convergence treatment. This option should only be used by "experts" who are already familiar with the program. It requires some experience in the methodology of light scattering analysis to produce reliable results.

Result Files

Depending on the chosen options and on the mode of operation *mieschka* generates different result files. The following description of the files is related to the base name specified by use of the option `-o` **{name}**.

Result files related to the input parameters:

- **name.inr:**
  This file contains the input parameters used in a certain program run.
- **name.surf:**
  This file contains the boundary surface of the scatterer in Cartesian coordinates. It may be used to plot the boundary surface with *xmgr* or *xmgrace*, respectively.
- **name_pol.surf:**
  This file contains the boundary surface of the scatterer in polar coordinates.

Result files related to the scattering analysis of particles in fixed orientations:

- **name_o<n>.ds:**
  This file contains the polarimetric differential scattering cross-sections belonging to the n'th fixed orientation of the scatterer. In the five columns the following data are given:
  - 1. column: scattering angle [degree]
  - 2. column: vv-polarized differential scattering cross-sections

  - 3. column: hh-polarized differential scattering cross-sections
  - 4. column: hv-polarized differential scattering cross-sections
  - 5. column: vh-polarized differential scattering cross-sections

- **name_o<n>.ts:**
  This file contains the total cross-sections belonging the n'th fixed orientation of the scatterer.
- **name.agr:**
  This file contains a *xmgr* or *xmgrace* plot of the vv- and hh-polarized differential cross-sections for all calculated orientations.

Please note that the extension "_o<n>" in the above given files is switched of if there is just one single orientation for which the scattering behaviour is calculated.

Result files related to the scattering analysis of particles in random orientation:

- **pm_name.dat:**
  This file contains the phase matrix of the scattering particle. The first column contains the scattering angle in [degree]. All other columns are the (1,1), (1,2), ..., (2,1), (2,2), ..., (4,4) elements of the phase matrix.
- **pf_name.dat:**
  This file contains the normalized phase function (second column) of the scattering particle dependent on the scattering angle in [degree] (first column). The normalized phase function is calculated from the (1,1)-element of the phase matrix by multiplication with $4\pi/(k_0^2 \cdot \sigma^s)$ with $\sigma^s = \sigma_h^s + \sigma_v^s$ being the unpolarized total scattering cross-section.
- **pm_name.ts:**
  This file contains the total cross-sections of the scattering particle in random orientation.
- **pf_name.agr:**
  This file contains an *xmgr* or *xmgrace* plot of the phase function.

Result files related to the scattering analysis in the presence of an aperture (this is accomplished only for particles in fixed orientations, so far):

- **name_o<n>.ads:**
  This file contains the unpolarized differential scattering cross-sections with aperture integration, belonging to the n'th fixed orientation of the scatterer. In the three columns the following data are given:

  - 1. column: scattering angle in [degree]
  - 2. column: differential scattering cross-section for a v-polarized incident plane wave (integrated over aperture)
  - 3. column: differential scattering cross-section for a h-polarized incident plane wave (integrated over aperture)

- **name_o<n>.as:**
  This file contains the unpolarized differential scattering cross-sections at each sensor specified in the scattering plane, and for a particle in the n'th fixed orientation.

Result files related to the convergence behaviour:

These files will be generated only if the verbose option **[-v]** is used. The relative errors are calculated from two successive *mieschka* runs with the pairs (n_{cut}, $n_{cut}+3$) or ($l_{cut}, l_{cut}+1$), respectively. n_{cut} and l_{cut} are the numbers given in the first and second column of the corresponding convergence files. Most of the generated convergence files are only of interest if the user will perform his own convergence tests, or if he intends to apply *mieschka* at higher size parameters or aspect ratios than it will be possible in the mode "automatic convergence strategy" with the default accuracy parameters, for example.

- **name.conv:**
  This file contains the convergence parameter n_{cut} and l_{cut}, the number of the used function calls to perform the surface integration as well as an estimate of the integration error.
- **name_n.conv:**
  This file contains the maximum relative error obtained in determining the convergence parameter n_{cut}. This file is generated for particles in fixed as well as in random orientation. The data of the six columns are:
  - 1. column: n_{cut}
  - 2. column: $l = 1$ (please, remember that only this azimuthal mode is used to determine n_{cut})
  - 3. column: maximum relative error of the vv-polarized differential scattering cross-sections
  - 4. column: maximum relative error of the hh-polarized differential scattering cross-sections
  - 5. column: maximum relative error of the hv-polarized differential scattering cross-sections
  - 6. column: maximum relative error of the vh-polarized differential scattering cross-sections
- **name_l.conv:**
  This file contains the maximum relative error obtained in determining the convergence parameter l_{cut} for a particle in fixed orientation (the file is generated only in this case!). The format is that of **name_n.conv** except that in columns 3–6 the maximum relative error of all orientations is given if the particle is analysed for multiple orientations. If there is just one orientation then columns 3–6 are equivalent to **name_n.conv**.
- **name_pm_l.conv:**
  This file is generated only for particles in random orientation. It contains the maximum relative error obtained in determining l_{cut}. The first two columns are the determined values of n_{cut} and l_{cut}. The remaining columns contain the maximum relative error of the corresponding phase matrix elements in the same order as given in **pm_name.dat**.

- **name_n<i>.ds:**
  This file contains the differential scattering cross-sections calculated in determining n_{cut}, but for $l = 1$ only! It is generated for particles in fixed and random orientation, as well. Its format is that of **name_o<n>.ds**. Please, note that the differential scattering cross-sections are artificial and never correct since they are related to this single azimuthal mode.
- **name_o<n>_n<i>_l<j>.ds:**
  This file contains the differential scattering cross-sections calculated in determining l_{cut}. Its format is that of **name_o<n>.ds**, and it is generated only for particles in fixed orientations. Please, note that the extension '_l<j>' convey the summation of all modes l<−j>, l<−j+1>, . . . , l<+j>, i.e., if convergence is achieved the correct differential cross-sections are listed in this file.
- **pm_name_n<i>_l<j>.dat:**
  This file is generated only for particles in random orientation. It contains the effective phase matrix elements or the analytically determined phase matrix elements, respectively, calculated in determining l_{cut}. Its format is that of **pm_name.dat**.
- **pf_name_n<i>_l<j>.dat:**
  This file is generated only for particles in random orientation. It contains the effective normalized phase function calculated in determining l_{cut}. Its format is that of **pf_name.dat**.

Environmental Parameter

The following two parameters can be used to set up a certain working environment:

- **MIESCHKA_INPUT**
  This parameter denotes name and path of an initialization or input file created by the user. All parameters specified in this file will be automatically adopted by *mieschka*. In this way, the user can match the program to his needs. For example, preparing an initialization file will allow the user to fix all the units and some of the necessary input parameters (length, frequency or wavelength, usage of refractive index or dielectric constant, etc.) according to the "world" he is familiar with. Only the remaining and/or frequently changing parameters can be specified afterwards via the interactive input. To generate an initialization or input file just copy the file *commented_initialization_file.eng* of the software package. The generic command to use this parameter is

  ```
  export MIESCHKA_INPUT={valid path and file name}
  ```

  (Please, note that the Linux command `export` may be possibly replaced by the command `setenv`).
- **MIESCHKA_PLOT**
  This parameter denotes name and path of the plot program. The default setting is **MIESCHKA_PLOT=xmgr**. The generic command to use this parameter is

```
export MIESCHKA_PLOT={valid path and name of the
plot program}
```

(Please, note that the Linux command `export` may be possibly replaced by the command `setenv`).

9.4.3 Content of the Software Package

The software package can be downloaded from the Springer's web page related to this book. It contains the executable scattering program *mieschka* (only the executable can be provided, due to licence restrictions regarding the NAG library), and a scattering database for spheroidal particles in random orientation with an interactive user interface. The database can be used without this interface, of course. But the interface was especially designed to meet the user's needs and to simplify the access to the amount of pre-calculated scattering data.

All the necessary executables and documents are organized in two folders. Folder MIESCHKA contains all the material needed to install and run *mieschka* successfully. The file *commented_initialization_file.eng*, for example, is a commented input file which allows the user to create his own input or initialization file simply by copy and paste. Moreover, folder MIESCHKA contains a subfolder with several benchmark tests together with the related input files. These benchmark results may support the proof of the correct installation of *mieschka*. For example, once he has copied the input file `sphd_oblate_fo.inp` to his actual working directory, with the command

```
mieschka -f sphd_oblate_fo.inp
```

the user should be able to generate exactly the same results one can find in the directory `benchmarks/spheroid/sphd_oblate_fo`. Afterwards, he may change the relevant parameters to perform the simulations presented in Sect. 8.2.

Folder SCATDB contains all the necessary documents and installation files to install (automatically or by hand) the database as well as the user interface correctly. It also includes two documents. "Scatdb.pdf" describes the database in detail with emphasize on its resolution with respect to morphology, size parameter, and scattering angle. The second document "usermanual.pdf" provides a detailed description of the user interface and contains several examples to demonstrate its functionality.

Both programs *mieschka* as well as the user interface *db_surf* have been developed under Linux operating systems. They should run on all x86 architectures without any problems. However, in case of any problems with the installation, questions, and suggestions for further improvements do not hesitate to contact the author via e-mail (**tom.rother@dlr.de**)!

9.5 Description of Program *Tsym*

The program *Tsym* (pronounced "tee-simm") is a freely available, open-source T-matrix program for non-axisymmetric, homogeneous particles. It has been developed as a research code for testing new model particles and novel numerical approaches in T-matrix computations. Therefore, the development of this code has strongly focused on flexibility rather than user-friendliness. By contrast to *mieschka*, it does not contain any automatic convergence routines. It is entirely the user's responsibility to test the convergence and ensure the correctness of the computational results, which is not a trivial task. For this reason, the program can be a useful research tool for experienced users in numerical methods and electromagnetic scattering theory, but it is not recommended for newcomers. Novices in the field are advised to start their apprenticeship with *mieschka*.

Among the new numerical approaches that have been implemented and tested in *Tsym* are the group-theoretical methods introduced in Chap. 8 and the perturbation T-matrix approach discussed in Sect. 9.3.1. The group-theoretical methods do not merely exploit the commutation relations of the T-matrix, but also irreducible representations of finite groups. To the best of the authors' knowledge, *Tsym* is the only T-matrix program with that capability.

The program has mainly been tested for regular polygonal prisms, as well as for 2D and 3D Chebyshev particles. High-order Chebyshev particles with small deformation parameters can be used as models for particles with small-scale surface roughness. Recently, 2D and 3D Gaussian random spheres (GRS) and GRS/Chebyshev hybrid geometries have been added for testing the effects of stochastic surface perturbations.

Differences between axisymmetric and non-axisymmetric shapes can be subtle in some cases, and rather significant in other cases, depending on the optical properties under investigation, and depending on the size parameter, refractive index, and ensemble properties. An illustration is given in Fig. 9.48; this shows a comparison of the phase matrix elements $< Z_{11} >$ and $< Z_{22} > / < Z_{11} >$ computed with *Tsym* for randomly oriented hexagonal prisms (solid line), and computed with *mieschka* for randomly oriented finite circular cylinders (dashed line). The size parameter is $kr_{eqv} = 14.9$, and the refractive index is $n = 1.51 + 0.079\mathrm{i}$ (typical for ice at a wavelength of $\lambda = 18.2\,\mu\mathrm{m}$). The circular cylinders and hexagonal prisms both have comparable aspect ratios. In this particular case, the phase functions of both types of particles agree remarkably well, while significant differences are observed in $< Z_{22} > / < Z_{11} >$, which is related to the degree of linear depolarisation $\delta_L = (< Z_{11} > - < Z_{22} >)/(< Z_{11} > + < Z_{22} >)$.

The development of *Tsym* over the past twelve years has very much benefited from vivid discussions with various colleagues. The code uses the same truncation scheme as *mieschka* given in Eq. (9.17), and a similar approach for the numerical quadrature of the surface integrals. Also, the weighting functions given in Eqs. (9.20) and (9.21) are used. The code has borrowed routines for orientation-averaging of non-axisymmetric particles, various routines for calculating Bessel functions, Legendre functions, Clebsch-Gordan coefficients, etc from the T-matrix codes by Mackowski

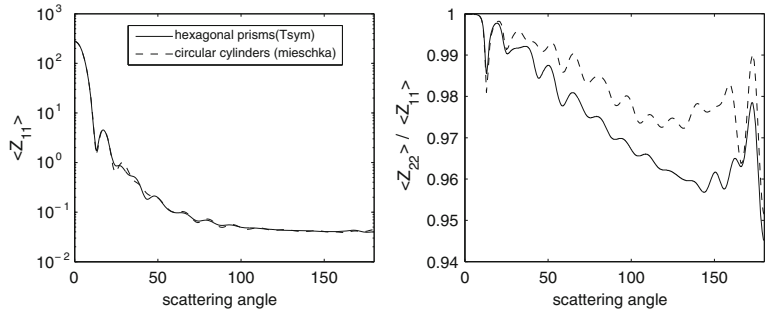

Fig. 9.48 Comparison of hexagonal prisms (computed with *Tsym*) with finite circular cylinders of comparable size and aspect ratio (computed with *mieschka*)

and Mishchenko, Laitinen and Lumme, and Mishchenko. The code for computing Gaussian random sphere geometries has been written by Muinonen and Nousiainen. These colleagues kindly gave their permission for including their routines in the distribution of *Tsym*.

9.5.1 Compilation and Input Parameters

The main directory contains the `Makefile`. The user needs to edit this file and specify the Fortran compiler prior to running the `make` command. The compilation will produce an executable file `tsym.x`. Before running the executable, one needs to edit the input file `params`, which specifies the particle properties and details about the computational methods. The file `params` contains comments that explain the meaning of the parameters that need to be specified. The file has to be placed in the same directory from which the executable is called. The user must not alter the number of lines in the file.

The use of irreducible representations can be turned on and off with a logical switch in the input file. Similarly, for particles with small-scale surface roughness, one can choose whether or not to use the iterative Lippmann-Schwinger approach for computing the T-matrix. Note that irreducible representations and the iterative method cannot be used simultaneously. If the iterative method is switched on, then one also needs to specify the maximum iteration order; the program makes no attempt to automatically determine the iteration order. If irreducible representations are used, then one has to specify the numerical method for constructing the transformation matrix $\mathbf{P}$ from the projection matrices $\tilde{\mathbf{P}}^{(\mu)}$ (see Sect. 8.4.5).

The code expedites the computations by making use of the commutation relations of the T-matrix and, if the user chooses so, by exploiting irreducible representations. To this end, one needs to specify in `params` the symmetry group to which the particle belongs. This is done by making appropriate choices for the parameters `Pgroup`

Table 9.4 Geometries implemented in *Tsym* and the corresponding settings for the parameters specifying the point group, `Pgroup`, and the index of the main rotational symmetry operation, `Nsym`

Geometry	Point group	`Pgroup`	`Nsym`
Prism, N-gonal cross section	$\mathcal{D}_{Nh}$	`Dnh`	N
2D Chebyshev, even order	$\mathcal{D}_{\infty h}$	`Dnh`	$2m_{cut}+1$
2D Chebyshev, odd order	$\mathcal{C}_{\infty v}$	`Cnv`	$2m_{cut}+1$
3D Chebyshev, even order ℓ	$\mathcal{D}_{\ell h}$	`Dnh`	ℓ
3D Chebyshev, odd order ℓ	$\mathcal{C}_{\ell v}$	`Cnv`	ℓ
2D Gaussian random sphere	$\mathcal{C}_{\infty v}$	`Cnv`	$2m_{cut}+1$
3D Gaussian random sphere	$\mathcal{C}_1$	`Cn`	1
GRS/Chebyshev hybrid, order ℓ	$\mathcal{C}_{\ell v}$	`Cnv`	ℓ

and `Nsym`. The former is a character string that indicates the family of point groups to which the particle belongs, while the latter indicates the index N of the main rotational symmetry operation C_N. Table 9.4 shows the various geometry options and the corresponding settings for the parameters `Pgroup` and `Nsym`.

Note that 3D GRS particles have no symmetry elements. The corresponding symmetry group is $\mathcal{C}_1$, which only contains the unit element. For those particles one should switch off the use of irreducible representations in the code.

Note further that *Tsym* is not optimised for axisymmetric geometries. The special symmetry structure of the T-matrix for axial symmetry given in Eq. (8.70) is hard-coded in *mieschka*, which makes this program highly efficient for particles with this particular symmetry. By contrast, *Tsym* uses the full machinery of irreducible representations described in Sect. 8.4 for block-diagonalising the matrices. This procedure is, to be sure, completely general and applies to arbitrary symmetry groups. However, for axisymmetric particles the symmetry structure of the T-matrix is quite trivial, and applying the procedures of Sect. 8.4 becomes unnecessarily complicated. The main purpose for including axisymmetric Chebyshev and GRS geometries in *Tsym* was to test the iterative Lippmann-Schwinger method described in Sect. 9.3.1, rather than to use the group theoretical methods. However, if, for some reason, one wishes to apply irreducible representations to axisymmetric particles in *Tsym*, then there is a straightforward way to do so. Table 9.4 shows that for axial symmetry the index of the main rotational symmetry axis becomes infinite, $N \to \infty$. The commutation relation of the T-matrix for infinite rotational symmetry is given in Eq. (8.70). The corresponding commutation relation for finite rotational symmetry is presented in Eq. (8.69). Numerically, Eq. (8.69) becomes *effectively* like Eq. (8.70) if $N > \max\{|l - l'|\}$. According to Eq. (9.17), l and l' vary, at most, between $-m_{cut}$ and m_{cut}, so $\max\{|l - l'| = 2m_{cut}$. For this reason, Table 9.4 recommends to set `Nsym`$=2m_{cut}+1$ for axisymmetric particles.

If one switches off the use of irreducible representations, one still needs to specify the parameters `Pgroup` and `Nsym` in the input parameter file; the program needs these parameters in order to apply the correct commutation relations.

Finally, one can run the program without exploiting symmetries by setting `Pgroup=Cn` and `Nsym=1`. For instance, one may want test the reduction in computation time due to the use of symmetries. This can be achieved by running the code twice, first with symmetries switched on, and a second time with symmetries switched off. More generally, it is possible to choose settings for `Pgroup` and `Nsym` that differ from those indicated in Table 9.4 if the chosen group is a subgroup of the particle's symmetry group. For instance, if a particle has $\mathcal{D}_{6h}$ symmetry, then examples of subgroups would be $\mathcal{D}_6$, $\mathcal{C}_{6h}$, $\mathcal{C}_6$, or, trivially, $\mathcal{C}_1$. Another important example in this regard are cubes, which belong to the octahedral symmetry group $\mathcal{O}_h$. At the time of writing, this rather special symmetry group is not yet implemented in *Tsym*. However, one can partially exploit the symmetries of a cube by using the subgroup $\mathcal{D}_{4h}$ (`Pgroup=Dnh`, `Nsym=4`).

9.5.2 Convergence Tests

The truncation parameters of the T-matrix, n_{cut} and l_{cut} (called `nmax` and `mmax` in *Tsym*) are specified in the file `params`. Similarly, the number of polar and azimuthal quadrature intervals (`th_nint` and `phi_nint`) need to be specified. The accuracy of the T-matrix results critically depends on the choices of these parameters. The user needs to test the convergence of the results by running computations for different settings of these parameters and analysing the stability of the results. The following procedure can be recommended.

- Set `mmax=nmax` throughout the testing procedure.
- Start with an initial guess for `nmax`, `th_nint`, and `phi_nint`. One may choose a relatively low value of `nmax` (depending on the size parameter), and vary `th_nint` and `phi_nint` until stable results are obtained. This way, one obtains a reasonable first-guess for `th_nint` and `phi_nint`. Experience shows that these first-guess values change very little after `nmax` has been determined (see next step).
- Increase `nmax=mmax` in steps of 3 from its initial value and compare the computational results. The goal is to find a value of this parameter such that the results computed for `nmax` and `nmax+3` are identical within the desired accuracy.
- Once `nmax` has been determined, double-check that the results are stable with respect to an increase in `th_nint` and `phi_nint`.

Usually, the results will be computationally stable for a range of `nmax` values. For values of `nmax` below that range, convergence has not yet been reached, while for values of `nmax` above that range, the results can start diverging. One would like to find the smallest value within the range of convergence, since the computation time rapidly increases with `nmax`.

Note that the code exploits particle symmetries to reduce the angular range of the surface integrals. `th_nint` is the number of polar quadrature intervals in the angular range $\theta \in [0, \pi]$, while `phi_nint` denotes the number of azimuthal quadrature

intervals in the range $\phi \in [0, 2\pi/\texttt{Nsym}]$. (Internally, the code will reduce the integration range even further in the presence of dihedral or reflection symmetries.) Thus, depending on the index of the main rotational symmetry, `Nsym`, the parameter `phi_nint` can be chosen smaller than the parameter `th_nint`.

Computations for size distributions of particles can be computationally highly demanding, as they often require computations for a large number of discrete sizes. It would be impractical to repeat the convergence tests for each and every discrete size in the distribution. Rather, one should choose only a few intermediate sizes $r_i < r_1 < \cdots < r_n = r_f$, where r_i and r_f are the lower and upper limits of the size range, and perform convergence tests only for $r_1, r_2, \ldots, r_n$. One thereby obtains for each size r_j parameters $\texttt{nmax}(j)$, $\texttt{th\_nint}(j)$ and $\texttt{phi\_nint}(j)$. These parameters can be used for performing calculations for all discrete sizes r in the range $r_{j-1} < r < r_j$, $j = 1, \ldots, n$. Each of these size intervals can contain a large number of discrete sizes. To expedite computations even further, one can perform additional convergence tests by trying to reduce $\texttt{mmax}(j)$ from its initial values $\texttt{mmax}(j)$=$\texttt{nmax}(j)$ to the smallest possible value that still gives convergent results.

9.5.3 Result Files

Depending on the choice of input parameters, the program generates two different sets of output files, one for particles in fixed orientation, and another for particles in random orientations. For particles in fixed orientation, the following files are generated.

- **C000001**, **C000002**, ...**:**
  These files contain integrated optical properties. There is one output file for each discrete orientation. The numbering of the files follows the same order in which the different orientations have been specified in the input file. The files contain the extinction, total scattering, and absorption cross sections, as well as the corresponding efficiencies.
- **D000001**, **D000002**, ...**:**
  These files contain the elements of the differential polarimetric scattering cross section, where

  – 1. column: scattering angle
  – 2. column: hh-polarized differential scattering cross-section
  – 3. column: hv-polarized differential scattering cross-section
  – 4. column: vh-polarized differential scattering cross-section
  – 5. column: vv-polarized differential scattering cross-section

  where each of the elements $\mathrm{d}\sigma_{\alpha\beta}/\mathrm{d}\Omega$ is scaled by k_0^2 to make the entries dimensionless.

- **F000001**, **F000002**, . . .**:**
  These files contain the elements of the phase matrix **Z**, where

  – 1. column: scattering angle
  – 2. column: non-normalized phase function Z_{11}
  – 3. column: Z_{22}/Z_{11}
  – 4. column: Z_{33}/Z_{11}
  – 5. column: Z_{44}/Z_{11}
  – 6. column: $-Z_{12}/Z_{11}$
  – 7. column: Z_{34}/Z_{11}

Computations for particles in random orientations produce the following output files.

- **C.dat:**
  This file contains the orientation-averaged extinction, scattering, absorption, and backscattering cross sections, the corresponding efficiencies, as well as the single-scattering albedo, the asymmetry parameter, and the linear and circular backscattering depolarization ratios.
- **F.dat:**
  This file contains the orientation-averaged phase matrix, where

  – 1. column: scattering angle
  – 2. column: normalized phase function $< Z_{11} >$
  – 3. column: $< Z_{22} > / < Z_{11} >$
  – 4. column: $< Z_{33} > / < Z_{11} >$
  – 5. column: $< Z_{44} > / < Z_{11} >$
  – 6. column: $- < Z_{12} > / < Z_{11} >$
  – 7. column: $< Z_{34} > / < Z_{11} >$

  The phase function is normalized according to $(1/2) \int_0^\pi \mathrm{d}(\cos\Theta) < Z_{11} > (\Theta) = 1$, where Θ denotes the scattering angle.
- **E.dat:**
  This file contains the expansion coefficients of the elements of the orientation-averaged phase matrix in the basis of generalized spherical functions. Many polarized radiative transfer codes, such as VDISORT, require the phase matrix in this format. The phase matrix is expanded according to

$$< Z_{11} > (\Theta) = \sum_{l=0}^{\infty} a_1^\ell P_{0,0}^\ell(\Theta) \tag{9.22}$$

$$< Z_{22} > (\Theta) + < Z_{33} > (\Theta) = \sum_{l=2}^{\infty} (a_2^\ell + a_3^\ell) P_{2,2}^\ell(\Theta) \tag{9.23}$$

$$< Z_{22} > (\Theta) - < Z_{33} > (\Theta) = \sum_{l=2}^{\infty} (a_2^\ell - a_3^\ell) P_{2,-2}^\ell(\Theta) \tag{9.24}$$

$$< Z_{44} > (\Theta) = \sum_{l=0}^{\infty} a_4^{\ell} P_{0,0}^{\ell}(\Theta) \tag{9.25}$$

$$< Z_{12} > (\Theta) = \sum_{l=2}^{\infty} b_1^{\ell} P_{0,2}^{\ell}(\Theta) \tag{9.26}$$

$$< Z_{34} > (\Theta) = \sum_{l=2}^{\infty} b_2^{\ell} P_{0,2}^{\ell}(\Theta), \tag{9.27}$$

where $P_{p,q}^{\ell}$ denote generalized spherical functions. The output file contains

- 1. column: Expansion order ℓ
- 2. column: Expansion coefficients a_1^{ℓ}
- 3. column: Expansion coefficients a_2^{ℓ}
- 4. column: Expansion coefficients a_3^{ℓ}
- 5. column: Expansion coefficients a_4^{ℓ}
- 6. column: Expansion coefficients b_1^{ℓ}
- 7. column: Expansion coefficients b_2^{ℓ}

Thus the *Tsym* output can be directly used as input to polarized radiative transfer calculations.

In addition, the code produces a logfile with runtime information, as well as three files named `matlab?.out` (`?=x,y,z`). The latter can be used by matlab to plot the particle geometry. The distribution of *Tsym* contains a subdirectory `MATLAB` with a script for plotting the particle in its standard orientation. The user needs to have Matlab on his system for running the script.

9.5.4 Resources

Program *Tsym* can be obtained at

http://www.rss.chalmers.se/kahnert/Tsym.html.

Apart from the source codes, the distribution of *Tsym* contains a few other useful resources. There is a subdirectory with several examples, test cases, and exercises for the novice who wants to become familiar with the program. One directory contains data files with pre-computed group character tables for several point groups. Another directory contains an interface to the GAP programming language. GAP is a script language for computational discrete algebra. It can, among many other things, be used to compute group character tables. As this can be quite non-trivial for

high-order symmetry groups, *Tsym* includes utility programs that automatize the use of GAP for computing character tables of point groups. If the user wishes to perform computations for particles for which the group character table is not contained in the list of pre-computed tables, then the utility programs can be employed to automatically generate GAP input scripts, call GAP, and post-process the output so that it can be directly read in by *Tsym*. GAP is free, open-source software that can be obtained at http://www.gap-system.org/.

Chapter 10
Recommended Literature

This chapter requires a clear statement at the beginning: **The recommended literature of this chapter is neither complete nor should it be understood as a ranking. It merely reflects the authors' very personal preferences.** Only those books and papers have been included which have been found most useful by the authors, and which were always in the near of their desk. Some aspects of electromagnetic wave scattering are not considered in the book at hand, and some aspects are only mentioned. The following list of recommended literature is therefore also aimed to provide the interested reader with additional information and more detailed considerations. It must also be stated that the following classification of the books and papers is not always unique. Even in the cited monographs there are often considered several of the subjects used in this chapter for the classification. The citation of a book in a certain section is again owed to the authors' personal point of view. Some of the cited literature are commented to emphasize those aspects which seem to be most important for a certain subject in conjunction with the book at hand.

10.1 Mie Theory

Born, M. and Wolf, E.: "Principles of Optics", Pergamon Press, Oxford, 1980.

In this book one can find a detailed representation of Mie's theory formulated in terms of the Debye potentials (*see especially Sect.* 13.5 *of this book*). *Please, note that instead of the* ϕ*-dependent function* $e^{il\phi}$ *the two real-valued functions* $cos(l\phi)$ *and* $sin(l\phi)$ *are used throughout this book.*

Debye, P.: "Der Lichtdruck auf Kugeln von beliebigem Material", Ann. Phys. **30**, p. 57, 1909.

In this famous paper Mie's theory is formulated for the first time by introducing the potentials named after Debye later on.

T. Rother and M. Kahnert, *Electromagnetic Wave Scattering on Nonspherical Particles*, Springer Series in Optical Sciences 145, DOI: 10.1007/978-3-642-36745-8_10,

Grandy, W.T.: “Scattering of Waves from Large Spheres”, Cambridge University Press, Cambridge (UK), 2000.

This book contains the classical Mie theory in Debye potential formulation, too. But as its title already indicates, the focus of the book is on large spherical scatterers (i.e., scattering on spheres at very high size parameters) for which the conventional Mie series (see (7.79–7.82) in the book at hand) becomes not or only very slowly convergent. It seems to be quite interesting to find out if some of the analysis presented in this book may be adopted for light scattering on nonspherical particles!

Mie, G.: “Beiträge zur Optik trüber Medien, speziell kolloidaler Metallösungen”, Ann. Phys. **25**, p. 377, 1908.

That is **the classical** *and important paper of G. Mie dealing with light scattering in turbid media. Therein, he developed the theory now known as Mie’s theory. It is listed at the end of this section only for the reason of alphabetic order!*

10.2 Mathematical Aspects of Scattering

Abramowitz, M. and Stegun, I.A.: “Handbook of Mathematical Functions”, Harri Deutsch, Frankfurt/Main, 1984.

Dallas, A.G.: “On the convergence and numerical stability of the second Waterman scheme for approximation of the acoustic field scattered by a hard object”, Technical Report Nr. 2000-7, Dept. of Mathematical Sciences, University of Delaware, 2000.

In this report one can find the proof of the norm convergence of the scattering quantities in the far-field (see Sect. 2.2.1 in the book at hand). This proof is restricted to one specific T-matrix method already derived by Waterman, and to spheroidal scatterer geometries. Even if the proof is hardly traceable for non-mathematicians it is one of the few profound papers dealing in detail with the convergence behaviour of the T-matrix approaches as well as with related misunderstandings.

Doicu, A., Eremin, Y. and Wriedt, T.: “Acoustic And Electromagnetic Scattering Analysis Using Discrete Sources”, Academic Press, New York, 2000.

In this book one can find the proofs of completeness and linearly independence of different classes of expansion functions at selected boundary surfaces. The Discrete Source Method treated in this book represents a specific T-matrix approach with a special choice of expansion functions.

Kleinman, R.E., Roach, G.F. and Ström, S.E.G.: “The null field method and modified Green functions”, Proc. R. Soc. Lond., A **394**, p. 121, 1984.

Relation (4.8), treated in the book at hand as a consequence of Huygens’ principle, was used in this paper for the first time as an appropriate ansatz of the Green function related to the scalar outer Dirichlet problem. It was shown afterwards how one can

calculate the unknown coefficients $[T_{\partial\Gamma}]_{i,k}$ *by use of the boundary condition* (1.10) *if applied in a least-squares sense. This paper was the driving force for the author's own considerations, especially for the introduction of the interaction operator presented in Chap.* 4. *This paper contains furthermore the proofs of completeness and linearly independence of the scalar eigensolutions of Helmholtz's equation as well as the proofs regarding the invertability of some infinite and finite matrices related to T-matrix approaches* (*see also Chap.* 2 *in the book at hand*).

Reed, M. and Simon, B.: "Methods of Modern Mathematical Physics", Vol. 3, Academic Press, San Diego, 1979.

Reading this book with benefit requires considerable mathematical expertise the authors of the book at hand do not possesses, unfortunately. But at the beginning of this book one can find a very helpful definition of "scattering" in general, the mathematical implications of this model, and the importance of the far-field.

Sommerfeld, A.: "Partial Differential Equations in Physics", Academic Press, New York, 1949.

This book is a bonanza for the reader who may be interested in mathematical and methodical aspects of solving partial differential equations. It introduces already Green functions in a clear and mathematically sound way. Especially the theory of Fourier series presented at the beginning of this book was very helpful for several considerations in the book at hand.

Varshalovich, D.A., Moskalev, A.N. and Khersonskii, V.K.: "Quantum Theory of Angular Momentum", World Scientific, Singapore, 1998.

In this book one can find a huge collection of properties, special cases, and representations of the scalar as well as vectorial eigensolutions of the Helmholtz and vector wave equation. This book can be used with benefit if one is interested in creating a T-matrix code.

10.3 Green Functions

Duffy, D.G.: "Green's Functions with Applications", Chappman & Hall/CRC, New York, 2001.

This book systematically describes different approaches of deriving Green's functions in different areas of physics. Moreover, it contains numerous examples thus making it especially appropriate for the practitioner.

Levine, H. and Schwinger, J.: "On the theory of electromagnetic wave diffraction in an infinite plane conducting screen", Appl. Math. **3**, p. 355, 1950.

Expression (2.321) *of the dyadic free-space Green function was derived in this paper for the first time.*

Morse, P.M. and Feshbach, H.: “Methods of Theoretical Physics”, McGraw-Hill, New York, 1953.

These two volumes have been an invaluable guidance to the authors in deriving the content of Chaps. 3, 4, and 8. They present an impressive demonstration of the importance of sophisticated analytical thinking to solve not only simple but more realistic physical problems of practical interest. Highly recommended are the chapters concerning Green functions. These have been frequently visited by the authors of the book at hand.

Tai, Chen-To: “Generalized Vector and Dyadic Analysis”, IEEE Press, NJ, 1992.

Here one can find the derivation of all the Green theorems related to vectorial and dyadic quantities.

Tai, Chen-To: “Dyadic Green Functions in Electromagnetic Theory”, IEEE Press, NJ, 1994.

This is one of the few books using Green functions throughout and in a consequent way to represent electrodynamic wave theory. It contains a lot of informative examples of how to use Green functions to solve electromagnetic wave problems, and it is highly recommended not only for modeller but also for the more practical interested reader.

10.4 T-Matrix Methods

Andreasen, M. G.:“ Comments on “Scattering by Conducting Rectangular Cylinders””, IEEE Trans. on Antennas and Propag. AP-12, p. 235, 1964.

Barber, P.W. and Hill, S.C.: “Light Scattering by Particles: Computational Methods”, World Scientific, Singapore, 1990.

The convergence strategy described in this book was partially overtaken in the program “mieschka”. The T-matrix program of Barber and Hill (that comes along with this book) was moreover used for intercomparison purposes with ”mieschka”.

Mei, K. K. and van Bladel, J.: “Scattering by Perfectly-Conducting Rectangular Cylinders”, IEEE Trans. on Antennas and Propag. AP-11, p.185, 1963.

Tsang, L., Kong, J.A. and Shin, R.T.: “Theory of Microwave Remote Sensing”, Wiley, New York, 1985.

Even if not suggested by its title this book contains a detailed representation of the T-matrix approach on the basis of the “Extended Boundary Condition” (see Sect. 3.5, of this book). Beside a lot of interesting applications of electromagnetic wave scattering in microwave remote sensing it employs already the operator formalism to model multiple scattering. But the interrelation between the used T-operator and

Waterman's T-matrix was not clarified. This situation was one of the trigger to introduce the interaction operator as part of the Green function related to the scattering problem on a single particle in the book at hand.

Waterman, P.C.: "Matrix formulation of electromagnetic scattering", Proceedings of IEEE **53**, p. 805, 1965.

Waterman, P.C.: "Symmetry, unitarity, and geometry in electromagnetic scattering", Phys. Rev. D **3**, p. 825, 1971.

These two papers are the flagships of the T-matrix method and a **must** *for every scientist who is interested in this method. The latter paper contains the description of an iterative orthogonalization technique to ensure the unitarity property for every finite-dimensional T-matrix if nonabsorbing nonspherical scatterers are considered.*

Wiscombe, J.A. and Mugnai, A.: "Single Scattering from Nonspherical Chebyshev Particles", NASA Reference Publ. 1157, 1986.

This report is a detailed treatment of the T-matrix method with emphasize on its numerical aspects and its application to light scattering modelling on Chebyshev particles. This report is especially recommended for practitioners. It contains also a short but informative section on Rayleigh's hypothesis. The included results for Chebyshev particles have been used for intercomparison purposes with our own T-matrix program "mieschka".

Schmidt, K., Rother, T. and Wauer, J.: "The equivalence of applying the Extended Boundary Condition and the continuity conditions for solving electromagnetic scattering problems", Opt. Comm. **150**, p. 1, 1998.

10.5 Method of Lines

Dreher, A. and Rother, T.: "New Aspects of the Method of Lines", IEEE Microwave and Guided Wave Letters **5**, p. 408, 1995.

Pregla, R. and Pascher, W.: "Method of Lines", in "Numerical Techniques for Microwave and Millimeter Wave Passive Structures", T. Itoh (Ed.), Wiley, New York, 1989.

Rother, T. and Schmidt, K.: "The discretized Mie-formalism for electromagnetic scattering", in "Progress in Electromagnetic Research", Kong, J.A. (Ed.), EMW Publishing, Cambridge, Massachusetts, 1997.

This book contribution originates from one of the author's (T.R.) younger days when he was an enthusiastic advocate of the Method of Lines. The reasons for his turning away from this method are explained in Chap. 5 of the book at hand. However, the intensive study of this method in conjunction with electromagnetic wave scattering on nonspherical particles and the clarification of occurring contradictions was of

some value for the later development of the Green function formalism as well as for a better understanding of the methodical backgrounds of other solution techniques.

Schulz, U.: "Die Methode der Geraden - ein neues Verfahren zur Berechnung planarer Mikrowellenstrukturen", Dissertation, Fernuniversität Hagen, 1980.

This Ph.D work is recommended for the reader who may be interested in the details of the Method of Lines. All essential aspects like the discretization error, boundary conditions and discretization, determination of the eigenvectors, etc. are discussed therein.

10.6 Integral Equation Methods and Singularities

Colton, D. and Kress, R.: "Integral Equation Methods in Scattering Theory", Wiley, New York, 1983.

Fikioris, J.G.: "Singular integrals in the source region", J. Electromagn.Waves Appl. **18**, p. 1505, 2004.

This article is concerned with the strong singularity of the dyadic free-space Green function and its impact on integral equation approaches. It is a concise and clearly written paper which reveals the risks if one disesteem this problem.

Fikioris, J.G. and Magoulas, A.N.: "Scattering from axisymmetric scatterers: A hybrid method of solving Maue's equation", PIER **25**, p. 131, 2000.

Hönl, H., Maue, A.W. and Westphal, K.: "Theorie der Beugung", in "Handbuch der Physik" Band 25/1, S. Flügge (Ed.), Springer, Berlin, 1961.

Existing only in German, unfortunately, this book represents one of the most detailed description of diffraction problems in physics the authors of the book at hand know. The integral equation formulation is within the focus of this book. Beside the conceptual fundamentals, it contains also several instructive examples. The detailed study of the boundary integral relation between the Dirichlet and von Neumann boundary value problem is highly recommended for the reader who may be interested in the methodical background of integral equation approaches. Waterman was already impressed by this book. Especially the derivation of Maue's integral equation presented therein can be considered to be the starting point for the development of his T-matrix approach by use of the Extended Boundary Condition to avoid problems at internal resonances.

Martin, P.A.: "On connections between boundary integral equations and T-matrix methods", Engineering Analysis with Boundary Elements **27**, p. 771, 2003.

Maue, A.W.: "Zur Formulierung eines allgemeinen Beugungsproblems durch eine Integralgleichung", Z. Physik **126**, p. 601, 1949.

Van Bladel, J.: "Singular Electromagnetic Fields and Sources", Clarendon Press, Oxford, 1991.

Wang, J.J.H.: "Generalized Moment Methods in Electromagnetics", Wiley, New York, 1991.

10.7 Rayleigh's Hypothesis

Bates, R.: "Rayleigh hypothesis, the Extended Boundary Condition and Point-Matching", Electron. Lett. **5**, p. 654, 1969.

Burrows, M.L.: "Equivalence of the Rayleigh solution and the Extended Boundary Condition solution for scattering problems", Electron. Lett. **5**, p. 277, 1969.

Keller, J.B.: "Singularities and Rayleigh's hypothesis for diffraction gratings", J. Opt. Soc. Am. **A 17**, p. 456, 2000.

Linton, C.M.: "The Green's function for the two-dimensional Helmholtz equation in periodic domains", J. Enging. Math. **33**, p. 377, 1998.

This article contains a collection of different expressions of the free-space Green function related to Helmholtz's equation in Cartesian coordinates if two-dimensional and periodic problems are considered (*see Chap.* 6 *in the book at hand*). *Their numerical advantages and disadvantages are discussed in detail.*

Lippmann, B.A.: "Note on the theory of gratings", J. Opt. Soc. Amer. **43**, p. 408, 1953.

This very short comment on Rayleigh's approach to solve plane wave scattering on periodic gratings can be considered as the date of birth of "Rayleigh's hypothesis". With this comment Lippmann expressed his doubts on the completeness of outgoing plane waves to solve this scattering problem.

Loewen, E.G. and Popov, E.: "Review of Electromagnetic Theory of Grating Efficiencies", CRC Press, New York, 1997.

Lord Rayleigh: "On the dynamical Theory of gratings", Proc. R. Soc. Lond. A **79**, p. 399, 1907.

This is the famous, frequently cited, and controversial discussed paper of Rayleigh regarding plane wave scattering on periodic gratings.

Millar, R.F.: "On the Rayleigh hypothesis in scattering problems", Electron. Lett. **5**, p. 416, 1969.

Millar, R.F. and Bates, R.: "On the legitimacy of an assumption underlying the point-matching methods", IEEE-MTT **18**, p. 325, 1970.

Millar, R.F.: “The Rayleigh hypothesis and a related least-squares solution to scattering problems for periodic surfaces and other scatterers”, Radio Science **8**, p. 785, 1973.

Petit, R. and Cadilhac, M.: “Sur la diffraction d’une onde plane par un reseau infiniment conducteur”, C. R. Acad. Sci. B **262**, p. 468, 1966.

Petit, R.: “A Tutorial Introduction”, in “Electromagnetic Theory of Gratings”, R. Petit (Ed.), Springer, Berlin, 1980.

van den Berg, P.M. and Fokkema, J.T.: “The Rayleigh hypothesis in the theory of reflection by a grating”, IEEE Trans. Antennas Propag. **27**, p. 577, 1979.

van den Berg, P.M. and Fokkema, J.T.: “The Rayleigh hypothesis in the theory of diffraction by a cylindrical obstacle”, J. Opt. Soc. Amer. **69**, p. 27, 1979.

Wauer, J. and Rother, T.: “Considerations to Rayleigh’s hypothesis”, Opt. Comm. **282**, p. 339, 2009.

Chapter 6 of the book at hand is based essentially on this paper we published very recently in Optics Communications. It compares for the first time (to the best of our knowledge!) numerical near-field results obtained by use of a T-matrix approach and a boundary integral equation method.

10.8 Electromagnetic Wave Theory

Jackson, J. D.: “Classical Electrodynamics”, Wiley, New York, 1975.

Kong, J.A.: “Electromagnetic Wave Theory”, Wiley, New York, 1986.

Lindell, I.V.: “Methods for Elelctromagnetic Field Analysis”, Oxford University Press, Oxford, 1992.

Müller, C.: “Foundations of the Mathematical Theory of Electromagnetic Waves”, Springer, Berlin, 1969.

Stratton, J.A.: “Electromagnetic Theory”, McGraw-Hill, New York, 1941.

Van Bladel, J.: “Electromagnetic Fields”, Hemisphere Publ. Corp., New York, 1985.

10.9 Scattering of Electromagnetic Waves and Applications

Barber, P.W. and Chang, R.K. (eds.): “Optical Effects Associated With Small Particles”, World Scientific, Singapore, 1988.

Bohren, C.F. and Huffman, D.R.: “Absorption and Scattering of Light by Small Particles”, Wiley, New York, 1983.

Hovenier, J.W. et al.: "Computations of scattering matrices of four types of non-spherical particles using diverse methods ", J. Quant. Spectrosc. Radiat. Transfer **55**, p. 695, 1996.

Kerker, M.: "The Scattering of Light", Academic Press, New York, 1969.

Mishchenko, M.I., Hovenier, J.W. and Travis, L.D. (Ed.): "Light Scattering by Non-spherical Particles: Theory, Measurements, and Applications", Academic Press, San Diego, 2000.

Mishchenko, M.I., Travis, L.D. and Lacis, A.A.: "Scattering, Absorption, and Emission of Light by Small Particles", Cambridge University Press, Cambridge (UK), 2002.

This book provides the reader with all the necessary electromagnetic aspects of light scattering. It contains moreover a detailed description of the analytical orientation averaging process together with the demonstration of its benefit in several instructive applications. The T-matrix method is within the focus of this book. The Appendices with their concise collection of all the relations, expressions, and properties of eigenfunctions which are of importance to create a T-matrix code may not be unmentioned!

Mugnai, A. and Wiscombe, W.J.: "Scattering of radiation by moderately nonspherical particles", Journal of Atm. Sci. **37**, p. 1291, 1980.

The examples presented therein are used for intercomparison purposes with "mieschka".

Nieto-Vesperinas, M.: "Scattering and Diffraction in Physical Optics", Wiley, New York, 1991.

The first chapter of this book is concerned with the extinction theorem and its equivalence to the "Extended Boundary Condition" used by Waterman to derive the T-matrix. The second chapter is a reprint of an article of Wolf regarding the importance of the extinction theorem in electromagnetic wave theory as well as in quantum mechanics. Beside several modern applications this book provides an up-to-date description and discussion of the basic concepts underlying physical optics.

Rother, T. et al.: "Light scattering on Chebyshev particles of higher order", Applied Optics **45**, p. 6030, 2006.

In this paper we could demonstrate that Chebyshev particles of higher orders exhibit a behaviour comparable to that of particles with an impressed surface roughness. Especially in the back scattering behaviour particles with a surface roughness differ significantly from regular nonspherical particles (i.e., particles with a smooth boundary surface) even if these are highly absorbing.

Saxon, D.S.: "Tensor Scattering Matrix for the Electromagnetic Field", Phys. Rev. **100**, p. 1771, 1955.

Schuerman, D.W. (Ed.): “Light Scattering by Irregularly Shaped Particles”, Plenum Press, New York, 1980.

This collection of articles marked the beginning of an intensive and critical examination of the importance of light scattering on nonspherical particles in remote sensing. The articles are concerned with experimental, methodical, as well as theoretical aspects. But also the opening contribution “Some Remarks on Science, Scientists, and the Remote Sensing of Particulates” by D. Deirmendjian is highly recommended since it is up-to-date even today!

van de Hulst, H.C.: “Light Scattering by Small Particles”, Dover, New York, 1981.

This has become the standard book on light scattering. It comprises experimental and physical/theoretical fundamentals as well, and it can be always read with benefit even if its emphasize is on light scattering on spherical particles.

Wauer, J. et al.: “MIESCHKA and CYL—two software packages for light scattering analysis on nonspherical particles in DLR’s Virtual Laboratory”, Appl. Opt. **43**, p. 6371, 2004.

10.10 Group Theory

Bishop, D.M.: “Group Theory and Chemistry”, Dover, Mineola, 1993.

This book offers a very readable introduction to point groups. It maintains sufficient mathematical rigour, while keeping the reader’s attention by providing many practical examples from theoretical chemistry. Only some basic knowledge of linear algebra, elementary quantum mechanics, and molecular physics is assumed.

Kahnert, M.: “Irreducible representations of finite groups in the T matrix formulation of the electromagnetic scattering problem”, J. Opt. Soc. Am. A **22**, p. 1187, 2005.

Kahnert, M. et al.: “Application of the extended boundary condition method to homogeneous particles with point group symmetries”, Appl. Opt. **40**, p. 3110, 2001.

Kahnert, M.: “Light scattering by particles with boundary symmetries”, in “Light Scattering Reviews 3”, Kokhanovsky, A. A. (Ed.), Springer, Berlin, 2008.

These articles discuss reducible and irreducible representations of point groups in T-matrix computations, practical aspects concerning their implementation, as well as boundary symmetries in general differential and integral equation problems, and their relation to the self-consistent Green function and T-matrix formulations of the electromagnetic scattering problem.

10.11 Miscellaneous

Dyson, F.: “George Green and Physics”, Physics World **6**, p. 33, 1993.

Ernst, T. et al.: “DLR’s Virtual Lab: Scientific Software Just a Mouse Click Away”, IEEE-CISE **5**, p. 70, 2003.

Heisenberg, W.: “Die beobachtbaren Grössen in der Theorie der Elementarteilchen”, Z. Phys. **120**, p. 513, 1943.

This is the second paper introducing (independently of Wheeler) the S-matrix to characterize scattering processes in quantum mechanics. The importance and the properties of this matrix are discussed in detail. However, its unitarity property is deduced from the principle of energy conservation. The S-matrix was introduced in electromagnetic wave scattering theory only later on.

Newton, R.G.: “Optical theorem and beyond”, American J. Phys. **44**, p. 639, 1976.

This is a quite interesting article regarding the history and importance of the so-called “optical theorem” (see Sect. 7.3 in the book at hand) in several fields of physics.

Wheeler, J.A.: “On the Mathematical Description of Light Nuclei by the Method of Resonating Group Structure”, Phys. Rev. **52**, p. 1107, 1937.

This is the first paper introducing the S-matrix to characterize scattering processes in quantum mechanics.

Index

A
Absorbing boundary conditions, 150
Amplitude matrix, 231
Asymmetry parameter, 323

B
Bessel functions, 33, 147, 184
Best approximation, 86
Boundary condition, 10, 18, 89, 204
  dielectric, 208
  homogeneous Dirichlet, 6, 67, 140, 148, 175
  homogeneous Neumann, 140
  ideal metallic, 207
  inhomogeneous, 6
  periodicity, 175
  transmission, 6, 67, 92
Boundary integral, 60, 61, 133, 154, 186
Boundary integral equation, 131, 151, 152, 158, 159, 173, 189, 212
Boundary value problem, 3, 5, 59, 130, 137

C
Chebyshev particle, 239, 306
  high-order, 319
Collocation method, 130
Completeness, 20, 33, 172
Convergence, 19
  criterion, 19
  norm, 19
  of improper integral, 153
  uniform, 19
  weak, 19, 124
Coordinate system
  rotation of, 50
Coordinates
  Cartesian, 31
  spherical, 31, 39, 42, 45, 62, 71, 74, 90, 144
Cross section
  absorption, 235, 323
  backscattering, 323
  extinction, 235
  scattering, 235, 323
Cylinders
  finitely extended circular, 304

D
Debye potentials
  boundary conditions, 31
  scalar potentials, 216, 217
  vector potentials, 214
Delta distribution, 61, 81
  dyadic, 76
  dyadic surface, 94
  surface, 83
Differential scattering cross section, 236
  reciprocity, 299
  shifted sphere, 292
  sphere, 289
  spheroid, 293
Diffraction, 203
Discretization operator, 140, 141
DLR Virtual Laboratory, 325
Dyadic, 70, 167
  far-field scattering function, 225
  identities, 72
  product, 71

E
Efficiency
  absorption, 236

T. Rother and M. Kahnert, *Electromagnetic Wave Scattering on Nonspherical Particles*, Springer Series in Optical Sciences 145, DOI: 10.1007/978-3-642-36745-8,

Efficiency (*cont.*)
extinction, 236
scattering, 236
Eigenresonances, 130
Eigensolutions, 121
incoming, 35, 45
radiating, 10, 35, 45, 84
regular, 12, 35, 45
Eigenvalue problem, 144, 147
Eigenvalues, 145, 148
Eigenvectors, 148
Equivalence principle, 151
Euler matrix, 52
Euler transformation, 52
Eulerian angles, 50
Expansion coefficients, 18, 22, 40, 57, 82, 97, 146
Expansion functions, 18, 20, 85, 86, 136, 180
entire domain, 21
linear independent, 20, 24, 133
orthogonal, 21
subdomain, 21
Extended boundary condition, 130, 132
Extinction Theorem, 131

F
Far-field, 221
Finite-difference method, 137, 138, 149
Fourier series, 177
Fourier transformation, 62

G
Gegenbauer representation, 40
Geometric optics, 1
Gram's matrix, 20, 22
Gram-Schmidt process, 29
Grating, 171
sinusoidal, 172
Green functions, 59, 108, 114, 116, 152, 177
approximation of, 65, 66
auxiliary, 67, 109
dyadic, 78
dyadic, 112, 118
outer Dirichlet problem, 100
outer transmission problem, 102
dyadic free-space, 74
dyadic surface, 98
free-space, 61, 88, 109, 177
iterative solution, 165, 166
magnetic, 212
of spherical scatterer, 90, 101
outer Dirichlet problem, 67, 85, 109
outer transmission problem, 67, 92, 93, 111
singularity of, 60, 64, 74, 76, 152, 178, 209
surface, 87, 90, 108
Green theorem, 60, 68, 87, 97, 161
dyadic-dyadic, 73, 75, 78, 99, 125
vector-dyadic, 73, 78, 98
Groove depth limit, 172
Group theory, 265
block diagonalisation of matrices, 283
conjucacy classes, 268
conjugate elements, 268
CPU time reductions, 267, 324
great orthogonality theorem, 277
group characters, 00
group generators, 265, 267, 276
implementation in T-matrix program, 336
invariant subspace, 273
dimension, 284
projection operator, 277
representations, 269
irreducible, 28, 270, 273, 275
reducible, 00
transformation into irreducible basis, 280

H
Hankel functions, 33, 147, 178
Helmholtz equation, 5, 9, 61, 138, 148
eigensolutions of, 30
scalar, 216
underlying assumptions, 205
Huygens' principle, 88, 89, 98, 99, 106, 109, 152

I
Idem factor, 71
Improper integral, 153, 158
Integral representation, 102
Interaction operator, 106, 107, 110, 118, 123, 133, 152, 163, 170, 173, 181, 189
dyadic, 113, 119, 168
outer Dirichlet problem, 111
outer Dirichlet problem, 153
outer transmission problem, 109
Irreducible representations, 270

L
Least-squares approach, 173, 185
Legendre polynomials, 33, 147
Lippmann-Schwinger equation, 152, 164, 166, 168, 169

Longitudinal fields, 45
Lorentz gauge, 215
Lorentzian line, 316

M
Maxwell's equations, 175, 206
Mean square error, 21, 22, 82
Method of Lines, 9
Mie theory, 90, 214
Mieschka program, 324
  automatic convergence, 327
  convergence strategy, 325
  operation, 329
  options, 330
  orientation averaging, 327
  software package, 335
Morphology dependent resonances, 316, 317

N
Near-field computation, 173
Neumann functions, 35
Norm, 187
Null-Field method, 130

O
Observation point, 60, 65, 67, 98, 154
Optical theorem, 229
Orientation averaging, 157
Outer Dirichlet problem, 5, 25, 27, 86, 98, 121, 127, 130, 152, 158
  integral representation of, 68
Outer transmission problem, 5, 27, 121, 152
  integral representation of, 68

P
Particles
  fixed orientation, 288
  random orientations, 302
Periodic surface, 171
Periodicity condition, 177, 180
Phase function
  size averaged, 314
  sphere, 302
  spheroid, 302
  spheres, 308
Phase matrix, 308
  symmetry relations, 308
Plane wave, 39, 53, 65, 76, 90, 102, 222
  inearly polarized, 58
  outgoing, 171, 176
Point matching method, 130, 172
Poisson integral, 40
Poynting vector
  time-averaged, 229
Principal axis transformation, 144
Principal value, 153, 162

R
Radiation condition, 7, 34, 39, 45, 61, 62, 64, 67, 74, 87, 98, 150, 176, 180
Rayleigh hypothesis, 76, 85, 107, 130, 157, 170, 171, 184, 186
Rayleigh method, 8, 90, 111, 130, 146
Rayleigh scattering, 1
Reciprocity, 62, 115, 295
Residual method, 62, 64
Resonance region, 1

S
Scalar product, 10, 86, 183
Scattering amplitude matrix, 231
Scattering quantities, 230
  orientation averaged, 236
Scattering
  electromagnetic, 203, 204
  scalability, 203, 237
Schauder basis, 187
Separation of Variables method, 29, 32, 138, 147, 149
Series expansion, 18
Similarity transformation, 144
Single-scattering albedo, 323
Singular value decomposition, 137, 283
Size parameter, 1, 238
S-matrix, 45, 115, 119, 122, 125
Solenoidal fields, 46
Source point, 60, 67
Sphere
  absorbing, 289, 303
  nonabsorbing, 289, 302
  shifted, 238, 292
Spherical harmonics, 32, 41
Spheroid, 238, 293
  absorbing, 303
  database, 313
  nonabsorbing, 302
  scattering quantities, 314
Stokes matrix, 232
Stokes vector, 232
Surface current, 133, 151, 157, 160, 170, 210
Surface roughness, 319
Symmetries

Symmetries (*cont.*)
axial, 261
CPU time reductions, 267, 324
free-space Green function, 61, 244
geometric, 241, 285
Green function
outer Dirichlet problem, 244, 245, 249
outer transmission problem, 250
groups, 265
interacton operator
outer Dirichlet problem, 243, 249
outer transmission problem, 250
inversion, 242, 259
outer Dirichlet problem, 242
outer transmission problem, 249
point groups, 266
reflections, 255
rotation-reflections, 259
rotations, 118, 119, 251
spherical, 262
T-matrix
commutation relations, 248–251, 261, 267
unitary representations, 251

T
Taylor expansion, 141
T-matrix
commutation relations, 248- 251, 261, 267
iterative solution method, 321
non-axisymmetric particles, 336
perturbation approach
implementation, 336
perturbation approach, 320
programs
mieschka, 287, 324
Tsym, 288, 336
T-matrix, 12, 26, 66, 86, 90, 92, 97, 103, 115, 128, 136, 157, 170, 173, 183
Transformation matrix, 24, 27, 89, 100, 144, 146, 183
Truncation parameter, 20, 40, 82
Tsym program, 336
geometries, 336
operation, 337
source code, 342
testing of convergence, 339

U
Unit source, 59, 65
Unit vector, 32, 41, 58, 65, 71
Unitarity, 26, 35, 45, 123, 127
relation to energy conservation, 115, 230

V
Vector spherical harmonics, 43
Vector-wave equation, 5, 9
igensolutions of, 42
Volume current, 151, 164, 170
Volume integral equation, 151, 164

W
Wave equation
for vector fields, 208
Weighting functions, 11, 13, 24, 174, 184
Wigner D functions, 50
Wigner functions, 50